# Hepatitis C virus induced perturbation of hepatic differentiation

Abigail Melissa Bloy

Submitted in accordance with the requirements for the degree of
Doctor of Philosophy

The University of Leeds
School of Medicine

September 2018

The candidate confirms that the work submitted is her own and that appropriate credit has been given where reference has been made to the work of others.

Chapter 3

Figure 3.1.1 Hepatic progenitor cell isolation, characterisation and HCV infection *ex vivo* carried out by Matthew Bentham

Figure 3.4.1 Huh7 cell FACS and CD24lo and CD24 high characterisation carried out by Matthew Bentham ; Huh7 cell mouse xenograft experiement carried out by Dr Adel Samson and Teklu Egnuni

Chapter 5

Figure 5.3.3, Figure 5.3.4 and Figure 5.3.5 RNA analysis and RNA seq library preparation carried out by Claire Morrisroe

Figure 5.3.6, Figure 5.3.8 and Figure 5.3.9 RNA seq initial analysis carried out by Dr Ping Wang

## Acknowledgements

I would like to thank my supervisor Dr Stephen Griffin for his support, patience and guidance throughout my PhD. Thanks also to Dr Matthew Bentham for letting me include some of his work, training me, answering my many questions and for being the optimist to my pessimism. I would like to thank Dr Andrew Macdonald and Dr Laura Matthews for their valuable input. I would like to thank Dr Luke Meredith for helping us set up the HepaRG cell culture. My thanks also go to all the past and present members of the Griffin lab, especially the Gryffindors, for listening to me, sharing my frustrations and for offering their moral support. I would also like to thank them for helping me out when I asked for a favour such as splitting cells or going to liquid nitrogen with (or without) me to bring up more cells. I would like to also extend my thanks to everyone else on Level 5 for welcoming me, making the years I spent at Leeds so fun and providing so many interesting lunch and coffee break conversations. So long, and thanks for all the cake. My thanks goes to my housemates Aarren and Rebecca for supporting me, listening to my worries and rants, and allowing me to practice my presentations too many times to count. Most of all I want to thank them for their friendship. I want to thank Becca for her friendship, support and most of all for all the laughter. Thanks also to the rest of my friends not in Leeds who supported me from afar. I want to thank my parents, siblings and nephew for believing in me and for their love and support throughout all my studies. Lastly I want to thank Alex for always being there for me, for laughing with me (or at me), and for filling our weekends with fun.

## Abstract

Despite being the only RNA virus listed as a class A carcinogen, attributing a direct oncogenic role for hepatitis C virus (HCV) infection during the development of hepatocellular carcinoma (HCC) is controversial: dogma attributes HCC development to increased cell turnover and the inflammatory microenvironment within the infected liver. Many studies focus upon the dedifferentiation of infected hepatocytes as a potential source of HCC cancer initiating cells (CICs), yet during chronic hepatitis the liver is mainly repopulated by immature hepatocytes arising from bi-potent hepatic progenitor cells (HPCs).

Previously, we have shown that HCV is capable of infecting patient-derived hepatic progenitors *ex vivo*, setting a precedent for these cells as a potential source of malignancy. Using Huh7 cells sorted for low expression of CD24 as a cell culture model of hepatic differentiation, we show that HCV infection led to increased expression of CIC-associated markers as well as a profound effect upon cellular differentiation. This manifested in delayed and diminished production of hepatocyte-like cells, instead resulting in maintenance of a mesenchymal-like morphology and altered gene and protein expression.

Enrichment analysis and cellular architecture led us to examine a potential link between HCV infection and the Hippo pathway, perturbation of which is a major driver of HCC development. In agreement with our hypothesis, infected cells displayed enhanced nuclear localisation of the YAP1 and increased levels of TAZ transcriptional regulators which correlated with their lack of differentiation. This potentially occurred as a result of disrupted expression and localisation of the regulatory kinases MST1, LATS1 and AMOT mediated by interactions between NS5A and components of the Hippo pathway. Taken together, our data support a novel cellular origin, and a potential mechanism for primary cancer arising within the HCV infected liver.

# Table of Contents

# Table of Figures

## Abbreviations

| | |
|---|---|
| 3-(4,5-Dimethylthiazol-2-yl)-2,5-Diphenyltetrazolium Bromide | MTT |
| Activating protein-1 | AP1 |
| Adenomatosis Polyposis Coli | APC |
| Adenosine triphosphate | ATP |
| Adenosine diphosphate | ADP |
| Alpha-1-antitrypsin | A1AT |
| Alpha-fetoprotein | AFP |
| AMOT-like protein 1 | AMOTL1 |
| AMOT-like protein 2 | AMOTL2 |
| Angiomotin | AMOT |
| Apolipoproteins | apo |
| Apoptosis-stimulating of p53 protein 2 | ASPP2 |
| Arbitrary densitometry units | ADU |
| Base mean | bm |
| Beta-actin | ACTB |
| Bicinchoninic acid | BCA |
| Biosafety level | BSL |
| Bone morphogenetic protein | BMP |
| Bovine serum albumin | BSA |
| Calcium/calmodulin-dependent protein kinase II | CAMK2 |
| Cancer-initiating cell marker | CIC |
| Casein kinase 1δ/1ε | CK1δ/ε |
| CCAAT/enhancer-binding protein alpha | c/EBPa |
| Chelerythrine | CHE |
| Chinese hamster ovary | CHO |
| ChIP-x Enrichment Analysis | ChEA |
| c-Jun N-terminal kinase | JNK |

| | |
|---|---|
| Cluster of differentiation | CD |
| Coiled-Coil | CC |
| Complementary DNA | cDNA |
| Connective tissue growth factor | CTGF |
| Cyclophilin A | CypA |
| Cytidine triphosphate | CTP |
| Cytochrome P450 Family 3 Subfamily A Member 4 | CYP3A4 |
| Cytokeratin | CK |
| Cytotracker green | CT-G |
| Daclatasvir | DCV |
| Deoxynucleotide | dNTP |
| Deoxyribonucleic acid | DNA |
| Dimethyl sulfoxide | DMSO |
| Direct acting antiviral | DAA |
| Dishevelled Segment Polarity Protein 2 | Dvl2 |
| Dithiothreitol | DTT |
| Dobutamine | Dob |
| Dulbecco’s Modified Eagle’s Medium | DMEM |
| Elbasvir | EBR |
| Embryonic day | E |
| Embryonic stem cell | ESC |
| Encephalomyocarditis virus | EMCV |
| Endoplasmic reticulum | ER |
| Enhanced chemiluminescence solution | ECL |
| Epidermal growth factor | EGF |
| Epidermal growth factor receptor | EGFR |
| Epithelial cell adhesion molecule | EpCAM |
| Epithelial to mesenchymal transition | EMT |
| Epstein-Barr virus | EBV |

| | |
|---|---|
| Ethylenediaminetetraacetic acid | EDTA |
| European Association for the Study of the Liver | EASL |
| Extracellular matrix | ECM |
| FADD-like IL1β-converting enzyme-like inhibitory protein | c-FLIP |
| Fas-associated protein with death domain | FADD |
| Fibroblast growth factor | FGF |
| Firefly luciferase + puromycin N-acetyl-transferase genes | Luc-PAC |
| Firefly luciferase control | Fluc |
| Fluorescence forming units | FFU |
| Fluorescence-activated cell sorting | FACS |
| Foetal bovine serum | FBS |
| Foot-and-mouth disease virus | FMDV |
| Foregut | fg |
| Forkhead box protein | FOX |
| Frizzled | FZD |
| Frizzled receptor 2 | FZD2 |
| G418 resistant plasmid | pcDNA3.1 |
| Gamma-actin | ACTG1 |
| Glecaprevir | GLE |
| Global Burden of Disease | GBD |
| Glyceraldehyde 3-phosphate dehydrogenase | GAPDH |
| Glycogen synthase kinase 3 beta | GSK-3β |
| G-protein coupled receptors | GPCR |
| Grazoprevir | GZR |
| Green fluorescent protein | GFP |
| Growth factor receptor-binding-protein 2 | Grb2 |
| GTPase-activating protein | GAP |
| Guanosine triphosphate | GTP |
| Guide RNA | gRNA |

| | |
|---|---|
| Hematopoietically-expressed homeobox protein | Hhex |
| Hepatic progenitor cell | HPC |
| Hepatic stellate cell | HSC |
| Hepatitis A virus | HAV |
| Hepatitis B virus | HBV |
| Hepatitis C Virus | HCV |
| Hepatitis D virus | HDV |
| Hepatitis E virus | HEV |
| Hepatocellular carcinoma | HCC |
| Hepatocyte growth factor | HGF |
| Hepatocyte nuclear factor | HNF |
| Hindgut | hg |
| Homeodomain-interacting protein kinas | HIPK2 |
| Horseradish peroxidase | HRP |
| Human immunodeficiency virus | HIV |
| Human papilloma virus | HPV |
| Immunofluorescence | IF |
| Induced pluripotent stem cell | iPSC |
| Injecting drug users | IDU |
| Interferon | IFN |
| Interferon-beta promoter stimulator 1 | IPS-1 |
| Interferon stimulated gene | ISG |
| Interleukin | IL |
| Internal ribosome entry site | IRES |
| Intrahepatic cholangiocarcinoma | ICCA |
| J6-JFH1 NS5A eGFP | J6-eGFP |
| Janus kinase | JAK |
| JFH1 replicon | JFH1-rep |
| Kyoto Encyclopaedia of genes and genomes | KEGG |

| | |
|---|---|
| Large tumour suppressor 1/2 | LATS1/2 |
| Ledipasvir | LDV |
| Lipoprotein receptor-related protein | LRP |
| Lipoviroparticle | LVP |
| Liver diverticulum | ld |
| Liver kinase B1 | LKB1 |
| Liver receptor homolog 1 | LRH1 |
| Liver sinusoidal endothelial cell | LSE |
| Low density lipoproteins | LDLs |
| Luria Bertani broth | LB |
| Mammalian Ste20-like kinases 1/2 | MST1/2 |
| Mammalian target of rapamycin | mTOR |
| Mean fluorescent intensity | MFI |
| Measles virus | MV |
| Messenger RNA | mRNA |
| Metalloproteinase | MMP |
| Micro RNA | miRNA |
| MicroRNA-122 | miR-122 |
| Midgut | mg |
| Mitochondrial antiviral-signalling protein | MAVS |
| Mitogen-activated protein kinase | MAPK |
| MOB kinase activator 1 | MOB1 |
| Modified Eagle's Medium | MEM |
| Multiplicity of infection | MOI |
| *N*-acetyl-D-glucosamine | GlcNAc |
| Neomycin Phosphotransferase | NPT |
| Neomycin phosphotransferase gene | Luc-Neo |
| Neurofibromin 2 | NF2 |
| Niemann-Pick C1-like1 cholesterol absorption receptor | NPC1L1 |

| | |
|---|---|
| Non-coding RNA | ncRNA |
| Non-structural | NS |
| Nuclear localisation sequence | NLS |
| Nucleoside triphosphate | NTP |
| O-GlcNAc transferase | OGT |
| Ombitasvir | OBV |
| Onecut | OC |
| Open reading frame | ORF |
| Paraformaldehyde | PFA |
| Parainfluenza 5 virus | PIV5 |
| Paritaprevir | PTV |
| Passive lysis buffer | PLB |
| Pattern recognition receptor | PRR |
| Pazopanib | Pazo |
| Peripheral blood mononuclear cells | PBMC |
| Phosphate buffered saline | PBS |
| Phosphatidylinositol 4-kinase III alpha | PI4KA |
| Phosphatidylinositol-4,5-bisphosphate 3-kinase | PI3K |
| Pibrentasvir | PIB |
| Polyethylenimine | PEI |
| Polymerase chain reaction | PCR |
| Polyvinylide fluoride | PVDF |
| Pregnane X receptor | PXR |
| Principal component analysis | PCA |
| Proliferating cell nuclear antigen | PCNA |
| Pro-Ser-Thr Phosphatase Interacting Protein 2 | PSTPIP2 |
| Prospero homeobox protein | Prox |
| Protein kinase B | Akt |
| Protein kinase C | PKC |

| | |
|---|---|
| Public Health England | PHE |
| Puromycin N-acetyl-transferase | PAC |
| Puromycin resistance gene | Puro |
| Ras-association domain family | RASSF |
| Red cell | RC |
| Red fluorescent protein | RFP |
| Resistance-associated variants | RAVs |
| Retinoblastoma | Rb |
| Retinoic acid-inducible gene I | RIG-I |
| Reverse transcriptase | rT |
| Reverse transcription | RT |
| Rho associated CC containing protein kinase | Rock |
| Ribonucleic acid | RNA |
| Ribonucleoside tri-phosphate | rNTP |
| Ritonavir | r |
| RNA Integrity number | RIN |
| RNA sequencing | RNA-seq |
| RNA-dependent RNA polymerase | RdRp |
| Room temperature | rt |
| Salvador family WW domain containing protein 1 | SAV1 |
| Scavenger receptor class B type 1 | SRB1 |
| Serine/Threonine kinase 4/3 | STK4/3 |
| Severe combined immunodeficient | SCID |
| Sex determining region Y | SRY |
| Signal transducer and activator of transcription | STAT |
| Single nucleotide polymorphism | SNP |
| Sodium dodecyl sulfate- | SDS- |
| Polyacrylamide gel electrophoresis | PAGE |
| Sofosbuvir | SOF |

| | |
|---|---|
| Special kidney stem cell media | SKSCM |
| SRC homology 3 | SH3 |
| SRY-box | SOX |
| Sterol regulatory element-binding protein | SREBP |
| Suppressor of cytokine signalling | SOCS |
| Sustained virologic response | SVR |
| T-box transcription factor | TBX |
| TEA Domain Transcription Factor | TEAD |
| TNF-alpha | TNF- α |
| Transcription factor | TF |
| Transcription factor 4 | TCF4 |
| Transcriptional activation domain | TAD |
| Transcriptional coactivator with PDZ-binding motif | TAZ |
| Transforming growth factor beta | TGFβ |
| Tripartite motif containing | TRIM |
| Tris buffered saline | TBS |
| Tris buffered saline with 0.1 % Tween 20 | TBST |
| Tumour necrosis factor | TNF |
| Twist-Related Protein | Twist |
| United Kingdom | UK |
| Untranslated region | UTR |
| Uridine triphosphate | UTP |
| Velpatasvir | VEL |
| very low density lipoproteins | VLDLs |
| Voxilaprevir | VOX |
| Wildtype | WT |
| World Health Organisation | WHO |
| WW Domain-Containing Adaptor 45 | WW45 |
| WW domain containing transcription regulator 1 | WWTR1 |

| | |
|---|---|
| XMU-MP-1 | XMU |
| Yes-associated protein | YAP1 |

# 1. Chapter: Introduction

## 1.1 Hepatitis viruses

Hepatitis viruses are as the name suggests viruses which infect the liver and lead to liver inflammation (hepatitis). The most common viruses to be responsible for viral hepatitis include: hepatitis A (HAV), hepatitis B (HBV), hepatitis C virus (HCV), hepatitis D (HDV) and hepatitis E (HEV). Despite the fact that these viruses all target the liver they are in fact unrelated. HAV is a picornavirus transmitted via contaminated food or water and causes acute hepatitis. Most people who become infected recover within 2 months (Lemon et al., 2017). HBV, a hepadnavirus and HCV of the f*laviviridae* family cause both acute and chronic hepatitis (Yuen et al., 2018). The risk of developing a chronic HBV infection varies with age with a risk of 90 % for infected infants under 1 year of age, 30 % for children between 1-5 years of age and 2 % for adults (Ozasa et al., 2006, Stevens et al., 1975), whereas HCV leads to chronic infection in about 60-80 % of cases (World Health Organization., 2017b). HCV and HBV combined were responsible for 1.34 million deaths in 2015 (World Health Organization., 2017b). Both HBV and HCV can be passed on sexually (although less common for HCV) and via blood transmission (World Health Organization., 2018a, World Health Organization., 2018b). In addition HBV and HCV can be passed from mother to child via breast feeding or by crossing the placenta respectively (World Health Organization., 2018a, World Health Organization., 2018b). HDV is a defective virus belonging to the *Deltavirus* genus and requires HBV infection to replicate (Botelho-Souza et al., 2017, Rizzetto et al., 1980). HEV of the *Hepeviridae* family, usually only causes acute hepatitis but can lead to a chronic infection in the immune compromised. For those with pre-existing liver disease or pregnant women the infection is more severe (Krzowska-Firych et al., 2018). HEV infection can cause rapid and severe liver failure (also known as fulminant hepatitis) in pregnant women leading to mother and infant mortality in up to 25 % of cases (Ranger-Rogez et al., 2002). HEV is spread in a similar way to HAV via the faecal-oral route (Krzowska-Firych et al., 2018). Vaccinations exist for HAV and HBV. Effective treatments now exist for HCV and will be discussed further in 1.2.3.

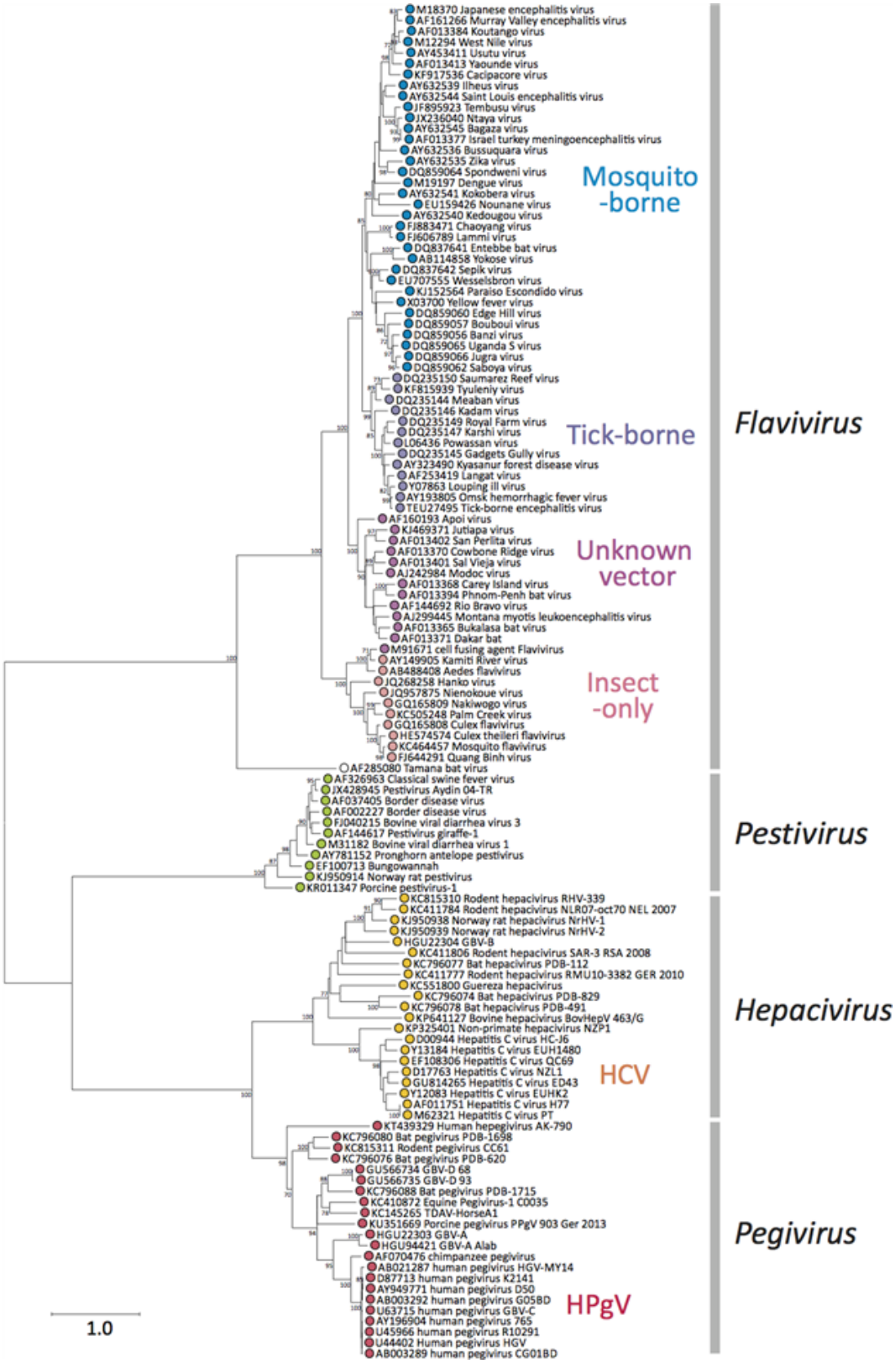


**Figure 1.1.1 Flaviviridae phylogeny.**

The phylogeny is mapped using the conserved amino acid sequence of the RdRp (NS5 or NS5B). Multiple alignment was created using MUSCLE (Edgar, 2004). From the sequence alignment an unrooted phylogenetic tree was constructed. The data underwent bootstrap re-sampling 100 times.

### 1.1.1 Flaviviridae phylogeny

Viruses belonging to the *Flaviviridae* family are enveloped RNA viruses about 40- 60 nm in size (Simmonds et al., 2017). The most well know viruses belonging to this family include; HCV, yellow fever virus and dengue virus. *Flaviviridae* viruses have a positive sense, non-segmented RNA genome between 9-13 kb in length. The genome contains a single open reading frame (ORF) flanked by two untranslated regions (UTRs) at the 5' and 3' termini which form important secondary structures required for genome replication and translation. The genome is translated into a polyprotein which is cleaved by host and viral factors into several structural proteins (including the capsid protein and envelope proteins) and non-structural proteins (NS) (including the RNA helicase and the RNA-dependent RNA polymerase (RdRp)). The Flaviviridae family contains 4 genera: *Flavivirus*, *Hepacivirus*, *Pestivirus* and *Pegivirus* (Figure 1.1.1) (Simmonds et al., 2017). The *Flaviviruses* are arthropod-borne viruses and primarily infect mammals and birds (Mukhopadhyay et al., 2005). *Pestiviruses* spread via infected secretions such as urine and respiratory droplets and usually infect pigs and ruminants (Tautz et al., 2015). *Pegiviruses* can lead to persistent infections in a range of mammals but as of yet have not been associated with disease (Stapleton et al., 2011). *Hepaciviruses* target the liver of horses, rodents, bats, cows and primates (Scheel et al., 2015) and include HCV and other more recently identified viruses. These newly identified Hepaciviruses have be classified further: Hepacivirus A (or non-primate Hepacivirus) which infects horses and dogs, Hepacivirus B (or GB virus B) which infects tamarins and other New World primates, Hepacivirus D which was identified in colobus monkeys, Hepacivirus E-I which infect rodents, Hepacivirus J-M identified in bats and Hepacivirus N which infects cows (Firth et al., 2014, Sibley et al., 2014, Walter et al., 2017, Corman et al., 2015, Baechlein et al., 2015, Kapoor et al., 2011, Burbelo et al., 2012, Kapoor et al., 2013, Drexler et al., 2013, Quan et al., 2013).

## 1.2 Hepatitis C Virus

### 1.2.1 Disease and Transmission

In the twentieth century it became established that most cases of hepatitis were caused by viral infection. Depending on the disease characteristics viral hepatitis was classified as either Hepatitis A or B. Hepatitis A caused an acute disease, spread via contaminated food and water and had a short

incubation period. Hepatitis B had a longer incubation period, could lead to chronic illness and was passed on via blood and other bodily fluids.

By the 1970s both HBV and HAV had been identified which enabled patients and blood products to be tested for the viruses. Screening for HBV and HAV lead to the realisation that another virus must exist which also causes liver inflammation, as a large proportion of hepatitis patients neither had HAV or HBV. Initially however, the agent responsible for the remaining cases could not be identified and was termed non- A, non- B hepatitis (Purcell et al., 1976).

HCV was finally identified in 1989 by molecular cloning (Choo et al., 1989). HCV infection can cause acute or chronic hepatitis. Acute hepatitis C is usually a mild asymptomatic illness and refers to the period immediately following infection (incubation period is two weeks – six months) up to six months after infection (World Health Organization., 2018b). Chronic hepatitis C can be a serious lifelong illness and refers to the continued presence of HCV six months after acquiring the infection. Although the acute infection is usually asymptomatic, for those infected persons that do develop symptoms, these include: fever, fatigue, nausea, abdominal pain, dark urine, grey-coloured faeces and jaundice (World Health Organization., 2018b); 15- 45 % of infected persons will spontaneously clear the virus within the first six months, however the remaining 60- 80 % of infected individuals will develop chronic hepatitis C (World Health Organization., 2018b).

For those suffering from chronic hepatitis C the risk of cirrhosis of the liver is 15- 30 % within 20 years of infection (World Health Organization., 2018b). The World Health organisation (WHO) estimates that 71 million people are living with chronic HCV and that about 399 000 people die each year from hepatitis C, usually due to liver cirrhosis and HCC (World Health Organization., 2017a), a 22 % increase since 2000. In the UK, Public Health England (PHE) estimates that 214 000 people have hepatitis C, which represents 0.4 % of the adult population, and 90 % of infections are acquired through injecting drug use (Public Health England. et al., 2018). HCV is a blood borne virus which can be transmitted via exposure to a small quantity of infectious blood, usually via injection drug use, unsafe healthcare practices or blood transfusion of unscreened blood products (World Health Organization., 2018b). Sexual transmission and transmission via an infected mother to her baby is also possible however these transmission modes are less common (World Health Organization., 2018b).

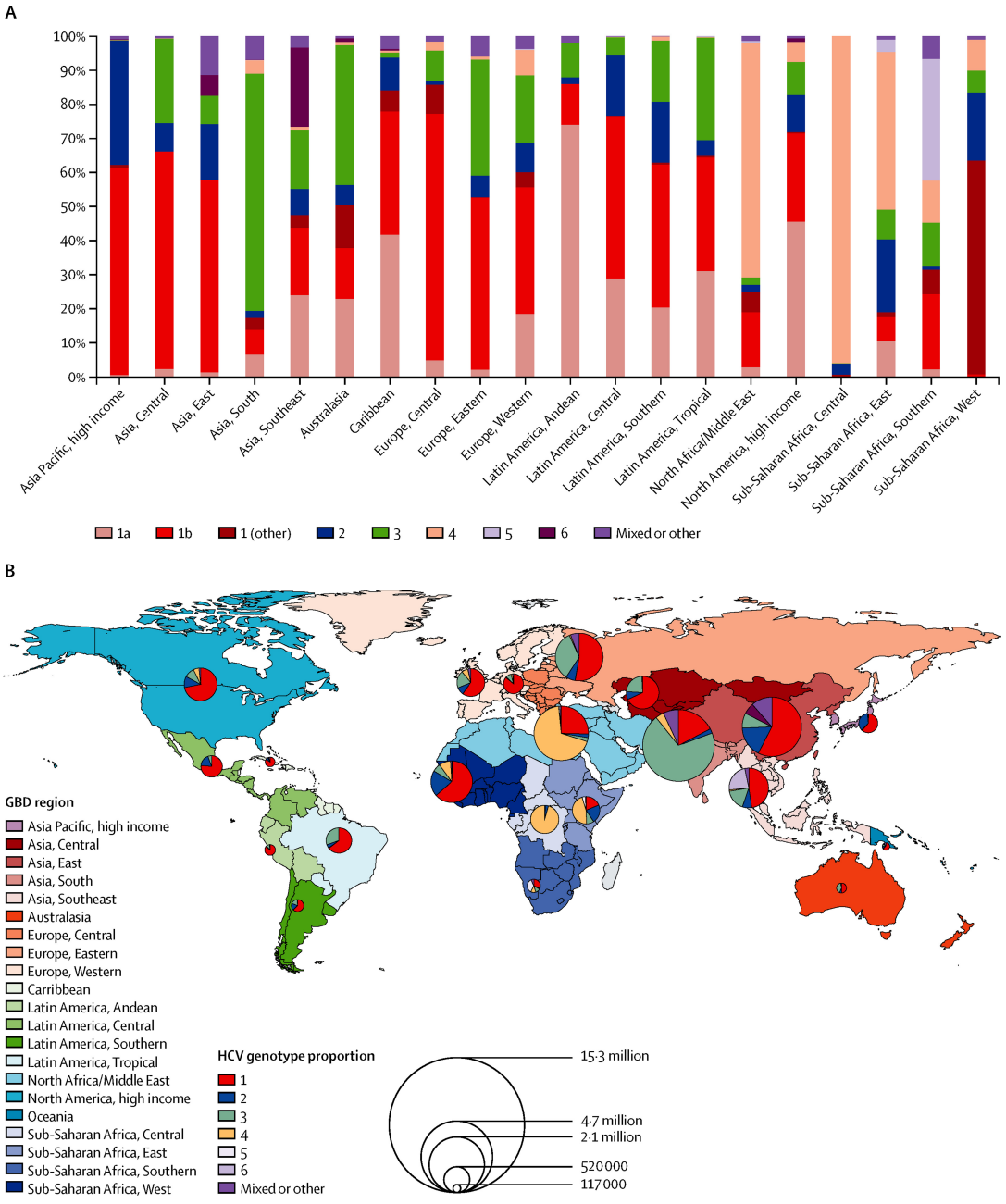


## Figure 1.2.1 Genotype distribution

A) By Global Burden of Disease (GBD) region B) Combined genotype distribution data with total viraemic HCV infections by GDB region. From: (Polaris Observatory HCV Collaborators., 2017).

Chronic HCV represents a leading cause of cirrhosis, HCC, liver transplantation and ultimately liver disease-related death. The 69th World Health Assembly in 2016 approved the Global Health Sector Strategy to eliminate hepatitis B and C infection by 2030 (World Health Organization., 2016b). Global targets for the care and management of HCV were introduced by the WHO: 90 % diagnosis of people living with a chronic viral hepatitis infection, 90 % reduction in new cases of chronic HCV infection, 65 % reduction in HCV related deaths and to achieve treatment of 80 % of eligible chronic HCV infected people (World Health Organization., 2016a).

### 1.2.2 Global Distribution

HCV is endemic worldwide with a total global prevalence of 1 %- 2.5 %, depending on the study (Polaris Observatory HCV Collaborators., 2017, Petruzziello et al., 2016). The WHO estimates that there were 1.75 million new HCV infections in 2015. Prevalence rates vary depending on the region with the highest prevalence rates in Central Asia, Sub-Saharan Africa and Eastern Europe (Polaris Observatory HCV Collaborators., 2017) (Figure 1.2.1). Depending on country, HCV infection can be prevalent throughout the general population, or concentrated in certain high risk populations such as in the UK where HCV prevalence is high amongst injecting drug users (IDU) (Public Health England. et al., 2018). There are several different genotypes and subtypes and global prevalence of these vary. Worldwide genotype 1 is the most prevalent (44 %), followed by genotype 3 (25 %) and genotype 4 (15 %) and 2 (11.0%). Genotype 4 is the most common in low-income countries, genotype 3 is common in middle-income countries and genotype 1 dominates in high-income and upper-middle income countries (Polaris Observatory HCV Collaborators., 2017) (Figure 1.2.1).

### 1.2.3 Diagnosis and Treatment

New direct-acting antiviral treatments can cure more than 95 % of infected people (Rockstroh, 2015). However access to diagnosis and treatment is low partly due to the asymptomatic nature of HCV infection. In 2015, only 20 % of the 71 million persons chronically infected with HCV knew their diagnosis (World Health Organization., 2017b). HCV diagnosis occurs in two steps. First a person is screened for anti-HCV antibodies by a serological test, this identifies whether the person has been exposed to the virus. In the case of a positive test result, a nucleic acid test for HCV RNA will confirm whether the person is suffering from a chronic infection (European Association for the Study of the Liver., 2018). After diagnosis the WHO recommends that an infected person should have an assessment to determine the degree of liver

damage (World Health Organization., 2017b). This is assessed by liver biopsy or via a variety of less invasive tests. The genotype with which the person is infected should be established. Infection with multiple genotypes is a possibility. Both the level of liver damage and the virus genotype will guide the treatment and disease management (Figure 1.2.2) (European Association for the Study of the Liver., 2018). With the development of new direct acting antivirals (DAAs), the standard of care has been changing rapidly.

WHO guidelines recommend regiments including Sofosbuvir (SOF), Daclatasvir (DCV) and the SOF/Ledipasvir (LDV) combination (World Health Organization., 2017b) SOF is an inhibitor of the non-structural protein NS5B polymerase with a high barrier to resistance (Bhatia et al., 2014).DCV and LDV are both NS5A inhibitors (Smith et al., 2016, Lawitz et al., 2012). European Association for the Study of the Liver (EASL) have recently updated their recommendations on the treatment of HCV in 2018 (European Association for the Study of the Liver., 2018). The choice of DAAs depends on genotype, treatment experience and stage of liver disease (Figure 1.2.2). A very limited role is now remaining for the pegylated interferon and ribavirin regimen. The cure rate depends on virus subtype and the type of treatment received amongst other factors. A patient is considered ‘cured’ when sustained virologic response (SVR), defined as undetectable HCV RNA at 24 weeks after treatment has ended, has been achieved (European Association for the Study of the Liver., 2018). Barriers exist to achieve the WHO target of eliminating hepatitis C by 2030. Although the cost of DAA production is low, the medicines remain very expensive in many high- and upper middle-income countries. The introduction of generic versions in some low-income countries has allowed the price of these medicines to drop. Access to HCV treatment is slowly improving however more needs to be done if the treatment target of 80 % is to be achieved by 2030. HCV resistance-associated variants (RAVs) are being identified which are associated with DAA treatment failure (European Association for the Study of the Liver., 2018, Pawlotsky, 2016, Sarrazin, 2016). Drug resistance is a common consequence of antiviral therapy however due to the genetic variability of HCV, RAVS have also been found to pre-exist in treatment naïve patients as naturally occurring variants (Harrington et al., 2018, Zeuzem et al., 2017).

| Genotype | Prior treatment | SOF/VEL | | GLE/PIB | | SOF/VEL/VOX | | SOF/LDV | | GZR/EBR | | OBV/PTV/r+DSV | |
|---|---|---|---|---|---|---|---|---|---|---|---|---|---|
| | | + C | - C | + C | - C | + C | - C | + C | - C | + C | - C | + C | - C |
| 1a | naïve | 12 wk | 12 wk | 8 wk | 12 wk | No | No | 8-12 wk | 12 wk | 12 wk | 12 wk | No | No |
| | experienced | 12 wk | 12 wk | 8 wk | 12 wk | No | No | No | No | 12 wk | 12 wk | No | No |
| 1b | naïve | 12 wk | 12 wk | 8 wk | 12 wk | No | No | 8-12 wk | 12 wk | 8-12 wk | 12 wk | 8-12 wk | 12 wk |
| | experienced | 12 wk | 12 wk | 8 wk | 12 wk | No | No | 12 wk | 12 wk | 12 wk | 12 wk | 12 wk | 12 wk |
| 2 | naïve | 12 wk | 12 wk | 8 wk | 12 wk | No | No | No | No | No | No | No | No |
| | experienced | 12 wk | 12 wk | 8 wk | 12 wk | No | No | No | No | No | No | No | No |
| 3 | naïve | 12 wk | No | 8 wk | 12 wk | No | 12 wk | No | No | No | No | No | No |
| | experienced | 12 wk | No | 12 wk | 16 wk | No | 12 wk | No | No | No | No | No | No |
| 4 | naïve | 12 wk | 12 wk | 8 wk | 12 wk | No | No | 12 wk | 12 wk | 12 wk | 12 wk | No | No |
| | experienced | 12 wk | 12 wk | 8 wk | 12 wk | No | No | No | No | No | No | No | No |
| 5 | naïve | 12 wk | 12 wk | 8 wk | 12 wk | No | No | 12 wk | 12 wk | No | No | No | No |
| | experienced | 12 wk | 12 wk | 8 wk | 12 wk | No | No | No | No | No | No | No | No |
| 6 | naïve | 12 wk | 12 wk | 8 wk | 12 wk | No | No | 12 wk | 12 wk | No | No | No | No |
| | experienced | 12 wk | 12 wk | 8 wk | 12 wk | No | No | No | No | No | No | No | No |

**Figure 1.2.2 EASL treatment recommendations for HCV infected patients**

Treatment recommendations for HCV mono-infected or HCV/HIV co-infected patients with cirrhosis (+C) or without cirrhosis (-C). Treatment recommendations also depends on the genotype the patient is infected with and whether the patient is treatment naïve (patient who has never been treated for HCV infection) or treatment experienced (patient who was previously treated with: pegylated IFN-α and ribavirin, pegylated IFN-α or ribavirin and Sofosbuvir. DSV- Dasabuvir, EBR- Elbasvir, GLE- Glecaprevir, GZR- Grazoprevir, LDV- Ledipasvir, OBV- Ombitasvir, PIB- Pibrentasvir, PTV- Paritaprevir, r- ritonavir, SOF- Sofosbuvir, VEL- Velpatasvir and VOX- Voxilaprevir.

### 1.2.4 HCV genome, genetic variation and evolution

HCV is an enveloped positive sense single- stranded RNA virus belonging to the *Hepacivirus* genus of the *Flaviviridae* family. The 9.6 kb genome with a single ORF encodes a single polyprotein of about 3000 amino acids, which is cleaved into 10 proteins: four structural proteins; E1, E2, core and p7 and six non-structural proteins; NS2, NS3, NS4A, NS4B, NS5A, NS5B (Penin et al., 2004) (Figure 1.2.3). Polyprotein processing into the distinct proteins occurs by cellular proteases signalase and signal peptide peptidase and the viral proteases: NS2- NS3 and NS3- NS4A (Scheel and Rice, 2013). Core maturation requires cleavage first by the cellular signal peptide peptidase and then by signalase. Signalase is also responsible for the cleavage of E1, E2 and p7 from the polyprotein. The NS2-NS3 protease is responsible for its own cleavage. The remaining non-structural proteins are cleaved by NS3-NS4A. An additional ORF overlapping the core gene has led to the detection of alternative translation products (Varaklioti et al., 2002). This alternate ORF, although present in all genotypes (Walewski et al., 2001), has only been studied in the context of genotype 1. HCV has short UTRs at either end of the genome (5'UTR and 3'UTR) (Figure 1.2.3). The UTRs are highly structured RNA elements (Brown et al., 1992) and are required for translation and replication (Friebe and Bartenschlager, 2002, Kieft et al., 2001, Zhang et al., 1999, Ito et al., 1998a). The 5'UTR contains an internal ribosome entry site (IRES) which allows cap-independent polyprotein translation by direct interaction with the 40S ribosomal subunit (Tsukiyama-Kohara et al., 1992, Wang et al., 1993, Pestova et al., 1998). Both the 5'UTR and the 3'UTR are important for viral RNA replication.

HCV is a heterogeneous virus with extensive genetic variation driven by the high error rate of the RdRp, the evolutionary pressure exerted by the immune system large viral population sizes and high replication rates (Domingo and Holland, 1997). Phylogenetic analysis led to the classification of seven HCV genotypes, further divided into a number of subtypes (Smith et al., 2014, Murphy et al., 2015). Over 30 % nucleotide sequence variation exists between genotypes and around 20 % between subtypes (Simmonds, 2004). The genotype with which an individual becomes infected impacts the disease course, the choice of and response to antiviral therapy (McHutchison et al., 2009, Ghany et al., 2009, Bochud et al., 2009, Zhu and Chen, 2013, Foster et al., 2011, Manns et al., 2017). The high degree of genetic variation is an important feature of HCV and contributes to immune evasion and the emergence of drug resistant variants (De Francesco and

Migliaccio, 2005). The HCV mutation rate per round of replication has been estimated at $10^{-4}$-$10^{-5}$ substitutions per site (Ribeiro et al., 2012, Bartenschlager and Lohmann, 2000). Mutation rates however vary in different regions of the genome. Genomic regions corresponding to essential viral functions and of structural importance (such as the 3' and 5'UTR) are more conserved. With 90 % sequence identity, the 5' UTR is the most conserved region of the HCV genome (Bukh et al., 1992). Whereas the genomic regions encoding proteins key to immune evasion, membrane glycoproteins E1 and E2 are the most variable with an evolution rate about up to nine times faster than the 5' UTR (Salemi and Vandamme, 2002). The high mutation and replication rate of HCV leads to the continuous production of a large number of related viral variants during infection and is referred to as a quasispecies (Martell et al., 1992, Domingo et al., 1998, Laskus et al., 2004). The quasispecies exists as a dynamic population and is subject to variation, competition and selection (Domingo and Gomez, 2007, Domingo et al., 2006).

### 1.2.5 HCV virion structure and protein function

The 50-80 nm in diameter HCV virion consists of a nucleocapsid surrounding the RNA genome (Catanese et al., 2013). Surrounding the nucleocapsid is a lipid bilayer (viral envelope). Some hypothesise that HCV circulates as a lipoviral particles (LVPs) in the bloodstream (Bartenschlager et al., 2011). However the exact nature of the interaction between HCV viral particles and lipoproteins is unclear. Viral RNA in human-infected plasma has been shown to co-elute with very low density lipoproteins (VLDLs) which range in size from 30 to 80 mm. A broad density profile is exhibited by HCV particles from 1.00 to 1.25 g/ml with the most infectious fractions displaying a low buoyant density of <1.1 g/ml. Antibodies against protein components of VLDLs and low density lipoproteins (LDLs) can be used to capture viral RNA, in the low-density fractions (Lindenbach, 2013). Apolipoproteins (apo) including apoE and apoB, apoA1 and apoC1-3 have been found to be associated with HCV particles. Furthermore HCV entry relies on lipoproteins and their corresponding receptors (see section 1.2.6).

The core protein is a RNA-binding protein which forms the nucleocapsid. Core often exists as dimeric or multimeric forms. HCV core protein has also been shown to interact with a number of cellular proteins and affect cellular signalling pathways (McLauchlan, 2000). E1 and E2 are glycoproteins which form heterodimers within the viral envelope. These structural proteins play

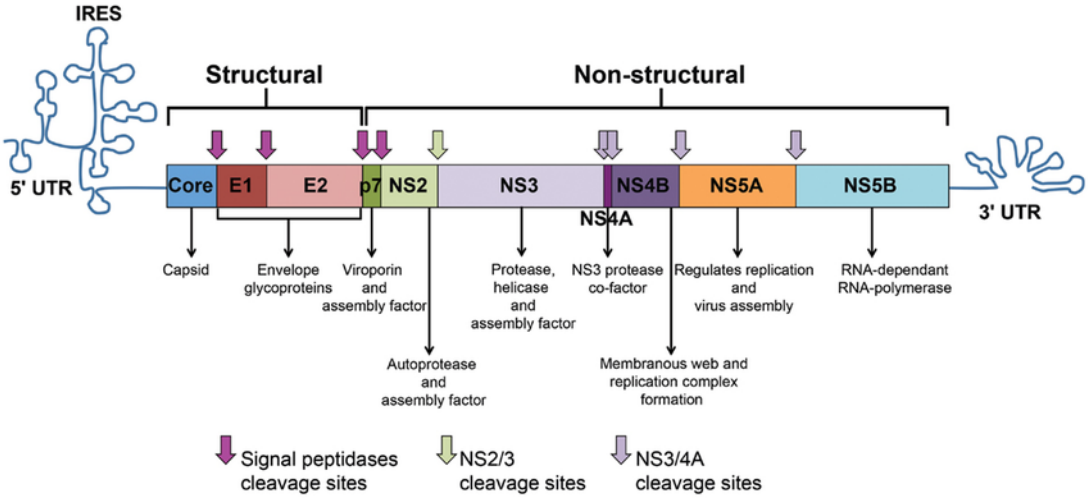


**Figure 1.2.3 HCV genome and polyprotein**

The HCV genome is flanked by two UTRs at the 5' and 3' end. The 5' UTR contains an IRES which directs translation of the ORF leading to the formation of a single polyprotein. The polyprotein is processed into 10 viral proteins classified into structural and non-structural by host and viral factors. Figure from (Abdel-Hakeem and Shoukry, 2014).

important roles during particle assembly, virus entry and endosomal membrane fusion (Lavillette et al., 2007, Mazumdar et al., 2011, Wahid et al., 2013). The structural proteins E1 and E2 have 5 and 11 glycosylation sites respectively. E2 also contains multiple hypervariable regions with great aa sequence variability between genotypes and subtypes (Weiner et al., 1991). This high variability represents a hurdle for vaccine development. E2 is believed to initiate viral attachment to the host cell whereas less is known about E1 but may play a role in the membrane fusion step during HCV entry (Flint and McKeating, 2000).

p7, located between E2 and NS2 in the viral polyprotein comprises a 63-amino acid protein that forms oligomers with cation channel activity and is a member of the viroporin family (Griffin et al., 2003). The p7 ion channel is important for viral particle assembly, release and *in vivo* infectivity (Jones et al., 2007, Steinmann et al., 2007, Sakai et al., 2003).

The N-terminus of NS2, like p7, is not involved in viral genome replication but is involved in virus assembly (Jirasko et al., 2010), whilst the NS2 C-terminus acts as an autoprotease which mediates cleavage between NS2 and NS3 along with the N-terminal end of NS3 (Schregel et al., 2009). NS2 is a small transmembrane protein which associates with the ER membrane (Yamaga and Ou, 2002).

NS3 encodes a serine protease at its N-terminus which along with its cofactor NS4A is responsible for 4 cleavage sites of the polyprotein. NS4A acts to stabilise the NS3 serine protease (Bartenschlager et al., 1995). The C-terminus of NS3 encodes a RNA helicase- NTPase required for HCV RNA replication but which also functions during viral particle assembly (Murray et al., 2008). The NS3 helicase- NTPase acts to unwind the secondary RNA structures using NTP hydrolysis (Tai et al., 1996). The helicase- NTPase activity can be modulated by both the protease domain of NS3 itself and NS5B (Zhang et al., 2005).

NS4B is a hydrophobic protein of 261 aa that is less well characterised. NS4B is a membrane protein which localises to the ER.(Hugle et al., 2001) NS4B is required for functional replication complex formation (Gouttenoire et al., 2009) specifically the formation of the membraneous web (Egger et al., 2002). NS4B may also play a role in modulating NS5B activity (Piccininni et al., 2002).

NS5A is a dimeric zinc-binding metalloprotein containing several phosphorylation sites. NS5A plays a role in HCV replication and particle

formation. NS5A exists as a basally phosphorylated 56 kDa and a hyperphosphorylated 58 kDa protein. NS5A has been shown to have a wide range of viral and cellular interaction partners, thus this protein must have numerous other potential functions. NS5A has 3 protein domains and within domain I is a zinc-binding motif (Tellinghuisen et al., 2004). NS5A is important for viral replication and mutations to the sequence inhibits RNA replication (Tellinghuisen et al., 2004, Elazar et al., 2003). The exact mechanism behind NS5A regulation of HCV replication however is not completely clear.

NS5B is responsible for viral genome replication as the RdRp via the synthesis of a complementary negative-strand RNA, followed by the synthesis of a genomic positive strand RNA. The c-terminal domain forms a α-helix which targets the protein to the ER (Moradpour et al., 2004). The rest of the protein forms the RdRp as a so called 'fingers, palm and thumb' structure (Ago et al., 1999, Bressanelli et al., 1999, Lesburg et al., 1999).

### 1.2.6 Viral life cycle

HCV virions circulate either as free particles or as a complex LVP by associating with LDLs, in the bloodstream (Andre et al., 2002). Viral entry proceeds in three steps: attachment, entry and fusion, involving a complex series of viral-host interactions (Figure 1.2.4). Viral attachment to the cell surface is a slow process and is mediated by the glycosylated structural proteins E1 and E2 interacting with host cell factors. Furthermore apolipoproteins on the surface of the LVP appear to also play a role in viral attachment. Many cellular proteins have been identified to be important for viral entry including the scavenger receptor class B type 1 (SRB1) (Scarselli et al., 2002), CD81 (Pileri et al., 1998), claudin-1 (Evans et al., 2007) and occludin (Ploss et al., 2009). More recently epidermal growth factor receptor (EGFR), ephrin A2 (Lupberger et al., 2011) and Niemann-Pick C1-like 1 cholesterol absorption receptor (NPC1L1) (Sainz et al., 2012) have been added to the list of potential HCV entry factors. Initial low affinity binding to the host cell has been hypothesised to be mediated by glycosaminoglycans and the LDL receptor (Figure 1.2.4). It is hypothesised that the interactions with glycosaminoglycans are mediated by apoE (Morozov and Lagaye, 2018). These initial interactions are then followed by E2 interacting with SRB1 and CD81 (Catanese et al., 2010, Sharma et al., 2011). The cellular proteins: claudin1, occludin, ephrin A2 and EGFR appear to be important for viral cell entry (Zeisel et al., 2013) (Figure 1.2.4). The E2-cell receptor complex then moves to the tight junction involving interactions with occludin

and claudin1, likely followed by interactions with NPC1L1 and EGFR to initiate cell entry. Following attachment, viral entry into the host cell proceeds via pH-dependent and clathrin-mediated endocytosis (Hsu et al., 2003, Blanchard et al., 2006). Following cell entry via endocytosis, the HCV genome is released into the cytoplasm by pH-dependent membrane fusion which requires acidification of the endoplasmic vesicle (Tscherne et al., 2006, Blanchard et al., 2006). E1 has been indicated as the viral protein which mediates fusion (Tong et al., 2017). The nucleocapsid is destroyed following membrane fusion and the viral RNA is released into the host cytoplasm (Figure 1.2.4).

Translation of the HCV genome occurs in the rough endoplasmic reticulum (ER), initiated by direct binding of the IRES to the 40S ribosomal subunit which induces assembly of the 80S ribosome (Spahn et al., 2001, Rijnbrand and Lemon, 2000, Kieft et al., 2001). Cis-acting RNA elements in the 3' UTR along with two stem loop structures in the core-coding region of the HCV genome are proposed to stimulate HCV RNA translation which proceeds via a cap-independent mechanism associated with direct binding of the IRES to the ribosome (Honda et al., 1996). The liver specific microRNA 122 (miR-122) plays an important role by binding at two sites within the 5' UTR leading to viral genome stabilisation, replication and translation (Jopling, 2008, Mortimer and Doudna, 2013). In conjunction with Argonaute (Ago) 2, miR-122 binds to the viral genome in the 5' UTR to protect the genome from host Xrn1 5' exonuclease activity thus protecting the genome from decay (Shimakami et al., 2012). This is an unusual function for a microRNA (miRNA) as usually miRNAs bind to the 3' UTR, recruit Ago proteins to initiate mRNA translation repression and destabilisation. How exactly miR-122 and Ago2 both binding to uncapped HCV RNA stimulates viral genome translation is unknown (Roberts et al., 2011). miR-122 also plays a role in increasing viral RNA synthesis, which appears to require the dissociation of Ago2 from the viral genome, to reduce the amount of viral RNA engaged in translation (Masaki et al., 2015). RNA replication occurs via a negative strand intermediate by the NS5B RdRp. Circulation of the HCV genome via motifs in the IRES and the NS5B sequence might function to prevent encounters between the ribosome and the viral replicase complex which move in the 5' to 3' and 3' to 5' direction respectively (Romero-Lopez et al., 2014, Paul et al., 2014). Translation produces a polyprotein which is about 3000 amino acid in length which (as already described in section 1.2.4) is processed by two host and two viral proteases. Viral assembly occurs via a multi-step process within the ER or

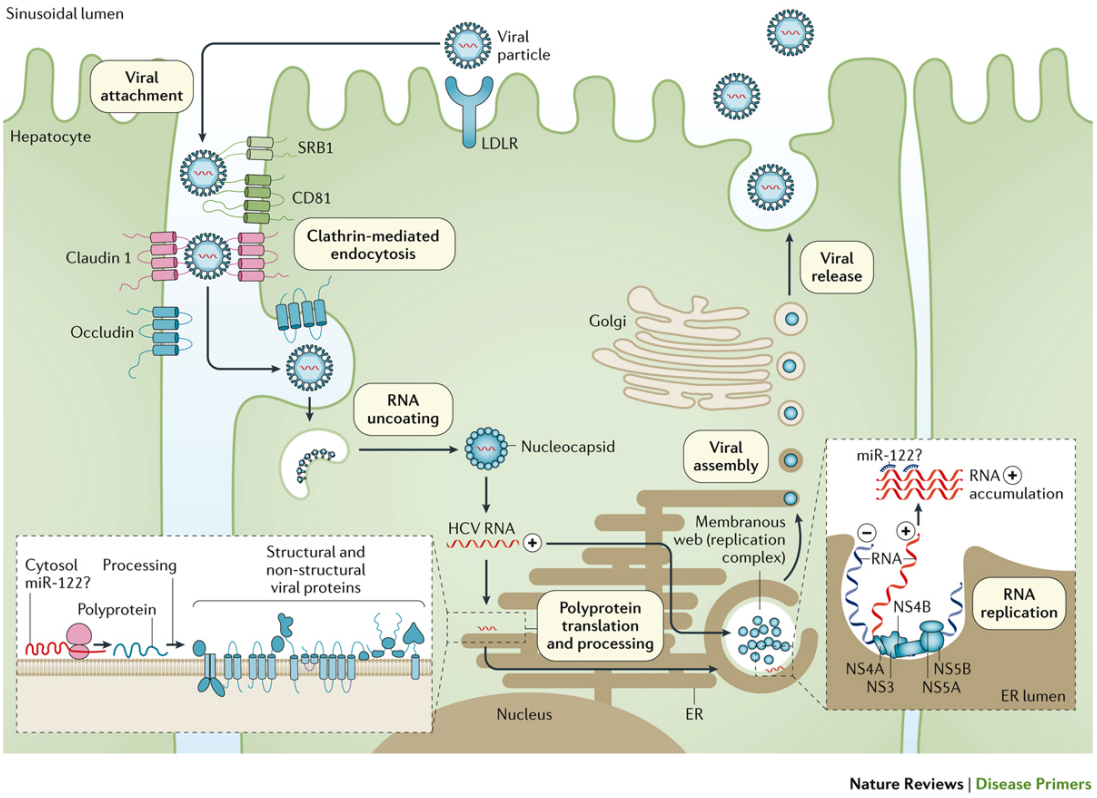


## Figure 1.2.4 HCV life cycle

Representation of the life cycle of HCV beginning with viral attachment mediated by apolipoproteins and HCV structural proteins E1 and E2 interacting with cellular proteins including LDLR, CD81 and SRB1. Attachment is followed by clathrin-mediated endocytosis. Acidification of the endoplasmic vesicle triggers membrane fusion thought to be mediated by E1. Membrane fusion is followed by nucleocapsid decay and viral RNA release into the cytoplasm. Viral RNA is translated via the HCV IRES binding to the host ribosome. The polyprotein is processed and cleaved by two cellular factors and two viral proteins. NS4B amongst other viral proteins lead to the formation of the membraneous web (from ER membrane) and viral replication complexes where the viral RNA is replicated by NS5B. Release of the progeny RNA leads to nucleocapsid formation after which the forming viral particle buds of the ER. Viral particles are thought to be released through the VLDL and LDL formation pathway. Schematic from (Manns et al., 2017).

on the surface of lipid droplets (Figure 1.2.4). The viral replicase complex is constructed of the non-structural proteins of NS3 to NS5B which associates with the viral genome. The NS3 helicase domain is responsible for unwinding the RNA in a ratchet-like or inchworm manner (Gu and Rice, 2010, Dumont et al., 2006). NS4A is responsible for localising NS3 to the ER membrane and regulating both its protease and helicase activities (Lindenbach et al., 2007). HCV infection leads to remodelling of intracellular membranes believed to be induced by NS4B, possibly in conjunction with NS5A (Romero-Brey et al., 2012, Egger et al., 2002). A membranous web is formed derived from the ER (Egger et al., 2002, Romero-Brey et al., 2012, Ferraris et al., 2013). The membraneous web is were RNA replication is thought to take place and are also referred to as viral replication factories (Paul et al., 2013) (Figure 1.2.4). Several cellular factors appear to be required or contribute towards the formation of the membraneous web and the viral replication factories such as Proline-Serine-Threonine Phosphatase Interacting Protein 2 (PSTPIP2) (Chao et al., 2012). NS4B and NS5A interact with PSTPIP2 which is an inducer of positive membrane curvature. The membraneous web includes altered cellular membranes, HCV non-structural proteins, viral RNA, and lipid droplets (Egger et al., 2002, Gosert et al., 2003, Romero-Brey et al., 2012). HCV infection has also been shown to induce de novo lipid and membrane biosynthesis. Induction appears to occur via the sterol regulatory element-binding protein (SREBP) pathway (Waris et al., 2007). Viral assembly is not yet fully understood however, nucleocapsid formation requires the viral progeny RNA to be released from the replication site. Viral particle production is initiated on the cytosolic side of the ER membrane and once nucleocapsid formation is initiated the viral particle buds and is released on the luminal side of the ER membrane (Figure 1.2.4). Maturation and viral particle release appears to be linked to the production of VLDLs and LDLs (Figure 1.2.4). The distribution of lipid droplets changes from a generalised cytoplasmic pattern to accumulation around the perinuclear region during HCV infection (Popescu et al., 2011). Indeed there appears to be a strong link between HCV and lipid metabolism throughout the virus life cycle (Alvisi et al., 2011).

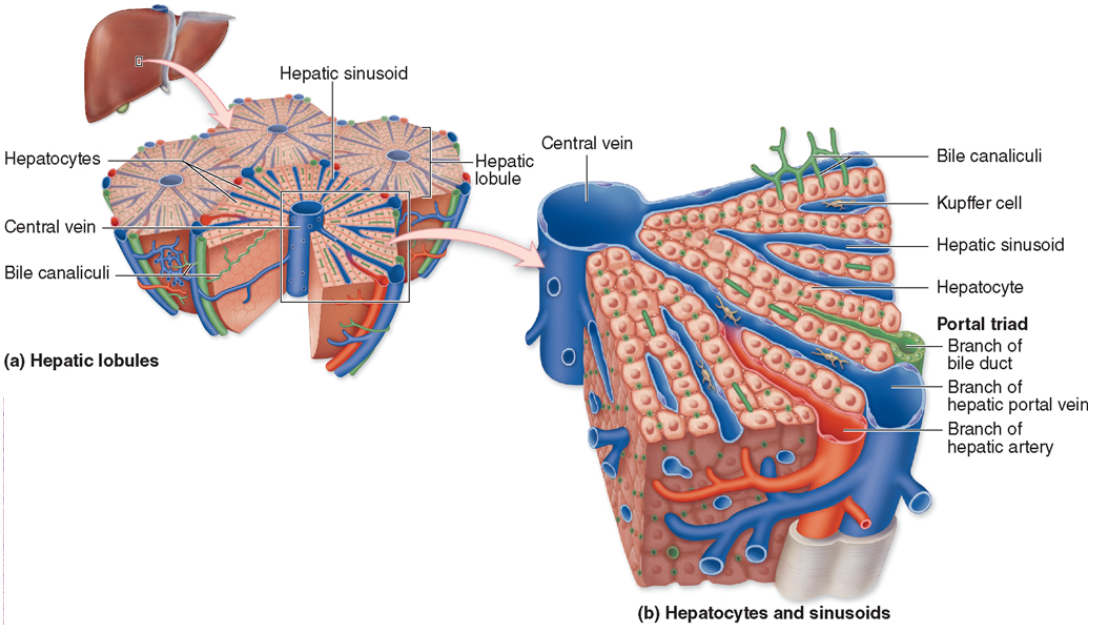


**Figure 1.2.5 Liver lobule and portal triad**

A) The liver is made up of liver lobules which represents the basic structural unit of the liver. B) A liver lobule consists of cords of hepatocytes separated by the sinusoidal capillaries which carry blood from the hepatic portal vein to the central vein. The portal vein is part of the portal triad which also contains a branch of the hepatic artery and a branch of the bile duct. At the apical side of the hepatocytes are the bile canaliculi which collect the bile and transport it to the bile duct. Figure from (Junqueira and Mescher, 2013)

## 1.3 The Liver

### 1.3.1 Liver architecture and function

The liver makes up about 2.5 % of total human body weight and is the largest gland in the body. The liver has many functions and is responsible for the synthesis, storage and breakdown of many substances. The liver consists of several different cell types divided into parenchymal and non-parenchymal cells. Parenchymal cells include hepatocytes and cholangiocytes (biliary epithelial cells). Non-parenchymal cells only make up about 6.3 % of the liver tissue volume and include endothelial cells, Kupffer cells (liver resident macrophages) and hepatic stellate cells (HSCs), whereas hepatocytes make up about 78 % of the volume (Blouin et al., 1977).

The liver lobule represents the basic structural unit of the liver (Figure 1.2.5). The lobule is made up of plates of hepatocytes between which are the sinusoidal capillaries carrying blood from the portal tract to the terminal hepatic venule. The portal tract or portal vein is part of a portal triad of vessels also consisting of the bile duct and hepatic artery. The portal vein and the hepatic artery both supply blood to the lobule. Hepatocytes metabolise, transform and store a range of substances absorbed by the intestine and secreted by the pancreas, and spleen. Functional and gene expression differences exist between hepatocytes located closer to the portal venule (periportal hepatocytes) and those located closer to the central hepatic venule (centrilobular hepatocytes) (Gumucio, 1989) leading to functional compartmentation along the porto-central axis of metabolic activities also known as liver zonation. Liver zonation is required for metabolic homeostasis (Torre et al., 2010). Blood perfusion from portal to hepatic venule thus allows progressive qualitative modification of the sinusoidal blood composition.

Hepatocytes are arranged in cords with tight junctions formed between cells. Hepatocytes are polarised epithelial cells where the basolateral surface faces the sinusoidal endothelial cells, whereas the apical surface is responsible for the transport of bile acid. Bile is collected by the canaliculi and carried to the bile duct within the portal triad, from which it is transported to the gall bladder. Canals of Hering are responsible for conducting bile from the canaliculi to the bile ducts in the portal triad and are lined with both cholangiocytes and hepatocytes. The Canals of Hering form the hepatocytic-

biliary interface and have been identified as the location of adult bi-potential progenitor cells (Figure 1.3.1).

### 1.3.2 Liver cell types

Hepatocytes are the main cell type of the liver and make up most of its mass. These specialised epithelial cells carry out many functions relating to the synthesis, detoxification, metabolism and storage a range of substances. Hepatocytes synthesise and secrete proteins such as albumin and clotting factors, produce bile and chemically process both exogenous substances such as drugs and medicines and endogenous substances such as hormones. Hepatocyte synthesis and storage functions are very important for nutrient homeostasis. Hepatocytes are cuboidal in shape and are highly polarised cells with a round nucleus and a large number of mitochondria (Treyer and Musch, 2013, Costa et al., 2003, Berasain and Avila, 2015).

Cholangiocytes are bile duct epithelial cells which play a role in bile duct formation (Boyer, 2013). Cholangiocytes are responsible for the modification of bile as it is transported through the bile ducts to the gall bladder for storage. Cholangiocytes transport various ions, solutes and water across their apical and basolateral membranes in a coordinated fashion (Boyer, 2013).

Endothelial liver cells include the vascular endothelial cells and the liver sinusoidal endothelial cells (LSEs). LSEs are highly specialised endothelial cells that form the liver sinusoid, which is a fenestrated, and so therefore highly permeable endothelial barrier (Sorensen et al., 2015). Liver sinusoids receive nutrient-rich blood from the portal vein (70 %) and oxygen-rich blood from the hepatic artery (30 %). Liver sinusoids act to equalise blood pressure and maintain the hepatic venous pressure at about 4 mmHg (Lee et al., 1988). The discontinuous nature of LSEs basement membrane allows blood plasma to enter the space between the LSEs and the hepatocyte, known as the space of Disse, or peri-sinusoidal space (Figure 1.3.1).

HSCs exist in the space of Disse with several protrusions which wrap around the sinusoids (Figure 1.3.1). HSCs are responsible for storing 80 % of retinoids within cytoplasmic lipid droplets (Hellerbrand, 2013). HSCs are usually quiescent however during liver injury these cells expand and play a prominent role in extracellular matrix (ECM) remodelling and liver fibrosis (Friedman, 2008). Recently HSCs have been suggested to be a form of non-professional antigen-presenting cells (Vinas et al., 2003).

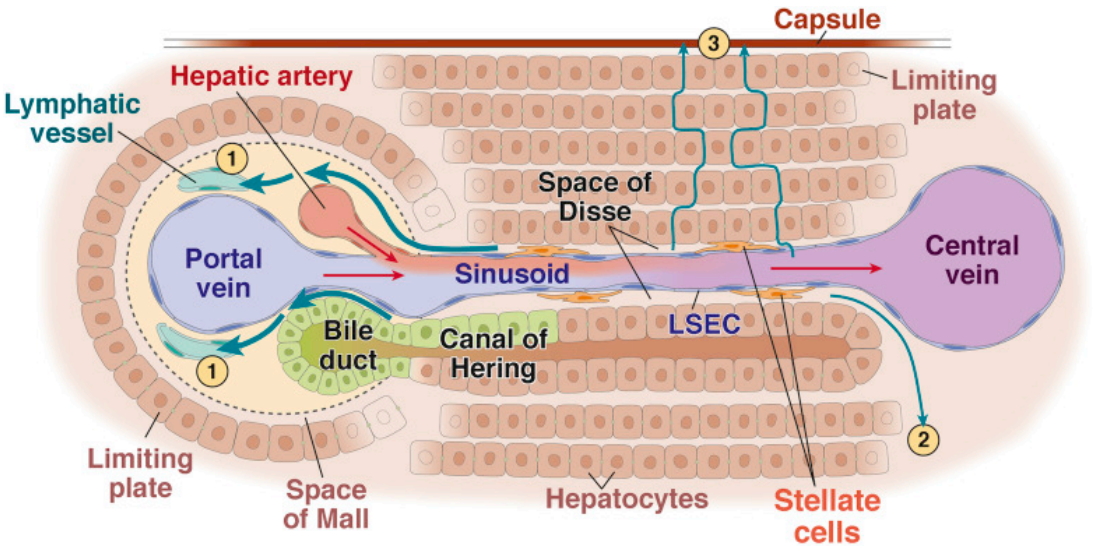


**Figure 1.3.1 Schematic of the cells and vascular system of the liver**

Diagram of the micro anatomy of the liver and liver cell types. Hepatocytes are polarised cells which form plates separated by sinusoids. The endothelial cells of the sinusoids are separated from the hepatocytes by the space of Disse. Plasma is filtered through the sinusoidal endothelial cells into the space of Disse, the lymph then drains into the portal tract lymphatics through the space of Mall. The apical surface of hepatocytes is the site of bile acid transportation. Bile is collected by the canaliculi and carried to the bile duct within the portal triad. The bile ducts are line with both cholangiocytes and hepatocytes. The sites of hepatocytic-biliary interface are named the Canals of Hering and have been suggested to harbour bi-potent adult liver progenitor cells. Blood flows from the portal vein and hepatic artery through the liver sinusoid to the central vein. HSCs are located in the Space of Disse and have several protrusions which wrap around sinusoidal cells. Schematic from (Tanaka and Iwakiri, 2016). The numbers 1-3 show the flow of lymphatic fluid, 1) highlights how the lymphatic fluid in the space of Disse flows through the space of Mall into the interstitium of the portal tract and then finally into the lymphatic capillaries. 2) some of the space of Disse lymphatic fluid also flows into the central vein interstitum and 3) also underneath the hepatic capsule.

Kupffer cells are the tissue resident specialised macrophages of the liver, located in the liver sinusoid. Kupffer cells represent about 80 % of tissue macrophages and play a crucial role in the innate immune response (Dixon et al., 2013). In addition to phagocytosing pathogens entering the liver from the portal or arterial circulation, Kupffer cells also represent a defence against immuno-reactive material entering from the intestinal tract. Kupffer cells are also responsible for clearing dead erythrocytes from the systemic circulation (Dixon et al., 2013).

### 1.3.3 Embryonic liver development

Hepatogenesis is a widely conserved process which has allowed much to be elucidated from the use of animal models. The embryonic origin of liver cells differs: hepatocytes and cholangiocytes arise from the endoderm whereas stromal, hepatic stellate, Kupffer and endothelial cells arise from the mesoderm. A series of reciprocal interactions between these two germ layers are required for hepatogenesis. At embryonic day (E) 7 of mouse development the endoderm forms a primitive gut tube which is initiated by Nodal signalling (Figure 1.3.2). Low doses of Nodal induce the mesoderm whereas higher doses induce the endoderm (Shen, 2007, Zorn and Wells, 2007) which leads to expression of the transcription factors SRY (sex determining region Y)-box (SOX)17 and Forkhead box protein (FOX) A1-3. These transcription factors in turn regulate a set of genes which commit cells to the endoderm lineage. The gut tube undergoes further patterning forming the foregut, midgut and hindgut domains (Figure 1.3.2), initiated by secreted factors which include fibroblast growth factor (FGF) (Dessimoz et al., 2006), Wnt (McLin et al., 2007), bone morphogenetic protein (BMP) (Tiso et al., 2002) and retinoic acid (Chen et al., 2004) from the adjacent mesoderm (Kumar et al., 2003). The posterior mesoderm secrets FGF4 and Wnt to repress the foregut fate and promote hindgut formation. Wnt and FGF4 signalling are inhibited in the anterior endoderm to allow foregut development (McLin et al., 2007, Wells and Melton, 2000, Dessimoz et al., 2006). The gall bladder, pancreas, lungs and liver arise from the foregut (Chalmers and Slack, 2000, Deutsch et al., 2001, Serls et al., 2005) which is identified by hematopoietically-expressed homeobox protein (Hhex) expression (Moore-Scott et al., 2007). Specifically the hepatic fate is induced to develop from the ventral foregut endoderm (Tremblay and Zaret, 2005) by FGF signals from the developing heart and BMPs from the septum transversum mesenchyme (Fukuda-Taira, 1981, Gualdi et al., 1996, Jung et al., 1999, Douarin, 1975, Rossi et al., 2001).

Hepatic specification occurs at E8.5- E9.0, and the epithelium begins to express liver genes such as albumin, alpha-fetoprotein (AFP) and hepatocyte nuclear factor (HNF) 4α and form the liver diverticulum (Bort et al., 2006) (Figure 1.3.2). Formation of the liver diverticulum is marked by the transition from simple cuboidal cells to a pseudostratified columnar epithelium. The anterior of the liver diverticulum goes on to form the liver and biliary tree whereas the gall bladder and extrahepatic bile ducts arise from the posterior. Several transcription factors and signals from endothelial cells, lead to liver bud formation, during which bi-potent hepatoblasts delaminate from the epithelium and invade the adjacent septum transversum mesenchyme (Bort et al., 2006) (Figure 1.3.2). Hepatoblasts express hepatocyte genes (such as HNF4a and albumin), cholangiocyte genes (such as *cytokeratin (CK) 19* and *foetal liver gene AFP*. Transcription factors including Hhex (Keng et al., 2000, Martinez Barbera et al., 2000), Gata4 (Watt et al., 2007), Gata6 (Zhao et al., 2005) and the later acting prospero homeobox protein (Prox) 1 (Sosa-Pineda et al., 2000), HNF6 (or Onecut (OC)-1) and OC-2 (Margagliotti et al., 2007) regulate liver bud formation. The hepatic vasculature development through angiogenesis and vasculogenesis accompanies the formation of the liver bud (Matsumoto et al., 2001, Gouysse et al., 2002). The liver bud undergoes a period of growth and vascularisation from E10-E15 during which the liver bud is also colonised with hematopoietic cells (Figure 1.3.2). Liver bud growth is regulated by intrinsic hepatoblast gene expression and by signals from the hepatic mesenchyme including FGF, BMP, hepatocyte growth factor (HGF), Wnt, transforming growth factor beta (TGFβ) and retinoic acid. These signals promote hepatoblast migration, proliferation and survival. Interestingly, during earlier stages of liver development Wnt signalling must be repressed to allow hepatic specification, however during liver bud growth Wnt signalling from the mesenchyme promotes liver development (Lade and Monga, 2011). Hepatoblasts which are in contact with the portal vein initially form a monolayer and then a bilayer and begin to commit to the cholangiocyte lineage by decreasing hepatic gene expression and increasing biliary gene expression. Hepatoblasts not in contact with the portal veins undergo hepatocyte differentiation. From E17 hepatocytes become arranged in characteristic hepatic cords and the intrahepatic bile ducts form (Figure 1.3.2).

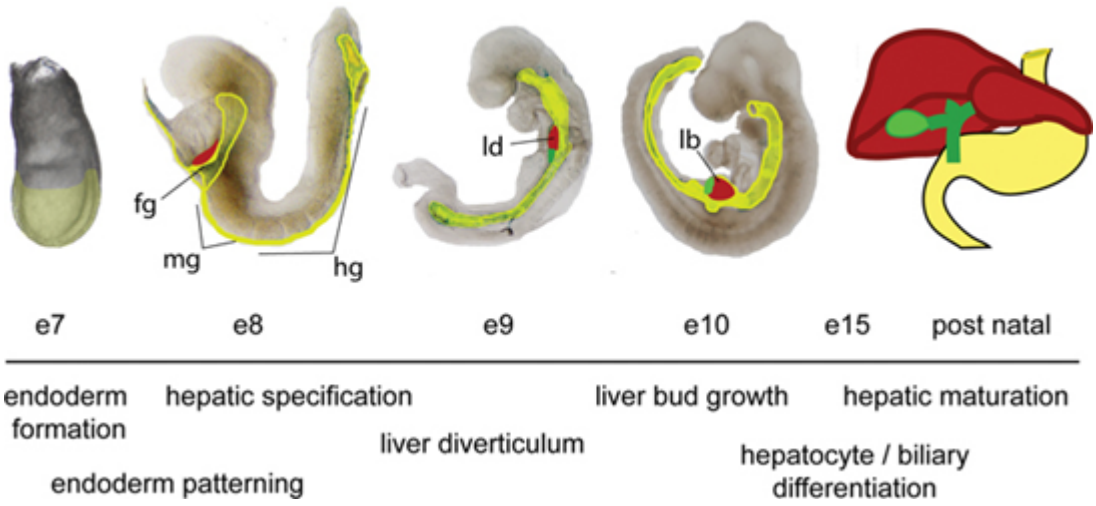


**Figure 1.3.2 Mouse model of embryonic liver development**

Diagram of mouse embryos at different developmental stages. The endoderm is highlighted in yellow, the liver in red and the gall bladder in green. Developmental events are listed below. During gastrulation (E6.5-E7.5 the endoderm is formed following which the endoderm is patterned into the foregut (fg), midgut (mg) and hindgut (hg) domains. The ventral foregut adjacent to the heart gives rise to the liver. Hepatic specification occurs by E8.5. By E9 the liver diverticulum (ld) is formed which grows and expands into the liver bud by E10. The liver bud undergoes a period of growth and hepatoblast differentiation into hepatocytes and cholangiocytes. The liver continues to develop and mature into the postnatal period. Figure from (Zorn, 2008)

### 1.3.4 Hepatocyte differentiation

Hepatocytes arise from bi-potential hepatoblasts which are also able to differentiate into cholangiocytes. The underlying mechanisms driving cell fate decision are unclear. It has been suggested however that signals from the periportal region including TGFβ, Notch, Wnt and FGFs lead to hepatoblasts committing to a cholangiocyte fate (Lemaigre, 2009, Zong and Stanger, 2012). However, lower level exposure to these signals for hepatoblasts located further away from the periportal region commit cells to a hepatocyte fate. Additionally, HGF is a growth factor that has been identified as an inducer of the hepatocytic lineage (Suzuki et al., 2003).

Hematopoietic cells that migrate to the liver around mouse E10 have been shown to play a role during deciding hepatocyte cell fate by secreting hepatocyte inducing signals such as Oncostatin M. Oncostatin M induces the expression of hepatocyte markers such as serum proteins via signal transducer and activator of transcription (STAT) 3 mediated signalling (Ito et al., 2000, Kamiya et al., 1999). The transcriptional repressor T-box transcription factor (TBX) 3 appears to be important to ensure continued expression of hepatocyte differentiation regulators HNFα and CCAAT/enhancer-binding protein alpha (c/EBPa), whereas TBX3 needs to be eliminated to ensure cholangiocyte differentiation (Ludtke et al., 2009, Suzuki et al., 2008).

Hepatocytes derived from hepatoblasts continue to differentiate and mature throughout the rest of embryonic development and into postnatal life. Maturing hepatocytes need to acquire several characteristic features to be able to support systemic homeostasis including quiescence, metabolic activation, cellular polarity and undergo a process of functional zonation. A set of core transcription factors have been identified that drive these processes, including HNF1α, HNF1β, FOXA2, HNF4, HNF6 and liver receptor homolog 1 (LRH1) (Kyrmizi et al., 2006, Schrem et al., 2002, Junqueira and Mescher, 2013). A model has been proposed where a threshold of each transcription factor is reached at a specific stage during development ensuring the correct temporal induction of target genes (Lemaigre, 2009). However extensive cross regulation exists between these transcription factors. Interestingly many of these transcription factors are also important for regulating gene transcription in the adult liver and it is unclear how these transcription factors fulfil different roles and induce different sets of genes during hepatogenesis compared with in the mature liver.

Genetic mouse models have highlighted a growing network of additional transcription factors, co-regulators and mRNA splicing factors that act alongside these core transcription factors to maintain hepatocyte gene expression in the adult liver (Wang et al., 1995, Flodby et al., 1996, Odom et al., 2004, Lokmane et al., 2008, Coffinier et al., 2002, Pontoglio et al., 1996, Le Lay and Kaestner, 2010, Bochkis et al., 2008). For example the transcription factor pregnane X receptor (PXR) which is regulated by HNF4α is required during foetal hepatocyte differentiation but is switched off in mature hepatocytes. Another study identified thousands of enhancers which were bound by HNF4α and FOX2A in a differentiation dependent manner. Enhancer switching was dependent on chromatin remodelling and led to differential expression of target genes. Hippo signalling appeared to play a crucial role in enhancer switching by influencing HNF4α and FOX2A interactions with temporal enhancers (Alder et al., 2014). Transcription factors may execute differential functions during development and in the adult liver by interacting with temporal enhancers. mRNA splicing can also play an important role as elucidated for HNF4α. HNF4α has at least nine isoforms which are generated by using two alternative promoters (P1 and P2) and the alternative splicing of the generated transcripts (Sladek et al., 1990, Torres-Padilla et al., 2001). Structural differences exist between the different isoforms which alter their interaction with transcriptional co-regulators and influence their gene-regulatory properties (Sladek et al., 1999, Wang et al., 1998, Torres-Padilla et al., 2002, Briancon and Weiss, 2006). Transcripts originating from the two different promoters appear to be sequentially expressed during development (Torres-Padilla et al., 2001).

A complex series of transcriptional mechanisms are essential for functional liver zonation (Braeuning et al., 2006) with an essential role having been assigned to the Wnt/ β-catenin pathway. In peri-central hepatocytes active β-catenin has been found whereas the β-catenin negative regulator, Adenomatosis Polyposis Coli (APC), has been discovered in periportal cells (Benhamouche et al., 2006). However other factors appear to play a role alongside β-catenin in modulating liver zonation including HNF4α.

### 1.3.5 Hepatocyte polarisation

Hepatocytes are highly organised cells are polarised with distinct luminal and basolateral compartments. The basal membrane faces the liver sinusoidal endothelial cells and mediates the interaction with the extracellular matrix. The apical side faces the bile canaliculi. Hepatocyte polarity is tightly regulated and is essential for the many functions of these

cells. Polarity is maintained and regulated by certain cell adhesion molecules, cytoskeletal factors and intracellular trafficking factors (Treyer and Musch, 2013). Hepatocytes form chains of cells sealed by tight junctions. Cell polarity allows hepatocytes to absorb and secrete proteins and other solutes in a directional manner. This is essential to the function of hepatocytes as they take up, process and secrete sinusoidal blood components and also synthesise and secrete bile. Unlike other epithelial cells which are polarised in the plane of the tissue (Bryant and Mostov, 2008), hepatocytes are unique in that two adjacent cells contribute towards an apical plasma membrane that form the bile canaliculi (Slim et al., 2013). Hepatocytes are organised into one or two cell thick plates which have multiple luminal and basal domains. Most epithelia establish a basal lamina however hepatocytes do not assemble extra cellular matrix molecules into a dense matrix. Basement membrane deposition during liver cirrhosis in fact disrupts tissue organisation and impairs hepatocyte function (Musch, 2014). Structural polarity is maintained by tight junctions which consist of claudins, occludins, and TJP proteins (Musch, 2014). E-cadherin is an important initiation factor for epithelial polarisation (Musch, 2014). E-cadherin is able to form a platform to assist the assembly of adherens junctions. Adherens junctions to link cell-cell contacts to the actin cytoskeleton and are essential in the maintenance of the actin belt (Treyer and Musch, 2013). Hepatocyte polarisation is tightly controlled during differentiation and liver development and abnormalities in hepatocyte polarisation can have major pathological consequences.

### 1.3.6 Response to liver damage & adult liver progenitor cells

The liver has extraordinary regenerative capability, which has likely evolved due to its role as first line of exposure to foreign substances and toxins absorbed from the intestine and delivered to the liver for biotransformation. Under normal homeostatic conditions, hepatocytes and other liver cells are largely quiescent; the liver has a low rate of cell turnover. Hepatocytes can persist for weeks and even up to months without dividing and less than 1-2 % of hepatocytes are cycling at any given time (Macdonald, 1961).

The liver response to acute liver injury, for example from drugs, alcohol, toxins or surgical removal of liver mass, occurs via the synchronised cell cycle re-entry of hepatocytes. Hepatocytes undergo several rounds of division until the original liver mass is restored (Michalopoulos, 2007, Michalopoulos, 2013). Malato et al., demonstrated the high efficiency of hepatocyte replication to a variety of acute injuries by using genetic labelling

to show that in response to acute injury, new hepatocytes are derived from pre-existing hepatocytes (Malato et al., 2011). Liver organ size is tightly regulated via several redundant and interacting signalling pathways. Liver regeneration in response to acute liver injury has commonly been investigated using animal models of partial hepatectomy. Non-parenchymal cells in the liver including HSCs, LSEs and Kupffer cells also play a role in the response to acute injury and help control the epithelial regeneration (Forbes and Rosenthal, 2014).

An alternative hypothesis of liver regeneration is that tissue resident stem cells help repopulate the liver after injury; this is known as the facultative stem cell hypothesis. Bi-potent HPCs appear to play a predominant role during chronic liver injury when hepatocyte replication is exhausted or inhibited, for example due to viral infection, metabolic disorders (e.g. diabetes) or persistent alcohol consumption (Blachier et al., 2013). Chronic liver injury induces what is commonly referred to as a ductular reaction during which adult liver progenitors emerge from the putative stem cell niche, the canals of Hering. The HPCs are able to differentiate into both hepatocytes and cholangiocytes, similar to hepatoblasts during development (Miyajima et al., 2014). These progenitors are able to differentiate into hepatocytes and contribute to liver regeneration (Stanger, 2015, Diehl and Chute, 2013, Williams et al., 2014), however the extent to which HPCs contribute to liver repair and hepatocyte replenishment is under research and still in debate (Diehl and Chute, 2013, Boulter et al., 2013, Huch et al., 2013). Yoon et al., showed that in cirrhotic livers hepatocytes which were positive for the progenitor marker epithelial cell adhesion molecule (EpCAM) also had longer telomere length than those hepatocytes which lacked EpCAM expression and associated close to ductular reactions (Yoon et al., 2011). Death of parenchymal cells due to liver injury induces cellular changes, leading to the infiltration of inflammatory cells and vascular alterations (Lawson et al., 1998). HPC associated liver regeneration is often accompanied by ECM remodelling and the deposition of collagens and laminins (Kallis et al., 2011, Klaas et al., 2016).

HSCs and portal fibroblasts are both ECM producing and modifying cells which contribute to liver fibrosis and cirrhosis during chronic liver injury. HSCs are thought to be the main contributors however (Mederacke et al., 2013). It is possible that HPCs may even contribute to profibrotic signals under certain circumstances (Chen et al., 2015b). The ECM may play a role in the regulation of HPC proliferation and differentiation (Tsukada et al.,

2009). Several inflammatory signalling molecules have been implicated in the induction of HPC proliferation, including tumour necrosis factor (TNF) α, interleukin (IL)-6 and interferon (IFN) γ (Knight et al., 2000, Yeoh et al., 2007, Akhurst et al., 2005). Growth factors such as HGF and epidermal growth factor (EGF) play a role in regulating both HPC proliferation and differentiation (Ishikawa et al., 2012, Kitade et al., 2013). Boulter et al., demonstrated that Notch induces cholangiocyte differentiation of HPCs and Wnt signalling by Kupffer cells, opposes Notch signalling to promote hepatocyte differentiation (Boulter et al., 2012).

### 1.3.7 Types of primary liver cancer

Primary liver cancer represents the sixth most common cancer worldwide, yet is the second leading cause of cancer related death with a growing disease burden (International Agency for Research on Cancer., 2014). Primary liver cancer comprise a heterogeneous group of tumours, including hepatocellular carcinoma, intrahepatic cholangiocarcinoma (ICCA), mixed HCC-ICCA, fibrolamellar HCC, angiosarcoma (or haemangiosarcoma) and hepatoblastoma (Lozano et al., 2012, International Agency for Research on Cancer., 2010). HCC was thought to have a hepatocellular origin and is often associated with cirrhosis and fibrosis. The main risk factors for HCC include viral hepatitis (HBV and HCV), excessive alcohol consumption, and non-alcoholic fatty liver disease in patients with metabolic diseases such as diabetes. ICCA has features of cholangiocyte origin and risk factors include primary sclerosing cholangitis, biliary duct cysts, hepatolithiasis, parasitic biliary infestation with flukes and HCV (Bridgewater et al., 2014, Li et al., 2015a). Fibrolamellar carcinoma is a rare subtype of HCC which is more common in younger adults and is not usually linked to cirrhosis or viral hepatitis. Angiosarcoma is an extremely rare primary liver cancer which begins in the blood vessels of the liver. Hepatoblastoma is also very rare and commonly affects young children under three. Hepatoblastoma cells have a mixed foetal hepatocyte, mature hepatocyte and cholangiocyte phenotype.

HCC and ICCA are the most common forms of primary liver cancer; with HCC alone accounting for 90 % of all primary liver cancer cases (Llovet et al., 2016). Viral hepatitis represents a common risk factor for HCC and ICCA (Palmer and Patel, 2012). Tumours of the liver have a heterogeneous morphology both within the same tumour and between different tumours. Classification is not always straight forward and some HCC and ICCA have progenitor cell features such as expression of the progenitor marker CK19

(Roskams et al., 2003, Lee et al., 2006, Wang et al., 2011a, Roskams, 2006). Mixed HCC-ICCA presents with a mixed hepatocyte & cholangiocyte phenotype (Singh et al., 2013). The cellular origin of HCC, ICCA and HCC-ICCA is much debated and possible cells of origin include HPCs and mature hepatocytes and cholangiocytes (Figure 1.3.3). HPCs may give rise to either HCC, ICCA or HCC-ICCA. Mature hepatocytes may undergo a process of dedifferentiation and transformation to give rise to HCC. Hepatocytes also have significant plasticity (Tarlow et al., 2014) and may undergo a process of transdifferentiation. Some hypothesise that cholangiocyte cells only give rise to ICCA and that cholangiocytes lack the same plasticity (Guest et al., 2014). However a study by Forbes and his group demonstrated that cholangiocytes are in fact able to dedifferentiate into HPCs and give rise to hepatocytes during liver regeneration (Raven et al., 2017).

Experimental evidence supports both a HPC and hepatocyte origin for HCC. For example genetic alterations of Hippo pathway genes in mice lead to the expansion of HPCs and ultimately the development of both HCC and ICCA (Lu et al., 2010, Lee et al., 2010, Fitamant et al., 2015). Alternatively, mature hepatocytes are able to dedifferentiate into nestin-positive HPC-like cells after the loss of tumour suppressor gene TP53, leading to HCC development after the acquisition of other subsequent oncogenic mutations (Tschaharganeh et al., 2014). Ultimately it is likely that both HPCs and mature hepatocytes are able to give rise to HCC, ICCA and HCC-ICCA primary liver cancer and this may vary depending upon the nature of the liver injury in question, or the hepatic background in which the cancer arises. Further research is needed to determine which circumstances give rise to tumours from HPCs or mature hepatocytes. Animal models are useful particularly for using cell fate tracing studies however discrepancies exist between mice and humans. The gap between cell fate tracing in animals and studies of patients with liver injury needs to be filled.

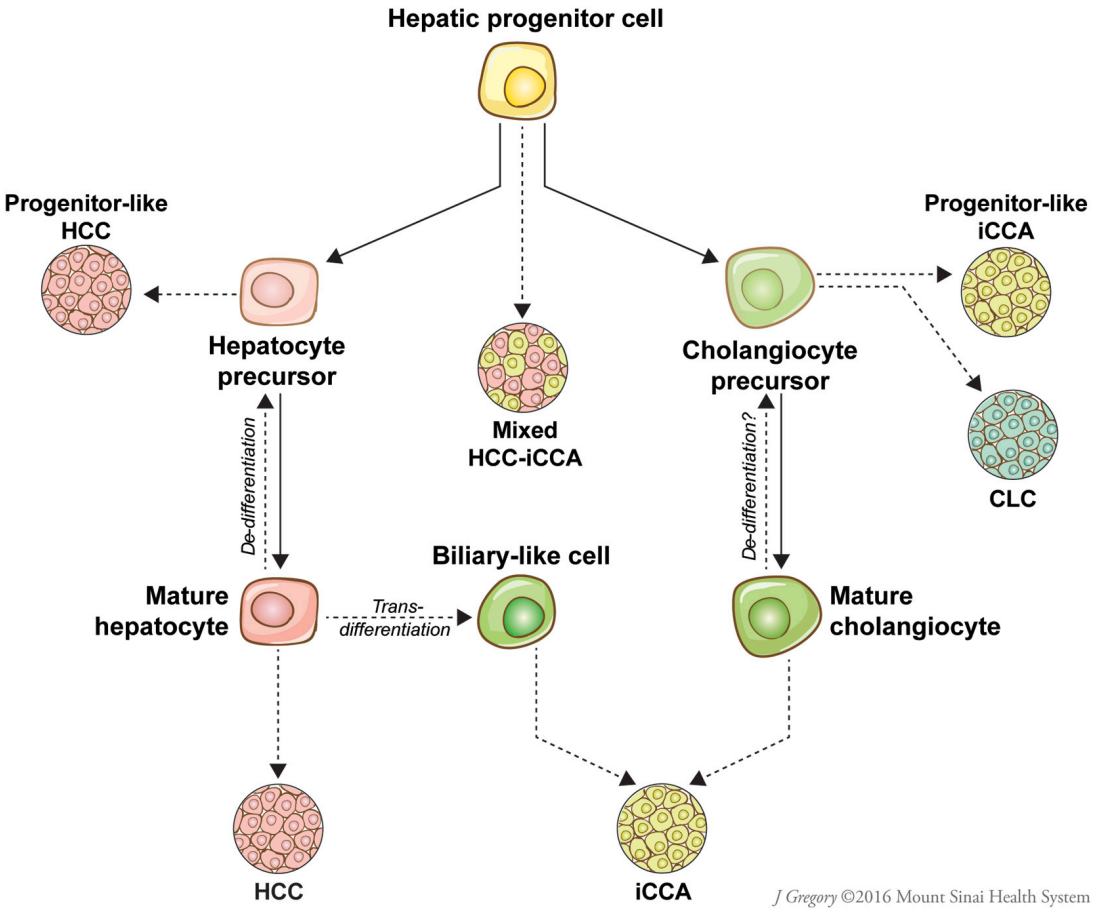


**Figure 1.3.3 Possible cells of origin of HCC and ICCA**

Multiple cells types may be the cell of origin of HCC and ICCA. HCC and ICCA can develop from mature hepatocytes and cholangiocytes respectively, via dedifferentiation and transformation. HPCs can also give rise to HCC, ICCA and mixed HCC-ICCA tumours. Mature hepatocytes are plastic and evidence suggests that these cells can be reprogrammed and transdifferentiate and also lead to the development of ICCA. From (Sia et al., 2017).

## 1.4 Hepatocellular carcinoma

### 1.4.1 General background and features

HCC commonly develops in patients with advanced hepatic fibrosis and cirrhosis due to chronic liver disease, particularly as a result of liver damage caused by viral hepatitis, HCV and HBV. Due to this HCC incidence is similar to the incidence of HCV and HBV, with the highest incidence rates in Asia and Sub-Saharan Africa. Development of HCC due to chronic HCV infection occurs almost exclusively in the presence of cirrhosis, however about 8 % HCC developed in patients with advanced fibrosis only (Lok et al., 2009). Most commonly HCC is classified into five stages of disease (0-very early, A, B, C and D- end stage) based on the Barcelona Clinic Liver Cancer staging classification (European Association for the Study of the Liver, 2012). Depending on the disease stage, the degree of liver impairment, and condition of the patient, patients undergo different treatments and the disease stage and chosen treatment impacts upon the prognostic outcome. Possible treatments include surgical resection, radiofrequency ablation, chemoembolization, Sorafenib (trade name Nexavar) treatment and liver transplantation (European Association for the Study of the Liver, 2012).

Only about 40 % of HCC patients are diagnosed in the early stages (stages 0 and A) of HCC and become eligible for potentially curative therapies such as resection and liver transplantation. Generally resection is recommended for patients with a single tumour and preserved liver function. Patients with single tumours of less than 5 cm or with up to three nodules of less than 3 cm are recommended for liver transplantation. The median survival rate for stage 0 and stage A patients is over 60 months and therapies include liver resection, transplantation or local ablation. Chemoembolization represents the recommended therapy for patients diagnosed at stage B and Sorafenib therapy is recommended at stage C. Median survival stand at 26 and 3 months for stages B and C, respectively. Patients diagnosed with end-stage HCC (stage D) receive symptomatic treatment only.

HBV vaccination has been shown to effectively reduce the incidence of HCC in those regions with a high prevalence of HBV. Interferon antiviral therapy can reduce the risk of HCC for patients living with chronic HCV infection (Singal et al., 2010). However new non-interferon-based DAAs will need to be assessed for their effectiveness at reducing the HCC risk; conflicting evidence has been published so far, with some reports suggesting DAA treatment reduces HCC risk whereas others finding no such risk reduction

(ANRS collaborative group on HCC, 2016, Finkelmeier et al., 2018, Ioannou et al., 2017, Reig et al., 2016, Waziry et al., 2017, Nault and Colombo, 2016).

There appears to be several stages of HCC development (Figure 1.4.1). HCC begins with the development of pre-cancerous cirrhotic nodules with low-grade dysplasia which then go on to progress into high-grade dysplastic nodules. These nodules may then subsequently transform into early stage HCC. As discussed in the previous section the cellular origin of HCC is unclear and HCC CICs may arise from mature hepatocytes, cholangiocytes or HPCs. The liver is rarely a target of classical cancer predisposition syndromes and genetic syndromes which predispose carriers to breast, ovarian or colorectal cancer are not often associated with liver tumours (Dragani, 2010). However there have been a number of single nucleotide polymorphisms (SNPs) associated with HCC risk (Nahon and Zucman-Rossi, 2012). These SNPs act at different disease stages and include SNPs which predispose carriers to HCC risk factors such as developing chronic, rather than acute HCV infection such as the IL28B SNPs (Ge et al., 2009, Suppiah et al., 2009, Tanaka et al., 2009). Other SNPs are associated with modulating the severity of liver disease, malignant transformation of cirrhotic nodules or the progression of hepatic tumours (Nahon and Zucman-Rossi, 2012). Furthermore the genetic condition call haemochromatosis which leads to increased iron storage in the liver is associated with an increased risk of developing HCC (Kowdley, 2004). HCC commonly develops by the accumulation of somatic genomic alterations. On average HCC nodules carry 40 functional somatic alterations in coding regions. This is reflected in the heterogeneous nature of HCC to which epigenetic modifications; including changes to DNA methylation, histone patterns, chromatin remodelling, miRNAs and long noncoding RNAs (ncRNAs) expression, also contribute (Guichard et al., 2012, Nault et al., 2013, Schulze et al., 2015).

The genetic alterations which accumulate in HCC do not appear to be entirely random. There appear to be common pathways which are altered and promote oncogenesis. Different pathways may be related to specific risk factors such as chronic HCV infection (Schulze et al., 2015). Whole genome sequencing has identified the pathways which are commonly altered in HCC. The pathways identified relate to telomere maintenance, the cell cycle such as p53 and the retinoblastoma (Rb) pathway, Wnt/β-catenin signalling, Hippo signalling, the oxidative stress pathway, the protein kinase B/mammalian target of rapamycin (Akt)/ (mTOR) pathway, Map kinase

signalling and epigenetic modification. The choice of HCC treatment currently relies mainly on phenotypic clinical staging; however molecular analysis has prognostic value using biomarkers and increases HCC understanding.

HCC can be divided into two subtypes on a molecular level: proliferative and non-proliferative class. The proliferative class is more aggressive and is enriched in signals relating to cell proliferation and cell cycle progression (Sia et al., 2017, Villanueva et al., 2012, Martinez-Quetglas et al., 2016, Sia et al., 2013). The non-proliferative class appears to retain normal hepatic features, shows lower levels of progenitor features and is dominated by activation of Wnt signalling (Lachenmayer et al., 2012). Several biomarkers have been identified for HCC and can help inform on treatment and prognosis. Biomarkers are also referred to cancer-stem cell markers or cancer-initiating cell markers (CICs). CICs have been identified as a small subset of tumour cells which are hypothesised to be responsible for treatment resistance, tumour recurrence and metastasis. This is often referred to as the cancer stem cell theory (Clarke et al., 2006). Any cancer treatment needs to target and eliminate this subpopulation of cells to ensure the cancer does not recur. Indeed in HCC CICs have been suggested to play a role in tumour growth, recurrence, metastasis and resistance to treatment (Xu et al., 2010a, Xu et al., 2010b). A set of CIC markers have been identified for HCC. Some CIC markers are common to many different cancers, whilst others are unique to a specific type of cancer and other markers appear to have opposing roles in different cancer types. CIC markers are used for prognostic purposes (to help to determine HCC stage) and to further our understanding of this specific cancer cell subpopulation in the hope of better targeting CICs. HCC CIC markers include: CK19 (Kawai et al., 2015), CD133 (Suetsugu et al., 2006, Ma et al., 2007, Ma et al., 2008), CD90 (Yamashita et al., 2013, Yang et al., 2008b), CD44 (Yang et al., 2008b, Zhu et al., 2010), EpCAM (Yamashita et al., 2009) and CD24 (Lee et al., 2011). Kawai et al., found that HCC lines expressing CK19 had higher proliferative capacity and when transplanted into immunodeficient mice generated large tumours. In addition CK19 positive patients had significantly poorer recurrence-free survival compared to CK19 negative patients (Kawai et al., 2015). Huh7 cells positive for CD133 have higher proliferative potential capacity and tumourigenic potential compared to CD133 negative Huh7 cells (Suetsugu et al., 2006). Ma et al., found when analysing HCC cell

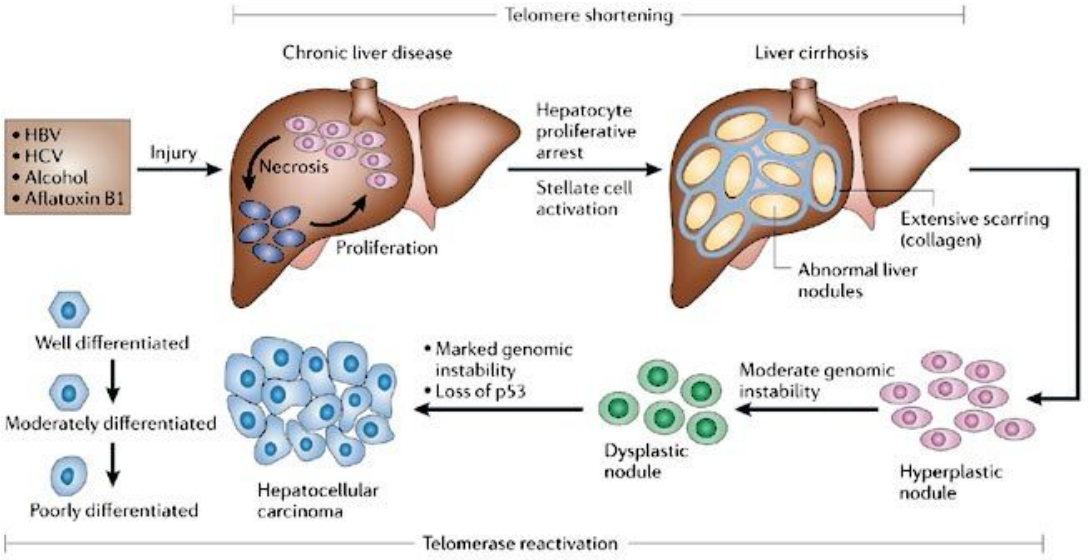




**Figure 1.4.1 Schematic of the multi-step development of HCC**

Chronic liver damage leads to fibrosis and cirrhosis via a continuous cycle of destruction and regeneration. Hepatocyte proliferation becomes exhausted and HSCs become activated. Abnormal pre-cancerous liver nodules develop with low-grade dysplasia. These cirrhotic nodules progress into high-grade dysplastic nodules and can eventually undergo transformation and lead to the development of HCC. Schematic from (Farazi and DePinho, 2006).

lines that CD133 positive cells had a greater tumour forming ability *in vivo*. CD133 positive cells were found to express a number of stem cell genes and shared characteristics with HPCs such as self-renewal (Ma et al., 2007, Ma et al., 2008). CD90 positive cells were associated with metastasis by Yamashita et al. Furthermore CD90 positive cells of different HCC cell lines had a higher tumourigenic capacity (Yang et al., 2008b). CD44 has been identified as a CIC marker in many different tumour types. Tumour cells expressing CD44 along with other CIC markers such as CD90 and CD133 display a more aggressive phenotype, are associated with metastasis and have stem cell properties (Yang et al., 2008b, Zhu et al., 2010). EpCAM is another CIC marker that is associated with a stem cell and HPC in tumour cells expression the marker (Yamashita et al., 2009). EpCAM positive cells were shown to be able to self-renew and differentiate. CD24 has been identified as a CIC marker for HCC and other tumours (Burgos-Ojeda et al., 2015, Huang and Hsu, 1995, Kristiansen et al., 2002, Liu et al., 2013, Salaria et al., 2015, Yang et al., 2014, Yang et al., 2009). CD24 is a heavily glycosylated cell membrane protein which is expressed by stem cells and progenitors. Chemoresistant CD24 positive HCC cells appear to be important for self-renewal, maintenance and metastasis of tumours, and expression is associated with poor patient prognosis (Lee et al., 2011). Furthermore this CD24 CIC phenotype appeared to be driven via STAT3 mediated NANOG regulation by inducing STAT3 phosphorylation at tyrosine 705 (Lee et al., 2011). Liu et al., found that the transcription factor twist-Related Protein (Twist) 2 was responsible for upregulation of CD24 in HCC cells (Liu et al., 2014).

### 1.4.2 Signalling Pathways involved in HCC development and progression

#### 1.4.2.1 Wnt Signalling Pathway

Wnt signalling is dysregulated in many types of cancer including HCC. Bengochea et al., found a potentially activating Frizzled (FZD) event in 95% of HCC resections (Bengochea et al., 2008). Wnt plays a role in a wide range of cellular processes such as proliferation, survival, migration, self-renewal, embryonic development and cell fate decision (Anastas and Moon, 2013), including during liver development and hepatocyte differentiation. Wnt signalling activation occurs via the canonical pathway which is β-catenin dependent or via the non-canonical pathway which is β-catenin independent. Non-canonical Wnt signalling includes the planar cell polarity pathway and the Wnt/Calcium pathway. The planar cell polarity pathway leads to

activation of Rho associated coiled-coil containing protein kinase (Rock) and c-Jun N-terminal kinase (JNK). For the Wnt/Calcium pathway Wnt5a binds to frizzled receptor 2 (FZD2) to activate phospholipase C eventually leading to increased intracellular calcium. Calcium then activates calcium/calmodulin-dependent protein kinase II (CAMK2) and protein kinase C (PKC). These kinases in turn inhibit the canonical Wnt pathway. A majority of HCC cases (up to 90 %) exhibit beta-catenin activation which promotes cell growth. The exact role of non-canonical Wnt signalling in HCC is less well understood (Liu et al., 2016).

#### 1.4.2.2 MAPK signalling

Mitogen-activated protein kinase (MAPK) signal transduction regulates many cellular processes such as cell survival and proliferation. MAPK pathways interact and modulate other signalling pathways such as Wnt/β-catenin and TGFβ/Smads. MAPK signalling is commonly dysregulated in malignancies including HCC (Min et al., 2011). Many studies have observed increased expression and activation of MEK1/2 and ERK1/2 in HCC tissue (Ito et al., 1998b, Schmidt et al., 1997, Huynh et al., 2003, Tsuboi et al., 2004). Indeed MEK inhibition has been shown to lead to reduced HCC cell growth and increased apoptosis, further supporting the role of the pathway in HCC tumour growth (Huynh et al., 2003, Klein et al., 2006). Dysregulation of the MAPK pathway in HCC occurs at different points along the signalling cascade. Ras and Raf activating mutations are rare in HCC, whereas downregulation of Ras/MAPK pathway inhibitors such as GTPase-activating protein (GAPs), Ras-association domain family (RASSF) proteins, Spred and Sprouty proteins appear to be largely responsible for aberrant MAPK signalling. The MAPK pathway is a therapeutic target in HCC; Sorafenib is an inhibitor of several tyrosine kinases including the RAF family kinases.

#### 1.4.2.3 TGF-β signalling

TGF-β appears to have dual and opposite roles in HCC, both tumour suppressive and tumour promoting. TGF-β regulates cell proliferation thereby acting as a tumour suppressor but TGF-β also enhances cancer cell motility and invasion. TGF-β and its intracellular mediators, the SMAD proteins, are responsible for the activation and proliferation of stromal fibroblasts, promoting fibrosis during chronic liver injury (Hellerbrand et al., 1999, Ueberham et al., 2003). The exact role of TGF-β signalling in HCC may depend on the stage of disease progression. As HCC progresses it appears that the tumour-suppressive activity of TGF-β are selectively

reduced whereas the pro-oncogenic activity is increased (Yoshida et al., 2016)

#### 1.4.2.4 STAT3 signalling

STAT3 is a member of the STAT family of proteins and is activated by Tyr705 and Ser727 phosphorylation (Wen et al., 1995). Activation and phosphorylation as a result of cytokine and growth factor signalling such as from IL-6, EGF and HGF (Takeda and Akira, 2000, Hirano et al., 2000) leads to STAT3 dimerization, nuclear translocation and DNA binding. Tyr705 phosphorylation is mediated by Janus kinases (JAKs), particularly JAK2. Ser727 phosphorylation appears to modulate STAT3 activity (Wen et al., 1995). In healthy cells STAT3 activation leads to a negative feedback loop with Suppressor of cytokine signalling (SOCS) 3 activation (Kubo et al., 2003) ensuring STAT3 activity is transient. However in cancer cells including HCC STAT3 is constitutively active which is generally associated with poor prognosis (Niwa et al., 2005, Ogata et al., 2006a, Ogata et al., 2006b, Li et al., 2006a, Liu et al., 2011c, Liu et al., 2011d). STAT3 target genes include pro-proliferative, anti-apoptotic and pro-invasion proteins such as cyclin D1, BCL-$x_L$ and metalloproteinases (MMPs) (Johnson et al., 2018).

### 1.4.3 HIPPO pathway

The Hippo signalling pathway is an important pathway involved in organ size regulation, cell fate decision and differentiation. The pathway was first identified and described in *Drosophila* (Wu et al., 2003); however since then a significant body of work has described the function and regulation of the Hippo pathway in mammalian cells. The core of the pathway consists of a central kinase cascade concerned with the inactivation of the transcriptional regulators Yes-associated protein (YAP1) and transcriptional coactivator with PDZ-binding motif (TAZ- gene name: WW domain containing transcription regulator 1- WWTR1). TAZ was identified as a paralog of YAP which shares almost 50 % sequence homology (Kanai et al., 2000). TAZ is only present in vertebrates. TAZ lacks several domains present on YAP: a second WW domain present, the N-terminal proline rich domain and the Src homology 3 (SH3) binding motif (Kanai et al., 2000) (Figure 1.4.2). In the absence of Hippo signalling, hypo-phosphorylated YAP1 and TAZ are present in the nucleus and bind to transcription factors including TEA Domain Transcription Factor (TEAD) 1-4, SMAD1-4 (activated by TGF-β) and p73 (Strano et al., 2001, Xiao et al., 2016, Papaspyropoulos et al., 2018, Kim et al., 2018, Ferrigno et al., 2002, Varelas et al., 2010b, Hau et al., 2013, Chen et al., 2010b) leading to a gene expression profile associated

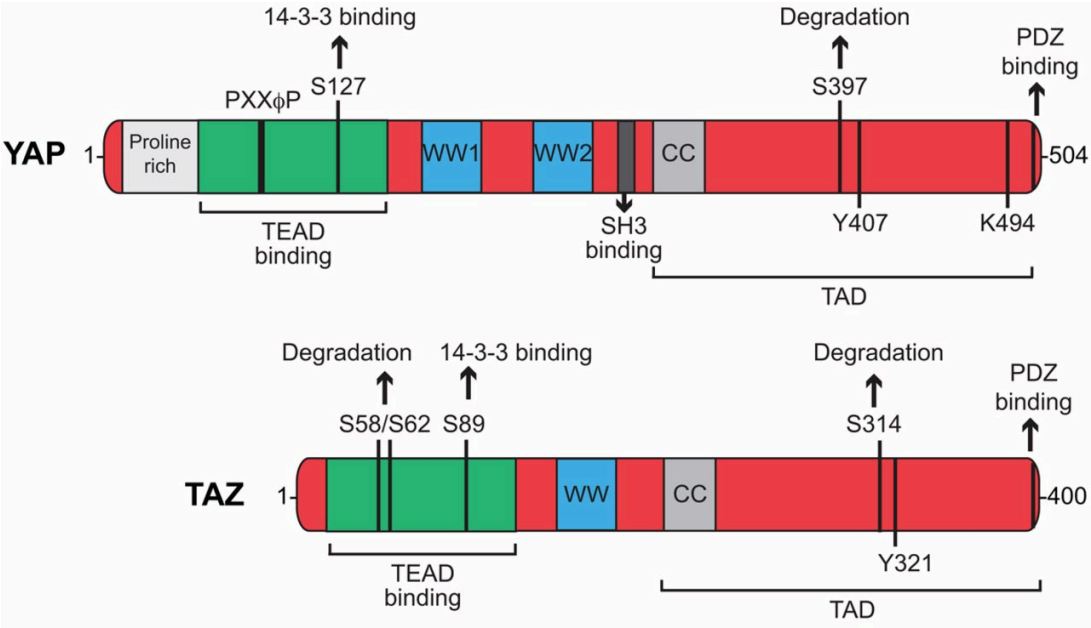


**Figure 1.4.2 Protein domains and regulatory sites of transcriptional regulators YAP1 and TAZ.**

TAZ is a paralog of YAP1 sharing almost 50 % sequence homology. Protein regions of note present in both YAP1 and TAZ include the WW domains (of which YAP1 has two), the coiled-coil (CC) domain, the TEAD-binding domain, the transcriptional activation domain (TAD), and the PDZ- binding motif. YAP1 also contains an SH3 domain and a proline rich motif. Also highlighted are the key residues which are targeted for post-translational modifications. These post-translational modifications regulate the cellular location and stability of YAP1 and TAZ. Diagram is from (Varelas, 2014).

with cell survival and proliferation (Zanconato et al., 2016, Zhi et al., 2012, Campbell et al., 2013). YAP1 and TAZ do not contain DNA- binding domains and function as regulators of transcription factors. The kinase cascade consists of the mammalian Ste20-like kinases 1/2 (MST1/2- gene name: Serine/Threonine kinase 4/3- STK4/3) which when activated phosphorylate in complex with Salvador family WW domain containing protein 1 (SAV1- gene name: WW45) and activate large tumour suppressor 1/2 (LATS1/2). LATS1/2 in complex with MOB kinase activator 1 (MOB1) phosphorylate YAP1 and TAZ. YAP1 and TAZ can be phosphorylated at several amino acid residues and phosphorylation of YAP1 and TAZ regulates the localisation and activity of these proteins. LATS1/2 phosphorylation at Ser89 for TAZ and Ser127 for YAP1 results in these proteins binding to 14-3-3 proteins, leading to their cytoplasmic retention (Zhao et al., 2007). Further phosphorylation at Ser397 and Ser11 for YAP1 and TAZ by LATS1/2 respectively, primes these proteins for further phosphorylation by casein kinase 1δ/ε at Ser314 on TAZ and Ser400/403 on YAP1. Phosphorylation at Ser314 on TAZ and Ser400/403 on YAP1 leads to proteasomal degradation by recruitment of the β-TrCP/SCF ubiquitin ligase (Liu et al., 2010, Zhao et al., 2010) (Figure 1.4.2). YAP1 and TAZ were first thought to be largely functionally redundant; however more evidence is emerging describing differences in their regulation and ensuing transcriptional activation between these two transcriptional regulators. TAZ can also be phosphorylated by glycogen synthase kinase 3β (GSK3β) on Ser58 and Ser62 which also leads to degradation after β-TrCP ubiquitination (Huang et al., 2012). Homeodomain-interacting protein kinase (HIPK2) seems to be a specific regulator of YAP1, acting to stabilise the protein and promote its nuclear activity possibly by regulating β-TrCP/SCF activity (Poon et al., 2012). In addition YAP1 and TAZ can be phosphorylated at a tyrosine residue in the C-terminal region (Y407 and Y321 on YAP1 and TAZ respectively) by c-ABL, Src and Yes (Figure 1.4.2). Phosphorylation at these tyrosine residues appear to regulate the transcriptional activity of YAP1 and TAZ by altering their binding selectivity to transcription factors (Zaidi et al., 2004, Levy et al., 2008, Jang et al., 2012). MST1/2 are activated by phosphorylation by upstream kinases such as RASSF1 and by autophosphorylation (Praskova et al., 2004). Autophosphorylation is enhanced by MST1/2 dimerization (Glantschnig et al., 2002).

#### 1.4.3.1 Regulation

Hippo signalling is activated and regulated by physical cues and biochemical signals. The Hippo pathway responds to changes in cell density via cell-cell contacts, cell- ECM interactions and cytoskeletal changes. The Hippo pathway is also regulated by secreted factors via G-protein coupled receptors (GPCRs). Serum deprivation and energy stress will also alter the Hippo pathway. A degree of crosstalk exist between the Hippo pathway and other pathways involved in development, proliferation and differentiation such as Wnt signalling, BMP signals, Notch and Hedgehog (Attisano and Wrana, 2013, Hsu et al., 2017, Watanabe et al., 2017, Young et al., 2015, Huang and Kalderon, 2014). The localisation and function of Hippo effector proteins YAP1 and TAZ are largely regulated by the upstream Hippo kinases however there are a number of proteins or pathways which can directly regulate YAP1 and TAZ independent of LATS1/2 such as Angiomotin (AMOT) and HIPK2 or GSK3β respectively.

Cell junctional protein complexes detect changes in cell density and tissue tension. Cell contact inhibition is believed to be largely mediated by Hippo signalling (Zhao et al., 2007, Ota and Sasaki, 2008). Furthermore regulation of the YAP1-TEAD transcription program in response to contact inhibition has been shown to be essential for embryonic development (Ota and Sasaki, 2008, Nishioka et al., 2009, Gumbiner and Kim, 2014). Cellular adherens and tight junctions influence LATS1/2 activity and YAP1/TAZ localisation and activity (Zhao et al., 2007, Silvis et al., 2011). YAP1 nuclear localisation has been reported to be induced via the activation of Rho-GTPases or the FAK-Src-PI3K (phosphatidylinositol-4,5-bisphosphate 3-kinase) pathway in response to cellular attachment to the ECM (Zhao et al., 2012, Kim and Gumbiner, 2015). In addition mechanical forces such as the stretching of the epithelial sheet regulate YAP1/TAZ via Rho-GTPases and F-actin capping and severing proteins (Aragona et al., 2013).

Neurofibromin 2 (NF2- also known as merlin) is one of the proteins identified to link cytoskeletal components and cell surface proteins with the Hippo pathway (Li et al., 2015c). NF2 knockout in mice led to the development of HCC via activation of YAP1 (Zhang et al., 2010). NF2 promotes phosphorylation of LATS1 and 2 by MST1/2-SAV by forming a complex with LATS1 and 2 at the cell membrane (Yin et al., 2013). Furthermore the interaction between NF2 and LATS1 and LATS2 is promoted by actin cytoskeleton disruption. Cytoskeletal and polarisation associated proteins including scribble and liver kinase B1 (LKB1) regulate proliferation by

inhibiting YAP1/TAZ activity (Skouloudaki et al., 2009, Ma et al., 2016). Adherens junction complex member α-catenin has also been linked to negative regulation of YAP1 by forming a complex with YAP1 and 14-3-3 leading to cytoplasmic YAP1 retention (Schlegelmilch et al., 2011). Interestingly AMOT, also an adherens junction protein, appears capable of carrying out opposing functions in respect to YAP1 regulation. AMOT has been described to both be able to promote nuclear YAP1 translocation and YAP1 retention in the cytoplasm. The expression of this family of proteins which includes the two AMOT isoforms p80 and p130, AMOT-like protein 1 (AMOTL1) and AMOT-like protein 2 (AMOTL2) differs depending on tissue-type, cell-type and developmental stage. AMOT interacts with YAP1 and TAZ via the WW domains. The p130 AMOT isoform interaction with YAP1 was shown to be able to prevent YAP1 phosphorylation by LATS1 and even associated with the YAP1-TEAD transcriptional complex to direct gene expression regulation (Yi et al., 2013). The same report showed that AMOT knockout in the liver resulted in reduced progenitor cell proliferation and tumorigenesis. In addition when liver-specific AMOT knockout mice were crossed with NF2 knockout mice, hepatomegaly and tumorigenesis usually associated with NF2 knockout was inhibited.

The Hippo pathway is also modulated by soluble factors and GPCRs. GPCRs can either lead to the activation or suppression of YAP1 activity. Rho-GTPases are responsible for mediating the GPCR action on the Hippo pathway. Important GPCR ligands to note are Wnt proteins. Noncanonical Wnt signalling is activated by Wnt5a/b binding to FZD receptors and activates YAP1 and TAZ (Park et al., 2015). Epinephrine, oestrogen, sphingosine and thrombin are some of the other ligands which can regulate Hippo signalling (Mo et al., 2012, Miller et al., 2012, Yu et al., 2012). However more studies are needed to understand the role GPCRs play in the liver to modulate Hippo signalling. The Hippo pathway is also modulated by stress signals, for example glucose deprivation will lead to phosphorylation and inactivation of YAP1 and TAZ via LATS1/2 activation (DeRan et al., 2014). During high glucose conditions O-GlcNAc (N-acetyl-D-glucosamine) transferase (OGT) attaches O-GlcNAc to Ser 109 of YAP1 which disrupts LATS1/2 ability to interact with YAP1 (Peng et al., 2017). Hypoxia induces YAP1/TAZ activation (Ma et al., 2015).

Genetic YAP1 and TAZ deletions demonstrate the importance of these transcriptional regulators during development. However individual knockouts result in differing phenotypes. Knocking out YAP1 results defects in yolk sac

vasculature and body axis elongation and results in embryonic lethality (Morin-Kensicki et al., 2006) whereas knocking out TAZ leads to the development of renal cysts and emphysema and the mice are able to survive (Hossain et al., 2007, Makita et al., 2008). YAP1 is expressed ubiquitously in the adult liver; however expression levels vary depending on cell type and cell position. Cholangiocytes express the highest levels of YAP1 and expression is graded depending on location of hepatocytes (Yimlamai et al., 2014, Li et al., 2012, Bai et al., 2012), with the highest expression described for hepatocytes in the portal area and lowest expression by hepatocytes found in the central venous region (Fitamant et al., 2015). Consistent with these findings is the observation that *in vitro* LATS1/2 knockout hepatoblasts preferentially differentiate into cholangiocyte-like cells (Lee et al., 2016). *In vivo* LATS1/2 knockout results in expansion of the ductal plate and an increase in cholangiocyte cells and fewer hepatocytes. YAP1/TAZ activity has been shown to play a crucial role during liver regeneration after injury. Overall YAP1 levels increase, as does YAP1 nuclear localisation whereas YAP1 phosphorylation levels decrease in response to partial hepatectomy leading to upregulation of known YAP1 target genes (Grijalva et al., 2014, Wu et al., 2013, Wang et al., 2012).

Due to its critical role in regulating liver cell proliferation and cell survival, alteration of the hippo pathway is also implicated in the liver oncogenesis and the development of HCC and ICCA (Bai et al., 2012, Li et al., 2015b, Marti et al., 2015, Pei et al., 2015, Sugihara et al., 2018, Sugimachi et al., 2017, Hayashi et al., 2015, Jie et al., 2013, Lee et al., 2010, Li et al., 2012, Patel et al., 2017, Sohn et al., 2016, Xiao et al., 2015, Xu et al., 2009, Zhou et al., 2009). Amplification of the genomic region encoding the YAP1 protein and YAP1 overexpression due to posttranscriptional regulation has been reported for several solid tumours, including liver cancer (Overholtzer et al., 2006, Zender et al., 2006, Li et al., 2012). Furthermore YAP1 overexpression led to hepatomegaly and HCC in mice; YAP1 is therefore a potent oncogene, contrasting the tumour suppressor phenotypes of upstream Hippo components (Camargo et al., 2007, Dong et al., 2007). Studies involving the genetic deletion of the upstream Hippo proteins MST1/2, SAV1, LATS1/2 and MOB1 further support these observations, and all led to decreased YAP1 phosphorylation, increased YAP1 nuclear activity and liver cancer (HCC and ICCA) (Zhou et al., 2009, Song et al., 2010, Lu et al., 2010, Chen et al., 2015c, Lee et al., 2010, Nishio et al., 2016, Nishio et al., 2012). In HCC patients a gene expression profile associated with a lack of Hippo signalling was identified and is associated with a reduced survival

time (Sohn et al., 2016). Increased levels of YAP1 and TAZ and the presence of nuclear YAP1 staining in HCC patients all associate with poor survival rates (Hayashi et al., 2015, Xiao et al., 2015, Reis et al., 2017).

### 1.4.4 HCV mediated manipulation of cellular signalling pathways associated with hepatocarcinogenesis

Chronic HCV infection is a leading risk factor for the development of HCC. However, the mechanisms underpinning HCV induced HCC development are poorly understood. Chronic HCV infection usually leads to progressive hepatic fibrosis and cirrhosis before the development of HCC. However HCV associated HCC can occur in the absence of cirrhosis (depending on cohort it appears to be between 10- 20 % (Lewis et al., 2013)). Worldwide an estimated 25 % of HCC occurrences are due to HCV infection (Webster et al., 2015). Many assume that HCC arises in this context mainly due to the indirect effects of chronic inflammation which causes oxidative stress leading to DNA damage (Okuda et al., 2002, Bartsch and Nair, 2004, Koike, 2007) and high cell turnover due to immune mediated killing of infected cells leading to repeated liver regeneration (Karidis et al., 2015). However, increasing evidence highlights the direct role played by the virus.

HCV contributes to HCC development by altering several host signalling pathways affecting the regulation of proliferation, energy metabolism, apoptosis and DNA repair. The oncogenic mechanism of HCV is less conspicuous than other better characterised oncogenic viruses such as Epstein- Barr virus (EBV) and human papilloma virus (HPV). The HCV RNA genome replicates outside of the nucleus and does not integrate into the host genome. Several HCV proteins have been described to manipulate and alter host cellular signalling pathways however, including core, NS2, NS3, NS5A and NS5B. In transgenic mice models HCV proteins either alone or together are able to promote cell growth and oncogenic transformation (Park et al., 2000, Lerat et al., 2002, Munakata et al., 2005, Moriya et al., 1998, Zemel et al., 2001). Core and NS5A are both implicated in interacting with a range of signalling pathways associated with regulating cell cycle, proliferation, apoptosis, lipid metabolism and epithelial to mesenchymal transition (EMT). HCV infection has been shown to profoundly affect cell cycle progression; for example, core was reported to increase proliferation of transfected Rat1 cells and upregulate the expression of Cyclin E mRNA (Cho et al., 2001). In addition the Core+1/ARF protein stemming from the alternative ORF was shown to modulate increase Cyclin D levels and

phosphorylated Rb levels (Moustafa et al., 2018). Cyclin E expression appears to be induced by NS2 also leading to increased cell growth.

HCV proteins also interact with tumour suppressor proteins; NS5B forms a complex with Rb resulting in Rb being targeted for degradation (Munakata et al., 2005). Rb regulates cellular proliferation and apoptosis. p53 has been found to be disrupted by several HCV proteins including by Core, NS3, NS2 and NS5A, however the underlying mechanisms these interactions have not been elucidated (McGivern and Lemon, 2011). NS2 sequesters p53 in the cytoplasm thereby altering the cellular localisation of the protein (Bittar et al., 2013). Core protein has been reported to interact with the p53 binding protein apoptosis-stimulating of p53 protein 2 (ASPP2) leading to inhibition of p53-mediated apoptosis (Cao et al., 2004). NS3 and NS5A appear to interact with p53 directly to suppress p53 mediated transcriptional activation (Deng et al., 2006, Lan et al., 2002). In addition core protein is able to interact with and form a complex with p21 (gene expression of which is regulated by p53) which results in abrogation of the proliferating cell nuclear antigen (PCNA) binding site (Wang et al., 2000). p21 interaction with PCNA is an important regulatory mechanism of cell cycle arrest (Cayrol et al., 1998).

HCV infection also leads to altered RAF/MAPK/ERK signalling. Core protein binds to 14-3-3 leading to an increase in Raf-1 kinase activity (Aoki et al., 2000). The core protein has also been described to activate MEK1 and Erk1/2 Map kinases. The activation of these kinases leads to a sustained response to EGF (Giambartolomei et al., 2001). Raf-1 was also identified as a binding partner of NS5A resulting increased Raf-1 phosphorylation (Burckstummer et al., 2006). NS5A has also been shown to interact with growth factor receptor-bound protein 2 (Grb2) via the SH3 domain (Tan et al., 1999). Grb2 is part of the MAPK cascade and NS5A interaction leads to activating protein-1 (AP1) inhibition (Macdonald et al., 2003). Activation of this pathway appears to facilitate viral replication by attenuating interferon signalling (Zhang et al., 2012). Taken together HCV perturbation of RAF/MAPK/ERK signalling may contribute to oncogenic transformation and proliferation.

NS5A contains a proline rich motif which mediates interaction with the SH3 domain of cellular proteins including the Src family of kinases, such as Hck, Lck, Lyn and Fyn (Macdonald et al., 2004). Lyn is known to activate STAT3 and is considered a proto-oncogene. STAT3 itself has also been described as an oncogene in HCC and STAT3 activation via serine and tyrosine

phosphorylation is associated with cell survival and proliferation (Xie et al., 2018, He and Karin, 2011). STAT3 is activated by cytokine signalling, particularly IL-6, via receptor tyrosine kinases including EGFR or non-receptor kinases such as Src (Porta et al., 2008, Mair et al., 2011). NS5A is also able to interact with EGFR (Street et al., 2004, Mankouri et al., 2008).

Wnt signalling is heavily implicated in hepatocarcinogenesis and both NS5A and Core have been shown to interact with this pathway. Expression of Core protein leads to activation of β-catenin/Transcription factor 4 (TCF4) - dependent transcription by upregulating expression of Wnt ligands including Wnt3a, and upregulating FZD receptors and Low-density lipoprotein receptor-related protein (LRP) 5/6 co-receptors (Liu et al., 2011b). Furthermore core protein leads to stabilisation of β-catenin and an increase in β-catenin levels by inactivating GSK-3β. In a mouse HCC xenograft model core protein expression was able to increase cellular proliferation and promote Wnt3a induced tumour growth (Liu et al., 2011a). NS5A protein binds to and activates PI3K leading to activation of Akt (Street et al., 2004, He et al., 2002). Akt activation results in suppression of FOX and phosphorylation of GSK-3β, causing its inactivation. Expression of the HCV polyprotein leads to accumulation of β-catenin and an increase in β-catenin-dependent gene expression (Street et al., 2005). It has also been shown that NS5A is able to interact directly with β-catenin and PI3K regulatory subunit p85 (Milward et al., 2010).

TNF-α signalling plays is an important role in host defence. HCV core protein has been shown to be able to inhibit TNF-α mediated apoptosis by inhibiting caspase-8 activation via sustained expression of Fas-associated protein with death domain (FADD)-like interleukin-1β-converting enzyme-like inhibitory protein (c-FLIP) (Saito et al., 2006). Furthermore NS5A appears to also be able to repress TNF-α mediated apoptosis by blocking the activation of caspase-3 and inhibiting cleavage of death substrate poly (ADP-ribose) polymerase (Ghosh et al., 2000).

The TGF-β signalling pathway is involved in liver regeneration, in liver fibrogenesis and the development of HCC. NS5A inhibits TGF-β signalling by interacting with TGF-β receptor 1 which diminished Smad2 phosphorylation, nuclear translocation of Smad2 and the hetero-dimerisation of Smad3 and Smad4 (Choi and Hwang, 2006). Whereas the core protein activates the TGF-β 1 promoter and upregulates TGF-β expression (Taniguchi et al., 2004).

## 1.5 Cell culture models of HCV

It took 10 years from when the HCV genome was first cloned (Choo et al., 1989) to develop the first cell culture system for HCV (Lohmann et al., 1999). Developing robust and reliable systems to culture HCV was very difficult. Initial attempts to inoculate human hepatocytes were unsuccessful or inefficient. In addition, culturing human hepatocytes has its own difficulties, for example primary hepatocytes quickly loose their normal function in 2D culture including their ability to support viral infection (Lazaro et al., 2003). Furthermore attempted infection of cell lines with serum derived HCV was also unsuccessful with HCV only replicating at very low levels, requiring a sensitive detection assay using reverse transcription (RT)- polymerase chain reaction (PCR) (Seipp et al., 1997, Kato et al., 1995, Nakajima et al., 1996, Shimizu et al., 1992, Tagawa et al., 1995). Transfection based assays became a possibility after the first full length HCV genomes were cloned (Choo et al., 1989, Kato et al., 1990). However, initially replication of these cloned genomes was undetectable even though several transfection assay conditions were tested. Once it was determined that these cloned genomes lacked the full 3' UTR sequence (Tanaka et al., 1995, Tanaka et al., 1996, Kolykhalov et al., 1996) and consensus HCV genomes were established which eliminated undesired or replication limiting mutations fully functional genomes were established based on a genotype 1a isolate named H77. These cloned genomes were demonstrated to be infectious and induced viremia in chimpanzees (Kolykhalov et al., 1997, Yanagi et al., 1997) but still did not replicate in cell culture. Subgenomic replicons were constructed based on the fact that for other related positive strand RNA viruses the structural proteins appeared unnecessary for genome replication (Kaplan and Racaniello, 1988, Khromykh and Westaway, 1997, Mittelholzer et al., 1997, Behrens et al., 1998). The replicons were constructed by replacing the core to NS2 sequence either with the firefly luciferase reporter gene or the neomycin phosphotransferase selection gene; hence subgenomic replicon cannot lead to the production of viral particles. When cell lines were screened for replication Huh7 cells were found to produce the highest number of G418 resistant cell colonies (Krieger et al., 2001, Lohmann et al., 2003, Lohmann et al., 1999). When these Huh7 clones were analysed it was found that the HCV subgenomic replicon replicated at high levels in these clones. The increased replication competency was revealed to be due to replication enhancing mutations or cell culture adaptive mutations (Lohmann et al., 2003, Lohmann et al., 2001).

More highly permissive cell clones which have included Huh7-Lunet (Friebe et al., 2005) and Huh7.5 cells (Blight et al., 2002). An increase in permissiveness results from higher expression of HCV dependency factors and from low expression of HCV restricting factors. Huh7.5 cells harbour a mutation in the gene encoding retinoic acid-inducible gene I (RIG-I). This cytoplasmic helicase recognises HCV RNA and then interacts with mitochondrial antiviral signalling protein (MAVS; also known as Interferon-beta promoter stimulator 1- IPS-1) to activate an interferon response (Sumpter et al., 2005). Huh7.5 cells also express higher level of CD81, which is a HCV entry factor, this is important for full length viral infection. Other cell lines such as the HepG2 and Hep3B cell lines only support low HCV replication even despite defective interferon signalling. Low level replication was found to be due to a lack of miR-122 and overexpression of miR-122 increases viral replication (Keskinen et al., 1999, Narbus et al., 2011, Thibault et al., 2013).

JFH1, a genotype 2a isolate was cloned from a Japanese patient with fulminant hepatitis, and sub-genomic replicons derived from this sequence found to replicate to high levels without requiring cell culture adaptive mutations (Kato et al., 2003). A chimera constructed using JFH1 NS3- NS5B protein sequence and the core to NS2 protein sequence from another genotype 2a J6 produced high titres of infectious HCV particles when transfected into Huh7.5 cells (Wakita et al., 2005, Lindenbach et al., 2005). All these discoveries (including the identification of permissive cell lines, identification of cell culture replication enhancing mutations, discovery of HCV dependent factors such as miR-122, and the identification of the JFH1 clone) contributed towards the development of robust and reliable cell culture models.

Most HCV cell culture models are based on Huh7 cells as replication is generally lower in other cells lines. However the Huh7 cell line is a hepatoma cell line and is transformed. Huh7 cell gene expression is not completely comparable to normal mature hepatocytes (e.g. Huh7 cells express lower levels of P450 genes (Guo et al., 2011)) and Huh7 cells do not exhibit the same characteristic cell polarisation as hepatocytes (Sainz et al., 2009b). Hence, Huh7 cells may not be ideally suited to study certain aspects of viral infection, such as carcinogenesis. Primary human hepatocytes may theoretically represent a better model to investigate these aspects of HCV infection, however its can be difficult to maintain their cellular phenotype and function, results are less reproducible (due to patient variability) and HCV

replication levels are lower due to a strong interferon response (Helle et al., 2013). It is important to note that the lower viral replication in primary hepatocytes likely represents the level of replication *in vivo* more accurately. Recently it has become possible to produce hepatocytes from induced pluripotent stem cells (iPSCs) and infect these with HCV (Roelandt et al., 2012, Schwartz et al., 2012, Wu et al., 2012).

## 1.6 Project Rationale

Chronic HCV infection represents a major risk factor for the development of HCC. An estimated 25 % of HCC occurrences worldwide are due to HCV infection (Webster et al., 2015). HCC commonly develops in the setting of hepatic fibrosis and cirrhosis due to chronic liver damage caused by viral hepatitis. The incidence of HCC matches with the incidence of HCV and HBV infection. The mechanisms underlying HCV associated HCC development are poorly understood. Many assume that chronic HCV causes HCC indirectly due to HCV induced chronic inflammation leading to oxidative stress induced DNA damage (Okuda et al., 2002, Bartsch and Nair, 2004, Koike, 2007) and high cell turnover due to immune mediated killing of infected cells (Karidis et al., 2015). However increasing evidence supports a more direct role played by the virus in the development of HCC. HCV proteins either alone or in combination promote cellular growth, lead to cellular transformation and tumour development when expressed in transgenic mice (Park et al., 2000, Lerat et al., 2002, Munakata et al., 2005, Moriya et al., 1998, Zemel et al., 2001, Fukutomi et al., 2005). The incidence of HCV associated HCC arising in the presence of cirrhosis is greater than autoimmune hepatitis associated cirrhosis (Yeoman et al., 2008, Lok et al., 2009). HCC occurs in the absence of cirrhosis in about 15 % of HCV associated HCC cases (Bralet et al., 2000). Elimination of viral infection by interferon treatment reduces an individual's risk of developing HCC even when cirrhosis persists (Hsu et al., 2015). The exact mechanism behind HCV induced oncogenesis is not obvious compared to other oncogenic viruses which often express clear oncogenes (e.g. HBV X protein (Shin Kim et al., 2016)) or integrate into the host genome (e.g. HPV (Munger et al., 2004)). However several HCV proteins have been shown to interact with and manipulate host signalling pathways (see section 1.4.4). Another aspect of HCC development which is uncertain is the origin of HCC CICs. Both mature hepatocytes (via a process of dedifferentiation and transformation) and HPCs (via perturbed differentiation and transformation) are hypothesised to

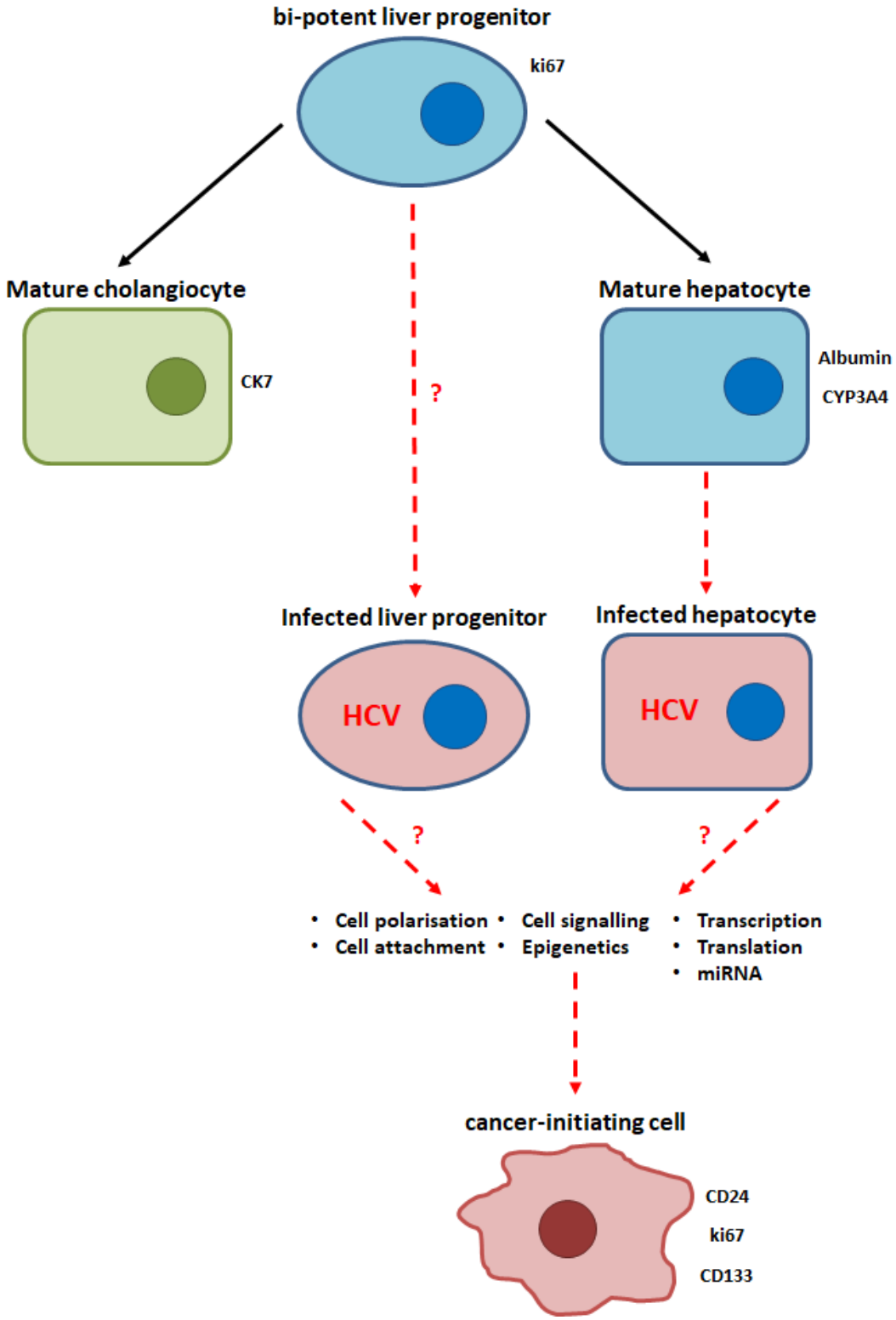


**Figure 1.6.1 Diagram of the possible origin of HCC CICs**

CIC cells (which express various markers including EpCAM, CD133, CD24, ki67 and CK19) may arise from the dedifferentiation and transformation of mature hepatocytes (which express hepatocyte proteins Albumin and CYP3A4) or from HPCs (express amongst other markers the proliferation marker ki67). HPCs can differentiate into hepatocytes and cholangiocytes (which express the marker CK7). CICs may arise from transformed HPCs.

give rise to HCC (possibly even cholangiocytes). Most studies investigating the link between HCV and HCC assume that mature hepatocytes are the cell of origin of CICs. However during chronic infection the liver will be largely repopulated by HPCs which can differentiate into both hepatocytes and cholangiocytes. Indeed HCV infection is also associated with and represents a risk factor for ICCA (Yamamoto et al., 2004, Li et al., 2015a). Furthermore HCC often has a mixed hepatocyte-cholangiocyte-progenitor phenotype. Thus we have been interested in examining whether HCV can infect HPCs. This project aimed to explore whether tissue resident bi potent liver progenitor cells are able to act as the cellular origin to HCV associated HCC (Figure 1.6.1). The first objective was to establish a cellular differentiation model to explore this hypothesis. The primary objective of this project was to explore whether HCV is able to perturb hepatocyte differentiation and whether this perturbation predisposes the cells to oncogenic transformation. The last objective of this project was to explore how the virus mediates this perturbation (i.e. which HCV protein(s) and cellular signalling pathway(s) are involved).

# 2. Chapter: Materials and Methods

## 2.1 Transformation of *Escherichia coli* DH5α

10 µl of transformation competent *E.coli* (DH5α, NEB) were thawed on ice. 500 ng of plasmid DNA was added, mixed gently and incubated on ice for 30 min. *E.coli* were heat shocked for 40 sec at 42 °C and placed back on ice for 5 min. 50 µl of S.O.C. media (supplied with NEB) was added and incubated in the shaker for 1 ½ hr at either 30 °C for replicon plasmids or 37 °C for any other plasmids. The transformation mixture was spread onto agar plates containing 100 mg/ml ampicillin using a sterile spreader. Plates were cultured overnight at 30 °C or 37 °C. Agar plates were prepared using ampicillin containing LB agar (for recipe see section 2.24) which was poured into 100 mm petri dishes and allowed to cool. Agar plates were stored at 4 °C but were warmed before use (for 1 hr at 30 °C).

## 2.2 Plasmid preparation

Single bacterial colonies were transferred into 2 ml of LB containing 100 mg/ml ampicillin in 15 ml falcon tubes (Corning) and incubated in the shaker overnight at either 30 °C or 37 °C. The starter culture was transferred into 200 ml of ampicillin (100 mg/ml) containing LB and incubated overnight in the shaker. Bacterial cells were pelleted by centrifugation at 4000 x *g* for 30 min at 4 °C in a falcon polypropylene 225 ml graduated conical centrifuge tube (Corning). Plasmids were purified using Qiagen Plasmid Maxi kit as per manufacturer's instructions and DNA was re-suspended in a suitable volume of distilled water to reach a final concentration of ~ 1 µg/µl

## 2.3 Plasmid linearization and extraction

The JFH1-replicon plasmid DNA was linearised using *Xba*I (NEB) restriction enzyme digest at 37 °C for 3-4hr. Following this, the reaction was inactivated by heating the reaction at 65 °C for 20 min. The linearization of the plasmid DNA was confirmed by running a sample on an agarose gel. The linearized DNA was then treated with Mungbean nuclease (NEB) for 40 min at 30 °C. The mung bean nuclease was inactivated by the addition of 1 % SDS. Phenol/Chloroform (Phenol:Chloroform:isomyl alcohol 25:24:1 saturated with

10 mM Tris pH 8.0 1mM EDTA, Sigma) was used to extract the linearised DNA.

## 2.4 *In vitro* RNA transcription and RNA extraction

RNA was synthesised from linearised template plasmid DNA using the RiboMAX™ large scale RNA T7 production system (Promega). The T7 reaction mixture contained 5 µg template DNA, 20 µl T7 Transcription 5X buffer, 30 µl rNTPs (25 mM each of ATP, CTP, GTP and UTP), 10 µl of the enzyme mix and was made up to 100 µl total volume using nuclease-free water. Reactions were incubated for 3-4 hr at 37 °C. To remove template DNA, 5 µl RQ1 RNase free DNase was added and incubated at 37 °C for 15 min. RNA was extracted using phenol:chloroform. An equal volume of acid phenol-chloroform (25:24:1 Phenol:Chloroform:Isoamyl alcohol pH 5.2, BDH) was added to the reaction mixture. Tubes were vortexed for 1 min and centrifuged in a microcentrifuge at top speed for 2 min. The upper aqueous phase was transferred to a new tube and an equal volume of chloroform (Merck Millipore) was added. The tube was vortexed for 1 min and centrifuged for 2 min. The upper phase was transferred to a fresh tube. 1/10 volume sodium acetate (3 M, pH 5.2) and 1 volume isopropanol was added, mixed, incubated on ice for 5 min and centrifuged for 10 min. The pellet was washed with 1 ml of 70 % ethanol and centrifuged for 2 min. The ethanol was removed and the pellet air dried before being re-suspended in a suitable volume of nuclease-free water. RNA was stored in aliquots at -80 °C.

## 2.5 RNA transfection by electroporation

8 x$10^6$ cells in 400 µl phosphate buffered saline (PBS) were mixed with 10 µg of RNA and transferred to an electroporation cuvette (4 mm electroporation cuvettes, Geneflow). The cells were pulsed using the Bio Rad gene pulser II (270 V, 950 microfarads) (Kato et al., 2003). After 6-18 hr the media was removed, the cells washed in PBS and fresh growth media added. Transfected cells were allowed to recover for at least 24 hr before further experiments or antibiotic selection.

## 2.6 Transfection

### 2.6.1 Transfection of DNA plasmids

Cells were seeded for transfection at 40 % confluence in either 10 $cm^2$ dishes or T75 flasks and allowed to settle overnight. The following morning

the transfection mixture was set up as follows: either 20 µg or 60 µg (depending on size of the dish) plasmid DNA in 500 µl Opti-MEM (Gibco) and in a separate tube 80 µl or 240 µl polyethylenimine (PEI -1 mg/ml in 20 mM HEPES pH 7.5) (in a ratio of 4:1) in 500 µl Opti-MEM and incubated at room temperature (rt) for 5 min. The DNA and PEI preparations were then combined, mixed and incubated for a further 20 min. The medium was removed and the cells washed with PBS. Depending on the size of the vessel (10 $cm^2$ dish or T75 flask) 9 ml or 10 ml Opti-MEM was added to the cells. After 20 min the PEI mixture was then added to the cell dishes and incubated for 4- 6hr. After the incubation period the PEI containing Opti-MEM medium is removed, the cells washed with PBS and growth medium was added. The cells were then incubated for 48 hr and then processed depending on the following experiment.

### 2.6.2 Transfection for production of *Lentivirus* stocks

*Lentivirus* stocks were created by transfecting HEK293T cells using PEI with three plasmids: the Gag-pol helper plasmid, the VSV-G envelope expressor plasmid and the vector containing the gene/construct of interest. The helper, expressor and the vector were combined in a ratio of 13:7:20 to a total of 20 µg of DNA and mixed with 300 µl of Opti-MEM (Gibco) and incubated for 5 min at rt. 40 µl of PEI was added to the DNA and incubated for a further 20 min. The DNA PEI mixture slowly added to a 10 mm dish of HEK293T cells in Opti-MEM and incubated for 4-6 hr. The Opti-MEM transfection mixture was then removed from the dish, the cells washed in PBS and fresh growth medium was added. *Lentivirus* containing supernatant was harvested at 24 and 48 hr post transfection. The *Lentivirus* containing growth medium was clarified by centrifugation at 400 x *g* for 5 min, filtered with a 0.22 µm filter (Millex-GP filter unit) and PEG concentrated. For PEG lentivirus concentration, 30 % w/w PEG8000 in PBS was added in a ratio of 1:3 and the mixture was incubated at 4 °C overnight. The following morning the mixture was centrifuged and re-suspended in an appropriate volume of growth media.

## 2.7 Transduction

Cells were seeded in 10 $cm^2$ dishes at 50 % confluency at left to set for 4-6 hr. After the cells had settled the growth medium was removed and the cells washed with PBS. After the wash step, clarified and PEG concentrated (see section 2.6.2) *Lentivirus*-containing supernatant was added to the cell culture dish and incubated overnight in the cell incubators. The following morning

the *Lentivirus* containing growth medium was removed, the cells washed and fresh growth medium was added to the cell culture dish. The cells were allowed to grow to confluence and bulked up as necessary for further experiments.

## 2.8 Tissue culture maintenance and cell lines

All cells were cultured at 37 °C in a humidified atmosphere containing 5 % $CO_2$. Cells were maintained in 25 $cm^2$, 75 $cm^2$ and 150 $cm^2$ vented plastic tissue culture flasks (Corning). Routine passaging of cells took place under aseptic conditions in a class II Microbiology Safety Cabinet. Adherent cells were passaged by removing the media and washing the cells with PBS. Cells were treated with an appropriate volume of Trypsin-EDTA (Sigma- 0.25 % Trypsin, 0.02 % EDTA) and incubated at 37 °C. The trypsin was inactivated by the addition of serum-containing culture media in a ratio of 2:1. An appropriate number of cells were then reseeded into a new flask. Viable cell counts were obtained using an improved Neubauer hoemocytometer (Marienfeld Superior) following dilution in 0.2 % trypan blue in PBS. All cell lines were routinely tested for Mycoplasma and found to be free of contamination.

Human hepatoma Huh7 (Nakabayashi et al., 1982), HLE (human hepatoma cell line; (Dor et al., 1975)), HepG2 cells ((Knowles et al., 1980) HCC cell line) and human embryonic kidney HEK293T cells (Graham et al., 1977, DuBridge et al., 1987) stably expressing the simian vacuolating virus 40 large T antigen) were cultured in glutamine containing Dulbecco's Modified Eagle's (DMEM high glucose- Sigma) with supplements (10 % Foetal bovine serum (FBS) (Gibco- heat inactivated), 1 % non-essential amino acids (Gibco), 50 000 units Penicillin and 50mg Streptomycin (Sigma). Human liver progenitor HepaRG cells (Gripon et al., 2002) were cultured in William's media E (Gibco) with supplements (10 % FBS- Hyclone FetalClone II Serum (Fisher Scientific), 50 000 units Penicillin, 50 mg Streptomycin (Sigma), 1x GlutaMAX-I (Gibco), 0.023 IE/ml human insulin (Gibco) and 4.7 µg/ml hydrocortisone (Sigma). Cells were not used above passage 20.

### 2.8.1 Subgenomic Replicon

The genotype 2a JFH1 clone (GeneBank accession number: AB047639.1) was isolated from a patient with fulminant hepatitis and a replicon was constructed by replacing the structural proteins core, E1 & E2, and proteins p7 and NS2 with the G418 resistance gene for selection and non-structural

proteins NS3-NS5B (GeneBank accession number: AB114136). The JFH1 replicon is able to replicate efficiently in Huh7 cells without common amino acid mutations (Kato et al., 2003).

Huh7 (and derivatives) replicon lines were generated using a T7 polymerase-derived RNA transcript of JFH1 (Kato et al., 2003) (See section 2.4). 8 x $10^6$ cells were electroporated with JFH1-replicon RNA (See section 2.5). Transfected cells were allowed to recover for at least 24 hr before beginning selection with 500 µg/ml G418 (Sigma-Aldrich). The growth media was replaced twice a week. The selection was considered complete once all mock electroporated cells died under G418 selection. G418 resistant cells were maintained thereafter with 500 µg/ml G418. However cells were not under G418 selection in any experimental conditions, G418 was usually withdrawn the night before.

### 2.8.2 Infectious HCV

The infectious viral J6-JFH1 clone used which is comprised of Core- NS2 of the genotype 2a J6 clone (GeneBank accession number D00944.1) and NS3-5B of the genotype 2a JFH1 clone (Lindenbach et al., 2005). For GFP (Green fluorescent protein) trap a version of this recombinant clone was used which expresses an NS5A-eGFP fusion protein (Gottwein et al., 2011) (kindly gifted by Jens Bukh). CD24lo cells were infected at a MOI (multiplicity of infection) of 10 FFU/cell (Focus forming units) and passaged twice before being used for further experiments. Infected cells were used up to passage 15. Level of infectivity was periodically measured by focus forming assay (see section 2.11).

## 2.9 Creation of Cured CD24lo control cell line

CD24lo JFH1-replicon and CD24lo cells were seeded in T25 flasks and treated with 1 µM DCV and 1 µM SOF in 5 ml of growth media for two weeks, changing the media twice a week and splitting the cells when needed. At the end of the treatment cells were reseeded for a G418 challenge experiment. Treated cells were seeded in a 6 well plate and challenged with 500 µg/ml G418 alongside CD24lo and JFH1-replicon CD24lo controls. Immunofluorescence (IF) (See section 2.15) and Western blot analysis (See section 2.14) using anti- NS5A antibodies was used to determine whether the DAA treatment was successful.

## 2.10 Culture of Infectious HCV

All infectious HCV cell culture was undertaken in biosafety level 3 (BSL3) containment following transfection of Huh7 cells with J6-JFH1 RNA (see section 2.5). Viral stocks were generated by seeding transfected cells into T150 flasks with 20 ml growth media buffered with 20 mM HEPES pH 7.5 (Gibco). Virus containing media was harvested every day and the titres determined by serial dilution onto naïve Huh7 cells (see section 2.11). The harvested supernatant containing the infectious virus was precipitated using 10 % PEG8000 in PBS (see section 2.6.2), snap frozen and stored at – 80 °C. Chronically infected CD24lo cells were generated by infecting the cells with the J6-JFH1 viral stock at MOI of 10 FFU/cell and incubating the cells for 48 hr. Following the 48 hr incubation with the virus stock the CD24lo cells were passaged as usual and bulked up for further experiments. The level of infectivity was measured periodically and fresh CD24lo cells were added if necessary.

## 2.11 Focus forming assay

To measure HCV infectivity uninfected Huh7 cells were seeded at 8000/well in a 96 well plate and left to settle overnight. The 96 well plate was taken to BCL3 to set up the assay. The growth media was removed from the 96 well plate and the HCV stock to be titered was then added to the Huh7 cells in a 10 fold serial dilution (covering a range of $10^1$- $10^6$) across the 96 well plate. The plate was then incubated for 48 hr. Following incubation the plate was fixed in 100 µl 4 % (w/v) Paraformaldehyde (PFA)/PBS per well for 20 min and then removed from the BCL3 laboratory. Following fixation the cells were lysed and stained for the HCV NS5A protein (For IF see section 2.15). The plate was then examined on a Microscope and wells scored positive if containing HCV infected cells and negative if lacking HCV infected cells and used to determine the titre of HCV stock. An uninfected well was used to determine the level of background staining.

## 2.12 Differentiation Assays

### 2.12.1 Huh7 CD24lo cells

Differentiation experiments were primarily assessed by Western blot and IF. For Western blot analysis (see section 2.14) cells were seeded at $6x10^5$ cells/well into 6 well plates and allowed to adhere overnight. For IF (see section 2.15) analysis cells were seeded at $2x10^5$ cells/well onto 19 mm

coverslips (Thermo Fisher Scientific) in 12 well plate and left to adhere overnight. Seeding density was determined based on cells reaching 90 % confluency after overnight adherence. Cells were either fixed using 1 ml of 4 % (w/v) PFA/PBS or lysed in 150 µl EBC buffer. The rest of the cells were washed with PBS and treated with growth media containing 1.8 % (v/v) DMSO (Dimethyl sulfoxide). The 1.8 % DMSO growth media was replaced every two days and samples for protein analysis were taken either every other day (during optimisation phase), or latterly more commonly on days one, five and nine post-DMSO addition.

### 2.12.2 HepaRG cells

HepaRG cells were seeded at $8x10^5$ cells/well into 6-well plates and allowed to adhere overnight (if not confluent cells were allowed to grow until they were. For IF analysis cells were seeded at $4x10^5$ cells/well onto 19 mm coverslips (Thermo Fisher Scientific) in 12 well plates and left to adhere overnight (or until confluent). Cells were either fixed using 1 ml 4 % PFA or lysed in 150 µl EBC buffer. The rest of the cells were washed with PBS and growth media replaced. Cells were maintained at confluence for two weeks with the growth media being replaced twice a week. After two weeks 1.8 % DMSO was added to the growth media and the cells were again maintained for two weeks with 1.8 % DMSO growth media changes twice a week. Samples for protein analysis were taken throughout the differentiation process.

### 2.12.3 DAAs and inhibitors

DAAs SOF and DCV, and pharmaceutical inhibitors were added to the differentiation assay 12 hr after seeding the cells. SOF and DCV were used at 1 µM, XMU-MP-1 was used at 5-2 µM, Verteporfin at 1 µM, Dobutamine at 20 µM, Pazopanib at 1 µM, and Chelerythrine at 5 µM.

### 2.12.4 De-differentiation

Cured and JFH1-replicon cells were de-differentiated by adding 1 ml Trypsin to the 6 well plate and reseeding the cells 1:5 into a new 6 well plate so that the cells were subconfluent. Cells were lysed two days after reseeding for western blot analysis.

## 2.13 Fluorescent cell-based reporter system for the detection of HCV gene expression

Huh7 and HepaRG cell lines expressing the fluorescent reporter system based on NS3-4A activity were created using a *Lentivirus* delivered plasmid. The reporter plasmid consisted of mitochondrial protein IPS-1, an internal nuclear localisation signal (NLS) and the red fluorescent protein (RFP) (Jones et al., 2010). The *Lentivirus* used in this system was a 2nd generation *Lentivirus* based on human immunodeficiency virus type 1 (HIV-1). Lentivirus stocks were created by transfecting HEK293T cells using PEI with three plasmids: the Gag-pol helper plasmid, the VSV-G envelope expression plasmid and the vector containing the RFP reporter. The helper, VSV-G expressor and the vector were combined at a ratio of 13:7:20 as a total of 20 µg of DNA, mixed with 300 µl of Opti-MEM (Gibco) and incubated for 5 min at rt. 40 µl of PEI was added to the DNA and incubated for a further 20 min. The DNA PEI mixture slowly added to a 10 mm dish of HEK293T cells in Opti-MEM and incubated overnight. The media was changed the next day to DMEM, harvested after 24- 48 hr, concentrated using PEG (see section 2.6.2) and transferred to either Huh7 or HepaRG cells which were incubated for 48 hr and visualised by direct fluorescence.

## 2.14 Western Blotting

To analyse cellular protein levels, cells were lysed in an appropriate amount of EBC lysis buffer (for recipe see section 2.24) (for 6 well plate cells were lysed in 150 µl lysis buffer). To lyse the cells, growth media was removed and cells were washed in PBS. PBS was then added (for a single well of a 6 well plate 1 ml PBS was added) and the cells were scraped off the cell culture dish. The cell suspension was centrifuged at 6200 x *g* and the pellet was re-suspended in lysis buffer. The lysate was clarified by pelleting the cell debris by centrifugation and removing the cell lysate supernatant to a fresh tube. Lysates were normalised by total protein concentration using the Pierce BCA (bicinchoninic acid) Protein Assay kit (Thermo Fisher Scientific) and diluted in an equal volume of 2 x Laemmli buffer (for recipe see section 2.24). Lysates were heated to 95 °C for 5-10 min. Following the boiling step, 5-15 µl of the cell lysate/laemmli sample was loaded onto hand-cast polyacrylamide gels (for recipes see section 2.24), alternatively pre- cast gels were used (Tris-Glycine precast- mini-protean and Criterion TGX stain-free 4-15 % polyacrylamide gradient gels). Depending on which protein of interest gels was blotted for, varying polyacrylamide concentrations were

used: either 8 %, 10 %, 12 % or 15 %. Lysates were resolved by SDS-PAGE (sodium dodecyl sulphate polyacrylamide gel electrophoresis) using Tris Glycine running buffer (for recipe see section 2.24) and electrophoresed at 120-160 V for 1-2 hr (Bio-Rad).

Proteins were transferred onto a PVDF (Polyvinylide fluoride- Immunoblot-FL Merck Millipore) membrane by semi dry blot transfer (Hoefer). Following pre-activation of the membrane in methanol the gel and membrane were placed between sponges pre-soaked with Towbin buffer (for recipe see section 2.24) and allowed to transfer for 1-2.5 hr at 60-240 mA (depending on the number of gels). Membranes were blocked in 5 % fat-free milk (Oxoid) in TBST-T (Tris buffered saline (for recipe see section 2.24) with 0.1 % Tween 20- Sigma-Aldrich) for 0.5-2 hr shaking at rt. Membranes were probed with primary antibody diluted in either 5 % fat-free milk or 5 % BSA (Bovine serum albumin, Fisher Scientific) in TBS-T overnight shaking at 4 °C. Secondary Horseradish peroxidase (HRP) conjugated antibodies (see section 2.23 for list of antibodies used) diluted in either 5 % fat-free milk or 5 % BSA were incubated with the membranes shaking at rt for 1 hr. The membranes were washed 3x 10 min with TBS-T shaking between each step. Immunoblots were visualised using either prepared enhanced chemiluminescence solution (ECL, for recipe see section 2.24) or ECL prime western blotting detection reagent (Amersham, GE Healthcare Life Sciences) on X-ray film using a Medical fil processor (SRX-101A, Konica Minolta Medical & Graphic, Inc.). Protein sample sizes were compared with pre-stained molecular weight markers (pre-stained Seeblue® Plus2, Invitrogen). X-ray films were scanned in as a TIF file image and band density was measured using Image J. The measured intensity for each sample for each different protein probed for were normalised to the GAPDH (Glyceraldehyde 3-phosphate dehydrogenase) reading for each sample. Results were presented as a percentage of the control (Cured or CD24lo) at day one of differentiation except for NS5A which was presented as the percentage of infected cell (JFH1-replicon or J6-JFH1) on day one. Statistical analysis was performed using a two- tailed paired Student’s t-test.

## 2.15 Immunofluorescence

Cells were seeded in either black walled flat bottom 96 well plates (Greiner Bio One) or on 19 mm coverslips (Thermo Fisher Scientific) in 12 well plates and allowed to settle and then treated/differentiated. Cells were washed 3x with PBS, fixed in 4 % (w/v) PFA/PBS for 10 min (BCL 3- 20 min) and

washed again 3x in PBS. If necessary cells were permeabilised with 0.1 % (v/v) Triton X-100/PBS for 10 min and washed 3x in PBS. Primary antibody (see 2.23 for a list of antibodies used) diluted in 10 % FBS in PBS was incubated for 1 hr at rt or overnight at 4 °C. Cells were washed in PBS and incubated with fluorescent secondary antibody (Alexa Fluor Invitrogen, see section 2.23) and Hoechst nuclear stain (Molecular Probes Hoechst 33342 used at 1/10000) diluted in 10 % FBS for 1 hr at rt. F-actin was stained using Phalloidin 594 (Invitrogen, 5 µl per coverslip was used) for 1 hr at rt. Cells were washed 3x in PBS and visualised using a fluorescence microscope (Nikon A1R confocal LSM) or the EVOS FL Cell Imaging System. Coverslips were mounted on slides in ProLong Gold anti-fade mountant solution (Invitrogen) before visualisation. Exposure times were determined for each primary antibody based on the negative control (coverslip exposed to secondary antibody only) and the positive control and then kept constant for all treatment conditions. Images were captured in a random pattern. Images were processed and quantified using image J either by counting the number of positive cells (by comparing number of cell positive for probed protein against number of Hoechst positive cells) or by measuring the mean fluorescent intensity (MFI) of each image. The MFI for each experiment normalised to the control and the mean normalised MFI for multiple experiments was presented. During the image processing any changes to the contrast or brightness was applied consistently to all images in all conditions. Statistical analysis was performed using a two- tailed paired Student's t-test.

## 2.16 Fluorescence- activated cell sorting (FACS) and flow-cytometry

### 2.16.1 Cell surface CD24 flow-cytometry

Cells were trypsinised and transferred to a FACS tube and centrifuged at 400x *g* for 5 min and washed in PBS. Following centrifugation the cell pellet was re-suspended in either 100 µl FACS buffer (for recipe see section 2.24) containing 10 µl anti-CD24-PE antibody or containing 10 µl IgG1-PE isotype control and incubated for 30 min. After 30 min the cell antibody suspension was topped up with 2 ml of FACS buffer and the cells were pelleted by centrifugation. The pellet was re-suspended in 1 % PFA and fixed for 10 min at rt. The suspension was topped up with PBS and centrifuged to wash the cells. The wash step was carried out twice. Finally the cell pellet was re-

suspended in 250 µl FACS buffer and either kept at 4 °C or ran on the flow-cytometer immediately (BD LSR II).

### 2.16.2 Intracellular ki67 flow-cytometry

Cells were trypsinised and transferred to a FACS tube and centrifuged at 400 x *g* for 5 min and re-suspended in 1 ml DMEM and 1 ml of pre-warmed Cytofix (BD) buffer. The cells were incubated for 10 min at 37 °C. Fixed cells were then pelleted by centrifugation and re-suspended in 1 ml pre-chilled Perm-buffer III (BD) and incubated on ice for 30 min. Following permeabilisation the cells were washed in Stain buffer (for recipe see section 2.24) three times. After the wash step, cells were re-suspended in 100 µl stain buffer containing 5 µl anti-ki67-BV421 or 5 µl IgG isotype control-BV421 and incubated at rt for 30 min. Following incubation the stained cells were washed in stain buffer twice and finally re-suspended in 250 µl stain buffer. The cells were either kept at 4 °C or ran on the flow-cytometer immediately (BD LSR II).

## 2.17 Reverse Transcription -Polymerase Chain Reaction

RNA was extracted from cells using TRIzol® (Invitrogen). $2x10^6$ cells were pelleted by centrifugation at 1400 rpm at 4 °C and re-suspended and lysed in 750 µl TRIzol. The sample was incubated at rt for 5 min. RNA was purified using phenol-chloroform extraction as in section 2.4. cDNA was synthesised from extracted RNA using SuperScript™ II reverse transcriptase (rT) (Invitrogen). The reaction mixture contained: 1 µg of RNA, 250 ng random primers and 1 µl dNTP mix (10 mM each) and was made up to 12 µl with nuclease-free water. The mixture was heated to 65 °C for 5 min. After a brief chill on ice, 4 µl 5X first strand buffer, 2 µl 0.1M DTT (Dithiothreitol) and 1 µL RNase OUT was added to the mixture. The reaction was mixed gently and incubated at 25 °C for 2 min. 1 µl of SuperScript II rT was added and incubated at 25 °C for 10 min. The reaction mixture was then incubated at 42 °C for 50 min and inactivated by heating it to 70 °C for 15 min. 2 µl of the cDNA reaction mixture was used in the PCR (Polymerase Chain Reaction). 2.5 µl 10X Standard Taq Reaction buffer, 10 mM dNTPs, 10 µM forward primer (AGCGTCTAGCCATGGCGT), 10 µM reverse primer (GGTGTACTCACCGGTTCCG) which recognise sequences in the 5' UTR and 0.125 µl Taq DNA polymerase were added to the cDNA template, made up to 25 µl with nuclease-free water, mixed and transferred to a PCR machine (Veriti 96 well Thermal cycler, Thermo Fisher Scientific) Programmed PCR cycle: Step1: 5 min at 95 °C, (Step 2: 30 sec at 95 °C,

Step 3: 30 sec at 63 °C, Step 4: 30 sec at 72 °C) X 30, followed by Step 5: 5 min at 72 °C. 15 µl of the reaction mixture was run on a 2 % agarose gel alongside 5 µl of a 25- 500 bp ladder (HyperLadder V, Bioline). 100 bp RNA bands were expected.

## 2.18 Immunoprecipitation of GFP-Fusion Proteins using GFP-Trap® _Agarose beads

Followed Chromotek Protocol for Immunoprecipitation of GFP-Fusion proteins using GFP-Trap® _A. CD24lo J6-JFH1 NS5A-GFP, CD24lo J6-JFH1 and CD24lo cells were seeded in T75 flasks (Corning) at 40 % confluence and allowed to settle overnight. CD24lo and CD24lo J6-JFH1 cells were transfected with GFP expression plasmid by PEI transfection (see section 2.6.1) and allowed to become confluent. After 48 hr $1x10^7$ CD24lo J6-JFH1 NS5A-GFP, CD24lo J6-JFH1 and CD24lo cells were harvested by removing the growth medium, washing the cells with PBS and scraping the cells from the dish into 5 ml PBS. Cells were transferred into a pre-cooled tube and span in a centrifuge at 500 x *g* for 3 min at 4 °C. Cells were washed in PBS again and re-suspended in 200 µl ice-cold lysis buffer by pipetting. The cells were placed on ice for 30 min and repeatedly pipetted every 10 min. Cell lysates were centrifuged at 20,000x *g* for 10 min at 4 °C. Cell lysates were transferred to a pre-cooled tube and diluted with 300 µl dilution buffer. Cell lysates were then either stored at – 80 °C or processed further. 25 µl of the GFP-Trap® _A bead slurry was diluted in 500 µl ice-cold dilution buffer and centrifuged at 2,500x *g* for 2 min at 4 °C. The supernatant was discarded and the wash step repeated twice more. 50 µl of diluted lysate was saved for immunoblot analysis and diluted in 50 µl SDS-sample buffer (input sample). The rest of the diluted lysate was added to the equilibrated GFP-Trap® _A beads and allowed to tumble end-over-end for 1 hr at 4 °C. The bead-lysate mixture was centrifuged at 2,500 x *g* for 2 min at 4 °C. 50 µl of the supernatant was saved for immunoblot analysis and diluted in 50 µl SDS-sample buffer (unbound sample). The rest of the supernatant was discarded. The GFP-Trap® _A beads were re-suspended in 500 µl ice-cold dilution buffer and centrifuged at 2,500x *g* for 2 min at 4 °C. The supernatant was discarded and the wash time was repeated twice more. The GFP-Trap® _A beads were re-suspended in 100 µl SDS-sample buffer (bound sample) and boiled for 10 min at 95 °C to dissociate the immuno complexes for the beads. The GFP-Trap® _A beads were then collected by centrifugation at 2,500x *g* for 2 min at 4 °C. SDS-PAGE and western blot

(see section 2.14) was performed with the input, unbound and bound samples.

## 2.19 Luciferase Assay

The luciferase assay was carried out using the Promega Firefly Luciferase Assay system. Growth medium was removed and the cells washed with PBS. Cells were lysed by scrapping the cells into an appropriate volume of Passive lysis buffer (PLB- provided by Promega) (e.g., 400 µl/60 mm culture dish, 900 µl/100 mm culture dish or 20 µl/well for a 96 well plate). Cell lysate was transferred to a tube and centrifuged to pellet the cell debris. After centrifugation the supernatant was transferred to a new tube. 20 µl cell lysate of each sample was transferred to a 96 well plate and 100 µl luciferase assay reagent was dispense by Berthold plate reader and the light produced was measured.

## 2.20 MTT Assay

Cell lines Huh7 CD24lo, JFH1-replicon CD24lo, CD24lo Cured, HLE and HepG2 were seeded at $8x10^3$ cells/well into 96 well plates and left to adhere overnight. Cells were treated with inhibitors (Verteporfin, Dobutamine, XMU-MP-1, Pazopanib, and Chelerythrine) for 24 hr. Following treatment 20 µl of 5 mg/ml MTT (3-(4,5-Dimethylthiazol-2-yl)-2,5-Diphenyltetrazolium Bromide) was added to each well and incubated for 4 hr. After the 4 hr incubation the media was removed from the wells and cells were solubilised using 150 µl DMSO. Plates were incubated for 10 min shaking and the optical density absorbance readings were determined at 550 nm.

## 2.21 *In vivo* tumourigenicity experiments

$1.4x10^6$ cells were re-suspended in 700 µl PBS in the lab and $1x10^5$ cells in 50 µl PBS were subcutaneously injected, into each severe combined immunodeficient (SCID) mouse in the animal house by Teklu Egnuni,. Seven mice were injected per group with Huh7, CD24lo or CD24hi cells. The size of tumours and survival (defined by tumour volume- V=[widthx2] x [length/2]) percentage were recorded.

## 2.22 RNA-Seq

Cured and JFH1-replcion cells were seeded $6x10^5$ cells/well into 6 well plate. Cells were differentiated for nine days by adding 1.8 % DMSO to the culture media and changing the media every two days. Cured cells were also treated with 2 µM XMU-MP-1 and JFH1-replicon cells were treated with 1 µM SOF and DCV. RNA was isolated using the Qiagen RNA easy mini kit protocol. The cells were initially washed in PBS. Following the wash step 600 µl RLT buffer was added to the cell monolayer to lyse the cells. Cells were collected using a cell scraper and transferred to a microcentrifuge tube. The tube was vortexed briefly to ensure no cell clumps were left. The lysate was then transferred into a QIAshredder spin column to homogenise the lysate and centrifuged for 2 min at full speed to collect the flow through. 600 µl of 70 % Ethanol was added to homogenised lysate and mixed by repeated pipetting. Up to 700 µl of the sample was transferred to an RNeasy spin column, centrifuged for 15 sec at over 8000 x *g* and the flow through was discarded. For on column DNase digestion 350 µl Buffer RW1 was added to the column, centrifuged at over 8000 x *g* for 15 sec and the flow through discarded. 80 µl DNase incubation mix was added to the spin column and incubated at rt for 15 min. Following incubation 350 µl Buffer RW1 was added to the spin column and the column was centrifuged for another 15 sec at over 8000 x *g*. The flow through was discarded. After DNase digestion the column was washed again using 700 µl Buffer RW1 and centrifuged again for 15 sec. 500 µl Buffer RPE was added to the column next and centrifuged for 15 sec. After a second wash step with RPE Buffer the column was centrifuged for 2 min. An additional spin step was carried out after placing the spin column in a fresh collection tube and centrifuging it for 1 min. The RNeasy spin column was then placed in a fresh 1.5 ml collection tube and 30 µl RNase-free water was added to the membrane. To elute the RNA the column was then centrifuged for 1 min at 8000 x *g*. Following RNA isolation the RNA was kept on ice and analysed on the NanoDrop to determine the concentration and the 280/260 and 230/260 ratios to check RNA purity. RNA samples were then sent to Manchester Genomic Technologies Core Facility for further quality assessment, RNA-seq library construction, sequencing and analysis.

## 2.23 List of Antibodies used

| Target | Clonality | Host | WB dilution | Size kDa | IF dilution | Product No | Clone |
|---|---|---|---|---|---|---|---|
| AFP | Mono | Mouse | 1/500 | 69 | 1/100 | Abcam ab114028 | 2A9 |
| Albumin | Mono | Mouse | 1/2500 | 66 | 1/1000 | Abcam ab10241 | 15C7 |
| CD24 | Mono | Mouse | 1/1000 | 35-45 | 1/200 | Santa Cruz sc-70598 | 2Q1282 |
| CD24 | Mono | Mouse | 1/1000 | 35-50 | 1/100 | Thermo MA5-11828 | SN3 |
| CD81 | Mono | Mouse | - | 26 | 1/100 | BD Pharmingen 555675 | JS-81 |
| CD90 | Mono | Rabbit | 1/1000 | 18 | 1/50 | Abcam ab92574 | EPR3132 |
| CK19 | Mono | Mouse | 1/1000 | 40 | 1/100 | Santa Cruz sc-376126 | A-3 |
| CK19 | Mono | Rabbit | 1/10000 | 44 | 1/100 | Abcam ab76539 | EPR1579Y |
| CK7 | Mono | Mouse | 1/1000 | 54 | 1/100 | Abcam ab9021 | RCK105 |
| CK8 | Mono | Mouse | 1/1000 | 50 | 1/100 | Abcam ab9023 | M20 |
| c-kit | Poly | Rabbit | 1/1000 | 117 | 1/300 | Abcam ab5506 | |
| CTGF | Poly | Rabbit | 1/1000 | 37-44 | 1/200 | Abcam ab6992 | |
| CYP3A4 | Poly | Rabbit | 1/1000 | 50 | 1/100 | Proteintech 18227-1-AP | 1576 |
| E-cadherin | | Mouse | 1/1000 | 120 | 1/50 | BD 610181 | 36/E-cad |
| EpCAM | Mono | Mouse | 1/1000 | 40 | 1/800 | Cell Sig 2929S | VU1D9 |
| GAPDH | Mono | Mouse | 1/20000 | 36 | - | Ambion AM4300 | 6C5 |
| GFP | Poly | Rabbit | 1/5000 | 27 | - | GeneTex GTX26556 | |
| HNF4a | Mono | Rabbit | 1/2000 | 53 | 1/100 | Abcam ab92378 | EPR3648 |
| ki67 | Mono | Rabbit | 1/200 | 395 | 1/50 | Abcam ab16667 | SP6 |
| LATS1 | Mono | Rabbit | 1/1000 | 140 | | Cell Sig 3477 | C66B5 |
| LATS1 | Mono | Mouse | 1/500 | 150 | 1/100 | Santa Cruz sc-398560 | G-12 |
| MOB1 | Mono | Rabbit | 1/1000 | 25 | - | Cell Sig 13730 | E1N9D |
| Mst1 | | Rabbit | 1/1000 | 59 | - | Cell Sig 3682 | |
| N-cadherin | | Mouse | 1/1000 | 130 | 1/50 | BD 610920 | 32/N-cad |
| Nestin | Mono | Mouse | 1/1000 | 200-220 | 1/200 | Millipore MAB5326 | 10C2 |
| NS5A | | Sheep | 1/5000 | 56 | 1/2000 | From Mark Harris | |
| Occludin | Mono | Mouse | 1/500 | 65 | 1/100 | Thermo 33-1500 | OC-3F10) |
| pMOB1 T35 | | Rabbit | 1/1000 | 24 | - | Cell Sig 8699 | D2F10 |
| pMST1 T183 | Poly | Rabbit | 1/1000 | 59 | - | Cell Sig 3681 | |
| pSTAT3 S727 | Mono | Rabbit | 1/1000 | 98 | 1/500 | Abcam ab32143 | E121-31 |
| pSTAT3 Y705 | Mono | Mouse | 1/1000 | 86/79 | 1/100 | Cell Sig 4113 | M9C6 |
| pYAP S127 | Mono | Rabbit | 1/1000 | 65-75 | - | Cell Sig 13008 | D9W2I |
| STK4/MST1 | Poly | Rabbit | 1/1000 | 56 | 1/100 | Proteintech 22245-1-AP | |
| V5-tag | Mono | Rabbit | 1/1000 | 20-30 | 1/1000 | Cell Sig 13202 | D3H8Q |
| YAP | Mono | Mouse | 1/1000 | 70 | 1/100 | Santa Cruz sc-101199 | 63.7 |
| YAP/TAZ | Mono | Rabbit | 1/1000 | 70/50 | - | Cell Sig 8418 | D24E4 |
| β-actin | Mono | Mouse | 1/10000 | 42 | - | Sigma Aldrich A1978 | AC15 |

| FACS antibodies | Species | Product number | for 0.5-1 x$10^6$ cells |
|---|---|---|---|
| Albumin-APC | Mouse | R&D IC1455A | 10 µl |
| IgG2A-APC control | Mouse | R&D IC003A | 10 µl |
| CD24-PE | Mouse | MACS 130-095-953 | 10 µl |
| IgG1-PE control | Mouse | MACS 130-092-212 | 10 µl |
| CYP3A4-PE | Rabbit | Bioorbyt 124579 | 10 µl |
| IgG-PE control | Rabbit | Bioorbyt 248104 | 10 µl |
| ki67-BV421 | Mouse | BD 562899 | 5 µl |
| BV421 control | Mouse | BD 562438 | 5 µl |

| Alexa Fluor Secondary Antibodies | | | |
|---|---|---|---|
| Target | Species | Dilution | Supplier |
| anti-Mouse 594 nm | Goat | 1/500 | Invitrogen |
| anti-Mouse 488 nm | Goat | 1/500 | Invitrogen |
| anti-Mouse 594 nm | Donkey | 1/500 | Invitrogen |
| anti-Mouse 488 nm | Donkey | 1/500 | Invitrogen |
| anti-Rabbit 594 nm | Goat | 1/500 | Invitrogen |
| anti-Rabbit 488 nm | Goat | 1/500 | Invitrogen |
| anti-Rabbit 594 nm | Donkey | 1/500 | Invitrogen |
| anti-Rabbit 488 nm | Donkey | 1/500 | Invitrogen |
| anti-Sheep 594 nm | Donkey | 1/500 | Invitrogen |
| anti-Sheep 488 nm | Donkey | 1/500 | Invitrogen |
| HRP Conjugated Secondary Antibodies | | | |
| anti-Mouse | Goat | 1/5000 | Sigma A4416 |
| anti-Rabbit | Goat | 1/5000 | Sigma A6154 |
| anti-Sheep | Donkey | 1/10000 | Sigma A3415 |

## 2.24 Buffers and Solutions

**DMEM** glutamine containing, high glucose (4500 mg/l) DMEM (Sigma) with 10 % (v/v) FBS (Gibco- heat inactivated), 1 % (v/v) non-essential amino acids (Gibco), 50 000 units Penicillin and 50mg Streptomycin (Sigma).

**William's E** (Gibco) with 10 % (v/v) FBS- Hyclone FetalClone II Serum (Fisher Scientific), 50 000 units Penicillin, 50 mg Streptomycin (Sigma), 1x GlutaMAX-I (Gibco), 0.023 IE/ml human insulin (Gibco) and 4.7 µg/ml hydrocortisone (Sigma).

**SKSCM** 60 % (v/v) low glucose (1000 mg/l) DMEM containing glutamine (Sigma), 40 % (v/v) MCDM-201 (Sigma) with 0.05 % (v/v) N-2 supplement (Gibco), 1 % (v/v) B-27 Supplement (Gibco), 10 ng/ml PDGF (Platelet-derived growth factor, Sigma), 20 ng/ml LIF (Leukaemia Inhibitory Factor, Sigma), 10 ng/ml EGF (Sigma), 0.1 mM L-ascorbic acid (Sigma)

**EBC lysis buffer:** 50 mM Tris HCl pH 8.0, 140 mM NaCl, 100 mM NaF, 200 µm $Na_3VO_4$, 0.1 % (w/v) SDS, 1 % (v/v) Triton X100, 1 tablet protease inhibitor per 50 ml (cOmplete ULTRA tablets, Roche)

**Luria Bertani broth (LB):** 1 % (w/v) NaCl, 1 % (w/v) Tryptone, 0.5 % (w/v) Yeast extract

**LB Agar plates:** 1 % (w/v) NaCl, 1 % (w/v) Tryptone, 0.5 % (w/v) Yeast extract, 0.75 % (w/v) Bacterio Agar

**Towbin:** 25 mM Tris base, 250 mM Glycine, 20 % (v/v) Methanol

**Tris Glycine:** 25 mM Tris base pH 8.0, 250 mM Glycine, 0.1 % (w/v) SDS

**Laemmli SDS PAGE gel loading buffer:** 100 mM Tris HCl pH 6.8, 4 % SDS, 20 % (v/v) Glycerol, 10 mM DTT, 0.025 % (w/v) Bromophenol Blue

**Tris-buffered Saline:** 50 mM Tris HCl pH 7.5, 150 mM NaCl

**FACS buffer** 0.5 % (w/v) BSA, 0.05 % (w/v) NaAz in PBS

**Stain Buffer** 2 % (w/v) FBS, 0.09 % (w/v) NaAz in PBS

**GFP-Trap® Lysis buffer:** 10 mM Tris/Cl pH 7.5; 150 mM NaCl; 0.5 mM EDTA; 0.5 % (v/v) NP-40

**GFP-Trap® Dilution buffer:** 10 mM Tris/Cl pH 7.5; 150 mM NaCl; 0.5 mM EDTA

**ECL Reagent:** Solution 1: 0.4 mM p-Coumaric acid, 2.5 mM Luminol, 0.1 Tris pH 8.5; Solution 2: 0.02 % (v/v) $H_2O_2$ 0.1 mM Tris pH 8.5

**PEI** 1 mg/ml stock solution in 20 mM HEPES pH 7.5

Pre- cast resolving gel recipe for Tris- glycine SDS- polyacrylamide Gel electrophoresis

8, 10, 12 or 15 % (v/v) Acrylamide

390 mM Tris (pH 8.8)

0.1 % (v/v) SDS
0.1 % (v/v) ammonium persulphate

0.04 % (v/v) Tetramethylethylenediamine

Pre- cast 5 % stacking gel recipe Tris- glycine SDS- polyacrylamide Gel electrophoresis

5 % (v/v) Acrylamide

130 mM Tris (pH 6.8)

0.1% (v/v) SDS

0.1 % (v/v) ammonium persulphate

0.1 % (v/v) Tetramethylethylenediamine

# 3. Chapter: Establishing laboratory models of hepatic differentiation amenable to hepatitis C virus infection

## 3.1 Introduction

Chronic HCV infection is a leading risk factor for developing HCC, which is one of the most common forms of primary liver cancer (Llovet et al., 2016). HCV is implicated in the development of HCC both indirectly, via the induction of chronic inflammation, and directly via the manipulation of host signalling pathways by viral proteins. Due to the fact HCV causes liver inflammation and disease, traditionally it was thought that HCV only infects hepatocytes however increasing evidence suggests that these cells are only one of many cell types HCV targets, which include B-cells (Ito et al., 2010b, Pham et al., 2008, Pham and Michalak, 2008), T-cells (Sarhan et al., 2012), monocytes, macrophages (Caussin-Schwemling et al., 2001) including other macrophage-like cells such as dendrocytes (Goutagny et al., 2003). Indeed HCV infection has also been associated with the development of lymphoproliferative disorders such as mixed cryoglobulinemia and non-Hodgkin's lymphoma (Mele et al., 2003, Monti et al., 2005, Ferri et al., 1994, Ferri et al., 1991, Zignego et al., 1997). It has also been suggested that peripheral blood mononuclear cells (PBMC) can serve as a reservoir for persistent infection (Ito et al., 2010a).

The origin of HCC CICs remains largely unclear. Parenchymal hepatocytes are the most abundant type of cell in the liver (80 % of liver volume). Non-parenchymal cells include: LSEs, which line the sinuses and regulate the passage of nutrients and other molecules from the blood vessels into the liver (Fraser et al., 1995, Wisse et al., 1985); Kupffer cells which are specialised macrophages (Naito et al., 1997), and stellate cells which reside in the perisinusoidal space between a hepatocyte and a sinusoid and are the body's main storage of retinoids (D'Ambrosio et al., 2011). Cholangiocytes are the epithelial cells which line the intra-hepatic bile ducts and function in bile formation. Bi-potent HPCs reside in the canal of Hering which is considered a putative hepatic stem cell niche in an adult liver (Theise et al., 1999). HPC are able to divide and differentiate to replenish both hepatocytes and cholangiocytes.

Following injury, the liver has the remarkable ability to regenerate (Taub, 2004). In response to acute injury, mature hepatocytes are able to re-enter

the cell cycle and replicate, being largely responsible for liver maintenance and regeneration as revealed by lineage-tracing studies (Malato et al., 2011). However, chronic liver injury and impairment of hepatocyte replicative potential (due to extreme hepatocyte loss, replicative exhaustion and chronic inflammation) induces mobilisation of HPCs via alteration of signalling pathways, including HGF/c-Met, TGF-β, Hedgehog and Hippo signalling which play key regulatory roles in defining HPC proliferation (Organ and Tsao, 2011, Zhao et al., 2008, Choi et al., 2011, Steiling et al., 2004, Ihn, 2002), known as a ductal reaction, to supply new hepatocytes and maintain the functional integrity of the liver (Theise et al., 1999).

Whilst the phenotype of murine HPCs and human embryonic bi-potent hepatoblasts (aka “oval cells”) are relatively well defined (Li et al., 2006b, Passman et al., 2016, Espanol-Suner et al., 2012, Haruna et al., 1996), the phenotype of adult human HPC is less clear. However, most studies of adult human HPC reveal multiple phenotypes involving numerous cellular biomarkers (Lee et al., 2012). However, some consensus is possible to discern, and it is generally accepted that HPCs express markers such as CD133, EpCAM and CK19, which are also considered markers of CIC. Both mature hepatocytes and HPCs have been suggested to be the cell of origin for HCC CIC. A recent HCC mouse model showed evidence that both hepatocytes and HPCs can lead to HCC formation and contribute to tumour heterogeneity (Tummala et al., 2017).

It is unclear whether HCV-associated HCC originates in the same way as other forms of HCC, or which cells give rise to HCC CICs in the context of a chronic HCV infection. It is conceivable that CICs either arise from the transformation and de-differentiation of mature infected hepatocytes, or that HCV may be able to infect HPCs cells and perturb their differentiation, thus predisposing cells towards transformation into HCC CICs. In support of the latter scenario, chronic HCV infection has also been associated with the development of ICCA (Li et al., 2015a), with HPCs being a potential common origin for both ICCA and HCC. Notably, classes of HCC and ICCA have been shown to harbour related gene transcription signatures despite histological differences (Marquardt et al., 2015), in accordance with their potential derivation from a common HPC ancestor. Thus we hypothesised that HCV may be able to infect HPCs, perturb their differentiation during chronic hepatitis and so predispose them towards transformation into HCC CICs. Accordingly, we pursued several options in order to establish a HPC-like cell culture model to explore whether HCV infection perturbs hepatic

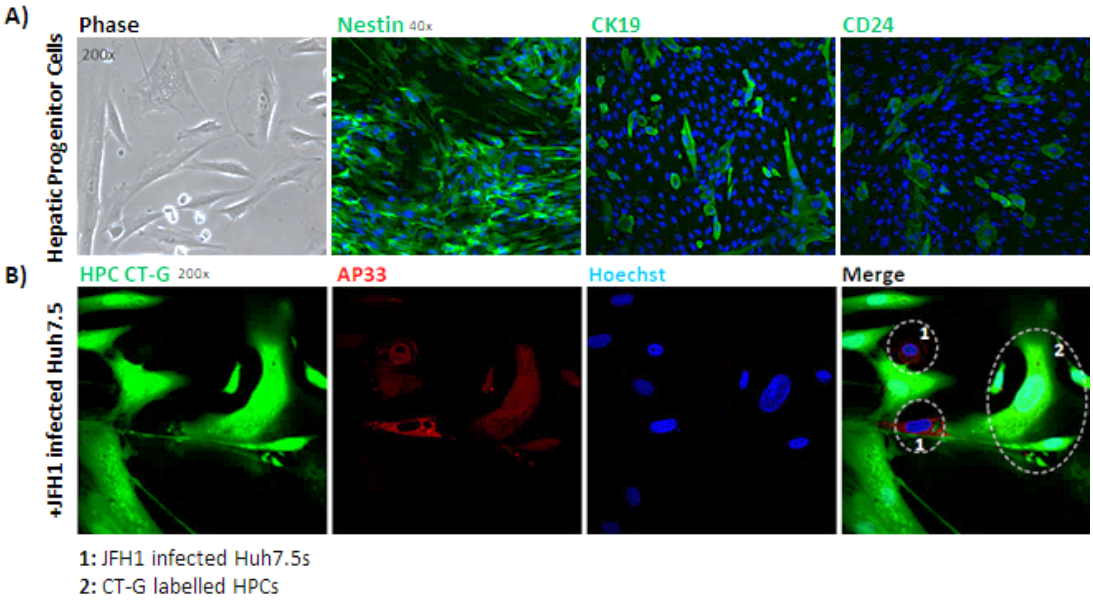


**Figure 3.1.1 Hepatic progenitor cell characterisation and HCV infection *ex vivo***

A) Immunofluorescence of HPCs stained with anti-Nestin, anti-CK19, anti-CD24 antibodies and 488 labelled secondary antibodies green). The nuclei were counterstained using DNA stain Hoechst (blue). Phase images were taken at a magnification of 200x and immunofluorescence were taken at 40x. Phase image is representative of cell density. B) HPCs were labelled with CT-G and co-cultured with JFH-1 infected Huh7.5 cells. Images were taken at 200x. Cells were fixed using 4 % PFA and stained for HCV structural protein E2 using the AP33 antibody and an Alexa Fluor 594 nm conjugated secondary antibody. Nuclei were counterstained using DNA stain Hoechst (blue) The merged image shows two infected Huh7.5 cell (1-red) and one infected CT-G labelled HPC (2- red & green). Work carried out by Dr Matthew Bentham.

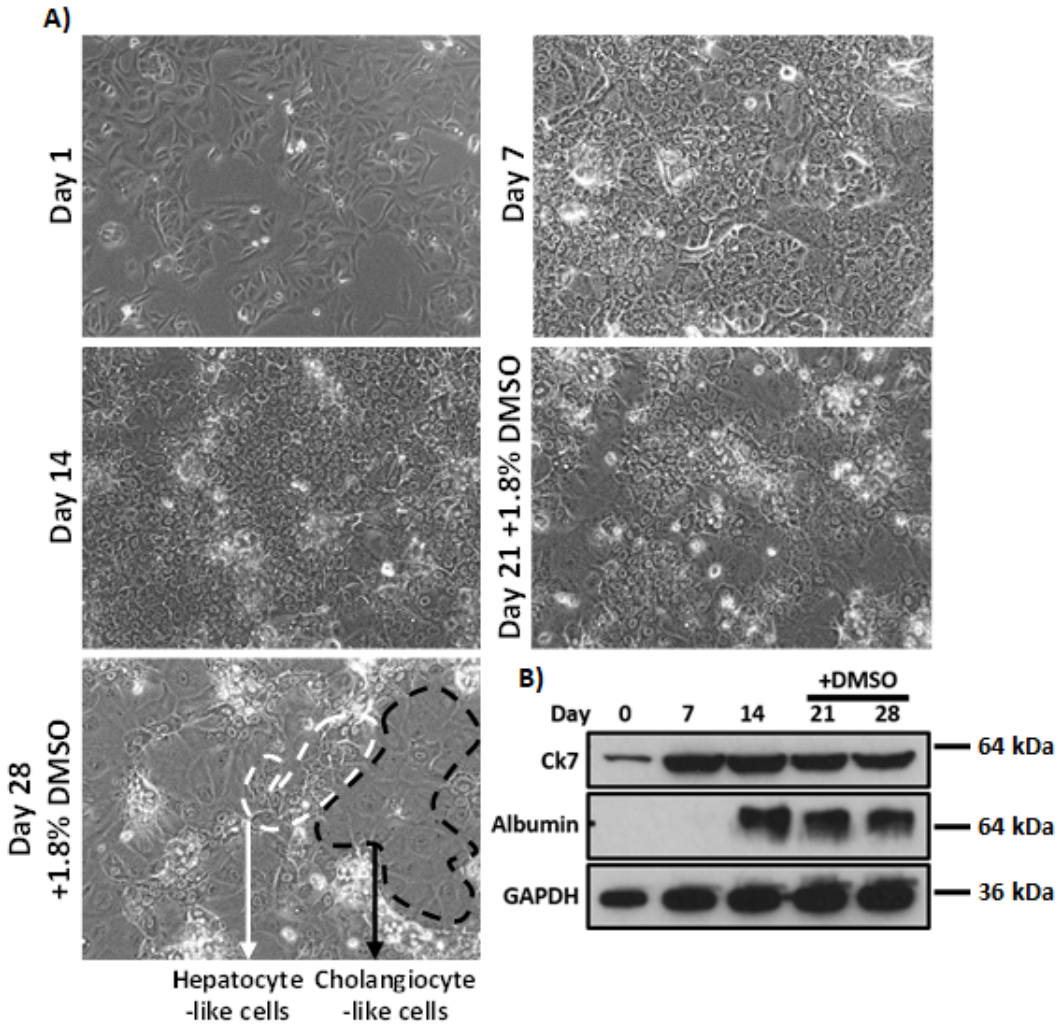


**Figure 3.1.2 HepaRG cell differentiation**

A) HepaRG cells were differentiated by seeding cells at confluence and changing the media twice a week for two weeks. After two weeks 1.8 % DMSO was added to the culture media and the cells were differentiated for another two weeks. Phase images were taken every seven days using an EVOS cell imaging system (20x objective). Islands of hepatocyte- and cholangiocyte-like cells are highlighted by white and black dotted lines, respectively. Images are representative of cell density. B) HepaRG cells were differentiated as described above with regular samples taken for whole cell protein lysates (Methods section 2.14). Lysates were separated by sodium dodecyl sulphate polyacrylamide gel electrophoresis (SDS-PAGE) and then immunoblotted using antibodies specific to CK7, albumin, CD24 and GAPDH.

differentiation, including the pathways involved and the HCV proteins that potentially mediate this effect.

## 3.2 A precedent for *ex vivo* infection of HPC by HCV

A key factor in establishing this PhD project was our laboratory's prior unpublished demonstration that cells retaining HPC-like properties, derived from primary adult liver tissue, were indeed permissive to HCV infection; this data is therefore summarised here in brief with kind permission from my supervisors Dr Matthew Bentham and Dr Stephen Griffin.

To isolate cells with the hallmarks of HPCs, healthy margins from hepatic colorectal metastasis resections were dissected and crudely dissociated using scalpels in collagenase-containing buffer. Resulting tissue aggregates were then cultured on fibronectin in a defined serum-free "stem cell media" in order to select for the growth of cells with inherent self-renewal capacity, without bias for particular biomarkers. After 8- 15 days, cellular outgrowths were evident from tissue, and these were subsequently expanded as polyclonal cell populations for up to seven passages; infection experiments described below were conducted using cells from passages 2 and 3.

Isolated cells were characterised by immunofluorescence, which showed expression of stem cell markers such Nestin, CK19 and CD24 (Figure 3.1.1A; work performed by Dr Matthew Bentham). Importantly, cells lacked expression of smooth muscle actin, ruling out contamination by fibroblasts or stellate cell precursors (data not shown). Overall, the cells isolated from patient liver samples shared characteristics with HPCs. To determine whether the isolated patient derived HPC were susceptible to HCV infection, cells were labelled with cytotracker green (CT-G) and co-cultured with HCV-infected (JFH-1 strain) Huh7.5 cells at a ratio of 10:1. Using this method a low level infection of progenitor cells was evident, with single or small groups of cells staining positively for HCV E2 antigen (AP33 monoclonal antibody) (Figure 3.1.1B; work carried out by Dr Matthew Bentham). However invasive liver biopsies are less common now, making it difficult to obtain liver samples from infected and non infected patients.

## 3.3 HepaRG immortalised hepatic progenitor cells- a potential new HCV model?

We have shown that adult patient derived HPC were in fact susceptible to infection by HCV *ex vivo*. This observation is in accordance with other studies describing that human foetal liver stem cells supported replication of blood-derived HCV (Guo et al., 2017) and another that showed susceptibility of human embryonic stem cells to HCV initially occurred at the stage of hepatic stem cells/hepatoblasts during differentiation towards mature hepatocytes (Yan et al., 2017, Wu et al., 2012). However, isolation and culture of adult patient derived liver progenitor cells described above is technically challenging, laborious, yields small cell numbers and leads to low level and frequency of infection. Hence a robust cell culture model was needed to test our hypothesis of whether HCV is able to infect HPCs and perturb their differentiation and so predispose towards HCC development.

### 3.3.1 Chemically induced differentiation of HepaRG cells into hepatocyte-like and cholangiocyte-like cells

HepaRG cells are immortal, but importantly not transformed, bi-potent progenitor-like cells which can be chemically induced (by DMSO) to differentiate into hepatocyte- and cholangiocyte-like cells over a period of four weeks (Parent et al., 2004). Ndongo-Thiam *et al*., demonstrated that HepaRG progenitor cells could support the infection and replication of serum-derived HCV (Ndongo-Thiam et al., 2011). Thus, HepaRG cells have the potential to be a model of hepatic differentiation to study the effect of HCV infection at various stages of differentiation, yet infection with cell culture HCV isolates has not been demonstrated in the literature. To use HepaRG cells as a model to study the effect of HCV on hepatic differentiation our first aim was to establish the HepaRG differentiation in our laboratory and characterise these cells at various stages of differentiation. The purpose of the characterisation was to determine whether they express similar markers to the HPCs and the patient derived HPCs isolated in our lab. The next aim was to determine whether HepaRG cells supported infection and replication of cell culture isolates of HCV.

Differentiation of HepaRG cells is induced in two stages, first by culturing the cells for two weeks at confluence, secondly by the addition of 1.8 % DMSO to the media and culturing the cells for a further two weeks. DMSO has been used to induce and maintain differentiation in multiple primary and tumour

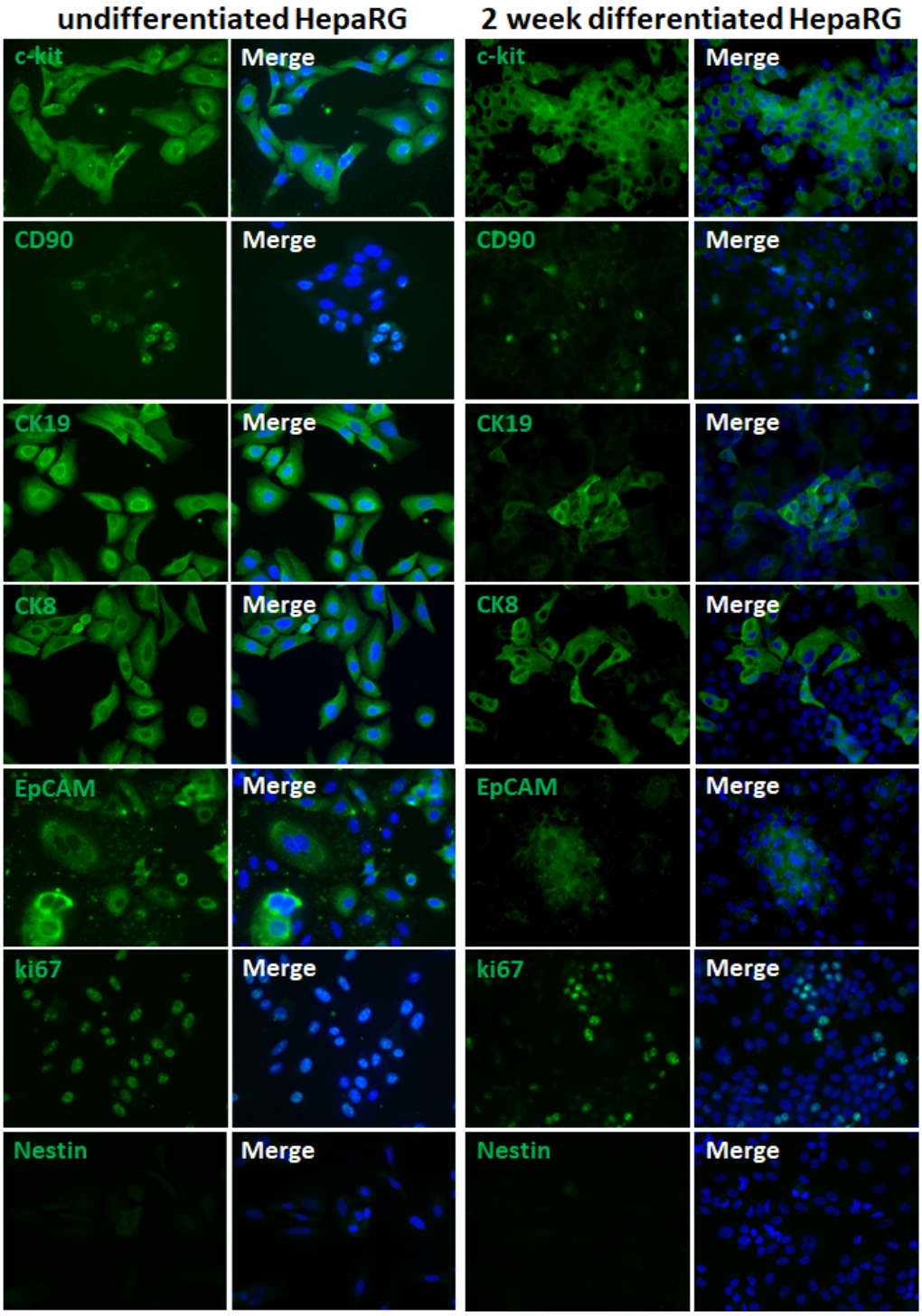


**Figure 3.3.1 Immunofluorescence of undifferentiated and differentiated HepaRG cells stained for c-kit, CD90 or CK19, CK8, EpCAM, ki67 and Nestin**

HepaRG cells were either seeded at sub-confluence, allowed to settle overnight or differentiated for 2 weeks and fixed using 4 % PFA in PBS. The cells were permeabilised using 0.2 % Triton X-100 in PBS and stained using antibodies against c-kit, CD90, CK19, CK8, EpCAM, ki67 and Nestin. Fluorescently labelled secondary antibodies with the fluorophore Alexa Fluor 488 nm (green) were used. Nuclei were counterstained using DNA stain Hoechst (blue). Images were taken using the 40x objective of the Nikon Eclipse Ti-E Widefield Fluorescent Inverted Microscope. Images are representative of cell density.

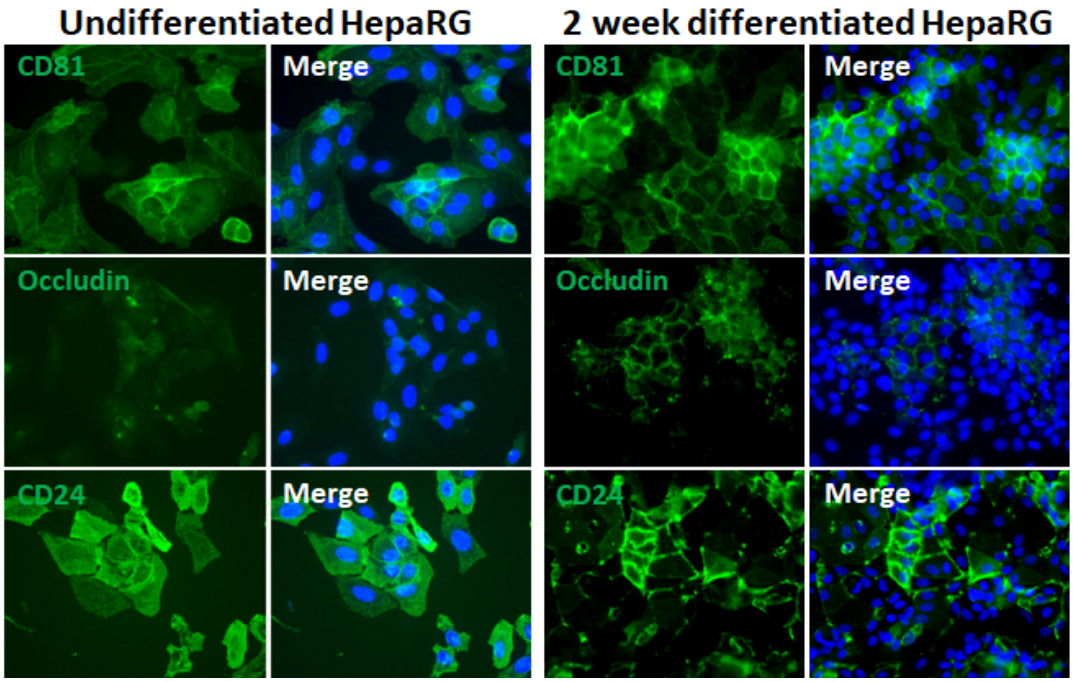


**Figure 3.3.2 Immunofluorescence of undifferentiated and differentiated HepaRG cells stained for CD81 and Occludin**

HepaRG cells were either seeded at sub-confluence ($8x10^3$/ml), allowed to settle overnight, then fixed using 4 % PFA in PBS either immediately, or after differentiation for two weeks. Cells were stained using antibodies against CD81, occludin, and CD24. Fluorescently labelled secondary antibodies with fluorophore Alexa Fluor 488 nm (green) were used to detect specific proteins. Nuclei were counterstained using DNA stain Hoechst (blue). Images were taken using the 40x objective of a Nikon Eclipse Ti-E Widefield Fluorescent Inverted Microscope. Images are representative of cell density.

cell lines (Cable and Isom, 1997, Azuma et al., 2003, Cheung et al., 2006, Villa et al., 1991). However, it's mode of action and the mechanism by which differentiation is induced remains unclear. The pleotropic effects of DMSO, such as; reducing cell membrane integrity (Melkonyan et al., 1996), altering intracellular signalling pathways including Wnt/β-catenin and TGF-β signalling (Fiore and Degrassi, 1999, Makowske et al., 1988, Choi et al., 2015) and affecting alternative mRNA splicing (Bolduc et al., 2001) have all been implicated in its ability to promote differentiation.

At low density, HepaRG cells appeared undifferentiated with an elongated morphology and unpronounced nuclei (Figure 3.1.2A). Once confluency was reached the cells differentiated into islands of hepatocyte-like cells surrounded by cholangiocyte-like cells (Figure 3.1.2A), as shown previously in the literature (Parent et al., 2004, Guillouzo et al., 2007), the islands of hepatocyte like cells displayed a more compact morphology with pronounced nuclei and a low nucleus-to-cytoplasm ratio. Correspondingly an increase in expression of the specific hepatocyte marker albumin and the cholangiocyte marker CK7 was observed by western blot (Figure 3.1.2B).

HepaRG cells were characterised by immunofluorescence for the expression of a panel of progenitor markers, which have been previously described as being expressed by HPC including; c-kit (also known as CD117), CD90, CK19, CK8, Nestin and EpCAM (Schmelzer et al., 2006, Weiss et al., 2008, Goldman et al., 2016). Ki67 was included as a marker of proliferation (Gerdes et al., 1984, Gerdes, 1990). 'Progenitor' or 'undifferentiated' and 2 week differentiated HepaRG cells expressed all progenitor markers tested, except Nestin (Figure 3.3.1); however the abundance and cell frequency of expression differs between progenitor and differentiated cells. Fewer HepaRG cells which had been cultured for 2 weeks in the absence of DMSO expressed the progenitor markers CD90, c-kit, CK19, EpCAM and ki67. HepaRG cells were also stained for HCV entry factors Occludin and CD81 (Figure 3.3.2). CD81 was expressed in the differentiated and progenitor stage however CD81 levels increased post differentiation. Progenitor HepaRG cells only expressed a low level of Occludin and the protein was not expressed by all cells. Expression of Occludin increased upon differentiation and more cells expressed the protein (Figure 3.3.2). This analysis largely mirrored similar studies of HepaRG cells in the literature (Parent et al., 2004, Gripon et al., 2002, Cerec et al., 2007, Narayan et al., 2009). Such studies also confirmed expression of liver specific mRNAs and protein such as albumin, transferrin, aldolase B and detoxification enzymes

such as Cytochrome P450 Family 3 Subfamily A Member 4 (CYP3A4) are generally absent in progenitor stage and increase over differentiation, especially after addition of DMSO (Parent et al., 2004, Gripon et al., 2002). HepaRG cells are negative for AFP at all stages (Gripon et al., 2002). Oval or progenitor markers analysed include CK19, CD90, c-kit, N-CAM, gp130 and CD34 (Cerec et al., 2007, Parent et al., 2004). CK19 is expressed throughout and accumulates in the cholangiocyte-like cells. Expression of CD34, CD90 and gp130 are lost during differentiation (Cerec et al., 2007).

### 3.3.2 Are HepaRG cells permissive to infection with cell culture derived HCV?

HepaRG cells could represent a novel cellular model for HCV infection. Unlike Huh7 cells, HepaRG cells are not transformed and are able to be differentiated from a bi-potent HPC-like cell into cholangiocyte-like and hepatocyte-like cells. However whilst others have shown patient-derived virus to infect these cells in a differentiated state (Ndongo-Thiam et al., 2011), no such studies have been reported using cell-culture derived viruses based on the JFH-1 isolate (Wakita et al., 2005, Kato et al., 2001). Initial experiments to determine whether HepaRG cells might be permissive to HCV comprised transfection of wildtype (WT) HepaRG cells with JFH-1 subgenomic replicon (Kato et al., 2003) RNA using transient electroporation. 48 hr post-electroporation, cells were analysed by immunofluorescence using a well-characterised polyclonal anti-HCV NS5A antibody (Macdonald et al., 2003). However, no NS5A staining was detected in the transfected HepaRG cells.

Ensuing experiments involved taking advantage of the Neomycin Phosphotransferase (NPT) selection marker expressed by the JFH1-replicon, conferring resistance to G418 (Figure 3.3.3). Following a G418 kill-curve titration on HepaRG cells (data not shown); a concentration of 500 µg/ml G418 was chosen for optimal selection of transfected HepaRG cells. Although transfected HepaRG cells survived under G418 selection while control mock transfected HepaRG cells died after 1-2 weeks of G418 selection, the transfected cells were sparse and grew slowly. Even in the selected HepaRG cells no HCV antigen was detectable by immunofluorescence. To circumvent growth inhibition within selected cells, a G418 pulse selection protocol was attempted, whereby cells were pulsed with 500 µg/ml G418 for one week and then released, to ensure selection of JFH-1 harbouring HepaRG and left to recover for another week, which again successfully selected resistant cells whilst controls were eliminated.

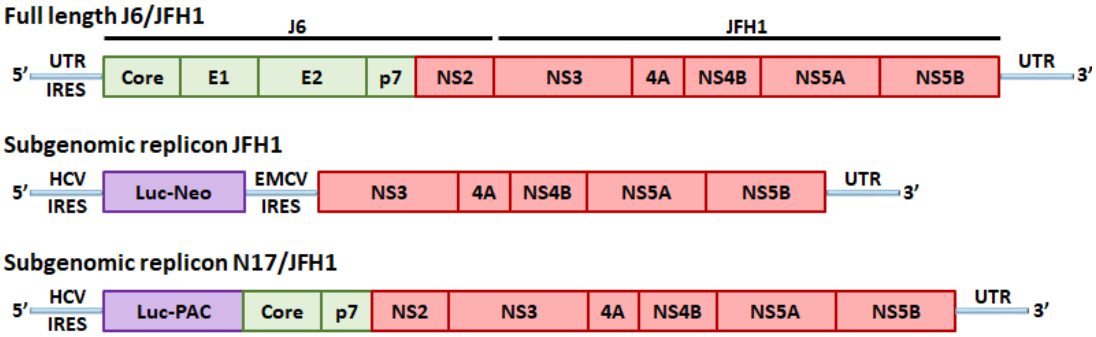


**Figure 3.3.3 Structures of HCV full length and subgenomic replicon constructs**

Diagram representing the structures of the full length J6/JFH1 (Lindenbach et al., 2006) and subgenomic replicon constructs JFH1-rep (Lohmann et al., 1999) and N17/JFH1-rep (Angus et al., 2012a). The HCV UTR regions flank the ORF. J6/JFH1 full length clone is a genotype 2a/2a intragenotypic chimaera, which contain the structural proteins Core, E1, E2, p7 and NS2 from the HC-J6 strain, which are linked to the remaining non-structural proteins NS3-NS5B from the JFH1 strain. The JFH1 replicon lacks the structural protein core, E1 and E2 in addition to proteins p7 and NS2. These proteins have been replaced by the firefly luciferase gene, the neomycin phosphotransferase gene (Luc-Neo) and the IRES of the encephalomyocarditis virus (EMCV). This IRES directs the expression of the HCV polyprotein. The Luc-Neo is under control of the HCV IRES present in the 5'UTR. The N17/JFH1 replicon construct encodes the firefly luciferase and the puromycin N-acetyl-transferase genes (Luc-PAC) in the JFH1 ΔE1/E2 background (Wakita et al., 2005) which lacks the genes encoding structural proteins E1 and E2.

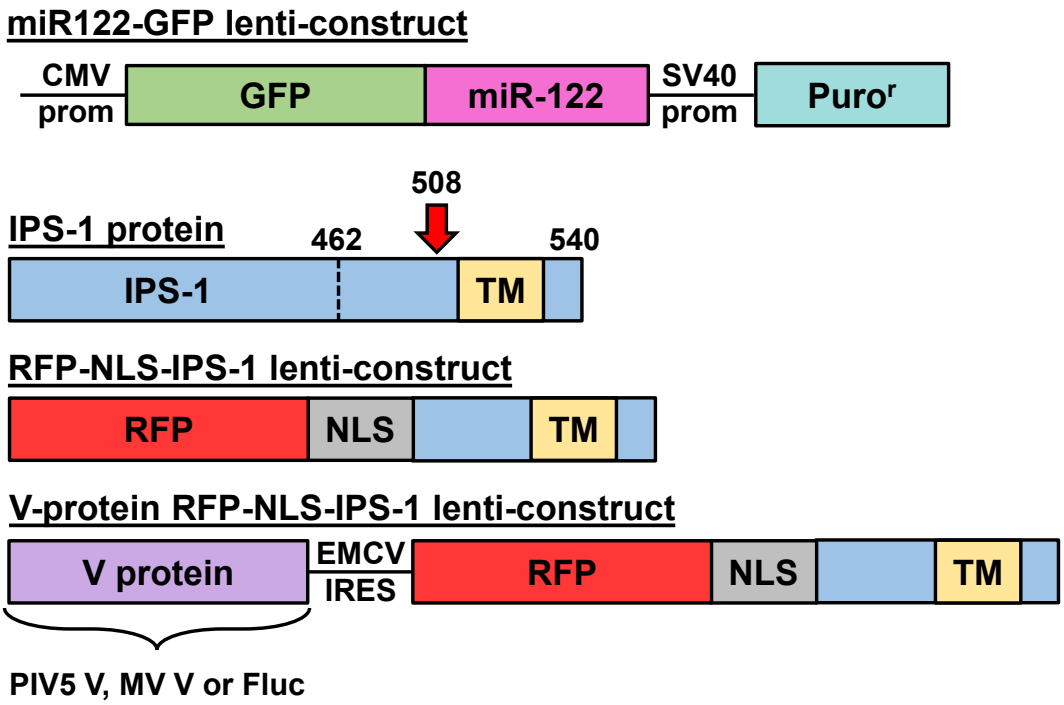


**Figure 3.3.4 Diagram of the constructs used to transduce the HepaRG cells**

The GFP-miR-122 lentivirus construct was obtained from abm and additionally encodes a puromycin resistance gene (Puro$^r$). The IPS-1 protein is cleaved by the HCV NS3-4A protease at amino acid 508 (arrow). The protein also contains a mitochondrial transmembrane domain leading to the protein being directed to the outer membrane of the mitochondria. The RFP-NLS-IPS lentivirus construct encodes a RFP and the SV40 NLS which have been fused to the 462-540 residue section of the IPS-1 gene. The V-protein RFP-NLS-IPS1 lentivirus construct is a bi-cistronic construct consisting of the V-protein from either PIV 5 or MV or the Firefly luciferase gene (Fluc) and the RFP-NLS-IPS-1 cassette.

However, semi-quantitative RT-PCR targeting a conserved region of the HCV 5' UTR was unable to detect any HCV RNA in any combination of the electroporated and G418 selected HepaRG cells (Figure 3.3.5B) (sensitivity down to 10 pg). To examine whether an alternative method of selection might be more successful, HepaRG cells were also transfected with the N17/JFH1 subgenomic replicon (Angus et al., 2012a), which contains both a Firefly luciferase reporter and puromycin N-acetyl-transferase (PAC), conferring puromycin resistance, preceding the HCV polyprotein carrying a deletion of the majority of the E1 and E2 sequences (Figure 3.3.3). However, following transfection luciferase activity again remained undetectable compared with baseline even after seemingly successful selection using 1 µg/ml puromycin (data not shown). Native HepaRGs grown as exponential 'progenitor-like' cells were poorly permissive for HCV infection. As they appeared to express major HCV receptors (such as CD81, Occludin), we reasoned that HepaRGs may either lack (or have low level expression) an essential cofactor(s) for HCV replication, or effectively suppress HCV replication via an innate interferon response to viral antigen. HepaRG have been shown to elicit potent IFNβ response to virus infection and to adopt robust interferon stimulated gene (ISG) responses (Maire et al., 2008). Accordingly, inhibition of type 1 IFN pathway, by neutralising anti-IFN β antibodies, results in enhanced HBV replication in these cells (Lucifora et al., 2010). In addition, the progenitor-like phenotype of these cells meant that they were unlikely to express significant levels of miR-122, an essential HCV cofactor, expression of which increases throughout liver development and hepatic differentiation (Jung et al., 2011). Thus, HepaRG were transduced using Lentiviruses expressing Paramyxovirus V proteins (Andrus et al., 2011), which are a potent antagonists for both IFN responses and production due to their action upon STAT1/2 signalling and cytosolic pattern recognition receptors (PRRs), respectively (Xu et al., 2012, Poole et al., 2002). Specifically, V proteins from parainfluenza 5 virus (PIV5) and the Measles virus (MV) were used; PIV5 V protein targets STAT1 for proteasomal degradation (Didcock et al., 1999) (Figure 3.3.4) and interacts with mda-5 to inhibit activation of the IFN-β promoter (Andrejeva et al., 2004) and the MV V protein targets both STAT1 and STAT2 to prevent their nuclear translocation (Caignard et al., 2009). Both the PIV5 and MV V proteins interact with the RIG-I/tripartite motif containing (TRIM) 25 regulatory complex to inhibit RIG-I signalling (Sanchez-Aparicio et al., 2018). HIV-based *lentivirus* stocks were established to transduce HepaRG cells with appropriate vectors.

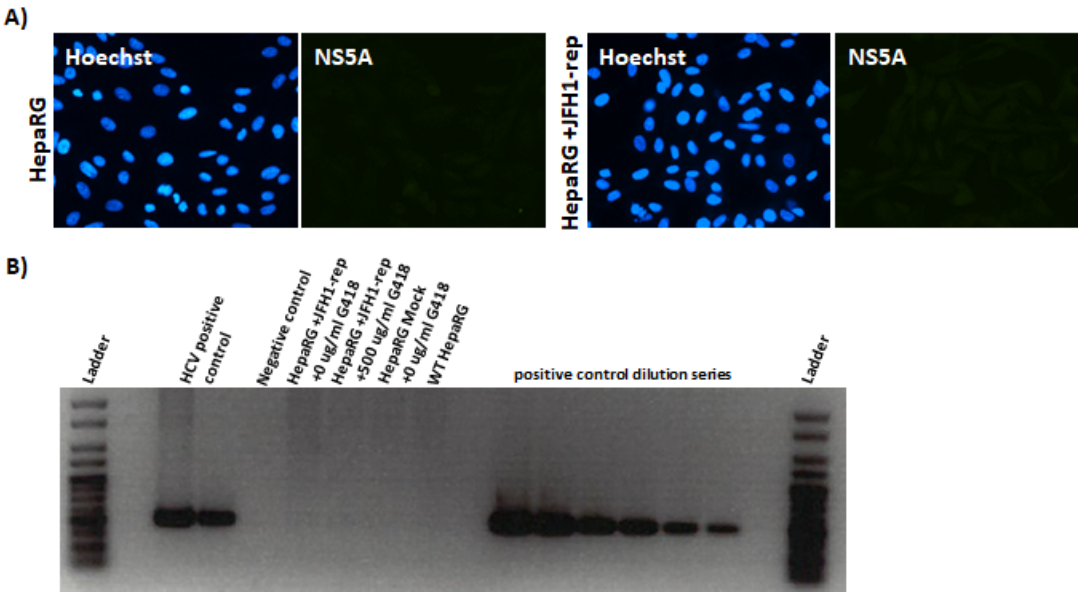


**Figure 3.3.5 Transfection of HepaRG cells with the JFH1 replicon**

A) Immunofluorescence of HepaRG cells which were fixed in 4 % PFA in PBS 48 hrs after electroporation +/- JFH1-replicon RNA ($8x10^6$ cells + 10 µg RNA). The cells were permeabilised using 0.2 % Triton-X100 in PBS and stained with DNA stain Hoechst (blue) and anti-NS5A antibody (green). Alexa fluor 488 nm fluorophore labelled secondary antibody was used. Images were taken using the 40x objective of the Nikon Eclipse Ti-E Widefield Fluorescent Inverted Microscope. Images are representative of cell density. B) HepaRG cells were either mock electroporated or with JFH1-replicon RNA ($8x10^6$ cells + 10 µg RNA) and treated +/- 500 µg/ml G418 for one week and left to recover for another week. An RT-PCR was performed to detect JFH1-replicon RNA in the cells. A band of about 100 bp was expected as seen for the positive control for which the HCV replicon was used. A DNA ladder with bands between 25- 500 bp was used. For the positive control dilution series 1 µg of HCV replicon RNA was used in the cDNA synthesis reaction and 1 µl of the cDNA reaction mixture followed by a 10 fold serial dilution was used in the RT-PCR reaction. No replicon RNA was detected in any of the HepaRG samples.

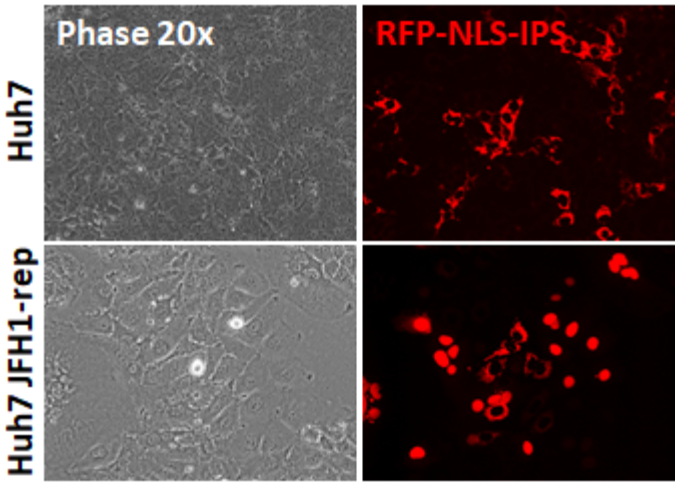


**Figure 3.3.6 Huh7 cells transduced with an RFP HCV reporter system**

Fluorescence microscopy (20x objective of the EVOS cell imaging system) of Huh7 cells transduced with a lentivirus encoding a real-time RFP cell-based reporter and transfected +/- the JFH1 replicon. The RFP construct contains a nuclear localisation sequence (NLS) in between the RFP protein sequence and the IPS-1. In the absence of HCV infection the RFP reporter exhibits mitochondrial localisation because of the IPS-1 mitochondrial targeting sequence, however in the presence of HCV infection the RFP translocates to the nucleus as the IPS-1 protein is recognised by the HCV NS3-4A protease and cleaved, revealing the nuclear localisation sequence. Images are representative of cell density.

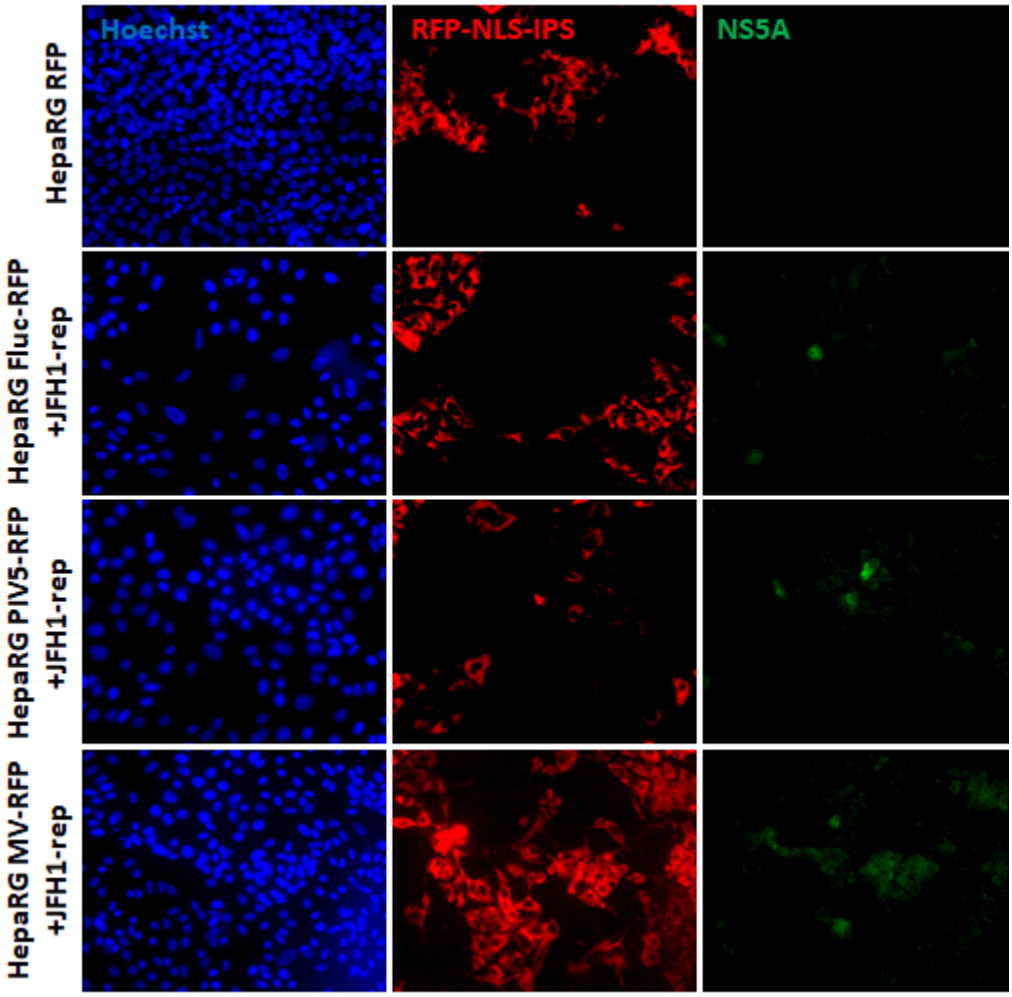


**Figure 3.3.7 HepaRG cells transduced with RFP-NLS-IPS and PMV V proteins**

Immunofluorescence (20x objective of the EVOS cell imaging system) of HepaRG cells transduced with a lentivirus encoded the RFP-NLS-IPS reporter system and PMV V proteins. The V proteins of either the MV or PIV5, or a firefly luciferase control (Fluc) were introduced using the same lentiviral vector encoding the RFP HCV reporter. After transduction with the RFP reporter, HepaRG cells were transfected with the JFH1 replicon, fixed (4 % PFA) 48 hr post electroporation and stained using an anti-NS5A antibody and Alexa Fluor 488 conjugated Donkey anti-sheep secondary antibody. Images are representative of cell density.

The miR-122 expression vector expresses precursor miR-122 linked to eGFP via a foot-and-mouth disease virus (FMDV) 2A translational inhibitory sequence to serve as an indirect marker of expression (Figure 3.3.4). The V proteins of PIV5 and MV were introduced into the HepaRG cells using a bi-cistronic Lentiviral vector, which also encoded a fluorescent reporter for HCV infection (Andrus et al., 2011) (Figure 3.3.4). The fluorescent reporter system allows real-time imaging of HCV infection and relies upon expression of the HCV NS3 protease to cleave a fusion protein consisting of IPS-1 fused to an NLS-tagged RFP. HCV infection therefore promotes release of the NLS-tagged RFP, translocating the RFP signal from the mitochondria to the nucleus (Jones et al., 2010). Initially the HCV-RFP reporter was tested in Huh7 cells and Huh7 cells transiently transfected with the JFH1-replicon. Obvious nuclear RFP localisation was visible for the Huh7 cells harbouring the JFH1-replicon (Figure 3.3.6).

HepaRG cells transduced with the PMV V protein HCV-RFP reporter viruses were subsequently transfected with the JFH1-replicon and stained for HCV NS5A protein. No nuclear RFP was detected in the transfected HepaRG cells, possibly due to a low transduction efficiency. However a low level of NS5A staining was detected (Figure 3.3.7). The JFH1-replicon construct contains the sequence for the firefly luciferase enzyme which is used as a bioluminescent reporter. By performing a luciferase assay to measure the relative light units produced from HepaRG lysates taken 4, 24 and 32 hr post electroporation we were unable to detect a luciferase signal after the initial sample taken 4 hr post electroporation, indicating that whilst initial translation of input RNA takes place, HCV RNA is unable to replicate efficiently within these cells (Figure 3.3.8). HepaRG cells were transduced with a combination of the MV V protein reporter and the miR-122 eGFP lentiviruses, followed by transfection with the JFH1-replicon. Interestingly following electroporation a very small number of cells with nuclear RFP re-localisation were visible (Figure 3.3.9). In addition, infection of the dual miR-122 and V protein transduced HepaRG cells using full length the J6-JFH1 virus again resulted in detection of a small number of nuclear RFP and NS5A positive cells (Figure 3.3.10). By virtue of the miR-122 lentiviral construct also containing a PAC puromycin resistance gene, these cells had first been pre-selected for puromycin resistance. These results suggest a combination of an increase in HCV cofactor expression and a reduction in anti-viral signalling can increase HepaRG HCV permissiveness.

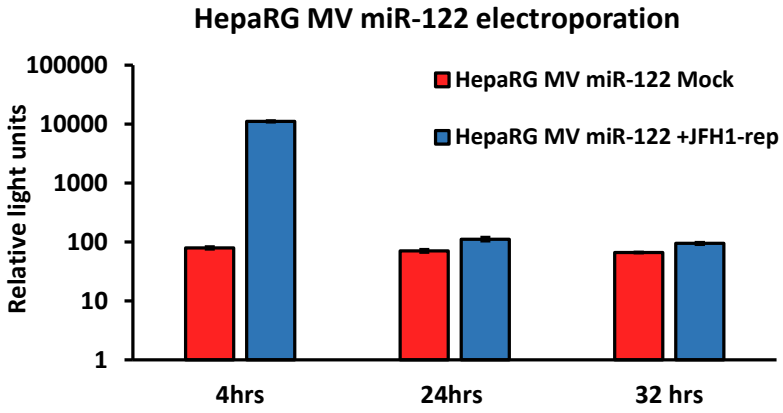


**Figure 3.3.8 Firefly luciferase measurement of electroporated HepaRG MV miR-122**

Firefly luciferase measurement of HepaRG MV miR-122 cells electroporated with JFH1-replicon RNA ($4x10^6$ cells, 5 µg RNA). Cells were lysed 4, 24 and 32 hr post electroporation in passive lysis buffer and the relative light units were measured after addition of the firefly substrate. Readings represent the mean ± standard deviation between replicate wells.

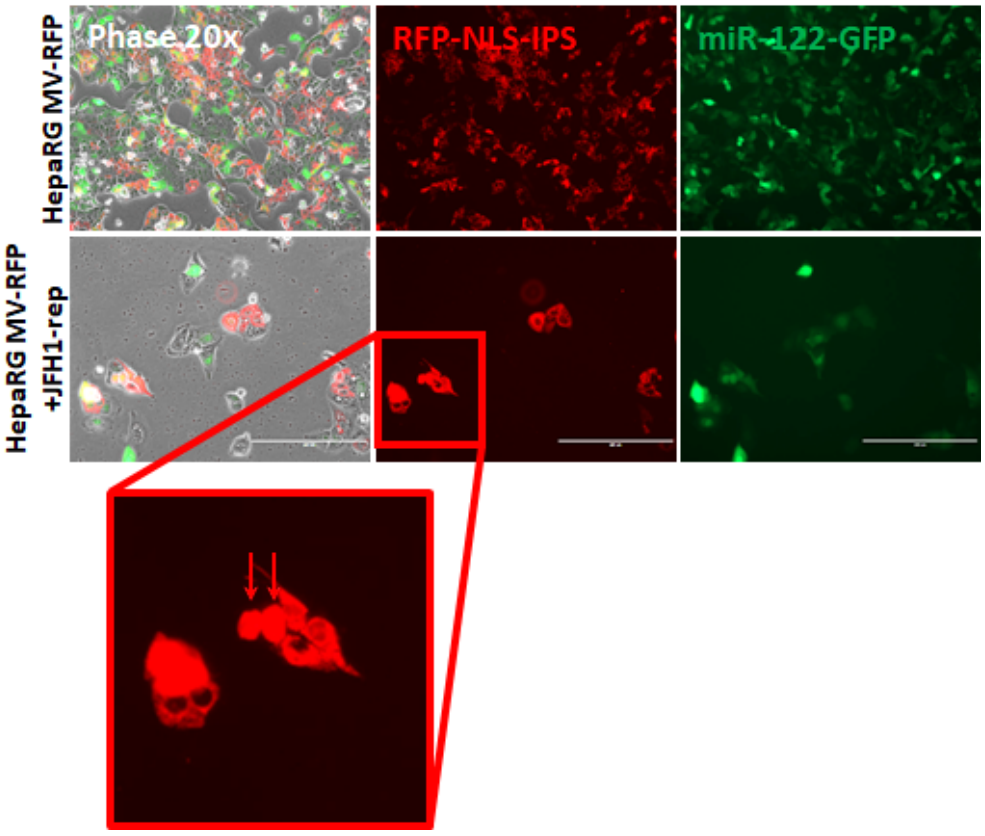


**Figure 3.3.9 HepaRG cells transduced with the RFP-NLS-IPS reporter and miR-122-GFP**

Fluorescence microscopy of HepaRG cells which have been transduced by two lentiviruses encoded either the MV RFP-NLS-IPS or a viral vector containing a miR-122-GFP sequence. After the HepaRG cells were transduced and undergone antibiotic selection for miR-122-GFP and MV RFP-NLS-IPS, HepaRG cells were transfected by electroporation with JFH1-replicon RNA ($4x10^6$ cells and 5 µg RNA). Images are representative of cell density.

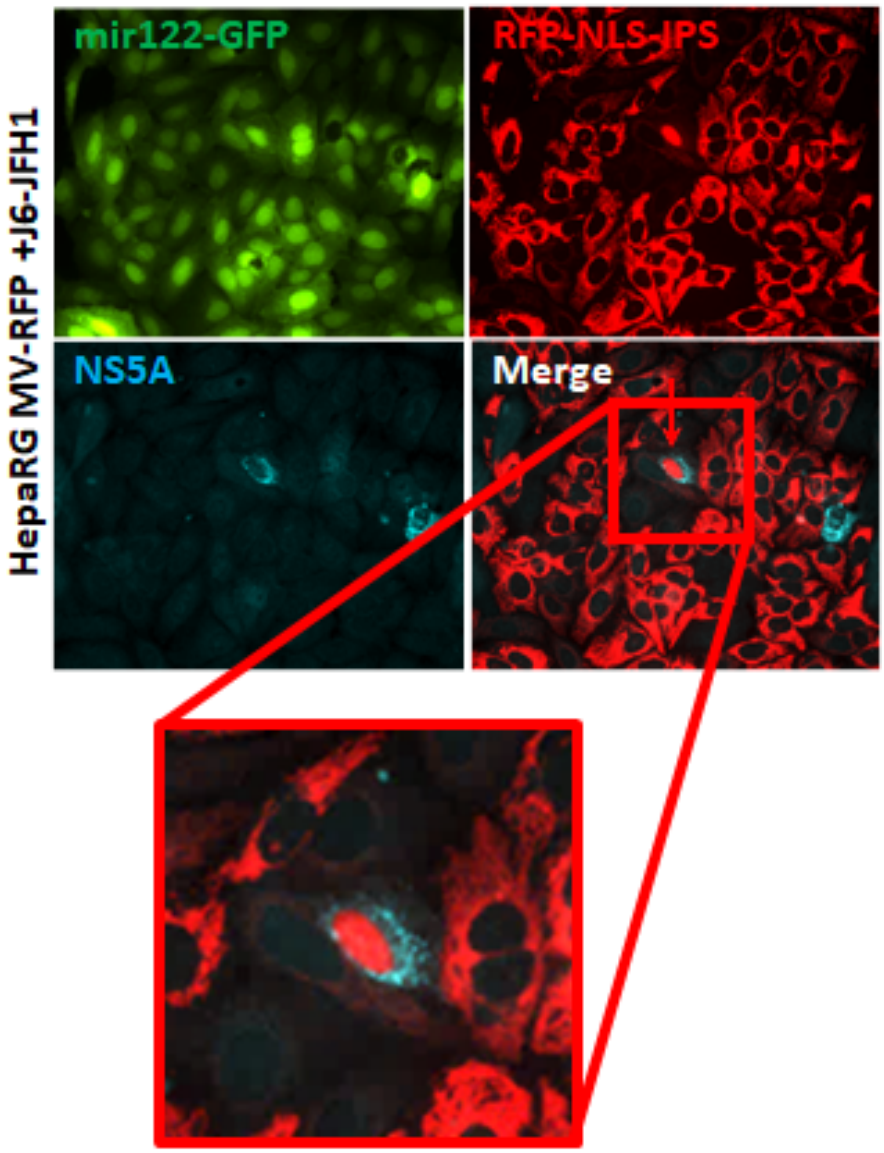


**Figure 3.3.10 RFP-LS-IPS and miR-122-GFP transduced HepaRG cells infected with J6-JFH1**

Immunofluorescence of HepaRG cells transduced by two lentiviruses encoded either the MV RFP-NLS-IPS or a viral vector containing a miR-122-GFP sequence. After transduction and selection for GFP positive cells the HepaRG cells were infected with J6-JFH1 and fixed in 4 % PFA in PBS, permeabilised with 0.2 % Triton-X100 in PBS 48 hr after infection and stained with an anti-NS5A antibody and Alexa Fluor 647 nm labelled secondary antibody. Images are representative of cell density.

## 3.4 Adaptation of Huh7 cells to use as a HPC model

### 3.4.1 CD24lo Huh7 cells- a less tumourigenic Huh7 cell model

HepaRG cells were found to be poorly permissive to HCV infection, even when supplemented with IFN antagonist proteins and over-expression of the mir122 cofactor. Thus, an *in vitro* model for hepatic differentiation remained elusive. Huh7 cells are the most common HCC-derived cell line used to study HCV infection as they are highly permissive to HCV as a result of expressing HCV entry factors including CD81, Occludin, Claudin-1 and SR-B1, high levels of essential HCV cofactor miR-122 and showing poor induction of interferon in the face of PRR stimulation (Yoo et al., 1995, Lohmann et al., 1999). However Huh7 cells are a transformed cell line with many genomic mutations, epigenetic modifications and copy number alterations (Bressac et al., 1990, Phillips et al., 2005, Keskinen et al., 1999, Kawai et al., 2001, Seow et al., 2001). Huh7 cells grow in 2D cell culture as a heterogeneous polyclonal population and previous studies have shown that they can be sub-defined into populations retaining greater or lesser tumour-promoting ability, based upon surface expression of CIC markers such as CD133 (Yang et al., 2011) and CD24 (Lee et al., 2011). CD24 is a sialoglycoprotein which modulates growth and differentiation, which is commonly over-expressed in many types of cancer including HCC (Huang and Hsu, 1995) and often correlates to poor patient prognosis (Lee et al., 2011). Thus, we hypothesised that selecting Huh7 cell sub-populations expressing low levels of CD24 would generate a cell culture model with a less transformed phenotype that better reflects resident HPCs rather than transformed CICs.

Huh7 cells were FACS sorted based upon cell surface CD24 expression (Figure 3.4.1) through two rounds, taking each time the top/bottom 20 % of cells (Figure 3.4.1A; experiment carried out by Dr Matthew Bentham). To confirm that the resultant two populations expressing high (CD24hi) and low (CD24lo) levels of CIC marker CD24, did indeed exhibit differences in tumourigenicity, we employed an established subcutaneous flank xenograft model (Samson et al., 2018) using SCID mice injected with low numbers of cells ($1x10^5$), comparing tumour growth over time alongside the parental Huh7 line. Pleasingly, CD24 expression correlated directly with Huh7 cell tumourigenicity as CD24lo cells were less tumourigenic than parental Huh7 cell (intermediate) and CD24hi cells (Figure 3.4.1B; Work carried out by Drs Matthew Bentham and Adel Samson). In addition, expression of other CIC

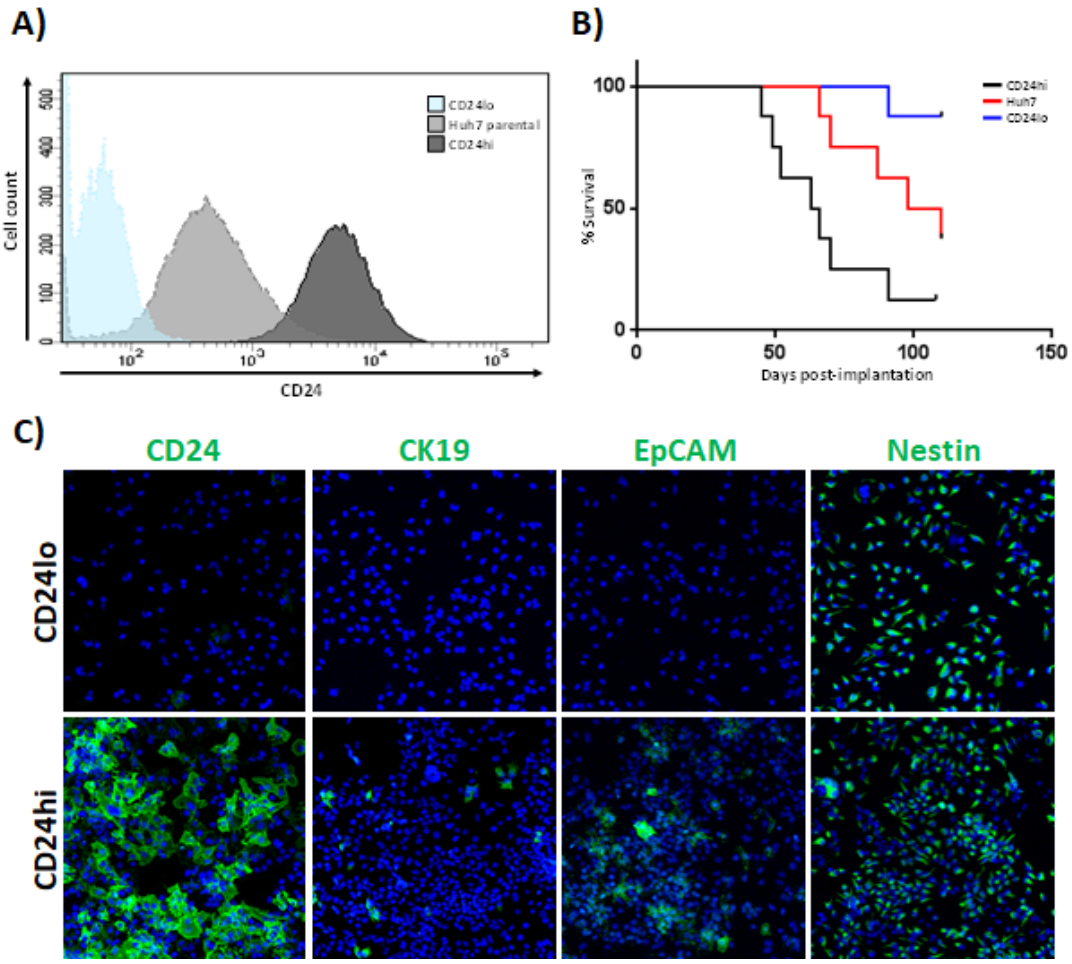


**Figure 3.4.1 Polyclonal Huh7 cells sorted for high and low expression of the cancer initiating cell marker CD24 by fluorescence-activated cell sorting**

A) Histogram of parental Huh7 cells (grey) sorted for high (dark grey) and low (light blue) expression of CIC marker CD24 (using an anti-CD24 antibody) by FACS. These results represent the second round of Huh7 cells sorting for CD24. B) Mouse xenograft experiment of CD24lo, CD24hi and parental Huh7 cells- Survival tumourigenicity SCID mouse xenografts experiment represented as percentage survival over the number of days post cell implantation. Eight mice were subcutaneously injected with either $1x10^5$ Huh7 parental cells, CD24hi cells or CD24lo cells (log rank test: CD24hi vs Huh7, p=0.0316, CD24hi vs CD24lo, p=0.0012, Huh7 vs CD24lo, p=0.0431). Experiments performed by Teklu Egnuni. C) Immunofluorescence of CD24hi and CD24lo Huh7 cells fixed in 4 % PFA in PBS and permeabilised. Cells were stained with DNA stain Hoechst (blue) and antibodies against CD24, Nestin, EpCAM or CK19. Alexa Fluor 488 nm fluorophore labelled secondary antibodies and images were taken using the 10x objective of the Nikon Eclipse Ti-E Widefield Fluorescent Inverted Microscope. Images are representative of cell density. Experiment performed by Matthew Bentham.

markers such as EpCAM and CK19 segregated with the CD24hi population (Figure 3.4.1C); Work carried out by Dr Matthew Bentham).

Thus, Huh7 CD24 low expressing cells were considered (hereafter referred to as CD24lo) as a more useful approximation to a non-transformed HPC compared with parental Huh7 cells or CD24hi cells, which bore the hallmarks of CICs. CD24lo cells supported HCV infection and replication to a similar degree as parental Huh7 cells (data not shown) and a polyclonal stable JFH1 replicon cell line was derived by G418 selection (referred to as CD24lo JFH1-replicon) (Figure 3.4.3). A control cell line to compare against G418 selected JFH1-replicon CD24lo cells was created by taking advantage of newly available DAAs (SOF and DCV) to 'cure' replicon cells of the viral RNA. This ensured that control cells retained the same provenance, with all subsequent experiments using equivalent stocks of these lines (Figure 3.4.3). In addition, Cured cells were more appropriate than an alternative control cell line where CD24lo cells were transfected with a G418 resistant plasmid (pcDNA3.1) and selected in parallel to replicons (Figure 3.4.3). These pcDNA3.1 CD24lo cells took on a distinct phenotype compared with either parental or control cells, with enhanced CIC marker expression and increased tumourigenicity (data not shown).

To confirm the complete removal of HCV RNA and antigen, Cured CD24lo cells re-challenged with G418 did not subsequently survive, unlike CD24lo JFH1-replicon cells. Moreover, western blotting and immunofluorescence for HCV NS5A protein and were both negative (Figure 3.4.2).

### 3.4.2 Differentiation of Huh7-derived cell sub-clones as a model of hepatic progenitor cell differentiation

DMSO has been shown to be effective for differentiating Huh7 cells (Sainz and Chisari, 2006, Choi et al., 2009, Mowbray et al., 2010). Reminiscent of HepaRG protocols, confluent (seeded at $3x10^5$/ml and left to settle overnight prior to the addition of DMSO) CD24lo and CD24hi cells were differentiated in the presence of 1.8 % DMSO for up to 11 days. Morphological changes were clearly observed in both CD24hi and CD24lo cells during differentiation; cells formed tightly packed islands, which displayed typical "cobblestone-like" features of primary hepatocytes (Herzog et al., 2016), alongside an obviously low nucleus-to-cytoplasm ratio (Figure 3.5.1). Such islands of hepatocyte-like cells were reminiscent of the islands that form during DMSO induced differentiation of HepaRG cells. Accordingly, expression of the hepatocyte marker CYP3A4 increased in both CD24hi and CD24lo cells as differentiation proceeded (Figure 3.5.2).

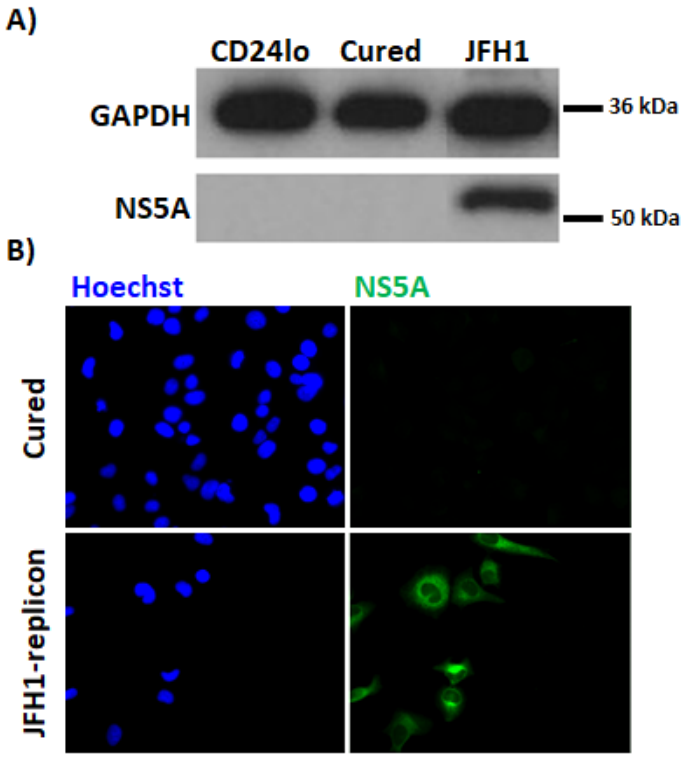


**Figure 3.4.2 Elimination of viral protein expression after DAA treatment of CD24lo cells harbouring the JFH1 replicon**

CD24lo cells harbouring the JFH1 replicon were treated with 1 µM SOF and DCV for two weeks. To confirm the CD24lo cells had been cured of the JFH1 replicon cells were analysed by western blot (A) and by immunofluorescence (B) and stained for viral protein NS5A (green) using an anti-NS5A antibody and an Alexa Fluor 488 nm fluorophore labelled secondary antibody. Images were taken using the 40x objective of the Nikon Eclipse Ti-E Widefield Fluorescent Inverted Microscope. Images are representative of cell density.

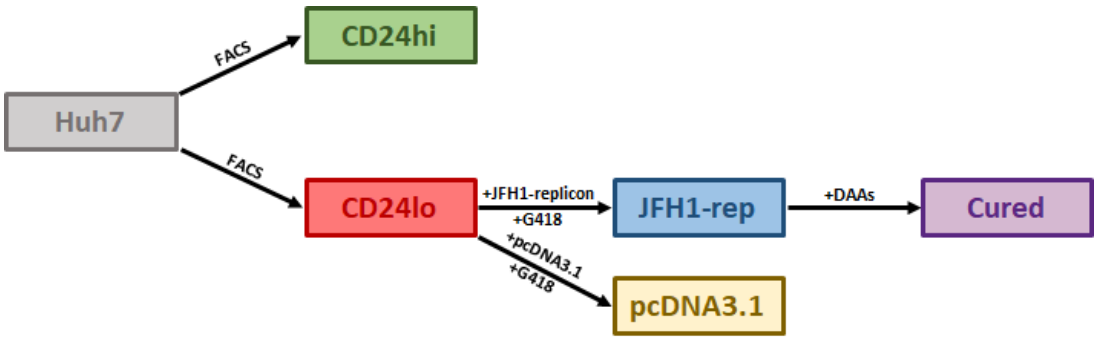


**Figure 3.4.3 Diagram of the derivation of cell culture models and lines used**

Huh7 cells were sorted by FACS for high and low cell surface expression of CD24, giving rise to two Huh7 lines: CD24hi and CD24lo. CD24lo Huh7 cells were transfected with the JFH1-replicon or the pcDNA3.1 plasmid and maintained under G418 selection to create a CD24lo cell line harbouring the JFH1 replicon named JFH1-rep and a G418 control line named pcDNA3.1 CD24lo cells. JFH1-rep CD24lo cells were then treated with 1 µM SOF and DCV for two weeks to cure the line of the JFH1 replicon and create the CD24lo Huh7 line named Cured. The Cured cells act as a control cell line to the CD24lo JFH1-rep cells.

Based on the observations that CD24lo cells were less tumourigenic in a mouse xenograft model and expressed lower levels of CIC markers, and that these cells can be induced to differentiate, CD24lo cells can be considered to be a robust HPC-like model for further experiments.

## 3.5 Discussion

To begin to understand our hypothetical link between chronic HCV infection and the development of HCC and to clarify which cells in the liver give rise to HCC CICs, we required a laboratory cell culture model. Relevant literature suggests that HCC CICs likely arise from dedifferentiated hepatocytes or from HPCs (Kitade et al., 2013, Chiba et al., 2007, Tschaharganeh et al., 2014, Shin et al., 2016, He et al., 2013a, Marquardt, 2016, Sia et al., 2017). HCC CICs cells have a mixed phenotype and express progenitor, hepatocyte and cholangiocyte markers such as CK19, AFP and EpCAM (Yamashita et al., 2008). During chronic HCV infection the liver is largely repopulated by the proliferation and differentiation of HPCs.

Our aim was to establish whether HCV is able to infect bi-potent HPCs and perturb the differentiation of these cells, thus potentially predisposing to the formation of HCC CICs. We were able to isolate HPCs from patient liver samples, based upon growth in defined media, rather than selection using one or more HPC markers. We determined that these cells were permissive to HCV infection via co-culture with J6-JFH1 chronically infected Huh7.5 cells. However HPC infection was sporadic and these cells were difficult to isolate in large numbers in order to conduct biochemical analysis.

Broadly speaking we took two approaches to developing an *in vitro* model system. In the first instance we took a non-transformed cell line which is well establish to mimic differentiation into both hepatocyte- and cholangiocyte-like cells (HepaRG) and tried to make it permissive for HCV infection. The alternative approach was to take the only known HCV permissive cell culture line (without the need of introducing HCV cofactors) (Huh7) and develop that towards a model mimicking hepatocyte differentiation. The HepaRG cell line appeared to be a useful alternative to *in vivo* derived HPC's to investigate whether HCV can perturb HPC differentiation. These cells behave similarly to bi-potent HPCs, plus whilst they are an immortal cell line they are not transformed, making them preferable to hepatoma-derived lines (Gripon et al., 2002, Parent et al., 2004).

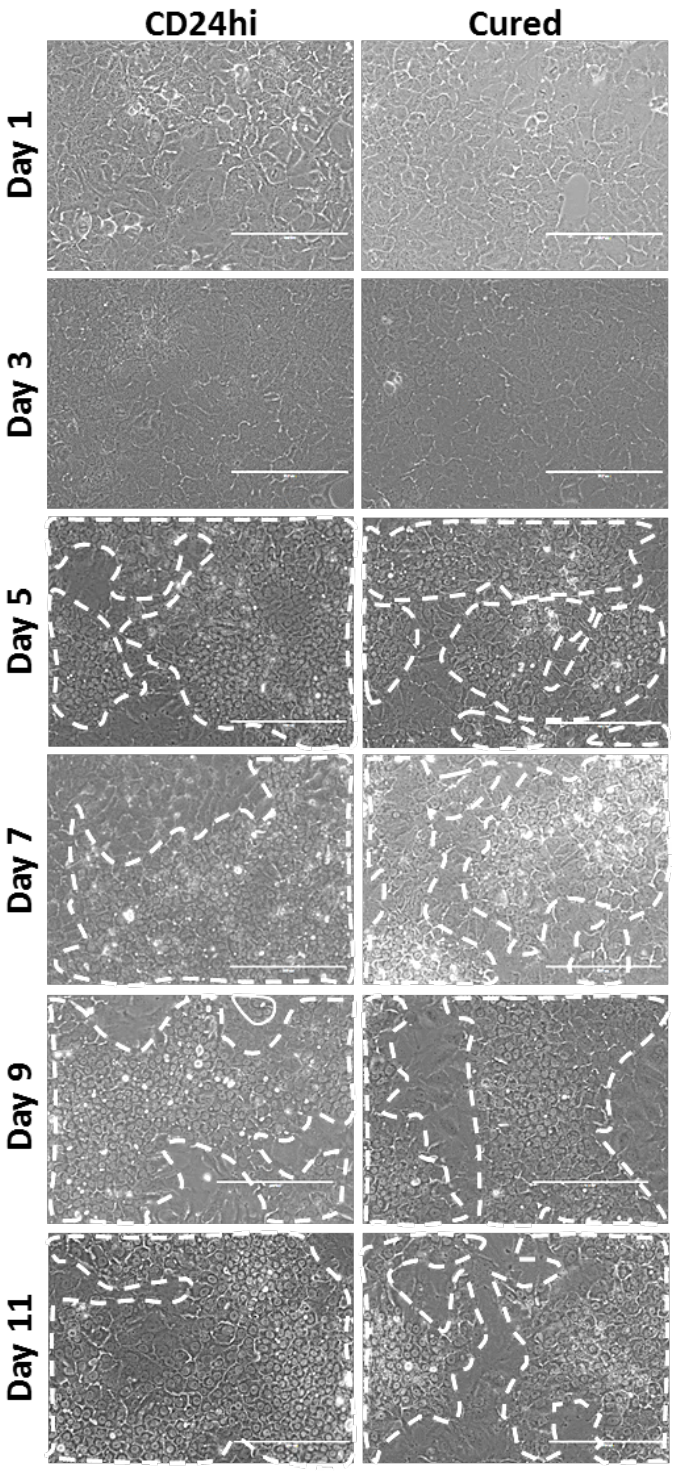


**Figure 3.5.1 Differentiation of CD24hi cells and Cured CD24lo cells**

Phase images of differentiating CD24hi and Cured CD24lo cells using the 20x objective of the EVOS cell imaging system. Images were taken on day one and every other day thereafter up to day eleven. Cells were seeding at $3x10^5$/ml and left to settle overnight. Confluent cells were differentiated by the addition of 1.8 % DMSO to the culture media. Hepatocyte-like cell islands which develop during differentiation are highlighted by the dashed lines. Images are representative of cell density.

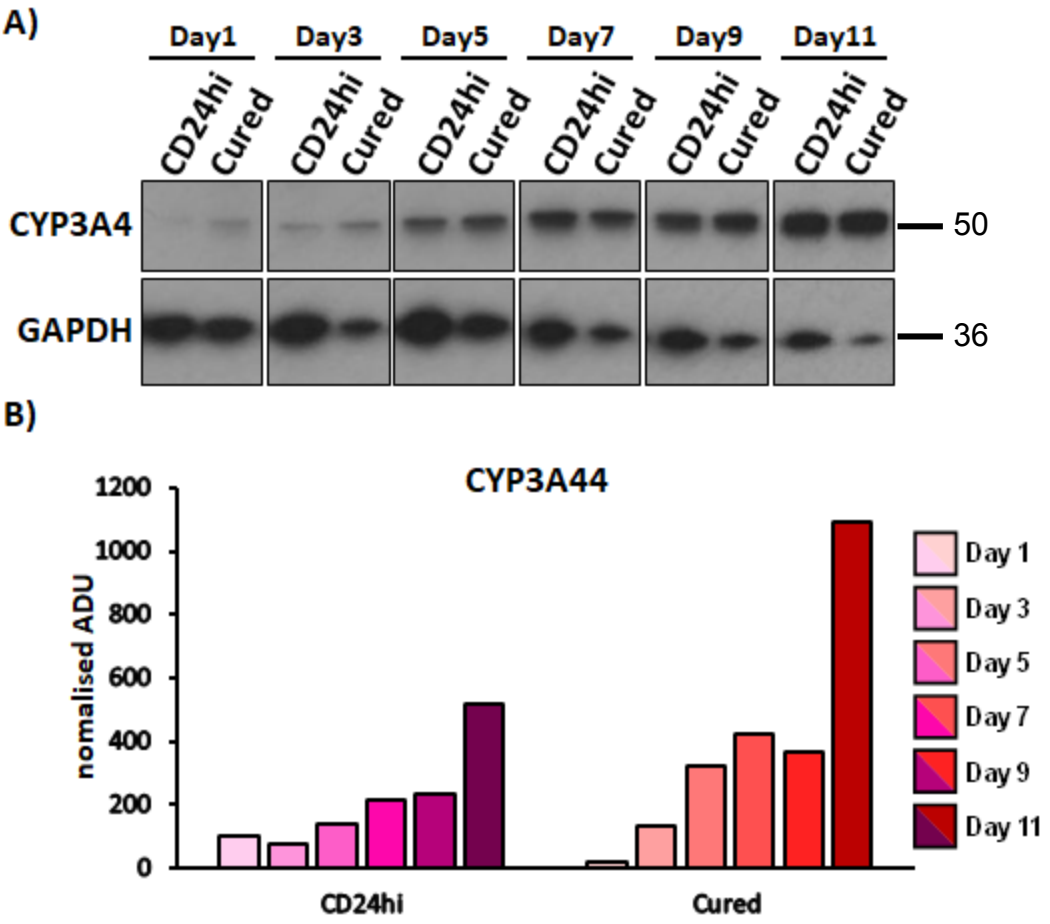


**Figure 3.5.2 Western blot for proteins CYP3A4 and GAPDH using differentiating CD24hi and CD24lo Cured cells**

CD24hi and CD24lo Cured cells were differentiated during which a well of a 6 well cell culture plate was lysed at day one and every two days up to day eleven for western blot analysis. A) Membranes were stained using anti-CYP3A4 and anti-GAPDH antibodies. B) Quantification of CYP3A4 western blot band intensity (Arbitrary densitometry units (ADU)) normalised to GAPDH band intensity using ImageJ and displayed as a percentage of Cured Day 1.

HepaRG cells have the ability to differentiate into hepatocyte-like and cholangiocyte-like cells, as well as then de-differentiating upon re-plating and retaining the capability to differentiate again in response to DMSO. Considerable effort was devoted to establish whether HepaRG cells are permissive to infection by cell culture HCV strains. Only one group so far have demonstrated HepaRG cells to be permissive to HCV using serum-derived HCV particles (Ndongo-Thiam et al., 2011). The infection was performed at day three post-plating (progenitor state); from day 14 post plating (differentiating HepaRG cells) extracellular HCV RNA was detected by qPCR. HCV particles released from the infected HepaRG cells were found to be infectious and able to infect naïve HepaRG cells. HepaRG cells were allowed to differentiate for these experiments whereas HepaRG cells were maintained at the progenitor cell state during our experiments. It would have been interesting to investigate how the infection compares at different stages along the differentiation and whether differentiation would have increased permissiveness.

We instead focused on whether HepaRG cells at the progenitor-like stage were permissive to cell culture derived HCV or the JFH1-replicon. Infection using cell culture derived HCV in comparison to serum-derived HCV samples can produce higher yields in other cell lines, the infection is more reproducible and supports the potential use of reverse genetics for future experiments. Wild-type ‘progenitor’-stage HepaRG cells were transfected with the G418 resistant JFH1-replicon and puromycin-resistant N17-replicon and subjected to antibiotic selection in an attempt to establish a stable HepaRG cell line harbouring a HCV replicon. Early signs during the antibiotic selection encouraged the belief that HepaRG cells were permissive, as HCV-replicon transfected cells had a prolonged survival time under antibiotic selection when compared to control cell. However after a prolonged culture of transfected HepaRGs, cells would become growth arrested and senescent and ultimately undergo cell death. In addition, transfected and selected HepaRG cells were found to not express viral protein NS5A and HCV RNA was undetectable by RT-PCR.

Due to the fact that transfected HepaRG cells appeared to survive under G418 and puromycin selection (depending on the construct used) but we were subsequently unable to detect any HCV antigen or luciferase activity may mean that the virus is unable to replicate in HepaRG cells but at such low levels to be beneath the limit of detection for IF, luciferase, or PCR assays. Indeed evidence exists that HCV can persist in cells at very low

levels even after treatment with interferon, DAAs or instances of spontaneous clearance resulting in apparent SVR (Chen et al., 2015a, Chen et al., 2013a, Pham et al., 2010, Pham et al., 2004). The development of a PCR assay which had enhanced sensitivity led to the identification of a form of HCV infection which has been shown to persist even in the presence of HCV antibodies and with apparent normal levels of liver enzymes after spontaneous clearance or antiviral therapy induced resolution. This has been referred to as occult HCV (Pham et al., 2010). During occult HCV infection HCV RNA is detected either in the liver or in PBMCs (Carreno, 2006). The existence of occult HCV is controversial, however increasing evidence supports the occurrence of this type of infection (Attar and Van Thiel, 2015). During occult infection HCV RNA was detected and found to not exceed 200 genome copies/ml of serum whereas during 'normal' infection HCV RNA levels are around $1x10^9$ copies/ml. Ndongo-Thiam et al., observed that 4-7 days after infection of HepaRG cells, HCV became undetectable using their PCR method but subsequently became detectable again after cells began to differentiate. It is plausible that in our experiments using JFH1 based virus and replicon, HCV RNA is able to infect progenitor-like HepaRG cells and persist at a low level. Our experiments showed us that HCV is able to infect HepaRGs which have been transduced with miR-122 and V protein and that replicon transfected HepaRG cells can persist during selection when the mock electroporated cells die, making it a possibility that HCV is able to persist at very low levels (below the limit of detection of our assays: Western blot, IF, PCR and luciferase).

It was possible that the intact and robust interferon response within HepaRG cells (Lucifora et al., 2010) was responsible for very low levels of HCV replicon replication, resulting in increasingly low levels of antibiotic resistance gene expression and eventual elimination of the virus from cell cultures. Thus, HepaRG cells were transduced with a lentivirus encoding the V proteins from either measles virus or parainfluenza virus 5, which are known to vigorously suppress both interferon production and responses. It is important to note that we did not confirm whether the interferon response was effectively suppressed, this would have been an important aspect to validate if we had taken the HepaRG line forward.

In addition we hypothesised that HepaRG cells may lack sufficient expression of HCV cofactors such as miR-122. Transcription of miR-122 is important for liver development and is switched on by liver enriched transcription factors (TFs) such as HNF6. HNF6 and miR-122 exist in a

positive feedback loop, which drives differentiation and leads to increased levels as differentiation proceeds (Laudadio et al., 2012). Thus HepaRG cells particularly at the progenitor-like stage may have an insufficient level of miR-122 transcription. Jung et al., showed that miR-122 was the most strongly upregulated miRNA upon HepaRG differentiation, by almost 2000 fold from day 2 to day 28 (Jung et al., 2016). However, according to Murrone et al., miR-122 was not the most abundant miRNA in terminally differentiated HepaRG cells (Marrone et al., 2016). Previous observations have demonstrated that hepatocellular cell lines express lower levels of miR-122 compared to primary hepatocytes however the cell lines tested only included HepG2, Huh7 and Hep3B cells (Song et al., 2013). These cell lines are however still able to support HCV replication. To determine whether a possible lack of miR-122 could enhance HepaRG cell permissiveness to HCV, miR-122 was also introduced by lentivirus transduction, however miR-122 on its own was not enough to increase HepaRG permissiveness to HCV.

Evidence of HCV replication was only obtained when HepaRGs were co-transfected with both miR-122 and the V protein, additionally a very high MOI (about 50 FFU/cell) was needed, yet the number of cells infected was low. HepaRG cells may lack expression of further HCV cofactors such as SEC14L2 (Saeed et al., 2015), phosphatidylinositol 4-kinase III alpha (PI4KA) (Berger et al., 2009, Borawski et al., 2009, Li et al., 2009) or cyclophilin A (CypA) (Kaul et al., 2009, Yang et al., 2008a) and are thus unable to support replication and virus production. However Huh7 and HepaRG cells have been shown to express higher amounts of PI4KA mRNA than normal hepatic specimens (Ilboudo et al., 2014). CypA is also detectable in both differentiated and non-differentiated HepaRG cells (Petrareanu et al., 2013). Moreover, we have shown that HepaRG cells express known HCV entry factors such as Occludin and CD81 (Figure 3.3.2). This leaves the possibility of unknown factors.

Another reason why we could not establish efficient HCV infection may be that HepaRG cells are not permissive to the viral clones used in cell culture and are unable to tolerate the cell culture adaptations of these strains. HepaRG cells appear to be closer to primary cells than other hepatocellular cell lines such as HepG2 and Huh7 cells. This may be the reason why cell culture adapted strains and JFH1 based viral constructs are unable to persist in these cells. Bukh et al., showed that a Con1 genome containing cell culture adaptive mutations led to increased replication levels in cell

culture. However the same transcript failed to achieve HCV infection of chimpanzees compared to the WT Con1 genome (Bukh et al., 2002).

Having exhausting the most likely co-factors to enhance HCV infection of HepaRG cells we next tried to take an permissive cell line and adapt that to a differentiation model. Huh7 cells are permissive to HCV infection and support a high level of replication however these cells are transformed. Huh7 cells are known to be polyclonal (Sainz et al., 2009a) which opens up the possibility of sorting these cells for low expression of CIC markers. Lee and colleagues found that HCC patients with high CD24 expressing tumours cells had a reduced survival rate compared to patients with CD24low expressing tumours (Lee et al., 2011). Huh7 cells sorted for low expression of CD24 were found to be less tumourigenic *in vivo* and expressed lower levels of other CIC markers such as EpCAM. CD24lo cells were found to support HCV replication to a similar level as parental Huh7 cells thus the CD24lo represents a better cellular model to investigate the link between HCV infection and the development of HCC. Lee et al., also found that cell populations expressing high levels of CD24 overlapped with other CIC markers including EpCAM and CD133 and suggested that these markers may share common self-renewal pathways (Lee et al., 2011), possibly via Nanog. The EpCAM locus is directly bound by Nanog (Polo et al., 2012) whereas CD133 is regulated by STAT3 which is itself amplified by Nanog (Ghoshal et al., 2016, Stuart et al., 2014). Other Huh7 subclones have in the past been isolated, however, these have usually been selected due to increased permissiveness to virus replication, for example Huh7.5s (Blight et al., 2002). We are unaware of a similar less tumourigenic Huh7 subclone.

Huh7 cells can be chemically induced to differentiate, as has been shown previously in the literature (Choi et al., 2009, Sainz and Chisari, 2006). The mechanism behind DMSO induced differentiation is unclear. DMSO is however, used in many differentiation protocols for both primary cells and cell lines (Cable and Isom, 1997, Azuma et al., 2003, Cheung et al., 2006, Villa et al., 1991). DMSO affects cell membrane integrity (Melkonyan et al., 1996), and alters intracellular signalling pathways such as Wnt/β-catenin and TGF-β signalling. Postulated to occur via upregulation of Wnt molecules such as Wnt2a and Wnt9a and TGF-β family members such as Tgfb1 and Gdf1 (Fiore and Degrassi, 1999, Makowske et al., 1988, Choi et al., 2015) and alternative mRNA splicing (Bolduc et al., 2001). The addition of DMSO to the culture medium induces several changes to CD24lo and CD24hi cells alike. Clear morphological changes became apparent; islands of hepatocyte-

like cells developed over the course of an 11 day differentiation. These islands consisted of cuboidal cells with a low nucleus-to-cytoplasm ratio and clear border definition which resembled primary hepatocytes more closely than proliferating Huh7 cells. Alongside these morphological changes both CD24lo and CD24hi Huh7 cells increased expression of the hepatocyte marker CYP3A4 which is an enzyme involved in drug metabolism and synthesis of cholesterol and steroids. Our results of differentiating CD24lo Huh7 cells confirmed previous findings of differentiating Huh7 cells. Similar morphological changes were observed by Sainz & Chisari, who also observed tightly packed monolayers with cells with a low nucleus-to-cytoplasm ratio and multiple distinct nucleoli. Similar to our observations of culturing CD24lo Huh7 cells in the absence of DMSO, Sainz & Chisari also observed how in the absence of DMSO Huh7 cells initially start to form a similarly tight monolayer however this monolayer becomes compromised and increased cell death follows. We observed that CD24lo Huh7 cells appear to continue to proliferate in the absence of DMSO, appear to lack cell contact induced growth arrest and followed by an increase in cell death. Concordant with our observations of increased hepatocyte marker expression (Figure 3.5.2) previous studies also measured an increase in albumin RNA levels alongside other markers such as alpha-1-antitrypsin (A1AT) and HNF4α. Choi *et al*., not only measured increased expression of P450 metabolic enzymes including CYP3A4 but also measured the activity of these enzymes which increased upon DMSO driven differentiation. These indicate that like polyclonal Huh7 cells CD24lo cells can be induced to differentiate further and can serve as a model of hepatic differentiation.

In summary, of the two potential cellular models evaluated to use to investigate whether HCV can perturb hepatocyte differentiation, only one was actually permissive for HCV replication to detectable levels. As the initial assays indicated that both model systems were amenable to differentiation (via DMSO) we therefore took the permissive CD24lo Huh7 line forward as a candidate model system.

# 4. Chapter: The influence of HCV infection on CD24lo Huh7 cellular differentiation

## 4.1 Introduction

As introduced in Chapter 3, DMSO can be used to differentiate Huh7 cells (Sainz and Chisari, 2006, Choi et al., 2009, Mowbray et al., 2010). Similar to previous studies of DMSO treated Huh7 cells, CD24lo cells become growth arrested and undergo morphological changes. These morphological changes manifested in the development of islands of hepatocyte-like cells which resembled the “cobblestone-like” features of primary hepatocytes (Herzog et al., 2016). In addition these hepatocyte-like cells displayed a low nucleus to cytoplasm ratio and multiple distinct nucleoli similar to primary hepatocytes. As well as exhibiting morphological changes reminiscent of hepatocytes; DMSO treated Huh7 cells expressed higher levels of hepatocyte markers such as albumin and drug-metabolising enzymes such as CYP3A4 (Choi et al., 2009). We observed a similar increase in expression of the metabolic enzyme CYP3A4 when CD24lo and CD24hi Huh7 cells were differentiated using DMSO. The next step was to determine what effect HCV infection, either using the JFH1-replicon or the J6-JFH1 full length virus, had upon DMSO induced differentiation of CD24lo cells.

## 4.2 HCV infection perturbs CD24lo cell differentiation

### 4.2.1 HCV infection delays and reduces CD24lo cell differentiation associated morphological changes

Huh7 cells were sorted into a subpopulation of cells expressing low levels of CD24, a CIC marker (see section 3.4.1). These CD24lo cells were found to be less tumourigenic in a mouse xenograft model compared to parental Huh7 and CD24high cells. Based on this, lower expression of selected CIC markers (EpCAM, CK19 etc.), and the fact that these cells can be induced to differentiate, CD24lo cells were considered to be a more useful approximation to HPCs compared with more heterogeneous cultures of parental Huh7 cells. CD24lo Huh7 cells were chosen as a tractable, robust model capable of accommodating HCV infection. Alternative models such as deriving HPC-like cells from iPSCs or from embryonic stem cells (ESCs) were considered but disregarded based on cost and time constraints. A CD24lo line stably expressing the JFH1-replicon was first derived by G418

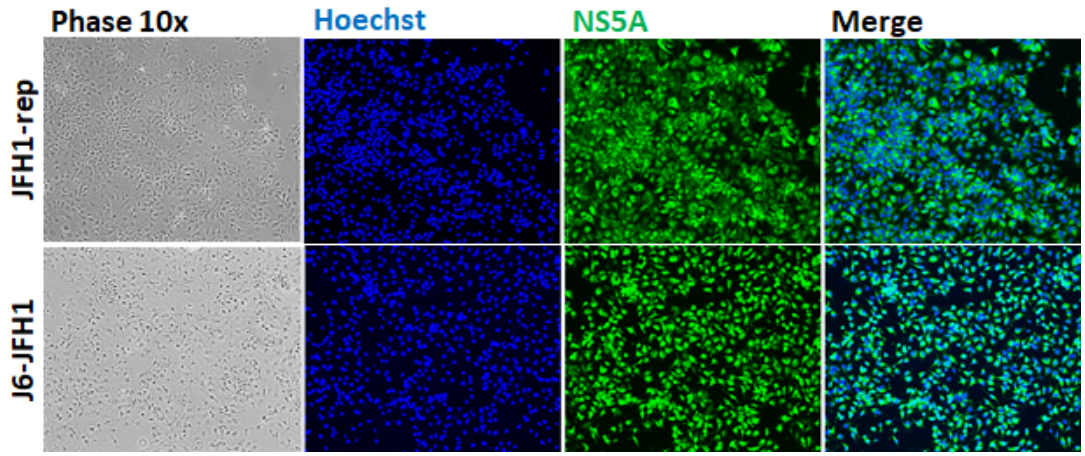


**Figure 4.2.1 NS5A expression of CD24lo JFH1-rep and chronically infected JFH1-J6 CD24lo cells**

CD24lo cells either harbouring the JFH1-replicon or chronically infected with full length JFH1-J6 were fixed using 4 % PFA, permeabilised and stained for HCV NS5A expression using polyclonal anti-NS5A antibodies and Alex Fluor 488 nm conjugated secondary antibodies. Images are representative of cell density.

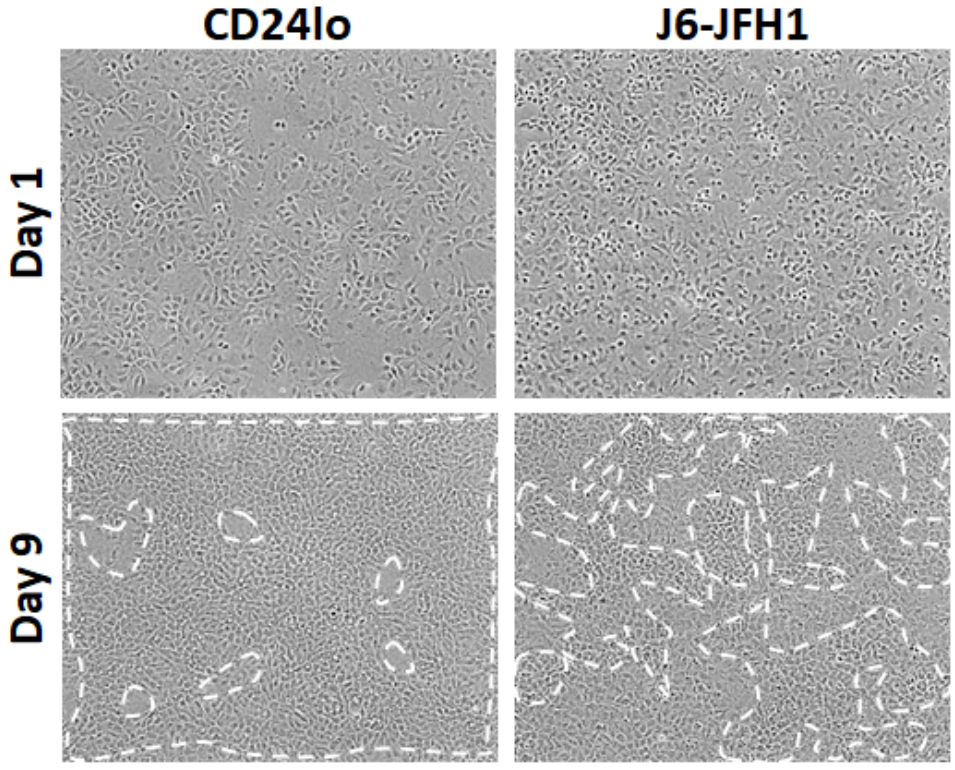


**Figure 4.2.2 Phase images of the differentiation of CD24lo cells and J6-JFH1 infected CD24lo cells**

CD24lo cells and chronically infected cells were differentiated over the course of nine days by the addition of 1.8 % DMSO to the culture media. The media was changed every two days and phase images were taken on the 10x objective of the Nikon Eclipse Ti-E Widefield Fluorescent Inverted Microscope from samples fixed in 4 % PFA in PBS on day one and nine of differentiation. Highlighted by white dashed lines are the islands of cells which have undergone a morphological change and are more hepatocyte-like in appearance. Images are representative of cell density.

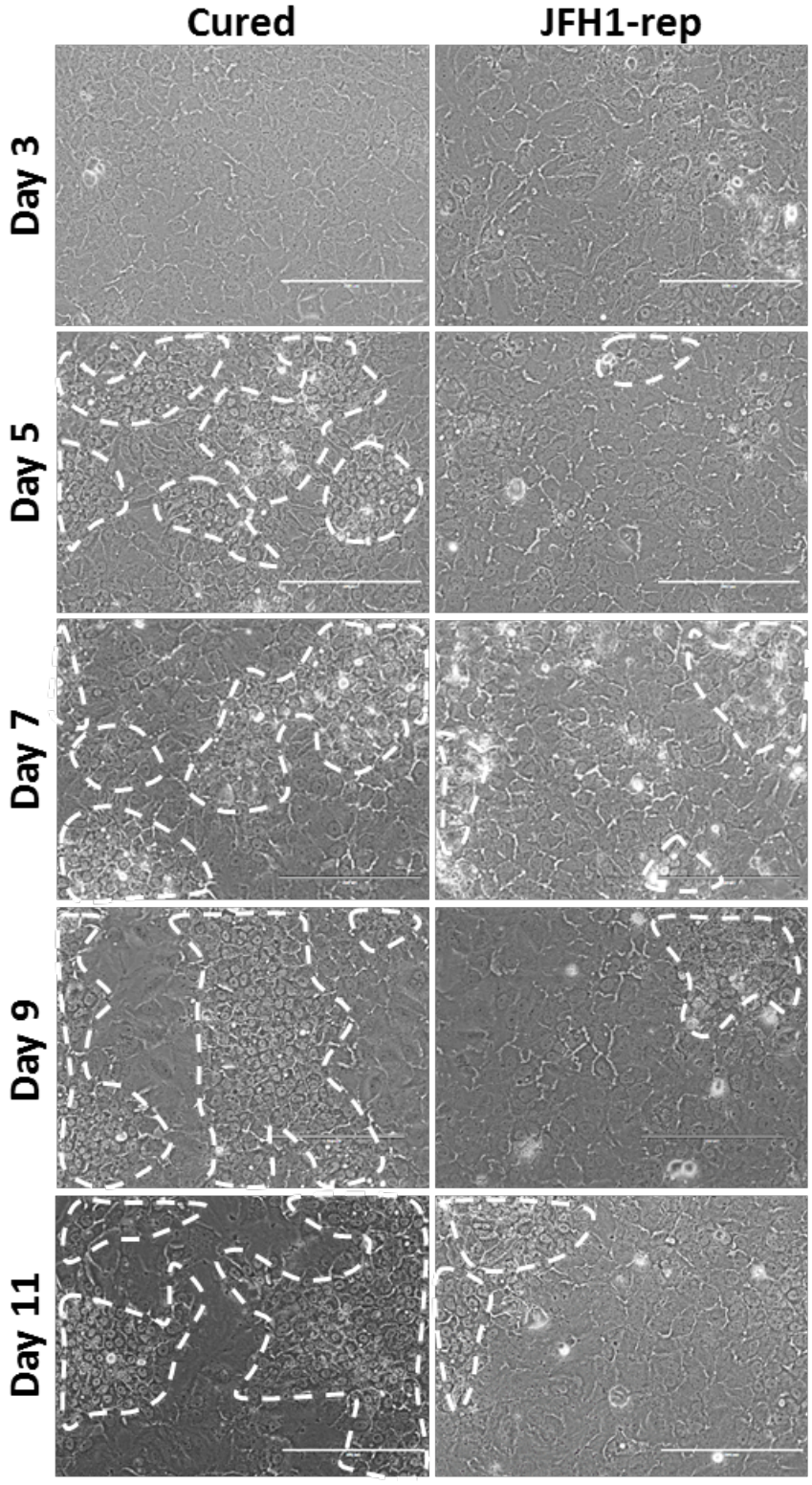


**Figure 4.2.3 Phase images of DMSO-differentiated Cured and JFH1-replicon containing CD24lo cells**

Cured and JFH1-replicon CD24lo cells were differentiated over the course of eleven days by the addition of 1.8 % DMSO to the culture media. The media was changed every two days and phase images were taken on the 20x objective of the EVOS cell imaging system. Highlighted by white dashed lines are the islands of cells which have undergone a morphological change and are more hepatocyte-like in appearance. Images are representative of cell density.

selection, followed by a control cell line where cells were “cured” of the replicon using DAAs (SOF & DCV), referred to hereafter as Cured. Using cell culture infection models also provides a measured and defined means of investigating the effect of HCV infection of differentiation. These replicon lines were compared to parental CD24lo chronically infected with the J6-JFH1 full length virus, providing a means to compare between the complete virus lifecycle and expression of the minimal HCV replicase (NS3, 4A/B, 5A/B).

When CD24lo JFH1-replicon cells were differentiated using DMSO alongside Cured CD24lo cells, we observed not only that the expected hepatocyte-like morphological changes were delayed, but that the JFH1-replicon cells developed far fewer islands of hepatocyte-like cells by day eleven of differentiation (Figure 4.2.3). These same morphological differences were observed when CD24lo and chronically infected J6-JFH1 CD24lo cells (Figure 4.2.1) were differentiated (Figure 4.2.2); further supporting the observed changes were dependent on viral infection.

### 4.2.2 Differentiation associated protein expression are altered by HCV infection

Previous studies have demonstrated that DMSO induced differentiation of Huh7 cells alters expression of multiple proteins, including albumin, A1AT, P450 enzymes and HNF4α and proliferation (Choi et al., 2009, Sainz and Chisari, 2006), indicative of cells both exiting the cell cycle and activating hepatocyte-like transcriptional programmes. We chose to monitor expression of ki67, albumin and CYP3A4 to serve as markers for cell cycle exit (into G0) and hepatocyte differentiation, respectively, with a view to determining whether morphological changes induced by HCV infection alters the outcome of chemical differentiation. Ki67 is a nuclear protein that is expressed during all active phases of the cell cycle from G1 to M phase (Gerdes et al., 1991), particularly M phase (Sobecki et al., 2017), and so is commonly used as a marker of proliferation (Scholzen and Gerdes, 2000). However, ki67 may still be expressed by $G_1$/S or $G_2$/M cell cycle arrested cells and it is therefore an indirect marker (van Oijen et al., 1998). As expected, the majority of proliferating CD24lo, Cured JFH1-replicon and J6-JFH1 cells expressed ki67 on day one of differentiation (Figure 4.2.4, Figure 4.2.5, Figure 4.2.6, Figure 4.2.7, Figure 4.2.9 & Figure 4.2.10). However, for CD24lo and Cured cells by day nine ki67 levels decreased close to the limit of detection (by western blot and immunofluorescence) (Figure 4.2.4, Figure 4.2.5, Figure 4.2.7 & Figure 4.2.9).

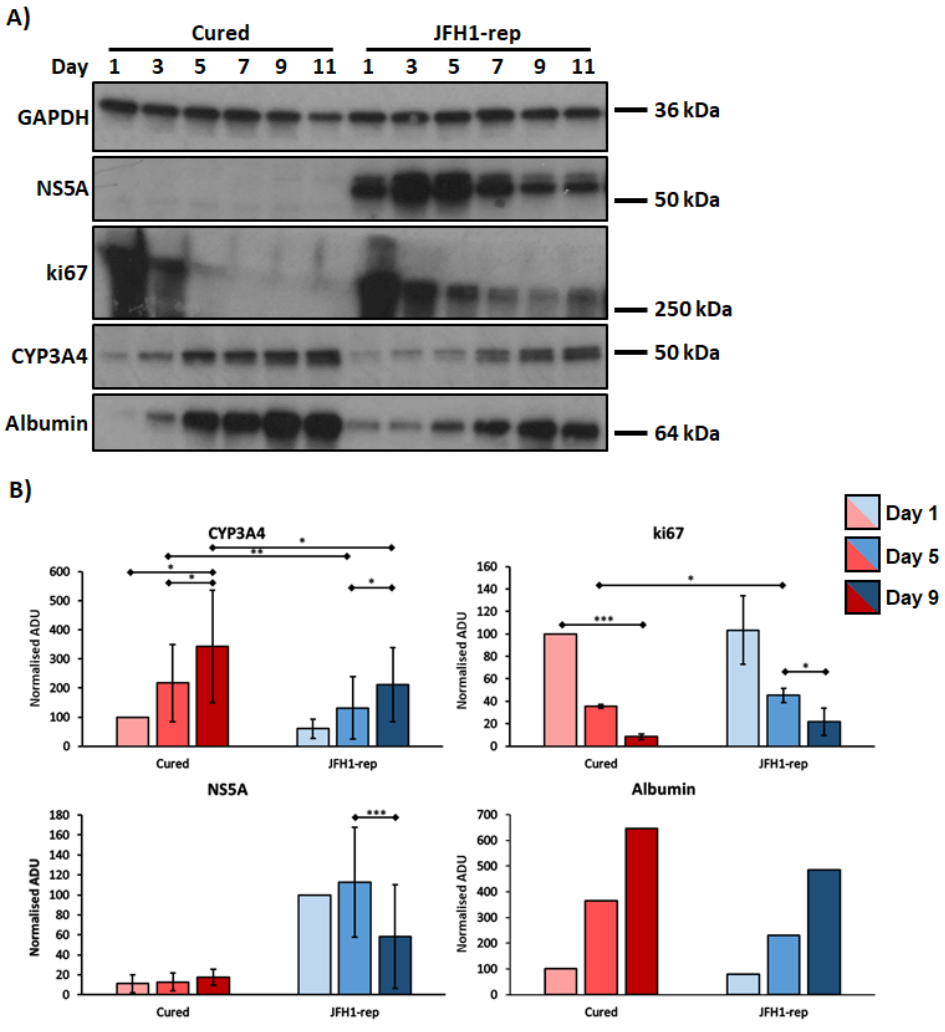


C)

| Two-tailed Student T-test | | | | | |
|---|---|---|---|---|---|
| NS5A | | ki67 | | CYP3A4 | |
| Conditions | p-value | Conditions | p-value | Conditions | p-value |
| | | C1- C5 | 0.008 | C1- C5 | 0.121 |
| | | C1-C9 | 0.0003 | C1-C9 | 0.048 |
| | | C1-J1 | 0.867 | C1-J1 | 0.051 |
| | | C1-J5 | 0.004 | C1-J5 | 0.554 |
| | | C1-J9 | 0.008 | C1-J9 | 0.123 |
| | | C5-C9 | 0.377 | C5-C9 | 0.017 |
| | | C5-J1 | 0.214 | C5-J1 | 0.058 |
| | | C5-J5 | 0.018 | C5-J5 | 0.010 |
| | | C5-C9 | 0.698 | C5-C9 | 0.771 |
| | | C9-J1 | 0.037 | C9-J1 | 0.032 |
| | | C9-J5 | 0.018 | C9-J5 | 0.010 |
| | | C9-J9 | 0.222 | C9-J9 | 0.019 |
| J1-J5 | 0.5589 | J1-J5 | 0.069 | J1-J5 | 0.187 |
| J1-J9 | 0.0781 | J1-J9 | 0.054 | J1-J9 | 0.061 |
| J5-J9 | 0.0002 | J5-J9 | 0.036 | J5-J9 | 0.030 |

**Figure 4.2.4 Protein levels of differentiated Cured and JFH1-rep cells**

A) Cells were differentiated over a course of nine days with media changes every two days. Approximately $1x10^6$ cells were lysed for Western blot analysis on days one, five and nine. Membranes were probed for GAPDH, NS5A, ki67, CYP3A4 or albumin. B) Quantification of NS5A, ki67, CYP3A4 and albumin western blot intensity (arbitrary densitometry units (ADU)) normalised to GAPDH band intensity using ImageJ. Displayed as the percentage of Cured Day 1 for except NS5A which is displayed as the percentage of JFH1-rep Day 1. Two-tailed Student t-test, * ≤0.05, **≤0.01, ***≤0.00; NS5A n=7, ki67 n=3, CYP3A4 n=5 and albumin n=2.

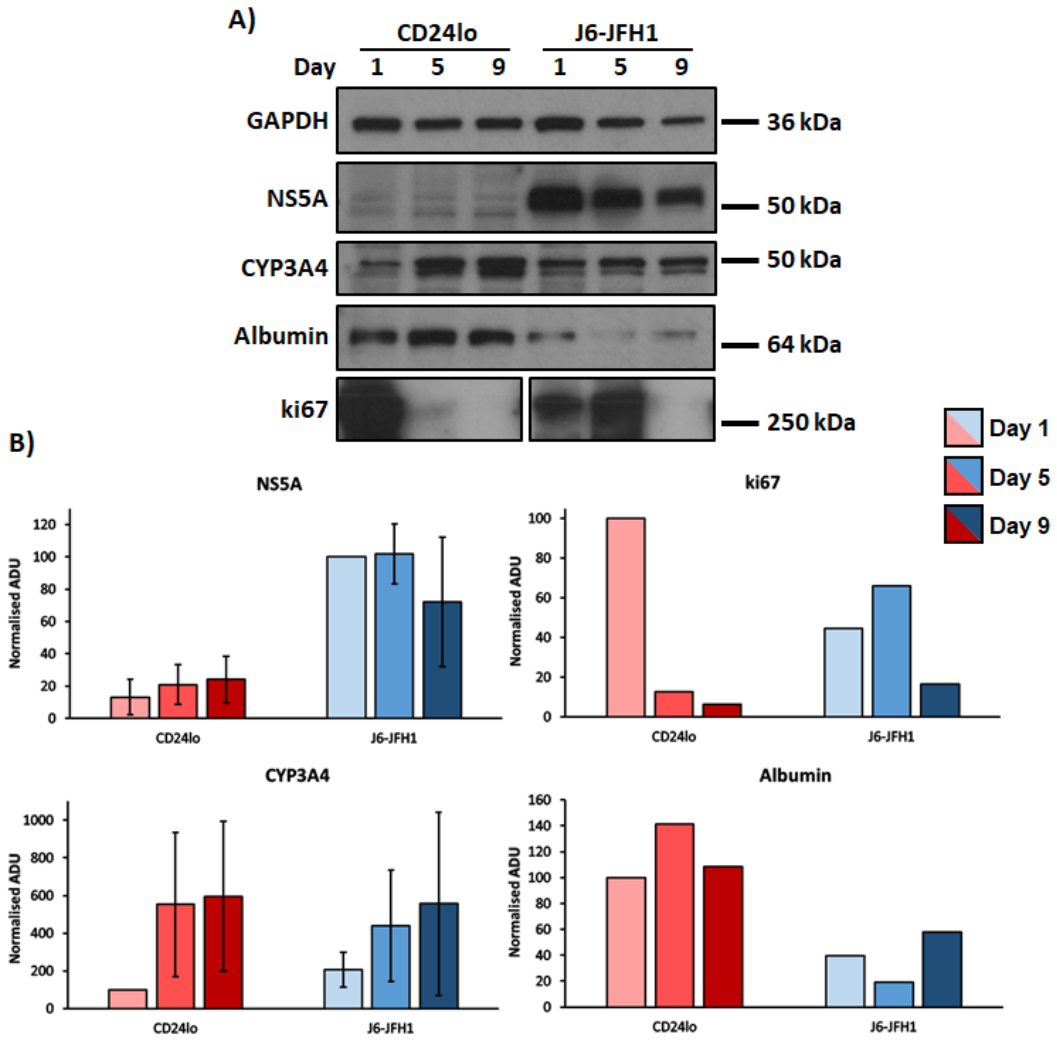


**Figure 4.2.5 Western blot of differentiated CD24lo and J6-JFH1 virus CD24lo cells**

A) Cells were differentiated over a course of nine days during which the media was changed every two days. About $1x10^6$ cells were lysed for Western blot analysis on days one, five and nine. Membranes were probed for GAPDH, NS5A, ki67, CYP3A4 or albumin. B) Quantification of NS5A, ki67, CYP3A4 and albumin western blot intensity measured as arbitrary densitometry units (ADU) normalised to GAPDH band intensity using ImageJ. Displayed as the percentage of CD24lo Day 1 for except NS5A which is displayed as the percentage of J6-JFH1 Day 1. Two-tailed Student t-test, *≤0.05, **≤0.01, ***≤0.001; NS5A n=3, ki67 n=2, CYP3A4 n=3 and albumin n=1. Results for NS5A and CYP3A4 were not statistically significant.

This decrease in ki67 was considerably less marked within HCV infected cells, with clear maintenance of ki67 levels compared with control cells. This trend was readily apparent on multiple western blots, with quantitation by densitometry attaining statistical significance on day five of differentiation (Figure 4.2.4, Figure 4.2.5, Figure 4.2.7 & Figure 4.2.9). By immunofluorescence we observed that JFH1-replicon cells and J6-JFH1 infected cells retained a significantly higher number (20.4 % and 11.2 % respectively) of ki67 positive cells on day nine of differentiation compared to Cured (3.3 %) and CD24lo cells (1.6 %) respectively (Figure 4.2.6, Figure 4.2.7 & Figure 4.2.9). We also confirmed these data on a single cell basis using flow-cytometry of differentiated Cured and JFH1-replicon cells, measuring both MFI and the percentage ki67 positive nuclei. The percentage of ki67 positive Cured cells dropped from 43 % at day one to just 4.2 % at day nine, whereas CD24lo cells harbouring the JFH1-replicon maintained 10.2 % ki67 positive cells at day nine from at 37.3 % at day one (Figure 4.2.10).

Hepatocyte function includes synthesis of the serum protein albumin (Zorn, 2008), as well as catabolic drug metabolism through the expression of xenobiotic enzymes such as CYP3A4. CYP3A4 is a member of the cytochrome P450 superfamily of enzymes and is involved in the metabolism of many commonly used drugs (Wilkinson, 2005). Accordingly, both are commonly used as hepatocyte markers. Differentiation of CD24lo cells led to an increase in expression for these hepatocyte markers (Figure 4.2.4 & Figure 4.2.5). Strikingly, the increase in CYP3A4 and albumin was dramatically reduced within HCV-infected (replicon or full length virus) CD24lo cells, including a statistically significant increase in CYP3A4 levels at day nine of differentiation in Cured cells compared to JFH1-replicon cells by western blot densitometry (Figure 4.2.4 & Figure 4.2.5). Measuring the MFI of IF images also confirmed that albumin expression was significantly higher in Cured and cells at day nine compared to JFH1-replicon cells (Figure 4.2.6 & Figure 4.2.7). The MFI was used as a measure of the level of Albumin expression. Due to the nature of the staining we were unable to measure the number of albumin positive cells.

The change in expression level of albumin, CYP3A4 and ki67 indicated that CD24lo cells are exiting the cell cycle and undergoing a process of differentiation however the altered pattern of HCV infected CD24lo cells suggested that the virus was perturbing this process and the cells were unable to differentiate to the same extent.

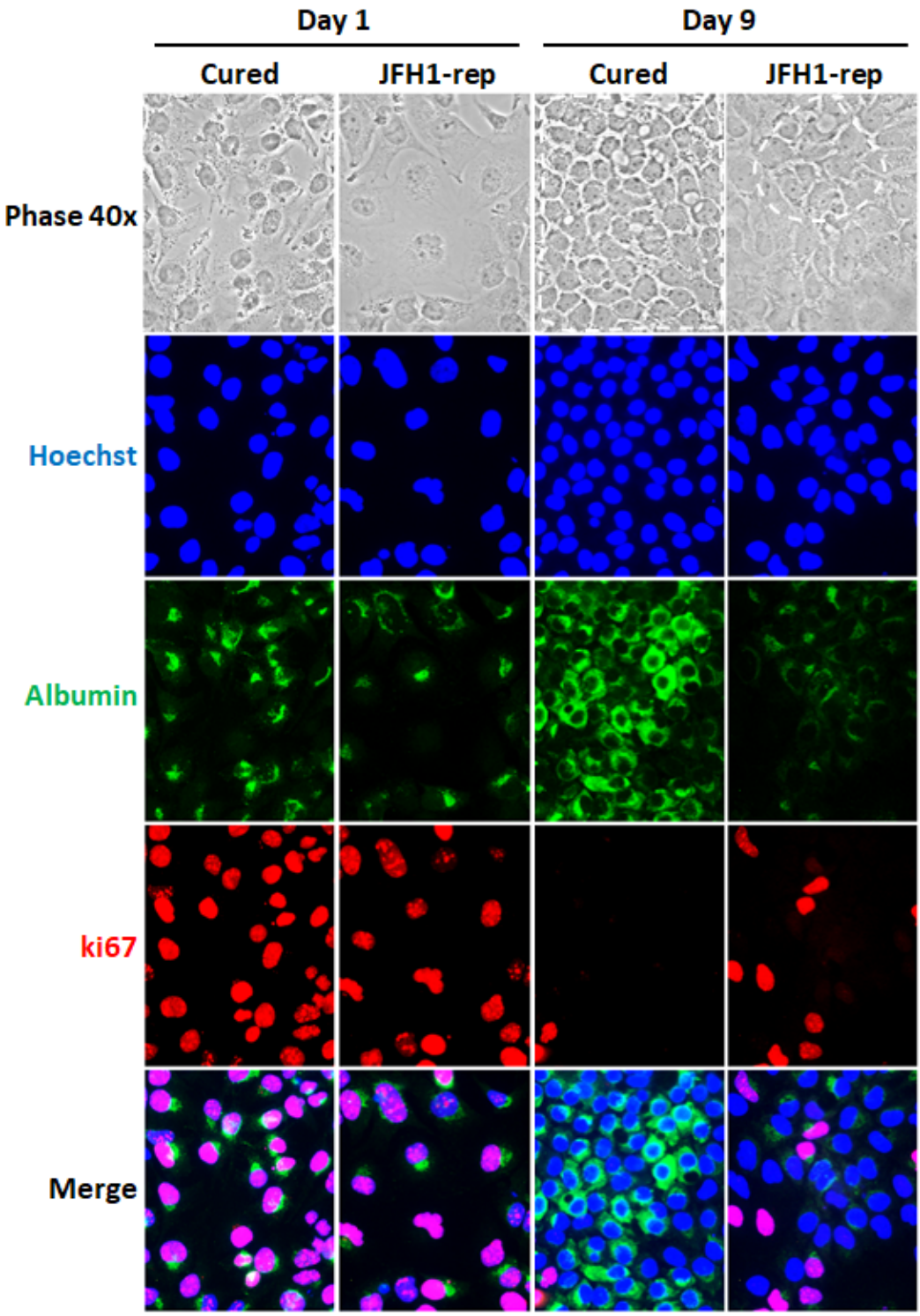


**Figure 4.2.6 Immunofluorescence of differentiated Cured and JFH1-replicon CD24lo cells**

Cells were differentiated on cover slips in a 12 well plate and fixed using 4 % PFA at day one and day nine of differentiation. The cells were then permeabilised using 0.2 % Triton-X100 and stained using antibodies against albumin (green) and ki67 (red) and 488 nm and 594 nm fluorescently labelled Alexa fluor secondary antibodies respectively. The nuclei were counterstained using DNA stain Hoechst. Images were taken using the 40x objective of the Nikon Eclipse Ti-E Widefield Fluorescent Inverted Microscope. Islands of hepatocyte-like cells are highlighted by dashed white lines. Images are representative of cell density.

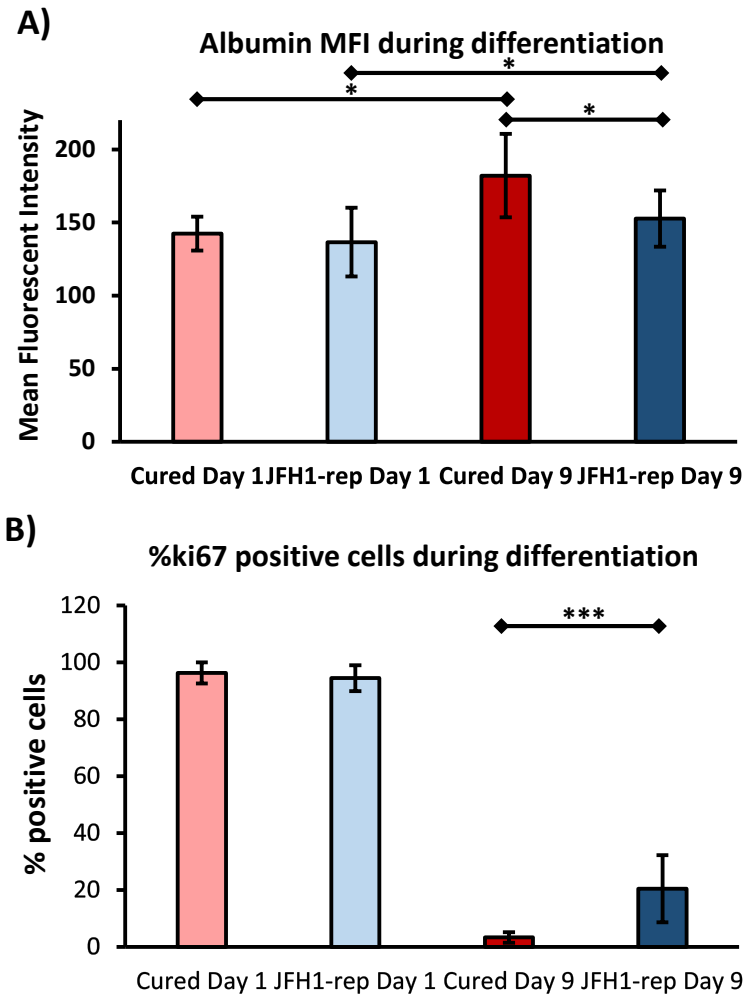


**Figure 4.2.7 Quantification of IF images of Cured and JFH1-replicon cells during differentiation.**

Quantification of immunofluorescence of Cured and JFH1-replicon CD24lo cells at day one and day nine of differentiation using Image J. A) ki67 staining was quantified as the mean percentage of ki67 positive cells (n=3; two-tailed t-test * ≤0.05, **≤0.01, ***≤0.001) B) Albumin staining was quantified as the MFI per image for albumin (n=3; two-tailed t-test * ≤0.05, **≤0.01, ***≤0.001).

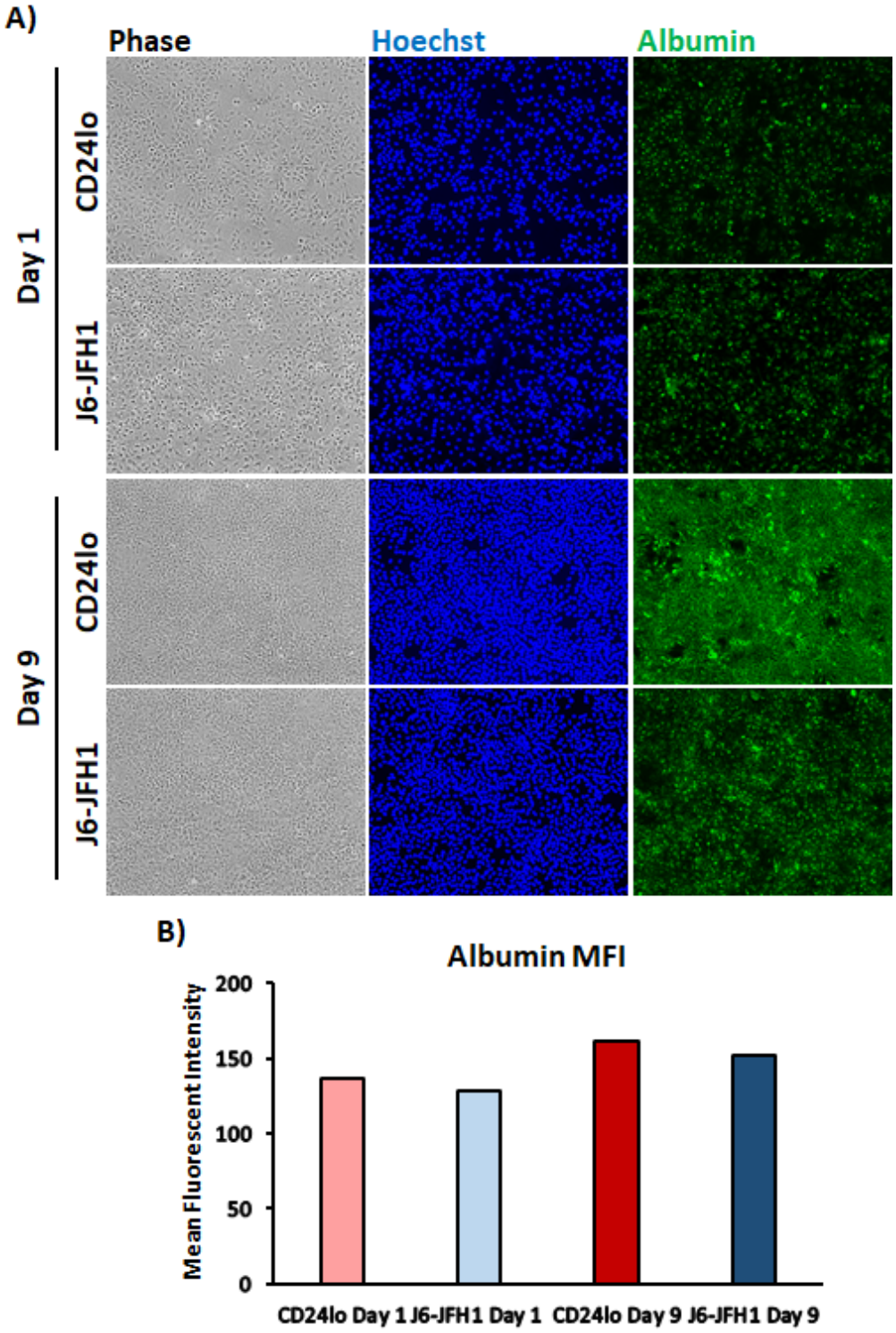


**Figure 4.2.8 Immunofluorescence of CD24lo and J6-JFH1 CD24lo cells for albumin**

Cells were differentiated on cover slips in a 12 well plate and fixed using 4 % PFA in PBS at day one and day nine of differentiation. The cells were then permeabilised using 0.2 % Triton-X100 in PBS and stained using antibodies against albumin (green) and 488 nm fluorescently labelled Alexa Fluor secondary antibodies. The nuclei were counterstained using the DNA stain Hoechst. Images were taken using the 40x objective of the Nikon Eclipse Ti-E Widefield Fluorescent Inverted Microscope. Images are representative of cell density. B) Albumin staining was quantified as the MFI intensity per image (n=2).

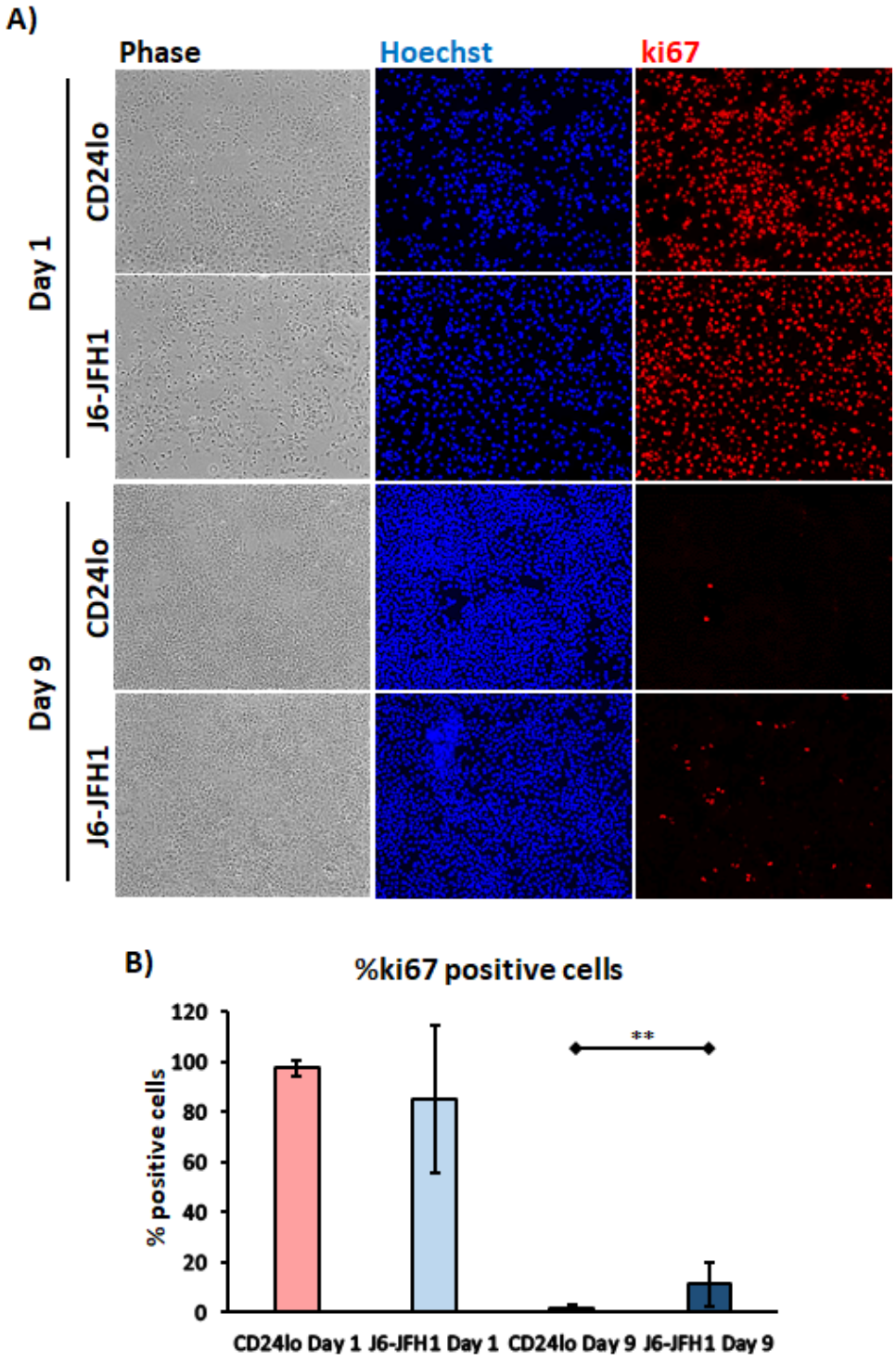


**Figure 4.2.9 Immunofluorescence of CD24lo and J6-JFH1 CD24lo cells for ki67**

Cells were differentiated on cover slips in a 12 well plate and fixed using 4 % PFA in PBS at day one and day nine of differentiation. The cells were then permeabilised using 0.2 % Triton-X100 in PBS probed using antibodies against ki67 (red) and 594 nm fluorescently labelled Alexa Fluor secondary antibodies. The nuclei were counterstained using the DNA stain Hoechst. Images were taken using the 40x objective of the Nikon Eclipse Ti-E Widefield Fluorescent Inverted Microscope. Images are representative of cell density. B) ki67 staining was quantified as the mean percentage of ki67 positive cells (n=3; two-tailed t-test * ≤0.05, **≤0.01, ***≤0.001).

### 4.2.3 The effect of differentiation on viral protein expression

NS5A is a HCV non-structural RNA binding protein that is required for both viral RNA replication as well as particle assembly (Fridell et al., 2011, Macdonald and Harris, 2004, Ross-Thriepland and Harris, 2015) and is often used as a surrogate marker of viral replication. NS5A also interacts with other HCV non-structural proteins and a wide variety of cellular proteins (He et al., 2006). An interesting protein expression pattern was observed for the viral NS5A protein during the course of differentiation (Figure 4.2.4 & Figure 4.2.5). NS5A levels initially increased at days three and five, suggestive of an increase in viral replication, yet then began to decrease below initial levels as differentiation continued (Figure 4.2.11). For five out of seven replicon experiments NS5A expression almost dropped below the threshold of detection entirely (Figure 4.2.11). A similar pattern was observed for J6-JFH1 infected cells with NS5A levels being much lower at day 9 compared to day 1. As we observed NS5A expression almost disappearing entirely in the majority of our experiments, differentiated (day 9 post-DMSO) JFH1-replicon cells were ‘de-differentiated’ by reseeding the cells at sub-confluent density in DMSO free media, to determine whether the virus persists during differentiation and whether viral replication and protein expression can be rescued. Both differentiation and de-dedifferentiation occurred in the absence of G418 selection. NS5A expression was rescued by allowing the CD24lo JFH1-replicon cells to ‘dedifferentiate’ (Figure 4.2.12). This indicates that HCV may preferentially replicate in cells which have been stimulated by DMSO but which have not yet become terminally differentiated. It also demonstrates that it is able to persist in the more terminally differentiated CD24lo cells, despite an obvious lack of replicase protein expression, and in the absence of selection. Both genome replication and gene expression are rescued when cells were no longer contact inhibited and allowed to proliferate.

### 4.2.4 Direct acting antiviral treatment during differentiation restores CD24lo differentiation phenotype

To elucidate whether the altered differentiation pattern observed in J6-JFH1 infected CD24lo cells and cells harbouring the JFH1-replicon was dependent upon ongoing HCV replication, differentiation experiments were repeated in the presence of the direct acting antivirals SOF and DCV which included a 24 hr pre-treatment prior to setting up the differentiation. DAA treatment was maintained throughout differentiation. Both of these DAAs are now commonly used in the clinic to treat patients (Section 1.2.3).

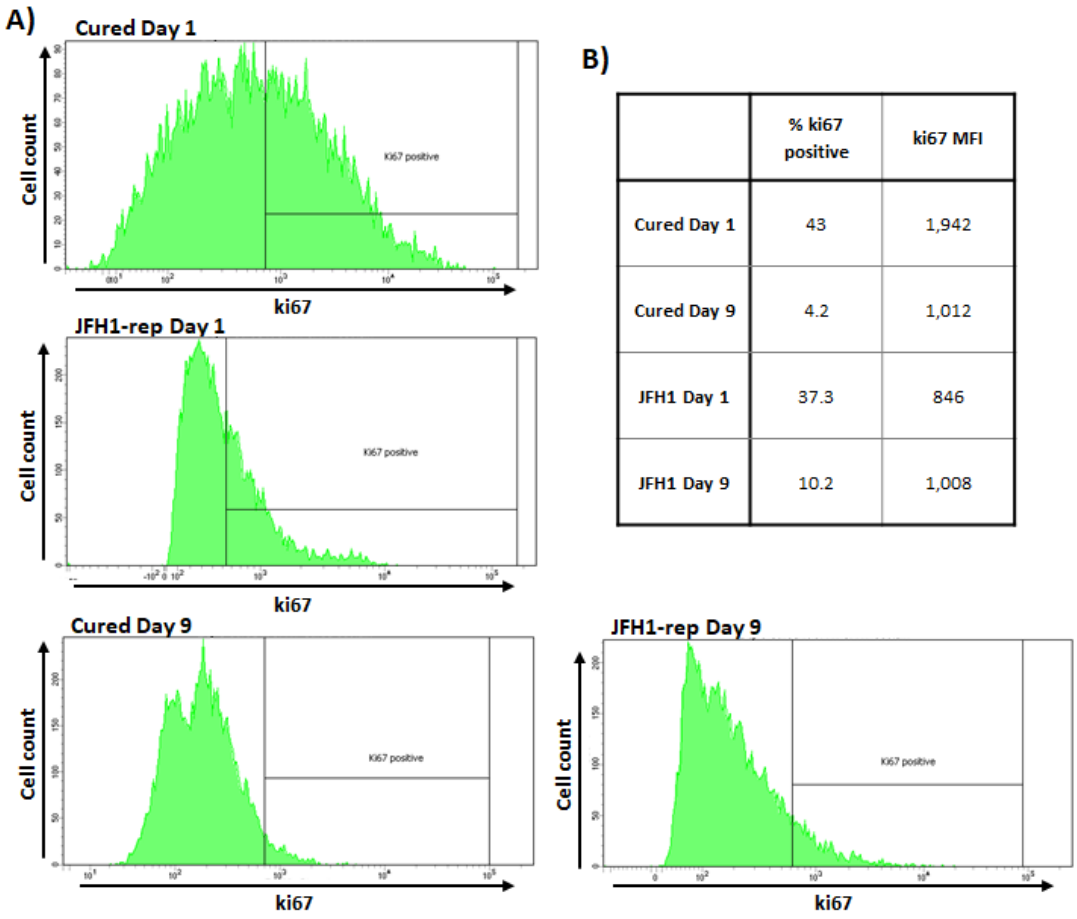


B)

| | % ki67 positive | ki67 MFI |
|---|---|---|
| Cured Day 1 | 43 | 1,942 |
| Cured Day 9 | 4.2 | 1,012 |
| JFH1 Day 1 | 37.3 | 846 |
| JFH1 Day 9 | 10.2 | 1,008 |

**Figure 4.2.10 Flow-cytometry for ki67 stained Cured and JFH1-replicon CD24lo cells over differentiation.**

Cured and JFH1-replicon cells were collected for flow-cytometry at day 1 and day 9 of differentiation. Cells were permeabilised stained for ki67 using BV421 conjugated anti-ki67 antibodies. After the cells were stained and fixed, the samples were analysed for ki67 expression by flow-cytometry. Gates are set based on 5 % of the isotope control of each sample B) Quantification of ki67 flow-cytometry of differentiated Cured and JFH1-replicon CD24lo cells. The percentage of ki67 positive cells and the MFI of the cells were recorded.

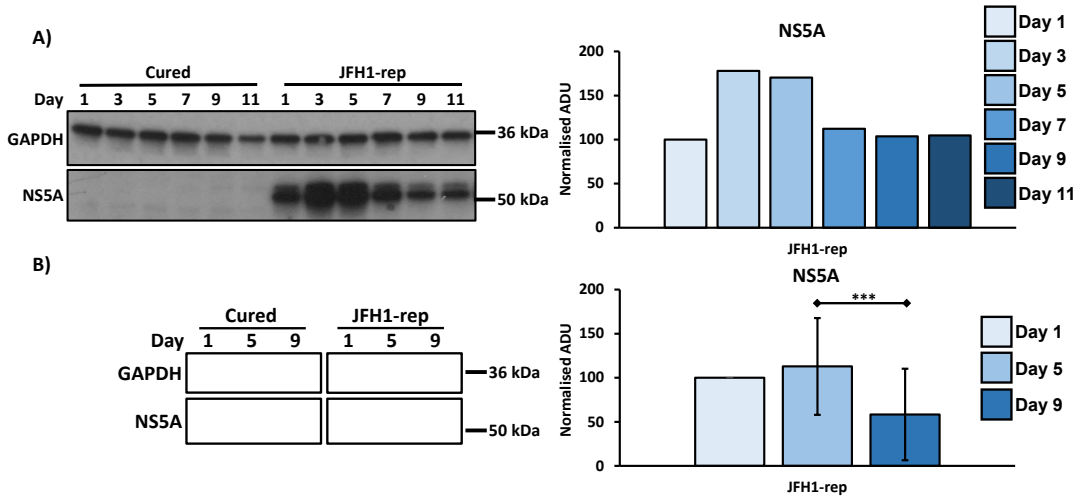


**Figure 4.2.11 Western blot of JFH1-replicon CD24lo cells over the course of differentiation**

A) Cells were differentiated over eleven days with media changes every two days. Lysates were also taken every two days for Western blot. Membranes were probed with anti-GAPDH and anti-NS5A antibodies. Quantification using ImageJ of NS5A western blot band intensities normalised to GAPDH band intensities. B) An example Western blot for NS5A of a differentiation experiment in which NS5A levels disappear almost entirely at day nine. Quantification of NS5A western blot intensity normalised to GAPDH band intensity using ImageJ (measured as Arbitrary densitometry units (ADU)). Displayed as percentage of JFH1-rep Day 1. Two tailed student t-test p=0.0002, n=7.

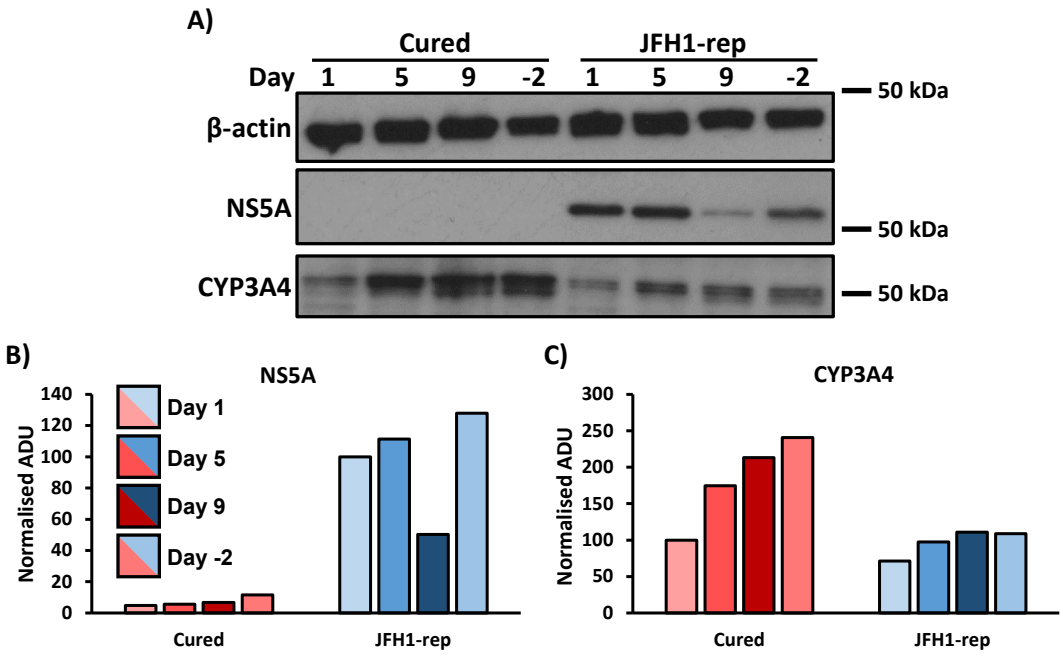


**Figure 4.2.12 Western blot of Cured and JFH1-replicon de-differentiation experiment**

A) Cured and JFH1-replicon CD24lo cells were differentiated for nine days and then trypsinized and re-seeded at sub-confluence in the absence of DMSO and G418. Lysates were taken at day one, five, nine and two days post re-seeding (day -2) for Western blot. Membranes were stained using anti-β-actin, NS5A, ki67 or CYP3A4 antibodies. B) NS5A western blot band intensity quantification using ImageJ normalised to β-actin band intensities. C) CYP3A4 western blot band intensity quantification using ImageJ normalised to β-actin band intensities (measured as Arbitrary densitometry units (ADU)). Displayed as percentage of JFH1-rep day 1 for NS5A and percentage of Cured day 1 for CYP3A4.

Based upon NS5A western blotting, DAA 24 hr pre-treatment of infected CD24lo cells cleared virus rapidly during differentiation experiments, with an initial decrease evident at day 1 (Figure 4.2.13 & Figure 4.2.14). DAA treatment and resulting elimination of HCV infection, restored the CD24lo differentiation phenotype. Specifically, we observed an increase in the number of hepatocyte-like islands in DAA treated cells to a level similar to CD24lo cells (Figure 4.2.15). In addition, DAA treated cells expressed higher levels of the hepatocyte marker CYP3A4 at day nine of the differentiation when compared to the infected cells (Figure 4.2.13 & Figure 4.2.14). DAA treatment of infected CD24lo cells also lead to a decrease in ki67 protein levels over the course of differentiation when compared to untreated control infections. This protein expression pattern of DAA treated cells resembled that of the uninfected CD24lo cells more closely than differentiated infected cells (Figure 4.2.13 & Figure 4.2.14). It is important to note that the CYP3A4 pattern for the untreated J6-JFH1 cells in the DAA J6-JFH1 experiment was not as pronounced, CYP3A4 levels were not as reduced as previously observed. These findings further support that the observed alteration of the differentiation phenotype is dependent upon HCV infection.

### 4.2.5 The effect of differentiation and HCV infection on cell-cell adhesion and cytoskeletal proteins

As hepatic cells differentiate, they become polarized and form sheets of tightly linked hepatocytes, a result of changes to cell adhesion, tight junction and cytoskeletal protein expression and rearrangement (Treyer and Musch, 2013, Braiterman and Hubbard, 2009). Differentiation of CD24lo cells drove clear changes in cell morphology and we observed that these were less marked in HCV infected compared with control cells. These observations led us to investigate whether cell cytoskeletal architecture and cell surface adhesion molecules might be differentially affected by HCV infection compared with controls during DMSO induced differentiation. Differentiated cells were analysed by immunofluorescence for selected cell adhesion, cell-cell contact and cytoskeletal proteins including; EpCAM, E-cadherin, N-cadherin, occludin and F-actin. Occludin is an important part of tight junctions and a HCV entry factor. E-cadherin and N-cadherin are important cell-cell adhesion molecules and the E/N-cadherin ratio is important marker of EMT. F-actin forms the actin cytoskeleton which is essential for many cellular functions. EpCAM is often used as a marker for HCC CICs.

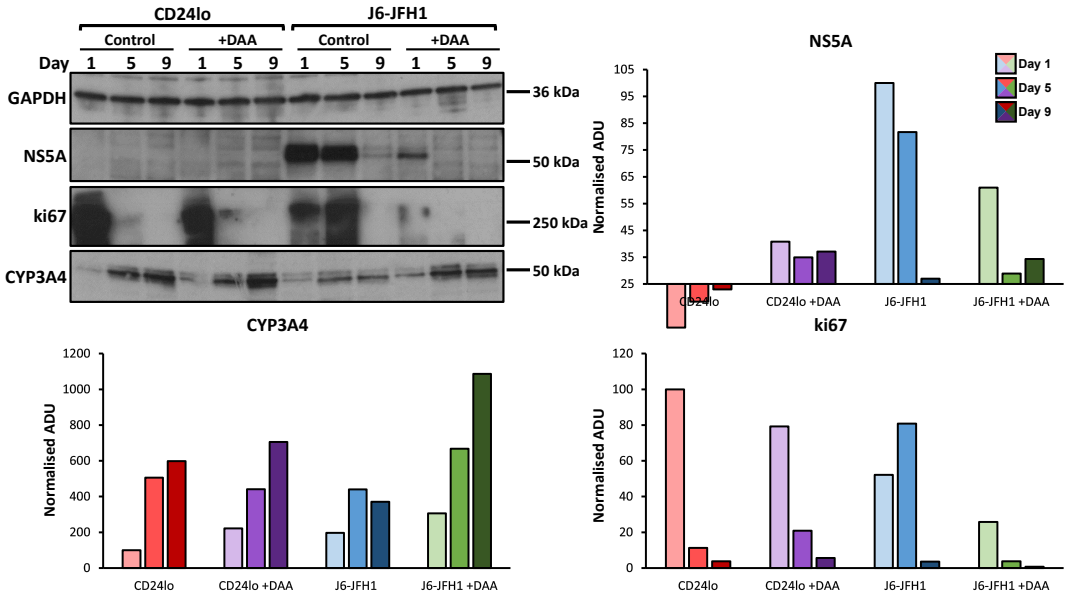


**Figure 4.2.13 Western blot of CD24lo and J6-JFH1 CD24lo cells +/- DAA over differentiation**

A) Cells were differentiated in the presence or absence of direct acting antivirals (DAAs) DCV (1 μM) and SOF (1 μM) and lysed for western blot analysis at day one, five and nine of differentiation. Membranes were stained using anti-GAPDH, anti-NS5A, anti-ki67 or anti-CYP3A4 antibodies. B) Quantification of NS5A, ki67 and CYP3A4 western blot intensity normalised to GAPDH band intensity measured using ImageJ (measured as Arbitrary densitometry units (ADU)) (n=1). Displayed as the percentage of CD24lo Day 1 except for NS5A which is the percentage of J6-JFH1 Day 1.

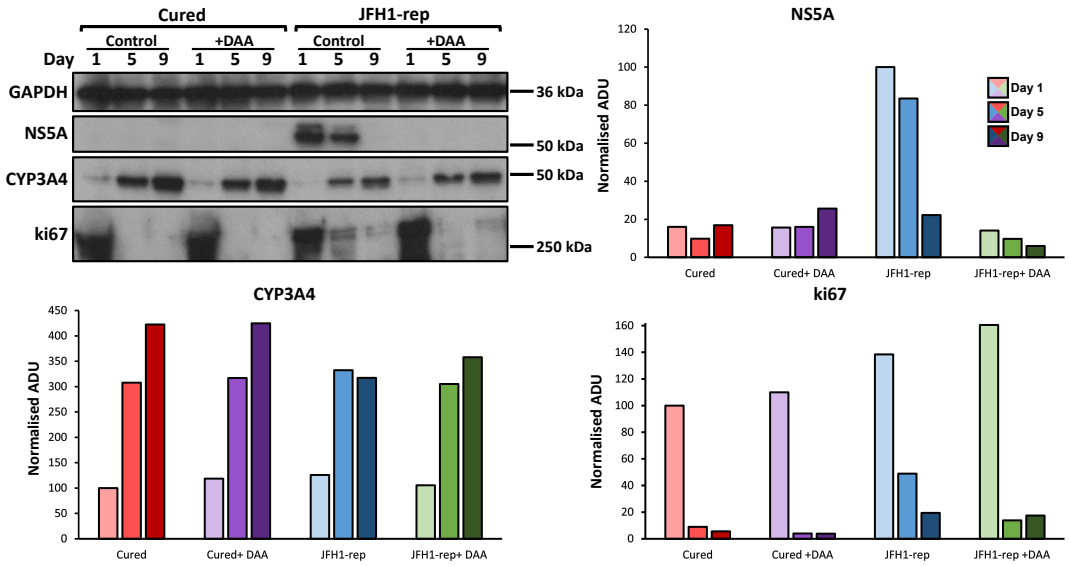


**Figure 4.2.14 Western blot of differentiated Cured and JFH1-replicon CD24lo cells +/- DAA**

A) Cells were differentiated in the presence or absence of direct acting antivirals (DAAs) DCV (1 μM) and SOF (1 μM) and lysed for western blot analysis at day one, five and nine of differentiation. Membranes were stained using anti-GAPDH, anti-NS5A, anti-ki67 or anti-CYP3A4 antibodies. B) Quantification of NS5A (n=2), ki67 (n=1) and CYP3A4 (n=2) western blot intensity normalised to GAPDH band intensity measured using ImageJ (measured as Arbitrary densitometry units (ADU)). Displayed as the percentage of CD24lo Day 1 except for NS5A which is the percentage of J6-JFH1 Day 1.

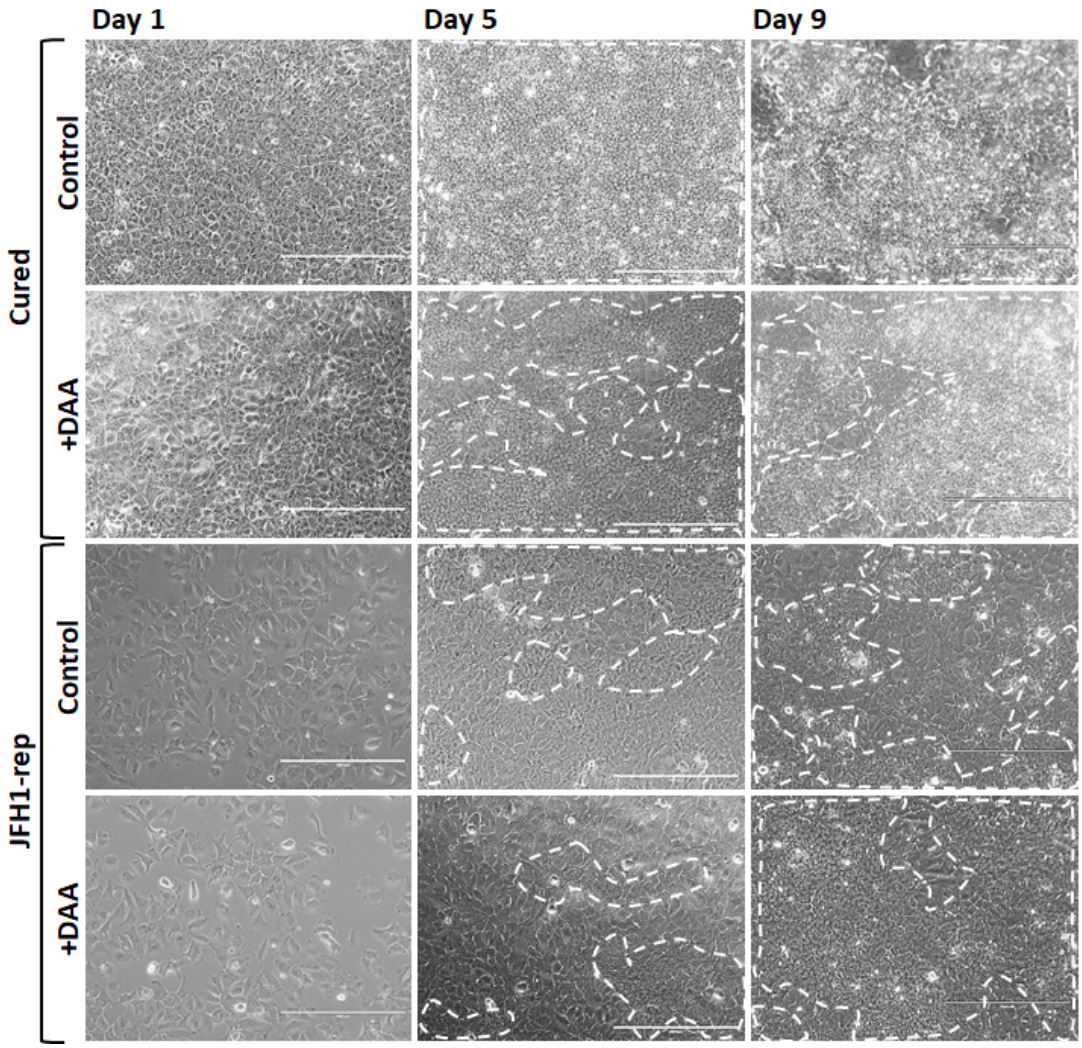


**Figure 4.2.15 Phase images of the differentiation of Cured and JFH1-replicon cells +/- DAAs**

Cells were differentiated in the presence or absence of direct acting antivirals DCV (1 μM) and SOF (1 μM) over nine days. After seeding and allowing the cells to settle overnight, DMSO was added to the culture media, which was replaced every two days. At days one, five and nine phase images were taken using the 20x objective of the EVOS cell imaging system. Images are representative of cell density.

(Figure 4.2.17) shows that expression of EpCAM increased over the course of differentiation, particularly within islands of hepatocyte-like cells. Correspondingly fewer JFH1-replicon cells expressed EpCAM at day nine of differentiation compared to the HCV negative Cured cells. Expression of the cell-cell adhesion protein E-cadherin, followed a similar trend to EpCAM, with the biggest difference observed between JFH1-replicon and Cured cells at day nine of differentiation. Again E-cadherin expression predominantly resided within the islands of hepatocyte-like cells, but was less punctate in the Cured cells at day nine of differentiation compared the JFH1-replicon cells (Figure 4.2.17).

Interestingly, JFH1-replicon cells expressed higher levels of N-cadherin at day one of differentiation compared to Cured cells. The localisation of N-cad changed over the course of the differentiation, becoming much more pronounced at the cell-cell junctions. It can be seen by comparing the day 9 images of (Figure 4.2.18) that JFH-replicon reduced this effect.

Occludin expression increased in both Cured and JFH1 cells over the course of differentiation (Figure 4.2.19). Expression of Occludin became more organised at day nine of differentiation and resided at the cell borders of non hepatocyte-like cells. Expression of occludin within the islands of hepatocyte-like cells localised to a single point, characteristic of the formation of tight junctions.

Analysis of the cytoskeletal protein F-actin revealed that stress fibres were more common in JFH1-replicon and J6-JFH1 CD24lo cells at day one of differentiation compared to HCV negative CD24lo cells (Figure 4.2.20 & Figure 4.2.21). Differentiated cells appear to form F-actin structures more similar to adhesion belts between cells.

Analysis of these proteins indicates that DMSO is able to induce some of the cytoskeletal and cell-adhesion changes associated with hepatocyte differentiation. For example the cell membrane associated N-cadherin and occludin tight junction formation. However we did observe differences in expression and localisation of some proteins compared to what is usually found in primary hepatocytes, such as the expression of EpCAM which is usually lost in primary hepatocytes. HCV infection was able to alter the expression and localisation pattern of E-cadherin, N-cadherin, occludin, EpCAM and F-actin during differentiation.

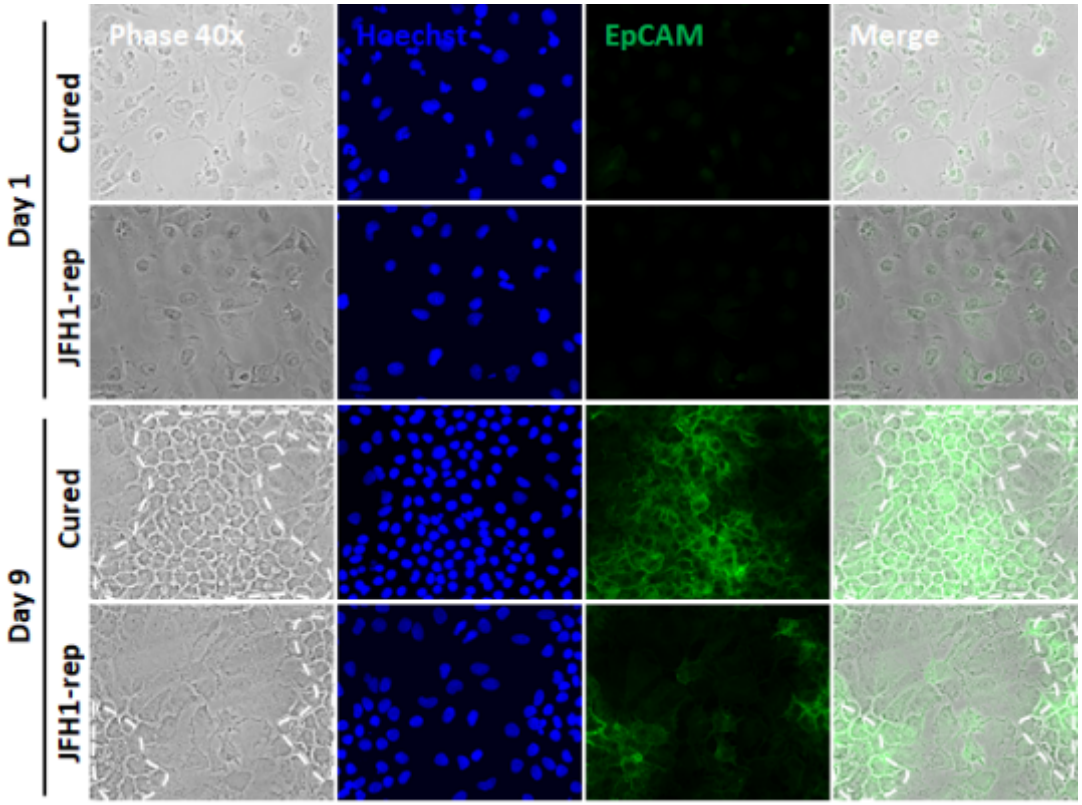


**Figure 4.2.16 Immunofluorescence of Cured and JFH1-replicon CD24lo cells for EpCAM**

Cells were differentiated on cover slips in a 12 well plate and fixed at day one and day nine of differentiation using 4 % PFA in PBS. The cells were then permeabilised using 0.2 % Triton-X100 in PBS and stained using antibodies against EpCAM (green) and 488 nm fluorescently labelled Alexa Fluor secondary antibodies. Nuclei were counterstained using DNA dye, Hoechst. Images were taken using the 40x objective of the Nikon Eclipse Ti-E Widefield Fluorescent Inverted Microscope. Islands of hepatocyte-like cells are highlighted by dashed white lines. Images are representative of cell density.

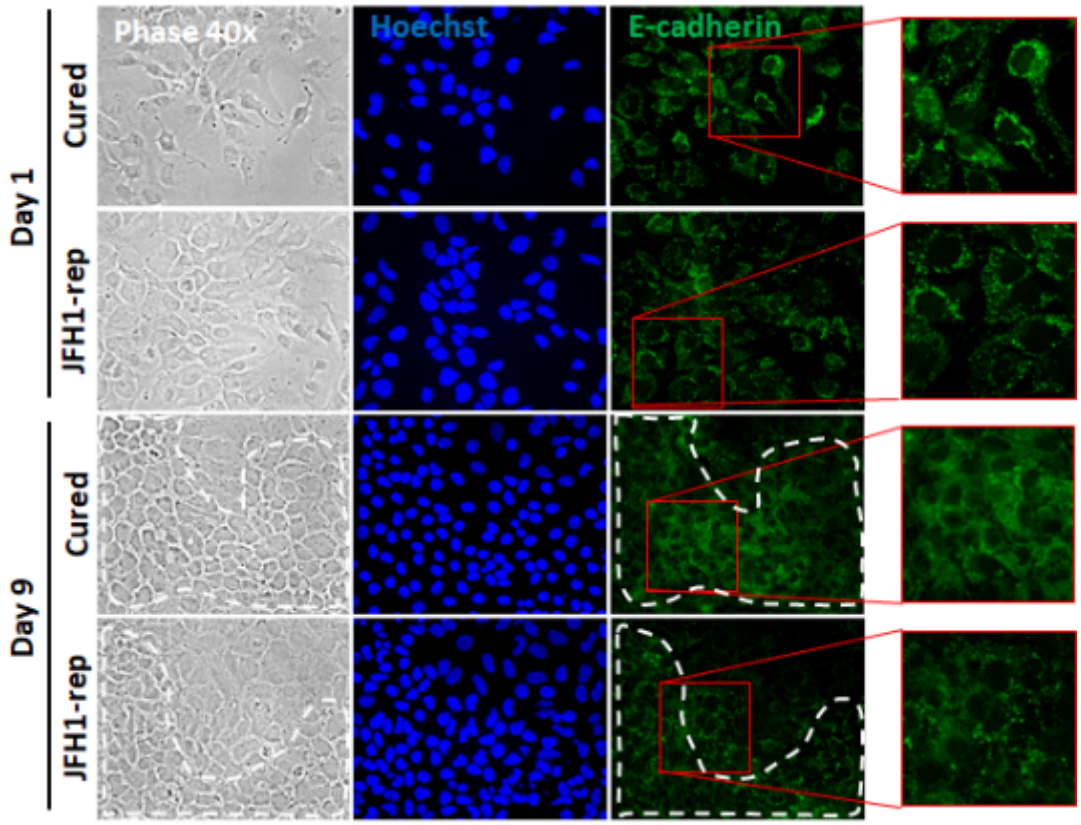


**Figure 4.2.17 Immunofluorescence of Cured and JFH1-replicon CD24lo cells for E-cadherin**

Cells were differentiated on cover slips in a 12 well plate and fixed at day one and day nine of differentiation using 4 % PFA in PBS. The cells were then stained using antibodies against E-cadherin (green) and 488 nm fluorescently labelled Alexa Fluor secondary antibodies. Nuclei were counterstained using DNA dye Hoechst. Images were taken using the 40x objective of the Nikon Eclipse Ti-E Widefield Fluorescent Inverted Microscope. Islands of hepatocyte-like cells are highlighted by dashed white lines. Images are representative of cell density.

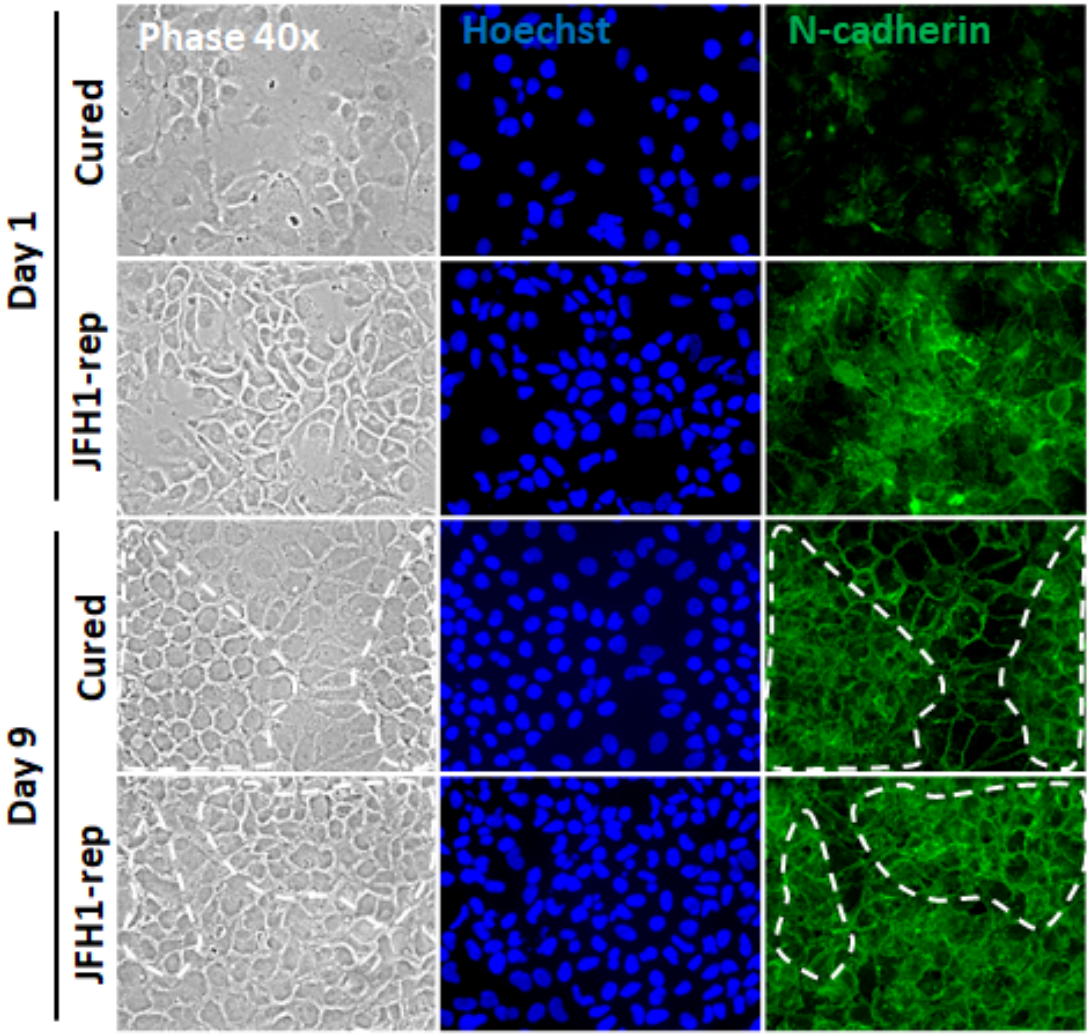


**Figure 4.2.18 Immunofluorescence of Cured and JFH1-replicon CD24lo cells for N-cadherin**

Cells were differentiated on cover slips in a 12 well plate and fixed at day one and day nine of differentiation using 4 % PFA in PBS. The cells were stained using antibodies against N-cadherin (green) and 488 nm fluorescently labelled Alexa Fluor secondary antibodies. Nuclei were counterstained using DNA dye Hoechst. Images were taken using the 40x objective of the Nikon Eclipse Ti-E Widefield Fluorescent Inverted Microscope. Islands of hepatocyte-like cells are highlighted by dashed white lines. Images are representative of cell density.

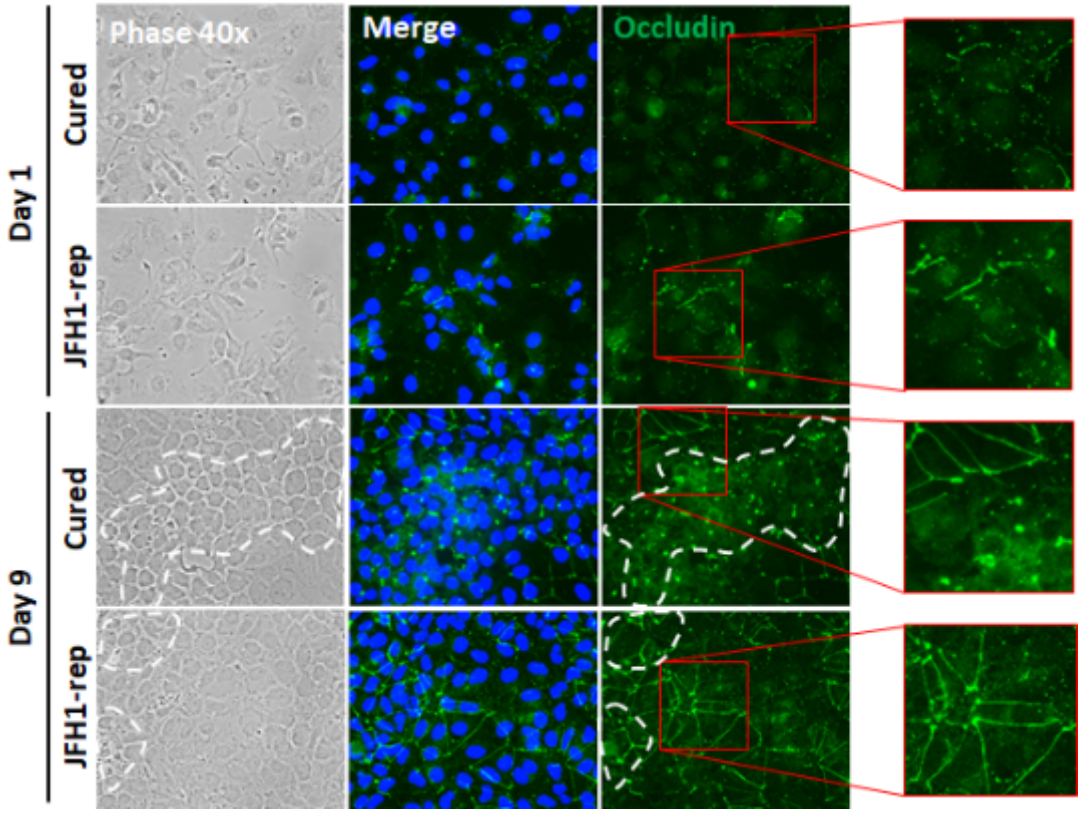


**Figure 4.2.19 Immunofluorescence of Cured and JFH1-replicon CD24lo cells for Occludin**

Cells were differentiated on cover slips in a 12 well plate and fixed at day one and day nine of differentiation using 4 % PFA in PBS. The cells were stained using antibodies against Occludin (green) and 488 nm fluorescently labelled Alexa Fluor secondary antibodies. Nuclei were counterstained using DNA dye Hoechst. Images were taken using the 40x objective of the Nikon Eclipse Ti-E Widefield Fluorescent Inverted Microscope. Islands of hepatocyte-like cells are highlighted by dashed white lines. Images are representative of cell density.

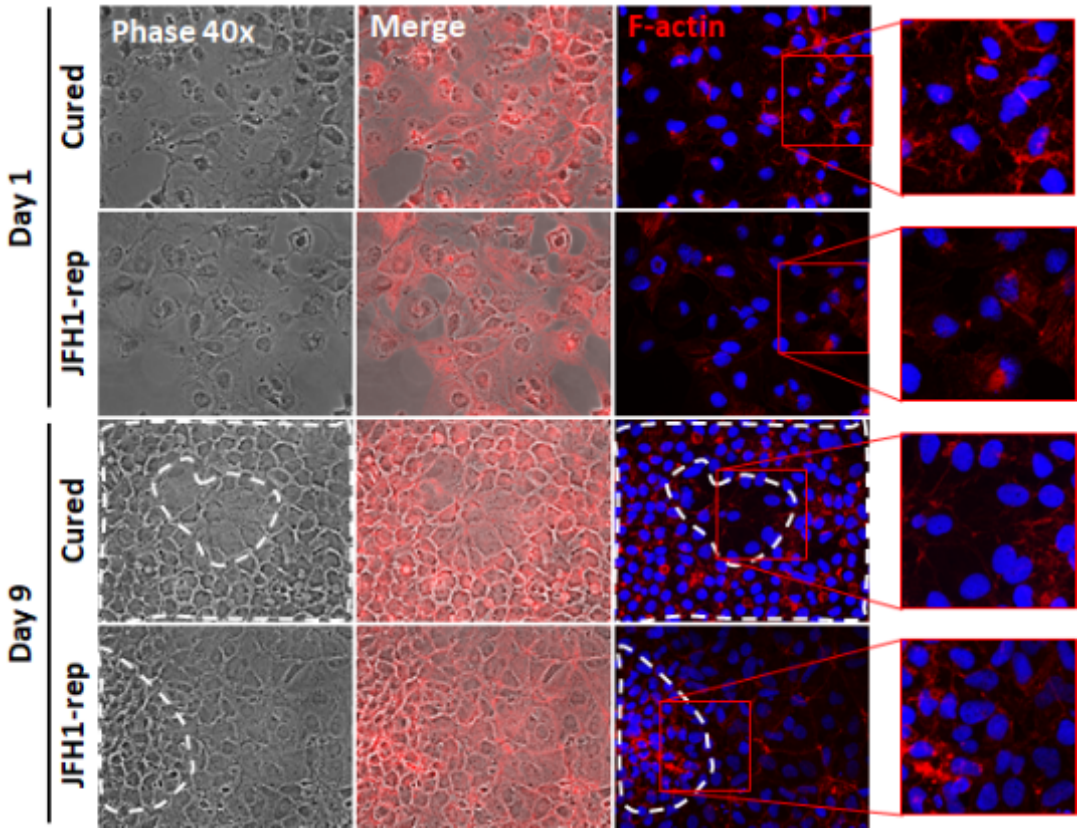


**Figure 4.2.20 Immunofluorescence of Cured and JFH1-replicon CD24lo cells for F-actin**

Cells were differentiated on cover slips in a 12 well plate and fixed at day one and day nine of differentiation using 4 % PFA in PBS. The cells were then permeabilised using 0.2 % Triton-X100 in PBS and stained using 594 nm fluorescently labelled Phalloidin for F-actin (red). Nuclei were counterstained using DNA dye Hoechst. Images were taken using the 40x objective of the Nikon Eclipse Ti-E Widefield Fluorescent Inverted Microscope. Islands of hepatocyte-like cells are highlighted by dashed white lines. Images are representative of cell density.

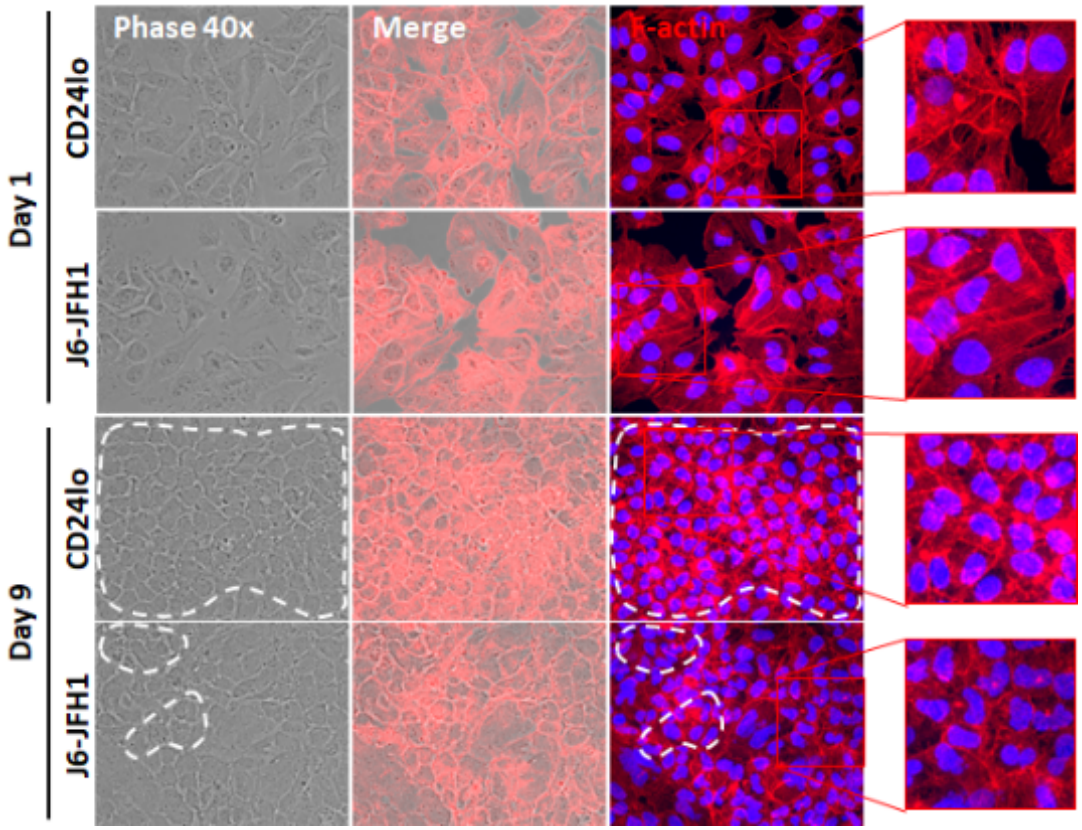


**Figure 4.2.21 Immunofluorescence of CD24lo and J6-JFH1 CD24lo cells for F-actin**

Cells were differentiated on cover slips in a 12 well plate and fixed at day one and day nine of differentiation using 4 % PFA in PBS. The cells were then permeabilised using 0.2 % Triton-X100 in PBS and stained using 594 nm fluorescently labelled Phalloidin for F-actin (red). Nuclei were counterstained using DNA dye Hoechst. Images were taken using the 40x objective of the Nikon Eclipse Ti-E Widefield Fluorescent Inverted Microscope. Islands of hepatocyte-like cells are highlighted by dashed white lines. Images are representative of cell density.

## 4.3 JFH1-replicon cells express higher levels of CIC marker CD24

CD24 is a well-accepted CIC marker and is over expressed on many human cancers such as ovarian (Kristiansen et al., 2002), bladder (Liu et al., 2013), and liver cancer (Lee et al., 2011). It is a small surface glycol-protein which has functions related to cell-cell and cell-matrix interactions, mainly binding to P-selectin. CD24 can be used as a marker of HCC patient prognosis (Yang et al., 2009) and is involved in cellular self-renewal and metastasis (Lee et al., 2011). Previous work in the lab showed that parental Huh7s harbouring the JFH1-replicon express higher levels of CD24 (data not shown). This increase in CD24 levels may be due to a selection artefact, in that JFH1 may replicate more efficiently in CD24 high expressing Huh7 cells leading to these cells being selected for under the G418 selection. This was another reason polyclonal Huh7 cells were sorted for high and low expression of CD24. Due to CD24 being an important 'stemness'/CIC marker and its involvement in many oncogenic pathways such as STAT3 and Hif1α signalling (Lee et al., 2011, Thomas et al., 2012), we wanted to investigate whether HCV was able to increase CD24 expression in the CD24lo background. CD24lo Cured and JFH1-replicon cells were probed for CD24 expression by flow-cytometry to determine whether CD24 expression was switched on and increased by the JFH1-replicon in a CD24lo background and whether CD24 levels change over the course of differentiation. Indeed, at day one of differentiation we found there was a higher percentage of CD24 positive JFH1-replicon cells (97 %) and that the MFI of these cells (7,463) was higher than for Cured cells for which the percentage of positive cells was 73 % and the MFI 4,143 (Figure 4.3.1). The percentage of CD24 positive Cured cells increased from 73 % to 92 % at day nine and the MFI increased very slightly to 4,482. The number of positive JFH1-replicon cells stayed at a similar level of 98 % at day nine however the MFI increase to 8,504 (Figure 4.3.1). A similar trend of differentiation induced increase in CD24 expression was observed in HepaRG cells (Figure 3.1.2). The same phenomenon was observed by Immunofluorescence with CD24 levels increasing over differentiation but with overall levels further elevated in JFH1-replicon cells compared to controls (Figure 4.3.2). This indicates that HCV is able to increase CD24 expression even in a CD24lo background and that differentiation has an impact on CD24 levels. This is interesting as Lee et al., observed an inability of FACS sorted CD24 negative PLC/PRF/5 cells

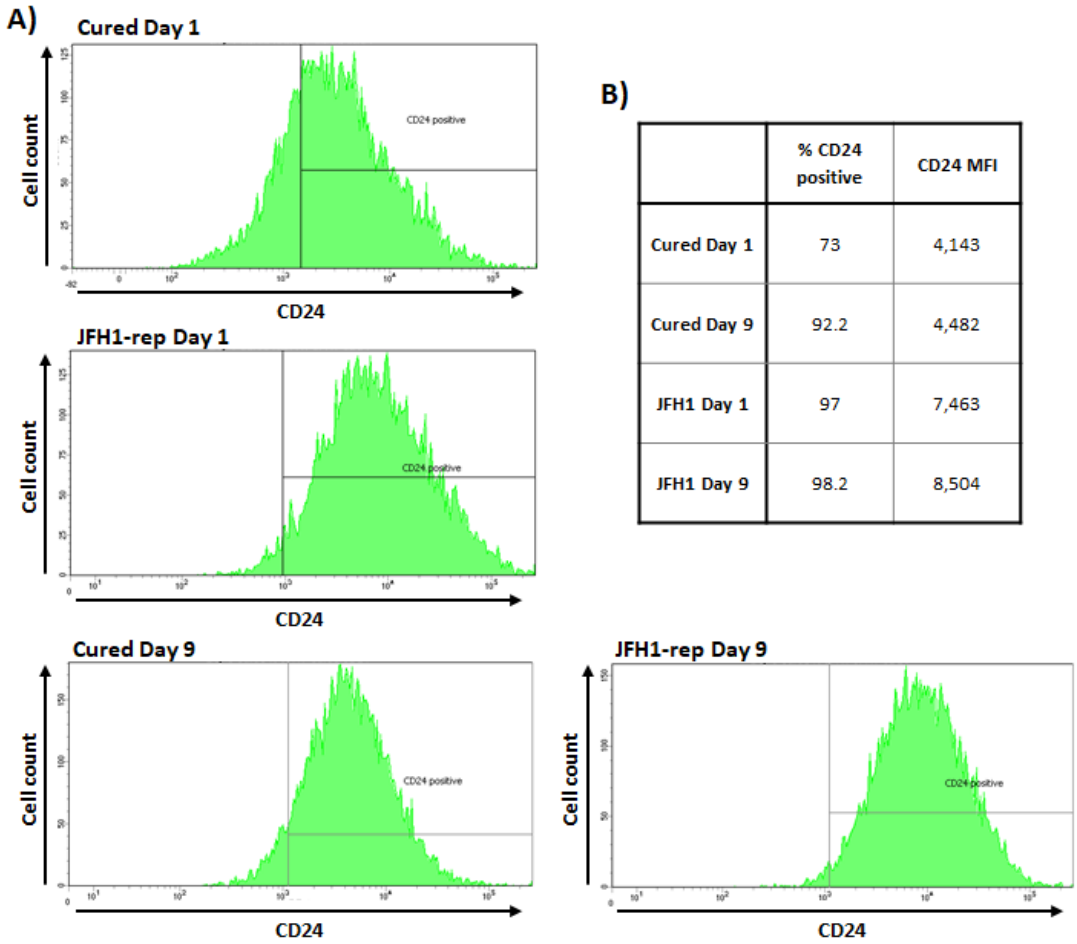


B)

| | % CD24 positive | CD24 MFI |
|---|---|---|
| Cured Day 1 | 73 | 4,143 |
| Cured Day 9 | 92.2 | 4,482 |
| JFH1 Day 1 | 97 | 7,463 |
| JFH1 Day 9 | 98.2 | 8,504 |

**Figure 4.3.1 Flow-cytometry for CD24 of Cured and JFH1-replicon CD24lo cells during differentiation**

Cured and JFH1-replicon CD24lo cells were differentiated and stained for CD24 using PE fluorescently labelled anti-CD24 antibodies. After the cells were stained and fixed, the samples were analysed for CD24 expression by flow-cytometry at day one and day nine of differentiation. Gates are set based on 5 % of the isotope control of each sample B) Quantification of CD24 flow-cytometry of differentiated Cured and JFH1-replicon CD24lo cells. The percentage of CD24 positive cells and the MFI of the cells were recorded.

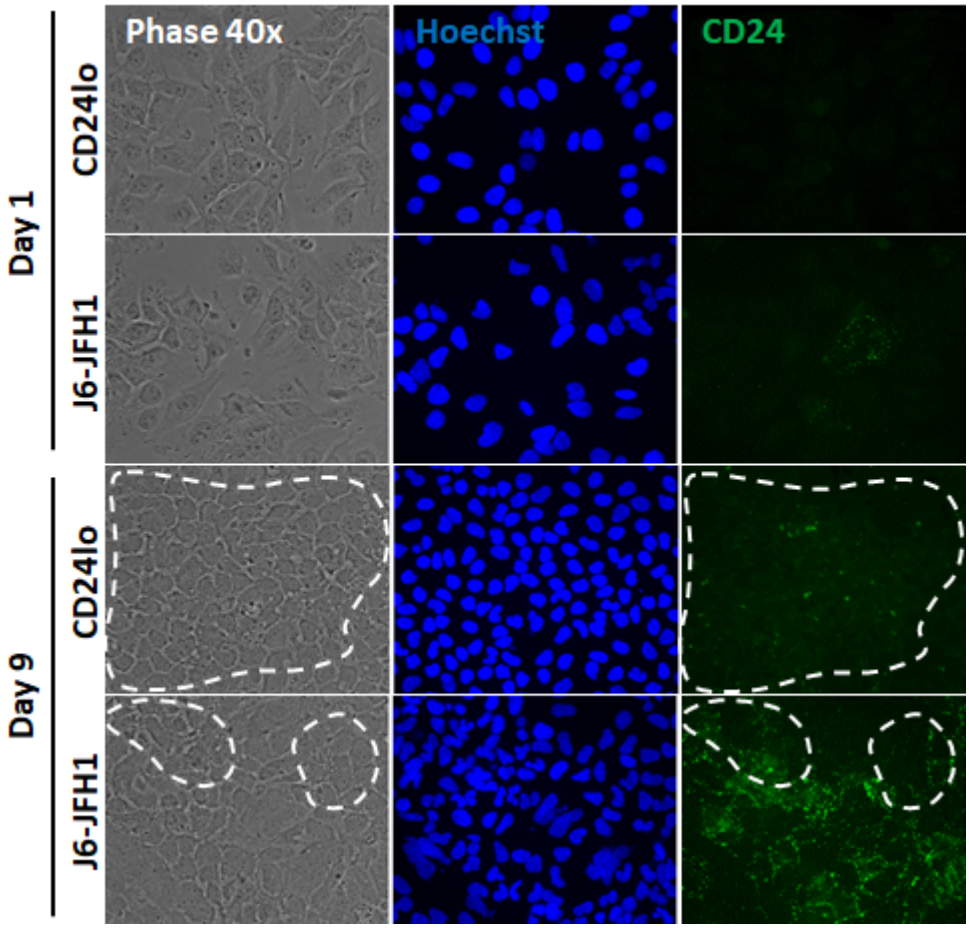


**Figure 4.3.2 Immunofluorescence of CD24lo and J6-JFH1 CD24lo cells for CD24lo**

Cells were differentiated on cover slips in a 12 well plate and fixed at day one and day nine of differentiation using 4 % PFA in PBS. The cells were stained using antibodies against CD24 (green) and 488 nm fluorescently labelled Alexa Fluor secondary antibodies. The nuclei were counter stained using the DNA stain Hoechst (blue). Images were taken using the 40x objective of the Nikon Eclipse Ti-E Widefield Fluorescent Inverted Microscope. Islands of hepatocyte-like cells are highlighted by dashed white lines. Images are representative of cell density.

to increase CD24 expression whereas a significant number of CD24 positive cells lost CD24 expression after a 2 weeks culture in 10 % serum supplemented media (Lee et al., 2011).

## 4.4 Discussion

Huh7 cells sorted for low expression of CIC marker CD24 serve as a useful approximation to a HPC as these cells are less tumourigenic than parental Huh7 cells (Figure 3.4.1) and yet remain amenable to *in vitro* differentiation. DMSO has been shown to be able to induce differentiation of various primary cells and cell lines (Czysz et al., 2015, Cheung et al., 2006, Choi et al., 2009, Mowbray et al., 2010). DMSO, via an unknown mechanism, induces changes to cell morphology, cell adhesion, cell junction and cytoskeletal protein expression (Pal et al., 2012). The addition of DMSO to the culture medium of CD24lo cells led to the development of cells which resemble hepatocytes more closely (Figure 4.2.2 & Figure 4.2.3). Identification of hepatocyte-like islands was based upon clear morphological differences. However, protein markers could be used to help measure and quantify these islands. We attempted using the Incucyte® Zoom to quantify the islands however the software was unable to distinguish between the hepatocyte-like islands and surrounding cells. One possible marker which could be used to define these hepatocyte-like islands is EpCAM, as our results indicated that EpCAM is predominantly expressed by the hepatocyte-like cells (Figure 4.2.16).

HCV infection perturbed CD24lo cell differentiation, evidenced by changes in cell morphology and an altered pattern of protein expression. Reduced expression of the hepatocyte markers albumin and CYP3A4, which our results suggest to be due to both a combination of fewer cells expressing these markers and reduced expression by individual cells, implies that HCV infection is able to resist/delay transcriptional programmes associated with hepatocyte differentiation. Moreover, a significant proportion of infected CD24lo cells seemingly did not exit the cell cycle and maintained expression of the proliferation marker ki67 despite DMSO treatment.

It is unclear from these results whether HCV infected cells are less likely to initiate a DMSO-induced differentiation programme (resist), or whether they are blocked/slowed at an early stage along this pathway (delay). It is also unclear why not all of the control cells undergo differentiation. The addition of DAAs SOF and DCV was able to partially restore differentiation and the associated hepatocyte protein marker expression pattern, supporting the

conclusion that resistance to differentiation was dependent upon ongoing viral replication. The perturbation of differentiation was observed in both CD24lo cells harbouring the JFH1-replicon and cells which were chronically infected with the J6-JFH1 full length cell culture

strain. This suggests that the viral protein or proteins responsible are HCV non-structural proteins NS3-NS5B, as the JFH1-replicon lacks genomic regions encoding the structural proteins (core, E1 & E2), the viral ion channel, p7, and non-structural protein NS2.

Fiore & Degrassi showed that DMSO was able to restore contact growth inhibition of Chinese hamster ovary (CHO) cells accompanied by changes to CHO cell morphology (Fiore and Degrassi, 1999). DMSO appears to have a similar effect on CD24lo Huh7 cells. Indeed, Choi *et al.* demonstrated that Huh7 cells remained viable without passaging for over 60 days in the presence of DMSO (Choi et al., 2009). By contrast, Huh7 cells cultured under standard conditions in the absence of DMSO continue proliferating and by day 10 post-seeding considerable cell death is observed (Sainz and Chisari, 2006). We observed CD24lo cell death at an earlier stage in the absence of DMSO at day five. The restoration of CHO cell contact inhibition was shown to potentially be due to an increase in E-cadherin and N-cadherin expression and ultimately an increase in cell-cell and cell-ECM adhesion capacity (Fiore and Degrassi, 1999).

Mature hepatocytes are polarised epithelial cells and polarisation is vital for their function (Treyer and Musch, 2013). Polarised epithelial cells require a closely linked system of cell-cell adhesion and structural organisation. Functional polarity is maintained by the cytoskeleton (Ezzell et al., 1993). Differentiated CD24lo cells were analysed for expression and localisation of cell adhesion/ tight junction proteins EpCAM, E-cadherin, N-cadherin and occludin and for the cytoskeletal protein F-actin. EpCAM is a transmembrane glycoprotein which is frequently overexpressed on CICs of epithelial origin (Yamashita et al., 2009) and adult stem cells. Its expression is usually absent in mature hepatocytes (de Boer et al., 1999). The functions of EpCAM relate to pluripotency maintenance, cell-cell adhesion, migration, proliferation and the regulation of differentiation (Schnell et al., 2013). Polyclonal Huh7 cells express EpCAM (Yamashita et al., 2009). However, after sorting Huh7 cells into subpopulations expressing high and low levels of CD24, EpCAM expression was found to co-segregate with high CD24 expression with minimal expression observed in CD24lo cells (Figure 3.4.1). Nevertheless, EpCAM expression was induced by the DMSO-mediated

differentiation and accumulated in the islands of hepatocyte-like cells. Accordingly, more Cured cells were positive for EpCAM expression than JFH1-replicon cells. Although it can not be excluded that this increase in EpCAM expression may be an artefact of chemically induced differentiation, it may represent a terminal differentiation marker in these cells. In renal cancer EpCAM expression is favourable and associated with a longer progression-free survival (Zimpfer et al., 2014). For HCC, however, EpCAM represents a CIC marker (Yamashita et al., 2008, Yamashita et al., 2013, Yamashita et al., 2009).

E-cadherin is a marker of epithelial cells and is expressed on mature hepatocytes (Ihara et al., 1996). E-cadherin is involved in cell-cell contact formation and has a role in cell signalling and differentiation (van Roy and Berx, 2008). Loss of E-cadherin expression is generally associated with poor patient prognosis in several cancers including HCC (Onder et al., 2008, He et al., 2013b, Chen et al., 2014). The loss of E-cadherin and increase in N-cadherin is usually associated with induction of epithelial-to-mesenchymal transition and has been observed to be a consequence of HCV infection (Li et al., 2016). E-cadherin is associated with tight junction proteins claudin-1 and occludin on the cell membrane (Hartsock and Nelson, 2008), both of which are considered HCV entry factors (Meertens et al., 2008, Ploss et al., 2009), and has been suggested to play a role in the proper localisation of these proteins for HCV entry (Li et al., 2016, Colpitts et al., 2016). Following infection E-cadherin is downregulated by core (Arora et al., 2008, Park and Jang, 2014). However HCV may have another mechanism of E-cadherin downregulation as we see similar effects for the JFH1-replicon (Figure 4.2.17). E-cadherin loss is a common feature associated with oncogenic virus such as for HBV via protein X (Shin Kim et al., 2016). Indeed DMSO induced differentiation of Cured cells did lead to an increase in cytoplasmic E-cadherin levels whereas this increase was not observed for JFH1-replicon cells (Figure 4.2.17). Furthermore E-cadherin appears to be predominantly associated with the cell membrane at day 9 for Cured cells whereas this is less apparent for infected cells.

N-cadherin is commonly used as a marker of EMT and an increase in N-cadherin levels during HCV infection has previously been described (Iqbal et al., 2013, Hu et al., 2017). We made the same observation in proliferating (day 1) JFH1-replicon cells compared to Cured cells (Figure 4.2.18). However N-cadherin has multiple functions depending on the cellular context (Derycke and Bracke, 2004). A gradient of N-cadherin expression exists

from high levels in perivenous hepatocytes, to low levels in periportal ones, at least in mouse livers (Hempel et al., 2015), and reflects the functional gradient of hepatocytes in the liver lobule. At day nine of differentiation we observed an apparent increase in expression of N-cadherin with it localising to the cell membrane in both Cured and JFH1-replicon cells. For HCC, down-regulation of N-cadherin has been linked with metastatic potential and poor surgical prognosis, compared to normal liver tissue where N-cadherin is strongly expressed on cell borders (Zhan et al., 2012). The ratio of E/N-cadherin may be a more helpful prognostic tool. Generally reduced expression and aberrant expression of N-cadherin have been associated with human carcinoma cells and poor patient prognosis. Cho et al., found that a loss of E-cadherin and discontinuous staining of N-cadherin in HCC was a predictive marker for HCC recurrence after resection (Cho et al., 2008).

Occludin is an integral part of tight junctions (Zona Occludens). Tight junctions are a regulator of polarisation and act as a measure of hepatic polarisation and maturation (Palakkan et al., 2015, Treyer and Musch, 2013). HCV has been shown to increase occludin expression in Huh7 cells during viral entry, however occludin is downregulated during infection to prevent super infection (Liu et al., 2009). Orban et al. found occludin was downregulated in HCC tissue compared to normal tissue (Orban et al., 2008). This downregulation is likely regulated by core (Liu et al., 2009), and may be the reason we did not observe a downregulation of Occludin in JFH1-rep cells at day 1 of differentiation (Figure 4.2.19). Differentiation of Cured cells lead to an increase in occludin expression with a localisation concentrated in a single point likely representing the formation of tight junctions between cells (Figure 4.2.19). This localisation was not discernible in JFH1-replicon cells.

The cytoskeletal protein F-actin localises along the plasma membrane in mature hepatocytes (Benkoel et al., 1992). The cytoskeleton is important for polarisation initiation and cell polarity maintenance (Treyer and Musch, 2013). This localisation pattern was not common for proliferating Cured cells and entirely absent for JFH1-replicon cells. In addition the F-actin appeared to form stress fibres in JFH1-replicon cells and J6-JFH1 cells (Figure 4.2.20 & Figure 4.2.21). Stress fibres are associated with motile and migratory cells (Tojkander et al., 2012, Hotulainen and Lappalainen, 2006). The F-actin in differentiated Cured cells, however, became more concentrated at the plasma membrane in regions of cell-cell contact. Stress fibres largely

disappeared in JFH1-replicon cells by day 9 of differentiation however we did not observe the same F-actin re-organisation as in Cured cells with the F-actin not localising to the plasma membrane as clearly when compared to Cured cells.

Alteration of cell-adhesion and cytoskeletal proteins due to HCV infection such as we have recorded could represent a predisposition step towards HCC CIC development. Indeed alteration to proteins such as EpCAM, E and N-cadherin have been recorded in HCC specimens (Yamashita et al., 2013, Chen et al., 2014, Zhan et al., 2012).

We showed that the HCC CIC marker protein levels were upregulated by HCV infection even in the CD24lo background. This is an interesting results as not only is CD24 associated with poor patient prognosis, tumour initiation/maintenance and metastasis but a previous report suggested that CD24 expression was unable to be switched on in CD24 negative cells. CD24 is involved in many oncogenic signalling pathways such as STAT3 and Hif1α signalling (Lee et al., 2011, Thomas et al., 2012), and upregulation of CD24 by HCV may be an important mediator of HCV driven oncogenesis. It is unclear however how HCV is able to increase CD24 protein levels. HCV could affect CD24 protein stability, mRNA translation or gene expression.

We have demonstrated that HCV infection perturbs/alters differentiation however it is important to consider why HCV would have evolved to do so. Is the perturbation a consequence of HCV interaction with cellular proteins to support replication viral production or is perturbation of differentiation a direct mechanism to improve viral replication and production? Differentiation and resultant senescence may represent a problem to HCV replication as to support viral gene expression and genome replication the virus requires the availability of the host translation and lipid biosynthesis machinery, such as eukaryotic translation initiation factors, ribosomal proteins and sterol regulatory element-binding proteins (Randall et al., 2007, Waris et al., 2007, George et al., 2012). It is likely that HCV requires a degree of hepatocyte differentiation in terms of requiring expression of essential cofactors such as miR-122 (likely already in excess however in Huh7 cells) and entry factors such as occludin however viral replication also requires access to cellular translation and lipid biosynthesis machinery hence requiring cells to be actively dividing and not in a senescent state associated with mature hepatocytes. The intermediate stage during differentiation may offer optimal conditions for HCV replication and gene expression. This may explain why we observed an initial increase in NS5A protein levels followed by a

decrease in protein level as the differentiation proceeds (Figure 4.2.12). However HCV induced alterations to cellular protein expression and localisation to maintain cells in this state may predispose these cells to oncogenic transformation.

# 5. Chapter: HCV effect on HIPPO signalling during CD24lo cell differentiation

## 5.1 Introduction

HCV infection perturbs DMSO induced differentiation of CD24lo Huh7 cells, apparent by the development of a reduced number of islands of hepatocyte-like cells, maintenance of proliferation marker ki67 expression and reduced expression of hepatocyte markers Albumin and CYP3A4. The next logical step was to determine which cellular pathway(s) are involved, and which viral protein(s) might be responsible.

The RNA genome of HCV replicates in the cytoplasm and does not integrate into the host genome. Accordingly, HCV proteins alone (for example core and NS5A) or together are able to promote cellular growth and lead to cellular transformation in transgenic mice (Park et al., 2000, Lerat et al., 2002, Wang et al., 2009, Moriya et al., 1998, Zemel et al., 2001, Fukutomi et al., 2005). HCV associated carcinogenesis appears to be complex and the oncogenic role of HCV is less conspicuous than other better characterised oncogenic viruses such as EBV and HBV. Carcinogenic mechanisms associated with HCV include the oncogenic effect of HCV proteins, chronic inflammation, fibrosis, oxidative stress and chromosomal instability (Okuda et al., 2002, Bartsch and Nair, 2004, Koike, 2007, Park et al., 2000, Lerat et al., 2002, Munakata et al., 2005, Moriya et al., 1998, Zemel et al., 2001, McGivern and Lemon, 2011, McGivern and Lemon, 2009). A number of viral proteins have been shown to interact with and alter cellular signalling pathways (Deng et al., 2006, Lan et al., 2002, Wang et al., 2000, Aoki et al., 2000, Burckstummer et al., 2006, Macdonald et al., 2004, Street et al., 2004, Mankouri et al., 2008, He et al., 2002, Cho et al., 2001, Moustafa et al., 2018, Munakata et al., 2005, McGivern and Lemon, 2011, Cao et al., 2004, Bittar et al., 2013).

HCV proteins have been associated with oncogenesis including core, NS3, NS5A and NS5B. HCV proteins have been shown to activate oncogenes, inactivate tumour-suppressor genes and alter signal-transduction pathways. NS3 transfected fibroblasts were shown to proliferate rapidly, lost contact inhibition and formed tumours in mice (Zemel et al., 2001). In addition NS3 interacts with p53 which leads to suppression of p53 mediated transcriptional activation (Deng et al., 2006, Kwun et al., 2001, Ishido et al.,

1998). Indeed Core (Ray et al., 1998, Otsuka et al., 2000), NS2 (Bittar et al., 2013), NS5A (Lan et al., 2002, Qadri et al., 2002, Majumder et al., 2001) and NS5B (Goh et al., 2004) have all been associated with p53 disruption. It is important to note however that Huh7 cells overexpress a defective p53 mutant and p53 has a prolonged half-life in these cells leading to the protein accumulating in the nucleus (Bressac et al., 1990).

Core and NS5A are both implicated interacting with a range of signalling pathways, leading to alterations to the cell cycle, cellular proliferation, cell survival, lipid metabolism and EMT. For example core protein can form a complex with p21 resulting in abrogation of the PCNA binding site (Wang et al., 2000). Core protein can also bind to 14-3-3 with a consequent increase in Raf-1 kinase activity (Aoki et al., 2000)

NS5A has been implicated in the dysregulation of many cell signalling pathways and can interact with a wide range of cellular signalling proteins. NS5A interacts with signalling proteins such as PI3K/Akt, NFκB and Wnt (Macdonald and Harris, 2004). NS5A contains a conserved proline rich motif that can interact with the SH3 domain of cellular proteins including the Src family of kinases (Macdonald et al., 2004).

NS5B is able to bind to Rb to form a complex which is targeted for degradation, leading to a reduction of Rb levels (Munakata et al., 2005). Rb is a key regulator of cellular proliferation and apoptosis and loss of Rb leads to expression of E2F responsive genes and cell proliferation.

However, as the subgenomic replicon induces the same perturbation of differentiation as full length virus, this suggests that the structural proteins, notably core, as well as NS2 are not responsible for changes observed in our experimental system. Here we attempted to determine the mechanism behind HCV-induced perturbation of DMSO stimulated Huh7 CD24lo cell differentiation caused by the NS3-NS5B region of the HCV polyprotein.

## 5.2 The Hippo pathway

We performed enrichment gene analysis using Enrichr and a published gene expression data set of J6-JFH1 infected cycling Huh7.5 cells (Woodhouse et al., 2010). The study from Woodhouse et al., also including DNA microarray analysis, it is important to note that we used the data from the RNA sequencing (RNA-seq) experiment for enrichment analysis. Enrichment analysis can be used to analyse gene data sets which have been generated

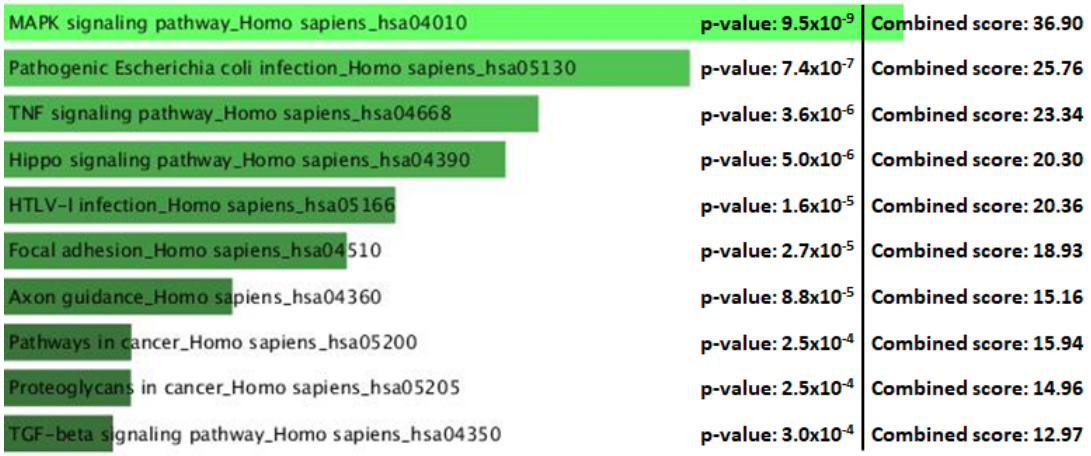


**Figure 5.2.1 Enrichr pathway analysis**

Enrichr pathway analysis using the KEGG signalling database. KEGG pathways predicted to be altered based on the input gene expression data, are ranked by p-value. The length and the brightness of the bar reflects the significance of that term/gene set, i.e. the longer and brighter the bar, the more significant the term/gene set is. A grey bar means the term/gene-set is not significant. The input data set is from Woodhouse et al., 2010. Bar Graph representation of the Enrichr KEGG pathway analysis. The p-value is calculated from the Fisher exact test which is commonly used by most enrichment analysis tools. The combined score represents a calculated combination of the p-value and the z-score. The z-score represents the deviation from an expected rank and is calculated using a modified Fisher's exact test. Sourced from Enrichr website and publications where further explanation of the different scores can be found (Chen et al., 2013b, Kuleshov et al., 2016).

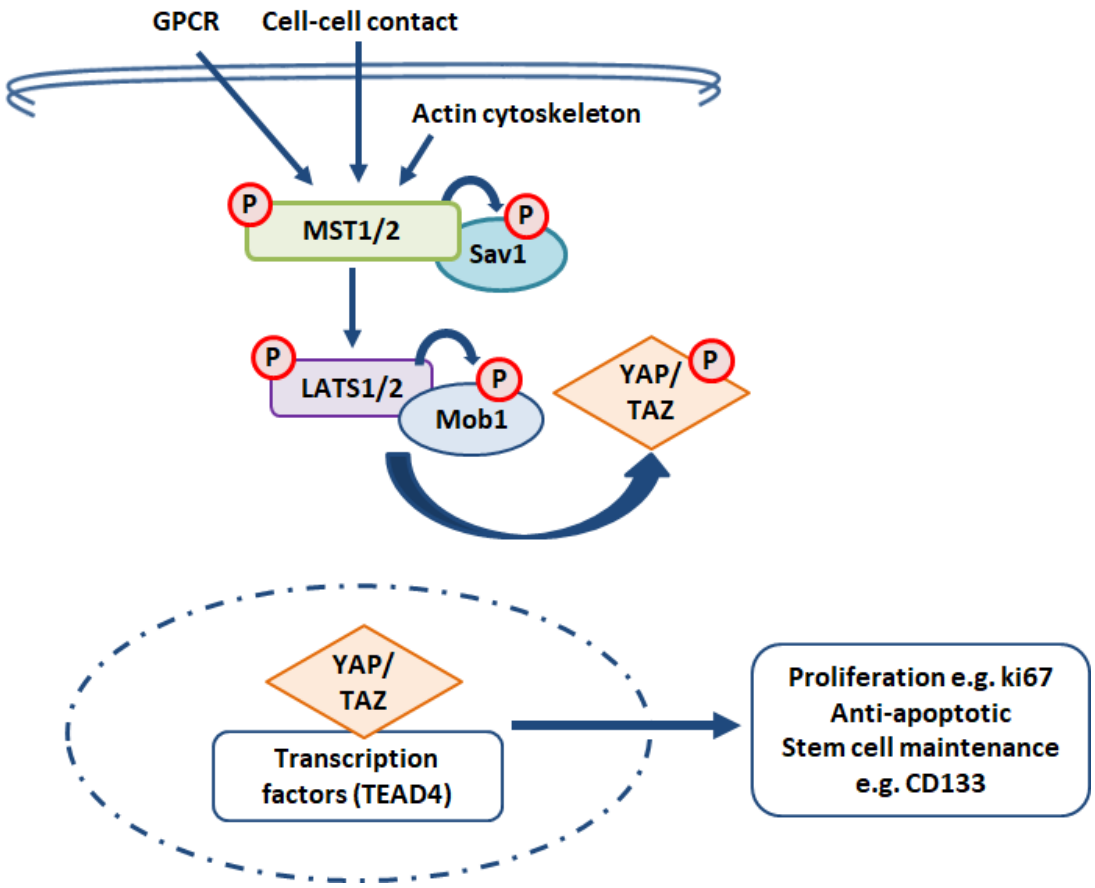


**Figure 5.2.2 Hippo pathway diagram**

Simplified diagram of the Hippo signalling pathway. In the absence of Hippo signalling YAP1/TAZ translocate to the nucleus and bind to transcription factors such as TEAD4 leading to the transcription of proliferative, pro-survival and stem cell maintenance genes. When Hippo signalling is activated in response to cell-cell contact via tight junctions, adherens junction or via TGF-ß signalling or Wnt signalling pathways, this leads to the phosphorylation and activation of MST1/2 which in turn phosphorylates SAV1. Next in the signalling pathway LATS1/2 is phosphorylated and activated which leads to the phosphorylation of Mob1. LATS1/2 phosphorylates YAP1 which leads to YAP1 being sequestered in the cytoplasm and being degraded.

by genome-wide experiments. Enrichment analysis draws upon curated and annotated gene-set libraries to visualise and better understand the input gene data set and associates a functional biological term to a collection of genes. This type of analysis compares the input gene data set to annotated gene sets. By comparing the input data set with annotated gene sets the analysis can calculate whether the input gene set significantly overlaps with the annotated gene set and infers knowledge about the input gene. Enrichr is a popular enrichment analysis tool (Chen et al., 2013b, Kuleshov et al., 2016). A functional term such as a pathway or disease has been associated with every gene set on the Enrichr database. This way Enrichr can predict which pathways may be leading to the observed gene profile of the input data set or which may be altered by the input gene data set by using annotated databases such as the Kyoto Encyclopaedia of genes and genomes (KEGG) (Kanehisa and Goto, 2000).

The top three pathways highlighted by the KEGG analysis when ranked by p-value were expected from the published literature, and included the MAPK signalling pathway ($p=9.5x10^{-9}$) and the TNF signalling pathway ($p=3.6x10^{-6}$) (Figure 5.2.1). MAPK signalling pathway has previously been shown to be activated by HCV infection. NS5A interacts directly with Grb2 via the SH3 domain which inhibits the activation of ERK1/2 by EGF (He et al., 2001, Tan et al., 1999, Macdonald et al., 2004). Core can activate the Raf/MEK/ERK cascade (Giambartolomei et al., 2001, Hayashi et al., 2000, Fukuda et al., 2001) independently to EGF and TGF-α signalling (Hayashi et al., 2000). TNF signalling was another pathway highlighted by the Enrichr analysis. TNF-alpha (TNF- α) plays a crucial role in the host immune response to infection and is activated by HCV infection apparent by elevated levels of circulating TNF- α and soluble TNF receptors (Nelson et al., 1997).

Interestingly, the $4^{th}$-ranked pathway highlighted by the Enrichr KEGG analysis was the Hippo pathway, which is an important signalling pathway during liver development, regeneration and hepatocyte differentiation (Meng et al., 2016). The pathway is regulated by cell-cell contact, cell polarity, the actin cytoskeleton, mechanical transduction and hormonal signals via G-protein coupled receptors (Meng et al., 2016). The core of the pathway consists of a kinase cascade which functions to inhibit the activation of the transcriptional co-activators YAP1 and TAZ. MST1/2 in complex with Sav1 phosphorylate and activate LATS1/2 and co-activator MOB1. The LATS1/2 kinases in turn phosphorylate transcriptional regulators YAP1 and TAZ (Figure 5.2.2). Phosphorylation of YAP1 and TAZ promotes their nuclear exit

and ultimately inhibits their function. LATS1/2 phosphorylation at TAZ(Ser89) and YAP1(Ser127) results in 14-3-3 binding and cytoplasmic retention of YAP1 and TAZ (Zhao et al., 2007). Further LATS1/2 phosphorylation at YAP1(Ser397) and TAZ(Ser11) primes these proteins for casein kinase 1δ/1ε (CK1δ/ε) phosphorylation at TAZ(Ser314) and on YAP1(Ser400/403). TAZ(Ser314) and YAP1(Ser400/403) phosphorylation leads β-TrCP/SCF dependent ubiquitination and proteasomal degradation (Liu et al., 2010, Zhao et al., 2010). Nuclear YAP1 and TAZ promote cell proliferation, cell survival and tissue growth by binding to and regulating transcription factors such as TEADs and SMADs (Hong and Guan, 2012). Since the pathway was first identified in *Drosophila* over 20 years ago many studies have revealed the Hippo pathway as a complex network with over 30 components with a large protein interactome (Moya and Halder, 2014). Abnormal Hippo signalling is associated with liver tumorigenesis (both HCC and ICCA) (Lu et al., 2010, Chakraborty and Hong, 2018, Lee et al., 2010, Patel et al., 2017, Sugimachi et al., 2017, Pei et al., 2015). MST1/2 ablation in mice leads to YAP1-dependent liver overgrowth and eventually HCC and ICCA (Zhou et al., 2009, Song et al., 2010).

### 5.2.1 HCV effects upon on Hippo pathway associated proteins

Hippo pathway inactivation and resultant nuclear localisation of transcriptional regulators YAP1 and TAZ is associated with proliferation, cell survival and stem cell maintenance (Pan, 2010). The Hippo pathway is an essential regulator of liver development, hepatocyte differentiation and so is a potent tumour suppressor pathway (Nguyen et al., 2015, Alder et al., 2014, Sebio and Lenz, 2015). Hepatocyte differentiation requires Hippo signalling activation and inactivation of YAP1 (Yimlamai et al., 2014). Activation signals come from tight junction and adherens junction proteins, Wnt signalling, GPCRs and the actin cytoskeleton (Meng et al., 2016). Differentiated CD24lo Huh7 cells were analysed for expression and localisation of Hippo pathway associated proteins. This analysis revealed that HCV infection altered both Hippo pathway protein expression and localisation during differentiation. We expected to observe an increase in MST1 and LATS1 activation over the course of CD24lo differentiation with a parallel drop in nuclear YAP1 and TAZ levels corresponding to the activation of the Hippo signalling pathway. An increase in Hippo signalling should lead to YAP1 and TAZ being sequestered in the cytoplasm and being degraded.

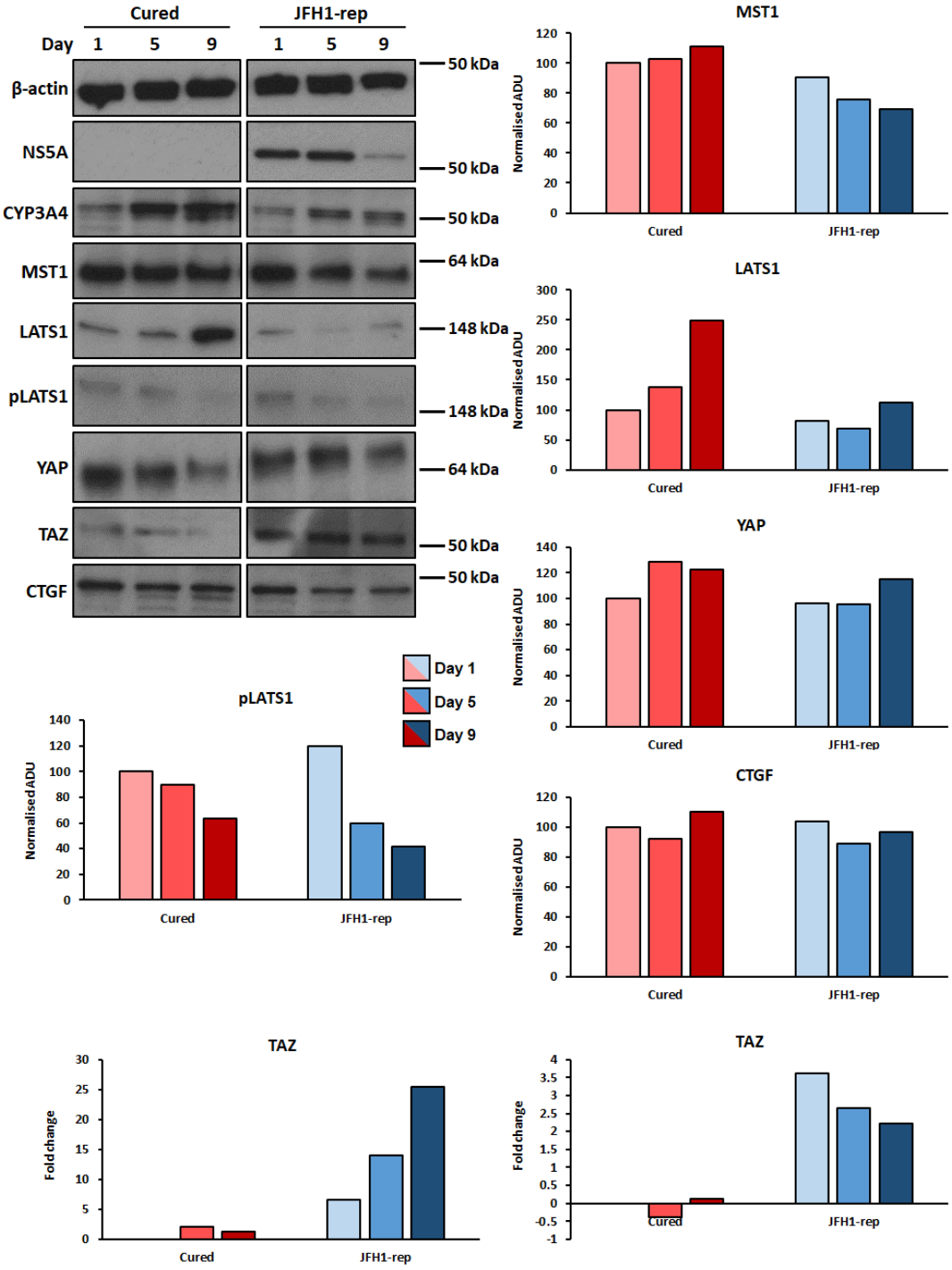


**Figure 5.2.3 Western blot of differentiated Cured and JFH1-rep CD24lo**

Cells were differentiated over a course of nine days during which the media was changed every two days. A well of a 6 well plate was lysed in 150 µ EBC buffer for Western blot analysis on day one, five and nine. Membranes were probed for β-actin, NS5A, CYP3A4, MST1, pLATS1, LATS1, YAP1, TAZ, or CTGF. Quantification of MST1 (n=2), LATS1 (n=2), pLATS1, YAP1 (n=2), TAZ (n=2) and CTGF western blot intensity normalised to β-actin band intensity (arbitrary densitometry units (ADU)) measured using ImageJ. Displayed as the percentage of Cured Day 1.

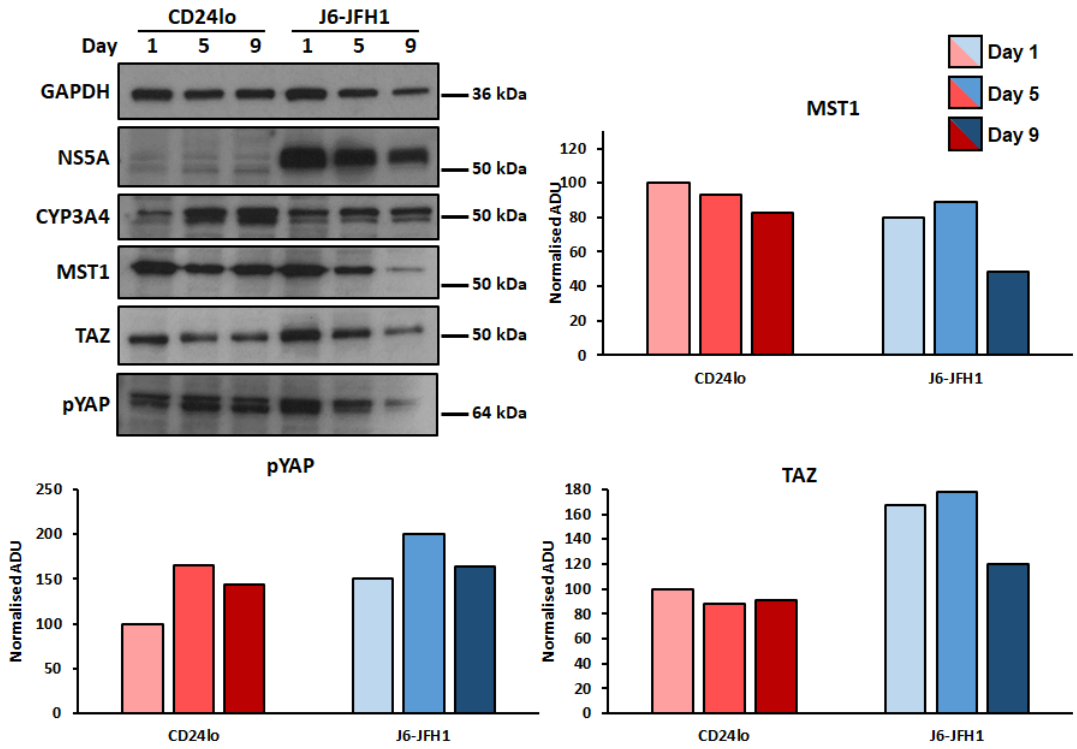


**Figure 5.2.4 Western blot of differentiated CD24lo and J6-JFH1 infected CD24lo**

Cells were differentiated over a course of nine days during which the media was changed every two days. A well of a 6 well plate was lysed in 150 µ EBC buffer for Western blot analysis on day one, five and nine. Membranes were probed for GAPDH, NS5A, CYP3A4, MST1, TAZ, or pYAP1. Quantification of MST1 (n=2), TAZ (n=1) and pYAP1 (n=2) western blot intensity normalised to GAPDH band intensity (arbitrary densitometry units (ADU)) measured using ImageJ. Displayed as the percentage of Cured Day 1. Two-tailed Student's t-test *≤0.05.

By Western blot we observed that MST1 levels are maintained over the course of differentiation in Cured and CD24lo cells (Figure 5.2.3 & Figure 5.2.4). However for virus infected cells (both J6-JFH1 and JFH1-replicon) there was a trend towards a reduction in MST1 levels over differentiation (Figure 5.2.3 & Figure 5.2.4) and MST1 protein levels were significantly lower in JFH1-replicon cells at day 5 and 9 compared to day 1 Cured cells. MST1 levels in J6-JFH1 infected cells followed a similar pattern (Figure 5.2.4). MST1 immunofluorescence revealed that the MFI of MST1 for Cured cells was significantly higher at day one of differentiation compared to JFH1-replicon cells (Figure 5.2.5 & Figure 5.2.7). The MFI increased for both Cured and JFH1-replicon cells over differentiation however the MFI remained significantly higher for Cured cells compared to JFH1-replicon cells at day 9 (Figure 5.2.7). At day one of differentiation the MST1 protein resided in both the nucleus and the cytoplasm in Cured and JFH1-replicon cells. At day nine of differentiation MST1 was concentrated to the centrosome in both Cured and JFH1-replicon cells (Figure 5.2.5). The centrosome staining remained for the JFH1-replicon cells whereas the cytoplasmic staining appeared diminished. A similar trend was observed when comparing differentiated CD24lo cells and J6-JFH1 infected cells (Figure 5.2.6 & Figure 5.2.7).

By western LATS1 levels increased over the course of differentiation. LATS1 levels were however significantly lower throughout the course of differentiation for JFH1-replicon cells (Figure 5.2.3). pLATS1 levels surprisingly dropped over the course of differentiation for both Cured and JFH1-replicon cells however this observation stemmed from one experiment (Figure 5.2.3). IF showed that on day one of differentiation, LATS1 was unexpectedly located in the nucleus in both CD24lo and JFH1-replicon cells (Figure 5.2.8). The consequence of LATS1 nuclear localisation is not fully understood, however the localisation does appear to impact on LATS1 activity, for example LATS1 targeting to the membrane increases LATS1 activity (Hergovich et al., 2006, Hergovich, 2013). By day nine of differentiation LATS1 localisation in Cured cells became predominantly cytoplasmic, whereas JFH1-replicon cells maintained LATS1 in the nucleus in (Figure 5.2.8). This same difference in localisation was not observed between CD24lo and J6-JFH1 cells (Figure 5.2.9). The same trend of lower LATS1 levels in the virus containing cells compared to control cells was observed for both the replicon and full length virus infected CD24lo cells (Figure 5.2.8 & Figure 5.2.9).

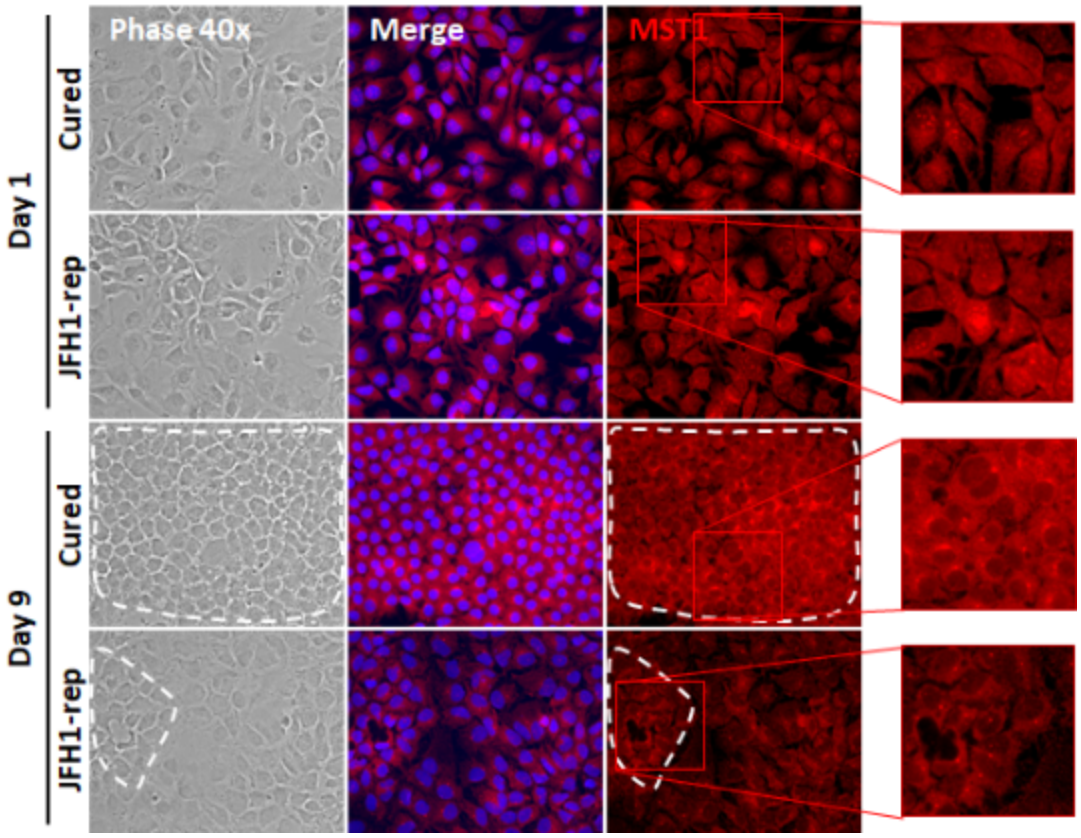


**Figure 5.2.5 Immunofluorescence of differentiated Cured and JFH1-rep CD24lo cells stained for MST1**

Cells were differentiated on cover slips in a 12 well plate and fixed in 4 % PFA in PBS at day one and day nine of differentiation. The cells were then permeabilised using 0.2 % Triton-X100 and stained using antibodies against MST1 (red) and 594 nm fluorescently conjugated Alexa Fluor secondary antibodies. The nuclei were counterstained using the DNA stain Hoechst (blue). Images were taken using the 40x objective of the Nikon Eclipse Ti-E Widefield Fluorescent Inverted Microscope. Islands of hepatocyte-like cells are highlighted by dashed white lines. Images are representative of cell density.

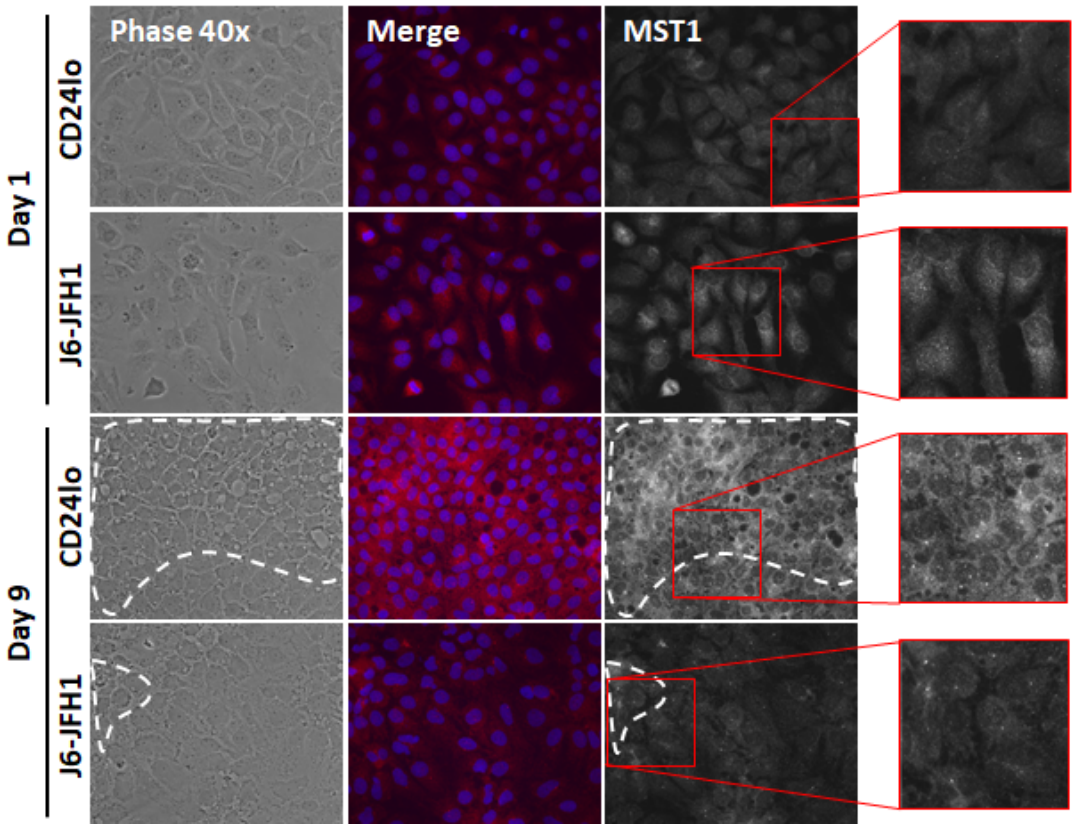


**Figure 5.2.6 Immunofluorescence of differentiated CD24lo and J6-JFH1 CD24lo cells stained for MST1**

Cells were differentiated on cover slips in a 12 well plate and fixed in 4 % PFA in PBS at day one and day nine of differentiation. The cells were then permeabilised using 0.2 % Triton-X100 and stained using antibodies against MST1 (gray) and 594 nm fluorescently conjugated Alexa Fluor secondary antibodies. The nuclei were counterstained using the DNA stain Hoechst (blue). Images were taken using the 40x objective of the Nikon Eclipse Ti-E Widefield Fluorescent Inverted Microscope. Islands of hepatocyte-like cells are highlighted by dashed white lines. Images are representative of cell density.

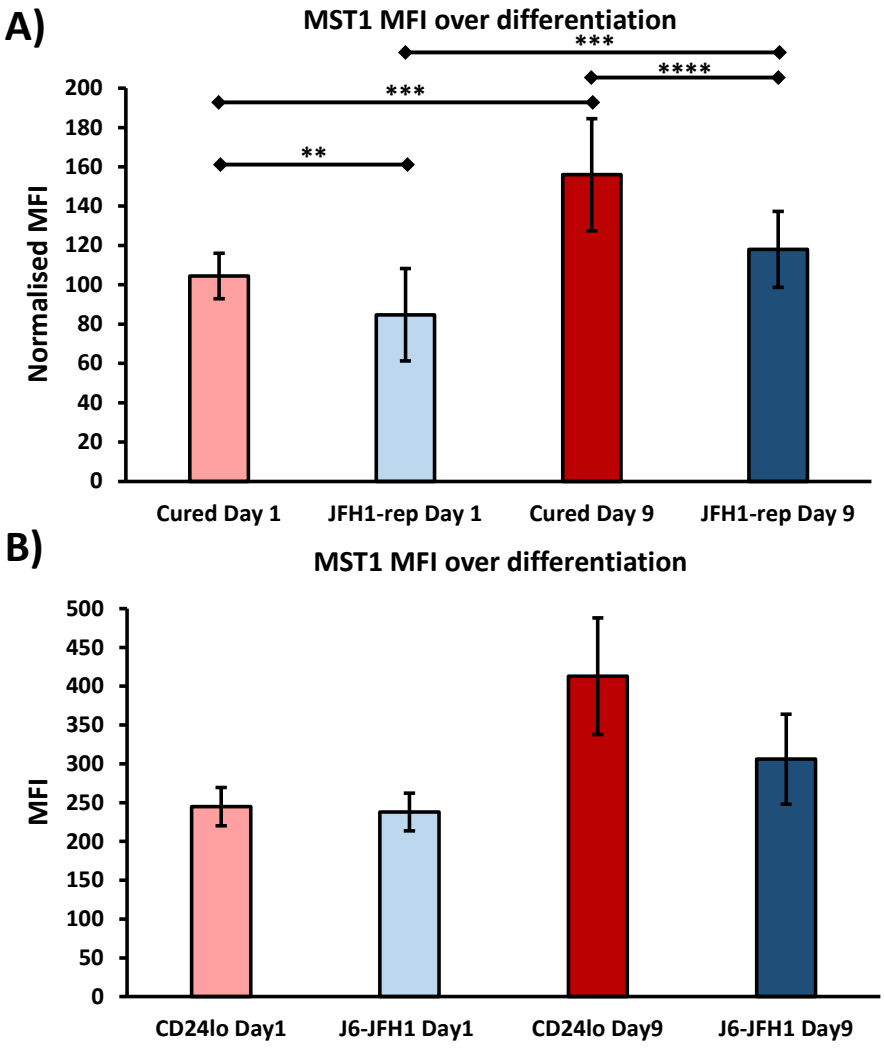


**Figure 5.2.7 Quantification of MST1 immunofluorescence**

A) Quantification of immunofluorescence of Cured and JFH1-replicon CD24lo cells at day one and day nine of differentiation using Image J. MST1 staining was quantified as the MFI per image for MST1 (two-tailed student t-test, *p≤0.05, **p≤0.01, ***p≤0.001, ***p≤0.0001 n=3). B) Quantification of immunofluorescence of CD24lo and J6-JFH1 infected CD24lo cells at day one and day nine of differentiation using Image J. MST1 staining was quantified as the MFI per image for MST1 (n=1).

YAP1 protein levels were unaffected over course of differentiation in both Cured and JFH1-replicon cells and overall levels were similar in both control and HCV containing cells (Figure 5.2.3). YAP1 becomes phosphorylated in the response to Hippo activation by LATS1/2 activity at up to five sites; S127 is one of the best characterised and results in 14-3-3 binding and cytoplasmic retention (Zhao et al., 2007). For J6-JFH1 infected and CD24lo cells pYAP1(S127) levels were probed and there was a trend towards a slight increase in pYAP1 levels over the course of differentiation in both control and infected cells (Figure 5.2.4), supporting an increase in Hippo signalling pathway activity.

The localisation of transcription regulator YAP1 is an important indicator of its activity (Zhao et al., 2007). At day one of differentiation YAP1 was located in the nucleus of HCV negative and HCV containing CD24lo cells (Figure 5.2.10 & Figure 5.2.11). At day nine of differentiation YAP1 was located predominantly in the cytoplasm of HCV control CD24lo lines. However, in HCV containing CD24lo cells more cells maintained nuclear YAP1 expression. YAP1 and TAZ share regulatory mechanisms, and are both phosphorylated and sequestered to the cytoplasm by Hippo activation. However, different regulatory mechanisms have been identified for these two transcriptional regulators and there appears to be a reciprocal regulatory feedback mechanism between the proteins (Moroishi et al., 2015). Interestingly we saw a maintenance in TAZ levels in JFH1-replicon cells compared to Cured cells and TAZ levels remained high throughout differentiation for the JFH1-replicon cells, when YAP1 levels appear unchanged and at a similar level in these cells lines (Figure 5.2.3). The same trend was observed in J6-JFH1 cells compared to CD24lo cells (Figure 5.2.4).

Connective tissue growth factor (CTGF) has been identified as one of the direct target genes of YAP1/TEAD interactions and plays an important protein mediating YAP1-dependent cell growth (Zhao et al., 2008). However, CTGF levels were similar in both Cured and JFH1-replicon cells and remained unaltered throughout differentiation (Figure 5.2.3). This is just one example of a YAP1/TAZ responsive gene. Activation of different genes will be cell type and context specific. Taken together these changes in protein expression and localisation suggest HCV infection is able to alter and perturb this signalling pathway but how this effect is mediated is not clear. It is important to bear in mind that Hippo signalling and YAP1 and TAZ activity and phosphorylation are regulated and altered by a range of proteins.

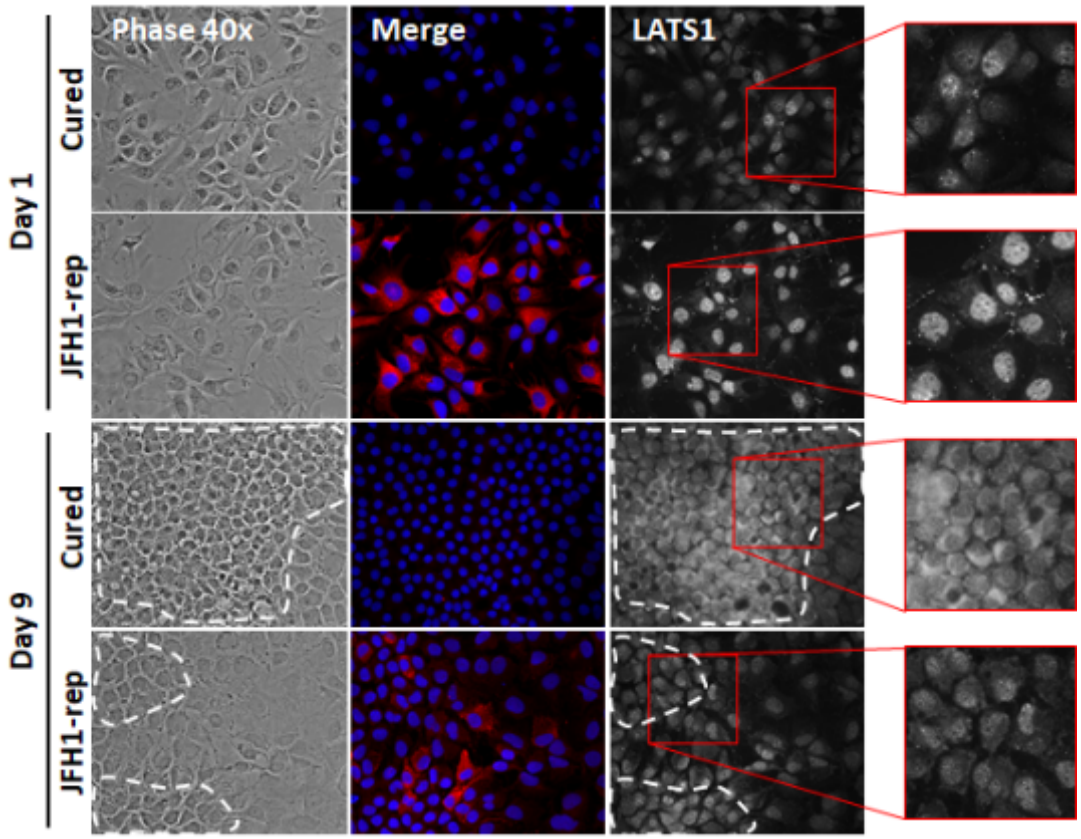


**Figure 5.2.8 Immunofluorescence of differentiated Cured and JFH1-rep CD24lo cells stained for NS5A and LATS1**

Cells were differentiated on cover slips in a 12 well plate and fixed in 4 % PFA in PBS at day one and day nine of differentiation. The cells were then permeabilised using 0.2 % Triton-X100 and stained using antibodies against LATS1 (gray) and NS5A (red) and 488 nm and 594 nm fluorescently conjugated Alexa Fluor secondary antibodies respectively. The nuclei were counterstained using the DNA stain Hoechst (blue). Images were taken using the 40x objective of the Nikon Eclipse Ti-E Widefield Fluorescent Inverted Microscope. Islands of hepatocyte-like cells are highlighted by dashed white lines. Images are representative of cell density.

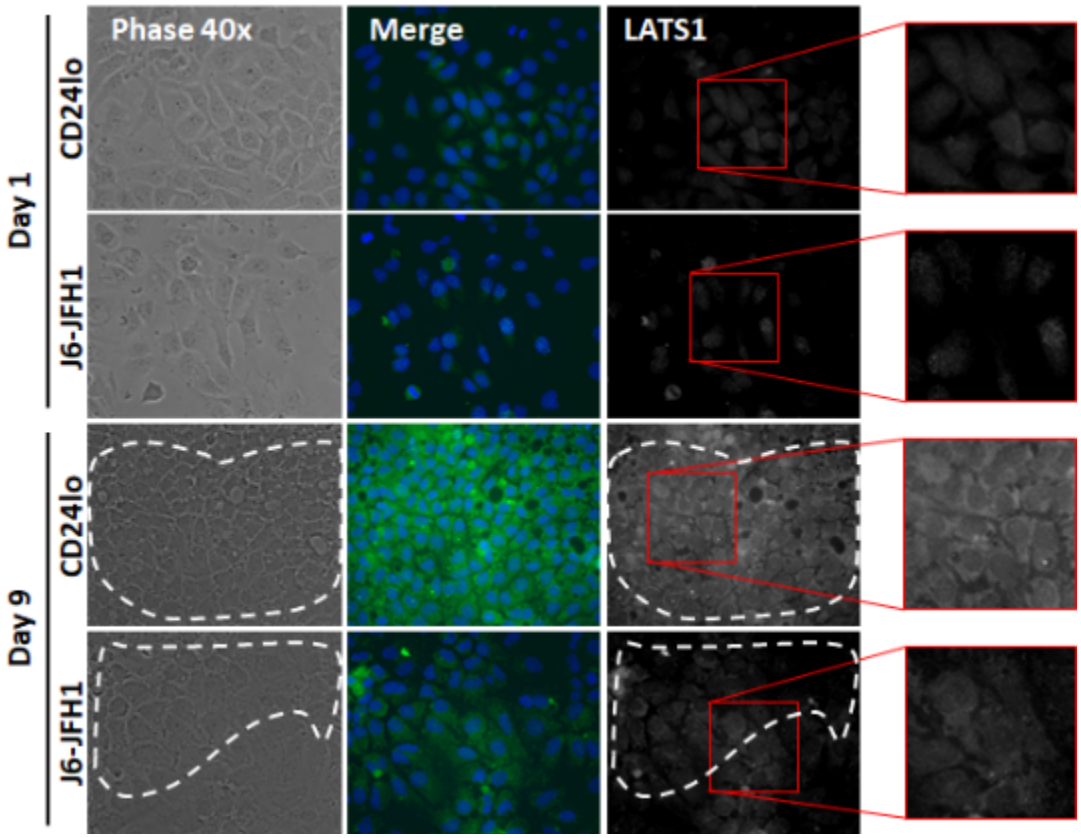


**Figure 5.2.9 Immunofluorescence of differentiated CD24lo and J6-JFH1 CD24lo cells stained for LATS1**

Cells were differentiated on cover slips in a 12 well plate and fixed in 4 % PFA in PBS at day one and day nine of differentiation. The cells were then permeabilised using 0.2 % Triton-X100 and stained using antibodies against LATS1 (grey) and 488 nm fluorescently labelled Alexa Fluor secondary antibodies. The nuclei were counterstained using the DNA stain Hoechst (blue). Images were taken using the 40x objective of the Nikon Eclipse Ti-E Widefield Fluorescent Inverted Microscope. Islands of hepatocyte-like cells are highlighted by dashed white lines. Images are representative of cell density.

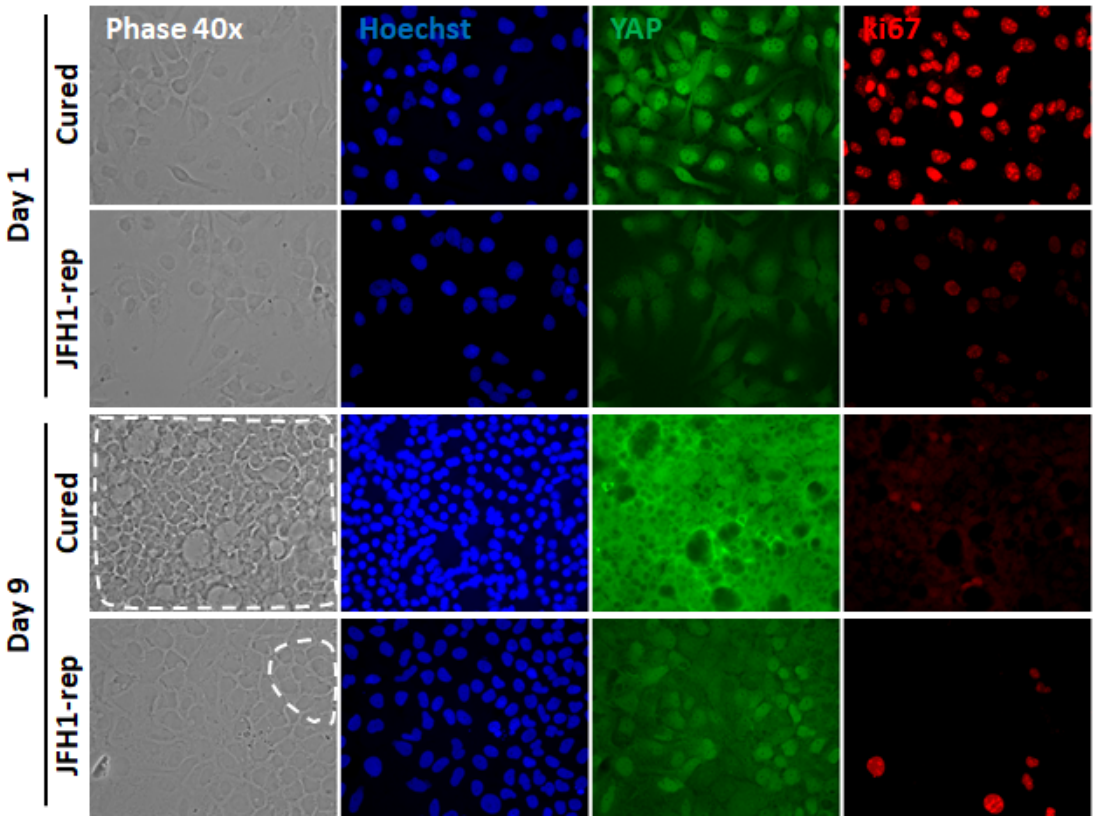


**Figure 5.2.10 Immunofluorescence of differentiated Cured and JFH1-J6 CD24lo cells stained for YAP1 and ki67**

Cells were differentiated on cover slips in a 12 well plate and fixed in 4 % PFA in PBS at day one and day nine of differentiation. The cells were then permeabilised using 0.2 % Triton-X100 and stained using antibodies against YAP1 (green) and ki67 (red) and 488 nm and 594 nm fluorescently conjugated Alexa Flour secondary antibodies respectively. The nuclei were counterstained using the DNA stain Hoechst (blue). Images were taken using the 40x objective of the Nikon Eclipse Ti-E Widefield Fluorescent Inverted Microscope. Islands of hepatocyte-like cells are highlighted by dashed white lines. Images are representative of cell density.

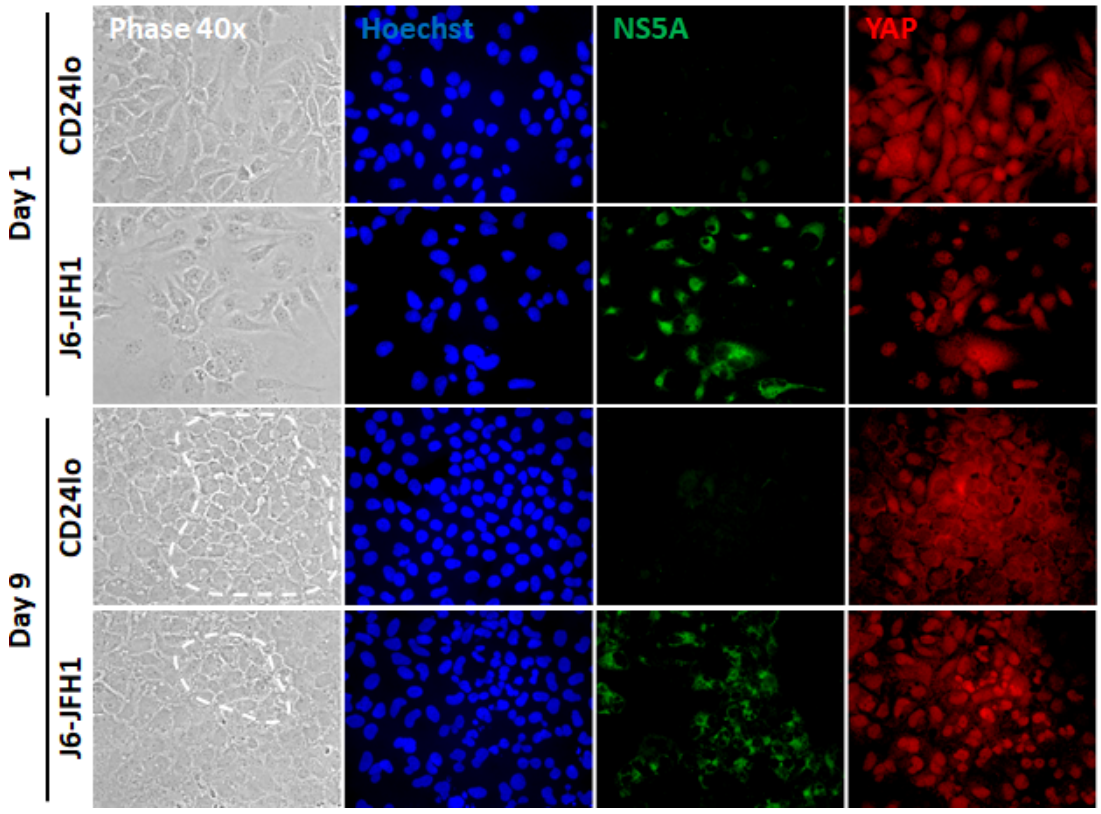


**Figure 5.2.11 Immunofluorescence of differentiated CD24lo and J6-JFH1 CD24lo cells stained for NS5A and YAP1**

Cells were differentiated on cover slips in a 12 well plate and fixed in 4 % PFA in PBS at day one and day nine of differentiation. The cells were then permeabilised using 0.2 % Triton-X100 and stained using antibodies against NS5A (green) and YAP1 (red) and 488 nm and 594 nm fluorescently conjugated Alexa Fluor secondary antibodies respectively. The nuclei were counterstained using the DNA stain Hoechst (blue). Images were taken using the 40x objective of the Nikon Eclipse Ti-E Widefield Fluorescent Inverted Microscope. Islands of hepatocyte-like cells are highlighted by dashed white lines. Images are representative of cell density.

### 5.2.2 Interaction between the HCV NS5A protein and Hippo pathway protein MST1

Immunofluorescence and western blot characterisation demonstrated that HCV infection alters Hippo protein expression and localisation however it is unclear how this effect is mediated. Our results showed that MST1 levels were reduced and that the cytosolic expression is reduced whereas centriole localisation remains in Control cells after differentiation. It is likely that this effect is mediated by a viral protein and, as we see the same trend in replicon cells and full length virus infected cells, the viral protein(s) responsible must be contained within the NS3-NS5B replicon polyprotein. As already mentioned, NS5A is known to interact with a range of cellular proteins so we hypothesised that it may also interact with and negatively regulate Hippo pathway components. To investigate this notion, we performed co-staining immunofluorescence using antibodies targeting NS5A as well as Hippo pathway proteins (LATS1, MST1 and YAP1). Immunofluorescent detection of NS5A and MST1 using a Widefield Fluorescent Inverted Microscope supported co-localisation between the two proteins within JFH1-replcion cells (Figure 5.2.12). To explore this further CD24lo cells were infected with a J6-JFH1 clone which contains enhanced green fluorescent protein inserted into domain III of NS5A (J6-eGFP) (Gottwein et al., 2011) (Figure 5.2.13). Differentiation of the J6-eGFP cells confirmed that the same differentiation pattern was observed with this HCV clone as cells infected with the WT J6-JFH1 clone (Figure 5.2.14), suggesting that domain III of NS5A is unlikely to be involved in manipulating relevant host cell pathways. However, the NS5A-eGFP fusion protein allowed us to take advantage of GFP-trap pulldowns to investigate potential interaction partners associated with the NS5A-eGFP fusion protein. Precipitates were probed for selected core Hippo pathway proteins for which reliable immunological reagents were available (MST1, LATS1, MOB1 and YAP1). Of these, MST1 specifically accumulated within the bound fragment of the GFP-trap pulldown (Figure 5.2.15) whereas other Hippo components did not (data not shown).

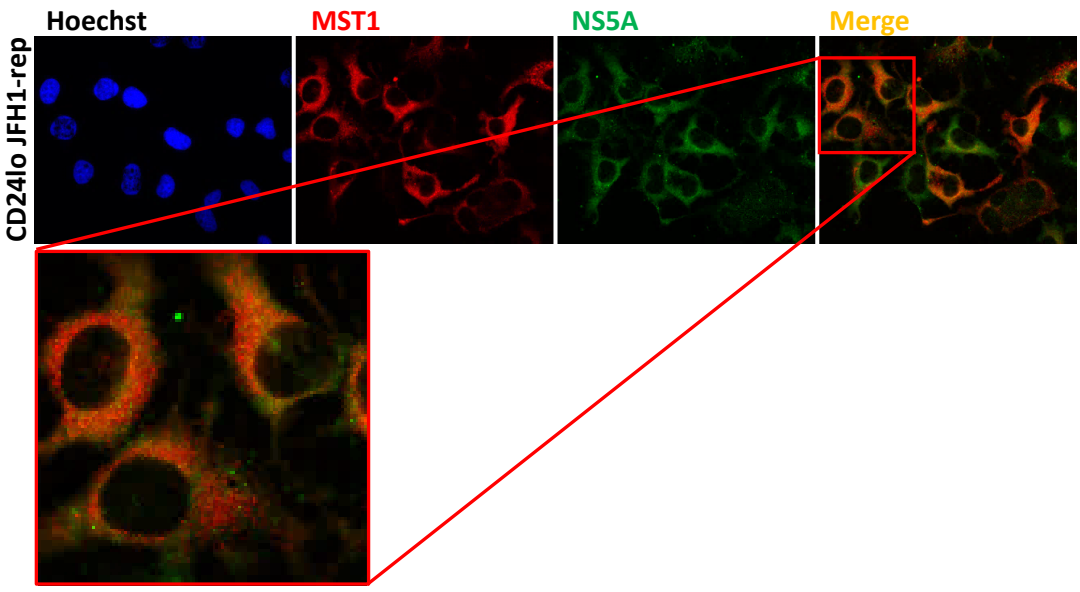


**Figure 5.2.12 Immunofluorescence showing the possible co-localisation of MST1 and NS5A in JFH1-replicon CD24lo cells**

Fluorescence microscopy of JFH1-replicon CD24lo cells using the 60x objective of the Nikon Eclipse Ti-E Widefield Fluorescent Inverted Microscope. Cells were fixed using 4 % PFA in PBS and permeabilised using 0.2 % Triton-X100 in PBS. Cells were stained using antibodies against MST1 (red) and NS5A (green) and 594 nm and 488 nm fluorescently conjugated secondary antibodies respectively.

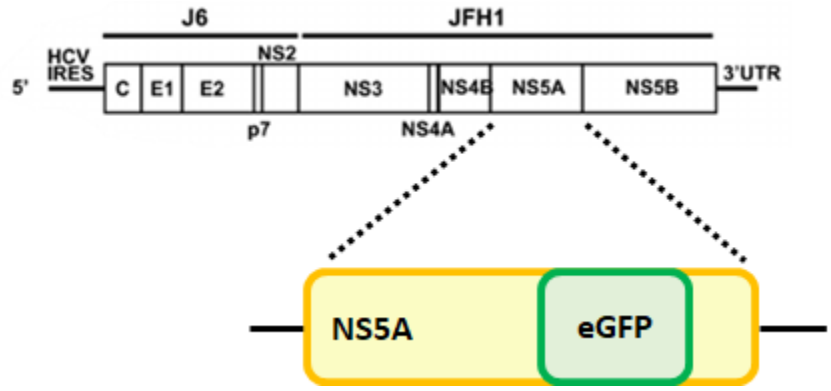


**Figure 5.2.13 Diagram of the J6-JFH1 clone expressing an NS5A-eGFP fusion protein (J6-eGFP)**

The enhanced green fluorescent protein was inserted into domain III of NS5A in the background of the J6-JFH1 viral construct. Diagram adapted from (Matsui et al., 2012).

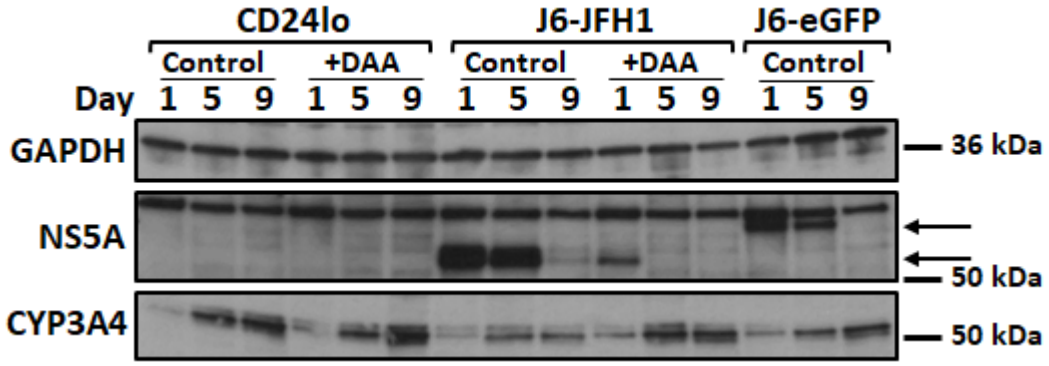


**Figure 5.2.14 Western blot of differentiated CD24lo cells and CD24lo cells infected with J6-JFH1 and J6-eGFP**

Cells were differentiated over a course of nine days with media changes every two days. About $1x10^6$ cells were lysed for Western blot analysis on day one, five and nine. Membranes were probed for GAPDH, NS5A and CYP3A4. Arrows on the NS5A blot indicate NS5A bands. The top band is a non specific band associated with the polyclonal anti-NS5A antibody. The top arrow indicates the NS5A-eGFP fusion protein with a higher molecular weight than the NS5A protein, marked by the bottom arrow.

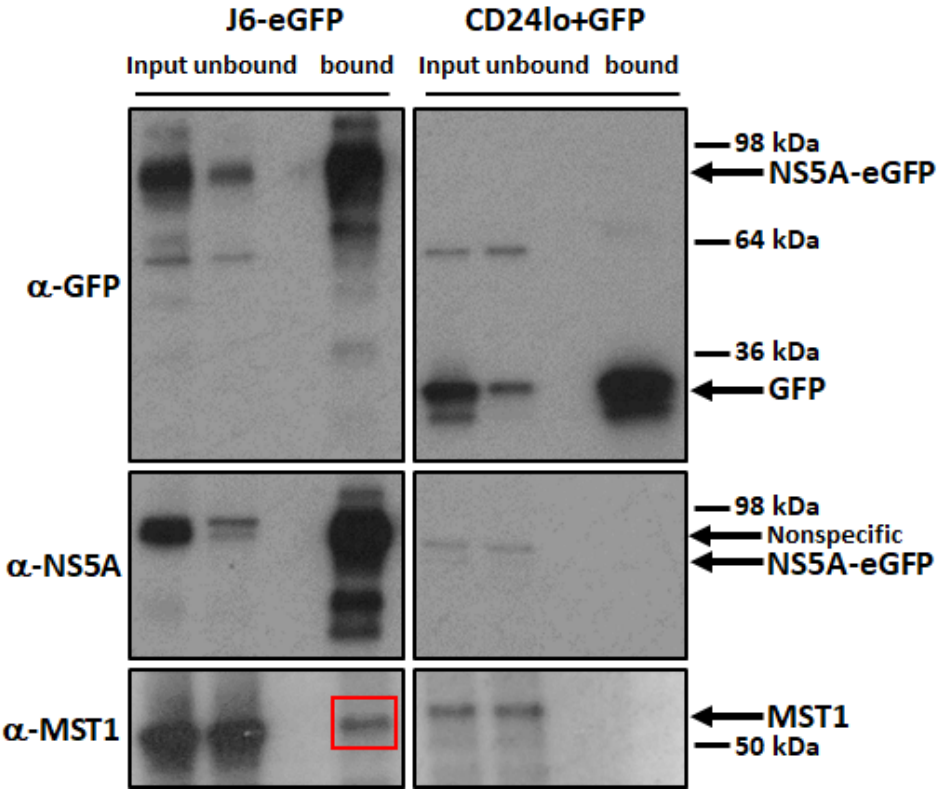


**Figure 5.2.15 Pulldown for NS5A-eGFP using the GFP-trap technique**

J6-eGFP infected CD24lo cells and CD24lo cells transfected with the GFP protein were lysed and incubated with agarose beads conjugated with anti-GFP antibodies. Samples were taken from the initial lysate (input), from the unbound fragment (unbound) and from the fragment eluted from the beads (bound). Western blot membranes were stained for GFP, NS5A or MST1. Representative blot from three experimental repeats.

### 5.2.3 Exploring the link between CD24lo differentiation and the Hippo pathway through Hippo protein inhibitors and RNA knockdown

### 5.2.4 Attempted shRNA- mediated knockdown of YAP1 expression and pharmaceutical manipulation of its activity

We have demonstrated that Hippo protein expression and localisation is altered during differentiation and in the presence of virus infection. However we wanted to explore whether differentiation was dependent on Hippo pathway signalling and whether the altered differentiation phenotype observed in infected CD24lo cells was due to perturbation of Hippo signalling. We explored interference of YAP1 expression via shRNA mediated knock down (Origene technologies), as well as attempting to remove YAP1 from the Huh7 genome using the ABM All-in-one CRISPR-Cas9 nuclease system with a panel of YAP1-targeted guide RNAs. CD24lo cells were transduced with Lentiviral vectors expressing short hairpin RNA designed to target YAP1. No observable YAP1 knockdown was noted after transduction by immunofluorescence (Figure 5.2.16) or by Western blot (data not shown).

Several drugs exist which are reported to inhibit YAP1 and/or TAZ activity such as Verteporfin, Dobutamine (Dob) and Pazopanib (Pazo). Verteporfin is a suppressor of the YAP1-TEAD complex via binding to YAP1 to alter the protein conformation and prevent YAP1 binding to TEAD (Liu-Chittenden et al., 2012). Dobutamine and Pazopanib prevent YAP1 nuclear translocation and lead to YAP1 phosphorylation (Bao et al., 2011, Oku et al., 2015). Dobutamine stimulates the β-adrenergic receptor which is a G-protein coupled receptor that regulates YAP1/TAZ phosphorylation (Yu et al., 2012). Pazopanib multi-kinase inhibitor not only prevents YAP1/TAZ nuclear translocation by increases their phosphorylation but also stimulates the proteasomal degradation of YAP1 and TAZ.

Cured cells were treated with YAP1 inhibitors Verteporfin (10 μM- 0.3 μM), Dobutamine (80 μM- 0.6 μM) and Pazopanib (20 μM- 0.2 μM) for 24 hr. However, by immunofluorescence these inhibitors appeared unable to induce a change in YAP1 nuclear localisation in Cured cells at a range of concentrations (Figure 4.2.17). Verteporfin induced significant cell death above 1 μM or in treatments longer than 48 hr. Indeed, differentiation of Cured and JFH1-replicon cells in the presence of 1 μM of the YAP1 inhibitor Verteporfin led to pronounced cytotoxicity to both cell lines (data not shown). Inhibitor concentrations were chosen based on the literature as well as

optimisation of assay windows using MTT assays (data not shown). Differentiation in the presence of Dobutamine (20 μM) and Pazopanib (1 μM) did not induce any morphological differences in terms of the number of hepatocyte islands observed between untreated or treated cells. Dobutamine, but not Pazopanib, did however induce an increase in CYP3A4 levels within JFH1-replicon cells, although the levels observed in control cells were not restored (Figure 5.2.18 & Figure 5.2.19).

### 5.2.5 Pharmaceutical manipulation of MST activity

Chemical inhibition or activation of upstream YAP1 regulators would help investigate the role of Hippo signalling in CD24lo differentiation. XMU-MP-1 (XMU) is the only published inhibitor of MST1/2 kinase activity. The potent and selective MST1/2 inhibitor was identified in a high-throughput screen and underwent rounds of structure-activity optimisation (Fan et al., 2016). XMU-MP-1, which is an ATP-competitive inhibitor for MST1/2, was shown to reduce phosphorylation of MST1/2, MOB1, LATS1/2 and YAP1 (Fan et al., 2016).

Excitingly, treatment of both Cured and JFH1-replicon cells with the MST1/2 inhibitor profoundly altered their differentiation pattern. Significantly fewer islands of hepatocyte-like cells were observed for both Cured and JFH1-replicon CD24lo cells (Figure 5.2.20). Furthermore differences in protein expression were evident by western blot (Figure 5.2.21). CYP3A4 protein levels remained low over the course of differentiation in treated Cured and JFH1-replicon cells and overall levels at day 9 were considerably lower in treated Cured and JFH1-replicon cells compared to untreated Cured and JFH1-replicon cells respectively. Interestingly NS5A protein levels remained high throughout differentiation of treated JFH1-replicon cells compared to untreated JFH1-replicon cells, for which we observed the usual drop in NS5A levels at day 9 (Figure 5.2.21).

In addition a decrease in levels of MST1, pMST1 and MOB1 were observed for XMU-MP-1 treated Cured and JFH1-replicon cells compared to the untreated cells. A decrease in pMST1 levels was an expected consequence of XMU-MP-1 treatment. As observed previously, LATS1 levels increased over differentiation in both Cured and JFH1-replicon cells, and overall levels appeared to be reduced in JFH1-replicon cells. Surprisingly pLATS1 levels decreased slightly over the course of differentiation in both Cured and JFH1-replicon cells. Differences in overall LATS1 levels between XMU-MP-1 treated cells and untreated cells were not apparent however pLATS1 levels

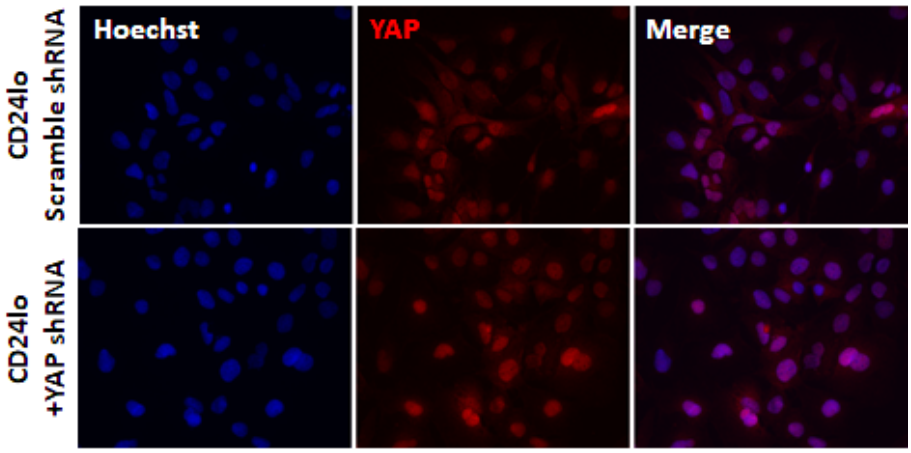


**Figure 5.2.16 Immunofluorescence CD24lo cells transduced with Lentivirus particles expressing shRNA designed to target YAP1.**

CD24lo cells were transduced with lentivirus particles either expressing four different shRNA to target YAP1 or a scrambled shRNA control. Transduced cells were selected using 1µg/ml puromycin for one week after which the mocks were dead. After selection cells were fixed using 4 % PFA, permeabilised using 0.2 % Triton-X100 and stained using anti-YAP1 (red) and 594 nm fluorescently conjugated Alexa Fluor secondary antibodies. The nuclei were counterstained using the DNA stain Hoechst (blue). Images were taken using the EVOS Cell Imaging System. Images are representative of cell density.

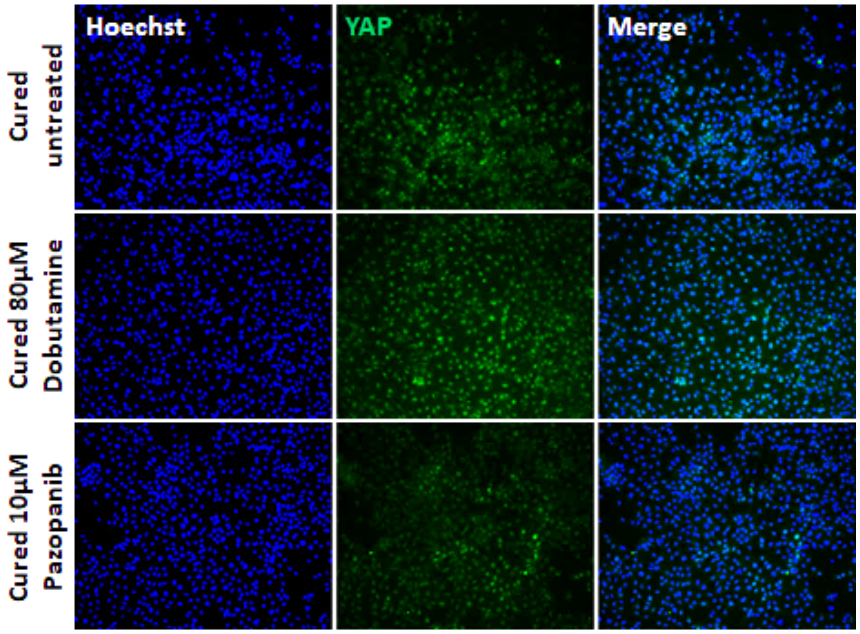


**Figure 5.2.17 CD24lo cells treated with YAP1 inhibitors Dobutamine and Pazopanib**

CD24lo cells were either left untreated or treated with Dobutamine (80 µM) or Pazopanib (10 µM) for 24hrs. Cells were then fixed using 4 % PFA and permeabilised using 0.2 % Triton-X100. The fixed CD24lo cells were stained with an anti-YAP1 (green) and 488 nm fluorescently conjugated Alexa Fluor secondary antibodies. The nuclei were counter stained using the DNA stain Hoechst (blue). Images were taken using an EVOS Cell Imaging System. Images are representative of cell density.

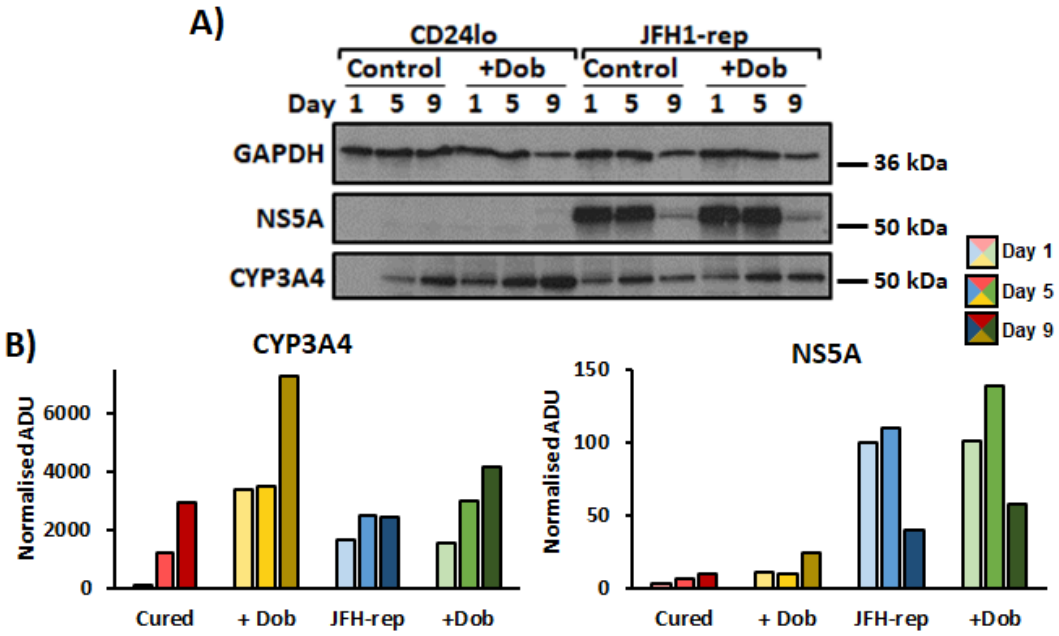


**Figure 5.2.18 Cured and JFH1-replicon CD24lo cells treated with YAP1 inhibitor Dobutamine during differentiation**

Cured or JFH1-rep cells were differentiated and treated with 20 μM Dobutamine. A) Lysates were taken at day one, five or nine of differentiation and western blot membranes were probed for β-actin, NS5A or CYP3A4. B) Quantification of CYP3A4 (n=1) and NS5A (n=1) western blot intensity normalised to β-actin band intensity (as arbitrary densitometry units (ADU)) measured using ImageJ. Displayed as the percentage of CD24lo Day 1 except for NS5A which is the percentage of JFH1-rep Day 1.

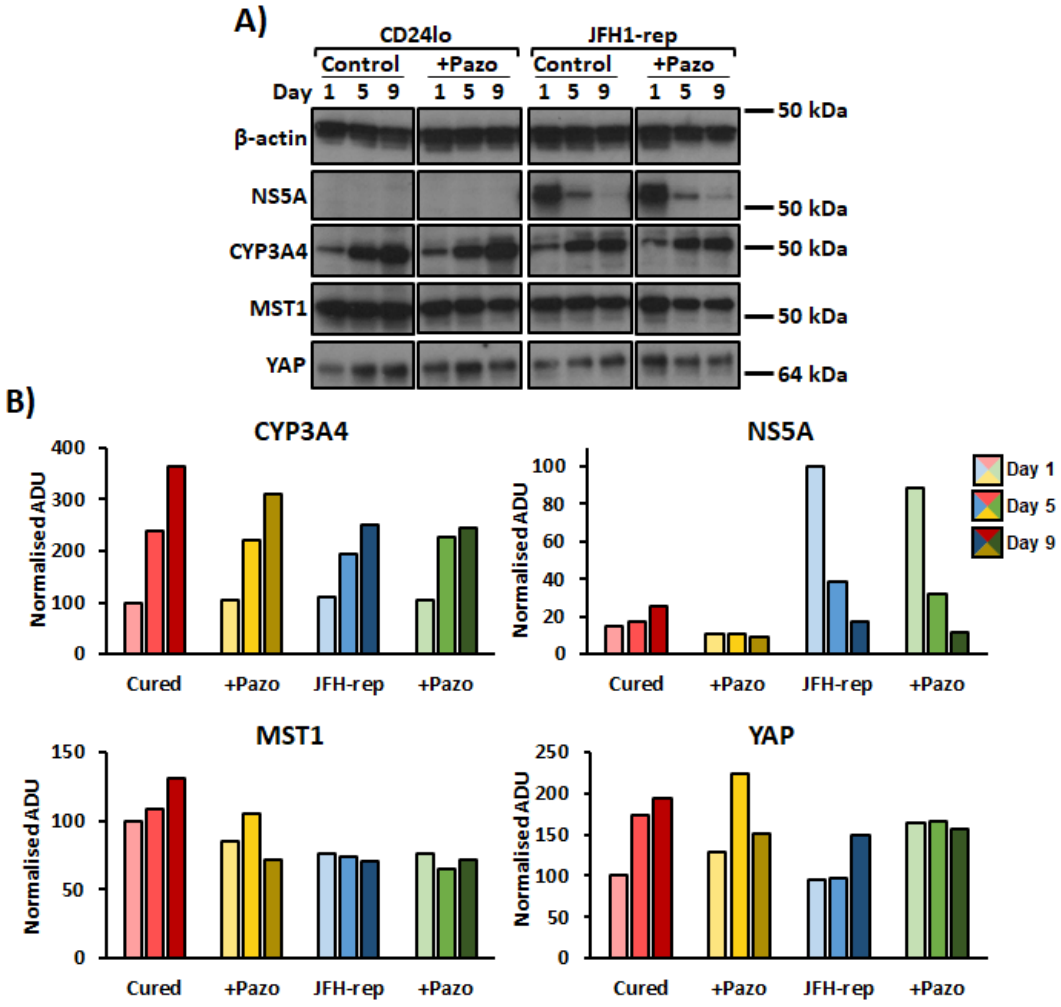


**Figure 5.2.19 Cured and JFH1-replicon CD24lo cells treated with YAP1 inhibitor Pazopanib during differentiation**

Cured or JFH1-rep CD24lo cells were differentiated and treated with 1 μM Pazopanib. A) Lysates were taken at day one, five or nine of differentiation and western blot membranes were probed for β-actin, NS5A, CYP3A4, MST1 or YAP1. B) Quantification of CYP3A4 (n=1), NS5A (n=1), MST1 (n=1) and YAP1 (n=1) western blot intensity normalised to β-actin band intensity (as arbitrary densitometry units (ADU)) measured using ImageJ. Displayed as the percentage of CD24lo Day 1 except for NS5A which is the percentage of JFH1-rep Day 1.

appeared further reduced at day 9 of differentiation in treated cells compared to untreated cells.

YAP1 levels were decreased in treated Cured cells throughout differentiation compared to untreated Cured cells however the same trend was not observed between treated and untreated JFH1-replicon cells. A complex pattern was observed for TAZ. Similarly as before overall TAZ levels were elevated in JFH1-replicon cells compared to Cured cells throughout differentiation. XMU-MP-1 treatment of Cured cells increased TAZ levels from day 1 to day 9 of differentiation, whereas treatment of JFH1-replicon cells caused TAZ to decrease over differentiation.

These results suggest that DMSO induced differentiation of CD24lo cells depends on Hippo signalling and MST1/2 activity. Inhibition of Hippo signalling in differentiating CD24lo cells appears to largely affect levels of the transcriptional regulator TAZ protein levels rather than YAP1. The protein expression profile of NS5A in MST1/2 inhibitor treated cells also suggests that an undifferentiated state is preferred for HCV replication and protein expression.

Chelerythrine (CHE) in the concentration range of 6- 10 μM induced apoptosis in cardiac myocytes (Yamamoto et al., 2001) and on further investigation was found be a potent MST1 activator (Yamamoto et al., 2003). Chelerythrine was shown to act upon caspase-cleaved MST1, which comprises a 34 kDa active kinase (Yamamoto et al., 2003). Differentiation of Cured and JFH1-replicon cells in the presence of 5 μM the MST1 activator Chelerythrine did not appear to alter the differentiation pattern (Figure 5.2.22). The concentration of 5 μM was chosen based on the literature. No apparent increase in CYP3A4 levels in treated Cured and JFH1-replicon cells compared to untreated Cured and JFH1-replicon cells respectively was observed. In addition there was no difference in NS5A levels of treated JFH1-replicon cells compared to untreated. This suggests that MST1 activation on its own is not enough to override the effect of HCV infection and ‘increase’ differentiation in JFH1-replicon cells. However it should be noted that we were unable to confirm whether Chelerythrine did indeed activate MST1 in CD24lo cells and further experiments are needed to measure the levels of pMST1, pLATS1, pMOB1, and both the phosphorylated and unphosphorylated forms of YAP1 and TAZ.

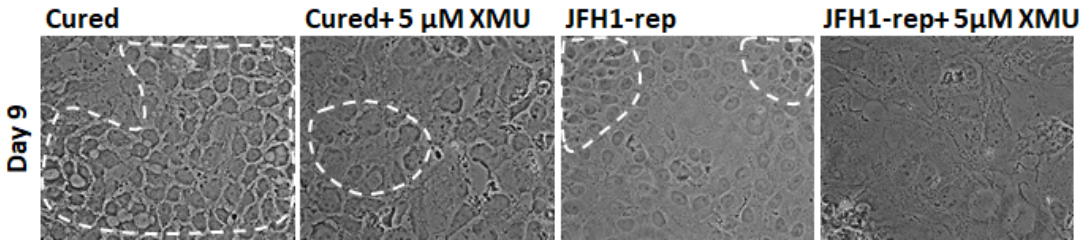


**Figure 5.2.20 Differentiated Cured and JFH1-replicon cells at day nine +/- XMU-MP-1**

Cells were differentiated over a course of nine days either in the absence or presence of 5 µM XMU-MP-1. During the differentiation the media was changed every two days. Phase images were taken on day nine using the EVOS cell Imaging System. Islands of hepatocyte-like cells are highlighted by white dashed lines. Images are representative of cell density.

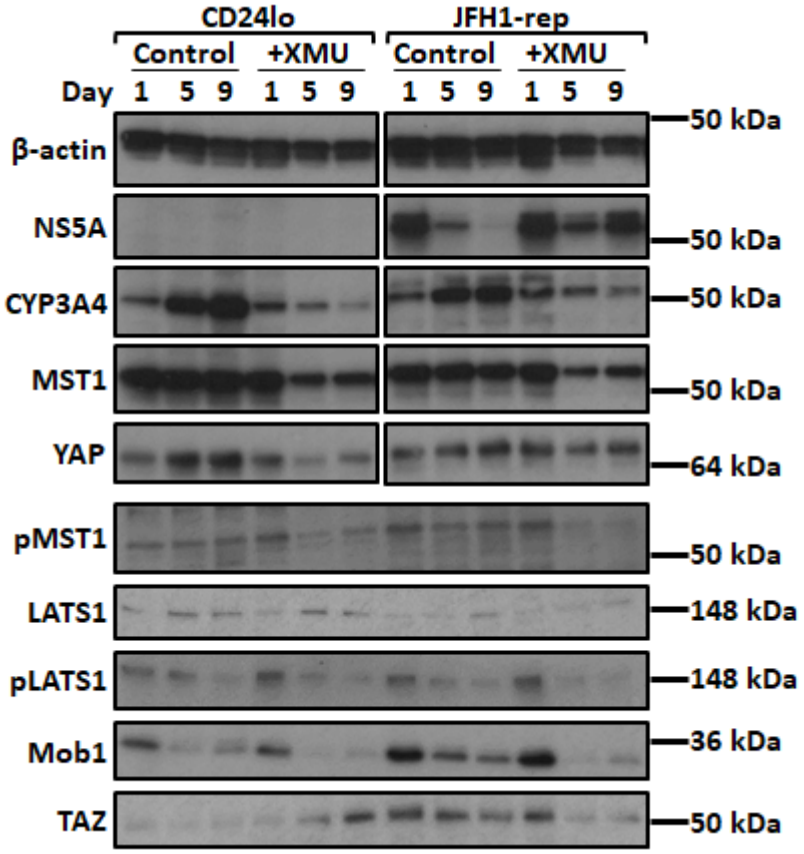


**Figure 5.2.21 Cured and JFH1-replicon CD24lo cells treated with MST1 inhibitor XMU-MP-1 during differentiation**

Cured or JFH1-rep CD24lo cells were differentiated and treated with 5 µM XMU-MP-1. Lysates were taken at day one, five or nine of differentiation and western blot membranes were probed for β-actin, NS5A, CYP3A4, MST1, YAP1, pMST1, LATS1, pLATS1, MOB1 or TAZ.

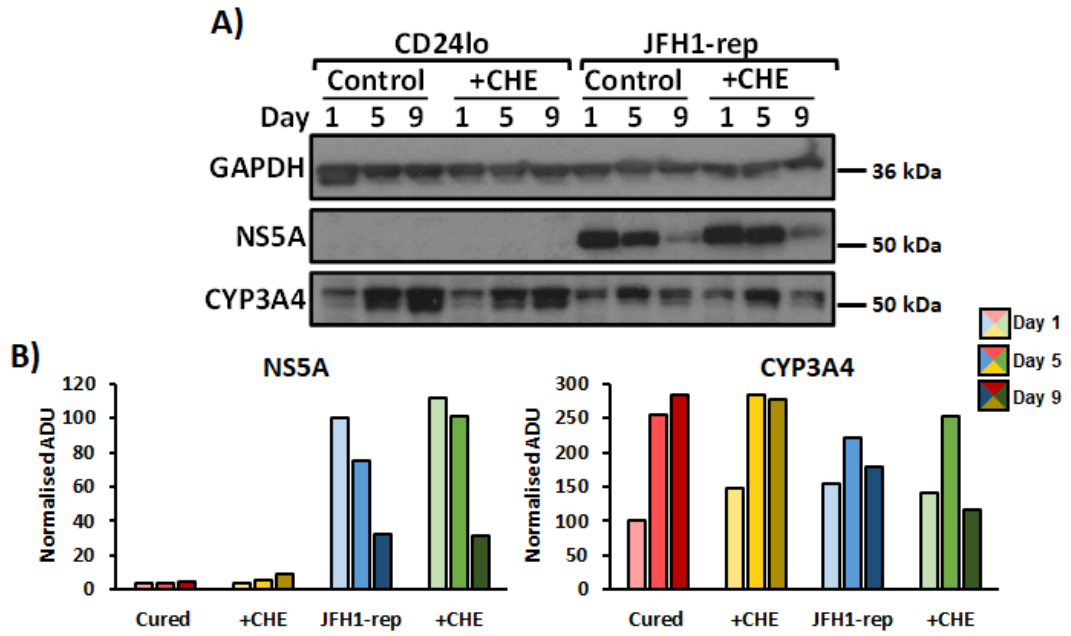


**Figure 5.2.22 Cured and JFH1-replicon CD24lo cells treated with MST activator CHE during differentiation**

Cured or JFH1-rep CD24lo cells were differentiated and treated with 5 μM Chelerythrine. A) Lysates were taken at day one, five or nine of differentiation and western blot membranes were probed for β-actin, NS5A or CYP3A4. Quantification of CYP3A4 (n=1) and NS5A (n=1) western blot intensity normalised to β-actin band intensity (as arbitrary densitometry units (ADU)) measured using ImageJ. Displayed as the percentage of CD24lo Day 1 except for NS5A which is the percentage of JFH1-rep Day 1.

## 5.3 RNA-seq analysis of differentiated Cured, JFH1-replicon, JFH1-replicon +DAA and Cured +MSTi cells

To better understand the effect of HCV on CD24lo differentiation we performed RNA sequencing (RNA-seq) analysis on RNA samples from day nine differentiated Cured (Control), JFH1-rep (HCV), JFH1-replicon cells differentiated in the presence of DAAs (1 μM SOF and 100 nM DCV) (HCV Cure) and Cured cells differentiated in the presence of the MST1/2 inhibitor XMU-MP-1 (2 μM) (MSTi). An RNA-seq analysis sequences the whole transcriptome and enables a global analysis of the gene expression changes induced in the different conditions. RNA-seq requires careful experimental design, RNA isolation and purification, library construction, sequencing, data analysis and interpretation (Figure 5.3.1).

RNA was isolated from six experimental replicates per condition followed by NanoDrop quantification and purity assessment (Figure 5.3.2). Three samples with the best RNA quality assessed by both the 260/280 and 260/230 ratios (for RNA both these ratios should be close to 2) were sent to the Manchester Genomic Technologies Core Facility for sequencing and analysis, carried out by Claire Morrisroe and Dr Ping Wang respectively. RNA quality was further assessed by the Bioanalyser, which analyses the samples using electrophoresis and assigns a RNA integrity number (RIN) based on the 18S and 28S bands. A RIN close to 10 indicates the highest RNA quality. All samples had a RIN between 9.6 and 10 (Figure 5.3.3). Sequencing libraries were created for each RNA sample by reverse transcribing the RNA into cDNA and adding sequencing adaptors. Sequencing library quality was assessed using electrophoresis on the TapeStation Agilent 2200. Using the D1000 ScreenTape assay the cDNA concentration and fragment average size was determined (Figure 5.3.4). qPCR was carried out to determine the cDNA library concentration (Figure 5.3.5). A summary of the RNA-seq analysis demonstrated that sufficient reads of around 50 million- 70 million were generated to analyse and compare gene expression of moderate to high expressed transcripts (Figure 5.3.6). The data was filtered and mapped to the human reference genome hg38. Pair-end sequencing involves the use of adaptors which contain sequencing priming sites at both ends and is used to increase the mapping accuracy. Principal Component analysis is used to assess the quality of the sample replicates and whether the gene expression data for each condition is distinct from one another.

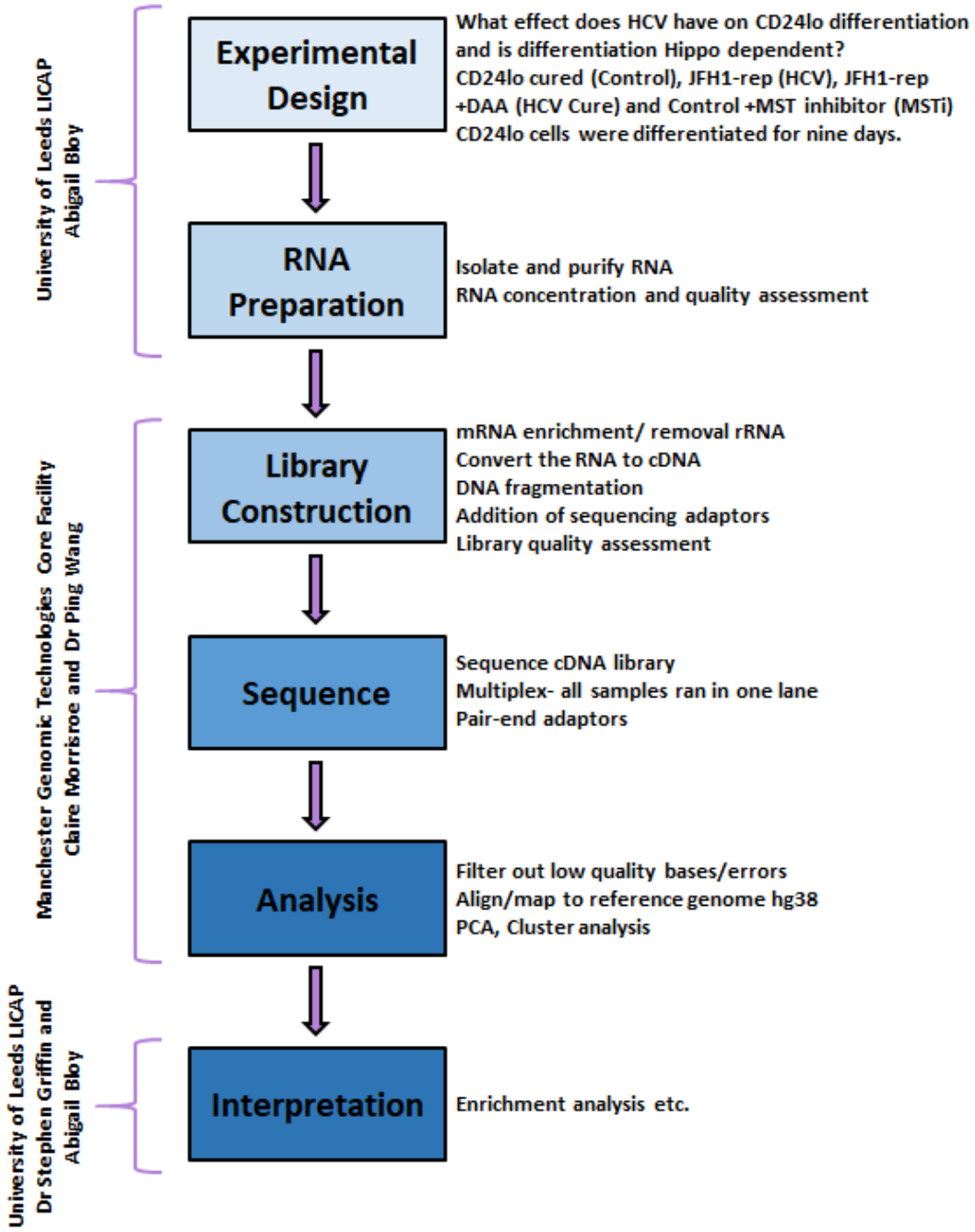


**Figure 5.3.1 RNA-seq Workflow**

CD24lo, JFH1-rep, JFH1-rep +DAA (1μM SOF and 100nM DCV) and CD24lo +MSTi (2 μM) cells were seeded in 6 well plates and differentiated for nine days according to the established differentiation protocol. RNA was isolated and purified using the Qiagen RNAeasy kit following the protocol provided. The isolated RNA quality was initially assessed using the NanoDrop. RNA samples were sent to the Manchester Genomic Technologies Core Facility for were the library was created, sequenced and analysed by Claire Morrisroe and Dr Ping Wang. Further analysis and data interpretation was carried out in Leeds on the data received from Dr Ping Wang.

| Sample | RNA Concentration (ng/µl) | Ratio 260/280 | Ratio 260/230 |
|---|---|---|---|
| Control 1- SG1 | 269.6 | 2.1 | 2.1 |
| Control 2 | 333.5 | 2.1 | 0.9 |
| Control 3- SG2 | 302.3 | 2.1 | 2.2 |
| Control 4 | 281.1 | 2.1 | 0.7 |
| Control 5 | 375 | 2.1 | 2.0 |
| Control 6- SG3 | 387.6 | 2.1 | 2.2 |
| MSTi 1- SG4 | 93.6 | 2.1 | 1.9 |
| MSTi 2 | 102.6 | 2.1 | 0.4 |
| MSTi 3 | 115 | 2.1 | 0.7 |
| MSTi 4- SG5 | 118.5 | 2.1 | 2.1 |
| MSTi 5 | 104.2 | 2.1 | 1.6 |
| MSTi 6- SG6 | 109.5 | 2.1 | 2.1 |
| HCV 1 | 174.6 | 2.1 | 1.5 |
| HCV 2- SG7 | 214.3 | 2.1 | 1.9 |
| HCV 3- SG8 | 190.8 | 2.1 | 2.2 |
| HCV 4- SG9 | 204.3 | 2.1 | 1.9 |
| HCV 5 | 235.9 | 2.1 | 1.8 |
| HCV 6 | 183.7 | 2.1 | 1.7 |
| HCV cure 1- SG10 | 198.8 | 2.1 | 2.1 |
| HCV cure 2 | 177.1 | 2.1 | 1.9 |
| HCV cure 3- SG11 | 244.6 | 2.1 | 1.9 |
| HCV cure 4 | 206.7 | 2.1 | 1.9 |
| HCV cure 5 | 254.6 | 2.1 | 0.9 |
| HCV cure 6- SG12 | 229.7 | 2.1 | 2.2 |

**Figure 5.3.2 NanoDrop RNA Quantification and Assessment**

RNA isolated from day 9 DMSO differentiated Cured (Control), JFH1-rep (HCV), JFH1-rep +DAA (HCV Cure) and Cured +MST inhibitor (MSTi) was quantified and assessed using the NanoDrop. Out of six isolated RNA samples per condition, three samples with the best purity (260/280 and 260/230 ratios) were chosen for RNA-seq analysis and sent to Manchester Genomic Technologies Core Facility, labelled SG1- SG12).

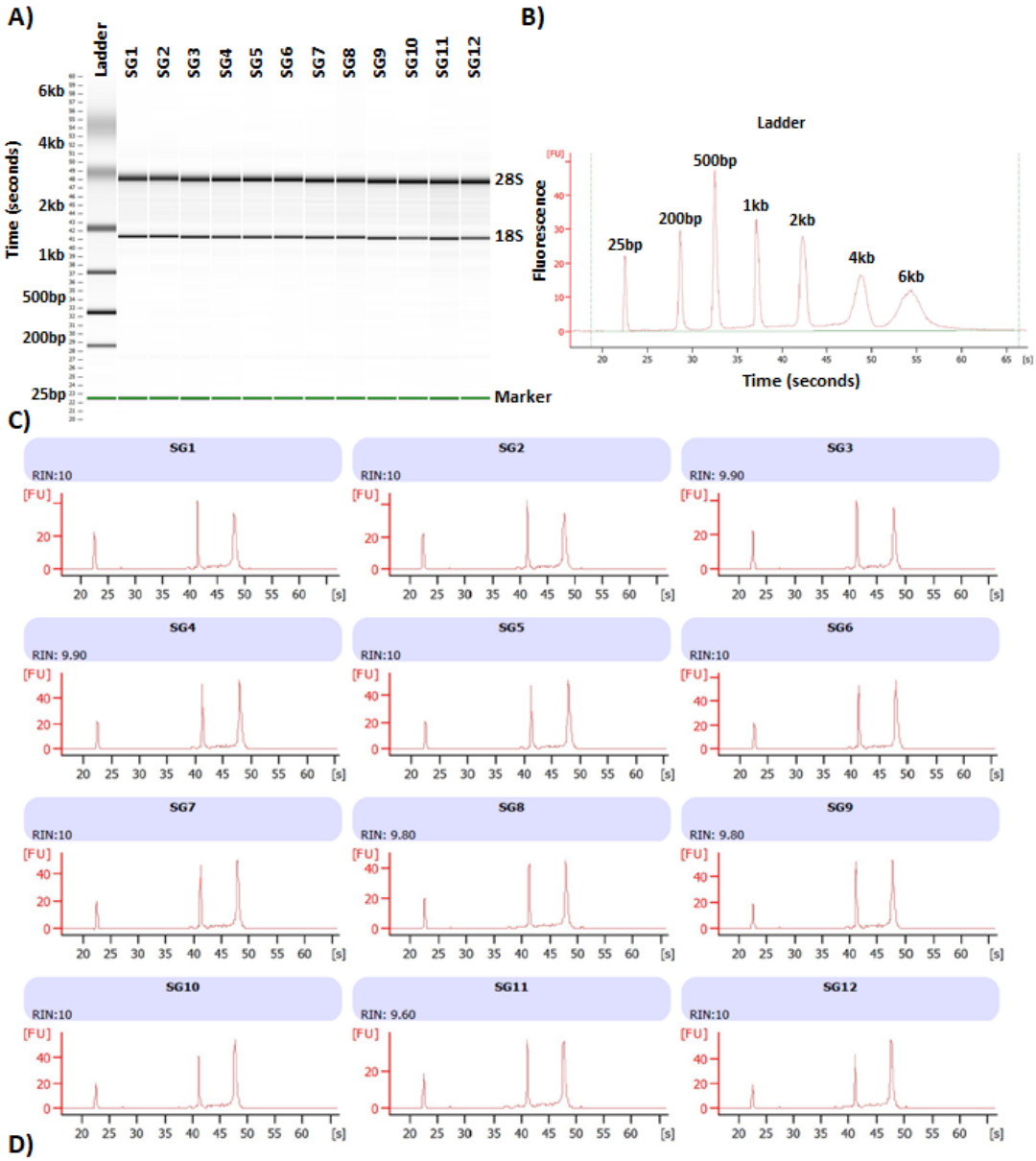


D)

| Sample | SG1-Control 1 | SG2-Control 2 | SG3-Control 3 | SG4-MSTi 1 | SG5-MSTi 2 | SG6-MSTi 3 | SG7-HCV 1 | SG8-HCV 2 | SG9-HCV 3 | SG10-HCV cure 1 | SG11-HCV cure 2 | SG12-HCV cure 3 |
|---|---|---|---|---|---|---|---|---|---|---|---|---|
| RNA Conc (ng/µl) | 47 | 45 | 45 | 58 | 50 | 59 | 50 | 53 | 60 | 57 | 46 | 62 |
| rRNA Ratio [28S/18S] | 1.7 | 1.7 | 1.7 | 1.8 | 1.9 | 1.8 | 1.9 | 1.8 | 1.8 | 2.3 | 2 | 2.2 |
| RIN | 10 | 10 | 9.9 | 9.9 | 10 | 10 | 10 | 9.8 | 9.8 | 10 | 9.6 | 10 |

**Figure 5.3.3 RNA sample Integrity**

Agilent Bioanalyzer 2100 electrophoresis run summary. The RNA samples were separated on a microfabricated chip by electrophoresis and detected by laser fluorescence. The Bioanalyzer produced a gel-like image (A) and electrograms for the ladder (B) and samples (C). D) RNA concentration, the ribosomal ratio and the RNA Integrity number (RIN) were measured for each sample.

A)

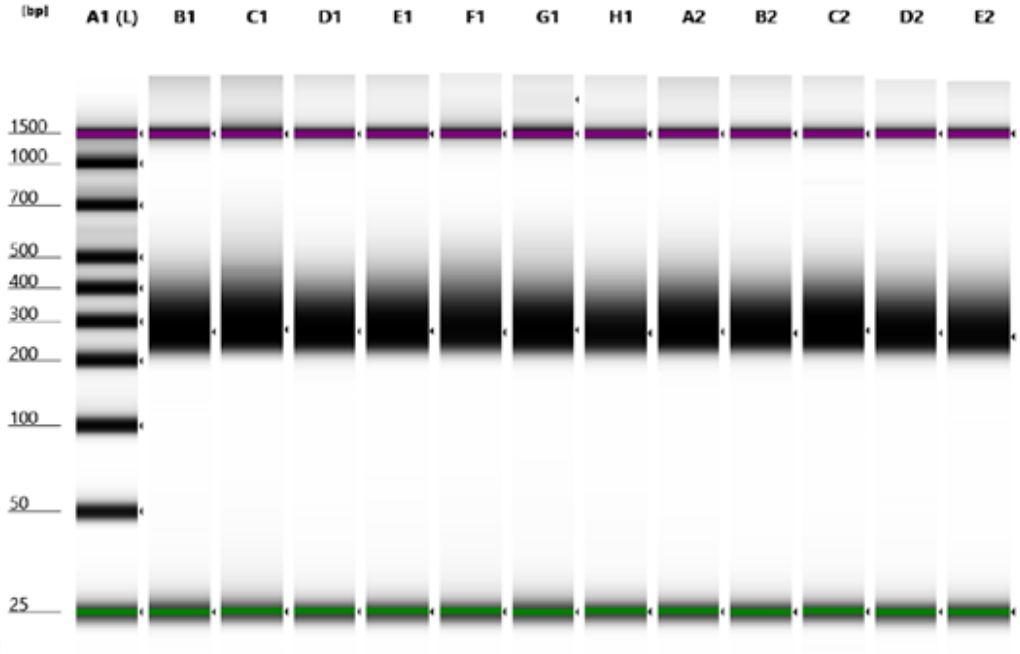


B)

| Well | Sample | From (bp) to (bp) | Average Size (bp) | Concentration (ng/µl) | Region Molarity (nmol/l) |
|---|---|---|---|---|---|
| A1 | Ladder | 25-1500 | | 56.2 | |
| B1 | SG1- Control 1 | 130-980 | 313 | 34.2 | 176 |
| C1 | SG2- Control 2 | 130-980 | 328 | 36.8 | 182 |
| D1 | SG3- Control 3 | 130-980 | 309 | 33.5 | 173 |
| E1 | SG4- MSTi 1 | 130-980 | 317 | 34.8 | 177 |
| F1 | SG5- MSTi 2 | 130-980 | 326 | 31.3 | 156 |
| G1 | SG6- MSTi 3 | 130-980 | 316 | 31.0 | 158 |
| H1 | SG7- HCV 1 | 130-980 | 308 | 27.8 | 145 |
| A2 | SG8- HCV 2 | 130-980 | 317 | 36.9 | 187 |
| B2 | SG9- HCV 3 | 130-980 | 310 | 32.6 | 169 |
| C2 | SG10- HCV cure 1 | 130-980 | 315 | 42.9 | 218 |
| D2 | SG11- HCV cure 2 | 130-980 | 307 | 31.7 | 166 |
| E2 | SG12- HCV cure 3 | 130-980 | 305 | 29.7 | 157 |

**Figure 5.3.4 cDNA library electrophoresis results**

The Agilent D1000 ScreenTape Assay was used to separate and analyse the DNA fragments of the cDNA library by electrophoresis. A) Gel-image of the cDNA electrophoresis. B) Sample concertation, average fragment size and molarity were measured for each sample.

Principal component analysis (PCA) demonstrated that based on two principal components the gene expression profile for each treatment group was distinctive and that there was considerable overlap between the experimental replicates of each condition, Control, HCV, HCV Cure and MSTi (Figure 5.3.8) demonstrating the quality of the RNA-seq data. By mapping the unfiltered sequencing reads to the JFH1 subgenomic replicon sequence (GeneBank accession number: AB047639), replicon HCV RNA was detected only in the HCV condition, which demonstrated the effective curing of the replicon in the JFH1-rep cells treated with DAAs over the course of differentiation (HCV Cure) (Figure 5.3.7). Stringent cut offs were applied to the filtered and mapped gene expression data and only genes with at least a 2fold increase/decrease, a p-value of 0.01 and a base mean over 100 were considered significantly regulated compared to the Control. The gene expression differences between HCV, HCV Cure and MSTi compared to the control were visually represented by plotting the analysed RNA-seq data on a MA plot which plots the $\log_2$ fold change against the $\log_{10}$ mean expression (Figure 5.3.9). There were 956 differentially regulated genes for HCV, 1087 and 2427 for HCV Cure and MSTi compared to Control respectively. As expected, the MSTi condition had the most pronounced effect and induced the most gene expression changes compared to the Control. Interestingly transcription of the proliferation marker ki67 gene was significantly increased in the HCV and MSTi condition but downregulated in the HCV Cure condition compared to the control (Figure 5.3.10). Albumin gene expression remained unaltered in HCV and HCV Cure conditions, but expression was significantly downregulated in the MSTi condition (Figure 5.3.10). CYP3A4 gene expression remained unaltered in all conditions compared to the control. However, expression of several other cytochrome P450 enzymes were altered in various condition. The expression of most cytochrome P450 enzyme genes followed a similar pattern, expression remained unaltered in the HCV and HCV Cure condition and was significantly downregulated in the MSTi condition compared to the control (Figure 5.3.10).

Next, the list of differentially regulated genes compared to the Control for each condition were analysed for overlapping differentially regulated genes (Figure 5.3.11). The three conditions, HCV, HCV Cure and MSTi shared 313 differentially regulated genes. HCV and HCV Cure shared a further 195 differentially regulated genes, HCV and MST1 and HCV Cure and MSTi shared a further 257 and 317 differentially regulated genes respectively. This suggests that all treatment conditions may induce some similar patterns of

gene expression changes but that each condition also induces some distinct changes via distinct mechanisms.

Enrichment analysis using the ChEA ChIP-seq database revealed that all three conditions, HCV, HCV Cure and MSTi, induced gene expression changes associated with the transcription factors FOXM1 and Sox2 (Figure 5.3.12). This was confirmed using enrichment analysis on the 313 genes which are differentially regulated in all three conditions (Figure 5.3.14). Interestingly gene expression of FOXM1 itself was significantly increased by the JFH1-replcion and MSTi treatment compared to Control cells at day 9 of differentiation (Figure 5.4.11). Other transcription factors which were likely to regulate these shared genes are E2F4 and TP63. Enrichment analysis using the KEGG signalling pathway database highlighted that the gene expression changes of each condition likely had an effect on cell cycle regulation. In addition enrichment analysis on the 313 genes which were differentially regulated in all three conditions that the expression changes of these genes were likely affecting the p53 pathway, amongst other signalling pathways (Figure 5.3.14).

The 195 differentially regulated genes shared between HCV and HCV cure were likely regulated by the transcription factors ESR1, ESR2, PRDM16 and SOX2 and affected key signalling pathways often involved in carcinogenesis such as P3IK-Akt signalling pathway, p53, TNF, inflammatory signalling and the Hippo pathway amongst other pathways (Figure 5.3.15). HCV infection was driving similar TFs as MSTi. The gene expression profile was not reversed completely by HCV Cure and similar TFs were predicted to be driving the expression changes.

Transcription factors associated with the 257 differentially regulated genes in the HCV and MSTi condition included FOXM1 again, KLF2/5/4, FOXO1, TP63 and HNF4α (Figure 5.3.16). The gene expression profiles likely lead to alteration of pathways involved in fatty acid metabolism and metabolism in general (Figure 5.3.16).

The genes which were uniquely differentially regulated in the HCV condition compared to the control appeared to be predominantly regulated by the transcription factor HIF1α (Figure 5.4.2) and likely lead to the alteration of pathways involved in viral pathogenesis, p53 signalling pathway, thyroid hormone signalling and regulation of focal adhesion (Figure 5.4.2). Gene expression changes induced by HCV were predicted to also affect signalling pathways involved in fatty acid metabolism and lipid metabolism. Amino acid

A)

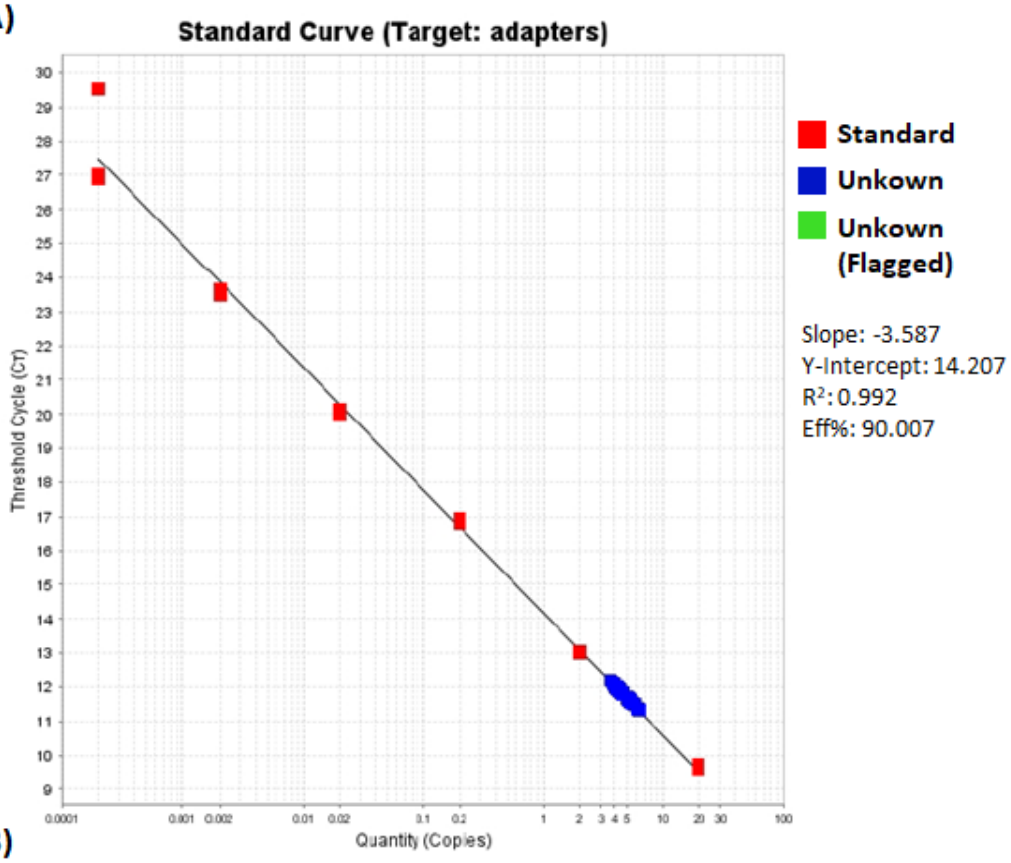


B)

| Sample | Target | Quantity (Mean) | Quantity (Std Dev) | $C_T$ (Mean) | $C_T$ (Std Dev) |
|---|---|---|---|---|---|
| SG1- Control 1 | adaptors | 5.13 | 0.35 | 11.66 | 0.11 |
| SG2- Control 2 | adaptors | 5.30 | 0.21 | 11.61 | 0.06 |
| SG3- Control 3 | adaptors | 4.56 | 0.20 | 11.84 | 0.07 |
| SG4- MSTi 1 | adaptors | 4.33 | 0.18 | 11.92 | 0.06 |
| SG5- MSTi 2 | adaptors | 4.22 | 0.12 | 11.97 | 0.05 |
| SG6- MSTi 3 | adaptors | 4.16 | 0.09 | 11.99 | 0.03 |
| SG7- HCV 1 | adaptors | 4.28 | 0.12 | 11.94 | 0.04 |
| SG8- HCV 2 | adaptors | 6.08 | 0.29 | 11.40 | 0.07 |
| SG9- HCV 3 | adaptors | 3.75 | 0.17 | 12.15 | 0.07 |
| SG10- HCV cure 1 | adaptors | 4.38 | 0.07 | 11.90 | 0.03 |
| SG11- HCV cure 2 | adaptors | 5.12 | 0.07 | 11.66 | 0.02 |
| SG12- HCV cure 3 | adaptors | 4.28 | 0.30 | 11.94 | 0.11 |
| Standard | adaptors | 20 | - | 9.69 | 0.06 |
| Standard | adaptors | 2 | - | 13.03 | 0.06 |
| Standard | adaptors | 0.2 | - | 16.84 | 0.08 |
| Standard | adaptors | 0.02 | - | 20.09 | 0.08 |
| Standard | adaptors | 0.002 | - | 23.58 | 0.09 |
| Standard | adaptors | 0.0002 | - | 27.82 | 1.49 |

**Figure 5.3.5 qPCR results**

Applied Biosystems StepOnePlus qPCR results. cDNA library assessment after adaptor addition. A) Standard Curve created using Cycle Threshold and concentration of standards. B) Sample quantitation was determined using the Standard Curve.

| Sample | Total read | Filtered read | Filtered% | Mapped reads | Mapped% | Pair | Pair% | Unique | Unique% |
|---|---|---|---|---|---|---|---|---|---|
| control_1 | 67423622 | 65680834 | 97 | 71999710 | 106 | 71998382 | 106 | 64619502 | 95 |
| control_2 | 64728606 | 63050788 | 97 | 68764317 | 106 | 68762890 | 106 | 62077685 | 95 |
| control_3 | 54164750 | 53011096 | 97 | 58765152 | 108 | 58764088 | 108 | 52252345 | 96 |
| HCV_1 | 61590396 | 60199164 | 97 | 65660035 | 106 | 65658868 | 106 | 58491485 | 94 |
| HCV_2 | 51423278 | 50143022 | 97 | 54641920 | 106 | 54640840 | 106 | 48720326 | 94 |
| HCV_3 | 62718766 | 61283100 | 97 | 67173204 | 107 | 67172020 | 107 | 59593775 | 95 |
| HCV_cure_1 | 68200520 | 66697932 | 97 | 73332227 | 107 | 73330798 | 107 | 65520416 | 96 |
| HCV_cure_2 | 66753292 | 65228396 | 97 | 72168824 | 108 | 72167488 | 108 | 64125172 | 96 |
| HCV_cure_3 | 70934198 | 69200646 | 97 | 76256516 | 107 | 76255246 | 107 | 68024479 | 95 |
| MST1_inhibitor_1 | 67743934 | 66298106 | 97 | 72442273 | 106 | 72440796 | 106 | 64552811 | 95 |
| MST1_inhibitor_2 | 68507618 | 66745068 | 97 | 72492140 | 105 | 72489484 | 105 | 64497567 | 94 |
| MST1_inhibitor_3 | 59347512 | 58097054 | 97 | 63906850 | 107 | 63905672 | 107 | 56588011 | 95 |

**Figure 5.3.6 RNA-seq data output**

The library was sequenced at Manchester Genomic Technologies Core Facility by Claire Morrisroe and analysed by Dr Ping Wang**.** The total number of reads represents the sequencing depth. Over 30 million reads is required to detect transcripts of moderate to high abundance and quantify gene expression. The total number of reads were filtered for suspected reads containing sequencing errors. The reads were then mapped to the human reference genome hg38. Some reads may align multiple times hence why the mapped reads were higher than the filtered reads. Pair-end reads were only counted as one read if both ends align to the genome. Unique reads represent reads which only align at one position of the genome.

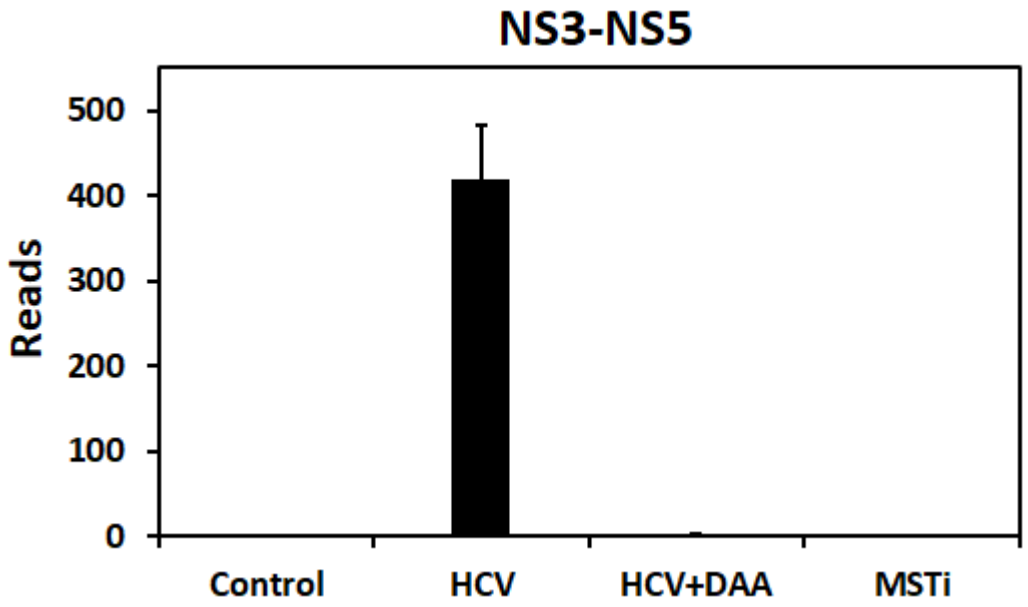


**Figure 5.3.7 The number of HCV NS3-5b (JFH1 SGR) reads**

The unfiltered RNA-seq data was analysed and mapped to the JFH1 subgenomic replicon sequence (GeneBank accession number: AB047639). Only in the JFH1-rep condition did any sequencing reads map to the JFH1 sequence, demonstrating that DAA treatment was able to eliminate the virus from the treated JFH1-rep cells.

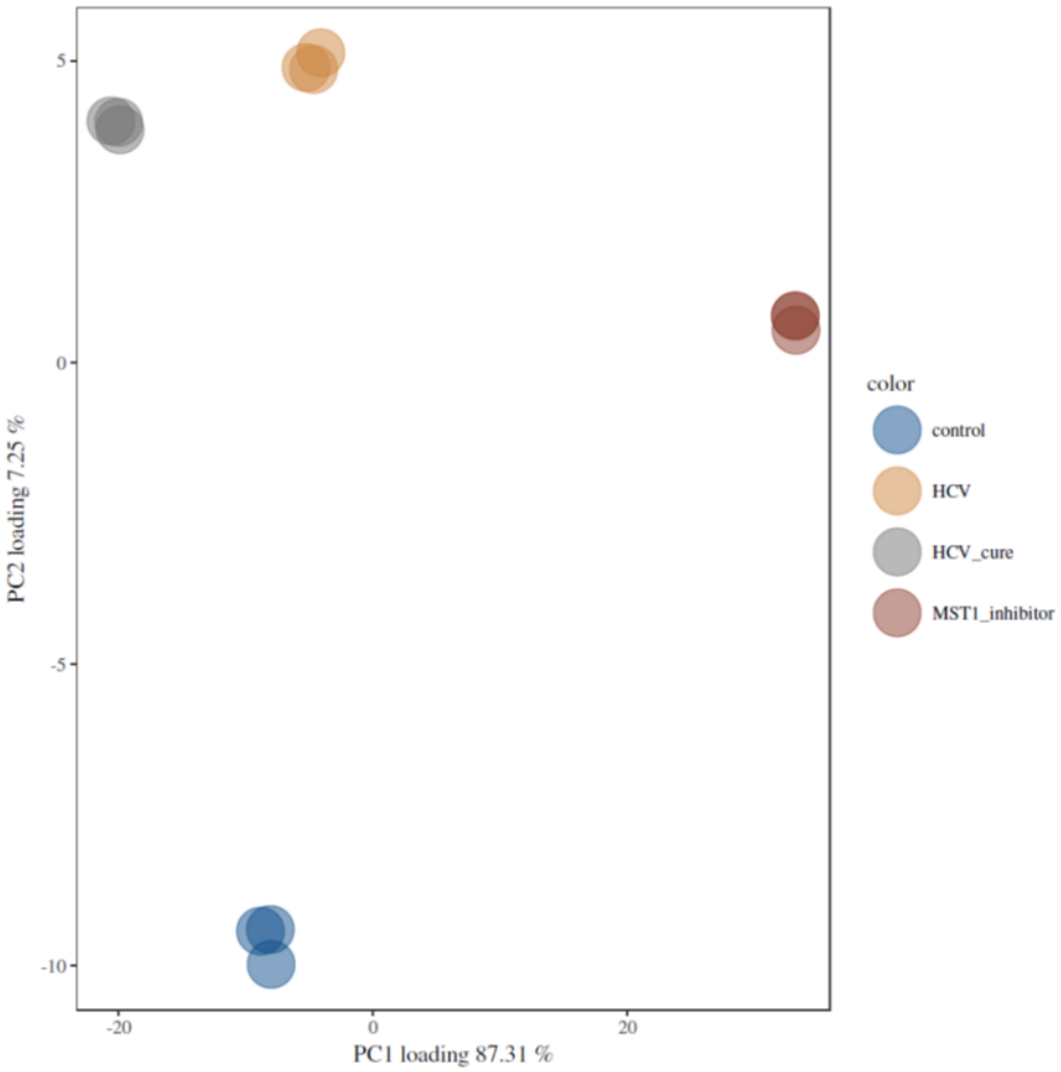


**Figure 5.3.8 RNA-seq Principal Component analysis**

PCA analysis reduces a dataset with multiple variables to two dimensions and gives an indication of the quality of the experimental replicates and how distinct the gene expression data is for each condition. PC analysis was applied to the RNA-seq data for differentiated Control, JFH1-rep (HCV), JFH1-rep+DAA (HCV cure) and Control+ MSTi cells. The analysis demonstrated that based on two principal components, the gene expression profile for each treatment group was different and there was considerable overlap between the replicates within each condition.

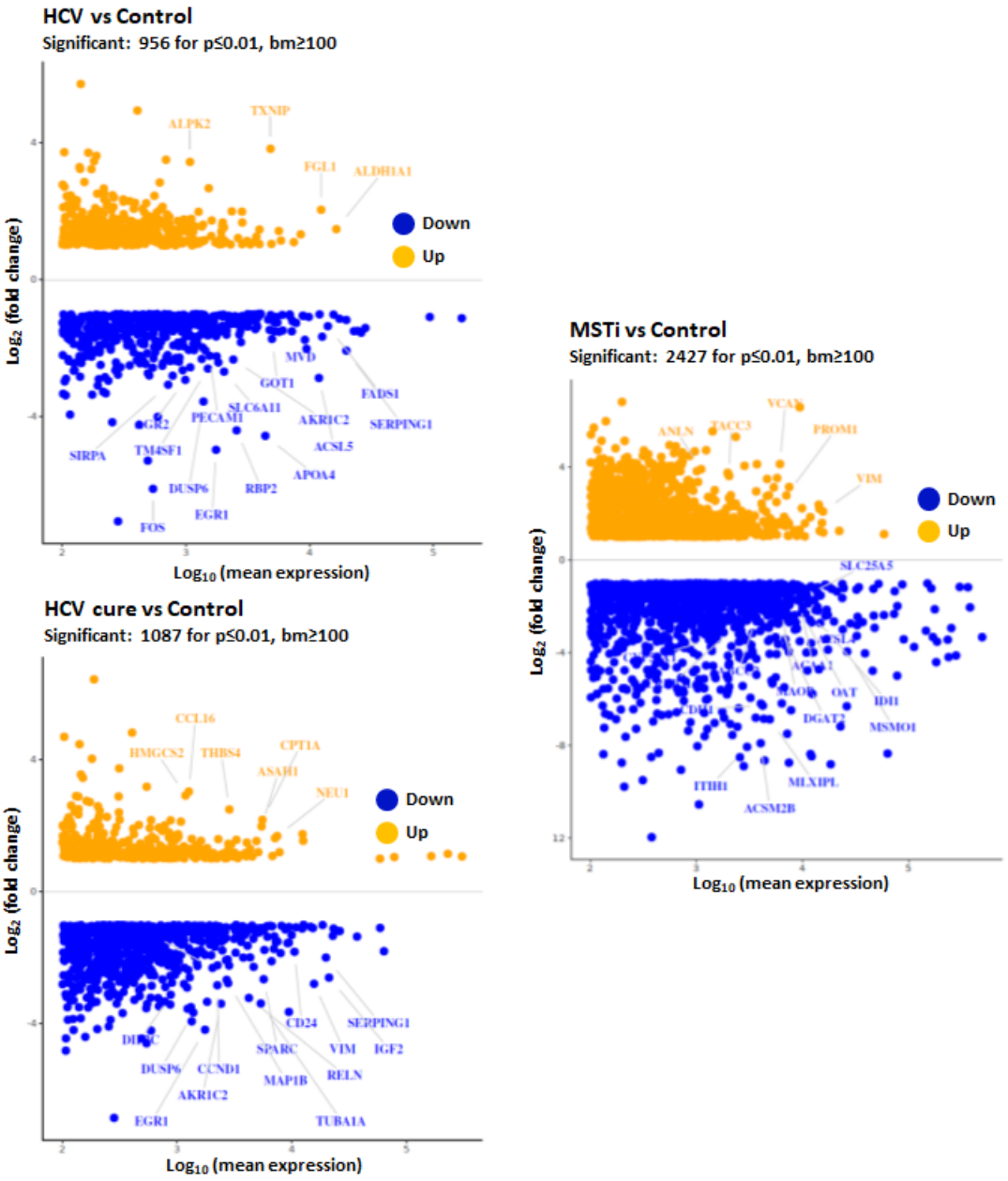


**Figure 5.3.9 MA plots of RNA-seq data**

Visual representation of the RNA gene expression differences between the Control and either HCV, HCV cure or MSTi by plotting mRNA fold change against the mean expression or base mean. Gene expression for which there was a fold increase are labelled orange and gene expression for which there was a fold decrease are labelled in blue. There were about 1000-2000 significantly differentially regulated genes in each condition with p≤0.01 and a minimum base mean expression of 100. RNA-seq reads were filtered and mapped to the human reference genome hg38 prior to MA analysis.

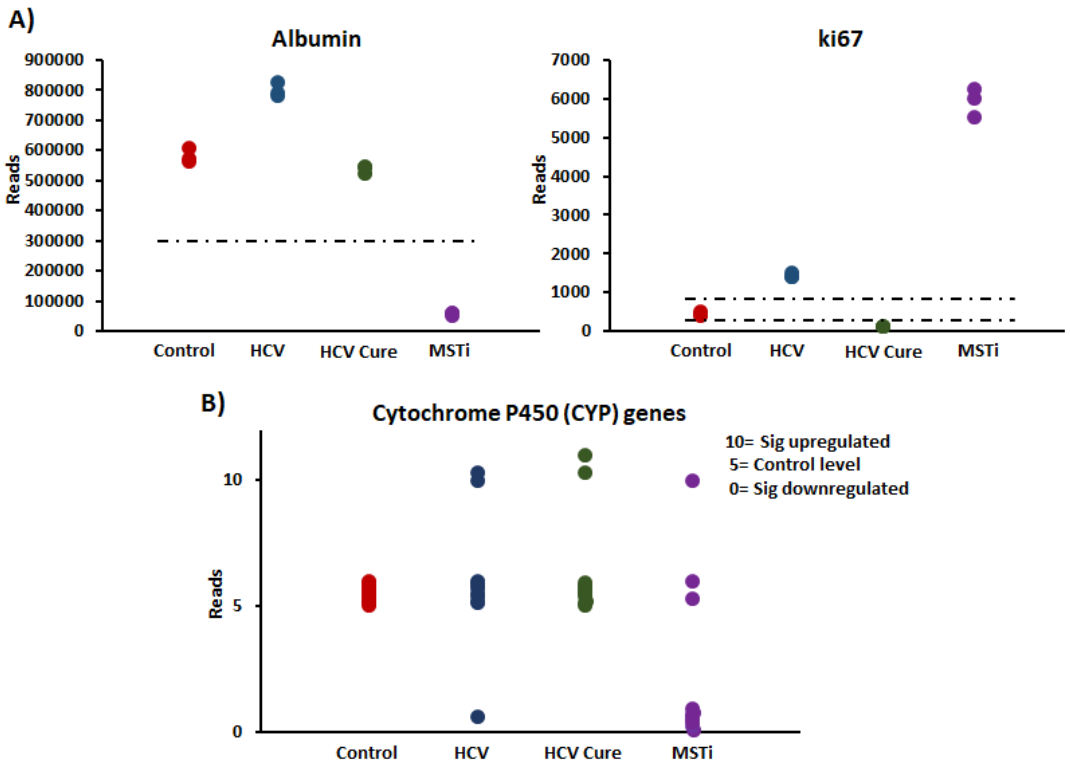


**Figure 5.3.10 Gene expression of hepatocyte markers and proliferation marker ki67**

A) RNA-seq analysis revealed the gene expression status of the hepatocyte marker albumin and the proliferation marker ki67 during HCV replicon infection at day 9 off differentiation at day 9. HCV replicon infection +DAA and under MSTi treatment. Albumin expression remained unaltered in the HCV and HCV Cure condition but was significantly downregulated in MSTi. Ki67 expression was significantly upregulated in the HCV and MSTi condition and downregulated in the HCV Cure condition. The dashed line serves to highlight in which conditions gene expression was significantly upregulated and is arbitrarily set on the graph. B) The expression of many Cytochrome P450 genes (CYP4V2, CYP3A5, CYP8B1, CYP19A1, CYP4F3, CYP4F12 and CYP27A1) followed a similar pattern of expression, remaining unaltered in HCV and HCV Cure and being downregulated in the MSTi condition. Expression of CYP26B1, CYP1A1, CYP51A1 and CYP2J2 did not follow the same pattern.

biosynthesis associated pathways were also included, and regulation of these pathways by HCV may be necessary for viral protein expression.

Genes which were uniquely differentially regulated in the MSTi condition are largely regulated by the transcription factors FOXA2, ESR1, PPARA and HNF4α (Figure 5.4.4). MSTi induced genes expression changes predicted to alter metabolic pathways and pathways involved in DNA replication (Figure 5.4.4).

Hierarchical cluster analysis was performed on the whole gene expression data set after the cut-offs of p≤0.01, bm≥100 and 2foldchange≥1 were applied. The Cluster analysis identified ten clusters with differential gene expression profiles compared to the Control (Figure 5.4.5). Some clusters showed shared patterns of gene expression changes between HCV and MSTi treatment, such as cluster 7 and 3 suggesting that HCV infection induces a set of gene expression changes also induced by Hippo signalling inhibition (Figure 5.4.5). Interestingly, whilst certain clusters demonstrated a gene expression profile associated with HCV that was reversed by DAA treatment in the HCV Cure condition (e.g. clusters 3 and 4 which contained 931 and 117 genes respectively) (Figure 5.4.6), others contained patterns of expression changes induced by HCV that were not reversed by DAA treatment; for example clusters 7 and 5, with 182 and 219 genes respectively (Figure 5.4.7). This implies that HCV may induce gene expression changes which last even after the virus is eliminated by DAA treatment. Cluster 1 is an interesting cluster which contains 359 genes which are similarly regulated in the HCV and HCV Cure conditions whereas gene expression remains similar to the Control for MSTi, indicating that these genes are not regulated by Hippo signalling (Figure 5.4.8). Analysis of the genes contained within this cluster reveals that these genes expression changes are associated with many signalling pathways implicated during carcinogenesis such as PI3K-Akt, Hippo and MAPK signalling pathways (Figure 5.4.8).

In terms of the Hippo pathway associated genes, the RNA-seq revealed several differentially regulated genes by HCV compared to the Control (Figure 5.4.11 & Figure 5.4.12). These genes included YAP1/TAZ responsive genes which were either downregulated (MYC, CCND1, SERPINE1 and CDKN1A -p21) or upregulated (BIRC5, AURKA, AURKB, CCNB1, CDC20, DKK1, CCNA2, PLK1, ANKRD1). Many of these responsive genes encode proteins which are anti-apoptotic (e.g. BIRC5 also known as Survivin), involved in cell cycle regulation (e.g. CCNB1- Cyclin B1,

CDC20 or CCNA2-Cyclin A2) or are involved in the regulation of other pathways (e.g. DKK1 which regulates Wnt signalling). BIRC5 inhibits caspase activation and thus negatively regulates apoptosis (Tamm et al., 1998). BIRC5 was also significantly upregulated by MSTi treatment but was found to be significantly downregulated in the HCV Cure condition compared to the Control (Figure 5.4.11). Cyclin B1, CDC20 and CCNA2 encode proteins which are all involved in cell cycle regulation and generally promote cell cycle progression. Cyclin B1 is expressed in the G2/M phase and is commonly overexpressed in different types of cancer (Yuan et al., 2006, Wang et al., 1997, Kawamoto et al., 1997, Mashal et al., 1996, Kushner et al., 1999). CDC20 activates APC and promotes cell cycles progression through the M phase (Fang et al., 1998b, Fang et al., 1998a). Cyclin A2 promotes transition through G1/S and G2/M phases of the cell cycle by interacting with CDK kinases (Pagano et al., 1992). DKK1 has been associated with HCC migration and invasion by promoting β-catenin expression (Chen et al., 2013c). Interestingly of all the YAP1/TAZ responsive genes highlighted here which were upregulated in the HCV condition were also upregulated in the MSTi condition however in the HCV Cure condition these genes were all downregulated except for AURKA for which the gene expression remained unaltered compared to the Control. Expression of MYC and CCND1 was also downregulated in the HCV Cure condition and unaltered in the MSTi condition compared to the Control. Expression of SERPIN1 was downregulated in all conditions. Yet expression of CDKN1A (p21) was downregulated by both the JFH1-replicon and by MST1/2 inhibition but unaffected by curing the JFH1-replicon (HCV Cure). p21 is a cyclin-dependent kinase inhibitor and expression of p21 is tightly regulated by p53 (Gartel and Tyner, 1999). p21 mediates p53 dependent cell cycle arrest in G1 (Cayrol et al., 1998). Loss of p21 is associated with carcinogenesis (Willenbring et al., 2008).

Several genes which encode Hippo regulatory proteins were either upregulated such as PPP2R2B and AMOT or downregulated such as RASSF6, FRMD6, ACTG1 (Gamma-actin) and ACTB (beta-actin) (Figure 5.4.9 & Figure 5.4.12). PPP2R2B and AMOT were also found to be upregulated in HCV Cure and MSTi conditions. ACTG1 downregulated in all conditions however RASSF6 was only downregulated in the HCV and MSTi condition. FRMD6 was also downregulated in HCV Cure but not in the MSTi condition and ACTB was only downregulated by HCV. Several of these genes encode proteins which regulate the function of MST1/2 by either inhibiting the kinase activity including RASSF6 (Ikeda et al., 2009) and

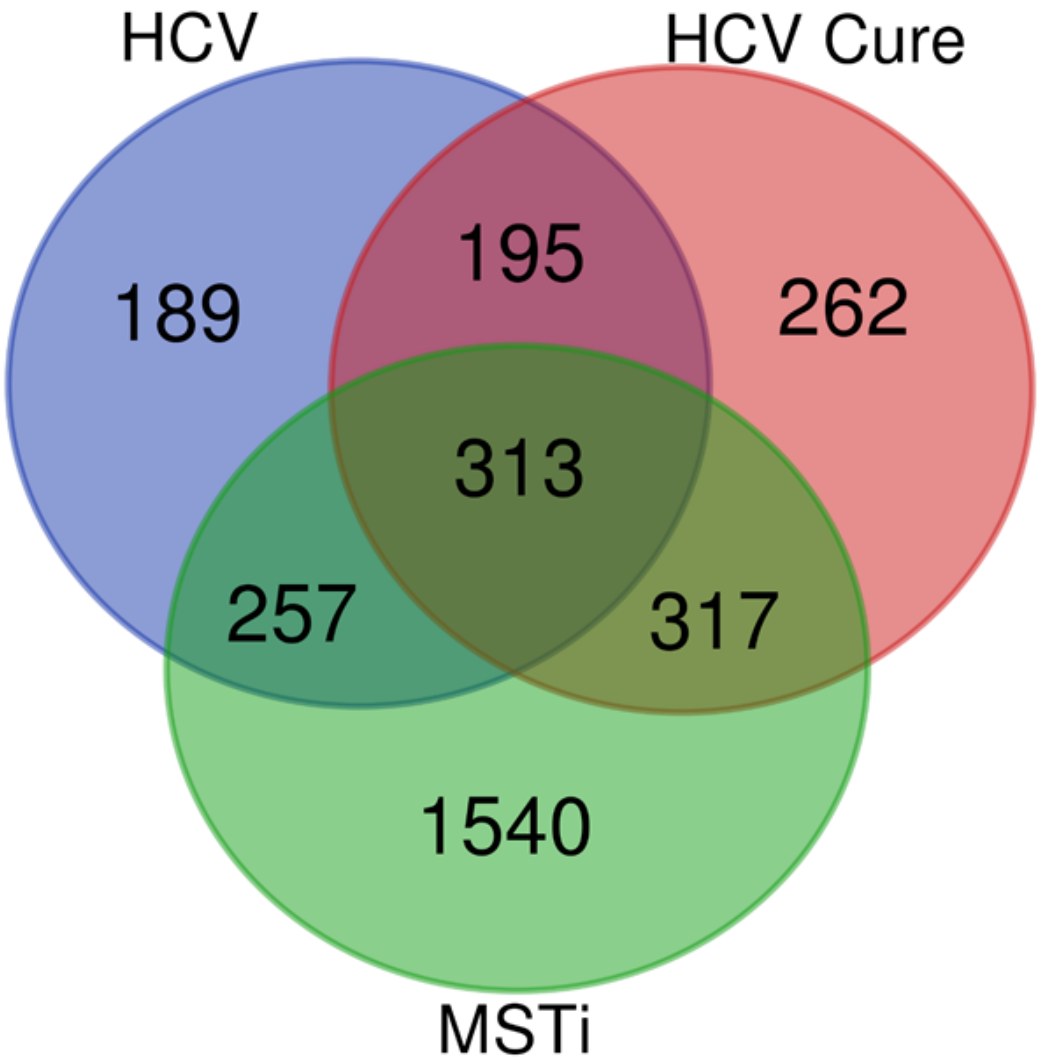


**Figure 5.3.11 Venn diagram of RNA-seq expression data**

The diagram displays the number of overlapping differentially regulated genes between each condition, HCV, HCV and MSTi. Genes were considered significantly differentially regulated compare to control for p≤0.01, ≥2fold change and Base mean≥100. All conditions shared 313 genes which were found to be differentially regulated compared to the control. HCV and HCV cure shared another 195 differentially regulated genes. HCV and MSTi shared another 257 differentially regulated genes and HCV cure and MSTi shared another 317. MSTi appeared to have the most uniquely regulated genes at 1540 compared to 189 for HCV and 262 for HCV cure. Overall HCV had 954 differentially regulated genes compared to control, HCV cure had 1087 and MSTi had 2427. The Venn diagram was created using UGent Bioinformatics & Evolutionary genomics Venn diagram tool.

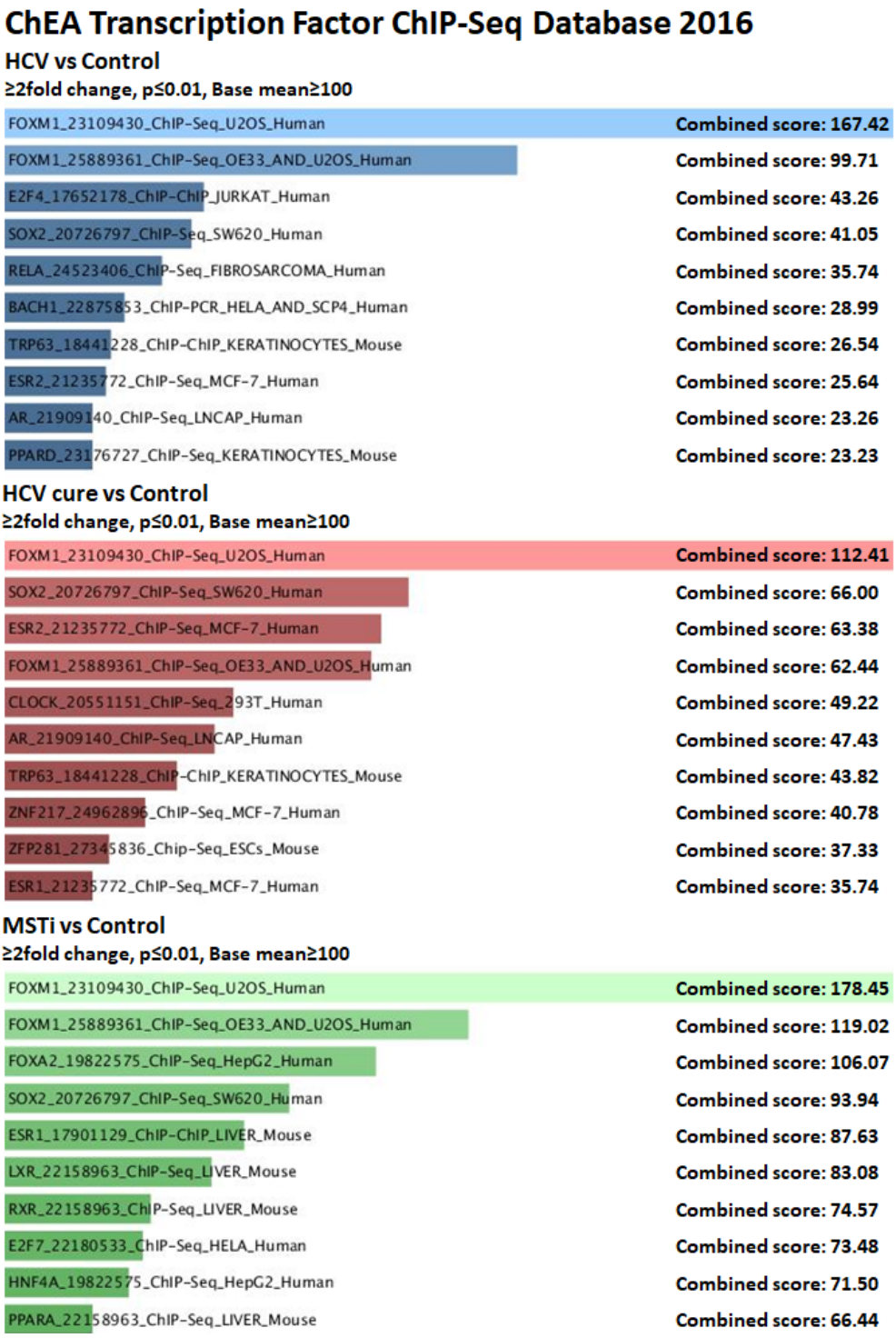


**Figure 5.3.12 ChEA Transcription Factor ChIP-Seq Database Enrichment analysis of significantly differentially regulated genes of HCV, HCV Cure and MSTi compared to Control**

Enrichment analysis using Enrichr and the ChEA TF Database to predict which transcription factors are responsible for the gene expression changes observed in the RNA-seq analysis. Transcription factors were ranked by combined score which takes into account the p-value (calculated using the Fisher's exact test) and the z-score (the z-score is a measure of the deviation from an expected rank). The length and the brightness of the bar reflects the significance of that term/gene set, i.e. the longer and brighter the bar, the more significant the term/gene set is. A grey bar means the term/gene-set is not significant.

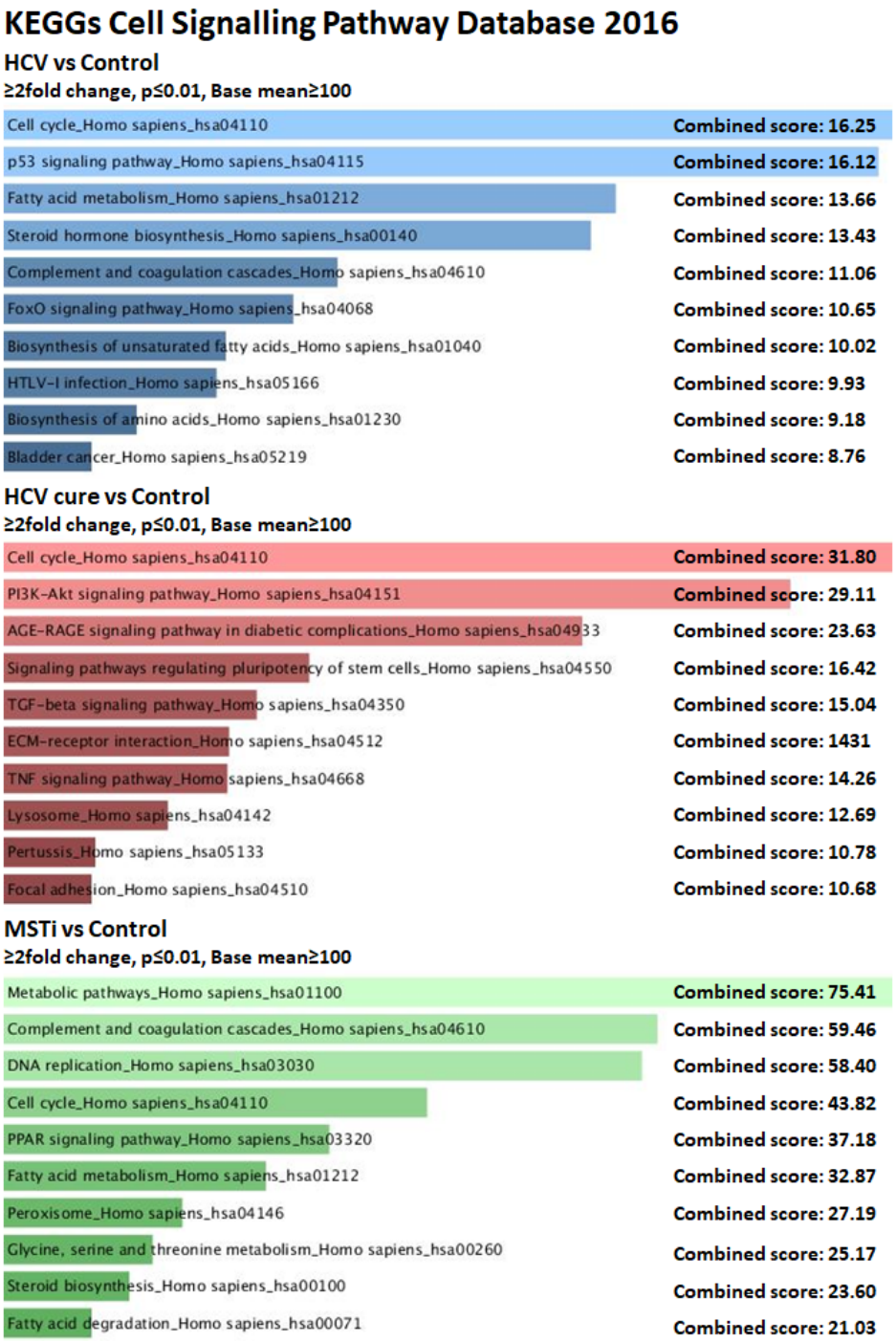


**Figure 5.3.13 KEGG Signalling Pathway Database Enrichment analysis of significantly differentially regulated genes of HCV, HCV Cure and MSTi compared to Control**

Enrichment analysis using Enrichr and the KEGG Signalling Pathway Database to predict which transcription factors are responsible for the gene expression changes observed and which signalling pathways are affected by the gene expression changes observed in the RNA-seq analysis. Transcription factors and signalling pathways were ranked by combined score which takes into account the p-value (calculated using the Fisher's exact test) and the z-score (the z-score is a measure of the deviation from an expected rank). The length and the brightness of the bar reflects the significance of that term/gene set, i.e. the longer and brighter the bar, the more significant the term/gene set is. A grey bar means the term/gene-set is not significant.

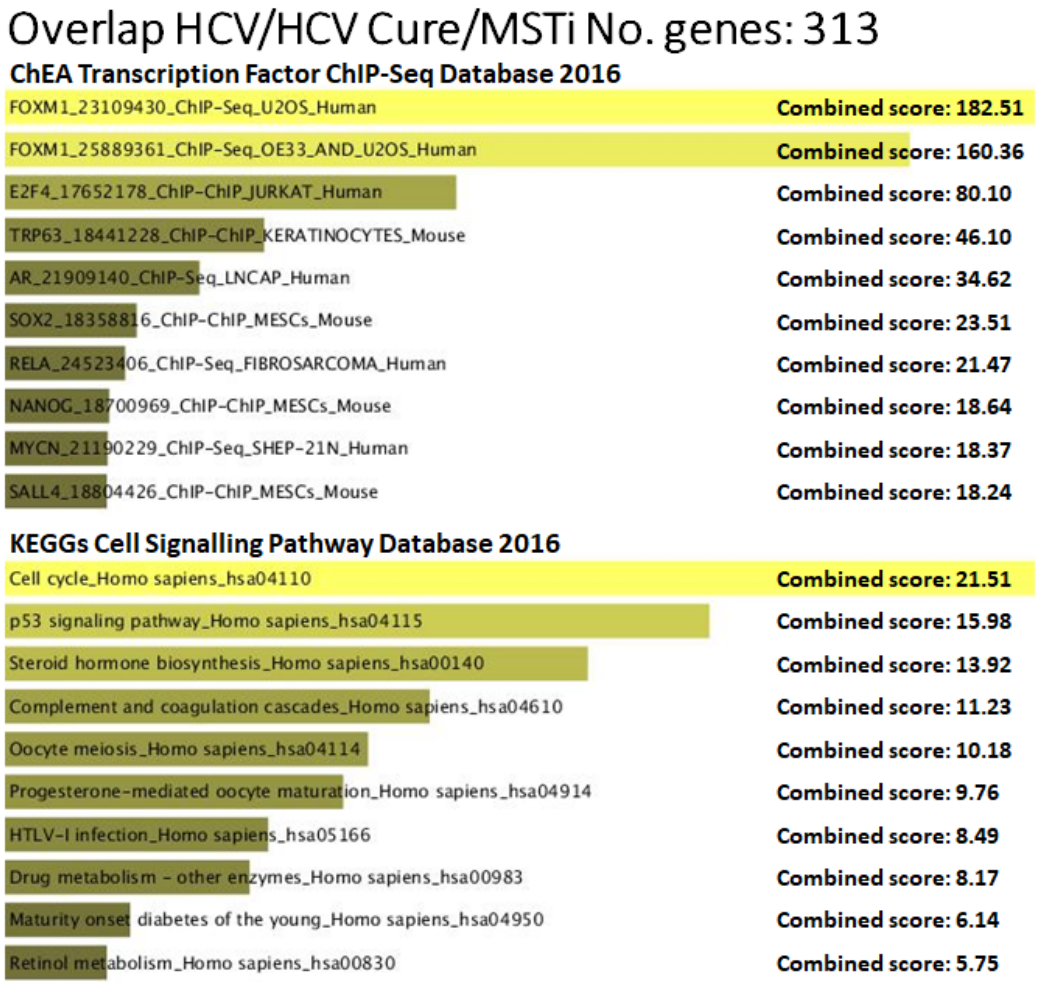


**Figure 5.3.14 Enrichment analysis of significantly differentially regulated genes of shared by HCV, HCV Cure and MSTi compared to Control**

Enrichment analysis using Enrichr, the ChEA Transcription Factor ChIP-seq Database and the KEGG Signalling Pathway Database to predict which transcription factors are responsible for the gene expression changes observed and which signalling pathways are affected by the gene expression changes observed in the RNA-seq analysis. Transcription factors and signalling pathways were ranked by combined score which takes into account the p-value (calculated using the Fisher's exact test) and the z-score (the z-score is a measure of the deviation from an expected rank). The length and the brightness of the bar reflects the significance of that term/gene set, i.e. the longer and brighter the bar, the more significant the term/gene set is. A grey bar means the term/gene-set is not significant.

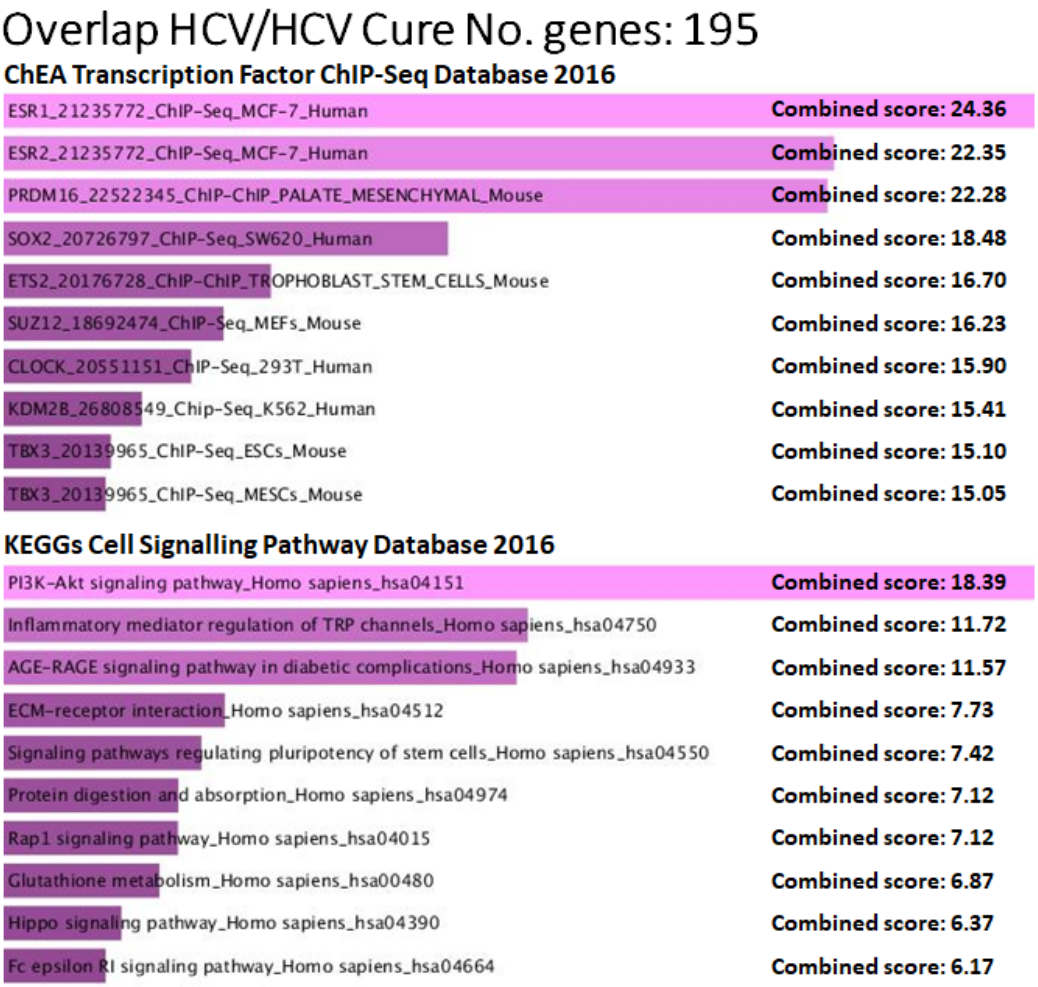


**Figure 5.3.15 Enrichment analysis of significantly differentially regulated genes shared by HCV and HCV Cure compared to Control**

Enrichment analysis using Enrichr, the ChEA Transcription Factor ChIP-seq Database and the KEGG Signalling Pathway Database to predict which transcription factors are responsible for the gene expression changes observed and which signalling pathways are affected by the gene expression changes observed in the RNA-seq analysis. Transcription factors and signalling pathways were ranked by combined score which takes into account the p-value (calculated using the Fisher's exact test) and the z-score (the z-score is a measure of the deviation from an expected rank). The length and the brightness of the bar reflects the significance of that term/gene set, i.e. the longer and brighter the bar, the more significant the term/gene set is. A grey bar means the term/gene-set is not significant.

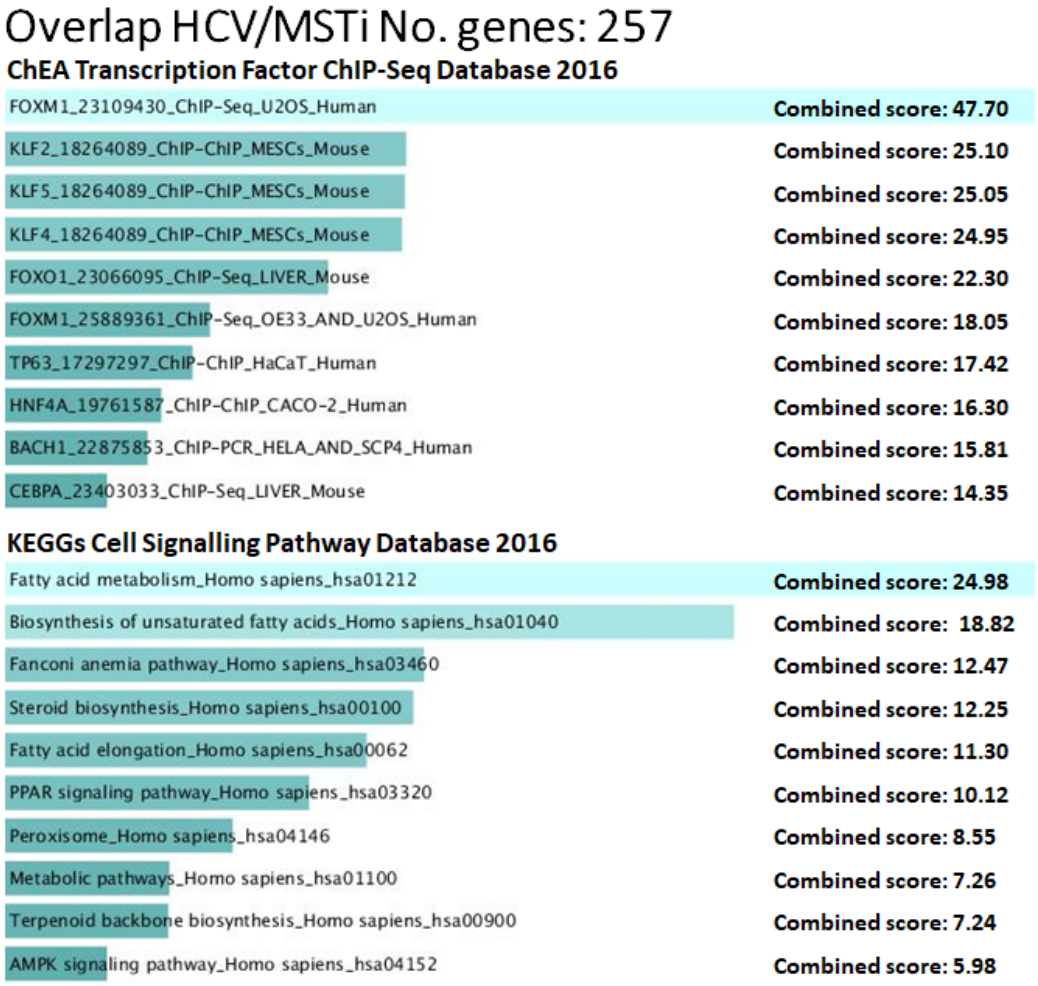


**Figure 5.3.16 Enrichment analysis of significantly differentially regulated genes shared by HCV and MSTi compared to Control**

Enrichment analysis using Enrichr, the ChEA Transcription Factor ChIP-seq Database and the KEGG Signalling Pathway Database to predict which transcription factors are responsible for the gene expression changes observed and which signalling pathways are affected by the gene expression changes observed in the RNA-seq analysis. Transcription factors and signalling pathways were ranked by combined score which takes into account the p-value (calculated using the Fisher's exact test) and the z-score (the z-score is a measure of the deviation from an expected rank). The length and the brightness of the bar reflects the significance of that term/gene set, i.e. the longer and brighter the bar, the more significant the term/gene set is. A grey bar means the term/gene-set is not significant.

PPP2R2B by regulating PP2A (Ribeiro et al., 2010) or by activating MST1/2 activity such as FRMD6 (Angus et al., 2012b). Indeed NS5A has been show to be a regulator of PP2A and increase PP2A activity (Georgopoulou et al., 2006). Overall the effects of these gene expression changes appeared to lead to a reduction in activation signals for MST1/2.

AMOT was the most highly upregulated gene within HCV-containing cells compared to the Control with a 2fold change of 5.7 (Figure 5.4.9). AMOT regulates the cellular localisation of YAP1 and TAZ and depending on cell polarity and cell state can either sequester YAP1 and/or TAZ to the cytoplasm, or promote nuclear translocation of YAP1 and/or TAZ (Zhao et al., 2011, Hong, 2013, Moleirinho et al., 2017). It will be important to determine whether the increase in gene expression translates to an increase in AMOT protein levels and what effect exactly AMOT is having on YAP1 and TAZ localisation in our CD24lo differentiation system.

FOXM1 was predicted by enrichment analysis to be the transcription factor largely responsible for the gene expression changes observed in all three conditions: HCV, HCV Cure and MSTi (Figure 5.3.12). Interestingly FOXM1 gene expression was upregulated in HCV , downregulated in HCV Cure and unchanged in MSTi compared to the control (Figure 5.4.11). Transcriptional regulators YAP1 and TAZ have been shown to interact with FOXM1 in a subset of soft-tissue sarcomas and be necessary for cell proliferation and tumorigenesis (Eisinger-Mathason et al., 2015). FOXM1 responsive genes highlighted by enrichment analysis included for example CDC20 and AURKB.

Of particular interest was the transcriptional upregulation of TAZ (Figure 5.4.10) but not YAP1 in the HCV condition compared to Control cells. This was especially interesting as we have demonstrated elevated protein levels of TAZ but not YAP1 in differentiated JFH1-replicon cells compared to Cured cells (Figure 5.2.3 & Figure 5.2.4). TAZ was not upregulated in either the HCV Cure condition however expression was also upregulated in response to Hippo signalling inhibition by the MST1/2 inhibitor (Figure 5.4.10). TAZ is an important transcriptional regulator which interacts with many transcription factors including TEAD1-4, SMAD1-4, and p73 (Varelas et al., 2008, Zhang et al., 2009, Kim et al., 2018). The only other Hippo protein with an altered expression profile was LATS2 which was interestingly upregulated in response to MST1/2 inhibition (Figure 5.4.10). TEAD4 the most commonly described transcription factor which YAP1 and TAZ bind to and alter but its

transcriptional activity was upregulated only in the MSTi condition compared to the Control (Figure 5.4.11).

The RNA-seq analysis has helped to reveal the gene expression differences between differentiated HCV, HCV Cure and MSTi compared to the Control. Some of these gene expression changes are shared between the different conditions and some gene expression changes are unique to the individual condition. In addition Cluster analysis highlighted that although HCV Cure was able to reverse some of the gene expression changes induced by HCV, DAA treatment did not reverse all gene expression changes compared to the control indicating that HCV infection may have a lasting effect on gene expression long after the virus is cured. By comparing HCV gene expression to the Control several genes associated with the Hippo pathway were found to be differentially regulated by HCV and overall appears to favour the inactivation of Hippo signalling and an increase of the transcriptional regulator TAZ.

## 5.4 Discussion

Our results showed that HCV infection perturbs DMSO induced CD24lo cell differentiation, evidenced by differences in cell morphology and altered expression of hepatocyte markers CYP3A4 and Albumin and the proliferation marker ki67. Thus, HCV appeared able to resist or delay the transcriptional programmes associated with DMSO-induced differentiation.

Following this observation we investigated how HCV perturbed differentiation by exploring which signalling pathway(s) and which viral protein(s) might be responsible using enrichment analysis. Enrichment analysis associates a functional term to a collection of genes by comparing the input gene data to databases of annotated gene sets and helps to infer which transcription factors may be responsible for the gene expression data and which pathways may be altered in response to the list of input genes by taking advantage of the Kyoto Encyclopaedia of genes and genomes (Kanehisa and Goto, 2000) and the ChEA Transcription factor ChIP-seq database (Lachmann et al., 2010). Enrichr is a popular and user-friendly enrichment analysis tool described by (Chen et al., 2013b, Kuleshov et al., 2016).

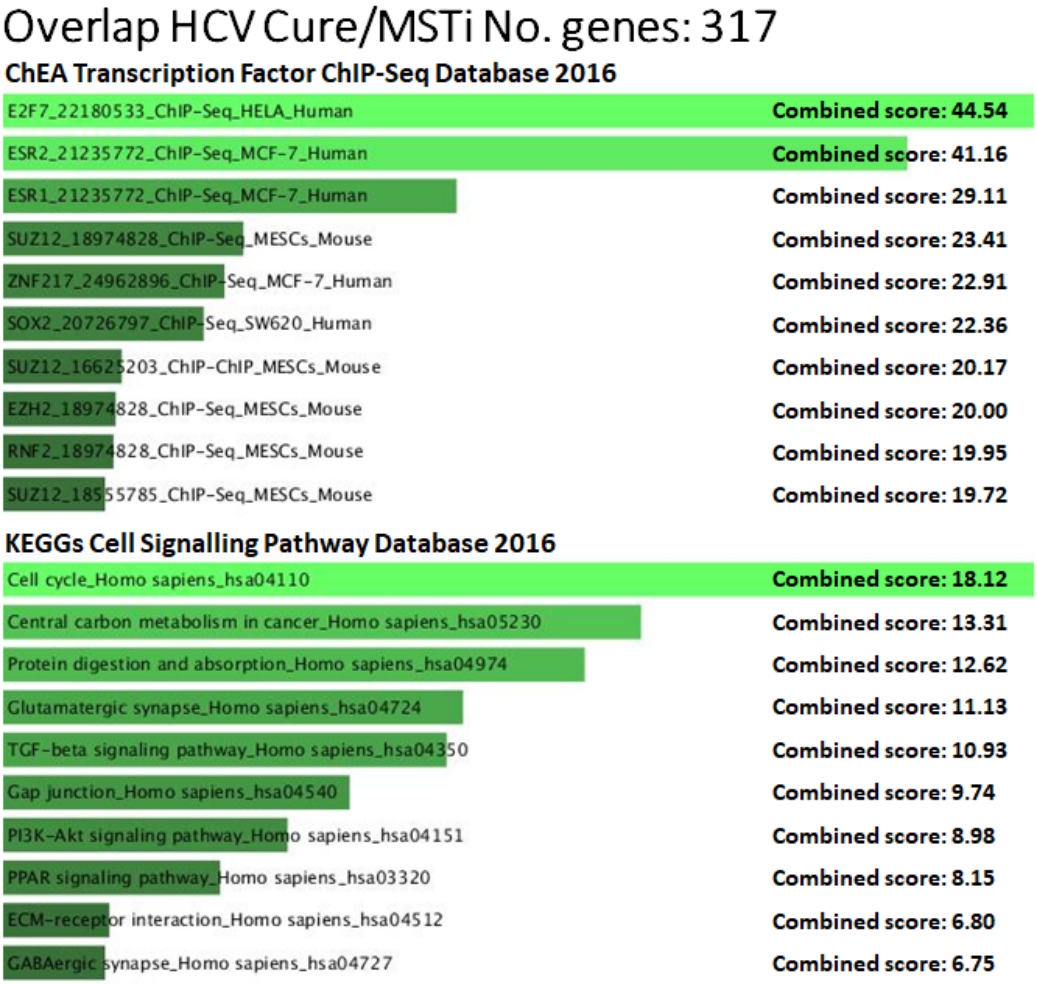


**Figure 5.4.1 Enrichment analysis of significantly differentially regulated genes shared by HCV Cure and MSTi compared to Control**

Enrichment analysis using Enrichr, the ChEA Transcription Factor ChIP-seq Database and the KEGG Signalling Pathway Database to predict which transcription factors are responsible for the gene expression changes observed and which signalling pathways are affected by the gene expression changes observed in the RNA-seq analysis. Transcription factors and signalling pathways were ranked by combined score which takes into account the p-value (calculated using the Fisher's exact test) and the z-score (the z-score is a measure of the deviation from an expected rank). The length and the brightness of the bar reflects the significance of that term/gene set, i.e. the longer and brighter the bar, the more significant the term/gene set is. A grey bar means the term/gene-set is not significant.

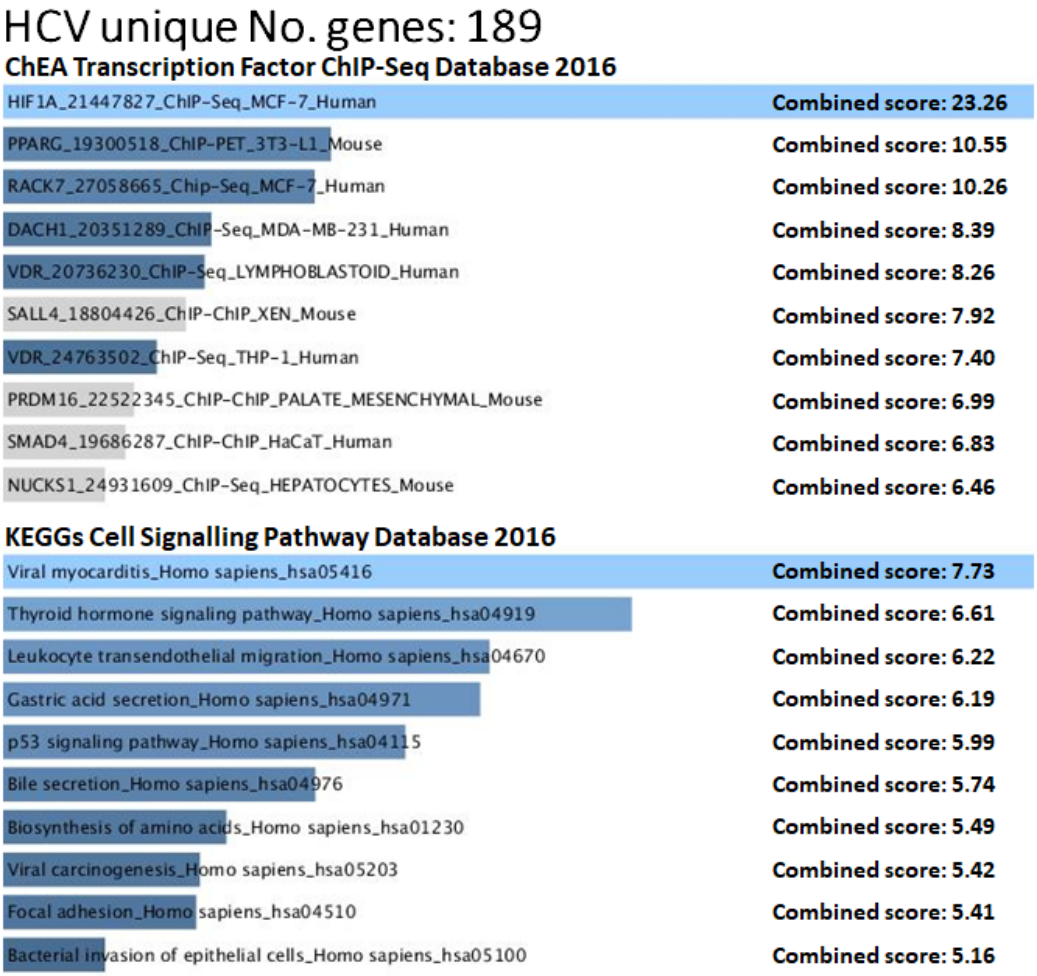


**Figure 5.4.2 Enrichment analysis of significantly differentially regulated genes unique to HCV compared to Control**

Enrichment analysis using Enrichr, the ChEA Transcription Factor ChIP-seq Database and the KEGG Signalling Pathway Database to predict which transcription factors are responsible for the gene expression changes observed and which signalling pathways are affected by the gene expression changes observed in the RNA-seq analysis. Transcription factors and signalling pathways were ranked by combined score which takes into account the p-value (calculated using the Fisher's exact test) and the z-score (the z-score is a measure of the deviation from an expected rank). The length and the brightness of the bar reflects the significance of that term/gene set, i.e. the longer and brighter the bar, the more significant the term/gene set is. A grey bar means the term/gene-set is not significant.

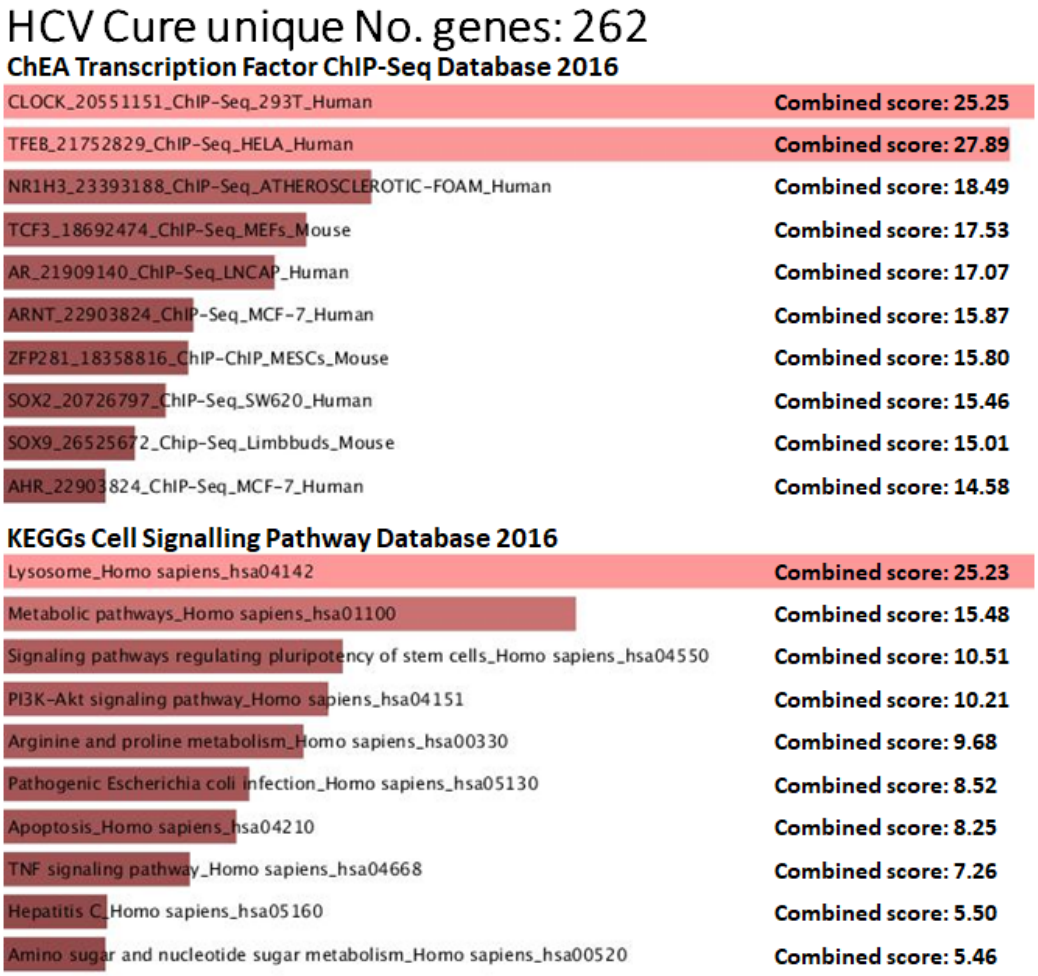


**Figure 5.4.3 Enrichment analysis of significantly differentially regulated genes unique to HCV Cure compared to Control**

Enrichment analysis using Enrichr, the ChEA Transcription Factor ChIP-seq Database and the KEGG Signalling Pathway Database to predict which transcription factors are responsible for the gene expression changes observed and which signalling pathways are affected by the gene expression changes observed in the RNA-seq analysis. Transcription factors and signalling pathways were ranked by combined score which takes into account the p-value (calculated using the Fisher's exact test) and the z-score (the z-score is a measure of the deviation from an expected rank). The length and the brightness of the bar reflects the significance of that term/gene set, i.e. the longer and brighter the bar, the more significant the term/gene set is. A grey bar means the term/gene-set is not significant.

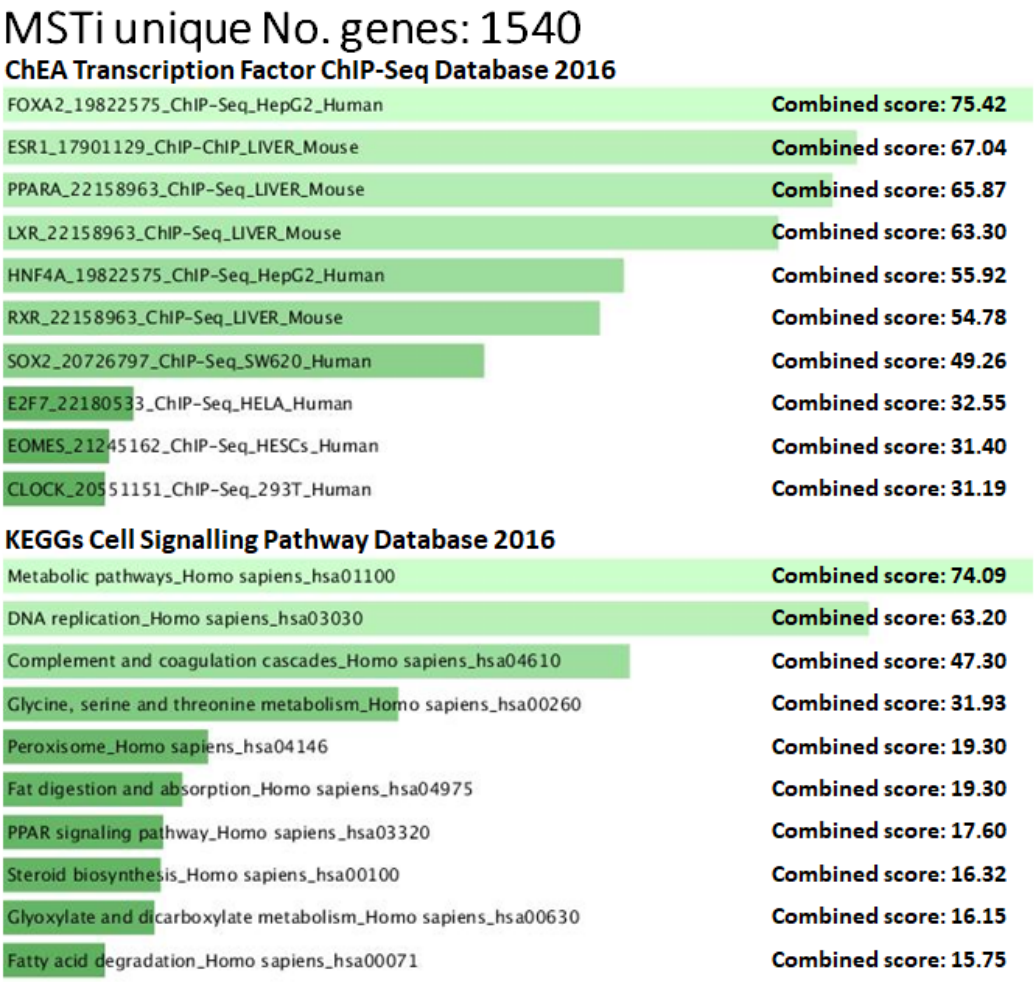


**Figure 5.4.4 Enrichment analysis of significantly differentially regulated genes unique to MSTi compared to Control**

Enrichment analysis using Enrichr, the ChEA Transcription Factor ChIP-seq Database and the KEGG Signalling Pathway Database to predict which transcription factors are responsible for the gene expression changes observed and which signalling pathways are affected by the gene expression changes observed in the RNA-seq analysis. Transcription factors and signalling pathways were ranked by combined score which takes into account the p-value (calculated using the Fisher's exact test) and the z-score (the z-score is a measure of the deviation from an expected rank). The length and the brightness of the bar reflects the significance of that term/gene set, i.e. the longer and brighter the bar, the more significant the term/gene set is. A grey bar means the term/gene-set is not significant.

We used Enrichr to carry out an enrichment analysis on a published gene expression data set of J6-JFH1 infected cycling Huh7.5 cells (Woodhouse et al., 2010) (Figure 5.2.1). The top pathways highlighted by the analysis were consistent with previous literature, including MAPK and TNF signalling (He et al., 2001, Tan et al., 1999, Macdonald et al., 2004, Giambartolomei et al., 2001, Hayashi et al., 2000, Fukuda et al., 2001, Nelson et al., 1997). However, Enrichr also highlighted the Hippo pathway, which is heavily implicated in liver development, hepatocyte differentiation and HCC development (Meng et al., 2016). To our knowledge, HCV-induced regulation of Hippo signalling has not been previously reported.

The Hippo pathway (Figure 5.4.12) is regulated by many different signals and responds to changes in cell-cell contact, cell-ECM interactions and cell polarity (Meng et al., 2016). The core of the pathway consists of two transcriptional regulators YAP1 and TAZ (gene name WWTR1) which, in the absence of Hippo signalling, translocate to the nucleus and interact with transcription factors such as TEADs and SMADs (Hong and Guan, 2012) and induce a transcriptional profile consistent with cell survival, proliferation and stem cell maintenance (Pan, 2010). YAP1 and TAZ are regulated by the kinase cascade consisting of MST1/2 which complexes with Sav1 to phosphorylate LATS1/2 and co-activator MOB1. LATS1/2 activation leads to phosphorylation of YAP1 and TAZ, cytoplasmic retention and eventually proteasomal degradation. Altered Hippo signalling and aberrant activation of YAP1 and TAZ is associated with liver tumorigenesis (Lu et al., 2010, Hong and Guan, 2012, Lee et al., 2010, Patel et al., 2017, Sugimachi et al., 2017, Pei et al., 2015). Hepatocyte differentiation and liver regeneration are dependent on Hippo signalling (Alder et al., 2014, Liu et al., 2012, Lu et al., 2018, Yimlamai et al., 2014). As previously stated, the Hippo pathway is regulated by many different signals including from tight junctions, adherens junctions, Wnt signalling, TGF-β signalling, GPCRs, the actin cytoskeleton and other intracellular proteins (Yu et al., 2012, Yang et al., 2015, Kim and Jho, 2014, Kim et al., 2017, Pefani et al., 2016, Sun and Irvine, 2016, Zhao et al., 2012). Indeed, during our characterisation of CD24lo differentiation we observed altered expression and localisation of junction proteins such as E-cadherin and EpCAM and cytoskeletal protein F-actin upon HCV infection (Figure 4.2.19). Our expectation was that Hippo signalling might be activated in differentiating CD24lo cells, sequestering and YAP1/TAZ to the cytoplasm and degrading them, but that this may not occur within cells harbouring HCV during DMSO induced differentiation.

Characterising the expression and localisation of Hippo pathway proteins in our differentiation model at day nine revealed a reduction of cytoplasmic MST1 levels whereas centrosome localisation was maintained, a reduction of LATS1 levels and altered localisation, an increase in TAZ levels and maintenance of nuclear YAP1 localisation during differentiation of HCV infected cells compared to Control cells. It will be important to further investigate any change in MST1 and also MST2 activity by further measuring the levels of phosphorylated MST1 and MST2 as this will give a clearer understanding of whether activity levels change in response to differentiation induction. The trend for MST1 levels in virus infected cells however was a reduction in MST1 levels over the course of differentiation and overall a significant reduction of MST1 protein levels. This indicates that virus infection is able to either alter the transcription or the protein stability of MST1, and thus influence Hippo signalling. As the MST1 gene was not downregulated in the HCV condition, the change in mST1 protein level is likely due to a change in protein stability. Further experiments involving qPCR analysis to measure MST1 and MST2 mRNA levels and protein stability assays such as by using the protein synthesis inhibitor Cyclohexamide (Schneider-Poetsch et al., 2010), will help us understand the effect of HCV infection better. Immunofluorescence of MST1 also revealed that differentiation induces an alteration in localisation of the protein in both control and HCV infected cells. At day one of differentiation MST1 was located in both the nucleus and cytoplasm however at day nine of differentiation MST1 was largely located in the cytoplasm and was concentrated to the centrosome. For HCV infected cells the centrosome MST1 expression/localisation was maintained however the cytoplasmic fraction was reduced. This observation is not completely surprising as MST1/MOB1 signalling controls centrosome duplication independent of the Hippo pathway by promoting phosphorylation of NDR which is required for centrosome duplication (Hergovich et al., 2009). NDR kinases are part of the same family of serine/threonine protein kinases as LATS1/2, however LATS1/2 are not directly involved in regulating centrosome duplication (Hergovich et al., 2007).

CD24lo cell differentiation induced an increase in LATS1 levels, yet LATS1 levels were significantly lower for HCV infected cells. This observation suggests that LATS1 protein stability is increased during differentiation and

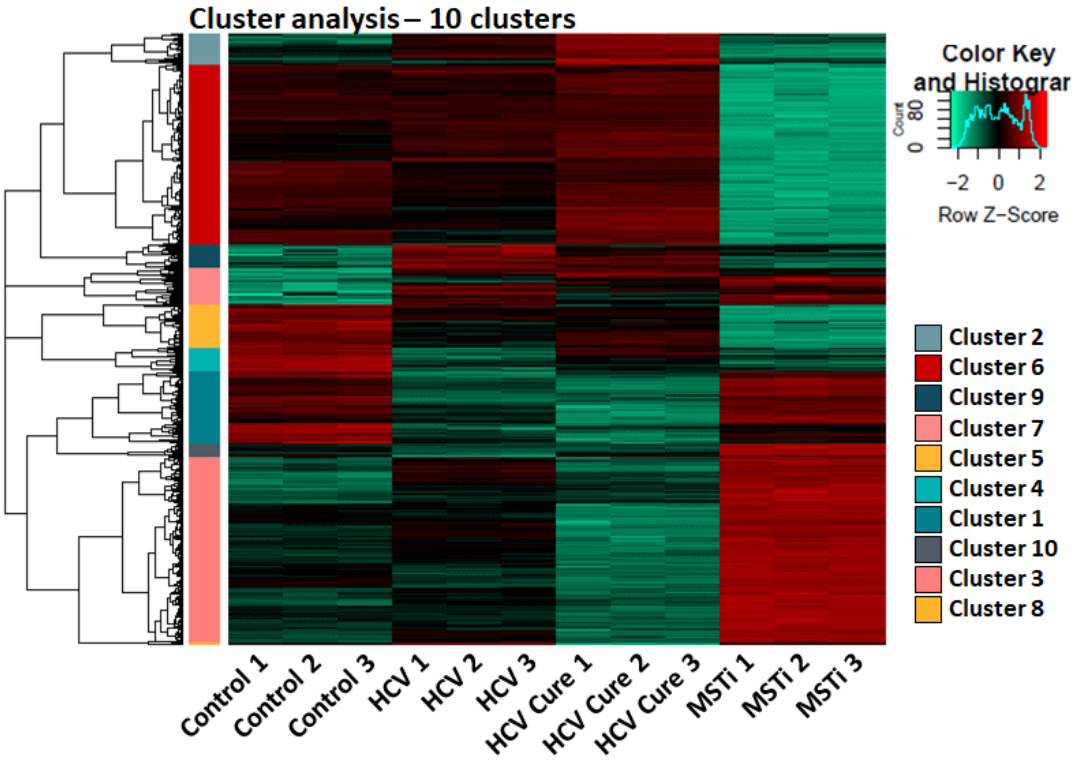


**Figure 5.4.5 Cluster analysis**

Cluster analysis found 10 different clusters of genes with similar expression profiles across the different conditions (HCV, HCV Cure, and MSTi) compared to the control. 3056 genes were included in the analysis based on stringent criteria: p≤0.01, 2foldchange≥1, bm≥100.

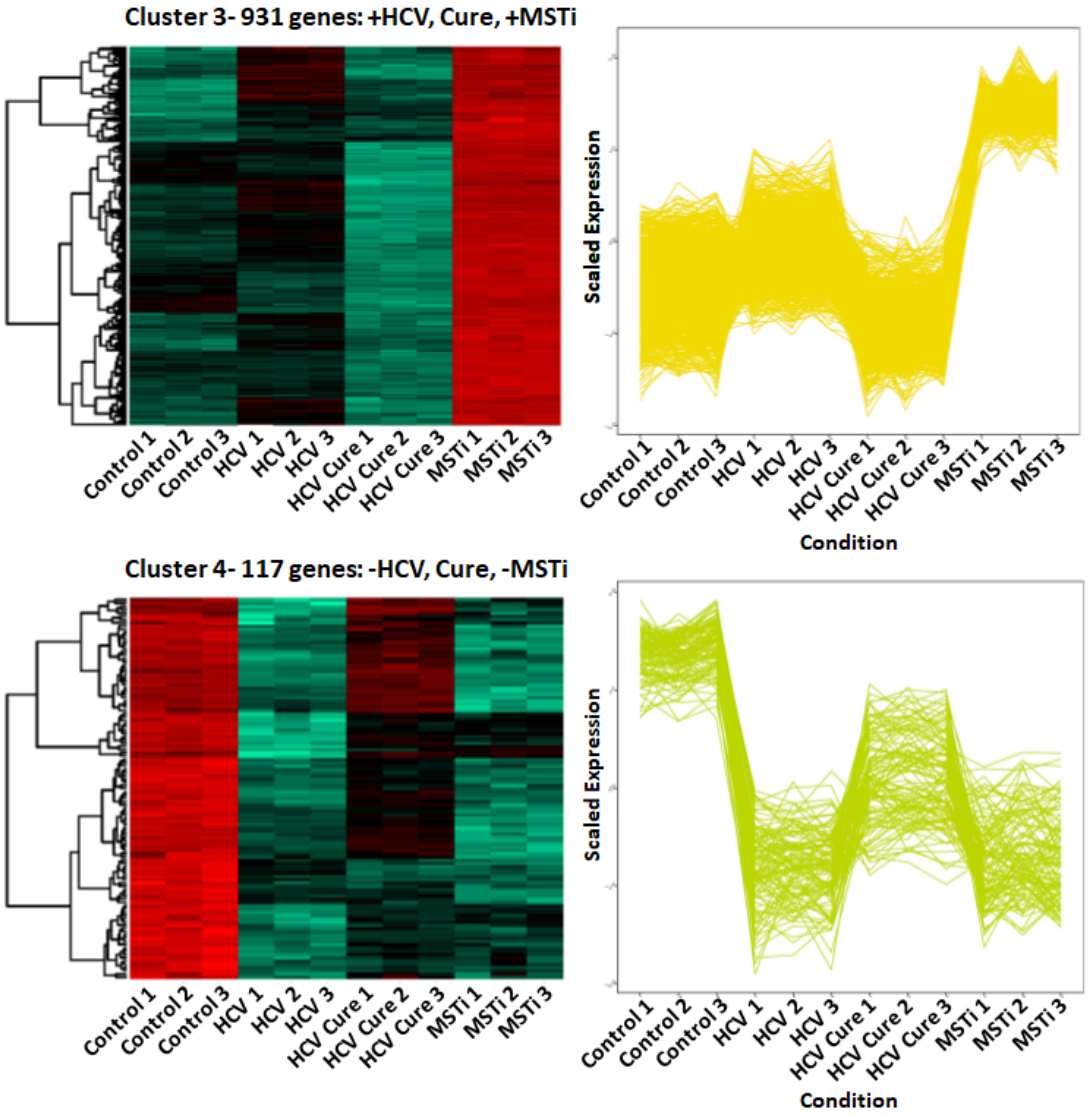


**Figure 5.4.6 Gene expression changes which are reversed by DAA treatment**

The cluster analysis revealed a few clusters of genes which were either upregulated (e.g. Cluster 3) or downregulated (e.g. Cluster 4) by HCV compared to the Control and for which the expression profile was reversed by DAA treatment.

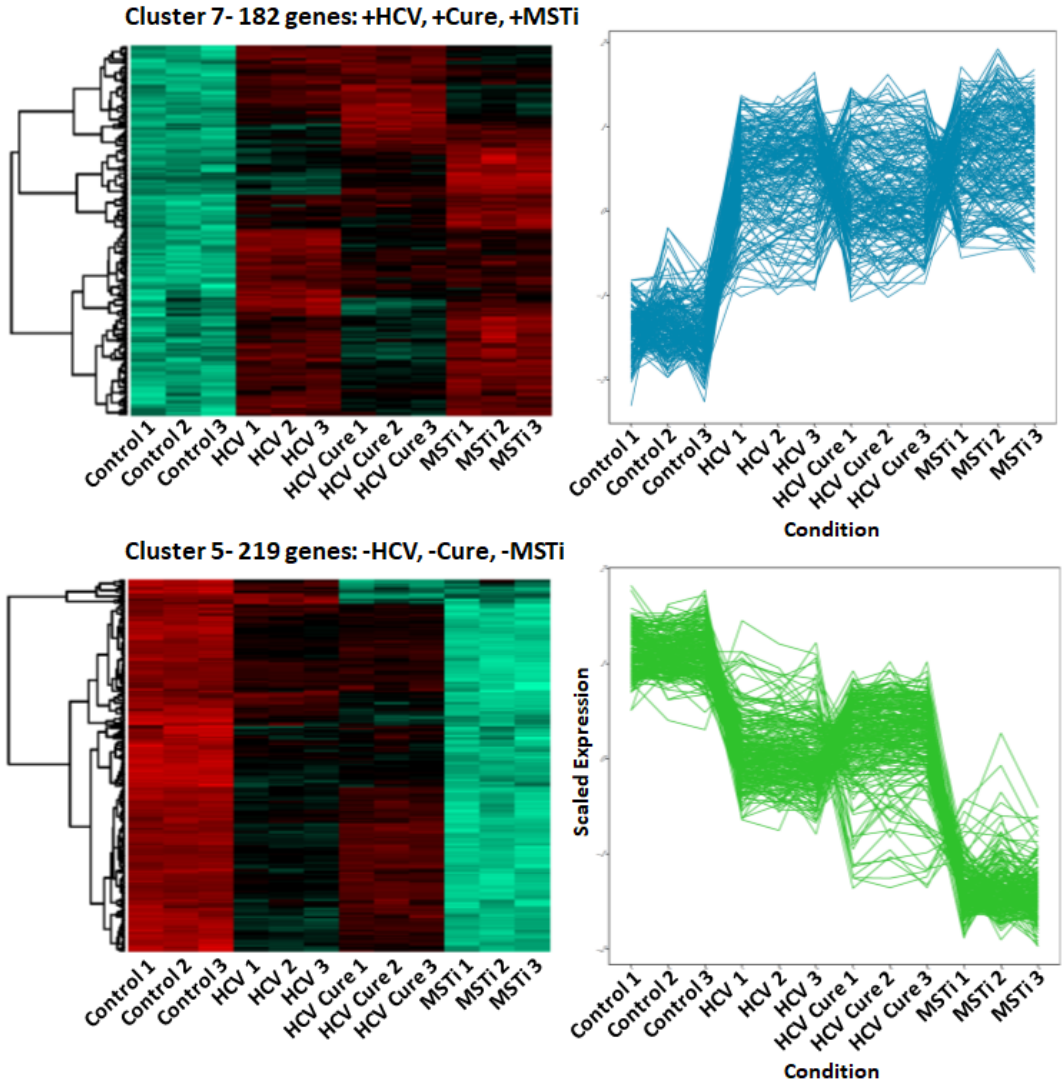


**Figure 5.4.7 Gene expression changes which are not reversed by DAA treatment**

The cluster analysis revealed a few clusters of genes which were either upregulated (e.g. Cluster 7) or downregulated (e.g. Cluster 5) by HCV compared to the Control and for which the expression profile was not reversed by DAA treatment.

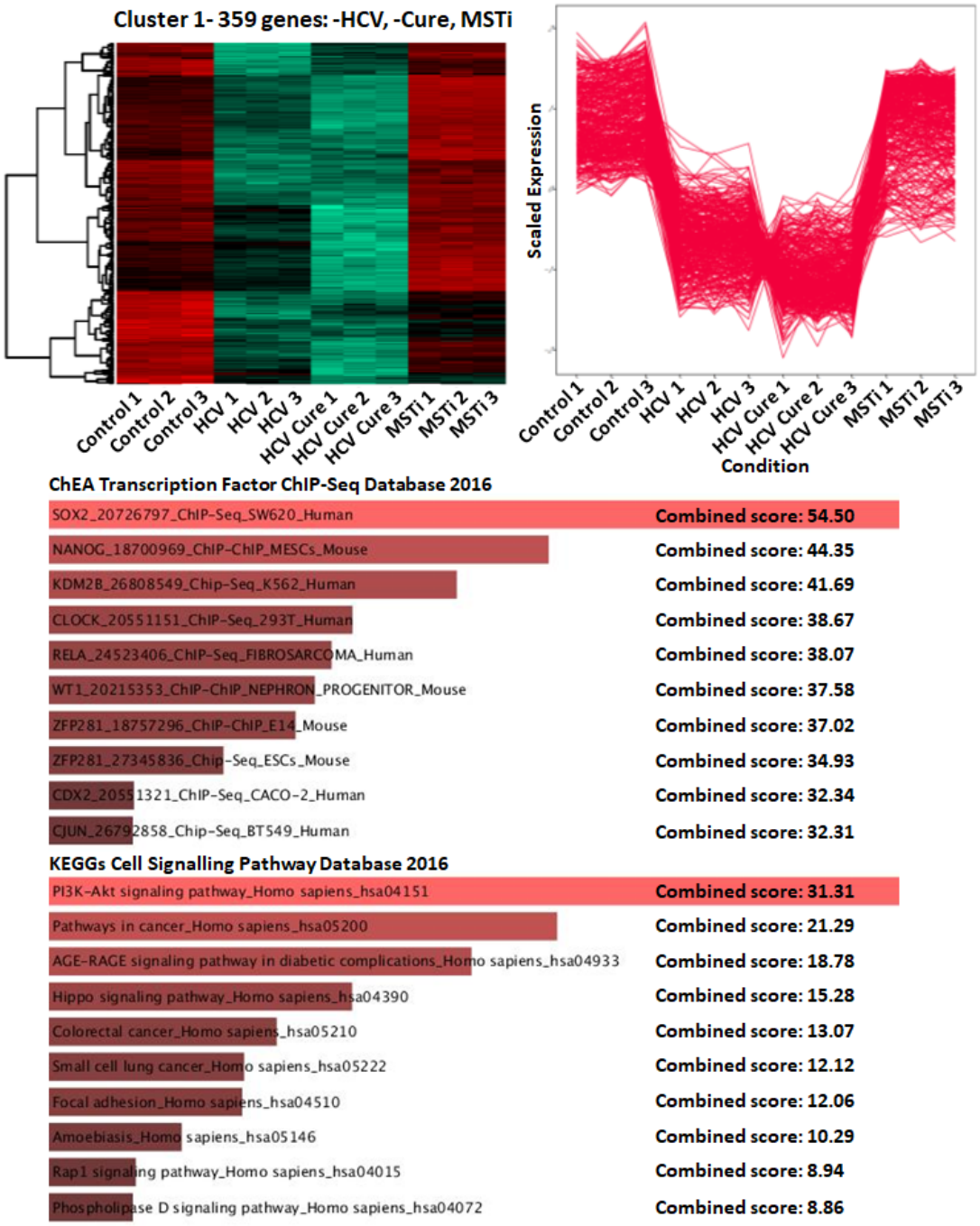


**Figure 5.4.8 Genes within cluster 1 are members of signalling pathways associated with carcinogenesis**

Further enrichment analysis using Enrichr, the ChEA Transcription Factor ChIP-seq Database and the KEGG Signalling Pathway Database to predict which transcription factors are responsible for the gene expression changes observed and which signalling pathways are affected by the gene expression changes of differentially regulated genes within cluster 1 revealed that this cluster contained many members of signalling pathways commonly associated with carcinogenesis. Transcription factors and signalling pathways were ranked by combined score which takes into account the p-value (calculated using the Fisher's exact test) and the z-score (the z-score is a measure of the deviation from an expected rank).

that HCV counteracts this as we did not see a decrease in LATS1 transcription for HCV in the RNA-seq experiment. However pLATS1 levels surprisingly decreased over the course of Cured and JFH1-replicon differentiation. This was particularly apparent for JFH1-replicon cells, indicating a drop in Hippo signalling activation. However, this was an observation based upon a single experiment and further experiments should continue to elucidate the pattern of phosphorylated LATS1 levels.

Interestingly immunofluorescence revealed a stark difference in LATS1 localisation at day nine of differentiation in HCV infected cells compared to control with LATS1 being maintained in the nucleus instead of translocating the cytoplasm as in Control cells. There are only few mentions of nuclear LATS1 in the literature. LATS1 is predominantly described to localise to the cytoplasm, yet the subcellular localisation of LATS1 plays a role in regulating LATS1 activity. For example membrane localised LATS1 appears to increase its kinase activity (Hergovich et al., 2006). Indeed membrane targeting of related kinases NDR1/2 is enough to promote phosphorylation and activation of these proteins (Hergovich et al., 2005). As already described, LATS1/2 also contain phosphorylation sites. LATS1 activity is regulated by PP2A-mediated de-phosphorylation to decrease its activity (Hergovich et al., 2006). However, LATS1/2 has been described to be activated by MST1/2 in the nucleus in mouse keratinocytes (Lee et al., 2008). To complicate the understanding of the relationship between subcellular localisation and LATS1 further Wei et al., describe that the CRL-DCAF1 ubiquitin ligase complex targets LATS1/2 in the nucleus in response to NF2 loss (Li et al., 2014). What exactly LATS1 subcellular localisation difference means in our experiment requires further investigation. In addition investigating the role, expression and localisation of LATS2 would help us understand the role of Hippo signalling better.

Surprisingly, YAP1 protein levels did not change over the course of differentiation for either Control or HCV infected cells and the overall levels were similar in these two conditions also. This indicated that in response to any upstream changes in Hippo signalling protein expression and stabilisation appeared to stay the same over differentiation and between Control and infected cells. However as with the upstream members of the Hippo pathway, MST/2 and LATS1/2, phosphorylation of YAP1 is an important indicator of YAP1 activity and Hippo signalling activation (Meng et al., 2016). Western blot analysis of CD24lo and infected cells revealed that YAP1 is phosphorylated at S127 at day one of differentiation in both J6-

JFH1 infected and in CD24lo cells. Furthermore there was a trend towards a slight increase in pYAP1(S127) levels in response to DMSO addition in both conditions, this suggests that Hippo signalling is indeed activated in response to DMSO induced differentiation, at least at day 5. To better understand the functional state of YAP1 during differentiation and between control and infected cells, immunofluorescence was used to examine protein localisation. As expected for cycling cells, YAP1 was located in the nucleus at day one for both control and infected cells. In response to differentiation, YAP1 was sequestered to the cytoplasm in almost all control cells. However, a large proportion of infected cells maintained nuclear YAP1 expression, suggesting that YAP1 is still active in these cells and able to bind to transcription factors in order to regulate transcription of YAP1 responsive genes. Aberrant activation of YAP1 is associated with tumorigenesis of many cancers, particular of the liver including HCC and ICCA (Xu et al., 2009, Li et al., 2015b). Total YAP1 levels and pYAP1 levels did not change dramatically during differentiation thus YAP1 localisation must be regulated by a different mechanism such as through binding to the YAP1/TAZ regulatory protein AMOT.

The paralogs YAP1 and TAZ can be considered the effector proteins of the Hippo pathway and are both transcriptional regulators. Often, these proteins are described interchangeably as both proteins share similar regulatory mechanisms and regulate a similar set of genes (Meng et al., 2016). They share about 45 % amino acid sequence identity but are located on separate chromosomes (located at 11q22.1 and 3q24 respectively for YAP1 and TAZ) (Kanai et al., 2000, Overholtzer et al., 2006). However, more recently, novel distinct regulatory mechanisms have also been identified for these proteins and a degree of reciprocal regulation also exists between them (Finch-Edmondson et al., 2015). These transcriptional regulators may also regulate the expression of a subset of unique genes to one another however this is has not been investigated thoroughly. Tissue specific, cell state specific mechanisms may guide YAP1 and TAZ gene regulation depending on the availability/expression of transcription factor binding partners. Thus it was interesting to observe an altered protein expression pattern of TAZ both as differentiation proceeded, and also between control and HCV infected cells, compared to seemingly invariant YAP1 expression. TAZ protein levels were significantly higher in HCV infected cells compared to control cells and remained elevated throughout differentiation. It would be interesting to explore these differences between YAP1 and TAZ further using

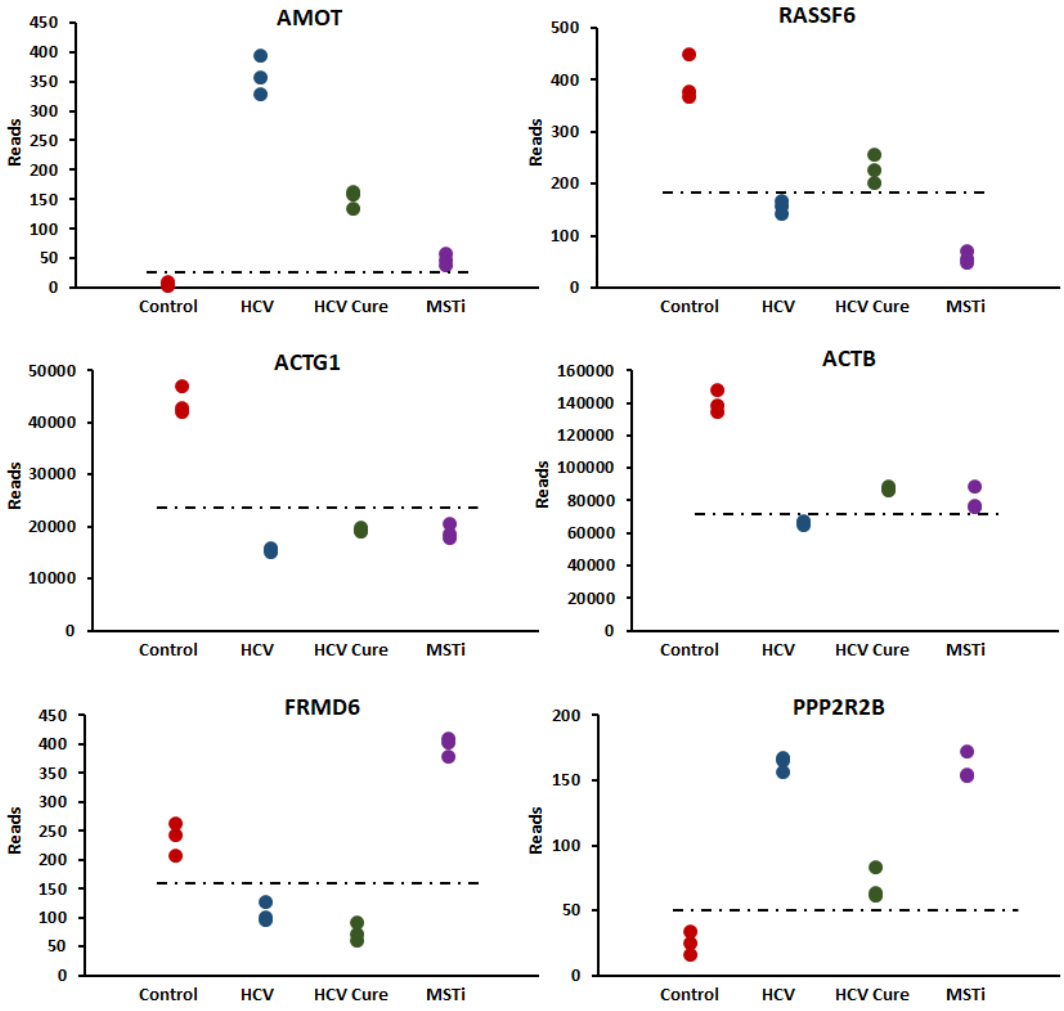


**Figure 5.4.9 Gene expression of Hippo signalling regulators**

RNA-seq analysis revealed that the gene expression of several Hippo signalling regulators is altered in the HCV, HCV Cure and MSTi conditions compared to Control at day9 of differentiation, including; AMOT, RASSF6, ACTG1, ACTB, FRMD6 and PPP2R2B. The dashed line serves to highlight in which conditions gene expression was significantly upregulated and is arbitrarily set on the graph.

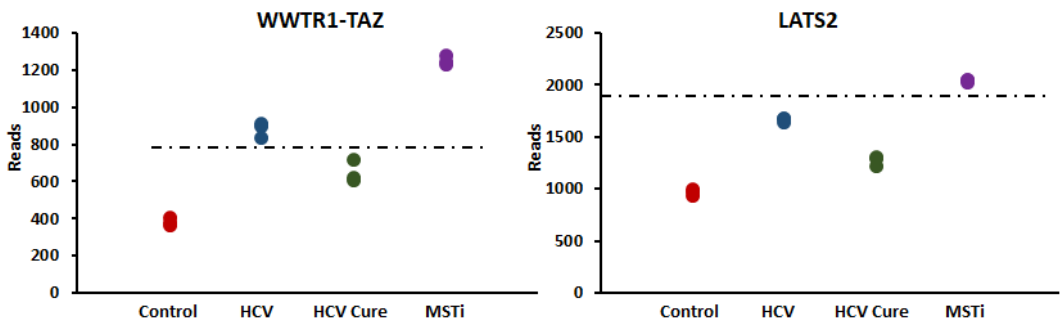


**Figure 5.4.10 WWTR1 (TAZ) and LATS2 gene expression**

RNA-seq analysis revealed that WWTR1 (TAZ) gene expression was significantly upregulated in HCV and MSTi conditions compared to the Control at day 9 of differentiation. LATS2 expression was significantly upregulated only by MST1/2 inhibition. The dashed line serves to highlight in which conditions gene expression was significantly upregulated and is arbitrarily set on the graph.

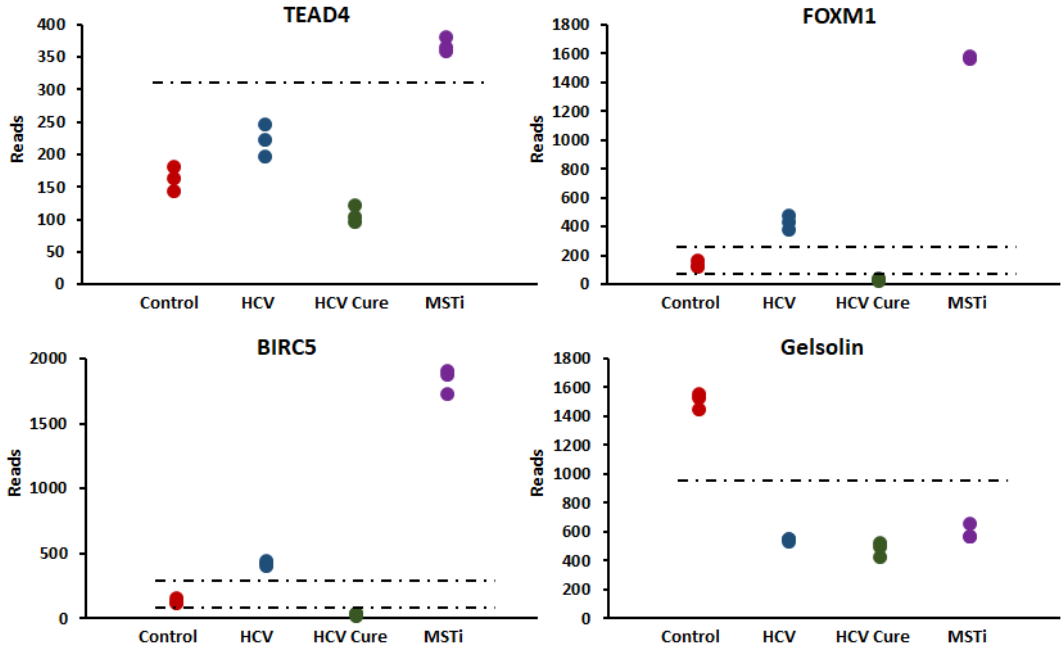


**Figure 5.4.11 Gene expression of YAP1/TAZ transcription factors and YAP1/TAZ responsive genes**

RNA-seq analysis revealed that the gene expression of several Hippo signalling regulators is altered in the HCV, HCV Cure and MSTi conditions compared to Control at day9 of differentiation, including; AMOT, RASSF6, ACTG1, ACTB, FRMD6 and PPP2R2B. The dashed line serves to highlight in which conditions gene expression was significantly upregulated and is arbitrarily set on the graph.

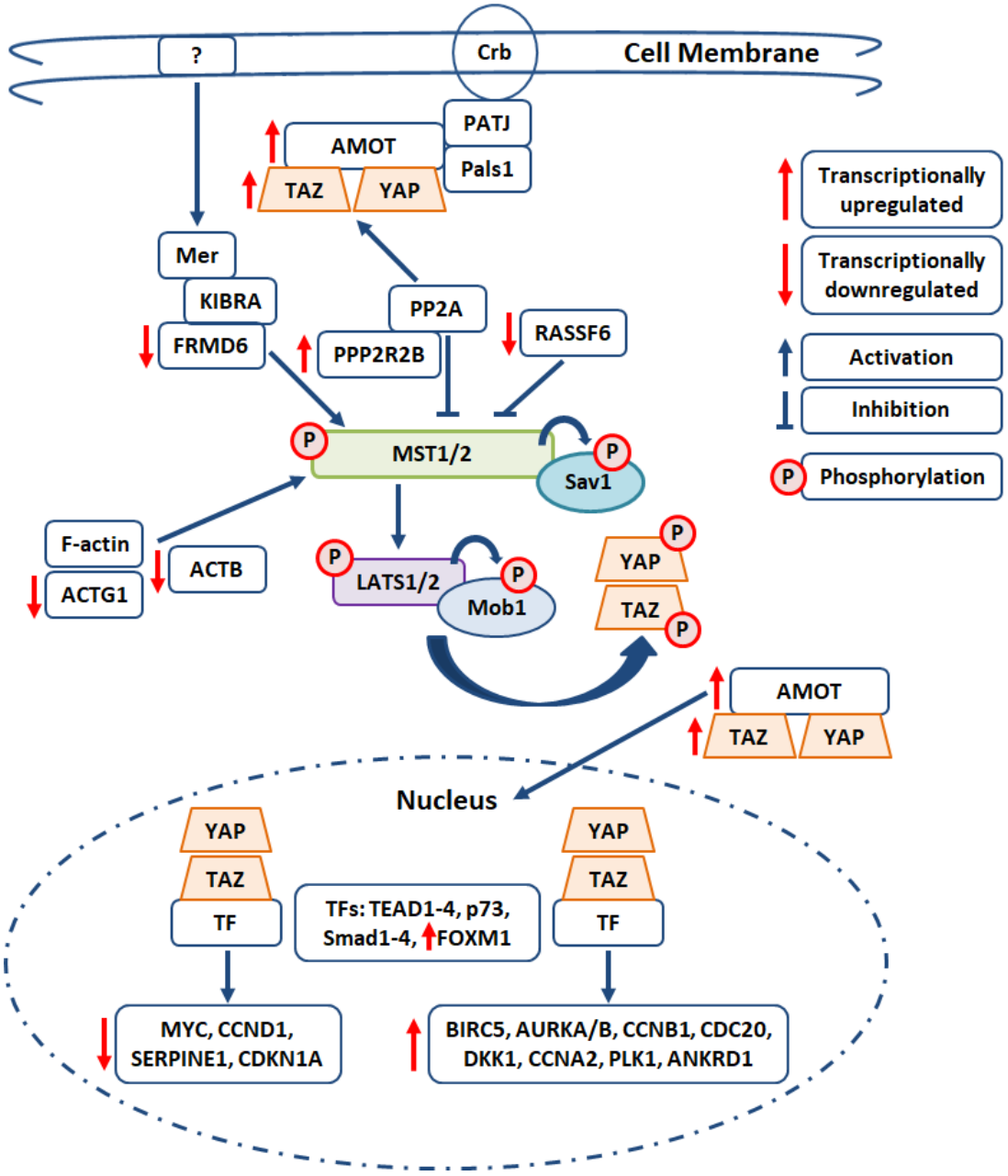


**Figure 5.4.12 Differentially regulated Hippo genes by HCV compared to Control**

After applying the stringent cut-offs p≤0.01 base mean≥100 and log2fold change≥1, several genes associated with the Hippo signalling pathway were found to be differentially regulated by HCV compared to the Control. Some genes were YAP1/TAZ responsive genes; others are involved in the regulation of Hippo signalling. Genes which are significantly differentially regulated by HCV are indicated by a red arrow. The blue arrows indicate protein activation or inhibition.

TAZ/pTAZ specific antibodies, although these are uncommon and we were unable to source examples during the course of this study.

As mentioned previously YAP1 and TAZ regulate the transcription of many genes by binding to various transcription factors including TEAD1-4, SMAD1-4, p73 and FOXM1 (Eisinger-Mathason et al., 2015) and regulating their activity. To better understand whether differentiation activated Hippo signalling it was important to examine the expression of YAP1/TAZ responsive genes. A very commonly described responsive gene which is often used as a marker of YAP1/TAZ activity is CTGF (Urtasun et al., 2011, Zhao et al., 2008). CTGF plays a role in modulating the cellular interaction with the ECM (Bornstein and Sage, 2002, Leask and Abraham, 2006, Shi-Wen et al., 2008), and is a direct target of YAP1/TAZ interaction with TEAD4 and helps mediate YAP1-dependent cell growth (Zhao et al., 2008). However western blot analysis revealed that intracellular CTGF levels remained unaltered during differentiation in both Cured and JFH1-replicon cells and overall levels were similar in both conditions. As CTGF is a secreted protein it will be important to validate this result using an ELISA assay.

Lack of the expected drop in CTGF levels during differentiation and no difference between infected and control cells does not necessarily mean that Hippo signalling is not being activated during differentiation, or that the observed differences Hippo protein expression and location are not having an effect on YAP1/TAZ transcriptional activity. YAP1 and TAZ activate, and also to a degree repress, the transcription of a large number of genes. Transcriptional regulation depends on transcription factor availability depending on cell type and state (Plouffe et al., 2018).

Interestingly the RNA-seq data revealed that many YAP1/TAZ responsive genes remained upregulated within HCV infected cells at day 9 of differentiation, such as BIRC5, AURKA/B, CCNB1, CDC20, CCNA2, DKK1, PLK1 and ANKARD1 whereas as some were also downregulated in response to HCV infection, such as MYC, CCND1, SERPINE1 and CDKN1A. CCND1 encodes the cyclin dependent kinase inhibitor also known as p21. p53 regulates p21 which mediates G1 cell cycle arrest. In addition p21 loss is associated with carcinogenesis (Cayrol et al., 1998, Gartel and Tyner, 1999, Willenbring et al., 2008). HCV is known to interact with p21 activity (Cao et al., 2004, Kwun et al., 2001, Majumder et al., 2001). YAP1 and TAZ are known to function in a tissue specific/ cell state specific way to alter gene expression. The observation that some known YAP1/TAZ

responsive genes are upregulated whereas others are downregulated by HCV may be a consequence of these cell type/state specific differences. In addition some genes may be exclusively or preferentially regulated by either YAP1 or TAZ, however not enough evidence exists to clearly define whether one gene is exclusively regulated by either YAP1 or TAZ. This may be particularly interesting as we found TAZ protein and mRNA levels to be elevated by HCV whereas YAP1 protein or mRNA levels were not.

WWTR1 (TAZ) is a paralog of YAP1 only present in vertebrates. As stated YAP1 and TAZ share almost 50 % sequence homology (Kanai et al., 2000) but TAZ compared to YAP1 lacks an additional WW domain, the N-terminal proline rich domain and the SH3 binding motif (Kanai et al., 2000) (Figure 1.4.2). Studies exploring the differences of YAP1/TAZ regulation and function are limited however and many studies either focus on YAP1 or less commonly just TAZ. In addition many refer to these proteins interchangeably due to their overlapping functions. YAP1 and TAZ do share many regulatory mechanisms, bind to many of the same transcription factors and are thought to regulate the transcription of a similar series of genes. However, whilst redundancy in their molecular activity clearly exists, evidence is mounting that these proteins have divergent functions. Even though YAP1 and TAZ share transcription factor targets it is still unclear how the individual proteins contribute to the function of these shared factors and the activation of unique targets is poorly studied. YAP1 and TAZ are not completely redundant and do not fully compensate each other when either is genetically knocked out. Different phenotypes emerged from YAP1 and TAZ knockout mice; knocking out YAP1 led to embryonic lethality, a shortened body axis and defects in the development of the yolk sac vasculature (Morin-Kensicki et al., 2006). TAZ knockout mice on the other hand were viable yet develop renal cysts, eventually leading to end stage kidney disease (Makita et al., 2008, Hossain et al., 2007). These differences suggest that either YAP1 and TAZ are expressed differently in different tissues or that tissue/cell- specific transcription factor binding partners exist or that differential regulatory mechanisms exist.

Relatively few studies exist specifically exploring the differences between YAP1 and TAZ in terms of how they effect transcriptional regulation, or are themselves regulated. For example, differences exist in the TEAD binding domain of both proteins, namely that TAZ lacks the extended PxxOP loop (O=hydrophobic residue) of YAP1 (Chen et al., 2010a, Li et al., 2010). TAZ possess two TEAD binding modes and is able to form a hetero-tetramer

complex with TEAD (Kaan et al., 2017) in addition to the hetero-dimer formed between YAP1 and TEAD (Chen et al., 2010a, Li et al., 2010). This additional interaction mode may be able to affect DNA target selectivity and potentially lead to a stronger induction of gene expression of certain targets . Different regulatory factors have been identified for YAP1 and TAZ, such as GSK3β which only targets TAZ to induced phosphorylation, leading to TAZ degradation in the absence of Wnt signalling (Huang et al., 2012). In addition, the HIPK2 is a specific regulator of YAP1 and can increase YAP1 cellular abundance. The mechanism by which HIPK2 increases YAP1 levels is unknown although HIPK2 has been shown to not interact with YAP1 directly (Poon et al., 2012). YAP1 has also been shown to be able to regulate the abundance of TAZ by proteasomal degradation in a GSK3β dependent manner, whereas TAZ expression was unable to affect YAP1 abundance (Finch-Edmondson et al., 2015). Furthermore, Parafibromin, which is a component of the RNA polymerase II associated factor, appears to regulate YAP1 and TAZ inversely; TAZ in complex with β-catenin interact with the dephosphorylated form of Parafibromin to stimulate TAZ/ β-catenin functions whereas YAP1 is activated by binding to the phosphorylated form of Parafibromin (Tang et al., 2018). Furthermore YAP1 does not interact with β-catenin.

The most highly upregulated protein by HCV in the RNA-seq experiment was AMOT (Figure 5.4.9). AMOT was also upregulated in HCV Cure and MSTi but not as highly. AMOT is a regulatory factor of YAP1 and TAZ, apparently able to regulate these two proteins in opposing ways. AMOT is recruited to the cellular junction Crumbs complex. AMOT has been shown to be able to bind to YAP1 and TAZ leading to cytoplasmic retention (Wang et al., 2011b, Zhao et al., 2011). However other work shows that p130-AMOT is able to bind to YAP1/TAZ-TEAD complexes in the nucleus. p130-AMOT also disrupted LATS1/2 interaction with YAP1, leading to reduced phosphorylation of YAP1 and increased nuclear YAP1 localisation (Yi et al., 2013). How these opposing roles are regulated however is not entirely clear and may be cell type specific.

Hippo signalling responds to cytoskeletal changes. For example loss of F-actin stress fibres has been associated with repression of nuclear activity of YAP1 and TAZ (Dupont et al., 2011). The RNA-seq analysis of differentiated CD24lo cells revealed that both beta-actin and gamma-actin transcription are downregulated by HCV infection. ACTG1 is also downregulated in HCV Cure and MSTi whereas ACTB is only downregulated in HCV (Figure 5.4.9).

However the exact impact of this upon Hippo signalling is unclear. F-actin assembly alterations by capping and severing proteins such as CapZ, cofilin or gelsolin are able to facilitate cytoplasmic retention of YAP1 and TAZ whereas depletion of these proteins has been associated with an increase in nuclear YAP1 and TAZ activity (Aragona et al., 2013). Gelsolin, the most potent actin filament severing protein is downregulated by HCV infection (and also in the MSTi and HCV Cure conditions) in our RNA-seq experiment (Figure 5.4.11). The fact that expression of this gene is also downregulated by MSTi suggests this gene may be regulated by Hippo signalling. Furthermore as the expression profile is not reversed by HCV Cure this may be an example of an gene which is epigenetically regulated by HCV infection similarly with beta-actin. Further experiments are needed to understand the exact effect of these observations on Hippo signalling and CD24lo differentiation.

Overall our results have shown that Hippo signalling, resultant YAP1/TAZ localisation, expression and ensuing transcription of responsive genes are altered by HCV in response to DMSO-induced differentiation. However, the next question was how did HCV mediate these effects? It is likely that the differences of Hippo protein localisation and expression are mediated via a viral protein interaction with a member of the core/canonical Hippo pathway, or potentially an associated regulatory protein. The viral protein(s) responsible must reside within the NS3-NS5B replicon polyprotein as the same perturbation of differentiation and Hippo pathway alteration was observed for both infection with full length J6-JFH1 HCV and the subgenomic JFH1-replicon. NS5A is known to interact with a range of cellular proteins (Macdonald and Harris, 2004, Ross-Thriepland and Harris, 2015). For example HCV is known to interact with PP2A to promote its activity. This is particularly interesting as PP2A is a known inhibitor of MST1/2 activity. This, combined with the unique ability of NS5A to accommodate genetic insertions, is why we first chose to investigate whether NS5A was able to interact with any of the main Hippo pathway proteins. Immunofluorescence of JFH1-replicon cells co-stained with anti-NS5A and anti-Hippo protein antibodies revealed an apparent co-localisation between MST1 and NS5A. To further investigate this possible interaction between the two proteins GFP pulldown was performed with cells infected with the J6-eGFP clone which encodes a NS5A-eGFP fusion protein (Gottwein et al., 2011). The pulldown assay indeed showed that MST1 accumulated in the bound fragment of the NS5A-eGFP pulldown sample, adding further evidence of an interaction between these proteins. We also

probed for LATS1, MOB1 and YAP1 but these proteins did not accumulate in the bound fragment of the pull down assay. To further confirm and understand the nature of this interaction further experiments are required. It would be interesting to know whether NS5A interacts directly with MST1 or in complex with other proteins. MST1 and MST2 contain a SARAH domain (named after the three classes of eukaryotic tumour suppressor proteins SAV, RASSF and Hpo) at the C terminus which mediates MST1 dimerization, interaction with SAV1 and interactions with RASSF proteins (Constantinescu Aruxandei et al., 2011, Hwang et al., 2007). Whether this binding domain plays a role in NS5A interaction can only be speculated. The interaction between NS5A and MST1 may underpin the observed decrease in MST1 levels within HCV infected cells at late time points, and may be a major factor in the ability of HCV to alter Hippo signalling. However it will be important to investigate the effect of HCV infection on pMST1 levels, MST2 and pMST2 levels also. Understanding the exact consequence of this interaction and how it is mediated would further elucidate the effect of HCV on CD24lo differentiation and Hippo signalling. It would be interesting to investigate whether NS5A or other viral proteins interact with other Hippo proteins and Hippo regulatory proteins.

Pharmaceutical manipulation of signalling pathway proteins can be a useful tool to understand a pathway better and the importance of that pathway for a given cellular function. By manipulating the Hippo pathway we wanted to further explore the importance/the role of the Hippo pathway during CD24lo differentiation and effect of HCV on differentiation and Hippo signalling. The specificity of pharmaceutical effectors however, can be limited and off target effects may make interpreting the results more difficult. This is one of the reasons we attempted to knockdown YAP1 expression by using targeted shRNA and the CRISPR-Cas9 system. Yet attempts to transduce CD24lo cells with either YAP1 shRNAs or YAP1 all-in-one CRISPR Cas9 lentiviruses and select stably knockdown or YAP1 knockout lines was unsuccessful. YAP1 expression was maintained in cells lines transduced with either YAP1 shRNAs or YAP1 gRNA even after antibiotic selection of successfully transduced cells. It is important to remember that Huh7 cells are a transformed cell line with a large list of genes with mutations or, perhaps more importantly with respect to CRISPR experiments, copy number alterations (Barretina et al., 2012). Although we were unable to find any references to alteration of Hippo pathway proteins in Huh7 cells, this may just represent a gap in the genetic characterisation of these cells. It will be

important to establish the genetic background for the Hippo pathway in Huh7 cell going forward.

Nonetheless a number of Hippo pathway inhibitors exist, largely targeting YAP1 activity indirectly. We chose to include a number of YAP1 inhibitors in our experiments with slightly different mechanisms but which have been described to lead to YAP1 cytoplasmic retention and a reduction in YAP1 dependent transcription. Verteporfin was the first YAP1 inhibitor identified and the most commonly described YAP1 inhibitor in the literature. Verteporfin targets the interaction between YAP1 and TEAD and thus inhibits YAP1-induced transcription (Liu-Chittenden et al., 2012). Dobutamine and Pazopanib induce the phosphorylation of YAP1 which leads to the protein being sequestered in the cytoplasm (Bao et al., 2011, Oku et al., 2015). Dobutamine acts on the β-adrenergic receptor which is a G-protein coupled receptor that regulates YAP1/TAZ phosphorylation (Yu et al., 2012). Pazopanib is a multi-kinase inhibitor which in addition to increasing YAP1/TAZ phosphorylation was also shown to increase proteasomal degradation of YAP1 and TAZ. However Verteporfin was found to be cytotoxic to CD24lo cells at similar concentrations used in the literature (10 μM- 2 μM) and after choosing the concentration of 1 μM, informed by an MTT assay, further experiments was found to not alter YAP1 localisation as described in the literature. Furthermore even at 1 μM considerable cell death was observed for experiments lasting over 48 hrs. Dobutamine and Pazopanib were also found to have little effect on YAP1 nuclear localisation in cycling CD24lo cells at a range of concentrations informed from the literature. CD24lo differentiation in the presence of Dobutamine but not Pazopanib did however induce a slight increase in CYP3A4 levels for treated cells compared to untreated cells. However it is important to note that this observation is based on a single experiment and at least for treated JFH1-replicon cells the increase in CYP3A4 levels was small compared to untreated JFH1-replicon cells at day nine. The reason why none of the YAP1 inhibitors chosen produced the expected effect upon YAP1 phenotype is unknown. Again Huh7 cells are a transformed cell line and genetic alteration or expression changes may explain our observations. However Verteporfin and Pazopanib inhibitors have been used on HepG2 cells (Chiou et al., 2010, Zhu et al., 2011, Simile et al., 2016) and when tested on this cell line, we still saw no effect on YAP1 localisation in the response to YAP1 inhibitor treatment (data not shown).

We chose to try to manipulate the Hippo pathway upstream of YAP1/TAZ, MST1 was a sensible target to begin with due to the identified interaction with NS5A. XMU-MP-1 is currently the only identified MST1/2 inhibitor (Fan et al., 2016). It acts as an ATP-competitive MST1/2 inhibitor and leads to the reduction in phosphorylation of MOB1, LATS1/2 and YAP1. Interestingly treatment of differentiating Cured and JFH1-replicon cells with the MST1/2 inhibitor altered the differentiation assay outcome, far fewer cells underwent the usual morphological changes and CYP3A4 levels did not increase over the course of DMSO induced differentiation. This indicates that Hippo signalling is indeed required for CD24lo differentiation and inhibition of Hippo signalling can prevent differentiation. Furthermore the observation that NS5A levels remained high in treated JFH1-replicon cells throughout differentiation but not in untreated JFH1-replicon cells adds additional evidence that differentiation and MST1/Hippo signalling activation negatively affects virus replication and protein expression and that HCV appears to prefer a less differentiated state but more differentiated than undifferentiated CD24lo cells due to the increase in NS5A levels at day 3/5 (Figure 4.2.11). It is important that future experiments explore the effect of this inhibitor upon differentiation further, specifically relating to the effect on the transcriptional regulators YAP1/TAZ in terms of the phosphorylation state and cellular localisation. It will be interesting to explore whether knockdown of MST1/2 and the downstream kinases LATS1/2 has a similar effect as MST1/2 inhibition. Similarly manipulating the Hippo pathway to promote Hippo signalling would be a helpful tool to investigate the link between the Hippo pathway and CD24lo differentiation further. With this in mind we chose to investigate the effects of Chelerythrine treatment upon Cured and JFH1-replicon differentiation. Chelerythrine was identified as a potent MST1 activator (Yamamoto et al., 2003). However initial experiments demonstrated no change to the differentiation outcome in response to Chelerythrine treatment, and further experiments are needed to assess whether Chelerythrine has the expected effect of MST1 activation on CD24lo cells by assessing the levels of phosphorylated and total MST1, LATS1, YAP1 and TAZ, to draw any conclusion from the experiment.

To truly begin to understand the effect of HCV infection upon CD24lo differentiation and the role Hippo signalling plays during differentiation we needed to obtain a more global view of the changes occurring in response to HCV infection and Hippo signalling inhibition. RNA-seq analysis generates a huge amount of data which needs to be appropriately analysed and interpreted. In our experiment we compared differentiated Cured, JFH1-

replicon, JFH1-replicon +DAA, and Cured +MSTi cells. RNA-seq analysis involves many steps including RNA isolation and purification, reverse transcription to create a cDNA library, sequencing adaptor addition followed by library sequencing and data analysis. Quality control assays are carried out at every step to confirm the RNA and cDNA library are of a sufficient quality to continue to the next step. These steps involved RNA quality assessment initially using the NanoDrop followed by the Bioanalyser which assigns a RIN to each sample indicating RNA integrity. All samples had a high RIN indicating high RNA quality and integrity. The cDNA library was assessed after initial reverse transcription from the input RNA and post sequencing adaptor addition. After cDNA library assessment the samples were sequenced generating between 50- 70 million reads which is considered sufficient to compare gene expression of moderate to high expressed transcripts. After data was filtered and mapped to the human reference genome hg38 which enables the identification of the genes expressed in the sample. The number of reads per gene specifies the expression level of that gene. Principal component analysis demonstrated that the gene expression profile of each condition was distinctive and considerable overlap between the experimental replicates existed. A huge number genes were identified by initial mapping of the reads to the human genome. Stringent cut-offs identified 1000-2000 differentially expressed genes in each condition (HCV, HCV Cure and MSTi) compared to the Control. The strict cut-offs to determine whether or not a gene was significantly differentially regulated, were used to ensure confidence in our results.

Comparison of the RNA-seq data of the different conditions HCV, HCV Cure and MSTi revealed that 313 significantly differentially regulated genes (either up or down compared to Control) were shared between the three conditions, however each condition also regulated a unique set of genes. MSTi produced the largest effect on gene expression in terms of the number of genes altered compared to the Control. This may reflect on the fact that a pharmacological inhibitor was used to reduce MST1/2 activity and there may be a number of off-target effects. On the other hand MST1/2 are known to regulate and phosphorylate a number of proteins including proteins involved in apoptosis and cell cycle. Interestingly there were 570 genes shared between MSTi and HCV which implies HCV infection may be causing similar pathways to be altered, leading to similar genes being acted upon as inhibition of the Hippo pathway. The overlap between HCV and HCV Cure of 508 genes in total may represent that DAA treatment does not reverse the

effect of HCV infection completely at least not over a nine day treatment. Interestingly enrichment analysis revealed that similar transcription factors appeared to be responsible for the gene expression patterns observed in all conditions.

FOXM1 was highlighted as the top transcription factor for HCV, HCV Cure and MSTi. FOXM1 is a transcription factor which plays a role in cell cycle progression (Wang et al., 2005, Wang et al., 2002, Leung et al., 2001). Interestingly FOXM1 is implicated as a proto-oncogene and upregulation is found in most solid cancers including liver cancer (Wierstra, 2013). FOXM1 is considered a prognostic marker for HCC and FOXM1 cooperates with YAP1/TEAD complexes to induce chromosomal instability in HCC and CCA (Weiler et al., 2017, Rizvi et al., 2018). FOXM1 gene expression was significantly upregulated HCV infection and downregulated in HCV Cure whereas FOXM1 expression was not significantly altered by MSTi treatment (Figure 5.4.11). HCV and HCV Cure shared more transcription factors in the enrichment analysis including SOX2 and p63. This suggests that HCV may have a hit and run effect upon cells, with the risk if liver disease and liver cancer persisting post SVR. SOX2 is a transcription factor important for stem cell maintenance and self-renewal and loss or inhibition of SOX2 in tumour cells leads to loss of tumourigenicity (Gangemi et al., 2009). p63 is a member of the p53 family and plays a role in epithelial stem cell maintenance, in preventing senescence but also in the induction of differentiation. However the regulation and function of p63 is complex and different isoforms have different functions (ΔNp63 & TAp63) (Bergholz and Xiao, 2012). Enrichment analysis also revealed that signalling associated with cell cycle regulation was likely to be altered in all conditions in response to the gene expression changes observed. In addition enrichment analysis also predicted the p53 signalling pathway to be altered by the gene expression changes induced by HCV infection which is interesting due to evidence describing how HCV viral proteins interact with p53 and associated proteins such as p21.

Cluster analysis of the RNA seq data revealed that DAA treatment did not completely reverse HCV induced gene expression changes, indicating that HCV infection is having a more long lasting effect on gene expression. This implies that HCV infection is able to alter the epigenetic regulation of these genes. Several studies have linked HCV infection with epigenetic modifications. One study showed that HCV infection enhanced promoter methylation of several genes in their panel, including p14, p73, RASSF1A,

RARB, CDH1 and APC (Zekri et al., 2014). It is interesting to note that p73 and RASSF1A are associated with the Hippo pathway. Furthermore two groups presented work at the international HCV meeting in 2017 demonstrating that HCV infection leaves an epigenetic signature which is not full reversed by DAA treatment (Hamdane et al., 2017, Perez et al., 2017). Epigenetic changes by HCV may help to explain why patients who have eradicated the virus by DAA treatment still develop HCC. Indeed Hamdane et al., presented that cells cured with DAA treatment displayed a pattern of gene regulation which is associated with a higher risk of HCC development (Hamdane et al., 2017). It would be interesting to include epigenetic analysis in future CD24lo +/-HCV differentiation experiments.

It should be noted that our RNA-seq analysis involved pooling all the cells in the well which had been expose to DMSO to induce differentiation, however it would be interesting to explore the differences between the hepatocyte-like cells and the surrounding cells which appear to not differentiate to begin to explain why some cells appear unable to differentiate. The proportion of cells which do not seem to undergo differentiation but also do not proliferate, is higher in HCV infected cells and cells exposed to the MSTi inhibitor. There still remains a proportion of cells that do differentiate in these conditions and it is possible to speculate that this may mask some of the differences between the Control and the HCV and MSTi conditions. However how we would separate the ‘differentiated’ cells from the cells which appear not to differentiate is unclear. EpCAM may be a useful marker to separate the two cells populations as EpCAM appears to only be expressed in the hepatocyte-like islands and flow-cytometry for EpCAM could help separately characterised the morphologically different cells.

In summary our results demonstrate that HCV is able to perturb CD24lo differentiation likely by acting upon the differentiation regulatory Hippo signalling pathway. It is likely that manipulating differentiation leads to more favourable conditions for virus replication, viral protein expression and particle production, but also potentially predisposes the infected cell to malignant transformation for example YAP1 and TAZ are oncogenes and whereas MST1 and 2 are tumour suppressors. It will be important to repeat our findings in a less transformed background possibly by infecting and differentiating liver progenitor cells derived from induced pluripotent stem cells. In addition it would be interesting to explore and compare Hippo pathway protein expression in HCV infected patient liver samples with uninfected individuals at different stages of liver disease and HCV disease

progression. The suggestion that HCV induces lasting epigenetic and gene expression patterns after DAA treatment may mean that individuals who have undergone DAA treatment and achieved SVR should continue to be monitored for liver disease and HCC development.

# 6. Final Discussion

We have shown that HCV is able to perturb the differentiation of hepatic cells using a model based on DMSO induced differentiation of CD24lo Huh7 cells. HCV infection and ensuing non-structural protein expression (observations consistent for both a subgenomic replicon and full-length infectious virus) leads to a reduction or delay in differentiation associated morphological changes and associated expression of hepatocyte/stem cell/proliferation markers, including an increased number of infected cells maintaining ki67 expression indicating that they do not exit the cell cycle. DMSO induced CD24lo differentiation is dependent on MST1/2 activity and we found HCV infection perturbs Hippo pathway proteins.

Enrichment analysis of J6-JFH1 infected Huh7.5 cells and cellular architecture led us to examine a potential link between HCV infection and the Hippo pathway, perturbation of which is a major driver of HCC development. Infected cells displayed altered expression and localisation of the YAP/TAZ regulatory kinases MST1 and LATS1 upon differentiation. Furthermore an increased number of infected cells maintained nuclear YAP localisation and RNA-seq analysis revealed higher levels of TAZ mRNA expression. This analysis also revealed that expression of a number of YAP/TAZ responsive genes was altered, such as BIRC5, along with a number of Hippo regulatory proteins such as AMOT which was the top most differentially regulated gene by HCV infection. HCV infection led to altered expression of a number genes also altered by the MST1/2 inhibitor XMU-MP-1. Enrichment analysis revealed that the transcription factor FOXM1 appears to be important mediator of the gene expression changes observed. Furthermore HCV infection induces a number of gene expression changes which were not reversible upon DAA treatment. There are emerging reports that HCV infection leads to epigenetic changes which last after DAA treatment (Hamdane et al., 2017, Perez et al., 2017). There appears to be some controversy as to whether DAA treatment reduces your risk of developing HCC as does interferon treatment (Kanwal et al., 2017, Singer et al., 2018, Ioannou et al., 2017, Reig et al., 2016). The epigenetic changes induced by HCV and which persist after DAA treatment are associated with a higher risk of HCC development (Hamdane et al., 2017).

An intermediate stage during differentiation may offer optimal conditions for HCV replication and gene expression and would begin to explain why we

observed an initial increase in NS5A protein levels followed by a decrease in protein level as the differentiation proceeds (Figure 4.2.11). The life-cycle of human papillomaviruses (HPVs) are particularly tied to cellular differentiation. HPVs infect basal cells of the stratified epidermis. HPV genomic DNA is kept to low-copy numbers within these cells and cellular differentiation is required for progression of the viral life cycle. Cross-talk exists between viral replication and cellular differentiation. Viral replication occurs in differentiated cells however HPV encodes oncogenes including E6 and E7 which can target Rb and p53 tumour suppressor proteins (Yim and Park, 2005). These proteins promote differentiated cells to re-enter the S phase of the cell cycle. Following from these observations it would be interesting to explore the levels of virus production in cells infected with full length J6-JFH1 over the course of differentiation to determine whether virus production and infectivity follows a similar trend to NS5A expression. Furthermore exploring at which stage during differentiation HCV replication is supported most effectively and measuring the expression of HCV cofactors such as miR-122, and entry factors such as CD81, occludin or NPC1L1 over the course of differentiation could help understand the relationship between HCV replication and differentiation further. The alterations to cellular proteins required to maintain cells in this state and in the cell cycle may predispose these cells to oncogenic transformation, such as the gross alterations we observed to cell cycle signalling (Figure 5.3.13), alteration in expression of oncogenes such as Cyclin B1 or alterations to growth regulatory pathways such as the Hippo pathway by upregulation of TAZ (Figure 5.4.10). Some viruses depend on the cell being in the cell cycle and infection is often linked to a differentiation state such as for HPV (Yim and Park, 2005). Several studies have found altered expression of cell cycle genes including p21, p27 and cyclin E, which are linked to carcinogenesis (Bassiouny et al., 2010, Sarfraz et al., 2009). Indeed we found the p21 gene CDKN1A downregulated by HCV compared to the control in our RNA-seq experiment. There are many examples of viruses which stimulate cells to enter the cell cycle such as Human T-lymphotropic virus 1 (HTLV-1) which increases gene expression of cellular proteins such as IL-2 by the viral *trans*-activator Tax protein (Farcet et al., 1991). Promoting cells to enter the cell cycle and proliferate by altering intracellular signalling pathways and by increasing levels of released stimulatory factors has the beneficial effect of promoting viral replication in an infected cell and make a neighbouring cell more suitable targets for infection. Virus induced cell cycle arrest in a certain stage of the cell cycle has been shown to be a beneficial mechanism

employed by some viruses such as HIV for which expression of the Vpr protein leads to infected cells arresting in G2 (Yoshizuka et al., 2005). This keeps the infected cells in a state which increases viral production. One study found that HCV induced cell cycle arrest at the level of mitosis imitation (Kannan et al., 2011).

The exact mechanism of CD24lo differentiation is unclear. Further investigation is needed to determine to what degree differentiation depends on Hippo signalling activation and could include knocking out components of the core pathway such as MST1, LATS1 and YAP/TAZ or overexpressing these proteins. Furthermore how Hippo signalling is exactly activated in this model needs to be clarified. It is possible that there are a number of regulatory elements including cues from the actin cytoskeleton, cell-cell junctions and signals relayed from GPCRs. How much crosstalk exists between Hippo signalling and other important pathways involved in differentiation such as Wnt? Several examples of interactions between the Wnt pathway and Hippo signalling have been described, for example TAZ inhibits the Wnt3a- induced phosphorylation of dishevelled segment polarity protein 2 (Dvl2) thereby leading to lower levels of β-catenin (Varelas et al., 2010a). Understanding how Hippo signalling is regulated during differentiation will help us understand how HCV infection alters Hippo signalling. Ideally this would be established in true HPCs derived from patient samples or in HPCs derived from iPSCs using established differentiation protocols using similar differentiation signals during hepatocyte specification rather than DMSO. Further experiments should focus on elucidating the activation state of Hippo kinases and proteins by focusing on the level of phosphorylation of MST1/2, LATS1/2 and YAP/TAZ. In addition including MST1/2 and LATS1/2 regulatory proteins such as the RASSF family of proteins and PP2A and YAP/TAZ regulatory proteins such as AMOT in future analysis will help us understand the role of this pathway during differentiation further. Interestingly PP2A is a known NS5A interaction partner which may play an important role during HCV perturbation of Hippo signalling during differentiation. AMOT is able to regulate YAP1 and TAZ in opposing ways. AMOT can bind to YAP and TAZ and retain these proteins in the cytoplasm (Wang et al., 2011b, Zhao et al., 2011). However p130-AMOT has also been shown to be able to disrupt the interaction between LATS1/2 and YAP1 thereby reducing YAP1 phosphorylation and increasing nuclear localisation (Yi et al., 2013). It is unclear however how these opposing functions of AMOT are regulated and may be cell type specific. Indeed the

p130 isoform of YAP appears to be necessary for hepatocyte proliferation and tumorigenesis (Yi et al., 2013).

Differences between the levels of YAP and TAZ were observed during HCV infection (Figure 5.2.3 & Figure 5.2.4), and it will be important to explore this difference further. It is starting to emerge that YAP and TAZ can be differentially regulated and so in turn regulate gene expression differently. It is important to understand what the transcriptional consequence of YAP and TAZ are in infected cells and the RNA-seq experiment has begun to elucidate this; indeed we see several YAP/TAZ responsive genes upregulated by HCV infection such as BIRC5.

It would be interesting to see which transcription factors are mediating this expression changes, and how YAP and TAZ are modulating the activity of these transcription factors. A chromatin immunoprecipitation analysis could help identify which transcription factors and gene promotors are being bound by YAP1 and TAZ. Enrichment analysis of our RNA-seq data highlighted FOXM1 as an important regulator of the gene expression changes observed in response to HCV infection. It will be interesting to see how inhibition of this transcription factor, by pharmacological modulation such as the FOXM1 inhibitor Thiostrepton, or by knocking out FOXM1 using shRNA or CRISPR, affects CD24lo differentiation.

To clarify how HCV alters Hippo signalling it will be important to validate and explore the interaction between cellular protein MST1 and viral protein NS5A further. Does NS5A interact with MST1 directly or in complex with other proteins and how this interaction is mediated including the binding domain involved are all questions to address. Expressing truncated NS5A constructs followed by pull-down assays could indicate which part of the viral protein mediates this interaction. Furthermore confocal microscopy and mass spectrometry of the bound fragment of the pulldown assay would be necessary to confirm the interaction between MST1 and NS5A. It would be interesting to probe whether any known interaction and regulatory proteins of MST1 also pulldown with NS5A. Over-expressing NS5A by itself in CD24lo cells and analysing whether this lead to a similar pattern of Hippo signalling perturbation as the HCV replicon would indicate the importance of the NS5A-MST1 interaction.

Modulation of Hippo signalling could therefore represent a common target of oncogenic viruses. Other oncogenic viruses are able to activate YAP and TAZ. For example Kaposi's sarcoma-associated herpesvirus encodes a viral GPCR which is able to activate a number of G-protein alpha subunits with

the consequence of inhibiting LATS1/2 (Liu et al., 2015). In the RNA-seq experiment we saw a number of GPCRs upregulated by HCV compared to the control differentiated cells, however whether this GPCRs regulate Hippo signalling could not be determined from the literature. Additionally the simian vacuolating virus 40 and Merkel cell polyomavirus both encode a small T antigen oncoprotein which inhibits NF2 and leads to activation of YAP (Nguyen et al., 2014). Modulation of Hippo signalling and activation of YAP/TAZ by these viruses were found to promote cellular tumorigenesis and transformation (Nguyen et al., 2014). The information gained from our RNA-seq analysis has helped us to understand the mechanisms behind CD24lo differentiation and HCV induced perturbation of CD24lo cell differentiation. To validate the results of the RNA-seq experiment and to contribute to the interpretation it will be important to determine whether the changes in gene transcription translate into changes in protein levels. AMOT was found to be the most highly upregulated gene by HCV compared to the control, it will be interesting whether we also see a big increase in AMOT protein levels, especially as this protein is an important regulator of YAP1 and TAZ.

Due to lack of an animal model of HCV infection it will be hard to replicate the differentiation model in vivo using a mouse xenograft model as we have observed from our experiments that differentiated CD24lo cells begin to de-differentiate once reseeded. It may be possible to selectively express HCV viral proteins in mouse or rat oval cells (possibly by putting the NS5A protein under control of a HNF4 responsive promoter) during liver development to determine whether HCV viral protein expression has an effect on tumourigenicity *in vivo*. However we must bear in mind that viral proteins are often overexpressed in these conditions compared to expression levels observed in infected patients. *In vitro* assays to assess self-renewal or proliferation may serve better to determine whether HCV infection during differentiation promotes tumourigenicity. A colony formation assay is a popular method to determine a cell ability to self-renew and forms colonies at low density. Seeding control, HCV infection cells or after treatment with Hippo pathway inhibitor after differentiation in a limiting dilution would help determine whether HCV infection or Hippo inhibition changes the cells ability to self-renew and potential tumour forming ability.

Lastly it is important to discuss the cellular model used. It is important to bear in mind that Huh7 cells are transformed and display many genetic mutations and copy number alterations. Whether any genes associated with the Hippo pathway are altered in Huh7 cells has not been established,

although our experiments indicate some alteration such as the observation of pLATS1 at day one of differentiation (Figure 5.2.3). Establishing whether the Hippo pathway is altered in Huh7 cells compared to primary hepatocytes or HPCs would be helpful to understand DMSO induced CD24lo differentiation further. Despite these limitations Huh7 cells are a helpful model particularly as it one of the only robust hepatocellular cell lines which support HCV replication without the need of introducing HCV cofactors. We explored the option of using HepaRG cells, as this cell line would be particularly suited for our experiments being a progenitor like cell line which is not transformed. However HepaRG cells appear to be but poorly permissive to HCV infection, which limits the application of the cell line. An option which is becoming more robust is the potential use of HPCs derived from iPSCs. Several studies show how iPSCs can be induced to differentiate along the hepatocellular fate to produce HPCs and furthermore mature hepatocytes using defined growth media at different stages of differentiation. Hepatocytes cells derived from iPSC have also been shown to be permissive to HCV infection (Wu et al., 2012), making it possible to replicate our findings in these cells by infected them at the HPC stage and inducing these cells to differentiate into mature hepatocytes. It would also be interesting to examine the expression of Hippo proteins in patient samples obtained from infected and non-infected patients. However invasive liver biopsies are less common now, making it more difficult to obtain patient liver samples. An additional problem includes the fact that histological detection of HCV in the liver is extremely difficult.

We have shown evidence that HCV is able to perturb the differentiation of CD24lo Huh7 cells the accompanying alterations to host signalling pathways such as the Hippo pathway may predispose or represent a step towards oncogenic transformation.

# Bibliography

ABDEL-HAKEEM, M. S. & SHOUKRY, N. H. 2014. Protective immunity against hepatitis C: many shades of gray. *Front Immunol,* 5**,** 274.

AGO, H., ADACHI, T., YOSHIDA, A., YAMAMOTO, M., HABUKA, N., YATSUNAMI, K. & MIYANO, M. 1999. Crystal structure of the RNA-dependent RNA polymerase of hepatitis C virus. *Structure,* 7**,** 1417-26.

AKHURST, B., MATTHEWS, V., HUSK, K., SMYTH, M. J., ABRAHAM, L. J. & YEOH, G. C. 2005. Differential lymphotoxin-beta and interferon gamma signaling during mouse liver regeneration induced by chronic and acute injury. *Hepatology,* 41**,** 327-35.

ALDER, O., CULLUM, R., LEE, S., KAN, A. C., WEI, W., YI, Y., GARSIDE, V. C., BILENKY, M., GRIFFITH, M., MORRISSY, A. S., ROBERTSON, G. A., THIESSEN, N., ZHAO, Y., CHEN, Q., PAN, D., JONES, S. J. M., MARRA, M. A. & HOODLESS, P. A. 2014. Hippo signaling influences HNF4A and FOXA2 enhancer switching during hepatocyte differentiation. *Cell Rep,* 9**,** 261-271.

ALVISI, G., MADAN, V. & BARTENSCHLAGER, R. 2011. Hepatitis C virus and host cell lipids: an intimate connection. *RNA Biol,* 8**,** 258-69.

ANASTAS, J. N. & MOON, R. T. 2013. WNT signalling pathways as therapeutic targets in cancer. *Nat Rev Cancer,* 13**,** 11-26.

ANDRE, P., KOMURIAN-PRADEL, F., DEFORGES, S., PERRET, M., BERLAND, J. L., SODOYER, M., POL, S., BRECHOT, C., PARANHOS-BACCALA, G. & LOTTEAU, V. 2002. Characterization of low- and very-low-density hepatitis C virus RNA-containing particles. *J Virol,* 76**,** 6919-28.

ANDREJEVA, J., CHILDS, K. S., YOUNG, D. F., CARLOS, T. S., STOCK, N., GOODBOURN, S. & RANDALL, R. E. 2004. The V proteins of paramyxoviruses bind the IFN-inducible RNA helicase, mda-5, and inhibit its activation of the IFN-beta promoter. *Proc Natl Acad Sci U S A,* 101**,** 17264-9.

ANDRUS, L., MARUKIAN, S., JONES, C. T., CATANESE, M. T., SHEAHAN, T. P., SCHOGGINS, J. W., BARRY, W. T., DUSTIN, L. B., TREHAN, K., PLOSS, A., BHATIA, S. N. & RICE, C. M. 2011. Expression of paramyxovirus V proteins promotes replication and spread of hepatitis C virus in cultures of primary human fetal liver cells. *Hepatology,* 54**,** 1901-12.

ANGUS, A. G., LOQUET, A., STACK, S. J., DALRYMPLE, D., GATHERER, D., PENIN, F. & PATEL, A. H. 2012a. Conserved glycine 33 residue in flexible domain I of hepatitis C virus core protein is critical for virus infectivity. *J Virol,* 86**,** 679-90.

ANGUS, L., MOLEIRINHO, S., HERRON, L., SINHA, A., ZHANG, X., NIESTRATA, M., DHOLAKIA, K., PRYSTOWSKY, M. B., HARVEY, K. F., REYNOLDS, P. A. & GUNN-MOORE, F. J. 2012b. Willin/FRMD6 expression activates the Hippo signaling pathway kinases in mammals and antagonizes oncogenic YAP. *Oncogene,* 31**,** 238-50.

ANRS COLLABORATIVE GROUP ON HCC 2016. Lack of evidence of an effect of direct-acting antivirals on the recurrence of hepatocellular carcinoma: Data from three ANRS cohorts. *J Hepatol,* 65**,** 734-740.

AOKI, H., HAYASHI, J., MORIYAMA, M., ARAKAWA, Y. & HINO, O. 2000. Hepatitis C virus core protein interacts with 14-3-3 protein and activates the kinase Raf-1. *J Virol,* 74**,** 1736-41.

ARAGONA, M., PANCIERA, T., MANFRIN, A., GIULITTI, S., MICHIELIN, F., ELVASSORE, N., DUPONT, S. & PICCOLO, S. 2013. A mechanical checkpoint controls multicellular growth through YAP/TAZ regulation by actin-processing factors. *Cell,* 154**,** 1047-1059.

ARORA, P., KIM, E. O., JUNG, J. K. & JANG, K. L. 2008. Hepatitis C virus core protein downregulates E-cadherin expression via activation of DNA methyltransferase 1 and 3b. *Cancer Lett,* 261**,** 244-52.

ATTAR, B. M. & VAN THIEL, D. 2015. A New Twist to a Chronic HCV Infection: Occult Hepatitis C. *Gastroenterol Res Pract,* 2015**,** 579147.

ATTISANO, L. & WRANA, J. L. 2013. Signal integration in TGF-beta, WNT, and Hippo pathways. *F1000Prime Rep,* 5**,** 17.

AZUMA, H., HIROSE, T., FUJII, H., OE, S., YASUCHIKA, K., FUJIKAWA, T. & YAMAOKA, Y. 2003. Enrichment of hepatic progenitor cells from adult mouse liver. *Hepatology,* 37**,** 1385-94.

BAECHLEIN, C., FISCHER, N., GRUNDHOFF, A., ALAWI, M., INDENBIRKEN, D., POSTEL, A., BARON, A. L., OFFINGER, J., BECKER, K., BEINEKE, A., REHAGE, J. & BECHER, P. 2015. Identification of a Novel Hepacivirus in Domestic Cattle from Germany. *J Virol,* 89**,** 7007-15.

BAI, H., GAYYED, M. F., LAM-HIMLIN, D. M., KLEIN, A. P., NAYAR, S. K., XU, Y., KHAN, M., ARGANI, P., PAN, D. & ANDERS, R. A. 2012. Expression of Yes-associated protein modulates Survivin expression in primary liver malignancies. *Hum Pathol,* 43**,** 1376-85.

BAO, Y., NAKAGAWA, K., YANG, Z., IKEDA, M., WITHANAGE, K., ISHIGAMI-YUASA, M., OKUNO, Y., HATA, S., NISHINA, H. & HATA, Y. 2011. A cell-based assay to screen stimulators of the Hippo pathway reveals the inhibitory effect of dobutamine on the YAP-dependent gene transcription. *J Biochem,* 150**,** 199-208.

BARRETINA, J., CAPONIGRO, G., STRANSKY, N., VENKATESAN, K., MARGOLIN, A. A., KIM, S., WILSON, C. J., LEHAR, J., KRYUKOV, G. V., SONKIN, D., REDDY, A., LIU, M., MURRAY, L., BERGER, M. F., MONAHAN, J. E., MORAIS, P., MELTZER, J., KOREJWA, A., JANE-VALBUENA, J., MAPA, F. A., THIBAULT, J., BRIC-FURLONG, E., RAMAN, P., SHIPWAY, A., ENGELS, I. H., CHENG, J., YU, G. K., YU, J., ASPESI, P., JR., DE SILVA, M., JAGTAP, K., JONES, M. D., WANG, L., HATTON, C., PALESCANDOLO, E., GUPTA, S., MAHAN, S., SOUGNEZ, C., ONOFRIO, R. C., LIEFELD, T., MACCONAILL, L., WINCKLER, W., REICH, M., LI, N., MESIROV, J. P., GABRIEL, S. B., GETZ, G., ARDLIE, K., CHAN, V., MYER, V. E., WEBER, B. L., PORTER, J., WARMUTH, M., FINAN, P., HARRIS, J. L., MEYERSON, M., GOLUB, T. R., MORRISSEY, M. P., SELLERS, W. R., SCHLEGEL, R. & GARRAWAY, L. A. 2012. The Cancer Cell Line Encyclopedia enables predictive modelling of anticancer drug sensitivity. *Nature,* 483**,** 603-7.

BARTENSCHLAGER, R. & LOHMANN, V. 2000. Replication of hepatitis C virus. *J Gen Virol,* 81**,** 1631-48.

BARTENSCHLAGER, R., LOHMANN, V., WILKINSON, T. & KOCH, J. O. 1995. Complex formation between the NS3 serine-type proteinase of the hepatitis C virus and NS4A and its importance for polyprotein maturation. *J Virol,* 69**,** 7519-28.

BARTENSCHLAGER, R., PENIN, F., LOHMANN, V. & ANDRE, P. 2011. Assembly of infectious hepatitis C virus particles. *Trends Microbiol,* 19**,** 95-103.

BARTSCH, H. & NAIR, J. 2004. Oxidative stress and lipid peroxidation-derived DNA-lesions in inflammation driven carcinogenesis. *Cancer Detect Prev,* 28**,** 385-91.

BASSIOUNY, A. E., NOSSEIR, M. M., ZOHEIRY, M. K., AMEEN, N. A., ABDEL-HADI, A. M., IBRAHIM, I. M., ZADA, S., EL-DEEN, A. H. & EL-BASSIOUNI, N. E. 2010. Differential expression of cell cycle regulators in HCV-infection and related hepatocellular carcinoma. *World J Hepatol,* 2**,** 32-41.

BEHRENS, S. E., GRASSMANN, C. W., THIEL, H. J., MEYERS, G. & TAUTZ, N. 1998. Characterization of an autonomous subgenomic pestivirus RNA replicon. *J Virol,* 72**,** 2364-72.

BENGOCHEA, A., DE SOUZA, M. M., LEFRANCOIS, L., LE ROUX, E., GALY, O., CHEMIN, I., KIM, M., WANDS, J. R., TREPO, C., HAINAUT, P., SCOAZEC, J. Y., VITVITSKI, L. & MERLE, P. 2008. Common dysregulation of Wnt/Frizzled receptor elements in human hepatocellular carcinoma. *Br J Cancer,* 99**,** 143-50.

BENHAMOUCHE, S., DECAENS, T., GODARD, C., CHAMBREY, R., RICKMAN, D. S., MOINARD, C., VASSEUR-COGNET, M., KUO, C. J., KAHN, A., PERRET, C. & COLNOT, S. 2006. Apc tumor suppressor gene is the "zonation-keeper" of mouse liver. *Dev Cell,* 10**,** 759-70.

BENKOEL, L., BRISSE, J., CAPO, C., BENOLIEL, A. M., BONGRAND, P., GARCIA, T. & CHAMLIAN, A. 1992. Localization of actin in normal human hepatocytes using fluorescent phallotoxins and immunohistochemical amplification. *Cell Mol Biol,* 38**,** 377-83.

BERASAIN, C. & AVILA, M. A. 2015. Regulation of hepatocyte identity and quiescence. *Cell Mol Life Sci,* 72**,** 3831-51.

BERGER, K. L., COOPER, J. D., HEATON, N. S., YOON, R., OAKLAND, T. E., JORDAN, T. X., MATEU, G., GRAKOUI, A. & RANDALL, G. 2009. Roles for endocytic trafficking and phosphatidylinositol 4-kinase III alpha in hepatitis C virus replication. *Proc Natl Acad Sci U S A,* 106**,** 7577-82.

BERGHOLZ, J. & XIAO, Z. X. 2012. Role of p63 in Development, Tumorigenesis and Cancer Progression. *Cancer Microenviron,* 5**,** 311-22.

BHATIA, H. K., SINGH, H., GREWAL, N. & NATT, N. K. 2014. Sofosbuvir: A novel treatment option for chronic hepatitis C infection. *J Pharmacol Pharmacother,* 5**,** 278-84.

BITTAR, C., SHRIVASTAVA, S., BHANJA CHOWDHURY, J., RAHAL, P. & RAY, R. B. 2013. Hepatitis C virus NS2 protein inhibits DNA damage pathway by sequestering p53 to the cytoplasm. *PLoS One,* 8**,** e62581.

BLACHIER, M., LELEU, H., PECK-RADOSAVLJEVIC, M., VALLA, D. C. & ROUDOT-THORAVAL, F. 2013. The burden of liver disease in Europe: a review of available epidemiological data. *J Hepatol,* 58**,** 593-608.

BLANCHARD, E., BELOUZARD, S., GOUESLAIN, L., WAKITA, T., DUBUISSON, J., WYCHOWSKI, C. & ROUILLE, Y. 2006. Hepatitis C virus entry depends on clathrin-mediated endocytosis. *J Virol,* 80**,** 6964-72.

BLIGHT, K. J., MCKEATING, J. A. & RICE, C. M. 2002. Highly permissive cell lines for subgenomic and genomic hepatitis C virus RNA replication. *J Virol,* 76**,** 13001-14.

BLOUIN, A., BOLENDER, R. P. & WEIBEL, E. R. 1977. Distribution of organelles and membranes between hepatocytes and nonhepatocytes in the rat liver parenchyma. A stereological study. *J Cell Biol,* 72**,** 441-55.

BOCHKIS, I. M., RUBINS, N. E., WHITE, P., FURTH, E. E., FRIEDMAN, J. R. & KAESTNER, K. H. 2008. Hepatocyte-specific ablation of Foxa2 alters bile acid homeostasis and results in endoplasmic reticulum stress. *Nat Med,* 14**,** 828-36.

BOCHUD, P. Y., CAI, T., OVERBECK, K., BOCHUD, M., DUFOUR, J. F., MULLHAUPT, B., BOROVICKA, J., HEIM, M., MORADPOUR, D., CERNY, A., MALINVERNI, R., FRANCIOLI, P., NEGRO, F. & SWISS HEPATITIS, C. C. S. G. 2009. Genotype 3 is associated with accelerated fibrosis progression in chronic hepatitis C. *J Hepatol,* 51**,** 655-66.

BOLDUC, L., LABRECQUE, B., CORDEAU, M., BLANCHETTE, M. & CHABOT, B. 2001. Dimethyl sulfoxide affects the selection of splice sites. *J Biol Chem,* 276**,** 17597-602.

BORAWSKI, J., TROKE, P., PUYANG, X., GIBAJA, V., ZHAO, S., MICKANIN, C., LEIGHTON-DAVIES, J., WILSON, C. J., MYER, V., CORNELLATARACIDO, I., BARYZA, J., TALLARICO, J., JOBERTY, G., BANTSCHEFF, M., SCHIRLE, M., BOUWMEESTER, T., MATHY, J. E., LIN, K., COMPTON, T., LABOW, M., WIEDMANN, B. & GAITHER, L. A. 2009. Class III phosphatidylinositol 4-kinase alpha and beta are novel host factor regulators of hepatitis C virus replication. *J Virol,* 83**,** 10058-74.

BORNSTEIN, P. & SAGE, E. H. 2002. Matricellular proteins: extracellular modulators of cell function. *Curr Opin Cell Biol,* 14**,** 608-16.

BORT, R., SIGNORE, M., TREMBLAY, K., MARTINEZ BARBERA, J. P. & ZARET, K. S. 2006. Hex homeobox gene controls the transition of the endoderm to a pseudostratified, cell emergent epithelium for liver bud development. *Dev Biol,* 290**,** 44-56.

BOTELHO-SOUZA, L. F., VASCONCELOS, M. P. A., DOS SANTOS, A. O., SALCEDO, J. M. V. & VIEIRA, D. S. 2017. Hepatitis delta: virological and clinical aspects. *Virol J,* 14**,** 177.

BOULTER, L., GOVAERE, O., BIRD, T. G., RADULESCU, S., RAMACHANDRAN, P., PELLICORO, A., RIDGWAY, R. A., SEO, S. S., SPEE, B., VAN ROOIJEN, N., SANSOM, O. J., IREDALE, J. P., LOWELL, S., ROSKAMS, T. & FORBES, S. J. 2012. Macrophage-derived Wnt opposes Notch signaling to specify hepatic progenitor cell fate in chronic liver disease. *Nat Med,* 18**,** 572-9.

BOULTER, L., LU, W. Y. & FORBES, S. J. 2013. Differentiation of progenitors in the liver: a matter of local choice. *J Clin Invest,* 123**,** 1867-73.

BOYER, J. L. 2013. Bile formation and secretion. *Compr Physiol,* 3**,** 1035-78.

BRAEUNING, A., ITTRICH, C., KOHLE, C., HAILFINGER, S., BONIN, M., BUCHMANN, A. & SCHWARZ, M. 2006. Differential gene expression in periportal and perivenous mouse hepatocytes. *Febs j,* 273**,** 5051-61.

BRAITERMAN, L. T. & HUBBARD, A. L. 2009. Hepatocyte Surface Polarity: Its Dynamic Maintenance and Establishment. *In:* ARIAS, I. M. (ed.) *The Liver: Biology and Pathobiology.* Fifth Edition ed.: John Wiley & Sons, Ltd.

BRALET, M. P., REGIMBEAU, J. M., PINEAU, P., DUBOIS, S., LOAS, G., DEGOS, F., VALLA, D., BELGHITI, J., DEGOTT, C. & TERRIS, B. 2000. Hepatocellular carcinoma occurring in nonfibrotic liver: epidemiologic and histopathologic analysis of 80 French cases. *Hepatology,* 32**,** 200-4.

BRESSAC, B., GALVIN, K. M., LIANG, T. J., ISSELBACHER, K. J., WANDS, J. R. & OZTURK, M. 1990. Abnormal structure and expression of p53 gene in human hepatocellular carcinoma. *Proc Natl Acad Sci U S A,* 87**,** 1973-7.

BRESSANELLI, S., TOMEI, L., ROUSSEL, A., INCITTI, I., VITALE, R. L., MATHIEU, M., DE FRANCESCO, R. & REY, F. A. 1999. Crystal structure of the RNA-dependent RNA polymerase of hepatitis C virus. *Proc Natl Acad Sci U S A,* 96**,** 13034-9.

BRIANCON, N. & WEISS, M. C. 2006. In vivo role of the HNF4alpha AF-1 activation domain revealed by exon swapping. *Embo j,* 25**,** 1253-62.

BRIDGEWATER, J., GALLE, P. R., KHAN, S. A., LLOVET, J. M., PARK, J. W., PATEL, T., PAWLIK, T. M. & GORES, G. J. 2014. Guidelines for the diagnosis and management of intrahepatic cholangiocarcinoma. *J Hepatol,* 60**,** 1268-89.

BROWN, E. A., ZHANG, H., PING, L. H. & LEMON, S. M. 1992. Secondary structure of the 5' nontranslated regions of hepatitis C virus and pestivirus genomic RNAs. *Nucleic Acids Res,* 20**,** 5041-5.

BRYANT, D. M. & MOSTOV, K. E. 2008. From cells to organs: building polarized tissue. *Nat Rev Mol Cell Biol,* 9**,** 887-901.

BUKH, J., PIETSCHMANN, T., LOHMANN, V., KRIEGER, N., FAULK, K., ENGLE, R. E., GOVINDARAJAN, S., SHAPIRO, M., ST CLAIRE, M. & BARTENSCHLAGER, R. 2002. Mutations that permit efficient replication of hepatitis C virus RNA in Huh-7 cells prevent productive replication in chimpanzees. *Proc Natl Acad Sci U S A,* 99**,** 14416-21.

BUKH, J., PURCELL, R. H. & MILLER, R. H. 1992. Sequence analysis of the 5' noncoding region of hepatitis C virus. *Proc Natl Acad Sci U S A,* 89**,** 4942-6.

BURBELO, P. D., DUBOVI, E. J., SIMMONDS, P., MEDINA, J. L., HENRIQUEZ, J. A., MISHRA, N., WAGNER, J., TOKARZ, R., CULLEN, J. M., IADAROLA, M. J., RICE, C. M., LIPKIN, W. I. & KAPOOR, A. 2012. Serology-enabled discovery of genetically diverse hepaciviruses in a new host. *J Virol,* 86**,** 6171-8.

BURCKSTUMMER, T., KRIEGS, M., LUPBERGER, J., PAULI, E. K., SCHMITTEL, S. & HILDT, E. 2006. Raf-1 kinase associates with Hepatitis C virus NS5A and regulates viral replication. *FEBS Lett,* 580**,** 575-80.

BURGOS-OJEDA, D., WU, R., MCLEAN, K., CHEN, Y. C., TALPAZ, M., YOON, E., CHO, K. R. & BUCKANOVICH, R. J. 2015. CD24+ Ovarian Cancer Cells Are Enriched for Cancer-Initiating Cells and Dependent on JAK2 Signaling for Growth and Metastasis. *Mol Cancer Ther,* 14**,** 1717-27.

CABLE, E. E. & ISOM, H. C. 1997. Exposure of primary rat hepatocytes in long-term DMSO culture to selected transition metals induces hepatocyte proliferation and formation of duct-like structures. *Hepatology,* 26**,** 1444-57.

CAIGNARD, G., BOURAI, M., JACOB, Y., TANGY, F. & VIDALAIN, P. O. 2009. Inhibition of IFN-alpha/beta signaling by two discrete peptides within measles virus V protein that specifically bind STAT1 and STAT2. *Virology,* 383**,** 112-20.

CAMARGO, F. D., GOKHALE, S., JOHNNIDIS, J. B., FU, D., BELL, G. W., JAENISCH, R. & BRUMMELKAMP, T. R. 2007. YAP1 increases organ size and expands undifferentiated progenitor cells. *Curr Biol,* 17**,** 2054-60.

CAMPBELL, K. N., WONG, J. S., GUPTA, R., ASANUMA, K., SUDOL, M., HE, J. C. & MUNDEL, P. 2013. Yes-associated protein (YAP) promotes cell survival by inhibiting proapoptotic dendrin signaling. *J Biol Chem,* 288**,** 17057-62.

CAO, Y., HAMADA, T., MATSUI, T., DATE, T. & IWABUCHI, K. 2004. Hepatitis C virus core protein interacts with p53-binding protein, 53BP2/Bbp/ASPP2, and inhibits p53-mediated apoptosis. *Biochem Biophys Res Commun,* 315**,** 788-95.

CARRENO, V. 2006. Occult hepatitis C virus infection: a new form of hepatitis C. *World J Gastroenterol,* 12**,** 6922-5.

CATANESE, M. T., ANSUINI, H., GRAZIANI, R., HUBY, T., MOREAU, M., BALL, J. K., PAONESSA, G., RICE, C. M., CORTESE, R., VITELLI, A. & NICOSIA, A. 2010. Role of scavenger receptor class B type I in hepatitis C virus entry: kinetics and molecular determinants. *J Virol,* 84**,** 34-43.

CATANESE, M. T., URYU, K., KOPP, M., EDWARDS, T. J., ANDRUS, L., RICE, W. J., SILVESTRY, M., KUHN, R. J. & RICE, C. M. 2013. Ultrastructural analysis of hepatitis C virus particles. *Proc Natl Acad Sci U S A,* 110**,** 9505-10.

CAUSSIN-SCHWEMLING, C., SCHMITT, C. & STOLL-KELLER, F. 2001. Study of the infection of human blood derived monocyte/macrophages with hepatitis C virus in vitro. *J Med Virol,* 65**,** 14-22.

CAYROL, C., KNIBIEHLER, M. & DUCOMMUN, B. 1998. p21 binding to PCNA causes G1 and G2 cell cycle arrest in p53-deficient cells. *Oncogene,* 16**,** 311-20.

CEREC, V., GLAISE, D., GARNIER, D., MOROSAN, S., TURLIN, B., DRENOU, B., GRIPON, P., KREMSDORF, D., GUGUEN-GUILLOUZO, C. & CORLU, A. 2007. Transdifferentiation of hepatocyte-like cells from the human hepatoma HepaRG cell line through bipotent progenitor. *Hepatology,* 45**,** 957-67.

CHAKRABORTY, S. & HONG, W. 2018. Linking Extracellular Matrix Agrin to the Hippo Pathway in Liver Cancer and Beyond. *Cancers (Basel),* 10.

CHALMERS, A. D. & SLACK, J. M. 2000. The Xenopus tadpole gut: fate maps and morphogenetic movements. *Development,* 127**,** 381-92.

CHAO, T. C., SU, W. C., HUANG, J. Y., CHEN, Y. C., JENG, K. S., WANG, H. D. & LAI, M. M. 2012. Proline-serine-threonine phosphatase-interacting protein 2 (PSTPIP2), a host membrane-deforming protein, is critical for membranous web formation in hepatitis C virus replication. *J Virol,* 86**,** 1739-49.

CHEN, A. Y., HOARE, M., SHANKAR, A. N., ALLISON, M., ALEXANDER, G. J. & MICHALAK, T. I. 2015a. Persistence of Hepatitis C Virus Traces after Spontaneous Resolution of Hepatitis C. *PLoS One,* 10**,** e0140312.

CHEN, A. Y., ZEREMSKI, M., CHAUHAN, R., JACOBSON, I. M., TALAL, A. H. & MICHALAK, T. I. 2013a. Persistence of hepatitis C virus during and after otherwise clinically successful treatment of chronic hepatitis C with standard pegylated interferon alpha-2b and ribavirin therapy. *PLoS One,* 8**,** e80078.

CHEN, E. Y., TAN, C. M., KOU, Y., DUAN, Q., WANG, Z., MEIRELLES, G. V., CLARK, N. R. & MA'AYAN, A. 2013b. Enrichr: interactive and collaborative HTML5 gene list enrichment analysis tool. *BMC Bioinformatics,* 14**,** 128.

CHEN, J., ZHANG, X., XU, Y., LI, X., REN, S., ZHOU, Y., DUAN, Y., ZERN, M., ZHANG, H., CHEN, G., LIU, C., MU, Y. & LIU, P. 2015b. Hepatic Progenitor Cells Contribute to the Progression of 2-Acetylaminofluorene/Carbon Tetrachloride-Induced Cirrhosis via the Non-Canonical Wnt Pathway. *PLoS One,* 10**,** e0130310.

CHEN, J., ZHAO, J., MA, R., LIN, H., LIANG, X. & CAI, X. 2014. Prognostic significance of E-cadherin expression in hepatocellular carcinoma: a meta-analysis. *PLoS One,* 9**,** e103952.

CHEN, L., CHAN, S. W., ZHANG, X., WALSH, M., LIM, C. J., HONG, W. & SONG, H. 2010a. Structural basis of YAP recognition by TEAD4 in the hippo pathway. *Genes Dev,* 24**,** 290-300.

CHEN, L., LI, M., LI, Q., WANG, C. J. & XIE, S. Q. 2013c. DKK1 promotes hepatocellular carcinoma cell migration and invasion through beta-catenin/MMP7 signaling pathway. *Mol Cancer,* 12**,** 157.

CHEN, L., LOH, P. G. & SONG, H. 2010b. Structural and functional insights into the TEAD-YAP complex in the Hippo signaling pathway. *Protein Cell,* 1**,** 1073-83.

CHEN, Q., ZHANG, N., XIE, R., WANG, W., CAI, J., CHOI, K. S., DAVID, K. K., HUANG, B., YABUTA, N., NOJIMA, H., ANDERS, R. A. & PAN, D. 2015c. Homeostatic control of Hippo signaling activity revealed by an endogenous activating mutation in YAP. *Genes Dev,* 29**,** 1285-97.

CHEN, Y., PAN, F. C., BRANDES, N., AFELIK, S., SOLTER, M. & PIELER, T. 2004. Retinoic acid signaling is essential for pancreas development and promotes endocrine at the expense of exocrine cell differentiation in Xenopus. *Dev Biol,* 271**,** 144-60.

CHEUNG, W. M., NG, W. W. & KUNG, A. W. 2006. Dimethyl sulfoxide as an inducer of differentiation in preosteoblast MC3T3-E1 cells. *FEBS Lett,* 580**,** 121-6.

CHIBA, T., ZHENG, Y. W., KITA, K., YOKOSUKA, O., SAISHO, H., ONODERA, M., MIYOSHI, H., NAKANO, M., ZEN, Y., NAKANUMA, Y., NAKAUCHI, H., IWAMA, A. & TANIGUCHI, H. 2007. Enhanced self-renewal capability in hepatic stem/progenitor cells drives cancer initiation. *Gastroenterology,* 133**,** 937-50.

CHIOU, J. F., WANG, Y. H., JOU, M. J., LIU, T. Z. & SHIAU, C. Y. 2010. Verteporfin-photoinduced apoptosis in HepG2 cells mediated by reactive oxygen and nitrogen species intermediates. *Free Radic Res,* 44**,** 155-70.

CHO, J. W., BAEK, W. K., SUH, S. I., YANG, S. H., CHANG, J., SUNG, Y. C. & SUH, M. H. 2001. Hepatitis C virus core protein promotes cell proliferation through the upregulation of cyclin E expression levels. *Liver,* 21**,** 137-42.

CHO, S. B., LEE, K. H., LEE, J. H., PARK, S. Y., LEE, W. S., PARK, C. H., KIM, H. S., CHOI, S. K. & REW, J. S. 2008. Expression of E- and N-cadherin and clinicopathology in hepatocellular carcinoma. *Pathol Int,* 58**,** 635-42.

CHOI, S., SAINZ, B., JR., CORCORAN, P., UPRICHARD, S. & JEONG, H. 2009. Characterization of increased drug metabolism activity in dimethyl sulfoxide (DMSO)-treated Huh7 hepatoma cells. *Xenobiotica,* 39**,** 205-17.

CHOI, S. C., CHOI, J. H., CUI, L. H., SEO, H. R., KIM, J. H., PARK, C. Y., JOO, H. J., PARK, J. H., HONG, S. J., YU, C. W. & LIM, D. S. 2015. Mixl1 and Flk1 Are Key Players of Wnt/TGF-beta Signaling During DMSO-Induced Mesodermal Specification in P19 cells. *J Cell Physiol,* 230**,** 1807-21.

CHOI, S. H. & HWANG, S. B. 2006. Modulation of the transforming growth factor-beta signal transduction pathway by hepatitis C virus nonstructural 5A protein. *J Biol Chem,* 281**,** 7468-78.

CHOI, S. S., OMENETTI, A., SYN, W. K. & DIEHL, A. M. 2011. The role of Hedgehog signaling in fibrogenic liver repair. *Int J Biochem Cell Biol,* 43**,** 238-44.

CHOO, Q. L., KUO, G., WEINER, A. J., OVERBY, L. R., BRADLEY, D. W. & HOUGHTON, M. 1989. Isolation of a cDNA clone derived from a blood-borne non-A, non-B viral hepatitis genome. *Science,* 244**,** 359-62.

CLARKE, M. F., DICK, J. E., DIRKS, P. B., EAVES, C. J., JAMIESON, C. H., JONES, D. L., VISVADER, J., WEISSMAN, I. L. & WAHL, G. M. 2006. Cancer stem cells--perspectives on current status and future directions: AACR Workshop on cancer stem cells. *Cancer Res,* 66**,** 9339-44.

COFFINIER, C., GRESH, L., FIETTE, L., TRONCHE, F., SCHUTZ, G., BABINET, C., PONTOGLIO, M., YANIV, M. & BARRA, J. 2002. Bile system morphogenesis defects and liver dysfunction upon targeted deletion of HNF1beta. *Development,* 129**,** 1829-38.

COLPITTS, C. C., LUPBERGER, J. & BAUMERT, T. F. 2016. Multifaceted role of E-cadherin in hepatitis C virus infection and pathogenesis. *Proc Natl Acad Sci U S A,* 113**,** 7298-300.

CONSTANTINESCU ARUXANDEI, D., MAKBUL, C., KOTURENKIENE, A., LUDEMANN, M. B. & HERRMANN, C. 2011. Dimerization-induced folding of MST1 SARAH and the influence of the intrinsically unstructured inhibitory domain: low thermodynamic stability of monomer. *Biochemistry,* 50**,** 10990-1000.

CORMAN, V. M., GRUNDHOFF, A., BAECHLEIN, C., FISCHER, N., GMYL, A., WOLLNY, R., DEI, D., RITZ, D., BINGER, T., ADANKWAH, E., MARFO, K. S., ANNISON, L., ANNAN, A., ADU-SARKODIE, Y., OPPONG, S., BECHER, P., DROSTEN, C. & DREXLER, J. F. 2015. Highly divergent hepaciviruses from African cattle. *J Virol,* 89**,** 5876-82.

COSTA, R. H., KALINICHENKO, V. V., HOLTERMAN, A. X. & WANG, X. 2003. Transcription factors in liver development, differentiation, and regeneration. *Hepatology,* 38**,** 1331-47.

CZYSZ, K., MINGER, S. & THOMAS, N. 2015. DMSO efficiently down regulates pluripotency genes in human embryonic stem cells during definitive endoderm derivation and increases the proficiency of hepatic differentiation. *PLoS One,* 10**,** e0117689.

D'AMBROSIO, D. N., WALEWSKI, J. L., CLUGSTON, R. D., BERK, P. D., RIPPE, R. A. & BLANER, W. S. 2011. Distinct populations of hepatic stellate cells in the mouse liver have different capacities for retinoid and lipid storage. *PLoS One,* 6**,** e24993.

DE BOER, C. J., VAN KRIEKEN, J. H., JANSSEN-VAN RHIJN, C. M. & LITVINOV, S. V. 1999. Expression of Ep-CAM in normal, regenerating, metaplastic, and neoplastic liver. *J Pathol,* 188**,** 201-6.

DE FRANCESCO, R. & MIGLIACCIO, G. 2005. Challenges and successes in developing new therapies for hepatitis C. *Nature,* 436**,** 953-60.

DENG, L., NAGANO-FUJII, M., TANAKA, M., NOMURA-TAKIGAWA, Y., IKEDA, M., KATO, N., SADA, K. & HOTTA, H. 2006. NS3 protein of Hepatitis C virus associates with the tumour suppressor p53 and inhibits its function in an NS3 sequence-dependent manner. *J Gen Virol,* 87**,** 1703-13.

DERAN, M., YANG, J., SHEN, C. H., PETERS, E. C., FITAMANT, J., CHAN, P., HSIEH, M., ZHU, S., ASARA, J. M., ZHENG, B., BARDEESY, N., LIU, J. & WU, X. 2014. Energy stress regulates hippo-YAP signaling involving AMPK-mediated regulation of angiomotin-like 1 protein. *Cell Rep,* 9**,** 495-503.

DERYCKE, L. D. & BRACKE, M. E. 2004. N-cadherin in the spotlight of cell-cell adhesion, differentiation, embryogenesis, invasion and signalling. *Int J Dev Biol,* 48**,** 463-76.

DESSIMOZ, J., OPOKA, R., KORDICH, J. J., GRAPIN-BOTTON, A. & WELLS, J. M. 2006. FGF signaling is necessary for establishing gut tube domains along the anterior-posterior axis in vivo. *Mech Dev,* 123**,** 42-55.

DEUTSCH, G., JUNG, J., ZHENG, M., LORA, J. & ZARET, K. S. 2001. A bipotential precursor population for pancreas and liver within the embryonic endoderm. *Development,* 128**,** 871-81.

DIDCOCK, L., YOUNG, D. F., GOODBOURN, S. & RANDALL, R. E. 1999. The V protein of simian virus 5 inhibits interferon signalling by targeting STAT1 for proteasome-mediated degradation. *J Virol,* 73**,** 9928-33.

DIEHL, A. M. & CHUTE, J. 2013. Underlying potential: cellular and molecular determinants of adult liver repair. *J Clin Invest,* 123**,** 1858-60.

DIXON, L. J., BARNES, M., TANG, H., PRITCHARD, M. T. & NAGY, L. E. 2013. Kupffer cells in the liver. *Compr Physiol,* 3**,** 785-97.

DOMINGO, E., BARANOWSKI, E., RUIZ-JARABO, C. M., MARTIN-HERNANDEZ, A. M., SAIZ, J. C. & ESCARMIS, C. 1998. Quasispecies structure and persistence of RNA viruses. *Emerg Infect Dis,* 4**,** 521-7.

DOMINGO, E. & GOMEZ, J. 2007. Quasispecies and its impact on viral hepatitis. *Virus Res,* 127**,** 131-50.

DOMINGO, E. & HOLLAND, J. J. 1997. RNA virus mutations and fitness for survival. *Annu Rev Microbiol,* 51**,** 151-78.

DOMINGO, E., MARTIN, V., PERALES, C., GRANDE-PEREZ, A., GARCIA-ARRIAZA, J. & ARIAS, A. 2006. Viruses as quasispecies: biological implications. *Curr Top Microbiol Immunol,* 299**,** 51-82.

DONG, J., FELDMANN, G., HUANG, J., WU, S., ZHANG, N., COMERFORD, S. A., GAYYED, M. F., ANDERS, R. A., MAITRA, A. & PAN, D. 2007. Elucidation of a universal size-control mechanism in Drosophila and mammals. *Cell,* 130**,** 1120-33.

DOR, I., NAMBA, M. & SATO, J. 1975. Establishment and some biological characteristics of human hepatoma cell lines. *Gan,* 66**,** 385-92.

DOUARIN, N. M. 1975. An experimental analysis of liver development. *Med Biol,* 53**,** 427-55.

DRAGANI, T. A. 2010. Risk of HCC: genetic heterogeneity and complex genetics. *J Hepatol,* 52**,** 252-7.

DREXLER, J. F., CORMAN, V. M., MULLER, M. A., LUKASHEV, A. N., GMYL, A., COUTARD, B., ADAM, A., RITZ, D., LEIJTEN, L. M., VAN RIEL, D., KALLIES, R., KLOSE, S. M., GLOZA-RAUSCH, F., BINGER, T., ANNAN, A., ADU-SARKODIE, Y., OPPONG, S., BOURGAREL, M., RUPP, D., HOFFMANN, B., SCHLEGEL, M., KUMMERER, B. M., KRUGER, D. H., SCHMIDT-CHANASIT, J., SETIEN, A. A., COTTONTAIL, V. M., HEMACHUDHA, T., WACHARAPLUESADEE, S., OSTERRIEDER, K., BARTENSCHLAGER, R., MATTHEE, S., BEER, M., KUIKEN, T., REUSKEN, C., LEROY, E. M., ULRICH, R. G. & DROSTEN, C. 2013. Evidence for novel hepaciviruses in rodents. *PLoS Pathog,* 9**,** e1003438.

DUBRIDGE, R. B., TANG, P., HSIA, H. C., LEONG, P. M., MILLER, J. H. & CALOS, M. P. 1987. Analysis of mutation in human cells by using an Epstein-Barr virus shuttle system. *Mol Cell Biol,* 7**,** 379-87.

DUMONT, S., CHENG, W., SEREBROV, V., BERAN, R. K., TINOCO, I., JR., PYLE, A. M. & BUSTAMANTE, C. 2006. RNA translocation and unwinding mechanism of HCV NS3 helicase and its coordination by ATP. *Nature,* 439**,** 105-8.

DUPONT, S., MORSUT, L., ARAGONA, M., ENZO, E., GIULITTI, S., CORDENONSI, M., ZANCONATO, F., LE DIGABEL, J., FORCATO, M., BICCIATO, S., ELVASSORE, N. & PICCOLO, S. 2011. Role of YAP/TAZ in mechanotransduction. *Nature,* 474**,** 179-83.

EDGAR, R. C. 2004. MUSCLE: a multiple sequence alignment method with reduced time and space complexity. *BMC Bioinformatics,* 5**,** 113.

EGGER, D., WOLK, B., GOSERT, R., BIANCHI, L., BLUM, H. E., MORADPOUR, D. & BIENZ, K. 2002. Expression of hepatitis C virus proteins induces distinct membrane alterations including a candidate viral replication complex. *J Virol,* 76**,** 5974-84.

EISINGER-MATHASON, T. S., MUCAJ, V., BIJU, K. M., NAKAZAWA, M. S., GOHIL, M., CASH, T. P., YOON, S. S., SKULI, N., PARK, K. M., GERECHT, S. & SIMON, M. C. 2015. Deregulation of the Hippo pathway in soft-tissue sarcoma promotes FOXM1 expression and tumorigenesis. *Proc Natl Acad Sci U S A,* 112**,** E3402-11.

ELAZAR, M., CHEONG, K. H., LIU, P., GREENBERG, H. B., RICE, C. M. & GLENN, J. S. 2003. Amphipathic helix-dependent localization of NS5A mediates hepatitis C virus RNA replication. *J Virol,* 77**,** 6055-61.

ESPANOL-SUNER, R., CARPENTIER, R., VAN HUL, N., LEGRY, V., ACHOURI, Y., CORDI, S., JACQUEMIN, P., LEMAIGRE, F. & LECLERCQ, I. A. 2012. Liver progenitor cells yield functional hepatocytes in response to chronic liver injury in mice. *Gastroenterology,* 143**,** 1564-1575 e7.

EUROPEAN ASSOCIATION FOR THE STUDY OF THE LIVER 2012. 2011 European Association of the Study of the Liver hepatitis C virus clinical practice guidelines. *Liver Int,* 32 Suppl 1**,** 2-8.

EUROPEAN ASSOCIATION FOR THE STUDY OF THE LIVER. 2018. EASL Recommendations on Treatment of Hepatitis C 2018. *J Hepatol,* 69**,** 461-511.

EVANS, M. J., VON HAHN, T., TSCHERNE, D. M., SYDER, A. J., PANIS, M., WOLK, B., HATZIIOANNOU, T., MCKEATING, J. A., BIENIASZ, P. D. & RICE, C. M. 2007. Claudin-1 is a hepatitis C virus co-receptor required for a late step in entry. *Nature,* 446**,** 801-5.

EZZELL, R. M., TONER, M., HENDRICKS, K., DUNN, J. C., TOMPKINS, R. G. & YARMUSH, M. L. 1993. Effect of collagen gel configuration on the cytoskeleton in cultured rat hepatocytes. *Exp Cell Res,* 208**,** 442-52.

FAN, F., HE, Z., KONG, L. L., CHEN, Q., YUAN, Q., ZHANG, S., YE, J., LIU, H., SUN, X., GENG, J., YUAN, L., HONG, L., XIAO, C., ZHANG, W., LI, Y., WANG, P., HUANG, L., WU, X., JI, Z., WU, Q., XIA, N. S., GRAY, N. S., CHEN, L., YUN, C. H., DENG, X. & ZHOU, D. 2016. Pharmacological targeting of kinases MST1 and MST2 augments tissue repair and regeneration. *Sci Transl Med,* 8**,** 352ra108.

FANG, G., YU, H. & KIRSCHNER, M. W. 1998a. The checkpoint protein MAD2 and the mitotic regulator CDC20 form a ternary complex with the anaphase-promoting complex to control anaphase initiation. *Genes Dev,* 12**,** 1871-83.

FANG, G., YU, H. & KIRSCHNER, M. W. 1998b. Direct binding of CDC20 protein family members activates the anaphase-promoting complex in mitosis and G1. *Mol Cell,* 2**,** 163-71.

FARAZI, P. A. & DEPINHO, R. A. 2006. Hepatocellular carcinoma pathogenesis: from genes to environment. *Nat Rev Cancer,* 6**,** 674-87.

FARCET, J. P., LEBARGY, F., LAVIGNAC, C., GAULARD, P., DAUTRY, A., GAZZOLO, L., ROMEO, P. H. & VAINCHENKER, W. 1991. Constitutive IL-2 expression in HTLV-I-infected leukaemic T cell lines. *Clin Exp Immunol,* 84**,** 415-21.

FERRARIS, P., BEAUMONT, E., UZBEKOV, R., BRAND, D., GAILLARD, J., BLANCHARD, E. & ROINGEARD, P. 2013. Sequential biogenesis of host cell membrane rearrangements induced by hepatitis C virus infection. *Cell Mol Life Sci,* 70**,** 1297-306.

FERRI, C., CARACCIOLO, F., ZIGNEGO, A. L., LA CIVITA, L., MONTI, M., LONGOMBARDO, G., LOMBARDINI, F., GRECO, F., CAPOCHIANI, E., MAZZONI, A. & ET AL. 1994. Hepatitis C virus infection in patients with non-Hodgkin's lymphoma. *Br J Haematol,* 88**,** 392-4.

FERRI, C., GRECO, F., LONGOMBARDO, G., PALLA, P., MORETTI, A., MARZO, E., MAZZONI, A., PASERO, G., BOMBARDIERI, S., HIGHFIELD, P. & ET AL. 1991. Association between hepatitis C virus and mixed cryoglobulinemia [see comment]. *Clin Exp Rheumatol,* 9**,** 621-4.

FERRIGNO, O., LALLEMAND, F., VERRECCHIA, F., L'HOSTE, S., CAMONIS, J., ATFI, A. & MAUVIEL, A. 2002. Yes-associated protein (YAP65) interacts with Smad7 and potentiates its inhibitory activity against TGF-beta/Smad signaling. *Oncogene,* 21**,** 4879-84.

FINCH-EDMONDSON, M. L., STRAUSS, R. P., PASSMAN, A. M., SUDOL, M., YEOH, G. C. & CALLUS, B. A. 2015. TAZ Protein Accumulation Is Negatively Regulated by YAP Abundance in Mammalian Cells. *J Biol Chem,* 290**,** 27928-38.

FINKELMEIER, F., DULTZ, G., PEIFFER, K. H., KRONENBERGER, B., KRAUSS, F., ZEUZEM, S., SARRAZIN, C., VERMEHREN, J. & WAIDMANN, O. 2018. Risk of de novo Hepatocellular Carcinoma after HCV Treatment with Direct-Acting Antivirals. *Liver Cancer,* 7**,** 190-204.

FIORE, M. & DEGRASSI, F. 1999. Dimethyl sulfoxide restores contact inhibition-induced growth arrest and inhibits cell density-dependent apoptosis in hamster cells. *Exp Cell Res,* 251**,** 102-10.

FIRTH, C., BHAT, M., FIRTH, M. A., WILLIAMS, S. H., FRYE, M. J., SIMMONDS, P., CONTE, J. M., NG, J., GARCIA, J., BHUVA, N. P., LEE, B., CHE, X., QUAN, P. L. & LIPKIN, W. I. 2014. Detection of zoonotic pathogens and characterization of novel viruses carried by commensal Rattus norvegicus in New York City. *MBio,* 5**,** e01933-14.

FITAMANT, J., KOTTAKIS, F., BENHAMOUCHE, S., TIAN, H. S., CHUVIN, N., PARACHONIAK, C. A., NAGLE, J. M., PERERA, R. M., LAPOUGE, M., DESHPANDE, V., ZHU, A. X., LAI, A., MIN, B., HOSHIDA, Y., AVRUCH, J., SIA, D., CAMPRECIOS, G., MCCLATCHEY, A. I., LLOVET, J. M., MORRISSEY, D., RAJ, L. & BARDEESY, N. 2015. YAP Inhibition Restores Hepatocyte Differentiation in Advanced HCC, Leading to Tumor Regression. *Cell Rep*.

FLINT, M. & MCKEATING, J. A. 2000. The role of the hepatitis C virus glycoproteins in infection. *Rev Med Virol,* 10**,** 101-17.

FLODBY, P., BARLOW, C., KYLEFJORD, H., AHRLUND-RICHTER, L. & XANTHOPOULOS, K. G. 1996. Increased hepatic cell proliferation and lung abnormalities in mice deficient in CCAAT/enhancer binding protein alpha. *J Biol Chem,* 271**,** 24753-60.

FORBES, S. J. & ROSENTHAL, N. 2014. Preparing the ground for tissue regeneration: from mechanism to therapy. *Nat Med,* 20**,** 857-69.

FOSTER, G. R., HEZODE, C., BRONOWICKI, J. P., CAROSI, G., WEILAND, O., VERLINDEN, L., VAN HEESWIJK, R., VAN BAELEN, B., PICCHIO, G. & BEUMONT, M. 2011. Telaprevir alone or with peginterferon and ribavirin reduces HCV RNA in patients with chronic genotype 2 but not genotype 3 infections. *Gastroenterology,* 141**,** 881-889 e1.

FRASER, R., DOBBS, B. R. & ROGERS, G. W. 1995. Lipoproteins and the liver sieve: the role of the fenestrated sinusoidal endothelium in lipoprotein metabolism, atherosclerosis, and cirrhosis. *Hepatology,* 21**,** 863-74.

FRIDELL, R. A., QIU, D., VALERA, L., WANG, C., ROSE, R. E. & GAO, M. 2011. Distinct functions of NS5A in hepatitis C virus RNA replication uncovered by studies with the NS5A inhibitor BMS-790052. *J Virol,* 85**,** 7312-20.

FRIEBE, P. & BARTENSCHLAGER, R. 2002. Genetic analysis of sequences in the 3' nontranslated region of hepatitis C virus that are important for RNA replication. *J Virol,* 76**,** 5326-38.

FRIEBE, P., BOUDET, J., SIMORRE, J. P. & BARTENSCHLAGER, R. 2005. Kissing-loop interaction in the 3' end of the hepatitis C virus genome essential for RNA replication. *J Virol,* 79**,** 380-92.

FRIEDMAN, S. L. 2008. Mechanisms of hepatic fibrogenesis. *Gastroenterology,* 134**,** 1655-69.

FUKUDA-TAIRA, S. 1981. Hepatic induction in the avian embryo: specificity of reactive endoderm and inductive mesoderm. *J Embryol Exp Morphol,* 63**,** 111-25.

FUKUDA, K., TSUCHIHARA, K., HIJIKATA, M., NISHIGUCHI, S., KUROKI, T. & SHIMOTOHNO, K. 2001. Hepatitis C virus core protein enhances the activation of the transcription factor, Elk1, in response to mitogenic stimuli. *Hepatology,* 33**,** 159-65.

FUKUTOMI, T., ZHOU, Y., KAWAI, S., EGUCHI, H., WANDS, J. R. & LI, J. 2005. Hepatitis C virus core protein stimulates hepatocyte growth: correlation with upregulation of wnt-1 expression. *Hepatology,* 41**,** 1096-105.

GANGEMI, R. M., GRIFFERO, F., MARUBBI, D., PERERA, M., CAPRA, M. C., MALATESTA, P., RAVETTI, G. L., ZONA, G. L., DAGA, A. & CORTE, G. 2009. SOX2 silencing in glioblastoma tumor-initiating cells causes stop of proliferation and loss of tumorigenicity. *Stem Cells,* 27**,** 40-8.

GARTEL, A. L. & TYNER, A. L. 1999. Transcriptional regulation of the p21((WAF1/CIP1)) gene. *Exp Cell Res,* 246**,** 280-9.

GE, D., FELLAY, J., THOMPSON, A. J., SIMON, J. S., SHIANNA, K. V., URBAN, T. J., HEINZEN, E. L., QIU, P., BERTELSEN, A. H., MUIR, A. J., SULKOWSKI, M., MCHUTCHISON, J. G. & GOLDSTEIN, D. B. 2009. Genetic variation in IL28B predicts hepatitis C treatment-induced viral clearance. *Nature,* 461**,** 399-401.

GEORGE, A., PANDA, S., KUDMULWAR, D., CHHATBAR, S. P., NAYAK, S. C. & KRISHNAN, H. H. 2012. Hepatitis C virus NS5A binds to the mRNA cap-binding eukaryotic translation initiation 4F (eIF4F) complex and up-regulates host translation initiation machinery through eIF4E-binding protein 1 inactivation. *J Biol Chem,* 287**,** 5042-58.

GEORGOPOULOU, U., TSITOURA, P., KALAMVOKI, M. & MAVROMARA, P. 2006. The protein phosphatase 2A represents a novel cellular target for hepatitis C virus NS5A protein. *Biochimie,* 88**,** 651-62.

GERDES, J. 1990. Ki-67 and other proliferation markers useful for immunohistological diagnostic and prognostic evaluations in human malignancies. *Semin Cancer Biol,* 1**,** 199-206.

GERDES, J., LEMKE, H., BAISCH, H., WACKER, H. H., SCHWAB, U. & STEIN, H. 1984. Cell cycle analysis of a cell proliferation-associated human nuclear antigen defined by the monoclonal antibody Ki-67. *J Immunol,* 133**,** 1710-5.

GERDES, J., LI, L., SCHLUETER, C., DUCHROW, M., WOHLENBERG, C., GERLACH, C., STAHMER, I., KLOTH, S., BRANDT, E. & FLAD, H. D. 1991. Immunobiochemical and molecular biologic characterization of the cell proliferation-associated nuclear antigen that is defined by monoclonal antibody Ki-67. *Am J Pathol,* 138**,** 867-73.

GHANY, M. G., STRADER, D. B., THOMAS, D. L., SEEFF, L. B. & AMERICAN ASSOCIATION FOR THE STUDY OF LIVER, D. 2009. Diagnosis, management, and treatment of hepatitis C: an update. *Hepatology,* 49**,** 1335-74.

GHOSH, A. K., MAJUMDER, M., STEELE, R., MEYER, K., RAY, R. & RAY, R. B. 2000. Hepatitis C virus NS5A protein protects against TNF-alpha mediated apoptotic cell death. *Virus Res,* 67**,** 173-8.

GHOSHAL, S., FUCHS, B. C. & TANABE, K. K. 2016. STAT3 is a key transcriptional regulator of cancer stem cell marker CD133 in HCC. *Hepatobiliary Surg Nutr,* 5**,** 201-3.

GIAMBARTOLOMEI, S., COVONE, F., LEVRERO, M. & BALSANO, C. 2001. Sustained activation of the Raf/MEK/Erk pathway in response to EGF in stable cell lines expressing the Hepatitis C Virus (HCV) core protein. *Oncogene,* 20**,** 2606-10.

GLANTSCHNIG, H., RODAN, G. A. & RESZKA, A. A. 2002. Mapping of MST1 kinase sites of phosphorylation. Activation and autophosphorylation. *J Biol Chem,* 277**,** 42987-96.

GOH, P. Y., TAN, Y. J., LIM, S. P., TAN, Y. H., LIM, S. G., FULLER-PACE, F. & HONG, W. 2004. Cellular RNA helicase p68 relocalization and interaction with the hepatitis C virus (HCV) NS5B protein and the potential role of p68 in HCV RNA replication. *J Virol,* 78**,** 5288-98.

GOLDMAN, O., COHEN, I. & GOUON-EVANS, V. 2016. Functional Blood Progenitor Markers in Developing Human Liver Progenitors. *Stem Cell Reports,* 7**,** 158-66.

GOSERT, R., EGGER, D., LOHMANN, V., BARTENSCHLAGER, R., BLUM, H. E., BIENZ, K. & MORADPOUR, D. 2003. Identification of the hepatitis C virus RNA replication complex in Huh-7 cells harboring subgenomic replicons. *J Virol,* 77**,** 5487-92.

GOTTWEIN, J. M., JENSEN, T. B., MATHIESEN, C. K., MEULEMAN, P., SERRE, S. B., LADEMANN, J. B., GHANEM, L., SCHEEL, T. K., LEROUX-ROELS, G. & BUKH, J. 2011. Development and application of hepatitis C reporter viruses with genotype 1 to 7 core-nonstructural protein 2 (NS2) expressing fluorescent proteins or luciferase in modified JFH1 NS5A. *J Virol,* 85**,** 8913-28.

GOUTAGNY, N., FATMI, A., DE LEDINGHEN, V., PENIN, F., COUZIGOU, P., INCHAUSPE, G. & BAIN, C. 2003. Evidence of viral replication in circulating dendritic cells during hepatitis C virus infection. *J Infect Dis,* 187**,** 1951-8.

GOUTTENOIRE, J., CASTET, V., MONTSERRET, R., ARORA, N., RAUSSENS, V., RUYSSCHAERT, J. M., DIESIS, E., BLUM, H. E., PENIN, F. & MORADPOUR, D. 2009. Identification of a novel determinant for membrane association in hepatitis C virus nonstructural protein 4B. *J Virol,* 83**,** 6257-68.

GOUYSSE, G., COUVELARD, A., FRACHON, S., BOUVIER, R., NEJJARI, M., DAUGE, M. C., FELDMANN, G., HENIN, D. & SCOAZEC, J. Y. 2002. Relationship between vascular development and vascular differentiation during liver organogenesis in humans. *J Hepatol,* 37**,** 730-40.

GRAHAM, F. L., SMILEY, J., RUSSELL, W. C. & NAIRN, R. 1977. Characteristics of a human cell line transformed by DNA from human adenovirus type 5. *J Gen Virol,* 36**,** 59-74.

GRIFFIN, S. D., BEALES, L. P., CLARKE, D. S., WORSFOLD, O., EVANS, S. D., JAEGER, J., HARRIS, M. P. & ROWLANDS, D. J. 2003. The p7 protein of hepatitis C virus forms an ion channel that is blocked by the antiviral drug, Amantadine. *FEBS Lett,* 535**,** 34-8.

GRIJALVA, J. L., HUIZENGA, M., MUELLER, K., RODRIGUEZ, S., BRAZZO, J., CAMARGO, F., SADRI-VAKILI, G. & VAKILI, K. 2014. Dynamic alterations in Hippo signaling pathway and YAP activation during liver regeneration. *Am J Physiol Gastrointest Liver Physiol,* 307**,** G196-204.

GRIPON, P., RUMIN, S., URBAN, S., LE SEYEC, J., GLAISE, D., CANNIE, I., GUYOMARD, C., LUCAS, J., TREPO, C. & GUGUEN-GUILLOUZO, C. 2002. Infection of a human hepatoma cell line by hepatitis B virus. *Proc Natl Acad Sci U S A,* 99**,** 15655-60.

GU, M. & RICE, C. M. 2010. Three conformational snapshots of the hepatitis C virus NS3 helicase reveal a ratchet translocation mechanism. *Proc Natl Acad Sci U S A,* 107**,** 521-8.

GUALDI, R., BOSSARD, P., ZHENG, M., HAMADA, Y., COLEMAN, J. R. & ZARET, K. S. 1996. Hepatic specification of the gut endoderm in vitro: cell signaling and transcriptional control. *Genes Dev,* 10**,** 1670-82.

GUEST, R. V., BOULTER, L., KENDALL, T. J., MINNIS-LYONS, S. E., WALKER, R., WIGMORE, S. J., SANSOM, O. J. & FORBES, S. J. 2014. Cell lineage tracing reveals a biliary origin of intrahepatic cholangiocarcinoma. *Cancer Res,* 74**,** 1005-10.

GUICHARD, C., AMADDEO, G., IMBEAUD, S., LADEIRO, Y., PELLETIER, L., MAAD, I. B., CALDERARO, J., BIOULAC-SAGE, P., LETEXIER, M., DEGOS, F., CLEMENT, B., BALABAUD, C., CHEVET, E., LAURENT, A., COUCHY, G., LETOUZE, E., CALVO, F. & ZUCMAN-ROSSI, J. 2012. Integrated analysis of somatic mutations and focal copy-number changes identifies key genes and pathways in hepatocellular carcinoma. *Nat Genet,* 44**,** 694-8.

GUILLOUZO, A., CORLU, A., ANINAT, C., GLAISE, D., MOREL, F. & GUGUEN-GUILLOUZO, C. 2007. The human hepatoma HepaRG cells: a highly differentiated model for studies of liver metabolism and toxicity of xenobiotics. *Chem Biol Interact,* 168**,** 66-73.

GUMBINER, B. M. & KIM, N. G. 2014. The Hippo-YAP signaling pathway and contact inhibition of growth. *J Cell Sci,* 127**,** 709-17.

GUMUCIO, J. J. 1989. Hepatocyte heterogeneity: the coming of age from the description of a biological curiosity to a partial understanding of its physiological meaning and regulation. *Hepatology,* 9**,** 154-60.

GUO, L., DIAL, S., SHI, L., BRANHAM, W., LIU, J., FANG, J. L., GREEN, B., DENG, H., KAPUT, J. & NING, B. 2011. Similarities and differences in the expression of drug-metabolizing enzymes between human hepatic cell lines and primary human hepatocytes. *Drug Metab Dispos,* 39**,** 528-38.

GUO, X., WANG, S., QIU, Z. G., DOU, Y. L., LIU, W. L., YANG, D., SHEN, Z. Q., CHEN, Z. L., WANG, J. F., ZHANG, B., WANG, X. W., GUO, X. F., ZHANG, X. L., JIN, M. & LI, J. W. 2017. Efficient replication of blood-borne hepatitis C virus in human fetal liver stem cells. *Hepatology,* 66**,** 1045-1057.

HAMDANE, N., JÜHLING, F., THUMANN, C., OUDOT, M., EL SAGHIRE, H., BANDIERA, S., SAVIANO, A., SCHMIDL, C., BOCK, C., DAVIDSON, I., PESSAUX, P., HABERSETZER, F., WIELAND, S., HERIM, M., PIARDI, T., SOMMACALE, D., FUCHS, B. C., BARDEESY, N., HOSHIDA, Y., ZEISEL, M. B. & BAUMERT, T. F. Hepatitis C Virus-Induced Epigenetic and Transcriptional Changes Persist Post Cure. 2017.

HARRINGTON, P. R., KOMATSU, T. E., DEMING, D. J., DONALDSON, E. F., O'REAR, J. J. & NAEGER, L. K. 2018. Impact of hepatitis C virus polymorphisms on direct-acting antiviral treatment efficacy: Regulatory analyses and perspectives. *Hepatology,* 67**,** 2430-2448.

HARTSOCK, A. & NELSON, W. J. 2008. Adherens and tight junctions: structure, function and connections to the actin cytoskeleton. *Biochim Biophys Acta,* 1778**,** 660-9.

HARUNA, Y., SAITO, K., SPAULDING, S., NALESNIK, M. A. & GERBER, M. A. 1996. Identification of bipotential progenitor cells in human liver development. *Hepatology,* 23**,** 476-81.

HAU, J. C., ERDMANN, D., MESROUZE, Y., FURET, P., FONTANA, P., ZIMMERMANN, C., SCHMELZLE, T., HOFMANN, F. & CHENE, P. 2013. The TEAD4-YAP/TAZ protein-protein interaction: expected similarities and unexpected differences. *Chembiochem,* 14**,** 1218-25.

HAYASHI, H., HIGASHI, T., YOKOYAMA, N., KAIDA, T., SAKAMOTO, K., FUKUSHIMA, Y., ISHIMOTO, T., KUROKI, H., NITTA, H., HASHIMOTO, D., CHIKAMOTO, A., OKI, E., BEPPU, T. & BABA, H. 2015. An Imbalance in TAZ and YAP Expression in Hepatocellular Carcinoma Confers Cancer Stem Cell-like Behaviors Contributing to Disease Progression. *Cancer Res,* 75**,** 4985-97.

HAYASHI, J., AOKI, H., KAJINO, K., MORIYAMA, M., ARAKAWA, Y. & HINO, O. 2000. Hepatitis C virus core protein activates the MAPK/ERK cascade synergistically with tumor promoter TPA, but not with epidermal growth factor or transforming growth factor alpha. *Hepatology,* 32**,** 958-61.

HE, G., DHAR, D., NAKAGAWA, H., FONT-BURGADA, J., OGATA, H., JIANG, Y., SHALAPOUR, S., SEKI, E., YOST, S. E., JEPSEN, K., FRAZER, K. A., HARISMENDY, O., HATZIAPOSTOLOU, M., ILIOPOULOS, D., SUETSUGU, A., HOFFMAN, R. M., TATEISHI, R., KOIKE, K. & KARIN, M. 2013a. Identification of liver cancer progenitors whose malignant progression depends on autocrine IL-6 signaling. *Cell,* 155**,** 384-96.

HE, G. & KARIN, M. 2011. NF-kappaB and STAT3 - key players in liver inflammation and cancer. *Cell Res,* 21**,** 159-68.

HE, X., CHEN, Z., JIA, M. & ZHAO, X. 2013b. Downregulated E-cadherin expression indicates worse prognosis in Asian patients with colorectal cancer: evidence from meta-analysis. *PLoS One,* 8**,** e70858.

HE, Y., NAKAO, H., TAN, S. L., POLYAK, S. J., NEDDERMANN, P., VIJAYSRI, S., JACOBS, B. L. & KATZE, M. G. 2002. Subversion of cell signaling pathways by hepatitis C virus nonstructural 5A protein via interaction with Grb2 and P85 phosphatidylinositol 3-kinase. *J Virol,* 76**,** 9207-17.

HE, Y., STASCHKE, K. A. & TAN, S. L. 2006. HCV NS5A: A Multifunctional Regulator of Cellular Pathways and Virus Replication. *In:* TAN, S. L. (ed.) *Hepatitis C Viruses: Genomes and Molecular Biology.* Norfolk (UK).

HE, Y., TAN, S. L., TAREEN, S. U., VIJAYSRI, S., LANGLAND, J. O., JACOBS, B. L. & KATZE, M. G. 2001. Regulation of mRNA translation and cellular signaling by hepatitis C virus nonstructural protein NS5A. *J Virol,* 75**,** 5090-8.

HELLE, F., BROCHOT, E., FOURNIER, C., DESCAMPS, V., IZQUIERDO, L., HOFFMANN, T. W., MOREL, V., HERPE, Y. E., BENGRINE, A., BELOUZARD, S., WYCHOWSKI, C., DUBUISSON, J., FRANCOIS, C., REGIMBEAU, J. M., CASTELAIN, S. & DUVERLIE, G. 2013. Permissivity of primary human hepatocytes and different hepatoma cell lines to cell culture adapted hepatitis C virus. *PLoS One,* 8**,** e70809.

HELLERBRAND, C. 2013. Hepatic stellate cells--the pericytes in the liver. *Pflugers Arch,* 465**,** 775-8.

HELLERBRAND, C., STEFANOVIC, B., GIORDANO, F., BURCHARDT, E. R. & BRENNER, D. A. 1999. The role of TGFbeta1 in initiating hepatic stellate cell activation in vivo. *J Hepatol,* 30**,** 77-87.

HEMPEL, M., SCHMITZ, A., WINKLER, S., KUCUKOGLU, O., BRUCKNER, S., NIESSEN, C. & CHRIST, B. 2015. Pathological implications of cadherin zonation in mouse liver. *Cell Mol Life Sci,* 72**,** 2599-612.

HERGOVICH, A. 2013. Regulation and functions of mammalian LATS/NDR kinases: looking beyond canonical Hippo signalling. *Cell Biosci,* 3**,** 32.

HERGOVICH, A., BICHSEL, S. J. & HEMMINGS, B. A. 2005. Human NDR kinases are rapidly activated by MOB proteins through recruitment to the plasma membrane and phosphorylation. *Mol Cell Biol,* 25**,** 8259-72.

HERGOVICH, A., KOHLER, R. S., SCHMITZ, D., VICHALKOVSKI, A., CORNILS, H. & HEMMINGS, B. A. 2009. The MST1 and hMOB1 tumor suppressors control human centrosome duplication by regulating NDR kinase phosphorylation. *Curr Biol,* 19**,** 1692-702.

HERGOVICH, A., LAMLA, S., NIGG, E. A. & HEMMINGS, B. A. 2007. Centrosome-associated NDR kinase regulates centrosome duplication. *Mol Cell,* 25**,** 625-34.

HERGOVICH, A., SCHMITZ, D. & HEMMINGS, B. A. 2006. The human tumour suppressor LATS1 is activated by human MOB1 at the membrane. *Biochem Biophys Res Commun,* 345**,** 50-8.

HERZOG, N., HANSEN, M., MIETHBAUER, S., SCHMIDTKE, K. U., ANDERER, U., LUPP, A., SPERLING, S., SEEHOFER, D., DAMM, G., SCHEIBNER, K. & KUPPER, J. H. 2016. Primary-like human hepatocytes genetically engineered to obtain proliferation competence display hepatic differentiation characteristics in monolayer and organotypical spheroid cultures. *Cell Biol Int,* 40**,** 341-53.

HIRANO, T., ISHIHARA, K. & HIBI, M. 2000. Roles of STAT3 in mediating the cell growth, differentiation and survival signals relayed through the IL-6 family of cytokine receptors. *Oncogene,* 19**,** 2548-56.

HONDA, M., PING, L. H., RIJNBRAND, R. C., AMPHLETT, E., CLARKE, B., ROWLANDS, D. & LEMON, S. M. 1996. Structural requirements for initiation of translation by internal ribosome entry within genome-length hepatitis C virus RNA. *Virology,* 222**,** 31-42.

HONG, W. 2013. Angiomotin'g YAP into the nucleus for cell proliferation and cancer development. *Sci Signal,* 6**,** pe27.

HONG, W. & GUAN, K. L. 2012. The YAP and TAZ transcription co-activators: key downstream effectors of the mammalian Hippo pathway. *Semin Cell Dev Biol,* 23**,** 785-93.

HOSSAIN, Z., ALI, S. M., KO, H. L., XU, J., NG, C. P., GUO, K., QI, Z., PONNIAH, S., HONG, W. & HUNZIKER, W. 2007. Glomerulocystic kidney disease in mice with a targeted inactivation of Wwtr1. *Proc Natl Acad Sci U S A,* 104**,** 1631-6.

HOTULAINEN, P. & LAPPALAINEN, P. 2006. Stress fibers are generated by two distinct actin assembly mechanisms in motile cells. *J Cell Biol,* 173**,** 383-94.

HSU, C. S., CHAO, Y. C., LIN, H. H., CHEN, D. S. & KAO, J. H. 2015. Systematic Review: Impact of Interferon-based Therapy on HCV-related Hepatocellular Carcinoma. *Sci Rep,* 5**,** 9954.

HSU, M., ZHANG, J., FLINT, M., LOGVINOFF, C., CHENG-MAYER, C., RICE, C. M. & MCKEATING, J. A. 2003. Hepatitis C virus glycoproteins mediate pH-dependent cell entry of pseudotyped retroviral particles. *Proc Natl Acad Sci U S A,* 100**,** 7271-6.

HSU, T. H., YANG, C. Y., YEH, T. H., HUANG, Y. C., WANG, T. W. & YU, J. Y. 2017. The Hippo pathway acts downstream of the Hedgehog signaling to regulate follicle stem cell maintenance in the Drosophila ovary. *Sci Rep,* 7**,** 4480.

HU, B., XIE, S., HU, Y., CHEN, W., CHEN, X., ZHENG, Y. & WU, X. 2017. Hepatitis C virus NS4B protein induces epithelial-mesenchymal transition by upregulation of Snail. *Virol J,* 14**,** 83.

HUANG, J. & KALDERON, D. 2014. Coupling of Hedgehog and Hippo pathways promotes stem cell maintenance by stimulating proliferation. *J Cell Biol,* 205**,** 325-38.

HUANG, L. R. & HSU, H. C. 1995. Cloning and expression of CD24 gene in human hepatocellular carcinoma: a potential early tumor marker gene correlates with p53 mutation and tumor differentiation. *Cancer Res,* 55**,** 4717-21.

HUANG, W., LV, X., LIU, C., ZHA, Z., ZHANG, H., JIANG, Y., XIONG, Y., LEI, Q. Y. & GUAN, K. L. 2012. The N-terminal phosphodegron targets TAZ/WWTR1 protein for SCFbeta-TrCP-dependent degradation in response to phosphatidylinositol 3-kinase inhibition. *J Biol Chem,* 287**,** 26245-53.

HUCH, M., DORRELL, C., BOJ, S. F., VAN ES, J. H., LI, V. S., VAN DE WETERING, M., SATO, T., HAMER, K., SASAKI, N., FINEGOLD, M. J., HAFT, A., VRIES, R. G., GROMPE, M. & CLEVERS, H. 2013. In vitro expansion of single Lgr5+ liver stem cells induced by Wnt-driven regeneration. *Nature,* 494**,** 247-50.

HUGLE, T., FEHRMANN, F., BIECK, E., KOHARA, M., KRAUSSLICH, H. G., RICE, C. M., BLUM, H. E. & MORADPOUR, D. 2001. The hepatitis C virus nonstructural protein 4B is an integral endoplasmic reticulum membrane protein. *Virology,* 284**,** 70-81.

HUYNH, H., NGUYEN, T. T., CHOW, K. H., TAN, P. H., SOO, K. C. & TRAN, E. 2003. Over-expression of the mitogen-activated protein kinase (MAPK) kinase (MEK)-MAPK in hepatocellular carcinoma: its role in tumor progression and apoptosis. *BMC Gastroenterol,* 3**,** 19.

HWANG, E., RYU, K. S., PAAKKONEN, K., GUNTERT, P., CHEONG, H. K., LIM, D. S., LEE, J. O., JEON, Y. H. & CHEONG, C. 2007. Structural insight into dimeric interaction of the SARAH domains from Mst1 and RASSF family proteins in the apoptosis pathway. *Proc Natl Acad Sci U S A,* 104**,** 9236-41.

IHARA, A., KOIZUMI, H., HASHIZUME, R. & UCHIKOSHI, T. 1996. Expression of epithelial cadherin and alpha- and beta-catenins in nontumoral livers and hepatocellular carcinomas. *Hepatology,* 23**,** 1441-7.

IHN, H. 2002. Pathogenesis of fibrosis: role of TGF-beta and CTGF. *Curr Opin Rheumatol,* 14**,** 681-5.

IKEDA, M., KAWATA, A., NISHIKAWA, M., TATEISHI, Y., YAMAGUCHI, M., NAKAGAWA, K., HIRABAYASHI, S., BAO, Y., HIDAKA, S., HIRATA, Y. & HATA, Y. 2009. Hippo pathway-dependent and -independent roles of RASSF6. *Sci Signal,* 2**,** ra59.

ILBOUDO, A., NAULT, J. C., DUBOIS-POT-SCHNEIDER, H., CORLU, A., ZUCMAN-ROSSI, J., SAMSON, M. & LE SEYEC, J. 2014. Overexpression of phosphatidylinositol 4-kinase type IIIalpha is associated with undifferentiated status and poor prognosis of human hepatocellular carcinoma. *BMC Cancer,* 14**,** 7.

INTERNATIONAL AGENCY FOR RESEARCH ON CANCER. 2010. *WHO Classification of Tumours* Geneva, World Health Organization.

INTERNATIONAL AGENCY FOR RESEARCH ON CANCER. 2014. World Cancer Reports. *In:* STEWART, B. W. & WILD, C. P. (eds.) *World Cancer Report 2014.*

IOANNOU, G. N., GREEN, P. K. & BERRY, K. 2017. HCV eradication induced by direct-acting antiviral agents reduces the risk of hepatocellular carcinoma. *J Hepatol*.

IQBAL, J., MCRAE, S., BANAUDHA, K., MAI, T. & WARIS, G. 2013. Mechanism of hepatitis C virus (HCV)-induced osteopontin and its role in epithelial to mesenchymal transition of hepatocytes. *J Biol Chem,* 288**,** 36994-7009.

ISHIDO, S., FUJITA, T. & HOTTA, H. 1998. Complex formation of NS5B with NS3 and NS4A proteins of hepatitis C virus. *Biochem Biophys Res Commun,* 244**,** 35-40.

ISHIKAWA, T., FACTOR, V. M., MARQUARDT, J. U., RAGGI, C., SEO, D., KITADE, M., CONNER, E. A. & THORGEIRSSON, S. S. 2012. Hepatocyte growth factor/c-met signaling is required for stem-cell-mediated liver regeneration in mice. *Hepatology,* 55**,** 1215-26.

ITO, M., MASUMI, A., MOCHIDA, K., KUKIHARA, H., MORIISHI, K., MATSUURA, Y., YAMAGUCHI, K. & MIZUOCHI, T. 2010a. Peripheral B cells may serve as a reservoir for persistent hepatitis C virus infection. *J Innate Immun,* 2**,** 607-17.

ITO, M., MURAKAMI, K., SUZUKI, T., MOCHIDA, K., SUZUKI, M., IKEBUCHI, K., YAMAGUCHI, K. & MIZUOCHI, T. 2010b. Enhanced expression of lymphomagenesis-related genes in peripheral blood B cells of chronic hepatitis C patients. *Clin Immunol,* 135**,** 459-65.

ITO, T., TAHARA, S. M. & LAI, M. M. 1998a. The 3'-untranslated region of hepatitis C virus RNA enhances translation from an internal ribosomal entry site. *J Virol,* 72**,** 8789-96.

ITO, Y., MATSUI, T., KAMIYA, A., KINOSHITA, T. & MIYAJIMA, A. 2000. Retroviral gene transfer of signaling molecules into murine fetal hepatocytes defines distinct roles for the STAT3 and ras pathways during hepatic development. *Hepatology,* 32**,** 1370-6.

ITO, Y., SASAKI, Y., HORIMOTO, M., WADA, S., TANAKA, Y., KASAHARA, A., UEKI, T., HIRANO, T., YAMAMOTO, H., FUJIMOTO, J., OKAMOTO, E., HAYASHI, N. & HORI, M. 1998b. Activation of mitogen-activated protein kinases/extracellular signal-regulated kinases in human hepatocellular carcinoma. *Hepatology,* 27**,** 951-8.

JANG, E. J., JEONG, H., HAN, K. H., KWON, H. M., HONG, J. H. & HWANG, E. S. 2012. TAZ suppresses NFAT5 activity through tyrosine phosphorylation. *Mol Cell Biol,* 32**,** 4925-32.

JIE, L., FAN, W., WEIQI, D., YINGQUN, Z., LING, X., MIAO, S., PING, C. & CHUANYONG, G. 2013. The hippo-yes association protein pathway in liver cancer. *Gastroenterol Res Pract,* 2013**,** 187070.

JIRASKO, V., MONTSERRET, R., LEE, J. Y., GOUTTENOIRE, J., MORADPOUR, D., PENIN, F. & BARTENSCHLAGER, R. 2010. Structural and functional studies of nonstructural protein 2 of the hepatitis C virus reveal its key role as organizer of virion assembly. *PLoS Pathog,* 6**,** e1001233.

JOHNSON, D. E., O'KEEFE, R. A. & GRANDIS, J. R. 2018. Targeting the IL-6/JAK/STAT3 signalling axis in cancer. *Nat Rev Clin Oncol,* 15**,** 234-248.

JONES, C. T., CATANESE, M. T., LAW, L. M., KHETANI, S. R., SYDER, A. J., PLOSS, A., OH, T. S., SCHOGGINS, J. W., MACDONALD, M. R., BHATIA, S. N. & RICE, C. M. 2010. Real-time imaging of hepatitis C virus infection using a fluorescent cell-based reporter system. *Nat Biotechnol,* 28**,** 167-71.

JONES, C. T., MURRAY, C. L., EASTMAN, D. K., TASSELLO, J. & RICE, C. M. 2007. Hepatitis C virus p7 and NS2 proteins are essential for production of infectious virus. *J Virol,* 81**,** 8374-83.

JOPLING, C. L. 2008. Regulation of hepatitis C virus by microRNA-122. *Biochem Soc Trans,* 36**,** 1220-3.

JUNG, C. J., IYENGAR, S., BLAHNIK, K. R., AJUHA, T. P., JIANG, J. X., FARNHAM, P. J. & ZERN, M. 2011. Epigenetic modulation of miR-122 facilitates

human embryonic stem cell self-renewal and hepatocellular carcinoma proliferation. *PLoS One,* 6**,** e27740.

JUNG, J., ZHENG, M., GOLDFARB, M. & ZARET, K. S. 1999. Initiation of mammalian liver development from endoderm by fibroblast growth factors. *Science,* 284**,** 1998-2003.

JUNG, K. H., MCCARTHY, R. L., ZHOU, C., UPRETY, N., BARTON, M. C. & BERETTA, L. 2016. MicroRNA Regulates Hepatocytic Differentiation of Progenitor Cells by Targeting YAP1. *Stem Cells,* 34**,** 1284-96.

JUNQUEIRA, L. C. U. & MESCHER, A. L. 2013. *Junqueira's Basic Histology: Text and Atlas,* New York, N.Y., McGraw-Hill Medical

KAAN, H. Y. K., CHAN, S. W., TAN, S. K. J., GUO, F., LIM, C. J., HONG, W. & SONG, H. 2017. Crystal structure of TAZ-TEAD complex reveals a distinct interaction mode from that of YAP-TEAD complex. *Sci Rep,* 7**,** 2035.

KALLIS, Y. N., ROBSON, A. J., FALLOWFIELD, J. A., THOMAS, H. C., ALISON, M. R., WRIGHT, N. A., GOLDIN, R. D., IREDALE, J. P. & FORBES, S. J. 2011. Remodelling of extracellular matrix is a requirement for the hepatic progenitor cell response. *Gut,* 60**,** 525-33.

KAMIYA, A., KINOSHITA, T., ITO, Y., MATSUI, T., MORIKAWA, Y., SENBA, E., NAKASHIMA, K., TAGA, T., YOSHIDA, K., KISHIMOTO, T. & MIYAJIMA, A. 1999. Fetal liver development requires a paracrine action of oncostatin M through the gp130 signal transducer. *Embo j,* 18**,** 2127-36.

KANAI, F., MARIGNANI, P. A., SARBASSOVA, D., YAGI, R., HALL, R. A., DONOWITZ, M., HISAMINATO, A., FUJIWARA, T., ITO, Y., CANTLEY, L. C. & YAFFE, M. B. 2000. TAZ: a novel transcriptional co-activator regulated by interactions with 14-3-3 and PDZ domain proteins. *EMBO J,* 19**,** 6778-91.

KANEHISA, M. & GOTO, S. 2000. KEGG: kyoto encyclopedia of genes and genomes. *Nucleic Acids Res,* 28**,** 27-30.

KANNAN, R. P., HENSLEY, L. L., EVERS, L. E., LEMON, S. M. & MCGIVERN, D. R. 2011. Hepatitis C virus infection causes cell cycle arrest at the level of initiation of mitosis. *J Virol,* 85**,** 7989-8001.

KANWAL, F., KRAMER, J., ASCH, S. M., CHAYANUPATKUL, M., CAO, Y. & EL-SERAG, H. B. 2017. Risk of Hepatocellular Cancer in HCV Patients Treated With Direct-Acting Antiviral Agents. *Gastroenterology,* 153**,** 996-1005 e1.

KAPLAN, G. & RACANIELLO, V. R. 1988. Construction and characterization of poliovirus subgenomic replicons. *J Virol,* 62**,** 1687-96.

KAPOOR, A., SIMMONDS, P., GEROLD, G., QAISAR, N., JAIN, K., HENRIQUEZ, J. A., FIRTH, C., HIRSCHBERG, D. L., RICE, C. M., SHIELDS, S. & LIPKIN, W. I. 2011. Characterization of a canine homolog of hepatitis C virus. *Proc Natl Acad Sci U S A,* 108**,** 11608-13.

KAPOOR, A., SIMMONDS, P., SCHEEL, T. K., HJELLE, B., CULLEN, J. M., BURBELO, P. D., CHAUHAN, L. V., DURAISAMY, R., SANCHEZ LEON, M., JAIN, K., VANDEGRIFT, K. J., CALISHER, C. H., RICE, C. M. & LIPKIN, W. I. 2013. Identification of rodent homologs of hepatitis C virus and pegiviruses. *MBio,* 4**,** e00216-13.

KARIDIS, N. P., DELLADETSIMA, I. & THEOCHARIS, S. 2015. Hepatocyte Turnover in Chronic HCV-Induced Liver Injury and Cirrhosis. *Gastroenterol Res Pract,* 2015**,** 654105.

KATO, N., HIJIKATA, M., OOTSUYAMA, Y., NAKAGAWA, M., OHKOSHI, S., SUGIMURA, T. & SHIMOTOHNO, K. 1990. Molecular cloning of the human

hepatitis C virus genome from Japanese patients with non-A, non-B hepatitis. *Proc Natl Acad Sci U S A,* 87**,** 9524-8.

KATO, N., NAKAZAWA, T., MIZUTANI, T. & SHIMOTOHNO, K. 1995. Susceptibility of human T-lymphotropic virus type I infected cell line MT-2 to hepatitis C virus infection. *Biochem Biophys Res Commun,* 206**,** 863-9.

KATO, T., DATE, T., MIYAMOTO, M., FURUSAKA, A., TOKUSHIGE, K., MIZOKAMI, M. & WAKITA, T. 2003. Efficient replication of the genotype 2a hepatitis C virus subgenomic replicon. *Gastroenterology,* 125**,** 1808-17.

KATO, T., FURUSAKA, A., MIYAMOTO, M., DATE, T., YASUI, K., HIRAMOTO, J., NAGAYAMA, K., TANAKA, T. & WAKITA, T. 2001. Sequence analysis of hepatitis C virus isolated from a fulminant hepatitis patient. *J Med Virol,* 64**,** 334-9.

KAUL, A., STAUFFER, S., BERGER, C., PERTEL, T., SCHMITT, J., KALLIS, S., ZAYAS, M., LOHMANN, V., LUBAN, J. & BARTENSCHLAGER, R. 2009. Essential role of cyclophilin A for hepatitis C virus replication and virus production and possible link to polyprotein cleavage kinetics. *PLoS Pathog,* 5**,** e1000546.

KAWAI, H. F., KANEKO, S., HONDA, M., SHIROTA, Y. & KOBAYASHI, K. 2001. alpha-fetoprotein-producing hepatoma cell lines share common expression profiles of genes in various categories demonstrated by cDNA microarray analysis. *Hepatology,* 33**,** 676-91.

KAWAI, T., YASUCHIKA, K., ISHII, T., KATAYAMA, H., YOSHITOSHI, E. Y., OGISO, S., KITA, S., YASUDA, K., FUKUMITSU, K., MIZUMOTO, M., HATANO, E. & UEMOTO, S. 2015. Keratin 19, a Cancer Stem Cell Marker in Human Hepatocellular Carcinoma. *Clin Cancer Res,* 21**,** 3081-91.

KAWAMOTO, H., KOIZUMI, H. & UCHIKOSHI, T. 1997. Expression of the G2-M checkpoint regulators cyclin B1 and cdc2 in nonmalignant and malignant human breast lesions: immunocytochemical and quantitative image analyses. *Am J Pathol,* 150**,** 15-23.

KENG, V. W., YAGI, H., IKAWA, M., NAGANO, T., MYINT, Z., YAMADA, K., TANAKA, T., SATO, A., MURAMATSU, I., OKABE, M., SATO, M. & NOGUCHI, T. 2000. Homeobox gene Hex is essential for onset of mouse embryonic liver development and differentiation of the monocyte lineage. *Biochem Biophys Res Commun,* 276**,** 1155-61.

KESKINEN, P., NYQVIST, M., SARENEVA, T., PIRHONEN, J., MELEN, K. & JULKUNEN, I. 1999. Impaired antiviral response in human hepatoma cells. *Virology,* 263**,** 364-75.

KHROMYKH, A. A. & WESTAWAY, E. G. 1997. Subgenomic replicons of the flavivirus Kunjin: construction and applications. *J Virol,* 71**,** 1497-505.

KIEFT, J. S., ZHOU, K., JUBIN, R. & DOUDNA, J. A. 2001. Mechanism of ribosome recruitment by hepatitis C IRES RNA. *Rna,* 7**,** 194-206.

KIM, M. & JHO, E. H. 2014. Cross-talk between Wnt/beta-catenin and Hippo signaling pathways: a brief review. *BMB Rep,* 47**,** 540-5.

KIM, M. K., JANG, J. W. & BAE, S. C. 2018. DNA binding partners of YAP/TAZ. *BMB Rep,* 51**,** 126-133.

KIM, N. G. & GUMBINER, B. M. 2015. Adhesion to fibronectin regulates Hippo signaling via the FAK-Src-PI3K pathway. *J Cell Biol,* 210**,** 503-15.

KIM, W., KHAN, S. K., GVOZDENOVIC-JEREMIC, J., KIM, Y., DAHLMAN, J., KIM, H., PARK, O., ISHITANI, T., JHO, E. H., GAO, B. & YANG, Y. 2017. Hippo signaling interactions with Wnt/beta-catenin and Notch signaling repress liver tumorigenesis. *J Clin Invest,* 127**,** 137-152.

KITADE, M., FACTOR, V. M., ANDERSEN, J. B., TOMOKUNI, A., KAJI, K., AKITA, H., HOLCZBAUER, A., SEO, D., MARQUARDT, J. U., CONNER, E. A., LEE, S. B., LEE, Y. H. & THORGEIRSSON, S. S. 2013. Specific fate decisions in adult hepatic progenitor cells driven by MET and EGFR signaling. *Genes Dev,* 27**,** 1706-17.

KLAAS, M., KANGUR, T., VIIL, J., MAEMETS-ALLAS, K., MINAJEVA, A., VADI, K., ANTSOV, M., LAPIDUS, N., JARVEKULG, M. & JAKS, V. 2016. The alterations in the extracellular matrix composition guide the repair of damaged liver tissue. *Sci Rep,* 6**,** 27398.

KLEIN, P. J., SCHMIDT, C. M., WIESENAUER, C. A., CHOI, J. N., GAGE, E. A., YIP-SCHNEIDER, M. T., WIEBKE, E. A., WANG, Y., OMER, C. & SEBOLT-LEOPOLD, J. S. 2006. The effects of a novel MEK inhibitor PD184161 on MEK-ERK signaling and growth in human liver cancer. *Neoplasia,* 8**,** 1-8.

KNIGHT, B., YEOH, G. C., HUSK, K. L., LY, T., ABRAHAM, L. J., YU, C., RHIM, J. A. & FAUSTO, N. 2000. Impaired preneoplastic changes and liver tumor formation in tumor necrosis factor receptor type 1 knockout mice. *J Exp Med,* 192**,** 1809-18.

KNOWLES, B. B., HOWE, C. C. & ADEN, D. P. 1980. Human hepatocellular carcinoma cell lines secrete the major plasma proteins and hepatitis B surface antigen. *Science,* 209**,** 497-9.

KOIKE, K. 2007. Pathogenesis of HCV-associated HCC: Dual-pass carcinogenesis through activation of oxidative stress and intracellular signaling. *Hepatol Res,* 37 Suppl 2**,** S115-20.

KOLYKHALOV, A. A., AGAPOV, E. V., BLIGHT, K. J., MIHALIK, K., FEINSTONE, S. M. & RICE, C. M. 1997. Transmission of hepatitis C by intrahepatic inoculation with transcribed RNA. *Science,* 277**,** 570-4.

KOLYKHALOV, A. A., FEINSTONE, S. M. & RICE, C. M. 1996. Identification of a highly conserved sequence element at the 3' terminus of hepatitis C virus genome RNA. *J Virol,* 70**,** 3363-71.

KOWDLEY, K. V. 2004. Iron, hemochromatosis, and hepatocellular carcinoma. *Gastroenterology,* 127**,** S79-86.

KRIEGER, N., LOHMANN, V. & BARTENSCHLAGER, R. 2001. Enhancement of hepatitis C virus RNA replication by cell culture-adaptive mutations. *J Virol,* 75**,** 4614-24.

KRISTIANSEN, G., DENKERT, C., SCHLUNS, K., DAHL, E., PILARSKY, C. & HAUPTMANN, S. 2002. CD24 is expressed in ovarian cancer and is a new independent prognostic marker of patient survival. *Am J Pathol,* 161**,** 1215-21.

KRZOWSKA-FIRYCH, J. M., LUCAS, C., LUCAS, G. & TOMASIEWICZ, K. 2018. Hepatitis E - A new era in understanding. *Ann Agric Environ Med,* 25**,** 250-254.

KUBO, M., HANADA, T. & YOSHIMURA, A. 2003. Suppressors of cytokine signaling and immunity. *Nat Immunol,* 4**,** 1169-76.

KULESHOV, M. V., JONES, M. R., ROUILLARD, A. D., FERNANDEZ, N. F., DUAN, Q., WANG, Z., KOPLEV, S., JENKINS, S. L., JAGODNIK, K. M., LACHMANN, A., MCDERMOTT, M. G., MONTEIRO, C. D., GUNDERSEN, G. W. & MA'AYAN, A. 2016. Enrichr: a comprehensive gene set enrichment analysis web server 2016 update. *Nucleic Acids Res,* 44**,** W90-7.

KUMAR, M., JORDAN, N., MELTON, D. & GRAPIN-BOTTON, A. 2003. Signals from lateral plate mesoderm instruct endoderm toward a pancreatic fate. *Dev Biol,* 259**,** 109-22.

KUSHNER, J., BRADLEY, G., YOUNG, B. & JORDAN, R. C. 1999. Aberrant expression of cyclin A and cyclin B1 proteins in oral carcinoma. *J Oral Pathol Med,* 28**,** 77-81.

KWUN, H. J., JUNG, E. Y., AHN, J. Y., LEE, M. N. & JANG, K. L. 2001. p53-dependent transcriptional repression of p21(waf1) by hepatitis C virus NS3. *J Gen Virol,* 82**,** 2235-41.

KYRMIZI, I., HATZIS, P., KATRAKILI, N., TRONCHE, F., GONZALEZ, F. J. & TALIANIDIS, I. 2006. Plasticity and expanding complexity of the hepatic transcription factor network during liver development. *Genes Dev,* 20**,** 2293-305.

LACHENMAYER, A., ALSINET, C., SAVIC, R., CABELLOS, L., TOFFANIN, S., HOSHIDA, Y., VILLANUEVA, A., MINGUEZ, B., NEWELL, P., TSAI, H. W., BARRETINA, J., THUNG, S., WARD, S. C., BRUIX, J., MAZZAFERRO, V., SCHWARTZ, M., FRIEDMAN, S. L. & LLOVET, J. M. 2012. Wnt-pathway activation in two molecular classes of hepatocellular carcinoma and experimental modulation by sorafenib. *Clin Cancer Res,* 18**,** 4997-5007.

LACHMANN, A., XU, H., KRISHNAN, J., BERGER, S. I., MAZLOOM, A. R. & MA'AYAN, A. 2010. ChEA: transcription factor regulation inferred from integrating genome-wide ChIP-X experiments. *Bioinformatics,* 26**,** 2438-44.

LADE, A. G. & MONGA, S. P. 2011. Beta-catenin signaling in hepatic development and progenitors: which way does the WNT blow? *Dev Dyn,* 240**,** 486-500.

LAN, K. H., SHEU, M. L., HWANG, S. J., YEN, S. H., CHEN, S. Y., WU, J. C., WANG, Y. J., KATO, N., OMATA, M., CHANG, F. Y. & LEE, S. D. 2002. HCV NS5A interacts with p53 and inhibits p53-mediated apoptosis. *Oncogene,* 21**,** 4801-11.

LASKUS, T., WILKINSON, J., GALLEGOS-OROZCO, J. F., RADKOWSKI, M., ADAIR, D. M., NOWICKI, M., OPERSKALSKI, E., BUSKELL, Z., SEEFF, L. B., VARGAS, H. & RAKELA, J. 2004. Analysis of hepatitis C virus quasispecies transmission and evolution in patients infected through blood transfusion. *Gastroenterology,* 127**,** 764-76.

LAUDADIO, I., MANFROID, I., ACHOURI, Y., SCHMIDT, D., WILSON, M. D., CORDI, S., THORREZ, L., KNOOPS, L., JACQUEMIN, P., SCHUIT, F., PIERREUX, C. E., ODOM, D. T., PEERS, B. & LEMAIGRE, F. P. 2012. A feedback loop between the liver-enriched transcription factor network and miR-122 controls hepatocyte differentiation. *Gastroenterology,* 142**,** 119-29.

LAVILLETTE, D., PECHEUR, E. I., DONOT, P., FRESQUET, J., MOLLE, J., CORBAU, R., DREUX, M., PENIN, F. & COSSET, F. L. 2007. Characterization of fusion determinants points to the involvement of three discrete regions of both E1 and E2 glycoproteins in the membrane fusion process of hepatitis C virus. *J Virol,* 81**,** 8752-65.

LAWITZ, E. J., GRUENER, D., HILL, J. M., MARBURY, T., MOOREHEAD, L., MATHIAS, A., CHENG, G., LINK, J. O., WONG, K. A., MO, H., MCHUTCHISON, J. G. & BRAINARD, D. M. 2012. A phase 1, randomized, placebo-controlled, 3-day, dose-ranging study of GS-5885, an NS5A inhibitor, in patients with genotype 1 hepatitis C. *J Hepatol,* 57**,** 24-31.

LAWSON, J. A., FISHER, M. A., SIMMONS, C. A., FARHOOD, A. & JAESCHKE, H. 1998. Parenchymal cell apoptosis as a signal for sinusoidal sequestration and transendothelial migration of neutrophils in murine models of endotoxin and Fas-antibody-induced liver injury. *Hepatology,* 28**,** 761-7.

LAZARO, C. A., CROAGER, E. J., MITCHELL, C., CAMPBELL, J. S., YU, C., FORAKER, J., RHIM, J. A., YEOH, G. C. & FAUSTO, N. 2003. Establishment,

characterization, and long-term maintenance of cultures of human fetal hepatocytes. *Hepatology,* 38**,** 1095-106.

LE LAY, J. & KAESTNER, K. H. 2010. The Fox genes in the liver: from organogenesis to functional integration. *Physiol Rev,* 90**,** 1-22.

LEASK, A. & ABRAHAM, D. J. 2006. All in the CCN family: essential matricellular signaling modulators emerge from the bunker. *J Cell Sci,* 119**,** 4803-10.

LEE, D. H., PARK, J. O., KIM, T. S., KIM, S. K., KIM, T. H., KIM, M. C., PARK, G. S., KIM, J. H., KUNINAKA, S., OLSON, E. N., SAYA, H., KIM, S. Y., LEE, H. & LIM, D. S. 2016. LATS-YAP/TAZ controls lineage specification by regulating TGFbeta signaling and Hnf4alpha expression during liver development. *Nat Commun,* 7**,** 11961.

LEE, J. H., KIM, T. S., YANG, T. H., KOO, B. K., OH, S. P., LEE, K. P., OH, H. J., LEE, S. H., KONG, Y. Y., KIM, J. M. & LIM, D. S. 2008. A crucial role of WW45 in developing epithelial tissues in the mouse. *EMBO J,* 27**,** 1231-42.

LEE, J. H., PARK, H. J., KIM, Y. A., LEE, D. H., NOH, J. K., KWON, C. H., JUNG, S. M. & LEE, S. K. 2012. The phenotypic characteristic of liver-derived stem cells from adult human deceased donor liver. *Transplant Proc,* 44**,** 1110-2.

LEE, J. S., HEO, J., LIBBRECHT, L., CHU, I. S., KAPOSI-NOVAK, P., CALVISI, D. F., MIKAELYAN, A., ROBERTS, L. R., DEMETRIS, A. J., SUN, Z., NEVENS, F., ROSKAMS, T. & THORGEIRSSON, S. S. 2006. A novel prognostic subtype of human hepatocellular carcinoma derived from hepatic progenitor cells. *Nat Med,* 12**,** 410-6.

LEE, K. P., LEE, J. H., KIM, T. S., KIM, T. H., PARK, H. D., BYUN, J. S., KIM, M. C., JEONG, W. I., CALVISI, D. F., KIM, J. M. & LIM, D. S. 2010. The Hippo-Salvador pathway restrains hepatic oval cell proliferation, liver size, and liver tumorigenesis. *Proc Natl Acad Sci U S A,* 107**,** 8248-53.

LEE, S. S., HADENGUE, A., MOREAU, R., SAYEGH, R., HILLON, P. & LEBREC, D. 1988. Postprandial hemodynamic responses in patients with cirrhosis. *Hepatology,* 8**,** 647-51.

LEE, T. K., CASTILHO, A., CHEUNG, V. C., TANG, K. H., MA, S. & NG, I. O. 2011. CD24(+) liver tumor-initiating cells drive self-renewal and tumor initiation through STAT3-mediated NANOG regulation. *Cell Stem Cell,* 9**,** 50-63.

LEMAIGRE, F. P. 2009. Mechanisms of liver development: concepts for understanding liver disorders and design of novel therapies. *Gastroenterology,* 137**,** 62-79.

LEMON, S. M., OTT, J. J., VAN DAMME, P. & SHOUVAL, D. 2017. Type A viral hepatitis: A summary and update on the molecular virology, epidemiology, pathogenesis and prevention. *J Hepatol*.

LERAT, H., HONDA, M., BEARD, M. R., LOESCH, K., SUN, J., YANG, Y., OKUDA, M., GOSERT, R., XIAO, S. Y., WEINMAN, S. A. & LEMON, S. M. 2002. Steatosis and liver cancer in transgenic mice expressing the structural and nonstructural proteins of hepatitis C virus. *Gastroenterology,* 122**,** 352-65.

LESBURG, C. A., CABLE, M. B., FERRARI, E., HONG, Z., MANNARINO, A. F. & WEBER, P. C. 1999. Crystal structure of the RNA-dependent RNA polymerase from hepatitis C virus reveals a fully encircled active site. *Nat Struct Biol,* 6**,** 937-43.

LEUNG, T. W., LIN, S. S., TSANG, A. C., TONG, C. S., CHING, J. C., LEUNG, W. Y., GIMLICH, R., WONG, G. G. & YAO, K. M. 2001. Over-expression of FoxM1 stimulates cyclin B1 expression. *FEBS Lett,* 507**,** 59-66.

LEVY, D., ADAMOVICH, Y., REUVEN, N. & SHAUL, Y. 2008. Yap1 phosphorylation by c-Abl is a critical step in selective activation of proapoptotic genes in response to DNA damage. *Mol Cell,* 29**,** 350-61.

LEWIS, S., ROAYAIE, S., WARD, S. C., SHYKNEVSKY, I., JIBARA, G. & TAOULI, B. 2013. Hepatocellular carcinoma in chronic hepatitis C in the absence of advanced fibrosis or cirrhosis. *AJR Am J Roentgenol,* 200**,** W610-6.

LI, H., HU, B., ZHOU, Z. Q., GUAN, J., ZHANG, Z. Y. & ZHOU, G. W. 2015a. Hepatitis C virus infection and the risk of intrahepatic cholangiocarcinoma and extrahepatic cholangiocarcinoma: evidence from a systematic review and meta-analysis of 16 case-control studies. *World J Surg Oncol,* 13**,** 161.

LI, H., WOLFE, A., SEPTER, S., EDWARDS, G., ZHONG, X., ABDULKARIM, A. B., RANGANATHAN, S. & APTE, U. 2012. Deregulation of Hippo kinase signalling in human hepatic malignancies. *Liver Int,* 32**,** 38-47.

LI, Q., BRASS, A. L., NG, A., HU, Z., XAVIER, R. J., LIANG, T. J. & ELLEDGE, S. J. 2009. A genome-wide genetic screen for host factors required for hepatitis C virus propagation. *Proc Natl Acad Sci U S A,* 106**,** 16410-5.

LI, Q., SODROSKI, C., LOWEY, B., SCHWEITZER, C. J., CHA, H., ZHANG, F. & LIANG, T. J. 2016. Hepatitis C virus depends on E-cadherin as an entry factor and regulates its expression in epithelial-to-mesenchymal transition. *Proc Natl Acad Sci U S A,* 113**,** 7620-5.

LI, W., COOPER, J., ZHOU, L., YANG, C., ERDJUMENT-BROMAGE, H., ZAGZAG, D., SNUDERL, M., LADANYI, M., HANEMANN, C. O., ZHOU, P., KARAJANNIS, M. A. & GIANCOTTI, F. G. 2014. Merlin/NF2 loss-driven tumorigenesis linked to CRL4(DCAF1)-mediated inhibition of the hippo pathway kinases Lats1 and 2 in the nucleus. *Cancer Cell,* 26**,** 48-60.

LI, W. C., YE, S. L., SUN, R. X., LIU, Y. K., TANG, Z. Y., KIM, Y., KARRAS, J. G. & ZHANG, H. 2006a. Inhibition of growth and metastasis of human hepatocellular carcinoma by antisense oligonucleotide targeting signal transducer and activator of transcription 3. *Clin Cancer Res,* 12**,** 7140-8.

LI, W. L., SU, J., YAO, Y. C., TAO, X. R., YAN, Y. B., YU, H. Y., WANG, X. M., LI, J. X., YANG, Y. J., LAU, J. T. & HU, Y. P. 2006b. Isolation and characterization of bipotent liver progenitor cells from adult mouse. *Stem Cells,* 24**,** 322-32.

LI, X., TAO, J., CIGLIANO, A., SINI, M., CALDERARO, J., AZOULAY, D., WANG, C., LIU, Y., JIANG, L., EVERT, K., DEMARTIS, M. I., RIBBACK, S., UTPATEL, K., DOMBROWSKI, F., EVERT, M., CALVISI, D. F. & CHEN, X. 2015b. Co-activation of PIK3CA and Yap promotes development of hepatocellular and cholangiocellular tumors in mouse and human liver. *Oncotarget,* 6**,** 10102-15.

LI, Y., ZHOU, H., LI, F., CHAN, S. W., LIN, Z., WEI, Z., YANG, Z., GUO, F., LIM, C. J., XING, W., SHEN, Y., HONG, W., LONG, J. & ZHANG, M. 2015c. Angiomotin binding-induced activation of Merlin/NF2 in the Hippo pathway. *Cell Res,* 25**,** 801-17.

LI, Z., ZHAO, B., WANG, P., CHEN, F., DONG, Z., YANG, H., GUAN, K. L. & XU, Y. 2010. Structural insights into the YAP and TEAD complex. *Genes Dev,* 24**,** 235-40.

LINDENBACH, B. D. 2013. Virion assembly and release. *Curr Top Microbiol Immunol,* 369**,** 199-218.

LINDENBACH, B. D., EVANS, M. J., SYDER, A. J., WOLK, B., TELLINGHUISEN, T. L., LIU, C. C., MARUYAMA, T., HYNES, R. O., BURTON, D. R., MCKEATING, J. A. & RICE, C. M. 2005. Complete replication of hepatitis C virus in cell culture. *Science,* 309**,** 623-6.

LINDENBACH, B. D., MEULEMAN, P., PLOSS, A., VANWOLLEGHEM, T., SYDER, A. J., MCKEATING, J. A., LANFORD, R. E., FEINSTONE, S. M., MAJOR, M. E., LEROUX-ROELS, G. & RICE, C. M. 2006. Cell culture-grown hepatitis C virus is infectious in vivo and can be recultured in vitro. *Proc Natl Acad Sci U S A,* 103**,** 3805-9.

LINDENBACH, B. D., PRAGAI, B. M., MONTSERRET, R., BERAN, R. K., PYLE, A. M., PENIN, F. & RICE, C. M. 2007. The C terminus of hepatitis C virus NS4A encodes an electrostatic switch that regulates NS5A hyperphosphorylation and viral replication. *J Virol,* 81**,** 8905-18.

LIU-CHITTENDEN, Y., HUANG, B., SHIM, J. S., CHEN, Q., LEE, S. J., ANDERS, R. A., LIU, J. O. & PAN, D. 2012. Genetic and pharmacological disruption of the TEAD-YAP complex suppresses the oncogenic activity of YAP. *Genes Dev,* 26**,** 1300-5.

LIU, A. Y., CAI, Y., MAO, Y., LIN, Y., ZHENG, H., WU, T., HUANG, Y., FANG, X., LIN, S., FENG, Q., HUANG, Z., YANG, T., LUO, Q. & OUYANG, G. 2014. Twist2 promotes self-renewal of liver cancer stem-like cells by regulating CD24. *Carcinogenesis,* 35**,** 537-45.

LIU, C., ZHENG, S., SHEN, H., XU, K., CHEN, J., LI, H., XU, Y., XU, A., CHEN, B., KAKU, H., NASU, Y., KUMON, H., HUANG, P. & WATANABE, M. 2013. Clinical significance of CD24 as a predictor of bladder cancer recurrence. *Oncol Lett,* 6**,** 96-100.

LIU, C. Y., ZHA, Z. Y., ZHOU, X., ZHANG, H., HUANG, W., ZHAO, D., LI, T., CHAN, S. W., LIM, C. J., HONG, W., ZHAO, S., XIONG, Y., LEI, Q. Y. & GUAN, K. L. 2010. The hippo tumor pathway promotes TAZ degradation by phosphorylating a phosphodegron and recruiting the SCF{beta}-TrCP E3 ligase. *J Biol Chem,* 285**,** 37159-69.

LIU, G., YU, F. X., KIM, Y. C., MENG, Z., NAIPAUER, J., LOONEY, D. J., LIU, X., GUTKIND, J. S., MESRI, E. A. & GUAN, K. L. 2015. Kaposi sarcoma-associated herpesvirus promotes tumorigenesis by modulating the Hippo pathway. *Oncogene,* 34**,** 3536-46.

LIU, H., JIANG, D., CHI, F. & ZHAO, B. 2012. The Hippo pathway regulates stem cell proliferation, self-renewal, and differentiation. *Protein Cell,* 3**,** 291-304.

LIU, J., DING, X., TANG, J., CAO, Y., HU, P., ZHOU, F., SHAN, X., CAI, X., CHEN, Q., LING, N., ZHANG, B., BI, Y., CHEN, K., REN, H., HUANG, A., HE, T. C. & TANG, N. 2011a. Enhancement of canonical Wnt/beta-catenin signaling activity by HCV core protein promotes cell growth of hepatocellular carcinoma cells. *PLoS One,* 6**,** e27496.

LIU, J., WANG, Z., TANG, J., TANG, R., SHAN, X., ZHANG, W., CHEN, Q., ZHOU, F., CHEN, K., HUANG, A. & TANG, N. 2011b. Hepatitis C virus core protein activates Wnt/beta-catenin signaling through multiple regulation of upstream molecules in the SMMC-7721 cell line. *Arch Virol,* 156**,** 1013-23.

LIU, L. J., XIE, S. X., CHEN, Y. T., XUE, J. L., ZHANG, C. J. & ZHU, F. 2016. Aberrant regulation of Wnt signaling in hepatocellular carcinoma. *World J Gastroenterol,* 22**,** 7486-99.

LIU, S., YANG, W., SHEN, L., TURNER, J. R., COYNE, C. B. & WANG, T. 2009. Tight junction proteins claudin-1 and occludin control hepatitis C virus entry and are downregulated during infection to prevent superinfection. *J Virol,* 83**,** 2011-4.

LIU, Y., LIU, A., LI, H., LI, C. & LIN, J. 2011c. Celecoxib inhibits interleukin-6/interleukin-6 receptor-induced JAK2/STAT3 phosphorylation in human hepatocellular carcinoma cells. *Cancer Prev Res (Phila),* 4**,** 1296-305.

LIU, Y., LIU, A., XU, Z., YU, W., WANG, H., LI, C. & LIN, J. 2011d. XZH-5 inhibits STAT3 phosphorylation and causes apoptosis in human hepatocellular carcinoma cells. *Apoptosis,* 16**,** 502-10.

LLOVET, J. M., ZUCMAN-ROSSI, J., PIKARSKY, E., SANGRO, B., SCHWARTZ, M., SHERMAN, M. & GORES, G. 2016. Hepatocellular carcinoma. *Nat Rev Dis Primers,* 2**,** 16018.

LOHMANN, V., HOFFMANN, S., HERIAN, U., PENIN, F. & BARTENSCHLAGER, R. 2003. Viral and cellular determinants of hepatitis C virus RNA replication in cell culture. *J Virol,* 77**,** 3007-19.

LOHMANN, V., KORNER, F., DOBIERZEWSKA, A. & BARTENSCHLAGER, R. 2001. Mutations in hepatitis C virus RNAs conferring cell culture adaptation. *J Virol,* 75**,** 1437-49.

LOHMANN, V., KORNER, F., KOCH, J., HERIAN, U., THEILMANN, L. & BARTENSCHLAGER, R. 1999. Replication of subgenomic hepatitis C virus RNAs in a hepatoma cell line. *Science,* 285**,** 110-3.

LOK, A. S., SEEFF, L. B., MORGAN, T. R., DI BISCEGLIE, A. M., STERLING, R. K., CURTO, T. M., EVERSON, G. T., LINDSAY, K. L., LEE, W. M., BONKOVSKY, H. L., DIENSTAG, J. L., GHANY, M. G., MORISHIMA, C. & GOODMAN, Z. D. 2009. Incidence of hepatocellular carcinoma and associated risk factors in hepatitis C-related advanced liver disease. *Gastroenterology,* 136**,** 138-48.

LOKMANE, L., HAUMAITRE, C., GARCIA-VILLALBA, P., ANSELME, I., SCHNEIDER-MAUNOURY, S. & CEREGHINI, S. 2008. Crucial role of vHNF1 in vertebrate hepatic specification. *Development,* 135**,** 2777-86.

LOZANO, R., NAGHAVI, M., FOREMAN, K., LIM, S., SHIBUYA, K., ABOYANS, V., ABRAHAM, J., ADAIR, T., AGGARWAL, R., AHN, S. Y., ALVARADO, M., ANDERSON, H. R., ANDERSON, L. M., ANDREWS, K. G., ATKINSON, C., BADDOUR, L. M., BARKER-COLLO, S., BARTELS, D. H., BELL, M. L., BENJAMIN, E. J., BENNETT, D., BHALLA, K., BIKBOV, B., BIN ABDULHAK, A., BIRBECK, G., BLYTH, F., BOLLIGER, I., BOUFOUS, S., BUCELLO, C., BURCH, M., BURNEY, P., CARAPETIS, J., CHEN, H., CHOU, D., CHUGH, S. S., COFFENG, L. E., COLAN, S. D., COLQUHOUN, S., COLSON, K. E., CONDON, J., CONNOR, M. D., COOPER, L. T., CORRIERE, M., CORTINOVIS, M., DE VACCARO, K. C., COUSER, W., COWIE, B. C., CRIQUI, M. H., CROSS, M., DABHADKAR, K. C., DAHODWALA, N., DE LEO, D., DEGENHARDT, L., DELOSSANTOS, A., DENENBERG, J., DES JARLAIS, D. C., DHARMARATNE, S. D., DORSEY, E. R., DRISCOLL, T., DUBER, H., EBEL, B., ERWIN, P. J., ESPINDOLA, P., EZZATI, M., FEIGIN, V., FLAXMAN, A. D., FOROUZANFAR, M. H., FOWKES, F. G., FRANKLIN, R., FRANSEN, M., FREEMAN, M. K., GABRIEL, S. E., GAKIDOU, E., GASPARI, F., GILLUM, R. F., GONZALEZ-MEDINA, D., HALASA, Y. A., HARING, D., HARRISON, J. E., HAVMOELLER, R., HAY, R. J., HOEN, B., HOTEZ, P. J., HOY, D., JACOBSEN, K. H., JAMES, S. L., JASRASARIA, R., JAYARAMAN, S., JOHNS, N., KARTHIKEYAN, G., KASSEBAUM, N., KEREN, A., KHOO, J. P., KNOWLTON, L. M., KOBUSINGYE, O., KORANTENG, A., KRISHNAMURTHI, R., LIPNICK, M., LIPSHULTZ, S. E., OHNO, S. L., et al. 2012. Global and regional mortality from 235 causes of death for 20 age groups in 1990 and 2010: a systematic analysis for the Global Burden of Disease Study 2010. *Lancet,* 380**,** 2095-128.

LU, L., FINEGOLD, M. J. & JOHNSON, R. L. 2018. Hippo pathway coactivators Yap and Taz are required to coordinate mammalian liver regeneration. *Exp Mol Med,* 50**,** e423.

LU, L., LI, Y., KIM, S. M., BOSSUYT, W., LIU, P., QIU, Q., WANG, Y., HALDER, G., FINEGOLD, M. J., LEE, J. S. & JOHNSON, R. L. 2010. Hippo signaling is a

potent in vivo growth and tumor suppressor pathway in the mammalian liver. *Proc Natl Acad Sci U S A,* 107**,** 1437-42.

LUCIFORA, J., DURANTEL, D., TESTONI, B., HANTZ, O., LEVRERO, M. & ZOULIM, F. 2010. Control of hepatitis B virus replication by innate response of HepaRG cells. *Hepatology,* 51**,** 63-72.

LUDTKE, T. H., CHRISTOFFELS, V. M., PETRY, M. & KISPERT, A. 2009. Tbx3 promotes liver bud expansion during mouse development by suppression of cholangiocyte differentiation. *Hepatology,* 49**,** 969-78.

LUPBERGER, J., ZEISEL, M. B., XIAO, F., THUMANN, C., FOFANA, I., ZONA, L., DAVIS, C., MEE, C. J., TUREK, M., GORKE, S., ROYER, C., FISCHER, B., ZAHID, M. N., LAVILLETTE, D., FRESQUET, J., COSSET, F. L., ROTHENBERG, S. M., PIETSCHMANN, T., PATEL, A. H., PESSAUX, P., DOFFOEL, M., RAFFELSBERGER, W., POCH, O., MCKEATING, J. A., BRINO, L. & BAUMERT, T. F. 2011. EGFR and EphA2 are host factors for hepatitis C virus entry and possible targets for antiviral therapy. *Nat Med,* 17**,** 589-95.

MA, B., CHEN, Y., CHEN, L., CHENG, H., MU, C., LI, J., GAO, R., ZHOU, C., CAO, L., LIU, J., ZHU, Y., CHEN, Q. & WU, S. 2015. Hypoxia regulates Hippo signalling through the SIAH2 ubiquitin E3 ligase. *Nat Cell Biol,* 17**,** 95-103.

MA, L. G., BIAN, S. B., CUI, J. X., XI, H. Q., ZHANG, K. C., QIN, H. Z., ZHU, X. M. & CHEN, L. 2016. LKB1 inhibits the proliferation of gastric cancer cells by suppressing the nuclear translocation of Yap and beta-catenin. *Int J Mol Med,* 37**,** 1039-48.

MA, S., CHAN, K. W., HU, L., LEE, T. K., WO, J. Y., NG, I. O., ZHENG, B. J. & GUAN, X. Y. 2007. Identification and characterization of tumorigenic liver cancer stem/progenitor cells. *Gastroenterology,* 132**,** 2542-56.

MA, S., LEE, T. K., ZHENG, B. J., CHAN, K. W. & GUAN, X. Y. 2008. CD133+ HCC cancer stem cells confer chemoresistance by preferential expression of the Akt/PKB survival pathway. *Oncogene,* 27**,** 1749-58.

MACDONALD, A., CROWDER, K., STREET, A., MCCORMICK, C. & HARRIS, M. 2004. The hepatitis C virus NS5A protein binds to members of the Src family of tyrosine kinases and regulates kinase activity. *J Gen Virol,* 85**,** 721-9.

MACDONALD, A., CROWDER, K., STREET, A., MCCORMICK, C., SAKSELA, K. & HARRIS, M. 2003. The hepatitis C virus non-structural NS5A protein inhibits activating protein-1 function by perturbing ras-ERK pathway signaling. *J Biol Chem,* 278**,** 17775-84.

MACDONALD, A. & HARRIS, M. 2004. Hepatitis C virus NS5A: tales of a promiscuous protein. *J Gen Virol,* 85**,** 2485-502.

MACDONALD, R. A. 1961. "Lifespan" of liver cells. Autoradio-graphic study using tritiated thymidine in normal, cirrhotic, and partially hepatectomized rats. *Arch Intern Med,* 107**,** 335-43.

MAIR, M., BLAAS, L., OSTERREICHER, C. H., CASANOVA, E. & EFERL, R. 2011. JAK-STAT signaling in hepatic fibrosis. *Front Biosci (Landmark Ed),* 16**,** 2794-811.

MAIRE, M., PARENT, R., MORAND, A. L., ALOTTE, C., TREPO, C., DURANTEL, D. & PETIT, M. A. 2008. Characterization of the double-stranded RNA responses in human liver progenitor cells. *Biochem Biophys Res Commun,* 368**,** 556-62.

MAJUMDER, M., GHOSH, A. K., STEELE, R., RAY, R. & RAY, R. B. 2001. Hepatitis C virus NS5A physically associates with p53 and regulates p21/waf1 gene expression in a p53-dependent manner. *J Virol,* 75**,** 1401-7.

MAKITA, R., UCHIJIMA, Y., NISHIYAMA, K., AMANO, T., CHEN, Q., TAKEUCHI, T., MITANI, A., NAGASE, T., YATOMI, Y., ABURATANI, H., NAKAGAWA, O., SMALL, E. V., COBO-STARK, P., IGARASHI, P., MURAKAMI, M., TOMINAGA, J., SATO, T., ASANO, T., KURIHARA, Y. & KURIHARA, H. 2008. Multiple renal cysts, urinary concentration defects, and pulmonary emphysematous changes in mice lacking TAZ. *Am J Physiol Renal Physiol,* 294**,** F542-53.

MAKOWSKE, M., BALLESTER, R., CAYRE, Y. & ROSEN, O. M. 1988. Immunochemical evidence that three protein kinase C isozymes increase in abundance during HL-60 differentiation induced by dimethyl sulfoxide and retinoic acid. *J Biol Chem,* 263**,** 3402-10.

MALATO, Y., NAQVI, S., SCHURMANN, N., NG, R., WANG, B., ZAPE, J., KAY, M. A., GRIMM, D. & WILLENBRING, H. 2011. Fate tracing of mature hepatocytes in mouse liver homeostasis and regeneration. *J Clin Invest,* 121**,** 4850-60.

MANKOURI, J., GRIFFIN, S. & HARRIS, M. 2008. The hepatitis C virus non-structural protein NS5A alters the trafficking profile of the epidermal growth factor receptor. *Traffic,* 9**,** 1497-509.

MANNS, M. P., BUTI, M., GANE, E., PAWLOTSKY, J. M., RAZAVI, H., TERRAULT, N. & YOUNOSSI, Z. 2017. Hepatitis C virus infection. *Nat Rev Dis Primers,* 3**,** 17006.

MARGAGLIOTTI, S., CLOTMAN, F., PIERREUX, C. E., BEAUDRY, J. B., JACQUEMIN, P., ROUSSEAU, G. G. & LEMAIGRE, F. P. 2007. The Onecut transcription factors HNF-6/OC-1 and OC-2 regulate early liver expansion by controlling hepatoblast migration. *Dev Biol,* 311**,** 579-89.

MARQUARDT, J. U. 2016. Deconvolution of the cellular origin in hepatocellular carcinoma: Hepatocytes take the center stage. *Hepatology,* 64**,** 1020-3.

MARQUARDT, J. U., ANDERSEN, J. B. & THORGEIRSSON, S. S. 2015. Functional and genetic deconstruction of the cellular origin in liver cancer. *Nat Rev Cancer,* 15**,** 653-67.

MARRONE, A. K., TRYNDYAK, V., BELAND, F. A. & POGRIBNY, I. P. 2016. MicroRNA Responses to the Genotoxic Carcinogens Aflatoxin B1 and Benzo[a]pyrene in Human HepaRG Cells. *Toxicol Sci,* 149**,** 496-502.

MARTELL, M., ESTEBAN, J. I., QUER, J., GENESCA, J., WEINER, A., ESTEBAN, R., GUARDIA, J. & GOMEZ, J. 1992. Hepatitis C virus (HCV) circulates as a population of different but closely related genomes: quasispecies nature of HCV genome distribution. *J Virol,* 66**,** 3225-9.

MARTI, P., STEIN, C., BLUMER, T., ABRAHAM, Y., DILL, M. T., PIKIOLEK, M., ORSINI, V., JURISIC, G., MEGEL, P., MAKOWSKA, Z., AGARINIS, C., TORNILLO, L., BOUWMEESTER, T., RUFFNER, H., BAUER, A., PARKER, C. N., SCHMELZLE, T., TERRACCIANO, L. M., HEIM, M. H. & TCHORZ, J. S. 2015. YAP promotes proliferation, chemoresistance, and angiogenesis in human cholangiocarcinoma through TEAD transcription factors. *Hepatology,* 62**,** 1497-510.

MARTINEZ-QUETGLAS, I., PINYOL, R., DAUCH, D., TORRECILLA, S., TOVAR, V., MOEINI, A., ALSINET, C., PORTELA, A., RODRIGUEZ-CARUNCHIO, L., SOLE, M., LUJAMBIO, A., VILLANUEVA, A., THUNG, S., ESTELLER, M., ZENDER, L. & LLOVET, J. M. 2016. IGF2 Is Up-regulated by Epigenetic Mechanisms in Hepatocellular Carcinomas and Is an Actionable Oncogene Product in Experimental Models. *Gastroenterology,* 151**,** 1192-1205.

MARTINEZ BARBERA, J. P., CLEMENTS, M., THOMAS, P., RODRIGUEZ, T., MELOY, D., KIOUSSIS, D. & BEDDINGTON, R. S. 2000. The homeobox gene Hex

is required in definitive endodermal tissues for normal forebrain, liver and thyroid formation. *Development,* 127**,** 2433-45.

MASAKI, T., AREND, K. C., LI, Y., YAMANE, D., MCGIVERN, D. R., KATO, T., WAKITA, T., MOORMAN, N. J. & LEMON, S. M. 2015. miR-122 stimulates hepatitis C virus RNA synthesis by altering the balance of viral RNAs engaged in replication versus translation. *Cell Host Microbe,* 17**,** 217-28.

MASHAL, R. D., LESTER, S., CORLESS, C., RICHIE, J. P., CHANDRA, R., PROPERT, K. J. & DUTTA, A. 1996. Expression of cell cycle-regulated proteins in prostate cancer. *Cancer Res,* 56**,** 4159-63.

MATSUI, C., SHOJI, I., KANEDA, S., SIANIPAR, I. R., DENG, L. & HOTTA, H. 2012. Hepatitis C virus infection suppresses GLUT2 gene expression via downregulation of hepatocyte nuclear factor 1alpha. *J Virol,* 86**,** 12903-11.

MATSUMOTO, K., YOSHITOMI, H., ROSSANT, J. & ZARET, K. S. 2001. Liver organogenesis promoted by endothelial cells prior to vascular function. *Science,* 294**,** 559-63.

MAZUMDAR, B., BANERJEE, A., MEYER, K. & RAY, R. 2011. Hepatitis C virus E1 envelope glycoprotein interacts with apolipoproteins in facilitating entry into hepatocytes. *Hepatology,* 54**,** 1149-56.

MCGIVERN, D. R. & LEMON, S. M. 2009. Tumor suppressors, chromosomal instability, and hepatitis C virus-associated liver cancer. *Annu Rev Pathol,* 4**,** 399-415.

MCGIVERN, D. R. & LEMON, S. M. 2011. Virus-specific mechanisms of carcinogenesis in hepatitis C virus associated liver cancer. *Oncogene,* 30**,** 1969-83.

MCHUTCHISON, J. G., LAWITZ, E. J., SHIFFMAN, M. L., MUIR, A. J., GALLER, G. W., MCCONE, J., NYBERG, L. M., LEE, W. M., GHALIB, R. H., SCHIFF, E. R., GALATI, J. S., BACON, B. R., DAVIS, M. N., MUKHOPADHYAY, P., KOURY, K., NOVIELLO, S., PEDICONE, L. D., BRASS, C. A., ALBRECHT, J. K., SULKOWSKI, M. S. & TEAM, I. S. 2009. Peginterferon alfa-2b or alfa-2a with ribavirin for treatment of hepatitis C infection. *N Engl J Med,* 361**,** 580-93.

MCLAUCHLAN, J. 2000. Properties of the hepatitis C virus core protein: a structural protein that modulates cellular processes. *J Viral Hepat,* 7**,** 2-14.

MCLIN, V. A., RANKIN, S. A. & ZORN, A. M. 2007. Repression of Wnt/beta-catenin signaling in the anterior endoderm is essential for liver and pancreas development. *Development,* 134**,** 2207-17.

MEDERACKE, I., HSU, C. C., TROEGER, J. S., HUEBENER, P., MU, X., DAPITO, D. H., PRADERE, J. P. & SCHWABE, R. F. 2013. Fate tracing reveals hepatic stellate cells as dominant contributors to liver fibrosis independent of its aetiology. *Nat Commun,* 4**,** 2823.

MEERTENS, L., BERTAUX, C., CUKIERMAN, L., CORMIER, E., LAVILLETTE, D., COSSET, F. L. & DRAGIC, T. 2008. The tight junction proteins claudin-1, -6, and -9 are entry cofactors for hepatitis C virus. *J Virol,* 82**,** 3555-60.

MELE, A., PULSONI, A., BIANCO, E., MUSTO, P., SZKLO, A., SANPAOLO, M. G., IANNITTO, E., DE RENZO, A., MARTINO, B., LISO, V., ANDRIZZI, C., PUSTERLA, S., DORE, F., MARESCA, M., RAPICETTA, M., MARCUCCI, F., MANDELLI, F. & FRANCESCHI, S. 2003. Hepatitis C virus and B-cell non-Hodgkin lymphomas: an Italian multicenter case-control study. *Blood,* 102**,** 996-9.

MELKONYAN, H., SORG, C. & KLEMPT, M. 1996. Electroporation efficiency in mammalian cells is increased by dimethyl sulfoxide (DMSO). *Nucleic Acids Res,* 24**,** 4356-7.

MENG, Z., MOROISHI, T. & GUAN, K. L. 2016. Mechanisms of Hippo pathway regulation. *Genes Dev,* 30**,** 1-17.

MICHALOPOULOS, G. K. 2007. Liver regeneration. *J Cell Physiol,* 213**,** 286-300.

MICHALOPOULOS, G. K. 2013. Principles of liver regeneration and growth homeostasis. *Compr Physiol,* 3**,** 485-513.

MILLER, E., YANG, J., DERAN, M., WU, C., SU, A. I., BONAMY, G. M., LIU, J., PETERS, E. C. & WU, X. 2012. Identification of serum-derived sphingosine-1-phosphate as a small molecule regulator of YAP. *Chem Biol,* 19**,** 955-62.

MILWARD, A., MANKOURI, J. & HARRIS, M. 2010. Hepatitis C virus NS5A protein interacts with beta-catenin and stimulates its transcriptional activity in a phosphoinositide-3 kinase-dependent fashion. *J Gen Virol,* 91**,** 373-81.

MIN, L., HE, B. & HUI, L. 2011. Mitogen-activated protein kinases in hepatocellular carcinoma development. *Semin Cancer Biol,* 21**,** 10-20.

MITTELHOLZER, C., MOSER, C., TRATSCHIN, J. D. & HOFMANN, M. A. 1997. Generation of cytopathogenic subgenomic RNA of classical swine fever virus in persistently infected porcine cell lines. *Virus Res,* 51**,** 125-37.

MIYAJIMA, A., TANAKA, M. & ITOH, T. 2014. Stem/progenitor cells in liver development, homeostasis, regeneration, and reprogramming. *Cell Stem Cell,* 14**,** 561-74.

MO, J. S., YU, F. X., GONG, R., BROWN, J. H. & GUAN, K. L. 2012. Regulation of the Hippo-YAP pathway by protease-activated receptors (PARs). *Genes Dev,* 26**,** 2138-43.

MOLEIRINHO, S., HOXHA, S., MANDATI, V., CURTALE, G., TROUTMAN, S., EHMER, U. & KISSIL, J. L. 2017. Regulation of localization and function of the transcriptional co-activator YAP by angiomotin. *Elife,* 6.

MONTI, G., PIOLTELLI, P., SACCARDO, F., CAMPANINI, M., CANDELA, M., CAVALLERO, G., DE VITA, S., FERRI, C., MAZZARO, C., MIGLIARESI, S., OSSI, E., PIETROGRANDE, M., GABRIELLI, A., GALLI, M. & INVERNIZZI, F. 2005. Incidence and characteristics of non-Hodgkin lymphomas in a multicenter case file of patients with hepatitis C virus-related symptomatic mixed cryoglobulinemias. *Arch Intern Med,* 165**,** 101-5.

MOORE-SCOTT, B. A., OPOKA, R., LIN, S. C., KORDICH, J. J. & WELLS, J. M. 2007. Identification of molecular markers that are expressed in discrete anterior-posterior domains of the endoderm from the gastrula stage to mid-gestation. *Dev Dyn,* 236**,** 1997-2003.

MORADPOUR, D., BRASS, V., BIECK, E., FRIEBE, P., GOSERT, R., BLUM, H. E., BARTENSCHLAGER, R., PENIN, F. & LOHMANN, V. 2004. Membrane association of the RNA-dependent RNA polymerase is essential for hepatitis C virus RNA replication. *J Virol,* 78**,** 13278-84.

MORIN-KENSICKI, E. M., BOONE, B. N., HOWELL, M., STONEBRAKER, J. R., TEED, J., ALB, J. G., MAGNUSON, T. R., O'NEAL, W. & MILGRAM, S. L. 2006. Defects in yolk sac vasculogenesis, chorioallantoic fusion, and embryonic axis elongation in mice with targeted disruption of Yap65. *Mol Cell Biol,* 26**,** 77-87.

MORIYA, K., FUJIE, H., SHINTANI, Y., YOTSUYANAGI, H., TSUTSUMI, T., ISHIBASHI, K., MATSUURA, Y., KIMURA, S., MIYAMURA, T. & KOIKE, K. 1998. The core protein of hepatitis C virus induces hepatocellular carcinoma in transgenic mice. *Nat Med,* 4**,** 1065-7.

MOROISHI, T., PARK, H. W., QIN, B., CHEN, Q., MENG, Z., PLOUFFE, S. W., TANIGUCHI, K., YU, F. X., KARIN, M., PAN, D. & GUAN, K. L. 2015. A YAP/TAZ-

induced feedback mechanism regulates Hippo pathway homeostasis. *Genes Dev,* 29**,** 1271-84.

MOROZOV, V. A. & LAGAYE, S. 2018. Hepatitis C virus: Morphogenesis, infection and therapy. *World J Hepatol,* 10**,** 186-212.

MORTIMER, S. A. & DOUDNA, J. A. 2013. Unconventional miR-122 binding stabilizes the HCV genome by forming a trimolecular RNA structure. *Nucleic Acids Res,* 41**,** 4230-40.

MOUSTAFA, S., KARAKASILIOTIS, I. & MAVROMARA, P. 2018. Hepatitis C Virus core+1/ARF Protein Modulates the Cyclin D1/pRb Pathway and Promotes Carcinogenesis. *J Virol,* 92.

MOWBRAY, C. A., HOWARD, A., MORSMAN, J. & HIRST, B. H. 2010. Differentiation of HepG2 and Huh7 cells using dimethyl sulfoxide. *The FASEB Journal,* 24**,** lb654-lb654.

MOYA, I. M. & HALDER, G. 2014. Discovering the Hippo pathway protein-protein interactome. *Cell Res,* 24**,** 137-8.

MUKHOPADHYAY, S., KUHN, R. J. & ROSSMANN, M. G. 2005. A structural perspective of the flavivirus life cycle. *Nat Rev Microbiol,* 3**,** 13-22.

MUNAKATA, T., NAKAMURA, M., LIANG, Y., LI, K. & LEMON, S. M. 2005. Down-regulation of the retinoblastoma tumor suppressor by the hepatitis C virus NS5B RNA-dependent RNA polymerase. *Proc Natl Acad Sci U S A,* 102**,** 18159-64.

MUNGER, K., BALDWIN, A., EDWARDS, K. M., HAYAKAWA, H., NGUYEN, C. L., OWENS, M., GRACE, M. & HUH, K. 2004. Mechanisms of human papillomavirus-induced oncogenesis. *J Virol,* 78**,** 11451-60.

MURPHY, D. G., SABLON, E., CHAMBERLAND, J., FOURNIER, E., DANDAVINO, R. & TREMBLAY, C. L. 2015. Hepatitis C virus genotype 7, a new genotype originating from central Africa. *J Clin Microbiol,* 53**,** 967-72.

MURRAY, C. L., JONES, C. T. & RICE, C. M. 2008. Architects of assembly: roles of Flaviviridae non-structural proteins in virion morphogenesis. *Nat Rev Microbiol.* England.

MUSCH, A. 2014. The unique polarity phenotype of hepatocytes. *Exp Cell Res,* 328**,** 276-83.

NAHON, P. & ZUCMAN-ROSSI, J. 2012. Single nucleotide polymorphisms and risk of hepatocellular carcinoma in cirrhosis. *J Hepatol,* 57**,** 663-74.

NAITO, M., HASEGAWA, G. & TAKAHASHI, K. 1997. Development, differentiation, and maturation of Kupffer cells. *Microsc Res Tech,* 39**,** 350-64.

NAKABAYASHI, H., TAKETA, K., MIYANO, K., YAMANE, T. & SATO, J. 1982. Growth of human hepatoma cells lines with differentiated functions in chemically defined medium. *Cancer Res,* 42**,** 3858-63.

NAKAJIMA, N., HIJIKATA, M., YOSHIKURA, H. & SHIMIZU, Y. K. 1996. Characterization of long-term cultures of hepatitis C virus. *J Virol,* 70**,** 3325-9.

NARAYAN, R., GANGADHARAN, B., HANTZ, O., ANTROBUS, R., GARCIA, A., DWEK, R. A. & ZITZMANN, N. 2009. Proteomic analysis of HepaRG cells: a novel cell line that supports hepatitis B virus infection. *J Proteome Res,* 8**,** 118-22.

NARBUS, C. M., ISRAELOW, B., SOURISSEAU, M., MICHTA, M. L., HOPCRAFT, S. E., ZEINER, G. M. & EVANS, M. J. 2011. HepG2 cells expressing microRNA miR-122 support the entire hepatitis C virus life cycle. *J Virol,* 85**,** 12087-92.

NAULT, J. C. & COLOMBO, M. 2016. Hepatocellular carcinoma and direct acting antiviral treatments: Controversy after the revolution. *J Hepatol,* 65**,** 663-665.

NAULT, J. C., DE REYNIES, A., VILLANUEVA, A., CALDERARO, J., REBOUISSOU, S., COUCHY, G., DECAENS, T., FRANCO, D., IMBEAUD, S., ROUSSEAU, F., AZOULAY, D., SARIC, J., BLANC, J. F., BALABAUD, C., BIOULAC-SAGE, P., LAURENT, A., LAURENT-PUIG, P., LLOVET, J. M. & ZUCMAN-ROSSI, J. 2013. A hepatocellular carcinoma 5-gene score associated with survival of patients after liver resection. *Gastroenterology,* 145**,** 176-87.

NDONGO-THIAM, N., BERTHILLON, P., ERRAZURIZ, E., BORDES, I., DE SEQUEIRA, S., TRÉPO, C. & PETIT, M. A. 2011. Long-term propagation of serum hepatitis C virus (HCV) with production of enveloped HCV particles in human HepaRG hepatocytes. *Hepatology,* 54**,** 406-17.

NELSON, D. R., LIM, H. L., MAROUSIS, C. G., FANG, J. W., DAVIS, G. L., SHEN, L., URDEA, M. S., KOLBERG, J. A. & LAU, J. Y. 1997. Activation of tumor necrosis factor-alpha system in chronic hepatitis C virus infection. *Dig Dis Sci,* 42**,** 2487-94.

NGUYEN, H. T., HONG, X., TAN, S., CHEN, Q., CHAN, L., FIVAZ, M., COHEN, S. M. & VOORHOEVE, P. M. 2014. Viral small T oncoproteins transform cells by alleviating hippo-pathway-mediated inhibition of the YAP proto-oncogene. *Cell Rep,* 8**,** 707-13.

NGUYEN, Q., ANDERS, R. A., ALPINI, G. & BAI, H. 2015. Yes-associated protein in the liver: Regulation of hepatic development, repair, cell fate determination and tumorigenesis. *Dig Liver Dis,* 47**,** 826-35.

NISHIO, M., HAMADA, K., KAWAHARA, K., SASAKI, M., NOGUCHI, F., CHIBA, S., MIZUNO, K., SUZUKI, S. O., DONG, Y., TOKUDA, M., MORIKAWA, T., HIKASA, H., EGGENSCHWILER, J., YABUTA, N., NOJIMA, H., NAKAGAWA, K., HATA, Y., NISHINA, H., MIMORI, K., MORI, M., SASAKI, T., MAK, T. W., NAKANO, T., ITAMI, S. & SUZUKI, A. 2012. Cancer susceptibility and embryonic lethality in Mob1a/1b double-mutant mice. *J Clin Invest,* 122**,** 4505-18.

NISHIO, M., SUGIMACHI, K., GOTO, H., WANG, J., MORIKAWA, T., MIYACHI, Y., TAKANO, Y., HIKASA, H., ITOH, T., SUZUKI, S. O., KURIHARA, H., AISHIMA, S., LEASK, A., SASAKI, T., NAKANO, T., NISHINA, H., NISHIKAWA, Y., SEKIDO, Y., NAKAO, K., SHIN-YA, K., MIMORI, K. & SUZUKI, A. 2016. Dysregulated YAP1/TAZ and TGF-beta signaling mediate hepatocarcinogenesis in Mob1a/1b-deficient mice. *Proc Natl Acad Sci U S A,* 113**,** E71-80.

NISHIOKA, N., INOUE, K., ADACHI, K., KIYONARI, H., OTA, M., RALSTON, A., YABUTA, N., HIRAHARA, S., STEPHENSON, R. O., OGONUKI, N., MAKITA, R., KURIHARA, H., MORIN-KENSICKI, E. M., NOJIMA, H., ROSSANT, J., NAKAO, K., NIWA, H. & SASAKI, H. 2009. The Hippo signaling pathway components Lats and Yap pattern Tead4 activity to distinguish mouse trophectoderm from inner cell mass. *Dev Cell,* 16**,** 398-410.

NIWA, Y., KANDA, H., SHIKAUCHI, Y., SAIURA, A., MATSUBARA, K., KITAGAWA, T., YAMAMOTO, J., KUBO, T. & YOSHIKAWA, H. 2005. Methylation silencing of SOCS-3 promotes cell growth and migration by enhancing JAK/STAT and FAK signalings in human hepatocellular carcinoma. *Oncogene,* 24**,** 6406-17.

ODOM, D. T., ZIZLSPERGER, N., GORDON, D. B., BELL, G. W., RINALDI, N. J., MURRAY, H. L., VOLKERT, T. L., SCHREIBER, J., ROLFE, P. A., GIFFORD, D. K., FRAENKEL, E., BELL, G. I. & YOUNG, R. A. 2004. Control of pancreas and liver gene expression by HNF transcription factors. *Science,* 303**,** 1378-81.

OGATA, H., CHINEN, T., YOSHIDA, T., KINJYO, I., TAKAESU, G., SHIRAISHI, H., IIDA, M., KOBAYASHI, T. & YOSHIMURA, A. 2006a. Loss of SOCS3 in the liver

promotes fibrosis by enhancing STAT3-mediated TGF-beta1 production. *Oncogene,* 25**,** 2520-30.

OGATA, H., KOBAYASHI, T., CHINEN, T., TAKAKI, H., SANADA, T., MINODA, Y., KOGA, K., TAKAESU, G., MAEHARA, Y., IIDA, M. & YOSHIMURA, A. 2006b. Deletion of the SOCS3 gene in liver parenchymal cells promotes hepatitis-induced hepatocarcinogenesis. *Gastroenterology,* 131**,** 179-93.

OKU, Y., NISHIYA, N., SHITO, T., YAMAMOTO, R., YAMAMOTO, Y., OYAMA, C. & UEHARA, Y. 2015. Small molecules inhibiting the nuclear localization of YAP/TAZ for chemotherapeutics and chemosensitizers against breast cancers. *FEBS Open Bio,* 5**,** 542-9.

OKUDA, M., LI, K., BEARD, M. R., SHOWALTER, L. A., SCHOLLE, F., LEMON, S. M. & WEINMAN, S. A. 2002. Mitochondrial injury, oxidative stress, and antioxidant gene expression are induced by hepatitis C virus core protein. *Gastroenterology,* 122**,** 366-75.

ONDER, T. T., GUPTA, P. B., MANI, S. A., YANG, J., LANDER, E. S. & WEINBERG, R. A. 2008. Loss of E-cadherin promotes metastasis via multiple downstream transcriptional pathways. *Cancer Res,* 68**,** 3645-54.

ORBAN, E., SZABO, E., LOTZ, G., KUPCSULIK, P., PASKA, C., SCHAFF, Z. & KISS, A. 2008. Different expression of occludin and ZO-1 in primary and metastatic liver tumors. *Pathol Oncol Res,* 14**,** 299-306.

ORGAN, S. L. & TSAO, M. S. 2011. An overview of the c-MET signaling pathway. *Ther Adv Med Oncol,* 3**,** S7-S19.

OTA, M. & SASAKI, H. 2008. Mammalian Tead proteins regulate cell proliferation and contact inhibition as transcriptional mediators of Hippo signaling. *Development,* 135**,** 4059-69.

OTSUKA, M., KATO, N., LAN, K., YOSHIDA, H., KATO, J., GOTO, T., SHIRATORI, Y. & OMATA, M. 2000. Hepatitis C virus core protein enhances p53 function through augmentation of DNA binding affinity and transcriptional ability. *J Biol Chem,* 275**,** 34122-30.

OVERHOLTZER, M., ZHANG, J., SMOLEN, G. A., MUIR, B., LI, W., SGROI, D. C., DENG, C. X., BRUGGE, J. S. & HABER, D. A. 2006. Transforming properties of YAP, a candidate oncogene on the chromosome 11q22 amplicon. *Proc Natl Acad Sci U S A,* 103**,** 12405-10.

OZASA, A., TANAKA, Y., ORITO, E., SUGIYAMA, M., KANG, J. H., HIGE, S., KURAMITSU, T., SUZUKI, K., TANAKA, E., OKADA, S., TOKITA, H., ASAHINA, Y., INOUE, K., KAKUMU, S., OKANOUE, T., MURAWAKI, Y., HINO, K., ONJI, M., YATSUHASHI, H., SAKUGAWA, H., MIYAKAWA, Y., UEDA, R. & MIZOKAMI, M. 2006. Influence of genotypes and precore mutations on fulminant or chronic outcome of acute hepatitis B virus infection. *Hepatology,* 44**,** 326-34.

PAGANO, M., PEPPERKOK, R., VERDE, F., ANSORGE, W. & DRAETTA, G. 1992. Cyclin A is required at two points in the human cell cycle. *EMBO J,* 11**,** 961-71.

PAL, R., MAMIDI, M. K., DAS, A. K. & BHONDE, R. 2012. Diverse effects of dimethyl sulfoxide (DMSO) on the differentiation potential of human embryonic stem cells. *Arch Toxicol,* 86**,** 651-61.

PALAKKAN, A. A., DRUMMOND, R., ANDERSON, R. A., GREENHOUGH, S., TV, K., HAY, D. C. & ROSS, J. A. 2015. Polarisation and functional characterisation of hepatocytes derived from human embryonic and mesenchymal stem cells. *Biomed Rep,* 3**,** 626-636.

PALMER, W. C. & PATEL, T. 2012. Are common factors involved in the pathogenesis of primary liver cancers? A meta-analysis of risk factors for intrahepatic cholangiocarcinoma. *J Hepatol,* 57**,** 69-76.

PAN, D. 2010. The hippo signaling pathway in development and cancer. *Dev Cell,* 19**,** 491-505.

PAPASPYROPOULOS, A., BRADLEY, L., THAPA, A., LEUNG, C. Y., TOSKAS, K., KOENNIG, D., PEFANI, D. E., RASO, C., GROU, C., HAMILTON, G., VLAHOV, N., GRAWENDA, A., HAIDER, S., CHAUHAN, J., BUTI, L., KANAPIN, A., LU, X., BUFFA, F., DIANOV, G., VON KRIEGSHEIM, A., MATALLANAS, D., SAMSONOVA, A., ZERNICKA-GOETZ, M. & O'NEILL, E. 2018. RASSF1A uncouples Wnt from Hippo signalling and promotes YAP mediated differentiation via p73. *Nat Commun,* 9**,** 424.

PARENT, R., MARION, M. J., FURIO, L., TREPO, C. & PETIT, M. A. 2004. Origin and characterization of a human bipotent liver progenitor cell line. *Gastroenterology,* 126**,** 1147-56.

PARK, H. W., KIM, Y. C., YU, B., MOROISHI, T., MO, J. S., PLOUFFE, S. W., MENG, Z., LIN, K. C., YU, F. X., ALEXANDER, C. M., WANG, C. Y. & GUAN, K. L. 2015. Alternative Wnt Signaling Activates YAP/TAZ. *Cell,* 162**,** 780-94.

PARK, J. & JANG, K. L. 2014. Hepatitis C virus represses E-cadherin expression via DNA methylation to induce epithelial to mesenchymal transition in human hepatocytes. *Biochem Biophys Res Commun,* 446**,** 561-7.

PARK, J. S., YANG, J. M. & MIN, M. K. 2000. Hepatitis C virus nonstructural protein NS4B transforms NIH3T3 cells in cooperation with the Ha-ras oncogene. *Biochem Biophys Res Commun,* 267**,** 581-7.

PASSMAN, A. M., LOW, J., LONDON, R., TIRNITZ-PARKER, J. E., MIYAJIMA, A., TANAKA, M., STRICK-MARCHAND, H., DARLINGTON, G. J., FINCH-EDMONDSON, M., OCHSNER, S., ZHU, C., WHELAN, J., CALLUS, B. A. & YEOH, G. C. 2016. A Transcriptomic Signature of Mouse Liver Progenitor Cells. *Stem Cells Int,* 2016**,** 5702873.

PATEL, S. H., CAMARGO, F. D. & YIMLAMAI, D. 2017. Hippo Signaling in the Liver Regulates Organ Size, Cell Fate, and Carcinogenesis. *Gastroenterology,* 152**,** 533-545.

PAUL, D., HOPPE, S., SAHER, G., KRIJNSE-LOCKER, J. & BARTENSCHLAGER, R. 2013. Morphological and biochemical characterization of the membranous hepatitis C virus replication compartment. *J Virol,* 87**,** 10612-27.

PAUL, D., MADAN, V. & BARTENSCHLAGER, R. 2014. Hepatitis C virus RNA replication and assembly: living on the fat of the land. *Cell Host Microbe,* 16**,** 569-79.

PAWLOTSKY, J. M. 2016. Hepatitis C Virus Resistance to Direct-Acting Antiviral Drugs in Interferon-Free Regimens. *Gastroenterology,* 151**,** 70-86.

PEFANI, D. E., PANKOVA, D., ABRAHAM, A. G., GRAWENDA, A. M., VLAHOV, N., SCRACE, S. & E, O. N. 2016. TGF-beta Targets the Hippo Pathway Scaffold RASSF1A to Facilitate YAP/SMAD2 Nuclear Translocation. *Mol Cell,* 63**,** 156-66.

PEI, T., LI, Y., WANG, J., WANG, H., LIANG, Y., SHI, H., SUN, B., YIN, D., SUN, J., SONG, R., PAN, S., SUN, Y., JIANG, H., ZHENG, T. & LIU, L. 2015. YAP is a critical oncogene in human cholangiocarcinoma. *Oncotarget,* 6**,** 17206-20.

PENG, C., ZHU, Y., ZHANG, W., LIAO, Q., CHEN, Y., ZHAO, X., GUO, Q., SHEN, P., ZHEN, B., QIAN, X., YANG, D., ZHANG, J. S., XIAO, D., QIN, W. & PEI, H.

2017. Regulation of the Hippo-YAP Pathway by Glucose Sensor O-GlcNAcylation. *Mol Cell,* 68**,** 591-604 e5.

PENIN, F., DUBUISSON, J., REY, F. A., MORADPOUR, D. & PAWLOTSKY, J. M. 2004. Structural biology of hepatitis C virus. *Hepatology,* 39**,** 5-19.

PEREZ, S., KASPI, A., DAVIDOVICH, A., NIMER, A., EL-OSTA, A., HAVIV, I. & GAL-TANAMY, M. Hepatitis C Virus Leaves Oncogenic Signatures on the Host Cell Following its Eradication by

DAAs Via Inducing an Epigenetic Memory Mechanism. 2017.

PESTOVA, T. V., SHATSKY, I. N., FLETCHER, S. P., JACKSON, R. J. & HELLEN, C. U. 1998. A prokaryotic-like mode of cytoplasmic eukaryotic ribosome binding to the initiation codon during internal translation initiation of hepatitis C and classical swine fever virus RNAs. *Genes Dev,* 12**,** 67-83.

PETRAREANU, C., MACOVEI, A., SOKOLOWSKA, I., WOODS, A. G., LAZAR, C., RADU, G. L., DARIE, C. C. & BRANZA-NICHITA, N. 2013. Comparative proteomics reveals novel components at the plasma membrane of differentiated HepaRG cells and different distribution in hepatocyte- and biliary-like cells. *PLoS One,* 8**,** e71859.

PETRUZZIELLO, A., MARIGLIANO, S., LOQUERCIO, G., COZZOLINO, A. & CACCIAPUOTI, C. 2016. Global epidemiology of hepatitis C virus infection: An up-date of the distribution and circulation of hepatitis C virus genotypes. *World J Gastroenterol,* 22**,** 7824-40.

PHAM, T. N., COFFIN, C. S. & MICHALAK, T. I. 2010. Occult hepatitis C virus infection: what does it mean? *Liver Int,* 30**,** 502-11.

PHAM, T. N., KING, D., MACPARLAND, S. A., MCGRATH, J. S., REDDY, S. B., BURSEY, F. R. & MICHALAK, T. I. 2008. Hepatitis C virus replicates in the same immune cell subsets in chronic hepatitis C and occult infection. *Gastroenterology,* 134**,** 812-22.

PHAM, T. N., MACPARLAND, S. A., MULROONEY, P. M., COOKSLEY, H., NAOUMOV, N. V. & MICHALAK, T. I. 2004. Hepatitis C virus persistence after spontaneous or treatment-induced resolution of hepatitis C. *J Virol,* 78**,** 5867-74.

PHAM, T. N. & MICHALAK, T. I. 2008. Hepatitis C virus in peripheral blood mononuclear cells of individuals with isolated anti-hepatitis C virus antibody reactivity. *Hepatology,* 48**,** 350-1; author reply 351-2.

PHILLIPS, A., HOOD, S. R., GIBSON, G. G. & PLANT, N. J. 2005. Impact of transcription factor profile and chromatin conformation on human hepatocyte CYP3A gene expression. *Drug Metab Dispos,* 33**,** 233-42.

PICCININNI, S., VARAKLIOTI, A., NARDELLI, M., DAVE, B., RANEY, K. D. & MCCARTHY, J. E. 2002. Modulation of the hepatitis C virus RNA-dependent RNA polymerase activity by the non-structural (NS) 3 helicase and the NS4B membrane protein. *J Biol Chem,* 277**,** 45670-9.

PILERI, P., UEMATSU, Y., CAMPAGNOLI, S., GALLI, G., FALUGI, F., PETRACCA, R., WEINER, A. J., HOUGHTON, M., ROSA, D., GRANDI, G. & ABRIGNANI, S. 1998. Binding of hepatitis C virus to CD81. *Science,* 282**,** 938-41.

PLOSS, A., EVANS, M. J., GAYSINSKAYA, V. A., PANIS, M., YOU, H., DE JONG, Y. P. & RICE, C. M. 2009. Human occludin is a hepatitis C virus entry factor required for infection of mouse cells. *Nature,* 457**,** 882-6.

PLOUFFE, S. W., LIN, K. C., MOORE, J. L., 3RD, TAN, F. E., MA, S., YE, Z., QIU, Y., REN, B. & GUAN, K. L. 2018. The Hippo pathway effector proteins YAP and TAZ have both distinct and overlapping functions in the cell. *J Biol Chem,* 293**,** 11230-11240.

POLARIS OBSERVATORY HCV COLLABORATORS. 2017. Global prevalence and genotype distribution of hepatitis C virus infection in 2015: a modelling study. *Lancet Gastroenterol Hepatol,* 2**,** 161-176.

POLO, J. M., ANDERSSEN, E., WALSH, R. M., SCHWARZ, B. A., NEFZGER, C. M., LIM, S. M., BORKENT, M., APOSTOLOU, E., ALAEI, S., CLOUTIER, J., BAR-NUR, O., CHELOUFI, S., STADTFELD, M., FIGUEROA, M. E., ROBINTON, D., NATESAN, S., MELNICK, A., ZHU, J., RAMASWAMY, S. & HOCHEDLINGER, K. 2012. A molecular roadmap of reprogramming somatic cells into iPS cells. *Cell,* 151**,** 1617-32.

PONTOGLIO, M., BARRA, J., HADCHOUEL, M., DOYEN, A., KRESS, C., BACH, J. P., BABINET, C. & YANIV, M. 1996. Hepatocyte nuclear factor 1 inactivation results in hepatic dysfunction, phenylketonuria, and renal Fanconi syndrome. *Cell,* 84**,** 575-85.

POOLE, E., HE, B., LAMB, R. A., RANDALL, R. E. & GOODBOURN, S. 2002. The V proteins of simian virus 5 and other paramyxoviruses inhibit induction of interferon-beta. *Virology,* 303**,** 33-46.

POON, C. L., ZHANG, X., LIN, J. I., MANNING, S. A. & HARVEY, K. F. 2012. Homeodomain-interacting protein kinase regulates Hippo pathway-dependent tissue growth. *Curr Biol,* 22**,** 1587-94.

POPESCU, C. I., ROUILLE, Y. & DUBUISSON, J. 2011. Hepatitis C virus assembly imaging. *Viruses,* 3**,** 2238-54.

PORTA, C., DE AMICI, M., QUAGLINI, S., PAGLINO, C., TAGLIANI, F., BONCIMINO, A., MORATTI, R. & CORAZZA, G. R. 2008. Circulating interleukin-6 as a tumor marker for hepatocellular carcinoma. *Ann Oncol,* 19**,** 353-8.

PRASKOVA, M., KHOKLATCHEV, A., ORTIZ-VEGA, S. & AVRUCH, J. 2004. Regulation of the MST1 kinase by autophosphorylation, by the growth inhibitory proteins, RASSF1 and NORE1, and by Ras. *Biochem J,* 381**,** 453-62.

PUBLIC HEALTH ENGLAND., COSTELLA, A., HARRIS, H., MANDAL, S. & RAMSAY, M. 2018. Hepatitis C in England and the UK. *In:* HARRIS, H. (ed.). London.

PURCELL, R. H., ALTER, H. J. & DIENSTAG, J. L. 1976. Non-A, non-B hepatitis. *Yale J Biol Med,* 49**,** 243-50.

QADRI, I., IWAHASHI, M. & SIMON, F. 2002. Hepatitis C virus NS5A protein binds TBP and p53, inhibiting their DNA binding and p53 interactions with TBP and ERCC3. *Biochim Biophys Acta,* 1592**,** 193-204.

QUAN, P. L., FIRTH, C., CONTE, J. M., WILLIAMS, S. H., ZAMBRANA-TORRELIO, C. M., ANTHONY, S. J., ELLISON, J. A., GILBERT, A. T., KUZMIN, I. V., NIEZGODA, M., OSINUBI, M. O., RECUENCO, S., MARKOTTER, W., BREIMAN, R. F., KALEMBA, L., MALEKANI, J., LINDBLADE, K. A., ROSTAL, M. K., OJEDA-FLORES, R., SUZAN, G., DAVIS, L. B., BLAU, D. M., OGUNKOYA, A. B., ALVAREZ CASTILLO, D. A., MORAN, D., NGAM, S., AKAIBE, D., AGWANDA, B., BRIESE, T., EPSTEIN, J. H., DASZAK, P., RUPPRECHT, C. E., HOLMES, E. C. & LIPKIN, W. I. 2013. Bats are a major natural reservoir for hepaciviruses and pegiviruses. *Proc Natl Acad Sci U S A,* 110**,** 8194-9.

RANDALL, G., PANIS, M., COOPER, J. D., TELLINGHUISEN, T. L., SUKHODOLETS, K. E., PFEFFER, S., LANDTHALER, M., LANDGRAF, P., KAN, S., LINDENBACH, B. D., CHIEN, M., WEIR, D. B., RUSSO, J. J., JU, J., BROWNSTEIN, M. J., SHERIDAN, R., SANDER, C., ZAVOLAN, M., TUSCHL, T. & RICE, C. M. 2007. Cellular cofactors affecting hepatitis C virus infection and replication. *Proc Natl Acad Sci U S A,* 104**,** 12884-9.

RANGER-ROGEZ, S., ALAIN, S. & DENIS, F. 2002. [Hepatitis viruses: mother to child transmission]. *Pathol Biol (Paris),* 50**,** 568-75.

RAVEN, A., LU, W. Y., MAN, T. Y., FERREIRA-GONZALEZ, S., O'DUIBHIR, E., DWYER, B. J., THOMSON, J. P., MEEHAN, R. R., BOGORAD, R., KOTELIANSKY, V., KOTELEVTSEV, Y., FFRENCH-CONSTANT, C., BOULTER, L. & FORBES, S. J. 2017. Cholangiocytes act as facultative liver stem cells during impaired hepatocyte regeneration. *Nature,* 547**,** 350-354.

RAY, R. B., STEELE, R., MEYER, K. & RAY, R. 1998. Hepatitis C virus core protein represses p21WAF1/Cip1/Sid1 promoter activity. *Gene,* 208**,** 331-6.

REIG, M., MARINO, Z., PERELLO, C., INARRAIRAEGUI, M., RIBEIRO, A., LENS, S., DIAZ, A., VILANA, R., DARNELL, A., VARELA, M., SANGRO, B., CALLEJA, J. L., FORNS, X. & BRUIX, J. 2016. Unexpected high rate of early tumor recurrence in patients with HCV-related HCC undergoing interferon-free therapy. *J Hepatol,* 65**,** 719-726.

REIS, H., BERTRAM, S., POTT, L., CANBAY, A., GALLINAT, A. & BABA, H. A. 2017. Markers of Hippo-Pathway Activity in Tumor Forming Liver Lesions. *Pathol Oncol Res,* 23**,** 33-39.

RIBEIRO, P. S., JOSUE, F., WEPF, A., WEHR, M. C., RINNER, O., KELLY, G., TAPON, N. & GSTAIGER, M. 2010. Combined functional genomic and proteomic approaches identify a PP2A complex as a negative regulator of Hippo signaling. *Mol Cell,* 39**,** 521-34.

RIBEIRO, R. M., LI, H., WANG, S., STODDARD, M. B., LEARN, G. H., KORBER, B. T., BHATTACHARYA, T., GUEDJ, J., PARRISH, E. H., HAHN, B. H., SHAW, G. M. & PERELSON, A. S. 2012. Quantifying the diversification of hepatitis C virus (HCV) during primary infection: estimates of the in vivo mutation rate. *PLoS Pathog,* 8**,** e1002881.

RIJNBRAND, R. C. & LEMON, S. M. 2000. Internal ribosome entry site-mediated translation in hepatitis C virus replication. *Curr Top Microbiol Immunol,* 242**,** 85-116.

RIZVI, S., FISCHBACH, S. R., BRONK, S. F., HIRSOVA, P., KRISHNAN, A., DHANASEKARAN, R., SMADBECK, J. B., SMOOT, R. L., VASMATZIS, G. & GORES, G. J. 2018. YAP-associated chromosomal instability and cholangiocarcinoma in mice. *Oncotarget,* 9**,** 5892-5905.

RIZZETTO, M., CANESE, M. G., GERIN, J. L., LONDON, W. T., SLY, D. L. & PURCELL, R. H. 1980. Transmission of the hepatitis B virus-associated delta antigen to chimpanzees. *J Infect Dis,* 141**,** 590-602.

ROBERTS, A. P., LEWIS, A. P. & JOPLING, C. L. 2011. miR-122 activates hepatitis C virus translation by a specialized mechanism requiring particular RNA components. *Nucleic Acids Res,* 39**,** 7716-29.

ROCKSTROH, J. K. 2015. HCV cure for everyone or which challenges remain? *J Virus Erad,* 1**,** 55-8.

ROELANDT, P., OBEID, S., PAESHUYSE, J., VANHOVE, J., VAN LOMMEL, A., NAHMIAS, Y., NEVENS, F., NEYTS, J. & VERFAILLIE, C. M. 2012. Human pluripotent stem cell-derived hepatocytes support complete replication of hepatitis C virus. *J Hepatol,* 57**,** 246-51.

ROMERO-BREY, I., MERZ, A., CHIRAMEL, A., LEE, J. Y., CHLANDA, P., HASELMAN, U., SANTARELLA-MELLWIG, R., HABERMANN, A., HOPPE, S., KALLIS, S., WALTHER, P., ANTONY, C., KRIJNSE-LOCKER, J. & BARTENSCHLAGER, R. 2012. Three-dimensional architecture and biogenesis of membrane structures associated with hepatitis C virus replication. *PLoS Pathog,* 8**,** e1003056.

ROMERO-LOPEZ, C., BARROSO-DELJESUS, A., GARCIA-SACRISTAN, A., BRIONES, C. & BERZAL-HERRANZ, A. 2014. End-to-end crosstalk within the hepatitis C virus genome mediates the conformational switch of the 3'X-tail region. *Nucleic Acids Res,* 42**,** 567-82.

ROSKAMS, T. 2006. Liver stem cells and their implication in hepatocellular and cholangiocarcinoma. *Oncogene,* 25**,** 3818-22.

ROSKAMS, T. A., LIBBRECHT, L. & DESMET, V. J. 2003. Progenitor cells in diseased human liver. *Semin Liver Dis,* 23**,** 385-96.

ROSS-THRIEPLAND, D. & HARRIS, M. 2015. Hepatitis C virus NS5A: enigmatic but still promiscuous 10 years on! *J Gen Virol,* 96**,** 727-38.

ROSSI, J. M., DUNN, N. R., HOGAN, B. L. & ZARET, K. S. 2001. Distinct mesodermal signals, including BMPs from the septum transversum mesenchyme, are required in combination for hepatogenesis from the endoderm. *Genes Dev,* 15**,** 1998-2009.

SAEED, M., ANDREO, U., CHUNG, H. Y., ESPIRITU, C., BRANCH, A. D., SILVA, J. M. & RICE, C. M. 2015. SEC14L2 enables pan-genotype HCV replication in cell culture. *Nature,* 524**,** 471-5.

SAINZ, B., JR., BARRETTO, N., MARTIN, D. N., HIRAGA, N., IMAMURA, M., HUSSAIN, S., MARSH, K. A., YU, X., CHAYAMA, K., ALREFAI, W. A. & UPRICHARD, S. L. 2012. Identification of the Niemann-Pick C1-like 1 cholesterol absorption receptor as a new hepatitis C virus entry factor. *Nat Med,* 18**,** 281-5.

SAINZ, B., JR., BARRETTO, N. & UPRICHARD, S. L. 2009a. Hepatitis C virus infection in phenotypically distinct Huh7 cell lines. *PLoS One,* 4**,** e6561.

SAINZ, B., JR. & CHISARI, F. V. 2006. Production of infectious hepatitis C virus by well-differentiated, growth-arrested human hepatoma-derived cells. *J Virol,* 80**,** 10253-7.

SAINZ, B., JR., TENCATE, V. & UPRICHARD, S. L. 2009b. Three-dimensional Huh7 cell culture system for the study of Hepatitis C virus infection. *Virol J,* 6**,** 103.

SAITO, K., MEYER, K., WARNER, R., BASU, A., RAY, R. B. & RAY, R. 2006. Hepatitis C virus core protein inhibits tumor necrosis factor alpha-mediated apoptosis by a protective effect involving cellular FLICE inhibitory protein. *J Virol,* 80**,** 4372-9.

SAKAI, A., CLAIRE, M. S., FAULK, K., GOVINDARAJAN, S., EMERSON, S. U., PURCELL, R. H. & BUKH, J. 2003. The p7 polypeptide of hepatitis C virus is critical for infectivity and contains functionally important genotype-specific sequences. *Proc Natl Acad Sci U S A,* 100**,** 11646-51.

SALARIA, S., MEANS, A., REVETTA, F., IDREES, K., LIU, E. & SHI, C. 2015. Expression of CD24, a Stem Cell Marker, in Pancreatic and Small Intestinal Neuroendocrine Tumors. *Am J Clin Pathol,* 144**,** 642-8.

SALEMI, M. & VANDAMME, A. M. 2002. Hepatitis C virus evolutionary patterns studied through analysis of full-genome sequences. *J Mol Evol,* 54**,** 62-70.

SAMSON, A., BENTHAM, M. J., SCOTT, K., NUOVO, G., BLOY, A., APPLETON, E., ADAIR, R. A., DAVE, R., PECKHAM-COOPER, A., TOOGOOD, G., NAGAMORI, S., COFFEY, M., VILE, R., HARRINGTON, K., SELBY, P., ERRINGTON-MAIS, F., MELCHER, A. & GRIFFIN, S. 2018. Oncolytic reovirus as a combined antiviral and anti-tumour agent for the treatment of liver cancer. *Gut,* 67**,** 562-573.

SANCHEZ-APARICIO, M. T., FEINMAN, L. J., GARCIA-SASTRE, A. & SHAW, M. L. 2018. Paramyxovirus V Proteins Interact with the RIG-I/TRIM25 Regulatory Complex and Inhibit RIG-I Signaling. *J Virol,* 92.

SARFRAZ, S., HAMID, S., ALI, S., JAFRI, W. & SIDDIQUI, A. A. 2009. Modulations of cell cycle checkpoints during HCV associated disease. *BMC Infect Dis,* 9**,** 125.

SARHAN, M. A., PHAM, T. N., CHEN, A. Y. & MICHALAK, T. I. 2012. Hepatitis C virus infection of human T lymphocytes is mediated by CD5. *J Virol,* 86**,** 3723-35.

SARRAZIN, C. 2016. The importance of resistance to direct antiviral drugs in HCV infection in clinical practice. *J Hepatol,* 64**,** 486-504.

SCARSELLI, E., ANSUINI, H., CERINO, R., ROCCASECCA, R. M., ACALI, S., FILOCAMO, G., TRABONI, C., NICOSIA, A., CORTESE, R. & VITELLI, A. 2002. The human scavenger receptor class B type I is a novel candidate receptor for the hepatitis C virus. *Embo j,* 21**,** 5017-25.

SCHEEL, T. K. & RICE, C. M. 2013. Understanding the hepatitis C virus life cycle paves the way for highly effective therapies. *Nat Med,* 19**,** 837-49.

SCHEEL, T. K., SIMMONDS, P. & KAPOOR, A. 2015. Surveying the global virome: identification and characterization of HCV-related animal hepaciviruses. *Antiviral Res,* 115**,** 83-93.

SCHLEGELMILCH, K., MOHSENI, M., KIRAK, O., PRUSZAK, J., RODRIGUEZ, J. R., ZHOU, D., KREGER, B. T., VASIOUKHIN, V., AVRUCH, J., BRUMMELKAMP, T. R. & CAMARGO, F. D. 2011. Yap1 acts downstream of alpha-catenin to control epidermal proliferation. *Cell,* 144**,** 782-95.

SCHMELZER, E., WAUTHIER, E. & REID, L. M. 2006. The phenotypes of pluripotent human hepatic progenitors. *Stem Cells,* 24**,** 1852-8.

SCHMIDT, C. M., MCKILLOP, I. H., CAHILL, P. A. & SITZMANN, J. V. 1997. Increased MAPK expression and activity in primary human hepatocellular carcinoma. *Biochem Biophys Res Commun,* 236**,** 54-8.

SCHNEIDER-POETSCH, T., JU, J., EYLER, D. E., DANG, Y., BHAT, S., MERRICK, W. C., GREEN, R., SHEN, B. & LIU, J. O. 2010. Inhibition of eukaryotic translation elongation by cycloheximide and lactimidomycin. *Nat Chem Biol,* 6**,** 209-217.

SCHNELL, U., CIRULLI, V. & GIEPMANS, B. N. 2013. EpCAM: structure and function in health and disease. *Biochim Biophys Acta,* 1828**,** 1989-2001.

SCHOLZEN, T. & GERDES, J. 2000. The Ki-67 protein: from the known and the unknown. *J Cell Physiol,* 182**,** 311-22.

SCHREGEL, V., JACOBI, S., PENIN, F. & TAUTZ, N. 2009. Hepatitis C virus NS2 is a protease stimulated by cofactor domains in NS3. *Proc Natl Acad Sci U S A,* 106**,** 5342-7.

SCHREM, H., KLEMPNAUER, J. & BORLAK, J. 2002. Liver-enriched transcription factors in liver function and development. Part I: the hepatocyte nuclear factor network and liver-specific gene expression. *Pharmacol Rev,* 54**,** 129-58.

SCHULZE, K., IMBEAUD, S., LETOUZE, E., ALEXANDROV, L. B., CALDERARO, J., REBOUISSOU, S., COUCHY, G., MEILLER, C., SHINDE, J., SOYSOUVANH, F., CALATAYUD, A. L., PINYOL, R., PELLETIER, L., BALABAUD, C., LAURENT, A., BLANC, J. F., MAZZAFERRO, V., CALVO, F., VILLANUEVA, A., NAULT, J. C., BIOULAC-SAGE, P., STRATTON, M. R., LLOVET, J. M. & ZUCMAN-ROSSI, J. 2015. Exome sequencing of hepatocellular carcinomas identifies new mutational signatures and potential therapeutic targets. *Nat Genet,* 47**,** 505-511.

SCHWARTZ, R. E., TREHAN, K., ANDRUS, L., SHEAHAN, T. P., PLOSS, A., DUNCAN, S. A., RICE, C. M. & BHATIA, S. N. 2012. Modeling hepatitis C virus infection using human induced pluripotent stem cells. *Proc Natl Acad Sci U S A,* 109**,** 2544-8.

SEBIO, A. & LENZ, H. J. 2015. Molecular Pathways: Hippo Signaling, a Critical Tumor Suppressor. *Clin Cancer Res,* 21**,** 5002-7.

SEIPP, S., MUELLER, H. M., PFAFF, E., STREMMEL, W., THEILMANN, L. & GOESER, T. 1997. Establishment of persistent hepatitis C virus infection and replication in vitro. *J Gen Virol,* 78 ( Pt 10)**,** 2467-76.

SEOW, T. K., LIANG, R. C., LEOW, C. K. & CHUNG, M. C. 2001. Hepatocellular carcinoma: from bedside to proteomics. *Proteomics,* 1**,** 1249-63.

SERLS, A. E., DOHERTY, S., PARVATIYAR, P., WELLS, J. M. & DEUTSCH, G. H. 2005. Different thresholds of fibroblast growth factors pattern the ventral foregut into liver and lung. *Development,* 132**,** 35-47.

SHARMA, N. R., MATEU, G., DREUX, M., GRAKOUI, A., COSSET, F. L. & MELIKYAN, G. B. 2011. Hepatitis C virus is primed by CD81 protein for low pH-dependent fusion. *J Biol Chem,* 286**,** 30361-76.

SHEN, M. M. 2007. Nodal signaling: developmental roles and regulation. *Development,* 134**,** 1023-34.

SHI-WEN, X., LEASK, A. & ABRAHAM, D. 2008. Regulation and function of connective tissue growth factor/CCN2 in tissue repair, scarring and fibrosis. *Cytokine Growth Factor Rev,* 19**,** 133-44.

SHIMAKAMI, T., YAMANE, D., JANGRA, R. K., KEMPF, B. J., SPANIEL, C., BARTON, D. J. & LEMON, S. M. 2012. Stabilization of hepatitis C virus RNA by an Ago2-miR-122 complex. *Proc Natl Acad Sci U S A,* 109**,** 941-6.

SHIMIZU, Y. K., IWAMOTO, A., HIJIKATA, M., PURCELL, R. H. & YOSHIKURA, H. 1992. Evidence for in vitro replication of hepatitis C virus genome in a human T-cell line. *Proc Natl Acad Sci U S A,* 89**,** 5477-81.

SHIN KIM, S., YEOM, S., KWAK, J., AHN, H. J. & LIB JANG, K. 2016. Hepatitis B virus X protein induces epithelial-mesenchymal transition by repressing E-cadherin expression via upregulation of E12/E47. *J Gen Virol,* 97**,** 134-43.

SHIN, S., WANGENSTEEN, K. J., TETA-BISSETT, M., WANG, Y. J., MOSLEH-SHIRAZI, E., BUZA, E. L., GREENBAUM, L. E. & KAESTNER, K. H. 2016. Genetic lineage tracing analysis of the cell of origin of hepatotoxin-induced liver tumors in mice. *Hepatology,* 64**,** 1163-1177.

SIA, D., HOSHIDA, Y., VILLANUEVA, A., ROAYAIE, S., FERRER, J., TABAK, B., PEIX, J., SOLE, M., TOVAR, V., ALSINET, C., CORNELLA, H., KLOTZLE, B., FAN, J. B., COTSOGLOU, C., THUNG, S. N., FUSTER, J., WAXMAN, S., GARCIA-VALDECASAS, J. C., BRUIX, J., SCHWARTZ, M. E., BEROUKHIM, R., MAZZAFERRO, V. & LLOVET, J. M. 2013. Integrative molecular analysis of intrahepatic cholangiocarcinoma reveals 2 classes that have different outcomes. *Gastroenterology,* 144**,** 829-40.

SIA, D., VILLANUEVA, A., FRIEDMAN, S. L. & LLOVET, J. M. 2017. Liver Cancer Cell of Origin, Molecular Class, and Effects on Patient Prognosis. *Gastroenterology,* 152**,** 745-761.

SIBLEY, S. D., LAUCK, M., BAILEY, A. L., HYEROBA, D., TUMUKUNDE, A., WENY, G., CHAPMAN, C. A., O'CONNOR, D. H., GOLDBERG, T. L. & FRIEDRICH, T. C. 2014. Discovery and characterization of distinct simian pegiviruses in three wild African Old World monkey species. *PLoS One,* 9**,** e98569.

SILVIS, M. R., KREGER, B. T., LIEN, W. H., KLEZOVITCH, O., RUDAKOVA, G. M., CAMARGO, F. D., LANTZ, D. M., SEYKORA, J. T. & VASIOUKHIN, V. 2011. alpha-catenin is a tumor suppressor that controls cell accumulation by regulating the localization and activity of the transcriptional coactivator Yap1. *Sci Signal,* 4**,** ra33.

SIMILE, M. M., LATTE, G., DEMARTIS, M. I., BROZZETTI, S., CALVISI, D. F., PORCU, A., FEO, C. F., SEDDAIU, M. A., DAINO, L., BERASAIN, C., TOMASI, M. L., AVILA, M. A., FEO, F. & PASCALE, R. M. 2016. Post-translational deregulation of YAP1 is genetically controlled in rat liver cancer and determines the fate and stem-like behavior of the human disease. *Oncotarget,* 7**,** 49194-49216.

SIMMONDS, P. 2004. Genetic diversity and evolution of hepatitis C virus--15 years on. *J Gen Virol,* 85**,** 3173-88.

SIMMONDS, P., BECHER, P., BUKH, J., GOULD, E. A., MEYERS, G., MONATH, T., MUERHOFF, S., PLETNEV, A., RICO-HESSE, R., SMITH, D. B., STAPLETON, J. T. & ICTV REPORT, C. 2017. ICTV Virus Taxonomy Profile: Flaviviridae. *J Gen Virol,* 98**,** 2-3.

SINGAL, A. K., SINGH, A., JAGANMOHAN, S., GUTURU, P., MUMMADI, R., KUO, Y. F. & SOOD, G. K. 2010. Antiviral therapy reduces risk of hepatocellular carcinoma in patients with hepatitis C virus-related cirrhosis. *Clin Gastroenterol Hepatol,* 8**,** 192-9.

SINGER, A. W., REDDY, K. R., TELEP, L. E., OSINUSI, A. O., BRAINARD, D. M., BUTI, M. & CHOKKALINGAM, A. P. 2018. Direct-acting antiviral treatment for hepatitis C virus infection and risk of incident liver cancer: a retrospective cohort study. *Aliment Pharmacol Ther,* 47**,** 1278-1287.

SINGH, S., CHAKRABORTY, S., BONTHU, N., RADIO, S., HUSSAIN, S. M. & SASSON, A. 2013. Combined hepatocellular cholangiocarcinoma: a case report and review of literature. *Dig Dis Sci,* 58**,** 2114-23.

SKOULOUDAKI, K., PUETZ, M., SIMONS, M., COURBARD, J. R., BOEHLKE, C., HARTLEBEN, B., ENGEL, C., MOELLER, M. J., ENGLERT, C., BOLLIG, F., SCHAFER, T., RAMACHANDRAN, H., MLODZIK, M., HUBER, T. B., KUEHN, E. W., KIM, E., KRAMER-ZUCKER, A. & WALZ, G. 2009. Scribble participates in Hippo signaling and is required for normal zebrafish pronephros development. *Proc Natl Acad Sci U S A,* 106**,** 8579-84.

SLADEK, F. M., RUSE, M. D., JR., NEPOMUCENO, L., HUANG, S. M. & STALLCUP, M. R. 1999. Modulation of transcriptional activation and coactivator interaction by a splicing variation in the F domain of nuclear receptor hepatocyte nuclear factor 4alpha1. *Mol Cell Biol,* 19**,** 6509-22.

SLADEK, F. M., ZHONG, W. M., LAI, E. & DARNELL, J. E., JR. 1990. Liver-enriched transcription factor HNF-4 is a novel member of the steroid hormone receptor superfamily. *Genes Dev,* 4**,** 2353-65.

SLIM, C. L., LAZARO-DIEGUEZ, F., BIJLARD, M., TOUSSAINT, M. J., DE BRUIN, A., DU, Q., MUSCH, A. & VAN IJZENDOORN, S. C. 2013. Par1b induces asymmetric inheritance of plasma membrane domains via LGN-dependent mitotic spindle orientation in proliferating hepatocytes. *PLoS Biol,* 11**,** e1001739.

SMITH, D. B., BUKH, J., KUIKEN, C., MUERHOFF, A. S., RICE, C. M., STAPLETON, J. T. & SIMMONDS, P. 2014. Expanded classification of hepatitis C virus into 7 genotypes and 67 subtypes: updated criteria and genotype assignment web resource. *Hepatology,* 59**,** 318-27.

SMITH, M. A., REGAL, R. E. & MOHAMMAD, R. A. 2016. Daclatasvir: A NS5A Replication Complex Inhibitor for Hepatitis C Infection. *Ann Pharmacother,* 50**,** 39-46.

SOBECKI, M., MROUJ, K., COLINGE, J., GERBE, F., JAY, P., KRASINSKA, L., DULIC, V. & FISHER, D. 2017. Cell-Cycle Regulation Accounts for Variability in Ki-67 Expression Levels. *Cancer Res,* 77**,** 2722-2734.

SOHN, B. H., SHIM, J. J., KIM, S. B., JANG, K. Y., KIM, S. M., KIM, J. H., HWANG, J. E., JANG, H. J., LEE, H. S., KIM, S. C., JEONG, W., KIM, S. S., PARK, E. S., HEO, J., KIM, Y. J., KIM, D. G., LEEM, S. H., KASEB, A., HASSAN, M. M., CHA, M., CHU, I. S., JOHNSON, R. L., PARK, Y. Y. & LEE, J. S. 2016. Inactivation of Hippo Pathway Is Significantly Associated with Poor Prognosis in Hepatocellular Carcinoma. *Clin Cancer Res,* 22**,** 1256-64.

SONG, H., MAK, K. K., TOPOL, L., YUN, K., HU, J., GARRETT, L., CHEN, Y., PARK, O., CHANG, J., SIMPSON, R. M., WANG, C. Y., GAO, B., JIANG, J. & YANG, Y. 2010. Mammalian Mst1 and Mst2 kinases play essential roles in organ size control and tumor suppression. *Proc Natl Acad Sci U S A,* 107**,** 1431-6.

SONG, K., HAN, C., ZHANG, J., LU, D., DASH, S., FEITELSON, M., LIM, K. & WU, T. 2013. Epigenetic regulation of MicroRNA-122 by peroxisome proliferator activated receptor-gamma and hepatitis b virus X protein in hepatocellular carcinoma cells. *Hepatology,* 58**,** 1681-92.

SORENSEN, K. K., SIMON-SANTAMARIA, J., MCCUSKEY, R. S. & SMEDSROD, B. 2015. Liver Sinusoidal Endothelial Cells. *Compr Physiol,* 5**,** 1751-74.

SOSA-PINEDA, B., WIGLE, J. T. & OLIVER, G. 2000. Hepatocyte migration during liver development requires Prox1. *Nat Genet,* 25**,** 254-5.

SPAHN, C. M., KIEFT, J. S., GRASSUCCI, R. A., PENCZEK, P. A., ZHOU, K., DOUDNA, J. A. & FRANK, J. 2001. Hepatitis C virus IRES RNA-induced changes in the conformation of the 40s ribosomal subunit. *Science,* 291**,** 1959-62.

STANGER, B. Z. 2015. Cellular homeostasis and repair in the mammalian liver. *Annu Rev Physiol,* 77**,** 179-200.

STAPLETON, J. T., FOUNG, S., MUERHOFF, A. S., BUKH, J. & SIMMONDS, P. 2011. The GB viruses: a review and proposed classification of GBV-A, GBV-C (HGV), and GBV-D in genus Pegivirus within the family Flaviviridae. *J Gen Virol,* 92**,** 233-46.

STEILING, H., MUHLBAUER, M., BATAILLE, F., SCHOLMERICH, J., WERNER, S. & HELLERBRAND, C. 2004. Activated hepatic stellate cells express keratinocyte growth factor in chronic liver disease. *Am J Pathol,* 165**,** 1233-41.

STEINMANN, E., PENIN, F., KALLIS, S., PATEL, A. H., BARTENSCHLAGER, R. & PIETSCHMANN, T. 2007. Hepatitis C virus p7 protein is crucial for assembly and release of infectious virions. *PLoS Pathog,* 3**,** e103.

STEVENS, C. E., BEASLEY, R. P., TSUI, J. & LEE, W. C. 1975. Vertical transmission of hepatitis B antigen in Taiwan. *N Engl J Med,* 292**,** 771-4.

STRANO, S., MUNARRIZ, E., ROSSI, M., CASTAGNOLI, L., SHAUL, Y., SACCHI, A., OREN, M., SUDOL, M., CESARENI, G. & BLANDINO, G. 2001. Physical interaction with Yes-associated protein enhances p73 transcriptional activity. *J Biol Chem,* 276**,** 15164-73.

STREET, A., MACDONALD, A., CROWDER, K. & HARRIS, M. 2004. The Hepatitis C virus NS5A protein activates a phosphoinositide 3-kinase-dependent survival signaling cascade. *J Biol Chem,* 279**,** 12232-41.

STREET, A., MACDONALD, A., MCCORMICK, C. & HARRIS, M. 2005. Hepatitis C virus NS5A-mediated activation of phosphoinositide 3-kinase results in stabilization of cellular beta-catenin and stimulation of beta-catenin-responsive transcription. *J Virol,* 79**,** 5006-16.

STUART, H. T., VAN OOSTEN, A. L., RADZISHEUSKAYA, A., MARTELLO, G., MILLER, A., DIETMANN, S., NICHOLS, J. & SILVA, J. C. 2014. NANOG amplifies STAT3 activation and they synergistically induce the naive pluripotent program. *Curr Biol,* 24**,** 340-6.

SUETSUGU, A., NAGAKI, M., AOKI, H., MOTOHASHI, T., KUNISADA, T. & MORIWAKI, H. 2006. Characterization of CD133+ hepatocellular carcinoma cells as cancer stem/progenitor cells. *Biochem Biophys Res Commun,* 351**,** 820-4.

SUGIHARA, T., WERNEBURG, N. W., HERNANDEZ, M. C., YANG, L., KABASHIMA, A., HIRSOVA, P., YOHANATHAN, L., SOSA, C., TRUTY, M. J., VASMATZIS, G., GORES, G. J. & SMOOT, R. L. 2018. YAP Tyrosine Phosphorylation and Nuclear Localization in Cholangiocarcinoma Cells is Regulated by LCK and Independent of LATS Activity. *Mol Cancer Res*.

SUGIMACHI, K., NISHIO, M., AISHIMA, S., KURODA, Y., IGUCHI, T., KOMATSU, H., HIRATA, H., SAKIMURA, S., EGUCHI, H., BEKKI, Y., TAKENAKA, K., MAEHARA, Y., SUZUKI, A. & MIMORI, K. 2017. Altered Expression of Hippo Signaling Pathway Molecules in Intrahepatic Cholangiocarcinoma. *Oncology,* 93**,** 67-74.

SUMPTER, R., JR., LOO, Y. M., FOY, E., LI, K., YONEYAMA, M., FUJITA, T., LEMON, S. M. & GALE, M., JR. 2005. Regulating intracellular antiviral defense and permissiveness to hepatitis C virus RNA replication through a cellular RNA helicase, RIG-I. *J Virol,* 79**,** 2689-99.

SUN, S. & IRVINE, K. D. 2016. Cellular Organization and Cytoskeletal Regulation of the Hippo Signaling Network. *Trends Cell Biol,* 26**,** 694-704.

SUPPIAH, V., MOLDOVAN, M., AHLENSTIEL, G., BERG, T., WELTMAN, M., ABATE, M. L., BASSENDINE, M., SPENGLER, U., DORE, G. J., POWELL, E., RIORDAN, S., SHERIDAN, D., SMEDILE, A., FRAGOMELI, V., MULLER, T., BAHLO, M., STEWART, G. J., BOOTH, D. R. & GEORGE, J. 2009. IL28B is associated with response to chronic hepatitis C interferon-alpha and ribavirin therapy. *Nat Genet,* 41**,** 1100-4.

SUZUKI, A., IWAMA, A., MIYASHITA, H., NAKAUCHI, H. & TANIGUCHI, H. 2003. Role for growth factors and extracellular matrix in controlling differentiation of prospectively isolated hepatic stem cells. *Development,* 130**,** 2513-24.

SUZUKI, A., SEKIYA, S., BUSCHER, D., IZPISUA BELMONTE, J. C. & TANIGUCHI, H. 2008. Tbx3 controls the fate of hepatic progenitor cells in liver development by suppressing p19ARF expression. *Development,* 135**,** 1589-95.

TAGAWA, M., KATO, N., YOKOSUKA, O., ISHIKAWA, T., OHTO, M. & OMATA, M. 1995. Infection of human hepatocyte cell lines with hepatitis C virus in vitro. *J Gastroenterol Hepatol,* 10**,** 523-7.

TAI, C. L., CHI, W. K., CHEN, D. S. & HWANG, L. H. 1996. The helicase activity associated with hepatitis C virus nonstructural protein 3 (NS3). *J Virol,* 70**,** 8477-84.

TAKEDA, K. & AKIRA, S. 2000. STAT family of transcription factors in cytokine-mediated biological responses. *Cytokine Growth Factor Rev,* 11**,** 199-207.

TAMM, I., WANG, Y., SAUSVILLE, E., SCUDIERO, D. A., VIGNA, N., OLTERSDORF, T. & REED, J. C. 1998. IAP-family protein survivin inhibits caspase activity and apoptosis induced by Fas (CD95), Bax, caspases, and anticancer drugs. *Cancer Res,* 58**,** 5315-20.

TAN, S. L., NAKAO, H., HE, Y., VIJAYSRI, S., NEDDERMANN, P., JACOBS, B. L., MAYER, B. J. & KATZE, M. G. 1999. NS5A, a nonstructural protein of hepatitis C virus, binds growth factor receptor-bound protein 2 adaptor protein in a Src homology 3 domain/ligand-dependent manner and perturbs mitogenic signaling. *Proc Natl Acad Sci U S A,* 96**,** 5533-8.

TANAKA, M. & IWAKIRI, Y. 2016. The Hepatic Lymphatic Vascular System: Structure, Function, Markers, and Lymphangiogenesis. *Cell Mol Gastroenterol Hepatol,* 2**,** 733-749.

TANAKA, T., KATO, N., CHO, M. J. & SHIMOTOHNO, K. 1995. A novel sequence found at the 3' terminus of hepatitis C virus genome. *Biochem Biophys Res Commun,* 215**,** 744-9.

TANAKA, T., KATO, N., CHO, M. J., SUGIYAMA, K. & SHIMOTOHNO, K. 1996. Structure of the 3' terminus of the hepatitis C virus genome. *J Virol,* 70**,** 3307-12.

TANAKA, Y., NISHIDA, N., SUGIYAMA, M., KUROSAKI, M., MATSUURA, K., SAKAMOTO, N., NAKAGAWA, M., KORENAGA, M., HINO, K., HIGE, S., ITO, Y., MITA, E., TANAKA, E., MOCHIDA, S., MURAWAKI, Y., HONDA, M., SAKAI, A., HIASA, Y., NISHIGUCHI, S., KOIKE, A., SAKAIDA, I., IMAMURA, M., ITO, K., YANO, K., MASAKI, N., SUGAUCHI, F., IZUMI, N., TOKUNAGA, K. & MIZOKAMI, M. 2009. Genome-wide association of IL28B with response to pegylated interferon-alpha and ribavirin therapy for chronic hepatitis C. *Nat Genet,* 41**,** 1105-9.

TANG, C., TAKAHASHI-KANEMITSU, A., KIKUCHI, I., BEN, C. & HATAKEYAMA, M. 2018. Transcriptional Co-activator Functions of YAP and TAZ Are Inversely Regulated by Tyrosine Phosphorylation Status of Parafibromin. *iScience,* 1**,** 1-15.

TANIGUCHI, H., KATO, N., OTSUKA, M., GOTO, T., YOSHIDA, H., SHIRATORI, Y. & OMATA, M. 2004. Hepatitis C virus core protein upregulates transforming growth factor-beta 1 transcription. *J Med Virol,* 72**,** 52-9.

TARLOW, B. D., PELZ, C., NAUGLER, W. E., WAKEFIELD, L., WILSON, E. M., FINEGOLD, M. J. & GROMPE, M. 2014. Bipotential adult liver progenitors are derived from chronically injured mature hepatocytes. *Cell Stem Cell,* 15**,** 605-18.

TAUB, R. 2004. Liver regeneration: from myth to mechanism. *Nat Rev Mol Cell Biol,* 5**,** 836-47.

TAUTZ, N., TEWS, B. A. & MEYERS, G. 2015. The Molecular Biology of Pestiviruses. *Adv Virus Res,* 93**,** 47-160.

TELLINGHUISEN, T. L., MARCOTRIGIANO, J., GORBALENYA, A. E. & RICE, C. M. 2004. The NS5A protein of hepatitis C virus is a zinc metalloprotein. *J Biol Chem,* 279**,** 48576-87.

THEISE, N. D., SAXENA, R., PORTMANN, B. C., THUNG, S. N., YEE, H., CHIRIBOGA, L., KUMAR, A. & CRAWFORD, J. M. 1999. The canals of Hering and hepatic stem cells in humans. *Hepatology,* 30**,** 1425-33.

THIBAULT, P. A., HUYS, A., DHILLON, P. & WILSON, J. A. 2013. MicroRNA-122-dependent and -independent replication of Hepatitis C Virus in Hep3B human hepatoma cells. *Virology,* 436**,** 179-90.

THOMAS, S., HARDING, M. A., SMITH, S. C., OVERDEVEST, J. B., NITZ, M. D., FRIERSON, H. F., TOMLINS, S. A., KRISTIANSEN, G. & THEODORESCU, D. 2012. CD24 is an effector of HIF-1-driven primary tumor growth and metastasis. *Cancer Res,* 72**,** 5600-12.

TISO, N., FILIPPI, A., PAULS, S., BORTOLUSSI, M. & ARGENTON, F. 2002. BMP signalling regulates anteroposterior endoderm patterning in zebrafish. *Mech Dev,* 118**,** 29-37.

TOJKANDER, S., GATEVA, G. & LAPPALAINEN, P. 2012. Actin stress fibers--assembly, dynamics and biological roles. *J Cell Sci,* 125**,** 1855-64.

TONG, Y., CHI, X., YANG, W. & ZHONG, J. 2017. Functional Analysis of Hepatitis C Virus (HCV) Envelope Protein E1 Using a trans-Complementation System Reveals a Dual Role of a Putative Fusion Peptide of E1 in both HCV Entry and Morphogenesis. *J Virol,* 91.

TORRE, C., PERRET, C. & COLNOT, S. 2010. Molecular determinants of liver zonation. *Prog Mol Biol Transl Sci,* 97**,** 127-50.

TORRES-PADILLA, M. E., FOUGERE-DESCHATRETTE, C. & WEISS, M. C. 2001. Expression of HNF4alpha isoforms in mouse liver development is regulated by sequential promoter usage and constitutive 3' end splicing. *Mech Dev,* 109**,** 183-93.

TORRES-PADILLA, M. E., SLADEK, F. M. & WEISS, M. C. 2002. Developmentally regulated N-terminal variants of the nuclear receptor hepatocyte nuclear factor 4alpha mediate multiple interactions through coactivator and corepressor-histone deacetylase complexes. *J Biol Chem,* 277**,** 44677-87.

TREMBLAY, K. D. & ZARET, K. S. 2005. Distinct populations of endoderm cells converge to generate the embryonic liver bud and ventral foregut tissues. *Dev Biol,* 280**,** 87-99.

TREYER, A. & MUSCH, A. 2013. Hepatocyte polarity. *Compr Physiol,* 3**,** 243-87.

TSCHAHARGANEH, D. F., XUE, W., CALVISI, D. F., EVERT, M., MICHURINA, T. V., DOW, L. E., BANITO, A., KATZ, S. F., KASTENHUBER, E. R., WEISSMUELLER, S., HUANG, C. H., LECHEL, A., ANDERSEN, J. B., CAPPER, D., ZENDER, L., LONGERICH, T., ENIKOLOPOV, G. & LOWE, S. W. 2014. p53-dependent Nestin regulation links tumor suppression to cellular plasticity in liver cancer. *Cell,* 158**,** 579-92.

TSCHERNE, D. M., JONES, C. T., EVANS, M. J., LINDENBACH, B. D., MCKEATING, J. A. & RICE, C. M. 2006. Time- and temperature-dependent activation of hepatitis C virus for low-pH-triggered entry. *J Virol,* 80**,** 1734-41.

TSUBOI, Y., ICHIDA, T., SUGITANI, S., GENDA, T., INAYOSHI, J., TAKAMURA, M., MATSUDA, Y., NOMOTO, M. & AOYAGI, Y. 2004. Overexpression of extracellular signal-regulated protein kinase and its correlation with proliferation in human hepatocellular carcinoma. *Liver Int,* 24**,** 432-6.

TSUKADA, Y., NAGAKI, M., SUETSUGU, A., OSAWA, Y. & MORIWAKI, H. 2009. Extracellular matrix is required for the survival and differentiation of transplanted hepatic progenitor cells. *Biochem Biophys Res Commun,* 381**,** 733-7.

TSUKIYAMA-KOHARA, K., IIZUKA, N., KOHARA, M. & NOMOTO, A. 1992. Internal ribosome entry site within hepatitis C virus RNA. *J Virol,* 66**,** 1476-83.

TUMMALA, K. S., BRANDT, M., TEIJEIRO, A., GRAÑA, O., SCHWABE, R. F., PERNA, C. & DJOUDER, N. 2017. Hepatocellular Carcinomas Originate Predominantly from Hepatocytes and Benign Lesions from Hepatic Progenitor Cells. *Cell Rep,* 19**,** 584-600.

UEBERHAM, E., LOW, R., UEBERHAM, U., SCHONIG, K., BUJARD, H. & GEBHARDT, R. 2003. Conditional tetracycline-regulated expression of TGF-beta1 in liver of transgenic mice leads to reversible intermediary fibrosis. *Hepatology,* 37**,** 1067-78.

URTASUN, R., LATASA, M. U., DEMARTIS, M. I., BALZANI, S., GONI, S., GARCIA-IRIGOYEN, O., ELIZALDE, M., AZCONA, M., PASCALE, R. M., FEO, F., BIOULAC-SAGE, P., BALABAUD, C., MUNTANE, J., PRIETO, J., BERASAIN, C. &

AVILA, M. A. 2011. Connective tissue growth factor autocriny in human hepatocellular carcinoma: oncogenic role and regulation by epidermal growth factor receptor/yes-associated protein-mediated activation. *Hepatology,* 54**,** 2149-58.

VAN OIJEN, M. G., MEDEMA, R. H., SLOOTWEG, P. J. & RIJKSEN, G. 1998. Positivity of the proliferation marker Ki-67 in noncycling cells. *Am J Clin Pathol,* 110**,** 24-31.

VAN ROY, F. & BERX, G. 2008. The cell-cell adhesion molecule E-cadherin. *Cell Mol Life Sci,* 65**,** 3756-88.

VARAKLIOTI, A., VASSILAKI, N., GEORGOPOULOU, U. & MAVROMARA, P. 2002. Alternate translation occurs within the core coding region of the hepatitis C viral genome. *J Biol Chem,* 277**,** 17713-21.

VARELAS, X. 2014. The Hippo pathway effectors TAZ and YAP in development, homeostasis and disease. *Development,* 141**,** 1614-26.

VARELAS, X., MILLER, B. W., SOPKO, R., SONG, S., GREGORIEFF, A., FELLOUSE, F. A., SAKUMA, R., PAWSON, T., HUNZIKER, W., MCNEILL, H., WRANA, J. L. & ATTISANO, L. 2010a. The Hippo pathway regulates Wnt/beta-catenin signaling. *Dev Cell,* 18**,** 579-91.

VARELAS, X., SAKUMA, R., SAMAVARCHI-TEHRANI, P., PEERANI, R., RAO, B. M., DEMBOWY, J., YAFFE, M. B., ZANDSTRA, P. W. & WRANA, J. L. 2008. TAZ controls Smad nucleocytoplasmic shuttling and regulates human embryonic stem-cell self-renewal. *Nat Cell Biol,* 10**,** 837-48.

VARELAS, X., SAMAVARCHI-TEHRANI, P., NARIMATSU, M., WEISS, A., COCKBURN, K., LARSEN, B. G., ROSSANT, J. & WRANA, J. L. 2010b. The Crumbs complex couples cell density sensing to Hippo-dependent control of the TGF-beta-SMAD pathway. *Dev Cell,* 19**,** 831-44.

VILLA, P., ARIOLI, P. & GUAITANI, A. 1991. Mechanism of maintenance of liver-specific functions by DMSO in cultured rat hepatocytes. *Exp Cell Res,* 194**,** 157-60.

VILLANUEVA, A., ALSINET, C., YANGER, K., HOSHIDA, Y., ZONG, Y., TOFFANIN, S., RODRIGUEZ-CARUNCHIO, L., SOLE, M., THUNG, S., STANGER, B. Z. & LLOVET, J. M. 2012. Notch signaling is activated in human hepatocellular carcinoma and induces tumor formation in mice. *Gastroenterology,* 143**,** 1660-1669 e7.

VINAS, O., BATALLER, R., SANCHO-BRU, P., GINES, P., BERENGUER, C., ENRICH, C., NICOLAS, J. M., ERCILLA, G., GALLART, T., VIVES, J., ARROYO, V. & RODES, J. 2003. Human hepatic stellate cells show features of antigen-presenting cells and stimulate lymphocyte proliferation. *Hepatology,* 38**,** 919-29.

WAHID, A., HELLE, F., DESCAMPS, V., DUVERLIE, G., PENIN, F. & DUBUISSON, J. 2013. Disulfide bonds in hepatitis C virus glycoprotein E1 control the assembly and entry functions of E2 glycoprotein. *J Virol,* 87**,** 1605-17.

WAKITA, T., PIETSCHMANN, T., KATO, T., DATE, T., MIYAMOTO, M., ZHAO, Z., MURTHY, K., HABERMANN, A., KRAUSSLICH, H. G., MIZOKAMI, M., BARTENSCHLAGER, R. & LIANG, T. J. 2005. Production of infectious hepatitis C virus in tissue culture from a cloned viral genome. *Nat Med,* 11**,** 791-6.

WALEWSKI, J. L., KELLER, T. R., STUMP, D. D. & BRANCH, A. D. 2001. Evidence for a new hepatitis C virus antigen encoded in an overlapping reading frame. *RNA,* 7**,** 710-21.

WALTER, S., RASCHE, A., MOREIRA-SOTO, A., PFAENDER, S., BLETSA, M., CORMAN, V. M., AGUILAR-SETIEN, A., GARCIA-LACY, F., HANS, A., TODT, D., SCHULER, G., SHNAIDERMAN-TORBAN, A., STEINMAN, A., RONCORONI, C.,

VENEZIANO, V., RUSENOVA, N., SANDEV, N., RUSENOV, A., ZAPRYANOVA, D., GARCIA-BOCANEGRA, I., JORES, J., CARLUCCIO, A., VERONESI, M. C., CAVALLERI, J. M., DROSTEN, C., LEMEY, P., STEINMANN, E. & DREXLER, J. F. 2017. Differential Infection Patterns and Recent Evolutionary Origins of Equine Hepaciviruses in Donkeys. *J Virol,* 91.

WANG, A., YOSHIMI, N., INO, N., TANAKA, T. & MORI, H. 1997. Overexpression of cyclin B1 in human colorectal cancers. *J Cancer Res Clin Oncol,* 123**,** 124-7.

WANG, A. G., LEE, D. S., MOON, H. B., KIM, J. M., CHO, K. H., CHOI, S. H., HA, H. L., HAN, Y. H., KIM, D. G., HWANG, S. B. & YU, D. Y. 2009. Non-structural 5A protein of hepatitis C virus induces a range of liver pathology in transgenic mice. *J Pathol,* 219**,** 253-62.

WANG, C., SARNOW, P. & SIDDIQUI, A. 1993. Translation of human hepatitis C virus RNA in cultured cells is mediated by an internal ribosome-binding mechanism. *J Virol,* 67**,** 3338-44.

WANG, C., ZHANG, L., HE, Q., FENG, X., ZHU, J., XU, Z., WANG, X., CHEN, F., LI, X. & DONG, J. 2012. Differences in Yes-associated protein and mRNA levels in regenerating liver and hepatocellular carcinoma. *Mol Med Rep,* 5**,** 410-4.

WANG, F., YOSHIDA, I., TAKAMATSU, M., ISHIDO, S., FUJITA, T., OKA, K. & HOTTA, H. 2000. Complex formation between hepatitis C virus core protein and p21Waf1/Cip1/Sdi1. *Biochem Biophys Res Commun,* 273**,** 479-84.

WANG, I. C., CHEN, Y. J., HUGHES, D., PETROVIC, V., MAJOR, M. L., PARK, H. J., TAN, Y., ACKERSON, T. & COSTA, R. H. 2005. Forkhead box M1 regulates the transcriptional network of genes essential for mitotic progression and genes encoding the SCF (Skp2-Cks1) ubiquitin ligase. *Mol Cell Biol,* 25**,** 10875-94.

WANG, J. C., STAFFORD, J. M. & GRANNER, D. K. 1998. SRC-1 and GRIP1 coactivate transcription with hepatocyte nuclear factor 4. *J Biol Chem,* 273**,** 30847-30850.

WANG, M., XIAO, J., JIANG, J. & QIN, R. 2011a. CD133 and ALDH may be the molecular markers of cholangiocarcinoma stem cells. *Int J Cancer,* 128**,** 1996-7.

WANG, N. D., FINEGOLD, M. J., BRADLEY, A., OU, C. N., ABDELSAYED, S. V., WILDE, M. D., TAYLOR, L. R., WILSON, D. R. & DARLINGTON, G. J. 1995. Impaired energy homeostasis in C/EBP alpha knockout mice. *Science,* 269**,** 1108-12.

WANG, W., HUANG, J. & CHEN, J. 2011b. Angiomotin-like proteins associate with and negatively regulate YAP1. *J Biol Chem,* 286**,** 4364-70.

WANG, X., KIYOKAWA, H., DENNEWITZ, M. B. & COSTA, R. H. 2002. The Forkhead Box m1b transcription factor is essential for hepatocyte DNA replication and mitosis during mouse liver regeneration. *Proc Natl Acad Sci U S A,* 99**,** 16881-6.

WARIS, G., FELMLEE, D. J., NEGRO, F. & SIDDIQUI, A. 2007. Hepatitis C virus induces proteolytic cleavage of sterol regulatory element binding proteins and stimulates their phosphorylation via oxidative stress. *J Virol,* 81**,** 8122-30.

WATANABE, Y., MIYASAKA, K. Y., KUBO, A., KIDA, Y. S., NAKAGAWA, O., HIRATE, Y., SASAKI, H. & OGURA, T. 2017. Notch and Hippo signaling converge on Strawberry Notch 1 (Sbno1) to synergistically activate Cdx2 during specification of the trophectoderm. *Sci Rep,* 7**,** 46135.

WATT, A. J., ZHAO, R., LI, J. & DUNCAN, S. A. 2007. Development of the mammalian liver and ventral pancreas is dependent on GATA4. *BMC Dev Biol,* 7**,** 37.

WAZIRY, R., HAJARIZADEH, B., GREBELY, J., AMIN, J., LAW, M., DANTA, M., GEORGE, J. & DORE, G. J. 2017. Hepatocellular carcinoma risk following direct-acting antiviral HCV therapy: A systematic review, meta-analyses, and meta-regression. *J Hepatol,* 67**,** 1204-1212.

WEBSTER, D. P., KLENERMAN, P. & DUSHEIKO, G. M. 2015. Hepatitis C. *Lancet,* 385**,** 1124-35.

WEILER, S. M. E., PINNA, F., WOLF, T., LUTZ, T., GELDIYEV, A., STICHT, C., KNAUB, M., THOMANN, S., BISSINGER, M., WAN, S., ROSSLER, S., BECKER, D., GRETZ, N., LANG, H., BERGMANN, F., USTIYAN, V., KALIN, T. V., SINGER, S., LEE, J. S., MARQUARDT, J. U., SCHIRMACHER, P., KALINICHENKO, V. V. & BREUHAHN, K. 2017. Induction of Chromosome Instability by Activation of Yes-Associated Protein and Forkhead Box M1 in Liver Cancer. *Gastroenterology,* 152**,** 2037-2051 e22.

WEINER, A. J., CHRISTOPHERSON, C., HALL, J. E., BONINO, F., SARACCO, G., BRUNETTO, M. R., CRAWFORD, K., MARION, C. D., CRAWFORD, K. A., VENKATAKRISHNA, S. & ET AL. 1991. Sequence variation in hepatitis C viral isolates. *J Hepatol,* 13 Suppl 4**,** S6-14.

WEISS, T. S., LICHTENAUER, M., KIRCHNER, S., STOCK, P., AURICH, H., CHRIST, B., BROCKHOFF, G., KUNZ-SCHUGHART, L. A., JAUCH, K. W., SCHLITT, H. J. & THASLER, W. E. 2008. Hepatic progenitor cells from adult human livers for cell transplantation. *Gut,* 57**,** 1129-38.

WELLS, J. M. & MELTON, D. A. 2000. Early mouse endoderm is patterned by soluble factors from adjacent germ layers. *Development,* 127**,** 1563-72.

WEN, Z., ZHONG, Z. & DARNELL, J. E., JR. 1995. Maximal activation of transcription by Stat1 and Stat3 requires both tyrosine and serine phosphorylation. *Cell,* 82**,** 241-50.

WIERSTRA, I. 2013. FOXM1 (Forkhead box M1) in tumorigenesis: overexpression in human cancer, implication in tumorigenesis, oncogenic functions, tumor-suppressive properties, and target of anticancer therapy. *Adv Cancer Res,* 119**,** 191-419.

WILKINSON, G. R. 2005. Drug metabolism and variability among patients in drug response. *N Engl J Med,* 352**,** 2211-21.

WILLENBRING, H., SHARMA, A. D., VOGEL, A., LEE, A. Y., ROTHFUSS, A., WANG, Z., FINEGOLD, M. & GROMPE, M. 2008. Loss of p21 permits carcinogenesis from chronically damaged liver and kidney epithelial cells despite unchecked apoptosis. *Cancer Cell,* 14**,** 59-67.

WILLIAMS, M. J., CLOUSTON, A. D. & FORBES, S. J. 2014. Links between hepatic fibrosis, ductular reaction, and progenitor cell expansion. *Gastroenterology,* 146**,** 349-56.

WISSE, E., DE ZANGER, R. B., CHARELS, K., VAN DER SMISSEN, P. & MCCUSKEY, R. S. 1985. The liver sieve: considerations concerning the structure and function of endothelial fenestrae, the sinusoidal wall and the space of Disse. *Hepatology,* 5**,** 683-92.

WOODHOUSE, S. D., NARAYAN, R., LATHAM, S., LEE, S., ANTROBUS, R., GANGADHARAN, B., LUO, S., SCHROTH, G. P., KLENERMAN, P. & ZITZMANN, N. 2010. Transcriptome sequencing, microarray, and proteomic analyses reveal cellular and metabolic impact of hepatitis C virus infection in vitro. *Hepatology,* 52**,** 443-53.

WORLD HEALTH ORGANIZATION. 2016a. Combating hepatitis B and C to reach elimination by 2030. Geneva.

WORLD HEALTH ORGANIZATION. 2016b. Global health sector strategy on viral hepatitis 2016-2021. Geneva.

WORLD HEALTH ORGANIZATION. 2017a. Global Health Report, 2017. Geneva.

WORLD HEALTH ORGANIZATION. 2017b. Global Hepatitis Report. Geneva

WORLD HEALTH ORGANIZATION. 2018a. *Fact Sheet- Hepatitis B* [Online]. Geneva: World Health Organization., . Available: http://www.who.int/en/news-room/fact-sheets/detail/hepatitis-b [Accessed 7th August 2018].

WORLD HEALTH ORGANIZATION. 2018b. *Fact Sheet- Hepatitis C* [Online]. Geneva: World Health Organization., . Available: http://www.who.int/en/news-room/fact-sheets/detail/hepatitis-c [Accessed 7th August 2018].

WU, H., XIAO, Y., ZHANG, S., JI, S., WEI, L., FAN, F., GENG, J., TIAN, J., SUN, X., QIN, F., JIN, C., LIN, J., YIN, Z. Y., ZHANG, T., LUO, L., LI, Y., SONG, S., LIN, S. C., DENG, X., CAMARGO, F., AVRUCH, J., CHEN, L. & ZHOU, D. 2013. The Ets transcription factor GABP is a component of the hippo pathway essential for growth and antioxidant defense. *Cell Rep,* 3**,** 1663-77.

WU, S., HUANG, J., DONG, J. & PAN, D. 2003. hippo encodes a Ste-20 family protein kinase that restricts cell proliferation and promotes apoptosis in conjunction with salvador and warts. *Cell,* 114**,** 445-56.

WU, X., ROBOTHAM, J. M., LEE, E., DALTON, S., KNETEMAN, N. M., GILBERT, D. M. & TANG, H. 2012. Productive hepatitis C virus infection of stem cell-derived hepatocytes reveals a critical transition to viral permissiveness during differentiation. *PLoS Pathog,* 8**,** e1002617.

XIAO, H., JIANG, N., ZHOU, B., LIU, Q. & DU, C. 2015. TAZ regulates cell proliferation and epithelial-mesenchymal transition of human hepatocellular carcinoma. *Cancer Sci,* 106**,** 151-9.

XIAO, Q., QIAN, Z., ZHANG, W., LIU, J., HU, E., ZHANG, J., LI, M., WANG, J., KONG, F., LI, Y., WANG, R., TAN, X., HE, D. & XIAO, X. 2016. Depletion of CABYR-a/b sensitizes lung cancer cells to TRAIL-induced apoptosis through YAP/p73-mediated DR5 upregulation. *Oncotarget,* 7**,** 9513-24.

XIE, Y., LI, J. & ZHANG, C. 2018. STAT3 promotes the proliferation and migration of hepatocellular carcinoma cells by regulating AKT2. *Oncol Lett,* 15**,** 3333-3338.

XU, M. Z., YAO, T. J., LEE, N. P., NG, I. O., CHAN, Y. T., ZENDER, L., LOWE, S. W., POON, R. T. & LUK, J. M. 2009. Yes-associated protein is an independent prognostic marker in hepatocellular carcinoma. *Cancer,* 115**,** 4576-85.

XU, P., LUTHRA, P., LI, Z., FUENTES, S., D'ANDREA, J. A., WU, J., RUBIN, S., ROTA, P. A. & HE, B. 2012. The V protein of mumps virus plays a critical role in pathogenesis. *J Virol,* 86**,** 1768-76.

XU, X., XING, B., HU, M., XU, Z., XIE, Y., DAI, G., GU, J., WANG, Y. & ZHANG, Z. 2010a. Recurrent hepatocellular carcinoma cells with stem cell-like properties: possible targets for immunotherapy. *Cytotherapy,* 12**,** 190-200.

XU, X. L., XING, B. C., HAN, H. B., ZHAO, W., HU, M. H., XU, Z. L., LI, J. Y., XIE, Y., GU, J., WANG, Y. & ZHANG, Z. Q. 2010b. The properties of tumor-initiating cells from a hepatocellular carcinoma patient's primary and recurrent tumor. *Carcinogenesis,* 31**,** 167-74.

YAMAGA, A. K. & OU, J. H. 2002. Membrane topology of the hepatitis C virus NS2 protein. *J Biol Chem,* 277**,** 33228-34.

YAMAMOTO, S., KUBO, S., HAI, S., UENISHI, T., YAMAMOTO, T., SHUTO, T., TAKEMURA, S., TANAKA, H., YAMAZAKI, O., HIROHASHI, K. & TANAKA, T.

2004. Hepatitis C virus infection as a likely etiology of intrahepatic cholangiocarcinoma. *Cancer Sci,* 95**,** 592-5.

YAMAMOTO, S., SETA, K., MORISCO, C., VATNER, S. F. & SADOSHIMA, J. 2001. Chelerythrine rapidly induces apoptosis through generation of reactive oxygen species in cardiac myocytes. *J Mol Cell Cardiol,* 33**,** 1829-48.

YAMAMOTO, S., YANG, G., ZABLOCKI, D., LIU, J., HONG, C., KIM, S. J., SOLER, S., ODASHIMA, M., THAISZ, J., YEHIA, G., MOLINA, C. A., YATANI, A., VATNER, D. E., VATNER, S. F. & SADOSHIMA, J. 2003. Activation of Mst1 causes dilated cardiomyopathy by stimulating apoptosis without compensatory ventricular myocyte hypertrophy. *J Clin Invest,* 111**,** 1463-74.

YAMASHITA, T., FORGUES, M., WANG, W., KIM, J. W., YE, Q., JIA, H., BUDHU, A., ZANETTI, K. A., CHEN, Y., QIN, L. X., TANG, Z. Y. & WANG, X. W. 2008. EpCAM and alpha-fetoprotein expression defines novel prognostic subtypes of hepatocellular carcinoma. *Cancer Res,* 68**,** 1451-61.

YAMASHITA, T., HONDA, M., NAKAMOTO, Y., BABA, M., NIO, K., HARA, Y., ZENG, S. S., HAYASHI, T., KONDO, M., TAKATORI, H., YAMASHITA, T., MIZUKOSHI, E., IKEDA, H., ZEN, Y., TAKAMURA, H., WANG, X. W. & KANEKO, S. 2013. Discrete nature of EpCAM+ and CD90+ cancer stem cells in human hepatocellular carcinoma. *Hepatology,* 57**,** 1484-97.

YAMASHITA, T., JI, J., BUDHU, A., FORGUES, M., YANG, W., WANG, H. Y., JIA, H., YE, Q., QIN, L. X., WAUTHIER, E., REID, L. M., MINATO, H., HONDA, M., KANEKO, S., TANG, Z. Y. & WANG, X. W. 2009. EpCAM-positive hepatocellular carcinoma cells are tumor-initiating cells with stem/progenitor cell features. *Gastroenterology,* 136**,** 1012-24.

YAN, F., WANG, Y., ZHANG, W., CHANG, M., HE, Z., XU, J., SHANG, C., CHEN, T., LIU, J., WANG, X., PEI, X. & WANG, Y. 2017. Human embryonic stem cell-derived hepatoblasts are an optimal lineage stage for hepatitis C virus infection. *Hepatology,* 66**,** 717-735.

YANAGI, M., PURCELL, R. H., EMERSON, S. U. & BUKH, J. 1997. Transcripts from a single full-length cDNA clone of hepatitis C virus are infectious when directly transfected into the liver of a chimpanzee. *Proc Natl Acad Sci U S A,* 94**,** 8738-43.

YANG, C. C., GRAVES, H. K., MOYA, I. M., TAO, C., HAMARATOGLU, F., GLADDEN, A. B. & HALDER, G. 2015. Differential regulation of the Hippo pathway by adherens junctions and apical-basal cell polarity modules. *Proc Natl Acad Sci U S A,* 112**,** 1785-90.

YANG, C. H., WANG, H. L., LIN, Y. S., KUMAR, K. P., LIN, H. C., CHANG, C. J., LU, C. C., HUANG, T. T., MARTEL, J., OJCIUS, D. M., CHANG, Y. S., YOUNG, J. D. & LAI, H. C. 2014. Identification of CD24 as a cancer stem cell marker in human nasopharyngeal carcinoma. *PLoS One,* 9**,** e99412.

YANG, F., ROBOTHAM, J. M., NELSON, H. B., IRSIGLER, A., KENWORTHY, R. & TANG, H. 2008a. Cyclophilin A is an essential cofactor for hepatitis C virus infection and the principal mediator of cyclosporine resistance in vitro. *J Virol,* 82**,** 5269-78.

YANG, X. R., XU, Y., YU, B., ZHOU, J., LI, J. C., QIU, S. J., SHI, Y. H., WANG, X. Y., DAI, Z., SHI, G. M., WU, B., WU, L. M., YANG, G. H., ZHANG, B. H., QIN, W. X. & FAN, J. 2009. CD24 is a novel predictor for poor prognosis of hepatocellular carcinoma after surgery. *Clin Cancer Res,* 15**,** 5518-27.

YANG, Z., ZHANG, L., MA, A., LIU, L., LI, J., GU, J. & LIU, Y. 2011. Transient mTOR inhibition facilitates continuous growth of liver tumors by modulating the maintenance of CD133+ cell populations. *PLoS One,* 6**,** e28405.

YANG, Z. F., HO, D. W., NG, M. N., LAU, C. K., YU, W. C., NGAI, P., CHU, P. W., LAM, C. T., POON, R. T. & FAN, S. T. 2008b. Significance of CD90+ cancer stem cells in human liver cancer. *Cancer Cell,* 13**,** 153-66.

YEOH, G. C., ERNST, M., ROSE-JOHN, S., AKHURST, B., PAYNE, C., LONG, S., ALEXANDER, W., CROKER, B., GRAIL, D. & MATTHEWS, V. B. 2007. Opposing roles of gp130-mediated STAT-3 and ERK-1/ 2 signaling in liver progenitor cell migration and proliferation. *Hepatology,* 45**,** 486-94.

YEOMAN, A. D., AL-CHALABI, T., KARANI, J. B., QUAGLIA, A., DEVLIN, J., MIELI-VERGANI, G., BOMFORD, A., O'GRADY, J. G., HARRISON, P. M. & HENEGHAN, M. A. 2008. Evaluation of risk factors in the development of hepatocellular carcinoma in autoimmune hepatitis: Implications for follow-up and screening. *Hepatology,* 48**,** 863-70.

YI, C., SHEN, Z., STEMMER-RACHAMIMOV, A., DAWANY, N., TROUTMAN, S., SHOWE, L. C., LIU, Q., SHIMONO, A., SUDOL, M., HOLMGREN, L., STANGER, B. Z. & KISSIL, J. L. 2013. The p130 isoform of angiomotin is required for Yap-mediated hepatic epithelial cell proliferation and tumorigenesis. *Sci Signal,* 6**,** ra77.

YIM, E. K. & PARK, J. S. 2005. The role of HPV E6 and E7 oncoproteins in HPV-associated cervical carcinogenesis. *Cancer Res Treat,* 37**,** 319-24.

YIMLAMAI, D., CHRISTODOULOU, C., GALLI, G. G., YANGER, K., PEPE-MOONEY, B., GURUNG, B., SHRESTHA, K., CAHAN, P., STANGER, B. Z. & CAMARGO, F. D. 2014. Hippo pathway activity influences liver cell fate. *Cell,* 157**,** 1324-38.

YIN, F., YU, J., ZHENG, Y., CHEN, Q., ZHANG, N. & PAN, D. 2013. Spatial organization of Hippo signaling at the plasma membrane mediated by the tumor suppressor Merlin/NF2. *Cell,* 154**,** 1342-55.

YOO, B. J., SELBY, M. J., CHOE, J., SUH, B. S., CHOI, S. H., JOH, J. S., NUOVO, G. J., LEE, H. S., HOUGHTON, M. & HAN, J. H. 1995. Transfection of a differentiated human hepatoma cell line (Huh7) with in vitro-transcribed hepatitis C virus (HCV) RNA and establishment of a long-term culture persistently infected with HCV. *J Virol,* 69**,** 32-8.

YOON, S. M., GERASIMIDOU, D., KUWAHARA, R., HYTIROGLOU, P., YOO, J. E., PARK, Y. N. & THEISE, N. D. 2011. Epithelial cell adhesion molecule (EpCAM) marks hepatocytes newly derived from stem/progenitor cells in humans. *Hepatology,* 53**,** 964-73.

YOSHIDA, K., MURATA, M., YAMAGUCHI, T., MATSUZAKI, K. & OKAZAKI, K. 2016. Reversible Human TGF-beta Signal Shifting between Tumor Suppression and Fibro-Carcinogenesis: Implications of Smad Phospho-Isoforms for Hepatic Epithelial-Mesenchymal Transitions. *J Clin Med,* 5.

YOSHIZUKA, N., YOSHIZUKA-CHADANI, Y., KRISHNAN, V. & ZEICHNER, S. L. 2005. Human immunodeficiency virus type 1 Vpr-dependent cell cycle arrest through a mitogen-activated protein kinase signal transduction pathway. *J Virol,* 79**,** 11366-81.

YOUNG, K., TWEEDIE, E., CONLEY, B., AMES, J., FITZSIMONS, M., BROOKS, P., LIAW, L. & VARY, C. P. 2015. BMP9 Crosstalk with the Hippo Pathway Regulates Endothelial Cell Matricellular and Chemokine Responses. *PLoS One,* 10**,** e0122892.

YU, F. X., ZHAO, B., PANUPINTHU, N., JEWELL, J. L., LIAN, I., WANG, L. H., ZHAO, J., YUAN, H., TUMANENG, K., LI, H., FU, X. D., MILLS, G. B. & GUAN, K. L. 2012. Regulation of the Hippo-YAP pathway by G-protein-coupled receptor signaling. *Cell,* 150**,** 780-91.

YUAN, J., KRAMER, A., MATTHESS, Y., YAN, R., SPANKUCH, B., GATJE, R., KNECHT, R., KAUFMANN, M. & STREBHARDT, K. 2006. Stable gene silencing of cyclin B1 in tumor cells increases susceptibility to taxol and leads to growth arrest in vivo. *Oncogene,* 25**,** 1753-62.

YUEN, M. F., CHEN, D. S., DUSHEIKO, G. M., JANSSEN, H. L. A., LAU, D. T. Y., LOCARNINI, S. A., PETERS, M. G. & LAI, C. L. 2018. Hepatitis B virus infection. *Nat Rev Dis Primers,* 4**,** 18035.

ZAIDI, S. K., SULLIVAN, A. J., MEDINA, R., ITO, Y., VAN WIJNEN, A. J., STEIN, J. L., LIAN, J. B. & STEIN, G. S. 2004. Tyrosine phosphorylation controls Runx2-mediated subnuclear targeting of YAP to repress transcription. *EMBO J,* 23**,** 790-9.

ZANCONATO, F., CORDENONSI, M. & PICCOLO, S. 2016. YAP/TAZ at the Roots of Cancer. *Cancer Cell,* 29**,** 783-803.

ZEISEL, M. B., FELMLEE, D. J. & BAUMERT, T. F. 2013. Hepatitis C virus entry. *Curr Top Microbiol Immunol,* 369**,** 87-112.

ZEKRI, A. R., BAHNASY, A. A., SHOEAB, F. E., MOHAMED, W. S., EL-DAHSHAN, D. H., ALI, F. T., SABRY, G. M., DASGUPTA, N. & DAOUD, S. S. 2014. Methylation of multiple genes in hepatitis C virus associated hepatocellular carcinoma. *J Adv Res,* 5**,** 27-40.

ZEMEL, R., GERECHET, S., GREIF, H., BACHMATOVE, L., BIRK, Y., GOLAN-GOLDHIRSH, A., KUNIN, M., BERDICHEVSKY, Y., BENHAR, I. & TUR-KASPA, R. 2001. Cell transformation induced by hepatitis C virus NS3 serine protease. *J Viral Hepat,* 8**,** 96-102.

ZENDER, L., SPECTOR, M. S., XUE, W., FLEMMING, P., CORDON-CARDO, C., SILKE, J., FAN, S. T., LUK, J. M., WIGLER, M., HANNON, G. J., MU, D., LUCITO, R., POWERS, S. & LOWE, S. W. 2006. Identification and validation of oncogenes in liver cancer using an integrative oncogenomic approach. *Cell,* 125**,** 1253-67.

ZEUZEM, S., MIZOKAMI, M., PIANKO, S., MANGIA, A., HAN, K. H., MARTIN, R., SVAROVSKAIA, E., DVORY-SOBOL, H., DOEHLE, B., HEDSKOG, C., YUN, C., BRAINARD, D. M., KNOX, S., MCHUTCHISON, J. G., MILLER, M. D., MO, H., CHUANG, W. L., JACOBSON, I., DORE, G. J. & SULKOWSKI, M. 2017. NS5A resistance-associated substitutions in patients with genotype 1 hepatitis C virus: Prevalence and effect on treatment outcome. *J Hepatol,* 66**,** 910-918.

ZHAN, D. Q., WEI, S., LIU, C., LIANG, B. Y., JI, G. B., CHEN, X. P., XIONG, M. & HUANG, Z. Y. 2012. Reduced N-cadherin expression is associated with metastatic potential and poor surgical outcomes of hepatocellular carcinoma. *J Gastroenterol Hepatol,* 27**,** 173-80.

ZHANG, C., CAI, Z., KIM, Y. C., KUMAR, R., YUAN, F., SHI, P. Y., KAO, C. & LUO, G. 2005. Stimulation of hepatitis C virus (HCV) nonstructural protein 3 (NS3) helicase activity by the NS3 protease domain and by HCV RNA-dependent RNA polymerase. *J Virol,* 79**,** 8687-97.

ZHANG, H., LIU, C. Y., ZHA, Z. Y., ZHAO, B., YAO, J., ZHAO, S., XIONG, Y., LEI, Q. Y. & GUAN, K. L. 2009. TEAD transcription factors mediate the function of TAZ in cell growth and epithelial-mesenchymal transition. *J Biol Chem,* 284**,** 13355-62.

ZHANG, J., YAMADA, O., ITO, T., AKIYAMA, M., HASHIMOTO, Y., YOSHIDA, H., MAKINO, R., MASAGO, A., UEMURA, H. & ARAKI, H. 1999. A single nucleotide insertion in the 5'-untranslated region of hepatitis C virus leads to enhanced cap-independent translation. *Virology,* 261**,** 263-70.

ZHANG, N., BAI, H., DAVID, K. K., DONG, J., ZHENG, Y., CAI, J., GIOVANNINI, M., LIU, P., ANDERS, R. A. & PAN, D. 2010. The Merlin/NF2 tumor suppressor

functions through the YAP oncoprotein to regulate tissue homeostasis in mammals. *Dev Cell,* 19**,** 27-38.

ZHANG, Q., GONG, R., QU, J., ZHOU, Y., LIU, W., CHEN, M., LIU, Y., ZHU, Y. & WU, J. 2012. Activation of the Ras/Raf/MEK pathway facilitates hepatitis C virus replication via attenuation of the interferon-JAK-STAT pathway. *J Virol,* 86**,** 1544-54.

ZHAO, B., LI, L., LU, Q., WANG, L. H., LIU, C. Y., LEI, Q. & GUAN, K. L. 2011. Angiomotin is a novel Hippo pathway component that inhibits YAP oncoprotein. *Genes Dev,* 25**,** 51-63.

ZHAO, B., LI, L., TUMANENG, K., WANG, C. Y. & GUAN, K. L. 2010. A coordinated phosphorylation by Lats and CK1 regulates YAP stability through SCF(beta-TRCP). *Genes Dev,* 24**,** 72-85.

ZHAO, B., LI, L., WANG, L., WANG, C. Y., YU, J. & GUAN, K. L. 2012. Cell detachment activates the Hippo pathway via cytoskeleton reorganization to induce anoikis. *Genes Dev,* 26**,** 54-68.

ZHAO, B., WEI, X., LI, W., UDAN, R. S., YANG, Q., KIM, J., XIE, J., IKENOUE, T., YU, J., LI, L., ZHENG, P., YE, K., CHINNAIYAN, A., HALDER, G., LAI, Z. C. & GUAN, K. L. 2007. Inactivation of YAP oncoprotein by the Hippo pathway is involved in cell contact inhibition and tissue growth control. *Genes Dev,* 21**,** 2747-61.

ZHAO, B., YE, X., YU, J., LI, L., LI, W., LI, S., LIN, J. D., WANG, C. Y., CHINNAIYAN, A. M., LAI, Z. C. & GUAN, K. L. 2008. TEAD mediates YAP-dependent gene induction and growth control. *Genes Dev,* 22**,** 1962-71.

ZHAO, R., WATT, A. J., LI, J., LUEBKE-WHEELER, J., MORRISEY, E. E. & DUNCAN, S. A. 2005. GATA6 is essential for embryonic development of the liver but dispensable for early heart formation. *Mol Cell Biol,* 25**,** 2622-31.

ZHI, X., ZHAO, D., ZHOU, Z., LIU, R. & CHEN, C. 2012. YAP promotes breast cell proliferation and survival partially through stabilizing the KLF5 transcription factor. *Am J Pathol,* 180**,** 2452-61.

ZHOU, D., CONRAD, C., XIA, F., PARK, J. S., PAYER, B., YIN, Y., LAUWERS, G. Y., THASLER, W., LEE, J. T., AVRUCH, J. & BARDEESY, N. 2009. Mst1 and Mst2 maintain hepatocyte quiescence and suppress hepatocellular carcinoma development through inactivation of the Yap1 oncogene. *Cancer Cell,* 16**,** 425-38.

ZHU, X. D., ZHANG, J. B., FAN, P. L., XIONG, Y. Q., ZHUANG, P. Y., ZHANG, W., XU, H. X., GAO, D. M., KONG, L. Q., WANG, L., WU, W. Z., TANG, Z. Y., DING, H. & SUN, H. C. 2011. Antiangiogenic effects of pazopanib in xenograft hepatocellular carcinoma models: evaluation by quantitative contrast-enhanced ultrasonography. *BMC Cancer,* 11**,** 28.

ZHU, Y. & CHEN, S. 2013. Antiviral treatment of hepatitis C virus infection and factors affecting efficacy. *World J Gastroenterol,* 19**,** 8963-73.

ZHU, Z., HAO, X., YAN, M., YAO, M., GE, C., GU, J. & LI, J. 2010. Cancer stem/progenitor cells are highly enriched in CD133+CD44+ population in hepatocellular carcinoma. *Int J Cancer,* 126**,** 2067-78.

ZIGNEGO, A. L., FERRI, C., GIANNINI, C., LA CIVITA, L., CARECCIA, G., LONGOMBARDO, G., BELLESI, G., CARACCIOLO, F., THIERS, V. & GENTILINI, P. 1997. Hepatitis C virus infection in mixed cryoglobulinemia and B-cell non-Hodgkin's lymphoma: evidence for a pathogenetic role. *Arch Virol,* 142**,** 545-55.

ZIMPFER, A., MARUSCHKE, M., REHN, S., KUNDT, G., LITZENBERGER, A., DAMMERT, F., ZETTL, H., STEPHAN, C., HAKENBERG, O. W. &

ERBERSDOBLER, A. 2014. Prognostic and diagnostic implications of epithelial cell adhesion/activating molecule (EpCAM) expression in renal tumours: a retrospective clinicopathological study of 948 cases using tissue microarrays. *BJU Int,* 114**,** 296-302.

ZONG, Y. & STANGER, B. Z. 2012. Molecular mechanisms of liver and bile duct development. *Wiley Interdiscip Rev Dev Biol,* 1**,** 643-55.

ZORN, A. M. 2008. Liver development. *StemBook.* Cambridge (MA): Harvard Stem Cell Institute



ZORN, A. M. & WELLS, J. M. 2007. Molecular basis of vertebrate endoderm development. *Int Rev Cytol,* 259**,** 49-111.